Analyses of Ship Collisions: Determination of Longitudinal Extent of Damage and Penetration

by

John A.W. Sajdak

Dissertation submitted to the faculty of the
Virginia Polytechnic Institute and State University
in partial fulfillment of the requirements for the degree of

Doctorate of Philosophy
in
Naval Architecture and Ocean Engineering

Dr. Alan J. Brown, Chairman

Dr. Rakesh K. Kapania

Dr. Owen F. Hughes

Dr. Eric Johnson

Dr. Bob West, Jr.

July 29, 2004
Virginia Tech, Blacksburg, VA, USA

Keywords: ship, collision, damage, bow, deformation, longitudinal

Analyses of Ship Collisions:
Determination of Longitudinal Extent of Damage and Penetration

John A.W. Sajdak

Abstract

The overall objective of this thesis is to develop, validate and assess a probabilistic collision damage model to support ongoing work by the Society of Naval Architecture and Marine Engineering (SNAME) Ad Hoc Panel #6 and IMO working groups. It is generally agreed that structural design has a major influence on tanker oil outflow and damaged stability in grounding and collision, but crashworthiness is not considered in present regulations. The proposed methodology provides a practical means of considering structural design in a regulatory framework, and when implemented would improve the safety and environmental performance of ships. This dissertation continues the development and applies a Simplified Collision Model (SIMCOL) to calculate damage extent (transverse, vertical and longitudinal) and oil outflow in ship collisions. The primary contribution of this dissertation is the development and validation of a theory for the determination of energy absorbed in longitudinal extent of damage, and the implementation of the theory within SIMCOL.

SIMCOL is sufficiently fast to be applied to thousands of collision cases as is required for a probabilistic analysis. The following specific tasks were completed using SIMCOL in support of this project:

- Completed the development of SIMCOL Version 3.0 including:
  1) Deformable Bow sub model
  2) Implementation and validation of theory for the determination of energy absorbed in longitudinal extent of damage.
- Developed the capability to model collision events using LSDYNA.
- Validated Virginia Tech LSDYNA ship collision modeling procedure.
- Validated SIMCOL using real collision data, and probabilistic collision data for penetrating collision

Table of Contents

Abstract ii

Table of Contents iii

List of Figures vi

List of Tables xi

Acknowledgements xii

1 Introduction and Motivation 1

2 The Collision Phenomenon 6

2.1 Ship-to-Ship Collisions 6

2.2 Collision Physics 7

2.3 Vessel Motion 12

2.4 Energy Absorbing Structure 14

3 Finite Element Modeling of Ship Collisions 21

3.1 Overview 21

3.2 Structural Geometry 22

3.3 Element Types 28

3.4 Finite Element Mesh 28

3.5 Smearing Techniques 29

3.6 External Dynamics and Constraints 35

3.7 Analysis Parameters 37

3.7.1 Contact and Friction 37

3.7.2 Material Properties 41

3.7.3 Element Failure 44

3.7.4 Strain Rate 55

3.8 Calibration 56

3.8.1 David E. Day - Marine Flier Collision 56

3.9 Summary of Finite Element Analysis in Ship-to-Ship Collisions 66

4 Simplified Methods 67

4.1 Timeline and Summary 67

4.2 Important Characteristics of a Ship-to-Ship Collision Model 68

4.3 Methods for Determining Energy Absorbed by the Struck Ship 69

4.3.1 Minorsky (Energy Coefficient) Method 69

4.3.2 Pederesen and Zhang Energy Coefficient 72

4.3.3 Paik and Pedersen Energy Coefficient 74

4.3.4 ALPS/SCOL 74

4.3.5 DAMAGE 76

4.4 Methods for Determining Energy Absorbed by the Striking Ship Bow 76

4.4.1 Amdahl's Method 76

4.4.2 Pedersen's Method 77

4.5 Methods for Determining Energy Absorbed the Striking and Struck Ships 78
4.5.1 DTU Collision Model 78
4.5.2 SIMCOL Version 2.1 80

4.6 Summary of Simplified Methods 105

5 SIMCOL Version 3.0 107

5.1 Energy Coefficient Method for use with Structural Decks ad Stringers 108

5.2 Energy Coefficient Method for use with Longitudinal and Transverse Bulkheads and Longitudinal Crushing of Side Shell 117

5.3 Deformable Bow Model 124

5.4 Longitudinal Deflection of Transverse Bulkheads and Webs 125
5.4.1 Flow Theory of Plasticity 141
5.4.2 Energy Absorption in Rectangular Region 145
5.4.3 Energy Absorption in Triangular Region 149
5.4.4 The Energy Absorbed from an Eight-Region Plate 153
5.4.5 The Energy Absorbed from a Twenty-Five-Region Plate 156
5.4.6 Validation of Energy Absorption of Twenty-Five-Region Plate 200

6 Correlation and Validation of SIMCOL 221

6.1 SIMCOL Correlation 221

6.2 SIMCOL Validation 225
6.2.1 David E. Day Marine Flier Collision 225
6.2.2 P&T Adventurer Tullahoma Collision 226

6.3 SIMCOL Probabilistic Validation 227

7 Conclusions 232

8 Future Work 233

References 234

Appendix A: 150K dwt Bulk Carrier Bow Structural Data 244

Appendix B: 40K dwt Container Ship Bow Structural Data 246

Appendix C: C4 Cargo Ship Bow Structural Data 248

Appendix D: Victory Cargo Ship Bow Structural Data 249

Appendix E: 150K dwt Double Hull Tanker Cargo Section Structural Data 254

Appendix F: T2 Tanker Cargo Section Structural Data 284

Appendix G: Amdahl Calculation of Energy Absorbed by Bow Damage 290

Appendix H: Pedersen Calculation of Energy Absorbed by Bow Damage 323

Appendix I: Example LSDYNA Finite Element Input File 325

Appendix J: Flowchart of Method of Lateral Deformation of Webs and Transverse Bulkheads 334

Appendix K: 100k dwt Single Hull Tanker Cargo Section Structural Data 380

Vita _____ *402*

List of Figures

Figure 1-1 Methodology to Determine Probabilistic Damage in Collision [3] *3*
Figure 2-1 Illustration of Damage Definition *7*
Figure 2-2 Collision of M/V Alexia and M/V Enif *9*
Figure 2-3 Damage to M/V Enif *10*
Figure 2-4 Collision of M/T Gas Roman and M/V Springbok *10*
Figure 2-5 Bow Penetration of Collision of M/T Gas Roman and M/V Springok *11*
Figure 2-6 Bow Damage of Collision of M/T Gas Roman and M/V Springbok *12*
Figure 2-7 Illustration of Constrained Vessel Yaw *14*
Figure 2-8 Actual Collision Bow Damage *19*
Figure 2-9 Bow Damage to Norwegian Dream *19*
Figure 2-10 Karisa Bow Damage *20*
Figure 3-1 Ship-to-Ship Collision as Modeled in LSDYNA *23*
Figure 3-2 Detailed LSDYNA Bow Model *23*
Figure 3-3 Struck Ship LSDYNA Model *25*
Figure 3-4 Struck Ship Cargo Section Mesh *26*
Figure 3-5 Struck Ship Cargo Section Geometry View from Outboard *27*
Figure 3-6 Struck Ship Cargo Section Geometry View from Centerline *27*
Figure 3-7 Rigid Bow Collision With Double-Sided Test Section *30*
Figure 3-8 Smearing Test Result Comparison of Energy vs. Penetration *33*
Figure 3-9 Smearing Cases 1,2 and 6 Result Comparison of Energy vs. Penetration *34*
Figure 3-10 Smearing Case 1 and 2 Hourglass Energy vs. Time *35*
Figure 3-11 Contact Nodal Requirement *38*
Figure 3-12 Friction and Kinetic Energy vs. Penetration [70] *39*
Figure 3-13 Coulomb Friction vs. Relative Velocity of Contact Surfaces *41*
Figure 3-14 Kinematic/Isotropic Elastic Plastic Material Stress Strain Curve *42*
Figure 3-15 Material Types 3 and 24 Stress/Strain Curves *44*
Figure 3-16 Comparison of Element Failure Criteria CB and CM *45*
Figure 3-17 Illustration of Ductile and Brittle Fractures *46*
Figure 3-18 Reported Failure Strains vs. Element Length Sizes [29,57,59,60,61,69,72,73,74,75] *47*
Figure 3-19 Kitamura Necessary Failure Strain Results [57] *48*
Figure 3-20 Charpy-V-Notch (CVN) Test *49*
Figure 3-21 Charpy-V-Notch (CVN) Sample Dimension *49*
Figure 3-22 Sample Charpy Test Data of ABS Grade B Steel [76] *50*
Figure 3-23 CVN FEM Mesh *51*
Figure 3-24 CVN FEM Analysis *52*
Figure 3-25 FEA Charpy Energy vs. Sample Thickness *53*
Figure 3-26 FEA Charpy Energy vs. L/T Ratio *53*
Figure 3-27 FEA Charpy Energy (divided by 10) vs. Failure Strain (FS) *54*
Figure 3-28 David E. Day - Marine Flier Collision Analysis FEA Model *57*
Figure 3-29 David E. Day Marine Flier FEA Damage at 0.5 Seconds *58*
Figure 3-30 David E. Day FEA Hull Damage at 0.5 Seconds *58*
Figure 3-31 Marine Flier FEA Bow Damage at 0.5 Seconds *58*
Figure 3-32 David E. Day - Marine Flier Damage at 1.0 Seconds *59*

Figure 3-33 David E. Day FEA Hull Damage at 1.0 Seconds *59*
Figure 3-34 Marine Flier FEA Bow Damage at 1.0 Seconds *59*
Figure 3-35 David E. Day - Marine Flier FEA Damage at 1.5 Seconds *60*
Figure 3-36 David E. Day FEA Hull Damage at 1.5 Seconds *60*
Figure 3-37 Marine Flier FEA Bow Damage at 1.5 Seconds *60*
Figure 3-38 David E. Day - Marine Flier FEA Damage at 2.0 seconds *61*
Figure 3-39 David E. Day FEA Hull Damage at 2.0 seconds *61*
Figure 3-40 Marine Flier FEA Bow Damage at 2.0 Seconds *61*
Figure 3-41 David E. Day - Marine Flier FEA Damage at 2.5 Seconds *62*
Figure 3-42 David E. Day FEA Hull Damage at 2.5 Seconds *62*
Figure 3-43 Marine Flier FEA Bow Damage at 2.5 Seconds *62*
Figure 3-44 David E. Day - Marine Flier FEA Damage at 3.0 Seconds *63*
Figure 3-45 David E. Day FEA Hull Damage at 3.5 Seconds *63*
Figure 3-46 Marine Flier FEA Bow Damage at 3.0 Seconds *63*
Figure 3-47 David E. Day - Marine Flier FEA Damage at 3.5 Seconds *64*
Figure 3-48 David E. Day FEA Hull Damage at 3.5 Seconds *64*
Figure 3-49 Marine Flier FEA Bow Damage at 3.5 Seconds *64*
Figure 3-50 David E. Day - Marine Flier FEA Damage at 4.0 Seconds *65*
Figure 3-51 Marine Flier FEA Bow Damage at 4.0 Seconds *65*
Figure 3-52 David E. Day FEA Hull Damage at 4.0 Seconds *65*
Figure 4-1 Reardon and Sprung Absorbed Energy vs. Damaged Volume *71*
Figure 4-2 Paik, Choe and Thayamballi Absobed Energy vs. Damaged Volume *72*
Figure 4-3 Pedersen and Zhang Absorbed Energy vs. Damaged Volume *73*
Figure 4-4 Damage from ALPS/SCOL Simulation *75*
Figure 4-5 SIMCOL Simulation Process *81*
Figure 4-6 SIMCOL External Ship Dynamics *82*
Figure 4-7 Web Deformation in SIMCOL *87*
Figure 4-8 Membrane Geometry *89*
Figure 4-9 Force Diagram for an Oblique Angle Collision *91*
Figure 4-10 Deflection and Forces in Distorted Web Frames *92*
Figure 4-11 Sweeping Segment Method *97*
Figure 4-12 Sweeping Segment Geometry *100*
Figure 5-1 Deck Crushing Showing Accordion Folding [21] *108*
Figure 5-2 Deck Crushing Showing Bow Impingement [21] *108*
Figure 5-3 Plate Crushing vs. Tearing (Cutting) [21] *109*
Figure 5-4 Rigid Wedge Cutting and Crushing Deck in Drop Test [89] *109*
Figure 5-5 FEA Deck Cutting and Crushing *109*
Figure 5-6 FEA Simplified Deck Crushing and Cutting Test Model *110*
Figure 5-7 FEA Deck Crushing and Tearing with HEA = 30 Degrees at 0.5 Seconds .. *112*
Figure 5-8 Deck Crushing and Tearing with HEA = 30 Degrees at 1.0 Seconds *112*
Figure 5-9 Deck Crushing and Tearing with HEA = 30 Degrees at 1.5 Seconds *113*
Figure 5-10 Deck Crushing and Tearing with HEA = 30 Degrees at 2.0 Seconds *113*
Figure 5-11 FEA Plate Mesh Showing Crushing and Tearing at 2.0 Seconds from HEA = 30 Degrees *114*
Figure 5-12 Absorbed Energy vs. Penetration at HEA = 30 Degrees *114*
Figure 5-13 Absorbed Energy vs. Penetration at HEA = 45 Degrees *115*

Figure 5-14 Absorbed Energy vs. Penetration at HEA = 60 Degrees *115*
Figure 5-15 Actual Longitudinal Bulkhead Crushing *117*
Figure 5-16 FEA Example of Longitudinal Bulkhead Crushing *118*
Figure 5-17 Simplified Longitudinal/Transverse Bulkhead Crushing Model *119*
Figure 5-18 Bulkhead Crushing at 0.5 Seconds *120*
Figure 5-19 Bulkhead Crushing at 1.0 Seconds *120*
Figure 5-20 Bulkhead Crushing at 1.5 Seconds *121*
Figure 5-21 Bulkhead Mesh Crushing at 1.5 Seconds *121*
Figure 5-22 Absorbed Energy vs. Time for Crushing of Bulkheads *122*
Figure 5-23 Damage Extent vs. Time for Bulkhead Crushing *122*
Figure 5-24 Absorbed Energy vs. Damage Extent for Bulkhead Crushing *123*
Figure 5-25 Crushing Force vs. Penetration for 150K Bulk Carrier Striking a rigid wall at 90 Degrees *124*
Figure 5-26 Actual Longitudinally Deformed Web [89] *126*
Figure 5-27 Ship Damage Showing Longitudinally Deflected Bulkhead and Impinging Bow Shape *127*
Figure 5-28 FEA Showing Longitudinal Deformation of Transverse Bulkhead *127*
Figure 5-29 Idealized Transverse Plate Model *128*
Figure 5-30 SIMCOL Wedge Model *129*
Figure 5-31 Contact Scenario 1 Geometry *130*
Figure 5-32 Contact Scenario 1 FEA Test Case at 0.1 Seconds *130*
Figure 5-33 Contact Scenario 1 FEA Test Case at 0.2 Seconds *130*
Figure 5-34 Contact Scenario 1 FEA Test Case at 0.3 Seconds *131*
Figure 5-35 Contact Scenario 1 FEA Test Case at 0.8 Seconds *131*
Figure 5-36 Contact Scenario 2 Geometry *131*
Figure 5-37 Contact Scenario 2 FEA Test Case at 0.2 Seconds *132*
Figure 5-38 Contact Scenario 2 FEA Test Case at 0.25 Seconds *132*
Figure 5-39 Contact Scenario 2 FEA Plate Mesh Deflection at 0.25 Seconds with 8 region model overlay *133*
Figure 5-40 Contact Scenario 3 Geometry *133*
Figure 5-41 Contact Scenario 3 FEA Test Case at 0.1 Seconds *134*
Figure 5-42 Contact Scenario 3 FEA Test Case at 0.2 Seconds *134*
Figure 5-43 Contact Scenario 3 FEA Test Case at 0.3 Seconds *134*
Figure 5-44 Contact Scenario 3 Plate Mesh Deformation at 0.3 Seconds *135*
Figure 5-45 Contact Scenario 4 Geometry *135*
Figure 5-46 Contact Scenario 4 FEA Test Case at 0.1 Seconds *135*
Figure 5-47 Contact Scenario 4 FEA Test Case at 0.2 Seconds *136*
Figure 5-48 Contact Scenario 4 Plate Mesh Deflection at 0.2 Seconds *136*
Figure 5-49 Longitudinal Deflection Simplified Argument Example Geometry *137*
Figure 5-50 Idealized Plate Geometry Definitions for Simplified Argument *137*
Figure 5-51 Centered Vertical Position of Wedge Striking Plate *138*
Figure 5-52 Lower Vertical Position of Wedge Striking Plate *139*
Figure 5-53 Upper Vertical Position of Wedge Striking Plate *139*
Figure 5-54 Simplified Plate Deflection (left) and Similar FEA Plate Mesh Deflection (right) *140*
Figure 5-55 Eight Region Plate Model *141*

Figure 5-56 Rectangular Region Geometry and Nomenclature *145*
Figure 5-57 Triangular Region Geometry and Nomenclature *149*
Figure 5-58 Eight Region Plate Absorbed Energy vs. Time Comparison to FEA *156*
Figure 5-59 Twenty-five Region Plate Overlaying FEA Plate Mesh Deformation *157*
Figure 5-60 Twenty-five Region Plate Geometry *158*
Figure 5-61 Striking Wedge Variable Definitions *173*
Figure 5-62 Collision Angle Definition *173*
Figure 5-63 Test Case 4 Twenty-Five Region Plate Deflection at 0.1 Seconds *201*
Figure 5-64 Test Case 4 FEA Deflection at 0.1 Seconds *202*
Figure 5-65 Test Case 4 Twenty-Five Region Plate Deflection at 0.2 Seconds *202*
Figure 5-66 Test Case 4 FEA Deflection at 0.2 Seconds *202*
Figure 5-67 Test Case 4 Twenty-Five Region Plate Deflection at 0.3 Seconds *203*
Figure 5-68 Test Case 4 FEA Deflection at 0.3 Seconds *203*
Figure 5-69 Test Case 4 Twenty-Five Region Plate Deflection at 0.35 Seconds *203*
Figure 5-70 Test Case 4 FEA Deflection at 0.35 Seconds *204*
Figure 5-71 Test Case 4 FEA Plate Mesh Deflection at 0.35 Seconds *204*
Figure 5-72 Case 1 Simplified Method and FEA Absorbed Energy vs. Time Comparison *204*
Figure 5-73 Case 2 Simplified Method and FEA Absorbed Energy vs. Time Comparison *205*
Figure 5-74 Case 3 Simplified Method and FEA Absorbed Energy vs. Time Comparison *205*
Figure 5-75 Case 4 Simplified Method and FEA Absorbed Energy vs. Time Comparison *206*
Figure 5-76 Case 5 Simplified Method and FEA Absorbed Energy vs. Time Comparison *206*
Figure 5-77 Case 6 Simplified Method and FEA Absorbed Energy vs. Time Comparison *207*
Figure 5-78 Case 7 Simplified Method and FEA Absorbed Energy vs. Time Comparison *207*
Figure 5-79 Case 8 Simplified Method and FEA Absorbed Energy vs. Time Comparison *208*
Figure 5-80 Case 9 Simplified Method and FEA Absorbed Energy vs. Time Comparison *208*
Figure 5-81 Case 10 Simplified Method and FEA Absorbed Energy vs. Time Comparison *209*
Figure 5-82 Case 11 Simplified Method and FEA Absorbed Energy vs. Time Comparison *209*
Figure 5-83 Case 12 Simplified Method and FEA Absorbed Energy vs. Time Comparison *210*
Figure 5-84 Case 13 Simplified Method and FEA Absorbed Energy vs. Time Comparison *210*
Figure 5-85 Case 14 Simplified Method and FEA Absorbed Energy vs. Time Comparison *211*
Figure 5-86 Case 15 Simplified Method and FEA Absorbed Energy vs. Time Comparison *211*

Figure 5-87 Case 16 Simplified Method and FEA Absorbed Energy vs. Time Comparison *212*
Figure 5-88 Case 17 Simplified Method and FEA Absorbed Energy vs. Time Comparison *212*
Figure 5-89 Case 18 Simplified Method and FEA Absorbed Energy vs. Time Comparison *213*
Figure 5-90 Case 19 Simplified Method and FEA Absorbed Energy vs. Time Comparison *213*
Figure 5-91 Case 20 Simplified Method and FEA Absorbed Energy vs. Time Comparison *214*
Figure 5-92 FEA Plate Crushing *215*
Figure 5-93 FEA Bending vs. Simplified Method Deformation *216*
Figure 5-94 Case 2 Simplified Method (With and Without Crushing) and FEA Comparison *216*
Figure 5-95 Case 7 Simplified Method (With and Without Crushing) and FEA Comparison *217*
Figure 5-96 Case 8 Simplified Method (With and Without Crushing) and FEA Comparison *217*
Figure 5-97 Case 12 Simplified Method (With and Without Crushing) and FEA Comparison *218*
Figure 5-98 Case 15 Simplified Method (With and Without Crushing) and FEA Comparison *218*
Figure 5-99 Case 18 Simplified Method (With and Without Crushing) and FEA Comparison *219*
Figure 5-100 Case 19 Simplified Method (With and Without Crushing) and FEA Comparison *219*
Figure 6-1 Penetration vs. Collision Location for BC150 Striking DH150 at 90 Degrees and 3 knots *221*
Figure 6-2 Penetration vs. Collision Location for BC150 Striking DH150 at 90 Degrees and 7 knots *222*
Figure 6-3 Penetration vs. Collision Location for BC150 Striking DH150 at 90 Degrees and 3 knots *222*
Figure 6-4 Penetration vs. Collision Location for BC150 Striking DH150 at 90 Degrees and 7 knots *223*
Figure 6-5 Penetration vs. Collision Angle for BC150 - DH150 at 3.5 m fwd Amidships and 3 knots *223*
Figure 6-6 Penetration vs. Collision Angle for BC150 - DH150 at 3.5 m fwd Amidships and 7 knots *224*
Figure 6-7: SIMCOL, MARPOL & HARDER SH100 Penetration Comparison *228*
Figure 6-8: SIMCOL, MARPOL & HARDER DH150 Penetration Comparison *228*
Figure 6-9: SIMCOL, MARPOL & HARDER SH100 LED Comparison *229*
Figure 6-10: SIMCOL, MARPOL & HARDER DH150 LED Comparison *229*

List of Tables

Table 2-1 Collision Energy Absorbing Structure *15*
Table 2-2 Collision Descriptions *16*
Table 2-3 Percentage of Energy Absorbed by Striking Ship Bow [15,36] *17*
Table 2-4 Percentage of Energy Absorbed by Striking Bow in Collisions [47] *18*
Table 3-1 Double-Sided Test Section Parameters *31*
Table 3-2 Smearing Test Case Nomenclature *33*
Table 3-3 Material Type 3 Definitions *42*
Table 3-4 Material Type 24 Definitions *43*
Table 4-1 Energy Absorbing Structure Method Summary for SIMCOL *102*
Table 4-2 Simplified Method Summary *105*
Table 5-1 FEA Simplified Deck Crushing and Cutting Test Parameters *111*
Table 5-2 Correlation Results of Energy Coefficient Methods to FEA at HEA = 30 Degrees *116*
Table 5-3 Simplified Longitudinal/Transverse Crushing Parameters *119*
Table 5-4 Correlation Results of Energy Coefficient Methods for Bulkhead Crushing *123*
Table 5-5 Eight Region Plate Analysis Initial Conditions *155*
Table 5-6 Constant Parameters for Twenty-Five Region Plate Test Cases *200*
Table 5-7 Twenty-Five Region Plate Test Case Variable Values *201*
Table 5-8 Correlation Coefficient of Simplified Method to FEA Energy vs. Time Curves *220*
Table 6-1 FEA - SIMCOL Validation Percent Difference *226*
Table 6-2: SIMCOL Validation Percent Difference *227*

Acknowledgements

The Completion of this dissertation would have been impossible without the support of many people. First of all, I would like to express appreciation to my advisor, Dr. Alan Brown, for his continuous support and guidance throughout the duration of this work.

This Dissertation is dedicated to my wife, Mindy, who has been a constant source of inspiration and encouragement. Her love and support has helped through difficult times and interesting challenges.

I would like to acknowledge my committee, Dr. Rakesh Kapania, Dr. Owen Hughes, Dr. Bob West, and Dr. Eric Johnson, for all their assistance, guidance and support.

Also I would like to acknowledge the following people for their much-appreciated support:

- Martin, Ottaway, van Hemmen & Dolan, Inc.
    - James Dolan
    - Rik van Hemmen
    - David Tantrum
    - Pierce Power
    - Wayne Thomas
- Livermore Software Technology Corporation
- Dr. Mike Allen
- Dr. Wayne Neu
- Jason Cordell
- Keith Webster
- Laura Waltham
- Gail Coe
- Betty Williams
- Wanda Foushee

1 Introduction and Motivation

The serious consequences of ship grounding and collision necessitate the development of regulations and requirements for the subdivision and structural design of ships to reduce damage and environmental pollution, and improve safety. This report addresses primarily oil tanker damage and oil pollution, but the process and damage calculations are directly applicable to damage stability calculations and regulations.

The International Maritime Organization (IMO) is responsible for regulating the design of oil tankers and other ships to provide for ship safety and environmental protection. Their ongoing transition to probabilistic performance-based standards requires the ability to predict the environmental performance and safety of specific ship designs. This is a difficult problem requiring the application of fundamental engineering principles and risk analysis [1,2,3,4].

IMO's first attempt at probabilistic performance-based standards for oil tankers was in response to the U.S. Oil Pollution Act of 1990 (OPA 90). In OPA 90, the U.S. requires that all oil tankers entering the U.S. waters must have double hulls. IMO responded to this unilateral action by requiring double hulls or their equivalent. Equivalency is determined based on probabilistic oil outflow calculations specified in the "Interim Guidelines for the Approval of Alternative Methods of Design and Construction of Oil Tankers Under Regulation 13F(5) of Annex I of MARPOL 73/78" [4], hereunder referred to as the Interim Guidelines.

The Interim Guidelines are an excellent beginning, but they have a number of significant shortcomings:

- They use a single set of damage extent probability density functions (pdfs) from limited single-hull accident data applied to all ships, independent of structural design.
- IMO damage pdfs consider only damage significant enough to breach the outer hull. This penalizes structures able to resist rupture.
- Damage extents are treated as independent random variables when they are actually dependent variables, and ideally should be described using a joint pdf.
- Damage pdfs are normalized with respect to ship length, breadth and depth when damage may depend largely on local structural features and scantlings vice global ship dimensions.

The overall objective of this dissertation is to develop, validate and assess a probabilistic collision damage model to support ongoing work by the Society of Naval Architecture and Marine Engineering (SNAME) Ad Hoc Panel #6 and IMO working groups.

It is generally agreed that structural design has a major influence on tanker oil outflow and damaged stability in grounding and collision, but crashworthiness is not considered in present regulations. The proposed methodology provides a practical means of considering structural design in a regulatory framework, and when implemented would improve the safety and environmental performance of ships.

Specific objectives are:

- Creation of a simplified collision model for the determination of longitudinal extent of damage.
- Creation of a simplified collision model for the determination of striking ship bow damage.
- To support ongoing work by SNAME Ad Hoc Panel #6 (Structural Design and Response in Collision and Grounding).
- To assess and integrate existing simplified collision-damage models and mechanisms into a single Simplified Collision Model (SIMCOL). This model will be used to predict probabilistic collision damage extents given a probabilistic description of collision scenarios. This requires that sub-model physics be sufficiently simple to support overall computational efficiency in probabilistic applications where thousands of runs are required.
- To validate SIMCOL in the context of a realistic collision simulation using real and finite element model data.
- To achieve international acceptance of this validation by publishing results and making all data and aspects of the research open for discussion and collaboration through SNAME and the Ship Structure Committee.
- To demonstrate the process and predict probabilistic structural damage for oil tankers. Identify important ship global and structural characteristics that impact collision damage extents.

- To provide the basis for further work in which a parametric analysis of probabilistic results would be incorporated in IMO oil outflow and damage stability regulations.

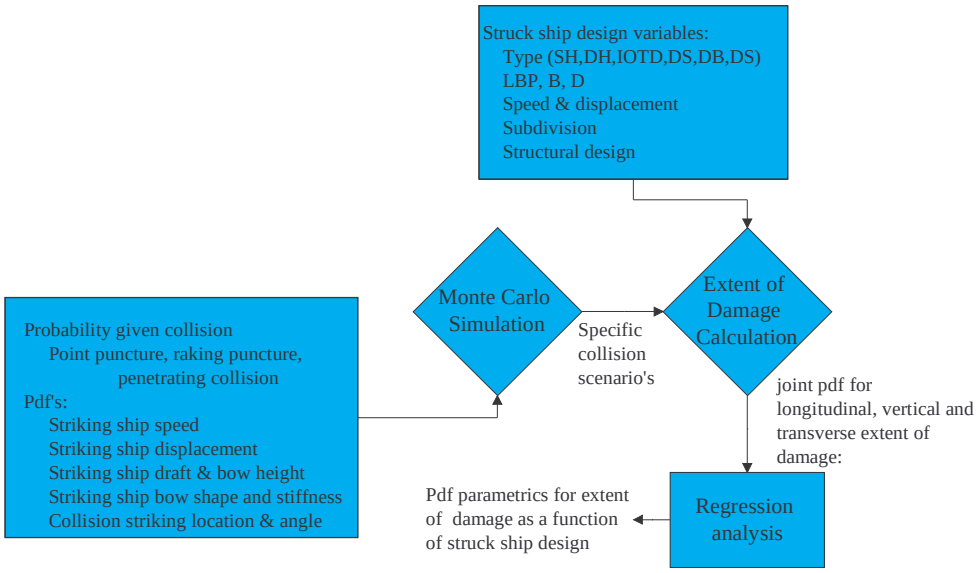

Figure 1-1 Methodology to Determine Probabilistic Damage in Collision [3]

Figure 1-1 illustrates the overall process proposed to predict probabilistic damage as a function of ship structural design. The process begins with a set of probabilities and probability density functions (pdfs) defining possible collision scenarios. Based on these pdfs, specific scenarios are selected in a Monte Carlo simulation, and, together with a specific ship structural design, provide the necessary input to predict damage using SIMCOL.

In the future, this process will be repeated for thousands of scenarios and a range of structural designs until sufficient data is generated to build a set of parametric equations relating probabilistic damage extent to structural design. These parametric equations can then be used in oil outflow or damage stability calculations. Critical to this process are a simple, but sufficient probabilistic definition of the collision scenario, including the striking ship, and a fast, but sufficient structural model to predict damage in a collision event.

The damage calculation is the most difficult step in the Figure 1-1 process. The simplified collision model (SIMCOL) performs this function. There are 3 major ship-to-ship collision classifications:

puncture, raking and penetrating. SIMCOL models penetrating collisions. SIMCOL is sufficiently fast to be applied to thousands of collision cases as is required for a probabilistic analysis, and is sufficient for a regulatory application. A simple and fast model is important in probabilistic analysis because thousands of different scenarios must be run to develop statistically significant results.

In 1979, the Ship Structure Committee (SSC) conducted a review of collision research and design methodologies [5,6,7]. They concluded that the most promising simplified collision analysis alternative was to extend Minorsky's original analysis of high-energy collisions by including consideration of shell membrane energy absorption.

A more recent review of the literature and of the applicability of available methods for predicting structural performance in collision and grounding was made at the 1997 International Ship and Offshore Structures Congress (ISSC 97) by Specialist Panel V.4 [8]. Their report states: "Knowledge of behavior on a global level only (i.e., total energy characteristics like the pioneering Minorsky formula) is not sufficient. The designer needs detailed knowledge on the component behavior (bulkheads, girders, plating, etc.) in order to optimize the design for accident loads."

The approach taken in this dissertation is to progressively increase the complexity of SIMCOL starting with a modified Minorsky approach followed by the inclusion of a deformable bow model and a new method for determining the energy absorbed through longitudinal extent of damage. SIMCOL version 3.0 represents the most recent product of this evolution.

Determination of the energy absorbed through longitudinal damage has often been neglected, treated as minimal compared to the energy absorbed through penetration. However, with oblique angle collisions (as occur more often than T-bone collisions) the energy absorbed in longitudinal damage may be greater than the energy absorbed due to penetration. Additionally, absorption of energy in the longitudinal direction removes energy from the entire system leaving less energy available for penetration.

The determination of the energy absorbed through longitudinal damage is additionally often neglected because of the complexity of: the additional degrees of freedom necessary for the system equations, the additional structural geometry that must be modeled and accounted for as energy absorbing structure and the formulation for the coupled solution of internal and external dynamics that properly considers longitudinal damage. Considering only the additional degrees of freedom necessary for the system equations, Pedersen and Zhang [14] derived expressions for both the longitudinal and transverse energy absorbed in ship-to-ship collisions. Pedersen and Zhang's expressions are however uncoupled from the internal deformation mechanics of the problem and do not consider the longitudinal damage of the transverse structure of the struck vessel. Thus, the determination of the energy absorbed through longitudinal damage and the development of a simplified longitudinal damage model is the primary original contribution of this dissertation.

2 The Collision Phenomenon

The high variability and complexity of damage behavior in ship-to-ship collisions precludes the ability to predict the exact behavior of the vessels during the collision event. However, as with most complex systems, various simplifications and assumptions based upon general behavior collected from multiple events can be made yielding a less complex and definable system. This Chapter is a collection and description of discovered and defined general behaviors, and the simplifications to which they lead.

2.1 Ship-to-Ship Collisions

A ship-to-ship collision is a high energy event occurring over a short period of time, often described mathematically through energy and momentum balance equations. Generally, from the time a collision between two vessels is determined imminent until the time of contact, several seconds or a few minutes pass. During this “pre-contact” time each vessel may attempt maneuvers to avoid contact. If successful, then the two vessels are involved in either a near miss or a light contact. If unsuccessful the vessels are involved in a collision. A near miss is the most desirable result of the pre-contact time where the vessels do not contact at all but miss each other by some small (centimeters to meters) distance. A light contact is an event where the vessels collide but either at such an oblique angle that penetration of one ship into the other does not occur or at such a low speed that again penetration does not occur. A light contact is best described as a collision in which neither of the hulls of the two vessels is compromised (ruptured or torn below the waterline). A collision is defined as any contact between two vessels resulting in the hull of one or both vessels being compromised (ruptured or torn below the waterline). For the duration of this report, a collision will refer to the contact between two vessels where significant penetration of one vessel into the hull of the other vessel occurs. This definition of collision is illustrated in Figure 2-1 where the striking ship has penetrated the struck ship. Note that the referring of the two vessels as the striking ship and struck ship does not imply fault of the collision on either vessel. As with automobile collisions, the fault of the accident is not always on the driver whose forward end is damaged.

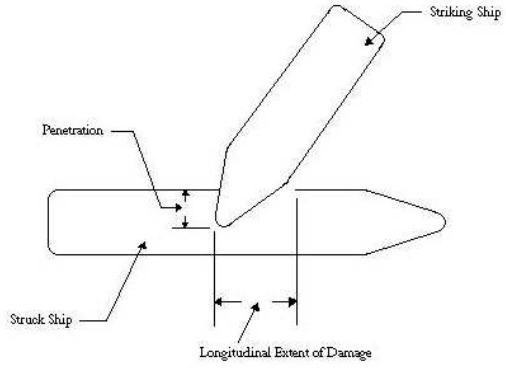

Figure 2-1 Illustration of Damage Definition

This definition of a collision narrows the study of ship-to-ship collisions to only the high energy less oblique "T" collisions, leaving the light contact and below waterline raking collisions for another investigation. Additionally, from the above definition of collision, the definition of damage extent follows directly as an indication of hull rupture with the following characteristics or metrics: 1) Extent of transverse penetration of striking ship into struck ship, 2) Longitudinal extent of outer hull opening, 3) Vertical extent of outer hull opening and 4) Tankage volume opened to sea. For clarity, the definitions of a collision and collision damage are restated as:

Collision: the contact between two vessels (striking and struck) where the penetration of one vessel (striking) into the hull of the other vessel (struck) occurs at an angle at which raking and sharp puncture are minimal energy absorbing components of the total energy balance.

Damage: an indication of hull rupture and if rupture then the measure of: 1) Extent of transverse penetration of striking ship into struck ship, 2) Longitudinal extent of outer hull opening 3) Vertical extent of outer hull opening and 4) Tankage volume opened to sea

2.2 Collision Physics

A collision between two vessels is modeled as an inelastic collision [9,10,13,15]. An inelastic collision is formally defined as a collision in which part of the initial kinetic energy of the colliding vessels changes to another form of energy (i.e. damage work and heat). For this dissertation, an

inelastic collision is specifically defined as a collision between two vessels that act and move as one body after damage penetration and where a significant part of the initial kinetic energy of the colliding vessels is converted to mechanical (deformation) energy.

For an inelastic collision the balance of momentum and energy are given by Equations 2.1 and 2.2.

$$M_1 \cdot V_1 + M_2 \cdot V_2 = (M_1 + M_2) \cdot V_3 \tag{2.1}$$

$$\frac{1}{2} \cdot \left(M_1 \cdot V_1^2 + M_2 \cdot V_2^2\right) = \frac{1}{2} \cdot (M_1 + M_2) \cdot V_3^2 + E_A + E_F \tag{2.2}$$

Where:

M_1 is the mass (plus added mass) tensor of the striking vessel

M_2 is the mass (plus added mass) tensor of the struck vessel

V_1 is the velocity vector of the striking vessel

V_2 is the velocity vector of the struck vessel

V_3 is the velocity vector of the combined striking and struck vessels after contact

E_A is the energy absorbed through structural deformation and damage

E_F is the energy imparted to the fluid (wave-making energy) during the collision

As with inelastic automobile collisions (car in tree), the damage to the struck vessel is often of the shape and form of the bow of the impinging striking vessel (i.e. local damage vice global damage). While damage is sustained to the striking vessel bow, this damage is often the result of heavy and dense cargo or substantial longitudinal structure within the struck ship. These generalities are supported by the realization that most vessel bows comprise additional strengthening structure designed to limit the deteriorative effects of slamming. As such, the bow of the striking vessel is treated as rigid in many analyses, while the damage sustained by the struck vessel is assumed to assume the shape and form of the penetrating rigid bow. These assumptions are supported by Figure 1-1 through Figure 2-6 and the works of Simonsen [10], Rosenblatt & Son, Inc. [18] and Chen [35].

Figure 2-2 Collision of M/V Alexia and M/V Enif

Figure 2-3 Damage to M/V Enif

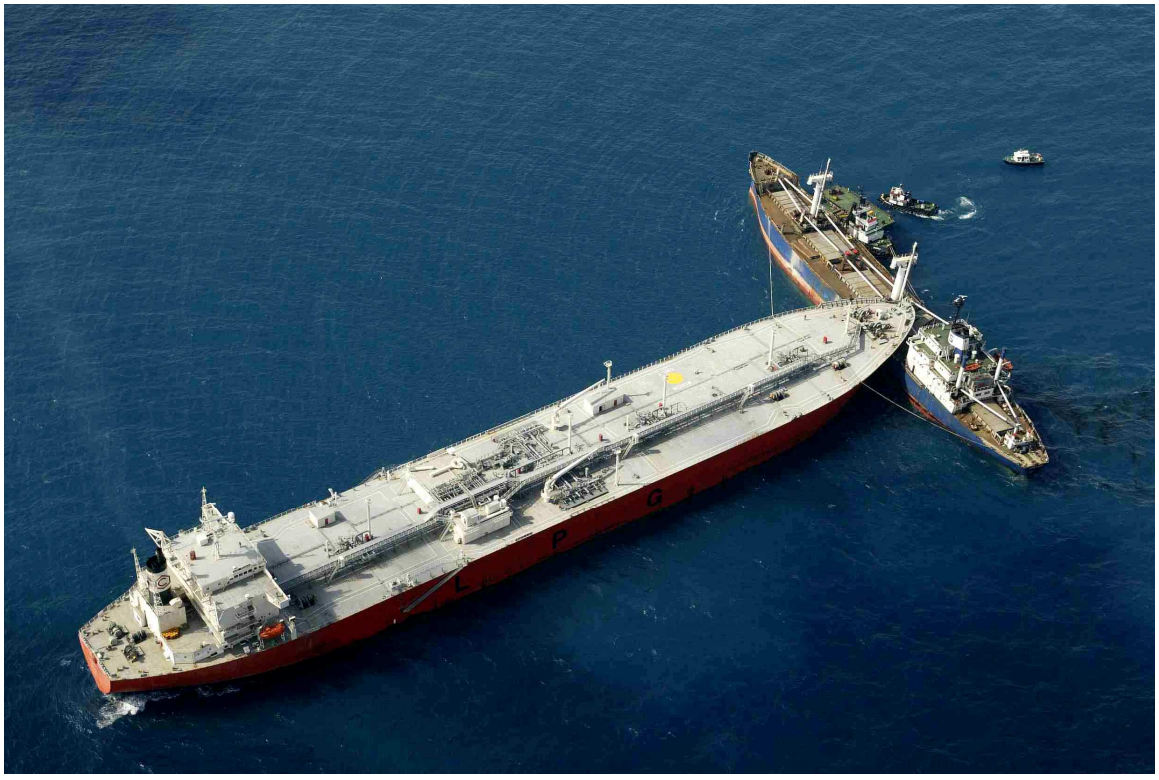

Figure 2-4 Collision of M/T Gas Roman and M/V Springbok

Figure 2-5 Bow Penetration of Collision of M/T Gas Roman and M/V Springok

Figure 2-6 Bow Damage of Collision of M/T Gas Roman and M/V Springbok

2.3 Vessel Motion

The motion of any vessel treated as a buoyant rigid body may be defined using a six degree of freedom system (surge, sway, heave, pitch, roll and yaw). However, as in maneuvering, a vessel involved in a collision event may be described using only three degrees of freedom (surge sway and yaw) where the motions of heave, pitch and roll may be neglected because the motion, and thus the energy, translated into these degrees of freedom are minimal compared to the motions in the surge, sway and yaw directions [9,10,13,14,16].

A vessel in a collision is induced to roll when a force is applied in the sway direction above or below the vessels vertical center of buoyancy. This statement is only true however if the vessel is not bound or constrained by other forces. As previously discussed, a collision is an inelastic event and as such, for most collisions, the roll of one vessel requires the pitch of the additional vessel about the combined center of buoyancy of the joined vessels. This coupling of the two vessels about the combined center of buoyancy limits the ability for either vessel to roll or pitch as the

restoring forces in these directions are high and therefore the only motions generally unconstrained are the in planer motions of surge, sway and yaw.

Often vessels involved in a collision continue to maneuver after contact occurs. The maneuvers are either from the attempt to pull away from the collision or from the continuation of a vessels momentum due to maneuvers performed prior to the contact. Because of the complicated dynamics involved during a collision these post contact maneuvers are often neglected [9,10,15] and the forces involved in the contact are assumed to include only those forces that are derived from each vessels respective forward momentum at the time of contact.

During an inelastic collision, the yaw of the struck vessel about it's own centroid is damped by the requirement to additionally sway and yaw the striking vessel about the struck vessels center of buoyancy (similar to the argument for a three degree of freedom system). A similar argument is made for the yaw of the striking vessel where the damping is provided by the requirement to surge and yaw the struck vessel. With this logical argument the continuation of the yaw momentums of either vessel are effectively damped by the addition of the second vessels mass (i.e. the two ships constrain each others motion). Figure 2-7 illustrates this phenomenon. The above logical argument does not however eliminate the ability of the combined vessels to yaw about the combine center of buoyancy nor does it preclude the yaw induced from non-amidships contacts, which are due to the initial forward momentum of the striking vessel and the contact location.

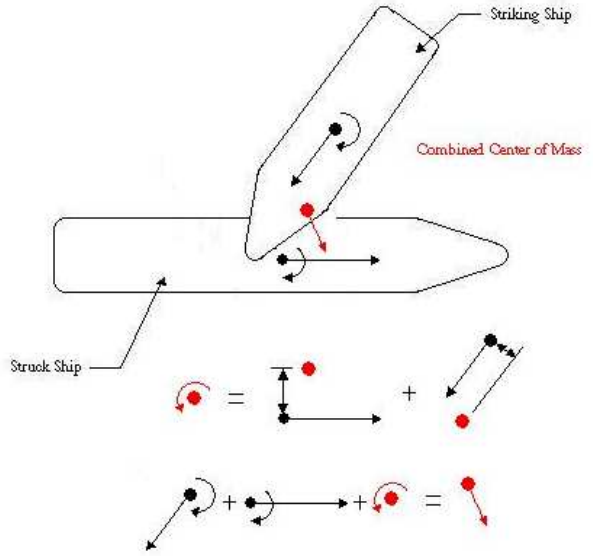

Figure 2-7 Illustration of Constrained Vessel Yaw

The argument for neglecting the propulsion forces of each vessel during a collision event is justified through the multitude of collision reports [84] where the vessels involved in collisions often attempt to limit the damage by shutting down the engines or clutching out the shaft and propeller near the time of contact. For those collisions where this does not occur, often the vessels are placed in full astern sometime near the time of contact [84]. In these situations the time at which the propulsion system of the vessel to change the propeller force direction (approximately 100 seconds) is often greater than the time of the entire collision event (less than ten seconds) and therefore the effect is similar to shutting down the engines or clutching out the shaft and propeller.

2.4 Energy Absorbing Structure

Recalling the energy balance of Equation 2.2, the energy absorbed through damage term (E_A) consists of all the energy absorbed through each structural and non-structural member of the vessel. For the duration of this report, the energy absorbed through damage will only refer to the energy absorbed through the structural components of the vessel, as such; the effects of cargo, ballast and outfit are neglected and saved for future investigations.

Examination of multiple collisions of varying speeds, collision angles, vessel types and collision locations relative to amidships on the struck vessel allows the general statement that the majority of

the energy absorbed by damage to structure within a ship-to-ship collision is absorbed by the following eight structural members; side shell, longitudinal bulkheads, decks, stringers, web frames, transverse bulkheads, longitudinal girders and transverse girders.

Table 2-1 presents the energy absorbed by each of the above structural components for multiple collisions where the struck ship is a tanker. The ships were modeled using finite element analysis as discussed in Chapter 3. Information regarding the structure of each vessel is provided in Appendices A through F.

The average percentage of the total energy absorbed within the collision by the eight structural members is approximately 95% or simply stated; the majority of the energy absorbed in a ship-to-ship collision is absorbed by the deformation and damage of the side shell, longitudinal bulkheads, decks, stringers, web frames, transverse bulkheads, longitudinal girders and transverse girders. Thus the energy absorbed by additional structure such as struts, columns and brackets may be neglected. While this is generally true, some non-standard structure or structural arrangements may need additional investigation to determine the relevance of the energy absorbing capacity within any individual collision.

Table 2-1 Collision Energy Absorbing Structure

		Collision 1	Collision 2	Collision 3	Collision 4
	Total Energy in Collision (J)	1.88E+08	6.32E+08	2.27E+08	3.83E+08
	Total Energy Absorbed by Structural Damage	4.98E+07	1.93E+08	3.95E+07	1.76E+08
	Energy Absorbed By Striking Ship Bow	1.34E+07	5.89E+07	1.45E+07	8.11E+07
	Energy Absorbed by Struck Ship	3.65E+07	1.34E+08	2.50E+07	9.49E+07
1	Side Shell	2.43E+07	4.17E+07	8.39E+06	3.66E+07
2	Longitudinal Bulkheads	2.37E+05	1.56E+07	4.95E+05	1.75E+07
3	Decks	4.04E+06	7.81E+06	9.45E+06	7.88E+06
4	Stringers		1.19E+07	4.74E+05	1.12E+07
5	Webs	3.78E+06	8.99E+06	3.90E+06	1.42E+07
6	Transverse Bulkheads	2.51E+06	4.04E+07	1.19E+05	2.77E+04
7	Longitudinal Girders		2.55E+05	1.80E+04	2.26E+05
8	Transverse Girders	8.80E+05	2.32E+05	1.76E+05	2.37E+06
	Total Energy from Parts 1 - 8	3.57E+07	1.27E+08	2.30E+07	8.99E+07
	% Energy 8 Parts of Struck Ship Energy Absorbed	97.96%	94.89%	92.12%	94.73%
	% Energy Bow of Total Energy Absorbed	26.83%	30.57%	36.68%	46.08%

The collisions used for Table 2-1 are described in Table 2-2.

Table 2-2 Collision Descriptions

Collision #	Striking Vessel	Struck Vessel	Collision Angle (Degrees)	Striking Ship Speed (knots)	Struck Ship Speed (knots)	Collision Location
1	C4 Cargo Vessel	T2 Tanker	55	5.5	6.81	9.923 m fwd amidships
2	150k dwt Bulk Carrier	150k dwt Double Hull Tanker	90	5	0	20 m fwd amidships
3	150k dwt Bulk Carrier	150k dwt Double Hull Tanker	45	3	0	20 m fwd amidships
4	40k dwt Container Ship	150k dwt Double Hull Tanker	90	7	0	3.5 m fwd amidships

Though the striking ship bow is often considered rigid as discussed in Section 2.4, this assumption is not always accurate as presented in Figure 2-8 and Figure 2-9. The bow when damaged may absorb a large quantity of the total energy of the collision. The energy absorbed through damage to a striking vessel bow is discussed and summarized by Vakkalanka [55]. Woison [17], Amdahl [23] and Pedersen [22] have also investigated the energy absorbed through damage of the striking vessel bow where it is shown that:

> "The almost universal assumption of a rigid striking ship bow in ship collision analysis is not valid. Differences in striking ship bow stiffness, draft, bow height and shape have an important influence on the allocation of absorbed energy between striking and struck ships and the extent of damage in the struck ship. The energy absorbed by the striking ship can be significant and varies in different collision scenarios." [83]

A reanalysis of Minorsky's [9] results discussed in Section 4.3.1 and presented in Table 2-3 shows that the percentage of energy absorbed by the striking ship in real collision cases is significant and is not constant. Using finite element analysis, Valsgard and Pettersen modeled a collision with a double hull struck ship and deformable striking bow that absorbed 55% of the total absorbed energy. Table 2-4 shows bow energy absorption of up to 46%. Using closed-form equations for bow stiffness, Lutzen., Simonsen, and Pedersen [47] show that bow energy absorption for a large striking ship with a longitudinally-stiffened bow is small. Bow energy absorption for smaller striking ships and for striking ships with transversely-stiffened bows is significant and variable (Table 2-4).

Table 2-3 Percentage of Energy Absorbed by Striking Ship Bow [15,36]

MINORSKY COLLISION CASE		Displacement (lton) [15,36]	n	t (in) [15,36]	V (knots) [15,36]	θ (deg) [15,36]	width (ft) [15,36]	penetration (ft) [15,36]	Struck Ship R_T (ft^2in)	Minirsky Total R_T (ft^2in) [9]	Bow R_T (ft^2in)	% Energy Absorbed in Bow
10	**Esso Greensboro**	21800	1	0.83	15	90	60	60	2988	3250	262	8.1
	Esso Suez	19500			15							
11	**Tullahoma**	21900	2	0.8	10	90	20	25	800	1100	300	27.3
	P&T Adventurer	8900			14							
21	**Gulf Glow**	21900	2	0.8	0	65	20	38	1216	1700	484	28.5
	Imperial Toronto	16000			14							
22	**Mojave**	5600	2	0.5	10	70	28	23	644	900	256	28.4
	Prometed	16000			14							
38	**Catawba Ford**	21800	1	0.8	10	90	27	10	216	250	34	13.6
	Hoegh Clair	6600			8							
46	**David E Day**	8700	2	0.7	16.3	55	35	17	833	1300	467	35.9
	Marine Flyer	20400			16.5							
B	**Andria Doria**	20900	6	0.375	15	90	50	30	3375	3800	425	11.2
	Stockholm	16200			18							

Table 2-4 Percentage of Energy Absorbed by Striking Bow in Collisions [47]

Striking Vessel / Struck Vessel	Bulk Carrier 150,000 DWT	Container Vessel 40,000 DWT	General Cargo 3,000 DWT	Tanker 2,000 DWT	Coaster 500 DWT
Tanker L = 103m	0	0	0	24	97
Tanker L=198m	0	0	36	95	89
Tanker L=317m	0	0	52	99	94
RoRo L=58m	0	0	0	98	91
RoRo L=150m	0	0	20	48	82
RoRo L=180m	0	0	0.4	46	86

Often a collision analysis is evaluated assuming either a rigid striking or a rigid struck vessel. A more appropriate approach is that for a single time step the vessel that is treated as the rigid vessel is the one that would absorb more energy given the same amount of relative deformation. This method is equivalent to a path of least resistance method where the damage is applied to the vessel which absorbs less energy in a given displacement or penetration in a given time step.

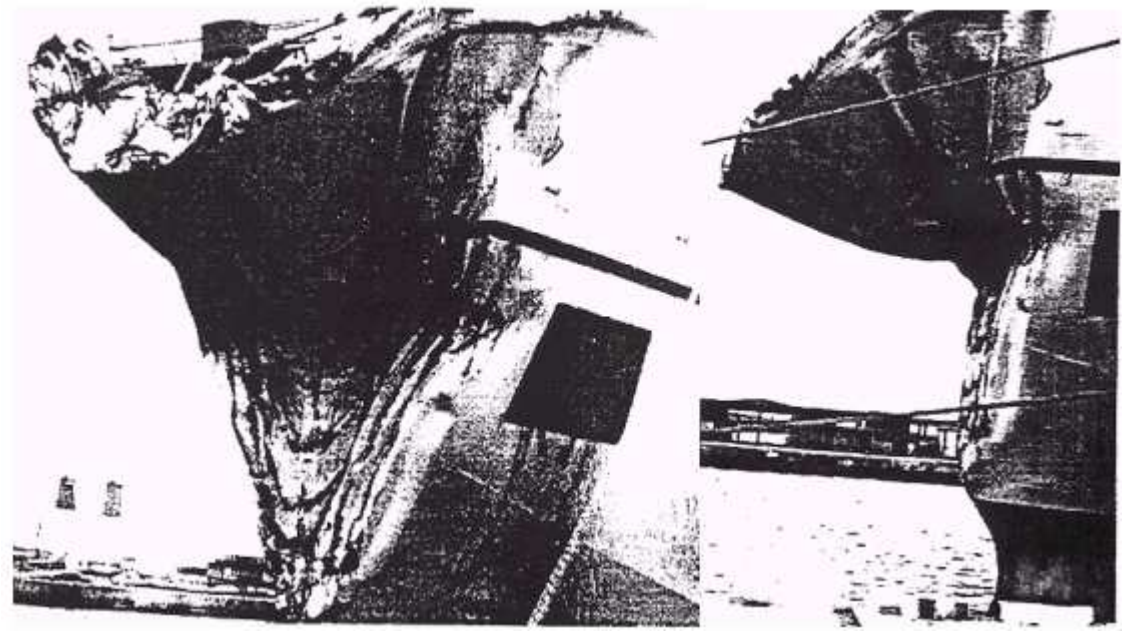

Figure 2-8 Actual Collision Bow Damage

Figure 2-9 Bow Damage to Norwegian Dream

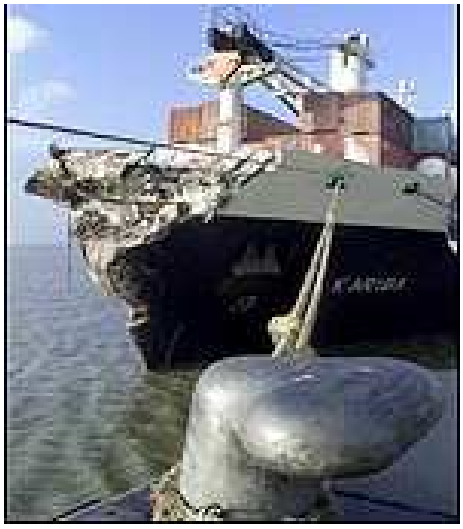

Figure 2-10 Karisa Bow Damage

Thus, a ship-to-ship collision is a high energy event occurring over a short time that can be modeled as an inelastic collision considering only the motions of surge, sway and yaw for each vessel. The initial kinetic energy is imparted to: 1) the remaining kinetic energy of the combined vessels, 2) radiation or wave making energy and 3) deformation energy. The deformation energy is suitably approximated by the summation of energy absorbed by 1) the striking ship bow and 2) the struck ship's side shell, longitudinal bulkheads, decks, stringers, webs, transverse bulkheads, longitudinal girders and transverse girders.

3 Finite Element Modeling of Ship Collisions

One of the important tools used in this research is finite element analysis (FEA). FEA is used throughout this report for developing and evaluating simplified methods. As previously discussed in Chapter 2, the cost of full scale collision testing and the inability to properly capture true collision behavior with physical scale modeling precludes live experimentation. The remaining methods of accident investigation and FEA must therefore be used to show and support the theories and simplified analysis described in this report.

LSDYNA is the primary FEA code used in this research, but many of the same issues that must be resolved to effectively use LSDYNA must be resolved for the efficient application of any FEA code. Other codes in common use for collision modeling include: ABAQUS-EXPLICIT, DYNA3D, and MSC-DYNA.

3.1 Overview

Finite element modeling of ship collisions cannot be performed with confidence without significant research, experimentation and validation of modeling techniques, element and material models, and careful model parameter value selection. The casual and undisciplined application of commercial software may produce impressive pictures, but be entirely wrong. The open literature and even detailed technical reports on the subject do not provide sufficient detail, analysis and validation to reproduce or defend many analyses, and “Calibration” of model parameters to one or two validation cases may only provide valid results for a very narrow range of problems.

LSDYNA is a general-purpose, explicit finite element program used to analyze the nonlinear dynamic response of three-dimensional inelastic structures. It was developed primarily for automotive collision applications, but can also be used for ship-to-ship collisions. It performs a fully dynamic analysis, not quasi-static. Crash behavior has large displacements, and is very non-linear with multiple point contact and rupture. Explicit time integration is best for these problems. The use of small time-steps is required for stability, but explicit integration does not require inversion of a large stiffness matrix as is required with implicit methods. Explicit integration also allows discontinuous failure criteria such as rupture strain. The run time required for an explicit

code is approximately proportional to the number of nodes vice the square of the number of nodes as with implicit codes.

Case studies in this Chapter use LSDYNA to model collisions between a striking ship and a struck oil tanker, and a striking ship and a double hull wall section. In some cases the striking ship bow is assumed to be rigid and in other cases the bow is deformable.

3.2 Structural Geometry

There are a number of important objectives to be considered when modeling the struck and striking ship structures:

- Minimize the number of nodes and elements to reduce computation time consistent with sufficient computational accuracy
- Minimize complexity
- Minimize ratio of triangular to quadrature elements
- Minimize numerical instabilities through the use of global parameterization controls
- Minimize numerical instabilities by modeling with a consistent, uniform mesh
- Have a minimum of 3 elements per side of any section in the entire vehicle and a minimum of 6 elements per buckle in the energy absorbing parts of the structure
- Have a time step sufficiently small to capture proper behavior and sufficiently large to minimize computational cost
- Minimize element warpage, but limit warpage to 10°
- Avoid edge-to-edge contacts
- Avoid initial penetration

Figure 3-1 shows a striking ship to struck ship collision as modeled in LSDYNA. The striking ship geometry is developed from an AutoCAD model. It includes a detailed bow model forward of the collision bulkhead and lumped beam elements aft of the collision bulkhead. The detailed portion of the bow model is shown in Figure 3-2 with side-shell, deck, stem, stringers, and primary girder components modeled using meshed shell elements. Stiffeners are smeared into plates as discussed in Section 3.5.

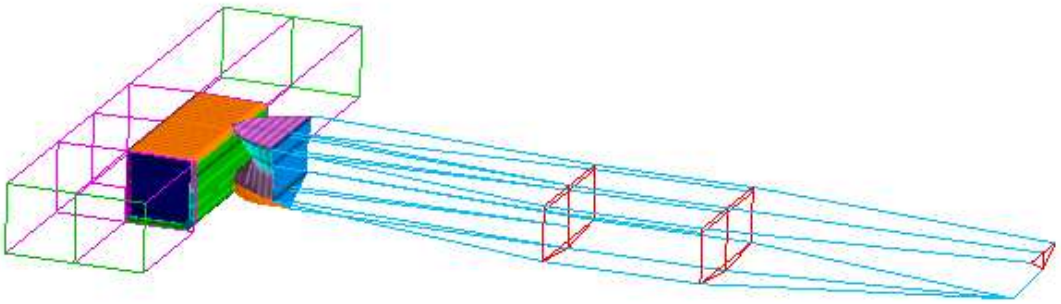

Figure 3-1 Ship-to-Ship Collision as Modeled in LSDYNA

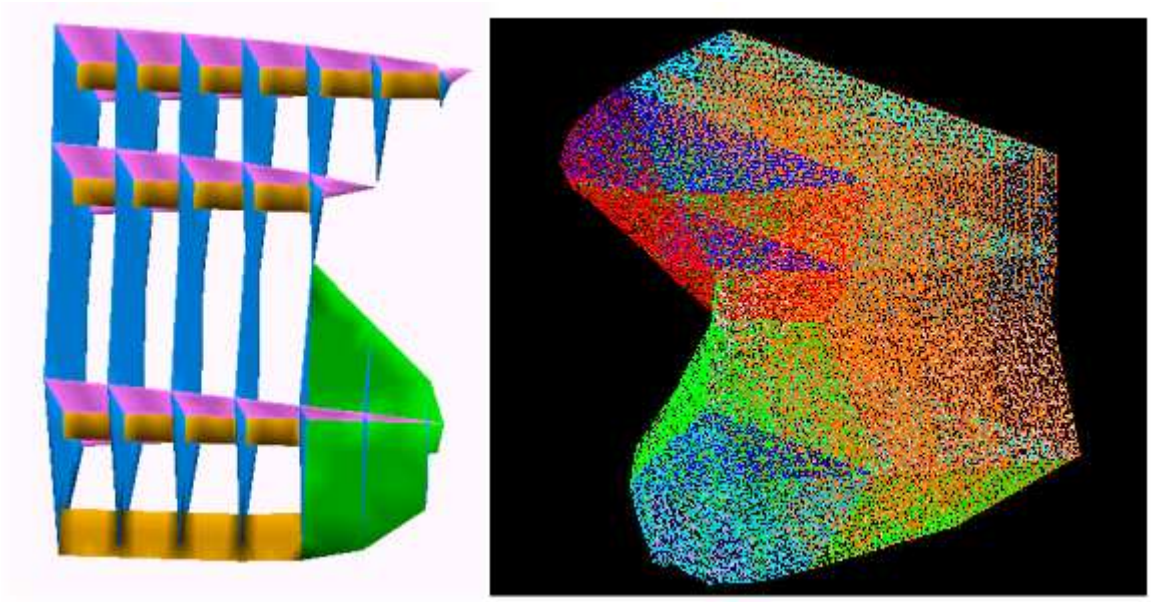

Figure 3-2 Detailed LSDYNA Bow Model

In order to simplify the bow model geometry of transverse frames, they are modeled as “stiff” transverse bulkheads using panel elements. “Stiff” is quantified as having increased element thickness or increased material density an order of magnitude beyond the actual structural or material value. Collision results using “stiff” transverse frames compare well with results using detailed transverse frame models. The collision bulkhead is the boundary between the detailed portion of the bow and the remainder of the striking ship. It is also modeled as a “stiff” transverse bulkhead. Fully rigid transverse frames and bulkheads were found to cause very high stresses and premature failure at their interface with the side shell and deck panel elements. They are not used.

The remainder of the striking ship aft of the collision bulkhead is modeled using “stiff” Hughes-Liu beam elements and concentrated masses such that the total mass and mass moment of inertia are the same as in the actual ship (including actual mass and added mass in the surge direction). The total cross sectional area of the longitudinal beam elements in this part of the model is determined such their sum is equal to the total longitudinal structure sectional area aft of the collision bulkhead in the real ship. Again, fully rigid beams were found to cause very high stresses and premature failure at their interface with the panel elements so stiff deformable beam elements are used.

The struck ship is usually modeled with only one side of the struck cargo tank, or tanks, in detail. Figure 3-4 and Figure 3-6 show the struck cargo tank section. The struck section includes shells, webs, girders, transverse and longitudinal bulkheads and stringers modeled as panel elements. Stiffeners are smeared into the plate thickness.
The remainder of the struck ship is modeled using “stiff” Hughes-Liu beam elements and concentrated masses, as with the bow model. This is based on the assumption that in ship collision cases local structural response dominates the collision results as determined through the results shown in Table 2-1. Dimensions of the longitudinal lumped beam elements are selected to model the horizontal moment of inertia at amidships. This allows some flexibility for hull girder horizontal bending (HGHB), although with a large struck ship, horizontal bending in collision is small [57]. Forward and aft transverse bulkheads are at the boundaries between the detailed cargo section model and the remainder of the struck ship. In order to simplify the geometry of the boundary transverse bulkheads, they are modeled as “stiff” transverse bulkheads using panel elements only. When a transverse bulkhead is in the way of or close to the collision contact, detailed tank structure is modeled on both sides of a detailed transverse bulkhead and the stiff bulkhead boundary is moved to the opposite end of an additional tank, shown in Figure 3-5. The centerline bulkhead model is also modeled using a “stiff” bulkhead unless it is in way of or close to the collision contact. When close to the collision contact the centerline bulkhead model is based on ship scantlings and geometry, supported with stiff beam elements that connect to nodes on the opposite deck edge at each frame, deck and stringer as shown in Figure 3-3. Again, fully rigid beams were found to cause very high stresses and premature failure at their interface with the panel elements so “stiff” deformable beam elements are used.

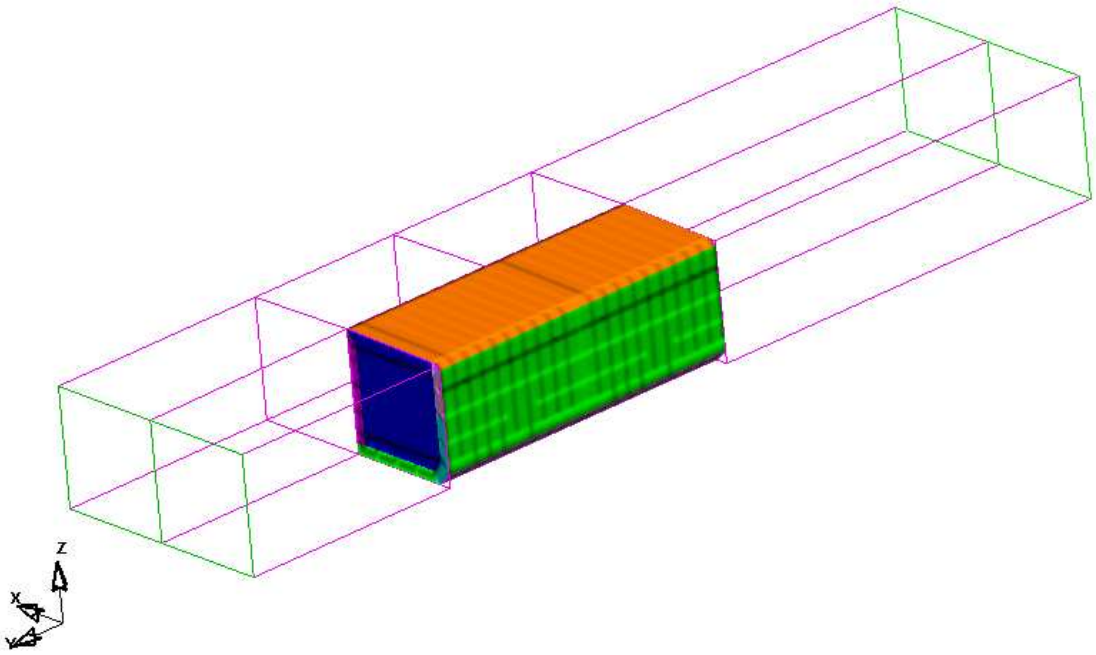

Figure 3-3 Struck Ship LSDYNA Model

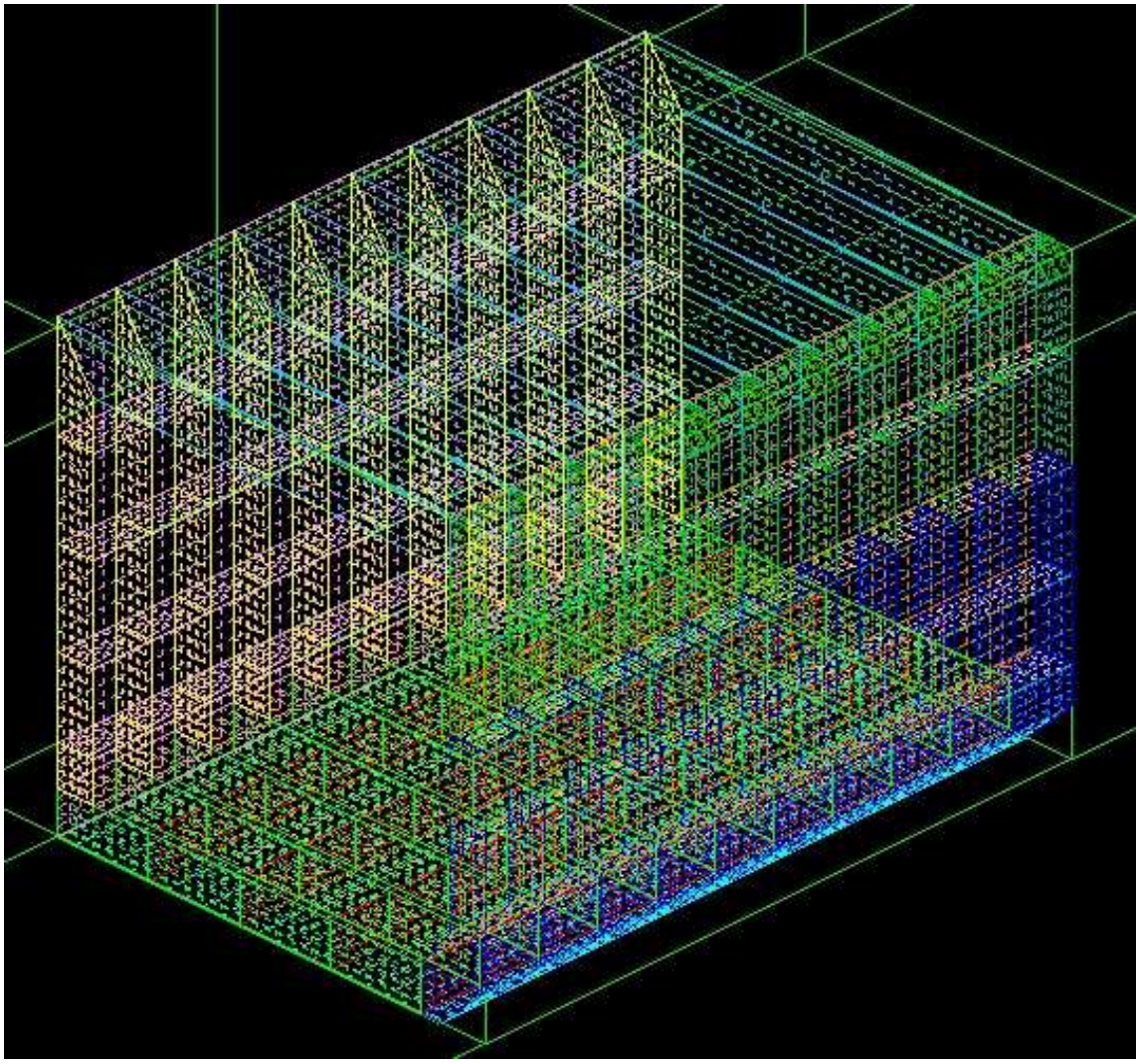

Figure 3-4 Struck Ship Cargo Section Mesh

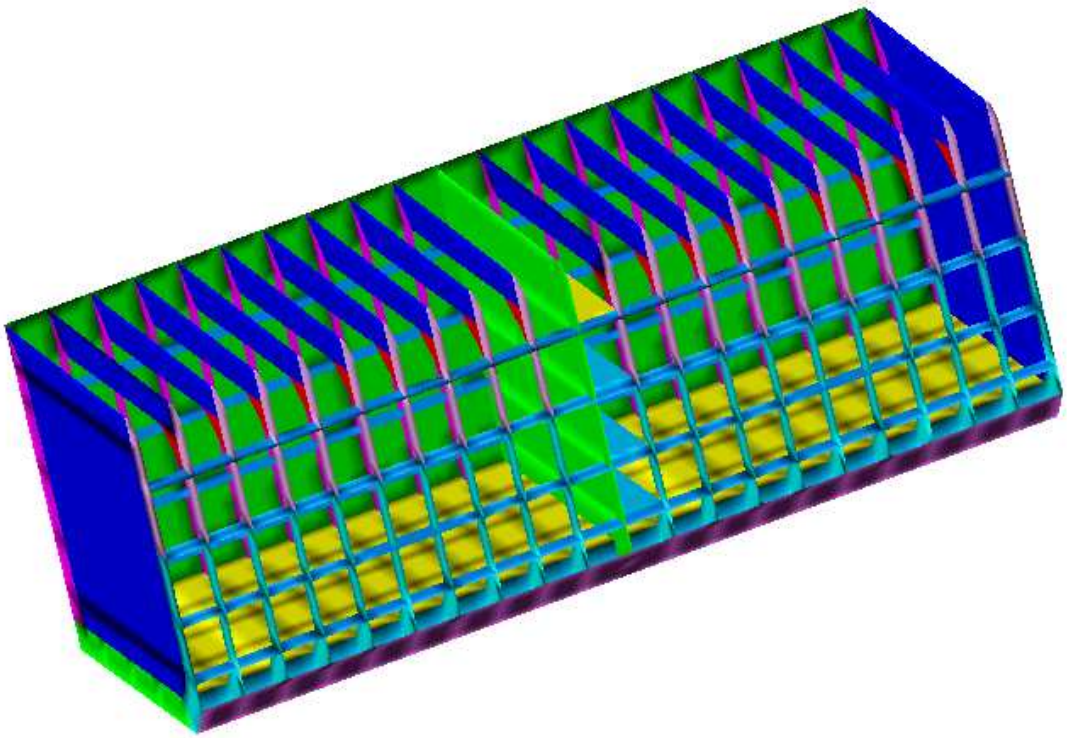

Figure 3-5 Struck Ship Cargo Section Geometry View from Outboard

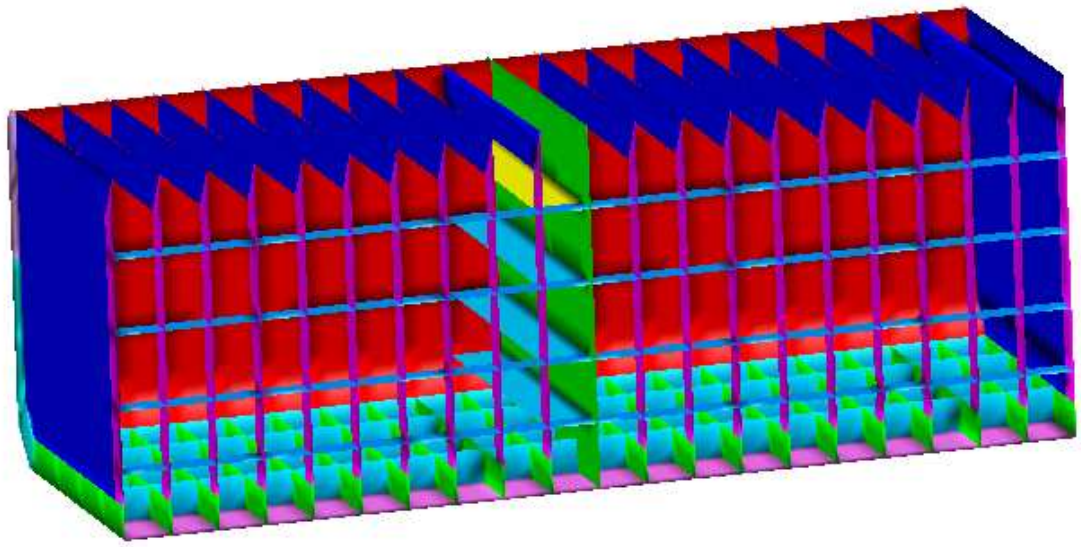

Figure 3-6 Struck Ship Cargo Section Geometry View from Centerline

3.3 Element Types

LSDYNA has many element types to choose from. In order to save CPU time, solid modeling and a fine mesh are avoided in favor of shell and beam elements and a more coarse mesh. The Hughes-Liu beam element is used for all struck and striking ship model beam elements. Hughes-Liu elements are designed not to fracture and provide out of plane bending not provided by truss elements. Belytschko-Tsay shell elements are used for all plate panels in both the struck and striking ship models. This element uses a local coordinate system that deforms with the element and provides a higher degree of numerical accuracy than a standard shell element at a lower time cost. Numerous runs with other element types available in LSDYNA were not as computationally efficient. Single point (reduced), standard Gauss integration is used and the panel reference location is taken at mid-plane.

Lemmen and Vredeveldt [72] found that two or three integration points through the thickness of a belytschko-tsay element were sufficient. Hourglassing[1] was not a problem with their small mesh (80x80mm). The LSDYNA manual recommends that hourglass energy be less than 10% of the internal energy. Otherwise, other methods should be used, such as triangle-elements instead of quadrilateral-elements or fully integrated elements instead of reduced integration elements. To reduce hourglassing while using the coarse elements, 5 integration points were found to be necessary to maintain the hourglass energy below 10% of the internal energy for most analysis.

3.4 Finite Element Mesh

Starting with an AutoCAD line model of the ship hull geometry, surfaces are created over the lines within the finite element model builder program (FEMB). Next, surfaces are partitioned and joined consistent with major energy absorbing structural members discussed in Chapter 2. The surfaces are auto-meshed with a minimum element dimension of 0.20 meters and a maximum element dimension of .3 meters. Element dimensions less than 0.5 meters are processing time prohibitive (3 to 5 days on a Pentium IV Desktop for the simplified models discussed in Section 3.8), however to obtain a true physical description of the deformed geometry of parts within the struck ship, elements of these sizes are required. Hourglassing is also an important concern with large mesh sizes and must be monitored closely. Finally, mesh problems are repaired manually. The resulting

[1] Numerical deformation modes other than rigid body that do not contribute to strains at the integration points

element length to thickness (L/t) ratio is typically 8:1 to 12:1. A uniform mesh throughout both the struck and striking ships detailed sections must be used to eliminate possible numerical errors within the contact due to translation of forces from element to element.

3.5 Smearing Techniques

To reduce computational time and to allow the use of a larger shell element mesh in the bow and cargo section models, plate stiffeners, flanges, and structural holes are smeared into plate panels. This is a common practice, but various methods can be used. Though smearing is not ideal, it is essential as a method to reduce the finite element computational time requirement. As such, the following smearing methods were compared:

- No smearing
- Equivalent Tensile Strength (Area) Smearing
- Equivalent Compression Strength Smearing
- Equivalent Membrane Strength Smearing
- Equivalent Moment of Inertia Smearing

This comparison is performed using an LSDYNA test case of a simple struck ship double-side configuration as shown in Figure 3-7. Table 3-1 provides details for the struck double-sided section.

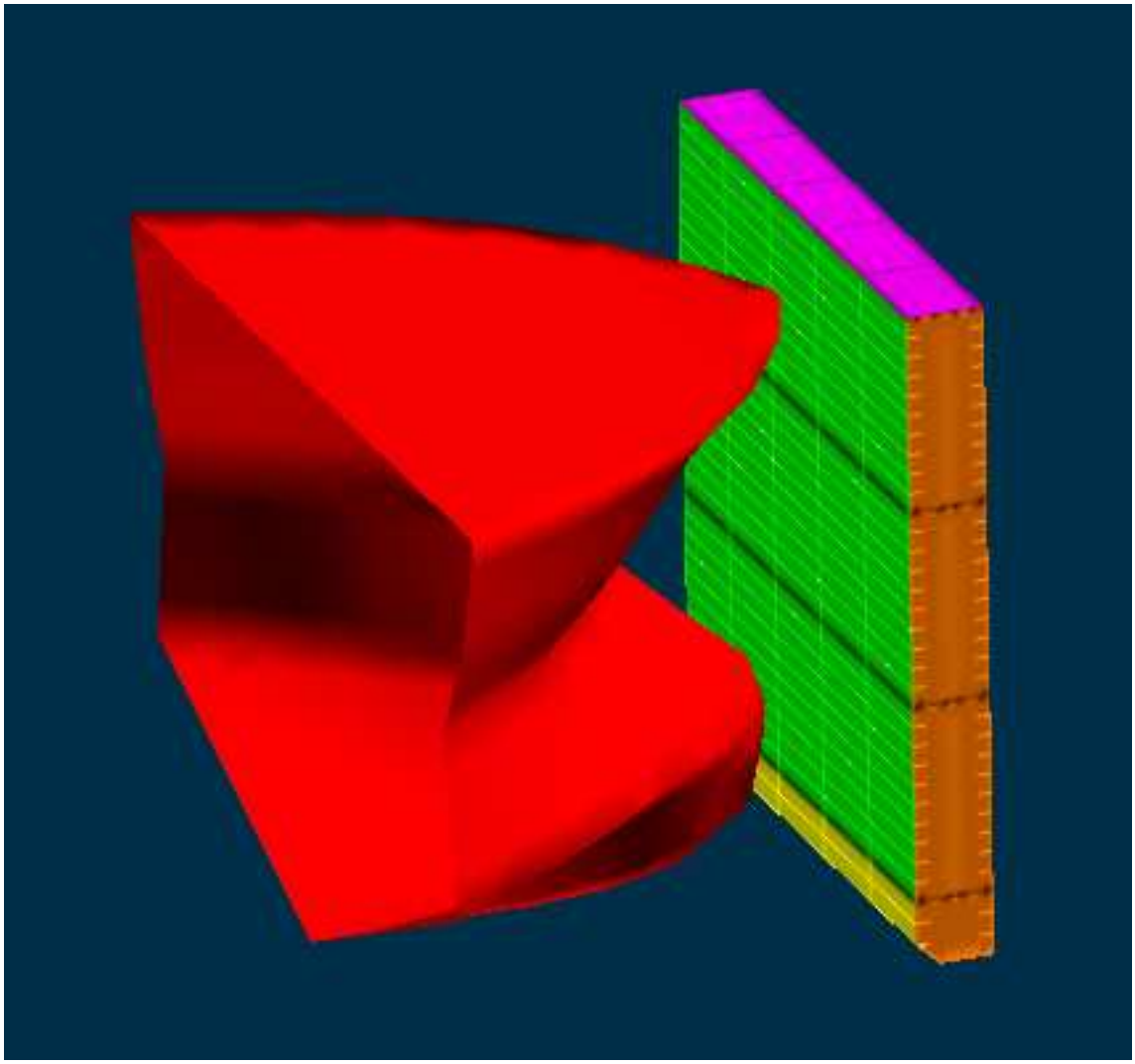

Figure 3-7 Rigid Bow Collision With Double-Sided Test Section

Table 3-1 Double-Sided Test Section Parameters

Global Dimensions	
Stringer Spacing	9 m
Double Bottom Height	3 m
Double Side Width	3.4m
Struck Section Depth	30 m
Struck Section Length	25 m
Web Spacing	5 m
Sideshell	
Thickness (3 m to 30 m)	20 mm
Stiffener Spacing (3 m to 30 m)	0.9 m
Stiffener Dimensions (3 m to 30 m)	T500,10,200,25
Innershell	
Thickness (0 m to 30 m)	16 mm
Stiffener Spacing (0 m to 3 m)	1 m
Stiffener Spacing (3 m to 30 m)	0.9 m
Stiffener Dimensions (0 m to 30 m)	T500,10,200,25 mm
Stringers and Deck	(3, 12, 21, 30 m)
Thickness	15 mm
Stiffener Spacing	0.875 m
Stiffener Dimensions	T250,10,100,15 mm
Bottom and Bilge Keel	
Thickness	21 mm
Stiffener Spacing	0.7 m
Stiffener Dimensions	600,25 mm
Webs	
Thickness	15 mm
Vertical Stiffener Spacing	1.7 m
Stiffener Dimensions	1000,20 mm

The traditional smearing method [56] provides equivalent tensile strength under longitudinal tension loading using area smearing. The equivalent plate (only) thickness, T_t, is calculated using Equation 3.1.

$$T_t = \frac{N_s \cdot (A_f + A_w) + A_p}{B} \tag{3.1}$$

N_s is the number of stiffeners and A_f, A_w and A_p are the stiffener flange, web and plate sectional areas, and B is the plate span.

Equivalent compressive strength smearing provides equivalent strength under a longitudinal compressive buckling loading. The equivalent compressive strength plate (only) thickness, T_c, is calculated using Equation 3.2.

$$T_c = b \cdot \sqrt{\frac{\pi^2}{3.62 \cdot (\frac{a}{\rho})^2}} \qquad (3.2)$$

The variable b is the stiffener spacing, a is the plate length, and a/ρ is the plate slenderness parameter [85].

The equivalent membrane strength smearing provides equivalent strength under transverse tension (perpendicular to stiffener direction) loading. Because the stiffeners do not provide any support in the transverse direction of the plate, the equivalent membrane strength thickness, Tm, is equal to the original plate thickness T_p. Thus the equivalent membrane strength plate has the dimensions of a and B with a thickness of T_m or T_p.

The equivalent Moment of Inertia smearing is based on plates under an out of plane loading. To develop the equivalent inertial thickness, T_i, the moment of inertia for the stiffened plate is set equal to that of an equivalent non-stiffened plate and the thickness, T_i, is solved. Equation 3.3 provides the value of T_i.

$$T_i = \sqrt[3]{\frac{12 \cdot I_X}{b}} \qquad (3.3)$$

Smearing test cases and a combination smearing case where the sideshell and innershell were tension smeared and the remaining parts were membrane smeared are summarized in Table 3-2. Figure 3-8 and Figure 3-9 compare absorbed energy vs. penetration results for each smearing method.

Table 3-2 Smearing Test Case Nomenclature

Case	Smearing Method
C1	NO SMEARING (AS BUILT)
C2	EQUIVILENT TENSILE STRENGTH (AREA) SMEARING
C3	EQUIVILENT COMPRESSION STRENGTH SMEARING
C4	EQUIVILENT MEMBRANE STRENGTH SMEARING
C5	EQUIVILENT MOMENT OF INERTIA SMEARING
C6	COMBINATION SMEARING

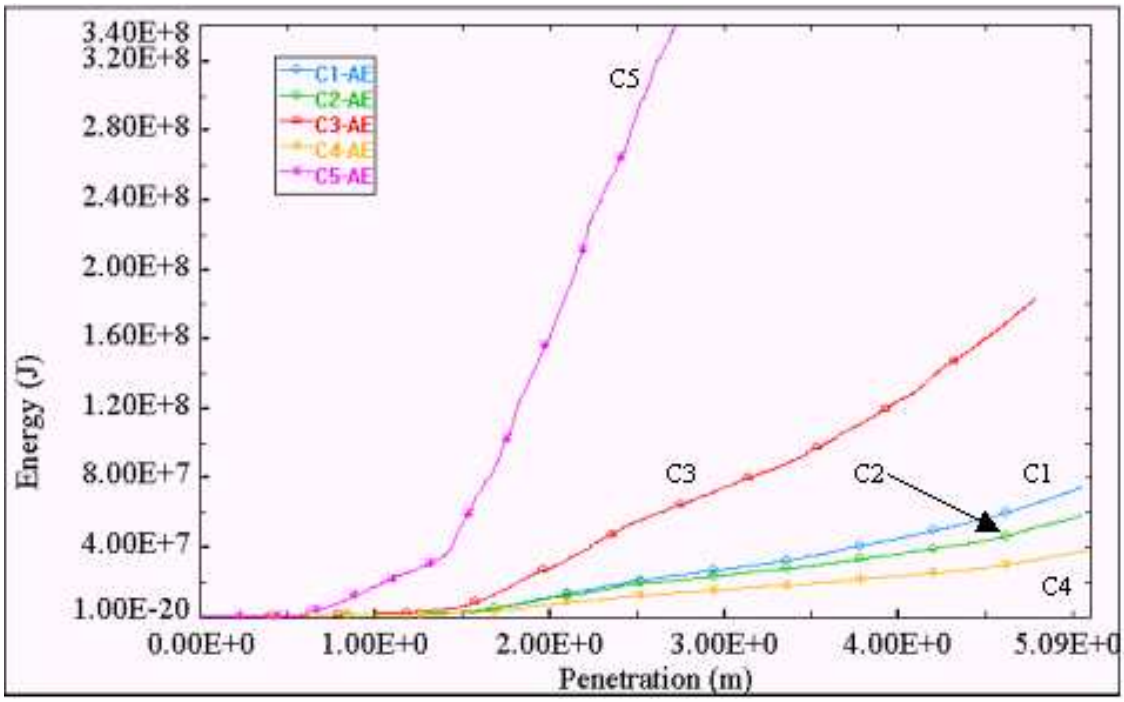

Figure 3-8 Smearing Test Result Comparison of Energy vs. Penetration

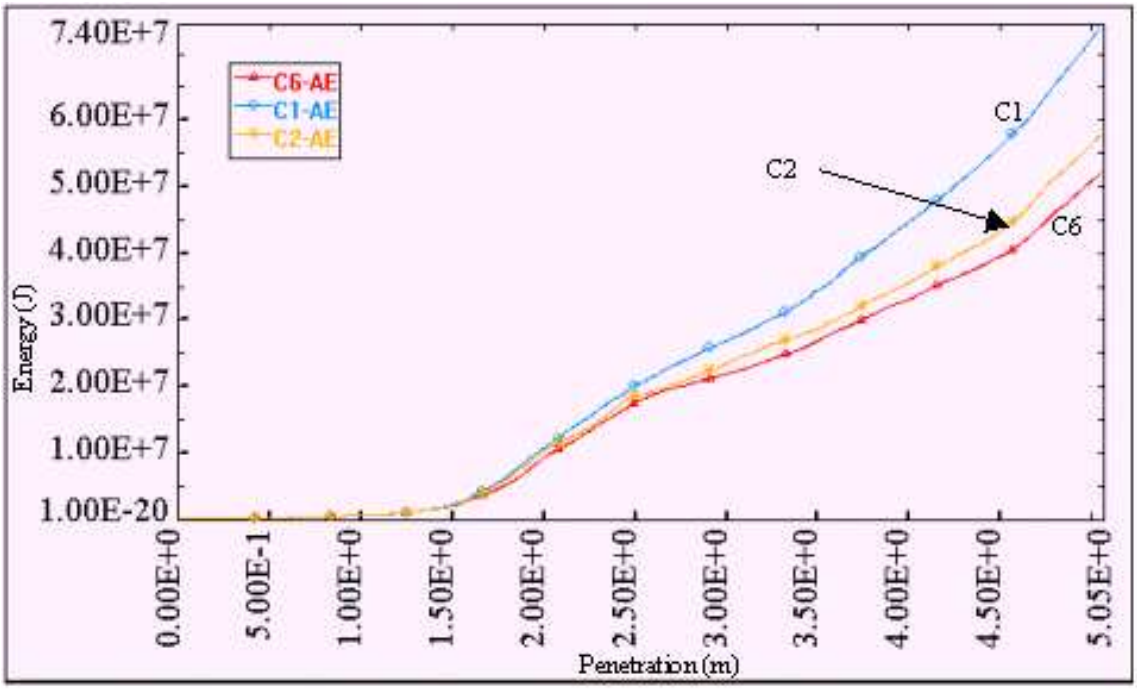

Figure 3-9 Smearing Cases 1,2 and 6 Result Comparison of Energy vs. Penetration

Comparison of smearing results to the unsmeared detailed structural model results indicates the following:

- Compression and Moment of Inertia smearing (C3 and C5 respectively) provide too stiff a structure resulting in an under-prediction of penetration and over-prediction of absorbed energy.
- Tension and membrane smearing (cases C2 and C4 respectively) under predict the energy absorbed and over predict the penetration.
- The average percent difference on penetration between C1 and C2 is less than one half of one percent. The average percent difference on Absorbed Energy between C1 and C2 is 22.00%. The variation in Absorbed Energy between C1 and C2 is due to the increase of Hourglass energy in C2 over C1 as shown in Figure 3-10 where the hourglass energy for C2 is approximately 27% higher than the hourglass energy at 0.3 seconds or 5.05 meters of penetration.

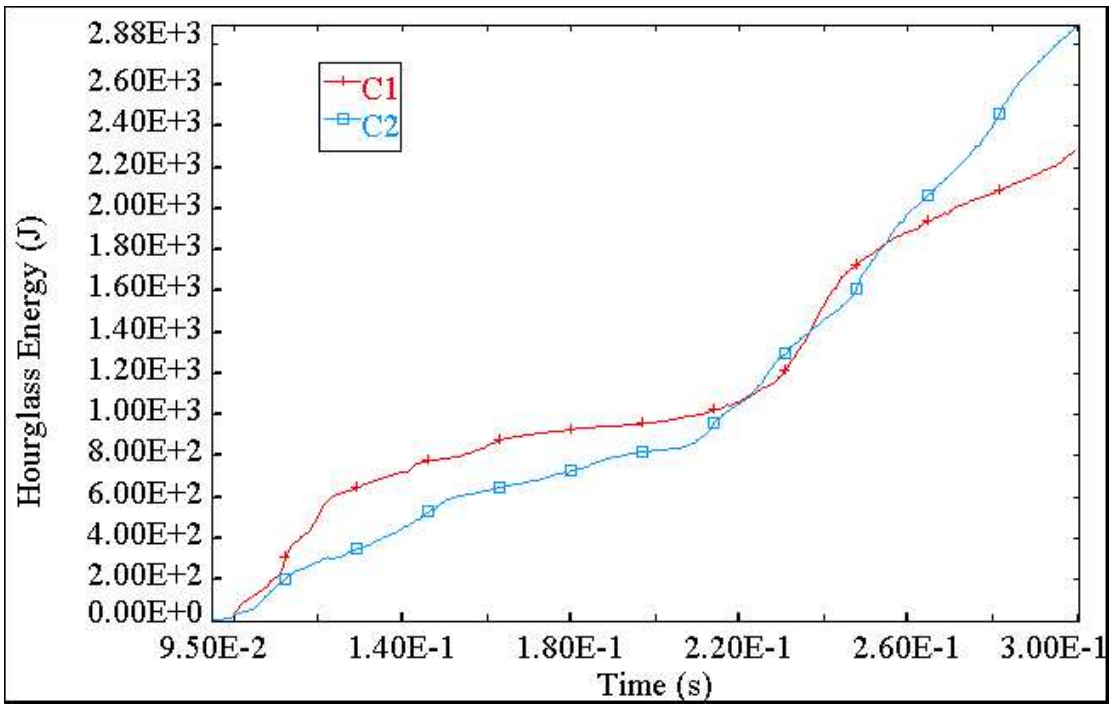

Figure 3-10 Smearing Case 1 and 2 Hourglass Energy vs. Time

Because callibration will be considered with regard to prediction of penetration, the equivilent tension strength smearing is considered to provide the best method for modelling ship structures vice other smearing methods considered. Tension strength smearing is used in all subsequent analysis.

3.6 External Dynamics and Constraints

An LSDYNA simulation is used to model both the internal structural response in collision and the external ship dynamics including hydrodynamics. To save CPU time, an inertia-equivalent method is used vice an explicit calculation of the fluid-structure interaction [58]. Masses and mass moments of inertia in surge, sway and yaw represent the virtual masses (actual plus added mass) for each ship. The masses of the striking ship outside of the bow section are assumed to be concentrated in three transverse section parts shown in Figure 3-1 in red. The masses of the bow parts are summed and the remaining mass is adjusted by assigning an appropriate mass density to the transverse section parts so that the total mass of the striking ship model is equivalent to the mass of the actual ship, plus the added mass in surge. The locations of the forward two transverse section masses are determined by matching the required added mass moment of inertia in yaw. A

similar procedure is followed for the struck ship when the vessel is anchored, moored or still at the time of collision, where the model mass is equivalent to the mass of the actual ship plus the added mass in sway. When the struck ship has forward velocity at the time of the collision, the inertia-equivalent method begins to break down as the mass of the vessel may only be adjusted within the model for a single degree of freedom. To overcome this problem, an equivalent momentum method is applied to the struck ship.

The equivalent momentum method requires that the actual mass (M_a) of the vessel times the actual forward velocity (V_a) of the vessel is equal to the model mass (M_m) times the model forward velocity (V_m). Defining the model mass as equivalent to the actual mass of the vessel plus the added mass in sway, then the forward velocity of the struck ship model is calculated using Equation 3.4.

$$V_m = \frac{Ma}{Mm} V_a \tag{3.4}$$

Similarly an equivalent energy method may be used where:

$$V_m = \sqrt{\frac{M_a}{M_m} \cdot V_a^2} \tag{3.5}$$

The equivalent momentum method provides the best results based on comparison of method results to the validation case study discussed in Section 3.8.

Added mass values vary over the duration of the collision and depend on hull form [13]. For model simplicity, average added mass coefficients are used where:

$$\begin{aligned} a_{11} &= c_{11} m_s \\ a_{22} &= c_{22} m_s \\ a_{33} &= c_{33} I_{s33} \end{aligned} \tag{3.6}$$

Coefficients values used in this report are selected to standardize results when compared to other models, specifically Pedersen [14], Simonsen [10] and Paik [29]. Assumed added mass coefficients are 0.05 in surge (c_{11}), 0.85 in sway (c_{22}) and 0.21 in yaw (c_{33}).

The motion of the striking ship is prevented in the 3, 4 and 5 directions (translation in the Z-axis, rotation around the X-axis and Y-axis or heave, pitch, and roll) by constraining the nodes in the collision bulkhead in these directions. These constraints allow the striking ship model to be very simple and provide for a faster solution. The striking ship motions in heave, pitch, and roll are relatively small and less significant in a collision event as discussed in Chapter 2. The motions of the struck ship are also constrained in these directions, allowing only sway, surge and yaw by constraining the nodes in the boundary transverse bulkheads and beam elements in these directions. This effectively limits ship global motion to the horizontal plane, but allows the deformable sections a full six degrees of freedom.

3.7 Analysis Parameters

Other FEM parameters requiring particular consideration include: contact types, failure strain, strain rate dependency, friction and other material properties. A very coarse finite element mesh using primarily panel elements to save CPU time also requires close attention to hourglassing.

Lemmen and Vredeveldt [59] also use LSDYNA to model full-scale collision tests. Their report identifies variable values that provide results consistent with their test results. Servis et. al. [60] and Naar [61] also provide some excellent general guidance. These are discussed in the following sections.

3.7.1 Contact and Friction

For the ship-to-ship collision analysis the NODES_TO_SURFACE and SINGLE_SURFACE contact types are used, allowing the master segments of the striking ship to penetrate into the struck ship, while ensuring deformation through the nodal requirement (i.e. compatibility). Figure 3-11 illustrates the nodal requirement where the red slave nodes are not allowed to penetrate through the blue master surface but must remain on the positive side (indicated by normal arrows) of the master segments.

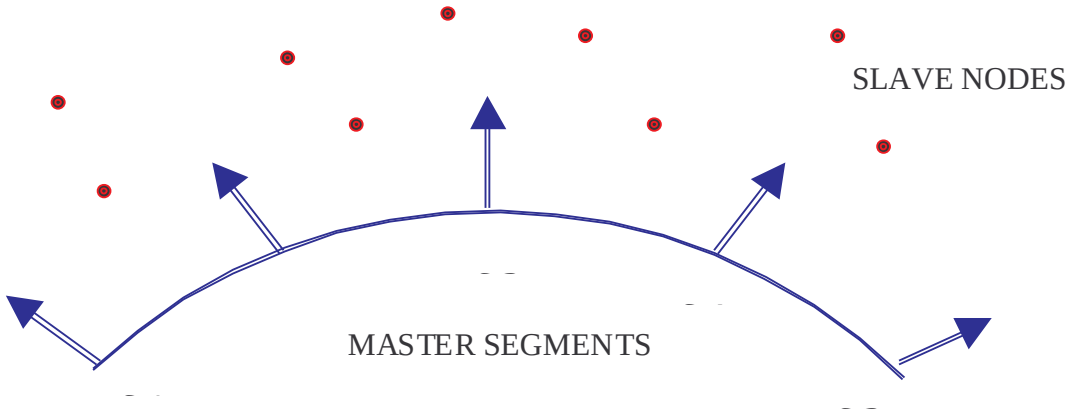

Figure 3-11 Contact Nodal Requirement

In NODES_TO_SURFACE contacts, nodes in the struck ship are assigned as slave nodes and surfaces within the striking ship are defined as master segments. The contact interface does not allow the slave nodes to penetrate the master segments. If the striking ship is defined as master segments then the penetration of the striking ship into the struck ship may occur and both are enabled to deform. If however, the struck ship is defined as the master segments then the striking ship cannot penetrate into the struck ship because slave nodes are not allowed to penetrate a master segment as defined by the compatibility requirement. Multiple NODES_TO_SURFACE contacts are defined within a single analysis.

Parts in the striking or struck ship are also defined as master segments over other parts in the same ship. As an example, the side shell is defined as a master surface while slave nodes define a web. Each contact is an independent interface such that a part defined by slave nodes in one contact interface may be defined by master segments within another contact interface.

In SINGLE_SURFACE contacts, a part within the striking and/or struck ship acts as both master surface and slave nodes to itself. This contact ensures proper physical behavior when the side shell is peeled back and contacts itself. Again SINGLE_SURFACE contact uses a similar approach as the NODES_TO_SURFACE contact where the part nodes are constrained to stay on the original side of the contact surface.

Care should be taken to ensure that all possible part-to-part contacts have been considered and accounted for as failure to properly define contacts where contacts exist will allow non-physical violations (i.e. striking ship passing through struck ship without resistance or deformation).

The correct consideration of friction in a ship-ship collision model is also important. As friction is increased the penetration of the striking ship into the struck ship is decreased or the absorbed energy per unit penetration is increased. Several considerations of friction and various static and dynamic friction coefficient values are reported in the literature. The most common value found in the literature for the dynamic friction coefficient is 0.3 [22,59,62,63,64,65]. Reported dynamic coefficients of friction vary from 0.0 to as high as 0.6 and static coefficients are reported at values between 0.5 and 0.8 [28,66,67,68,69]. Wisniewski et al [70] modeled collisions with a 40K dwt container ship striking a 105K dwt double hull crude oil carrier using ABAQUS-EXPLICIT. The dynamic coefficient of friction was varied from 0.0 to 0.6 in a parametric study. Plots of Wisniewski's results are provided in Figure 3-12 where it is shown that the higher the friction coefficient the faster the loss of kinetic energy of the striking ship. The difference between the friction curves for 0.3 and 0.6 is much smaller than between the curves for 0.0 and 0.3. As a result Wisniewski states, "The effect of friction will not increase significantly for larger values (greater than .6) of the coefficient."

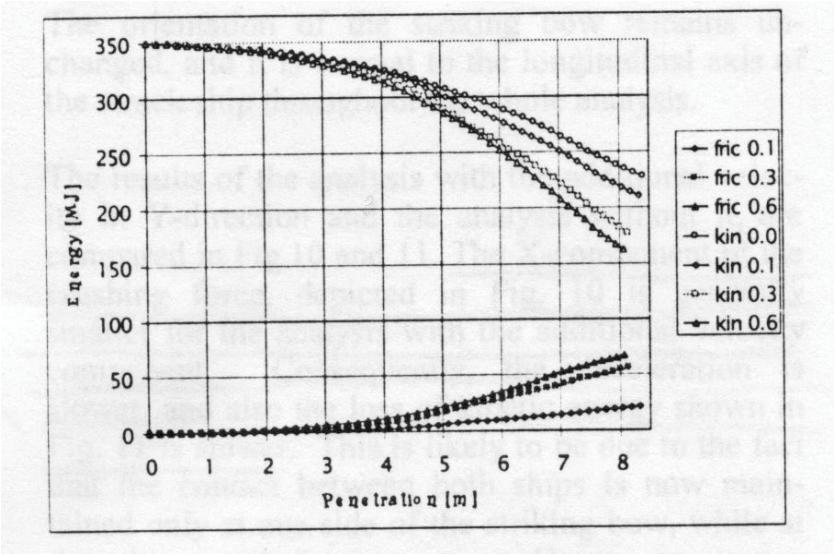

Figure 3-12 Friction and Kinetic Energy vs. Penetration [70]

The friction model in LSDYNA is based on the Coulomb friction relation given by Equation 3.7.

$$\mu_c = FD + (FS - FD)e^{-DC \cdot ABS(V_{rel})} \quad (3.7)$$

Where:

μ_c coulomb friction coefficient

FS static coefficient of friction for mild steel on steel

FD dynamic coefficient of friction for mild steel on steel

$\mathbf{V_{rel}}$ relative velocity of contact surfaces

DC exponential friction decay coefficient

The LSDYNA User's Manual [71] suggests a value of 0.74 for the static friction coefficient (FS) of dry mild steel on steel. An average value from the literature for FS of wet mild steel on steel is 0.7. The LSDYNA User's Manual suggests a value of 0.57 for the dynamic friction coefficient (FD) of dry mild steel on steel. An average value from the literature for FD is 0.3, for wetted, mild steel on steel. Figure 3-13 shows the Coulomb Friction value as a function of the change in relative velocity of the contact surfaces in meters per second with a DC value of 7.0. By increasing the value of DC the value of the relative velocity at which the steel on steel contact acts in a dynamic manner is decreased, i.e. the rate of change from the static friction coefficient to the dynamic is increased. Values selected for these coefficients in this dissertation are FS = 0.7, FD = 0.3 and DC = 7.0.

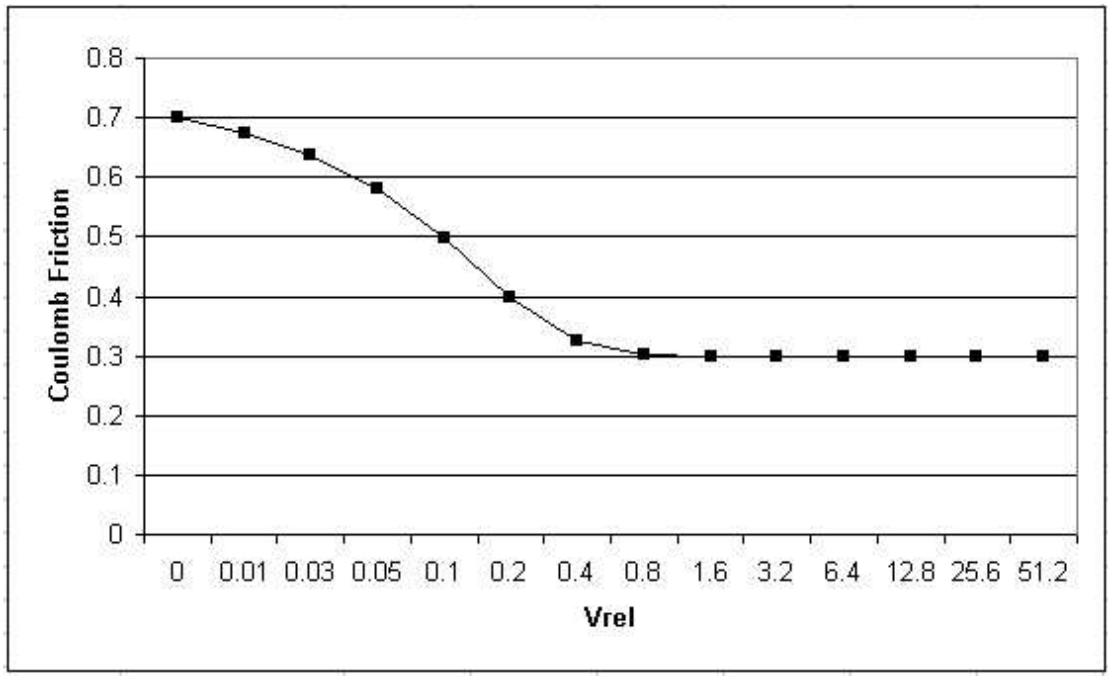

Figure 3-13 Coulomb Friction vs. Relative Velocity of Contact Surfaces

3.7.2 Material Properties

Only three of many (nearly 100) material types available in LSDYNA were found to be suitable or necessary for ship collision analyses:

- Type 24 – Elastic/Plastic Isotropic with Piecewise Linear Plasticity – This material type allows strain rate effects and complete material fracture. All panels in the struck ship are modeled using LSDYNA Material Type 24. Material behavior is specified using the following parameters: Young's modulus, yield stress, tangent modulus, failure strain and Cowper and Symonds strain rate parameters.
- Type 3 – Elastic/Plastic Isotropic with Kinematic Plastic Hardening - All transverse beams in the struck and striking ship and panels in the striking ship are modeled using LSDYNA Material Type 3. Material Type 3 is used in the striking ship because of the "No Fracture" behavior in its stress-strain curve shown in Figure 3-14. It was found that Master Elements modeled with Material Type 24 confuse the contact algorithm in the rare cases when these elements fracture. Model elements away from damaged areas must remain intact for model integrity. The use of Type 3 material avoids these problems.

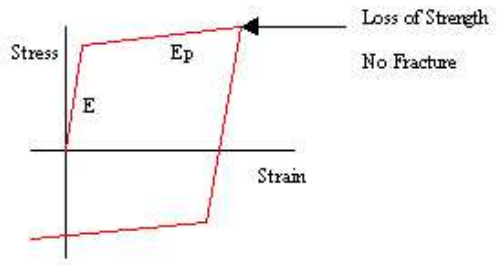

Figure 3-14 Kinematic/Isotropic Elastic Plastic Material Stress Strain Curve

- Type 20 – Rigid – Material Type 20 is used in special model cases specifying a rigid bow. Rigid elements are bypassed in deformation processing and are very time efficient.

Parameter values for modeling ABS materials Grade B, AH32 and AH36 using Material Types 3 and 24 are listed in Table 3-3 and Table 3-4. Figure 3-15 shows the resulting stress verses strain curves for Type 3 and Type 24 Material at each grade.

Table 3-3 Material Type 3 Definitions

MATERIAL TYPE 3				
NAME	(Material Name)	M3GB	M3GAH32	M3GAH36
TYPE	(Material Type)	3	3	3
MID	(Material Identification Number)	601	602	603
RO	(Material Density)	7.78E+03	7.83E+03	7.85E+03
E	(Material Modulus of Elasticity)	1.90E+11	2.00E+11	2.10E+11
PR	(Material Poissons Ratio)	0.281	0.292	0.303
SIGY	(Material Tension Yeild Stress)	2.35E+08	3.15E+08	3.55E+08
ETAN	(Material Tangent Modulus)	3.75E+09	3.05E+09	3.22E+09
BETA	(Material Hardening Parameter)	0	0	0
SRC	(Cowper-Symmonds Strain Rate Parameter C)	40.4	40.4	40.4
SRP	(Cowper-Symmonds Strain Rate Parameter P)	5	5	5
FS	(Material Failure Strain)	0	0	0
VP	(Material Formulation for rate effects)	0	0	0

Table 3-4 Material Type 24 Definitions

MATERIAL TYPE 24				
NAME	(Material Name)	M24GB	M24GAH32	M24GAH36
TYPE	(Material Type)	24	24	24
MID	(Material Identification Number)	701	702	703
RO	(Material Density)	7.78E+03	7.83E+03	7.85E+03
E	(Material Modulus of Elasticity)	1.90E+11	2.00E+11	2.10E+11
PR	(Material Poissons Ratio)	0.281	0.292	0.303
SIGY	(Material Tension Yeild Stress)	2.35E+08	3.15E+08	3.55E+08
ETAN	(Material Tangent Modulus)	3.75E+09	3.05E+09	3.22E+09
FAIL	(Plastic Strain to Failure)	0.1	0.1	0.1
TDEL	(Minimum Time Step Size for Automatic Deletion)	0	0	0
C	(Cowper-Symmonds Strain Rate Parameter C)	40.4	40.4	40.4
P	(Cowper-Symmonds Strain Rate Parameter P)	5	5	5
LCSS	(Load Curve Identification Number for Effective Stress verses Plastic Strain)	0	0	0
LCSR	(Load Curve Identification Number for Strain Rate Scaling Effect on Yeild Stress)	0	0	0
VP	(Material Formulation for rate effects)	1	1	1
EPS1	(Effective Plastic Strain Value 1)	0	0	0
EPS2	(Effective Plastic Strain Value 2)	0	0	0
EPS3	(Effective Plastic Strain Value 3)	0	0	0
EPS4	(Effective Plastic Strain Value 4)	0	0	0
EPS5	(Effective Plastic Strain Value 5)	0	0	0
EPS6	(Effective Plastic Strain Value 6)	0	0	0
EPS7	(Effective Plastic Strain Value 7)	0	0	0
EPS8	(Effective Plastic Strain Value 8)	0	0	0
ES1	(Corresponding Yeild Stress Value to EPS1)	0	0	0
ES2	(Corresponding Yeild Stress Value to EPS2)	0	0	0
ES3	(Corresponding Yeild Stress Value to EPS3)	0	0	0
ES4	(Corresponding Yeild Stress Value to EPS4)	0	0	0
ES5	(Corresponding Yeild Stress Value to EPS5)	0	0	0
ES6	(Corresponding Yeild Stress Value to EPS6)	0	0	0
ES7	(Corresponding Yeild Stress Value to EPS7)	0	0	0
ES8	(Corresponding Yeild Stress Value to EPS8)	0	0	0

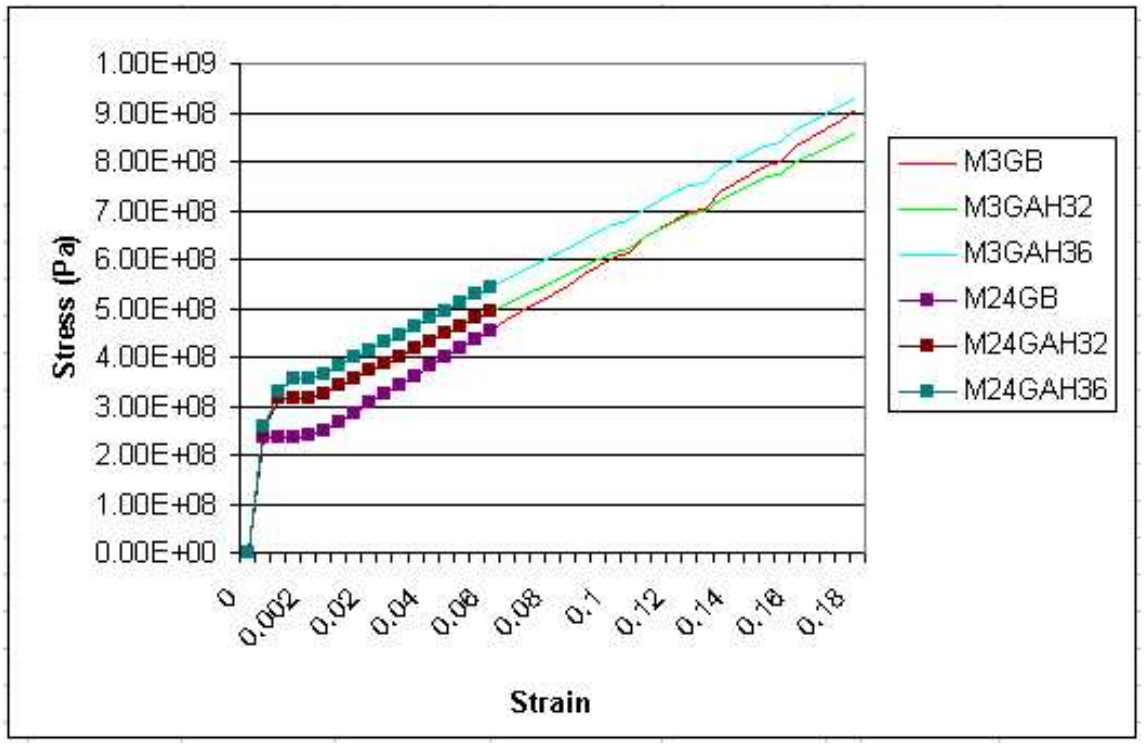

Figure 3-15 Material Types 3 and 24 Stress/Strain Curves

3.7.3 Element Failure

The difficulty in material modeling within finite elements is the determination of the plastic strain at which the element fails, fractures or ruptures (effectively losing strength and the ability to maintain a stress loading). In this dissertation, the point at which an element is no longer able to provide resistance to loading is referred to as failure. At failure, the element is eliminated from the analysis providing no further resistance to the global deformation.

Lemmen and Vredeveldt [59] used Material Type 24 as discussed in Section 3.7.2 and considered two element failure criteria: 1) criteria with bending (CB) - elements fail at specific integration points (stress then set to zero) when specific integration point equivalent plastic strain reaches the failure value - fails layer by layer; and 2) criteria with membrane strains only (CM) - stresses at all element integration points are set to zero when equivalent plastic strain reaches the failure value in the central layer – the element fails over its full thickness. CB was found to provide results more consistent with their tests and is used throughout this report. Figure 3-16 illustrates the differences between CB and CM.

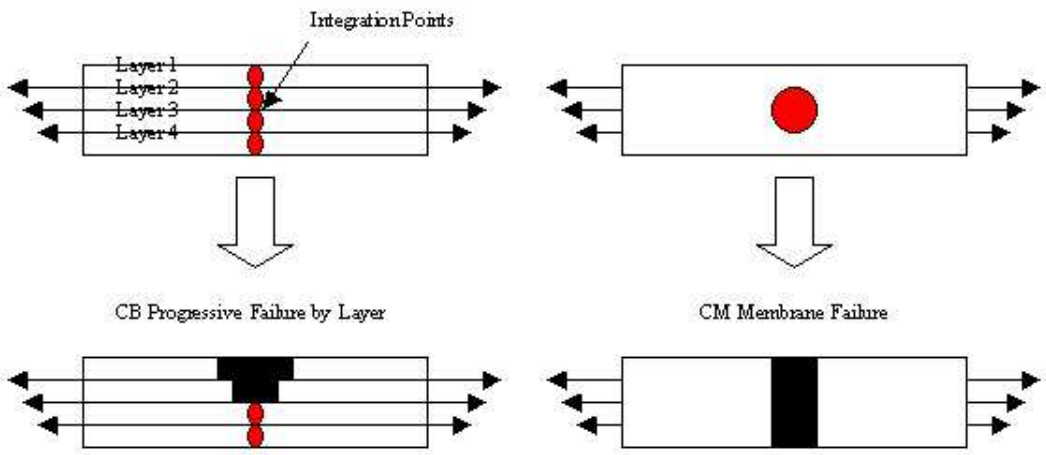

Figure 3-16 Comparison of Element Failure Criteria CB and CM

Still, the determination of the element strain at failure is necessary and is discussed in the following section.

3.7.3.1 Determination of Failure Strain

Failure of a material may be either ductile or brittle. Ductile failure is defined as failure that occurs after significant material thinning and is illustrated in Figure 3-17. Brittle failure is defined as failure that occurs without significant material thinning and is also shown in Figure 3-17.

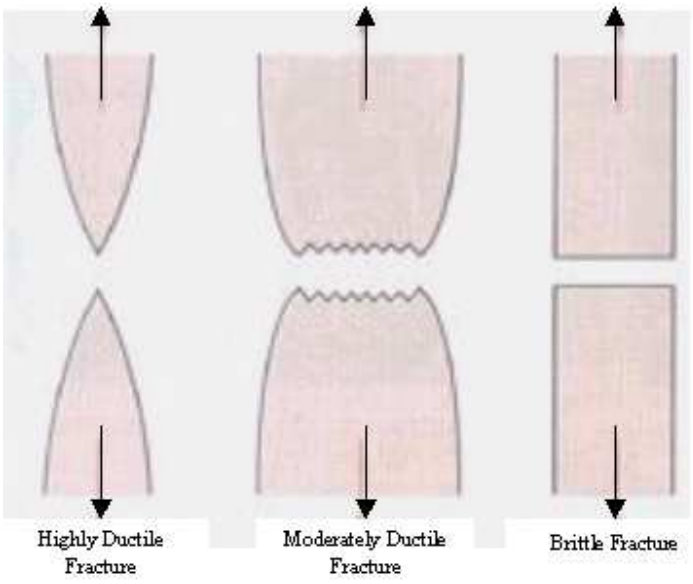

Figure 3-17 Illustration of Ductile and Brittle Fractures

In ship-to-ship collisions either ductile or brittle failure may occur. Which type of failure occurs is dependant on many variables such as temperature, loading, homogeneity, welds, eccentricity, and many others. Because of the complexity of failure, most research is concentrated in the development of a single parameter (failure strain) that accounts for both ductile and brittle fracture on a global scale (i.e. applicable to all material in a vessel).

Failure strain is the value of effective plastic strain at which a material fails and is based on the St. Venant theory of fracture mechanics [86]. Effective plastic strain E_{eff}^{P} is calculated using Equation 3.8 for each element. Where E_p is the plastic strain rate given as the difference between the total strain rate and the elastic strain rate.

$$E_{eff}^{p} = \int_0^t (\tfrac{2}{3} \dot{E}p \dot{E}\ p) \cdot dt \qquad (3.8)$$

In the initial phases of using the finite element method the material failure strain as determined by static tension tests or equivalent was used in the models. Various material tests performed include the static tension tests of mild steel performed by Naar et al [61] yielding a failure strain of 18% and agreeing with the value of Lehmann et al [46]. Wisniewski et al [70] reports a material failure

strain of 17% for both mild steel and high tensile steel. Simonsen and Lauridsen [73] report a material failure strain of 19% determined via a tension test on mild steel. Kitamura [57] reports “a lot of material tests have shown that [failure strain] of ordinary mild steel is about 30%.” Finally, Servis et al [60] report a tested material failure strain for mild steel at 46.1%.

However, comparison of finite element models to experiment shows that the numerical failure strain (the value used in the model) is a function of the element size [29,57,59,60,61,69,72,73,74,75] and therefore is not purely a material property. Much research has been performed to determine the proper value of the failure strain. Agreement as to the proper value or relation has yet to be shown though it is generally agreed that the larger the element size the smaller the numerical failure strain value should be. Figure 3-18 shows a collection of reported failure strains verses element sizes as used by various authors [29,57,59,60,61,69,72,73,74,75].

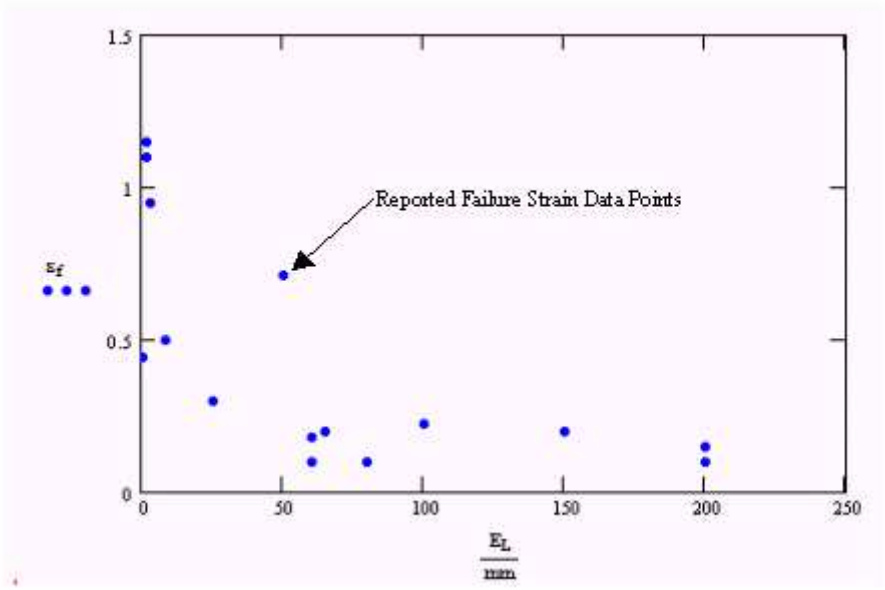

Figure 3-18 Reported Failure Strains vs. Element Length Sizes [29,57,59,60,61,69,72,73,74,75]

Paik and Pederson [29] and Kitamura [57] explain that the lower values of failure strain are used with larger element sizes to numerically account for stress concentration factors such as cracks, corrosion and impact loadings etc… within the model that larger size elements do not properly capture. For this reason, the use of small material samples for the determination of the failure strain

is invalid as small material samples do not provide a true representation of actual distributions of imperfections, stress concentrations or provide information as to an average stress state which occurs within larger elements. Paik and Pederson also state, “ship collisions are essentially dynamic problems and dynamic effects may not be neglected.” For this reason, the use of static or quasi-static experiments to validate the numerical failure strain to be used within a dynamic model is invalid.

Kitamura [57] performed a series of dynamic drop tests and quasi-static penetrations where either scale models were struck repeatedly by a free falling rigid bow model of 8.44 tons or slowly indented by the same rigid bow. Modeling these tests by finite elements a relation as shown in Figure 3-19 for failure strain verses average element edge length was determined. However it is unclear whether this relation was developed based on the dynamic tests or the quasi-static.

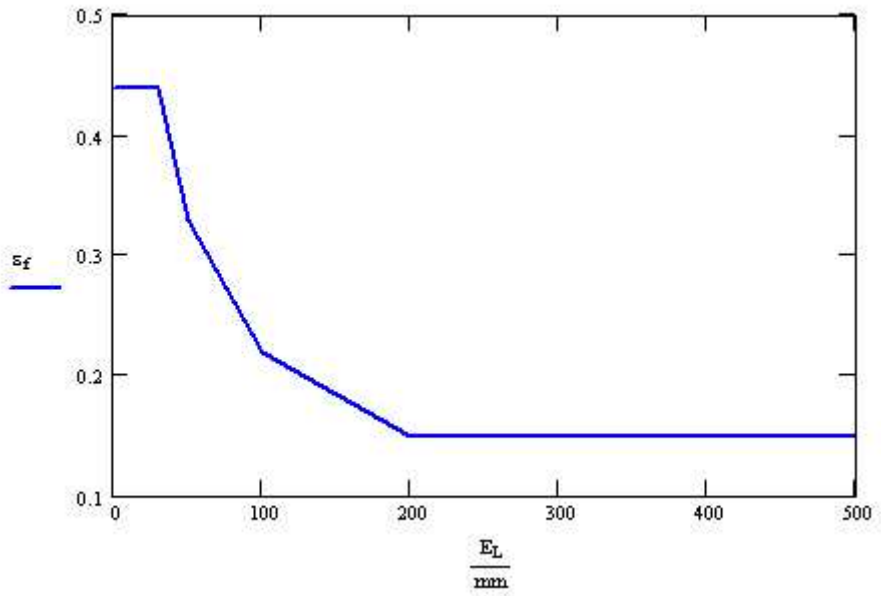

Figure 3-19 Kitamura Necessary Failure Strain Results [57]

To further examine the relationship between the element edge length and the numerical failure strain while incorporating strain rate effects a solely dynamic yet simplified test is desired. The simplest dynamic test to which a finite element model is easily implemented and maintains little computational and modeling effort is the Charpy-V-Notch (CVN) test which measures the total material absorbed energy (Charpy energy) prior to fracture. The disadvantage of using the CVN

test is that the material sample is small and the distributions of imperfections; stress concentrations or average stress state is not considered.

The Charpy energy, often called the impact energy, is determined by impacting a material sample using a pendulum device as shown in Figure 3-20. A Pendulum of a known mass is released from a known height and allowed to swing into the material sample located at the bottom of the pendulum's arc. The absorbed energy is calculated by measuring the height to which the pendulum swings after the impact.

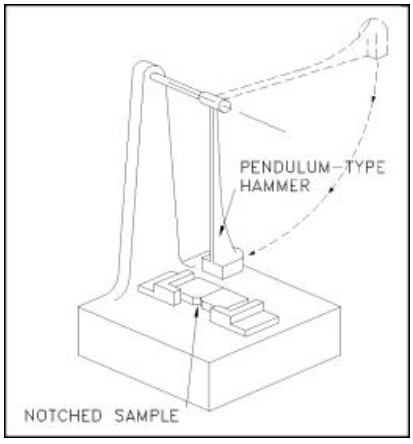

Figure 3-20 Charpy-V-Notch (CVN) Test

The standard size of a CVN test specimen is set by ASTM E23 and has the dimensions as shown in Figure 3-21. The long dimension of the sample (55-mm) is cut parallel to the rolling direction of the steel.

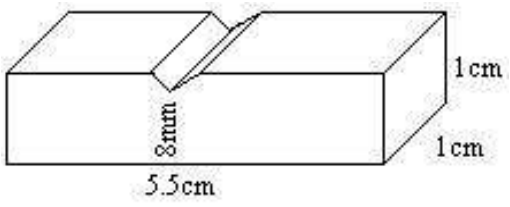

Figure 3-21 Charpy-V-Notch (CVN) Sample Dimension

CVN impact tests conducted on ABS GR. B materials at various temperatures by Francis, Cook and Nagy in SSC Report 276 [76] yield an impact energy verses temperature plot (Figure 3-22)

where the transition from brittle to ductile behavior of the material occurs at 0 degrees Fahrenheit and the upper shelf impact energy (absorbed energy in full ductile behavior range) is approximately 57 ft-lb or Approximately 77.0 Joules. The CVN test is not however the most accurate measure of the energy required to fracture a material sample. A large statistical error is present in most tests, and reproducibility is a common problem between facilities. (SSC Report no. 235 [77] reports a CVN upper shelf impact energy of 112 ft-lb for the ABS GR. B material.)

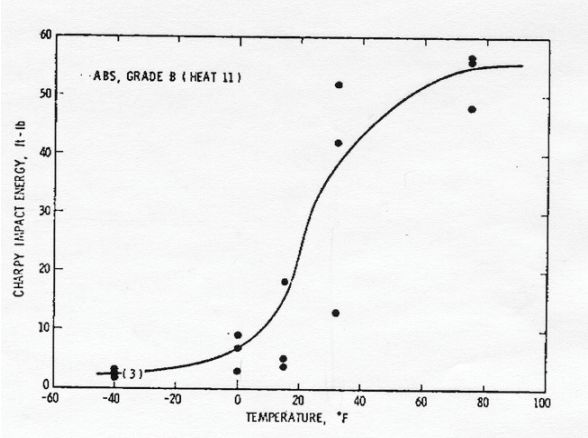

Figure 3-22 Sample Charpy Test Data of ABS Grade B Steel [76]

Though statistically abhorrent with a low number of samples, the CVN test is still a very cheap and affordable way to determine a statistical impact energy for a specified temperature for a material and as such is still used by many steel manufacturer's and ship building firms to classify the reliability of specific materials for designed tasks such as ice-breaking, cold-weather transport, and recently collision survivability and damage prediction.

To correlate the FEM to the CVN test data, the FEA absorbed energy is compared to the absorbed energy from the actual material (ABS GR. B) at an average service temperature of 60°F. The finite element model of the CVN test specimen consists of a flat plate comprised of varying number of elements and fixed on either end with a constant width of 10 mm and length of 55 mm (an example model shown in Figure 3-23). This model is developed for the general application to deck fracture and uses the Belytschko-Tsay shell element vice a solid element formulation as the shell element is used in the global ship-to-ship finite element model. The use of the shell element is valid because the stresses developed in the model are all planar and do not vary through the thickness.

The finite element model of the pendulum impactor is modeled by a rigid structure matching the dimensions as specified by ASTM E23. The test specimen is modeled having the material properties of ABS Grade B mild steel as provided in Table 3-4, where the plastic strain to failure (failure strain) is varied.

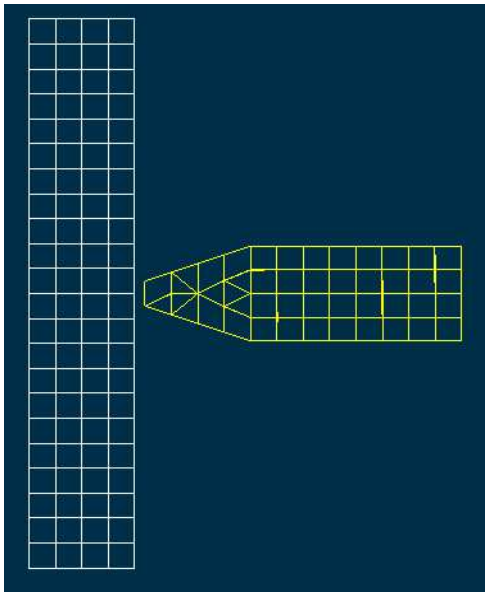

Figure 3-23 CVN FEM Mesh

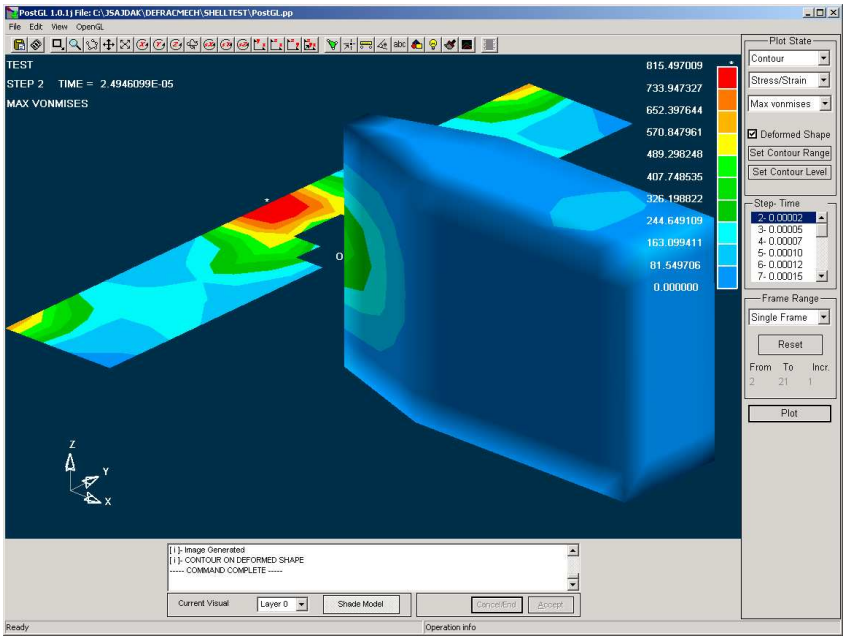

Figure 3-24 CVN FEM Analysis

Figure 3-24 shows that the material sample does not have a uniform planar state of stress and supports the conclusions that the failure strain is not a pure material property but is sensitive to the test configuration and geometry in finite element analysis.

The average computational time on a standard Pentium III Desktop computer for the CVN model was under a minute. After several variations of failure strain (FS), element thickness (t) and average element edge length (L) the absorbed energy (AE) was found to be a function of t, L, element type and material properties. By maintaining constant element type (Belytschko-Tsay shell element) and all material properties except failure strain, the absorbed energy becomes a function of t, L and FS only. Noting that the absorbed energy is a linear function of element thickness as shown by Figure 3-25 the effects of element thickness may be eliminated such that the dimensional parameter AE/t becomes only a function of the dimensionless parameters L/t and FS as shown by Equation 3.9.

$$AE/t = F((L/t), FS) \qquad (3.9)$$

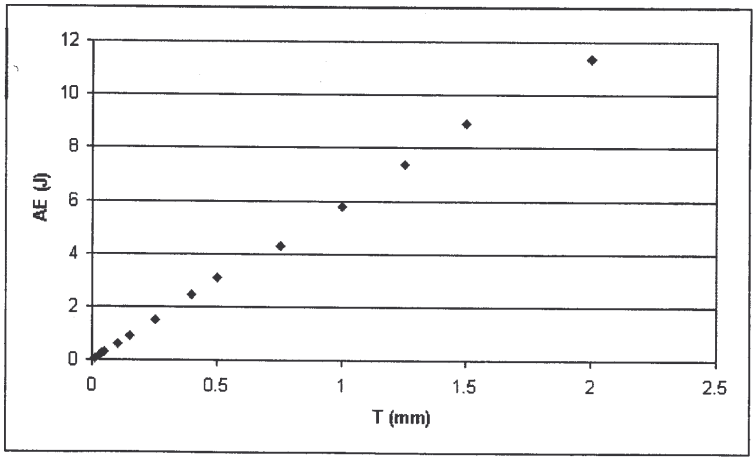

Figure 3-25 FEA Charpy Energy vs. Sample Thickness

Maintaining a constant failure strain of 5% (for simplicity) and varying the average element edge length and thickness of the elements within the test specimen numerical convergence of the AE/t parameter is shown to occur in Figure 3-26 for L/t ratios greater than 2.5.

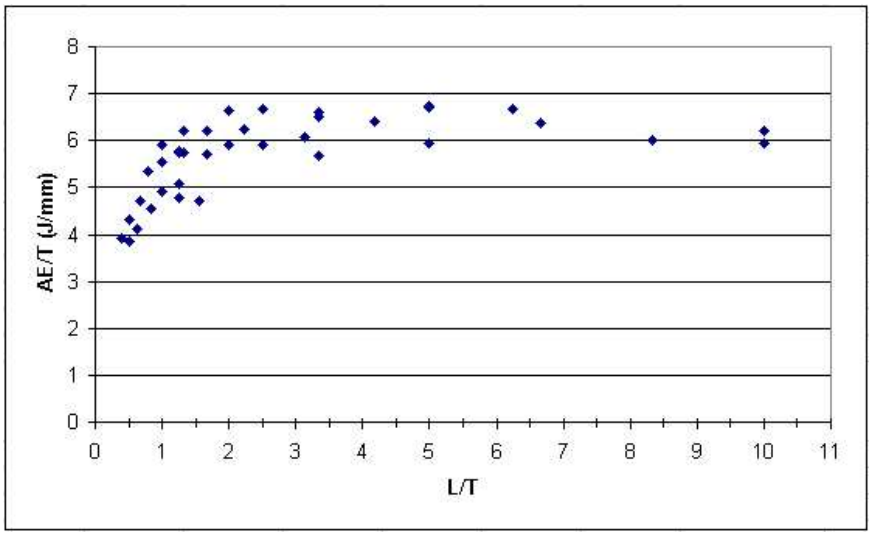

Figure 3-26 FEA Charpy Energy vs. L/T Ratio

Thus, the functional dependence of the absorbed energy on L of elements whose average element edge length is greater than 2.5 times the element thickness may be neglected. At some L/T ratio much greater than 2.5 the element size will not capture the physics of the material sample used within the CVN test and this approximation method will break down. Therefore, as long as the

above conditions are true, L/t ≥ 2.5 and L/t not >>2.5, then the absorbed energy is only a function of the failure strain and the element thickness as shown by Equation 3.10.

$$AE = F(FS) \text{ if } L/t \geq 2.5 \text{ and not } >>2.5 \qquad (3.10)$$

Examination of the effect of failure strain on the absorbed energy in the Charpy-V-Notch model, for the ABS GR. B material shows that the absorbed energy is linearly related to the failure strain (Figure 3-27, where AE is the absorbed energy in Joules divided by 10 and FS is the failure strain).

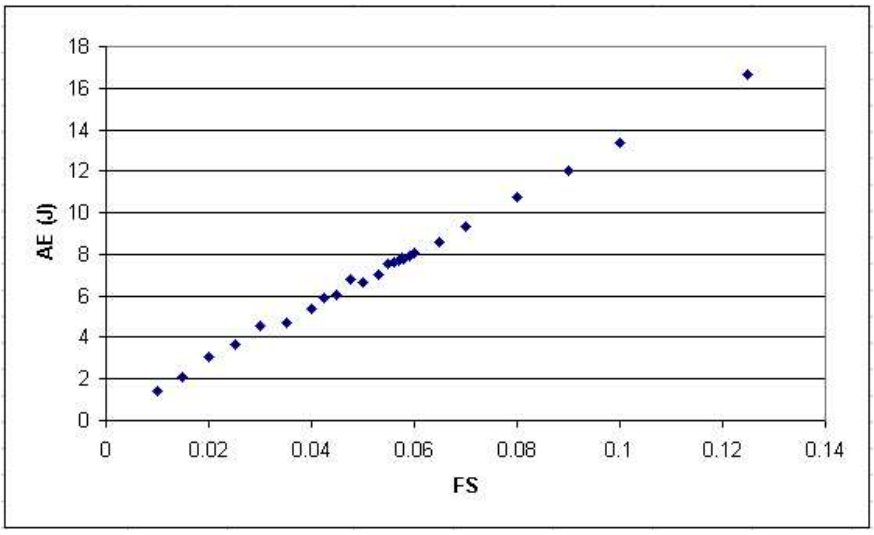

Figure 3-27 FEA Charpy Energy (divided by 10) vs. Failure Strain (FS)

By matching the average of reported Charpy energy for mild steel at 60°F [76,77] to Figure 3-27 where the thickness of both test specimens (numerical and actual) is equal to 10 mm, the numerical failure strain to properly model ABS Gr. B mild steel using Belytchko-tsay elements with material model and properties as given by Table 3-4 and Figure 3-15 is approximately 10% (between 6 and 14% to match the actual material test values of [76 and 77]), as long as the L/t ≥ 2.5 condition is met. For ship-to-ship collision analysis a failure strain of 10% will therefore be used for most analyses.

3.7.4 Strain Rate

The Cowper and Symonds strain rate model accounts for the effect of stain rate on yield strength. Lemmen and Vredeveldt [59] found this model to give good results. The influence of material inertia forces was found to be negligible, i.e. other than the effect of strain rate, material properties are not sensitive to velocity.

The Cowper-Symonds constitutive equation, Equation 3.11, is widely used and has been found adequate for many theoretical and numerical calculations [29]:

$$\sigma_D = \sigma_y[1+(\frac{\varepsilon_r}{C})]^{\frac{1}{P}} \quad (3.11)$$

Where:

σ_D dynamic yield stress

σ_y material static yield stress

ε_r plastic strain rate when the LSDYNA viscous-plasticity option flag is set at 1

C, P material constants

The plastic strain rate, ε_r, is calculated using Equation 3.12. The material properties C and P are most often taken as 40.4 sec^{-1} and 5.0 respectively for mild steel [28,29,72]. Paik et al. [28] used C equal to 3200 sec^{-1} and P equal to 5.0 for high tensile steel materials based on unidentified test data. These values of C and P for mild steel and high strength steel are used in the collision analysis presented here. Ship to ship collision strain rates in this project reach maximum values of approximately 0.1 sec^{-1}. These result in a dynamic yield stress that is 1.3 times the static yield stress in mild steel and can have a significant effect on the results.

$$\varepsilon_r = \frac{\Delta\varepsilon_P}{\Delta r} \quad (3.12)$$

Where:

$\Delta\varepsilon_P$ is the change in plastic strain;

Δt is the time step.

3.8 Calibration

The LSDYNA methodology presented above is calibrated (time step, damping factors and analysis control parameters adjusted) using one real collision event described by Minorsky's [9] collision data as this was the only near complete set of data required for an FE analysis after two years of search. The calibration case is the collision between the David E. Day and the Marine Flier [84] in the Pacific Ocean on May 17, 1952. Only one collision event is used for the calibration of the finite element analysis of ship-to-ship collisions because the majority of the information necessary for the modeling of the collision event is difficult to obtain. Structural design drawings, specific ship data and collision parameters are often not reported or available to the open public.

3.8.1 David E. Day - Marine Flier Collision

On May 17, 1952 the C4 cargo vessel "Marine Flier" struck the T2 tanker "David E. Day" at a reported 55-degree collision angle between frames 59 and 62 of the David E. Day, approximately 9 meters forward of amidships. The reported vessel speeds at the time of the collision were 16.3 knots for the David E. Day and 16.5 knots for the Marine Flier causing a reported 17 ft of penetration and 35 ft of damage length. However, extensive examination of documents related to the collision reveal that the actual speeds of the Marine Flier and David E. Day at the time of the collision were closer to 5 to 7 knots and the collision angle was in actuality between 50 and 55 degrees. In part these changes are due to last minute "Full Astern" and "Hard Right Rudder" orders given by the masters of each vessel in the effort to avoid the collision.

Structural drawings for both ships were obtained through the National Archives and Records Administration and specific data was used within the LSDYNA FEM model shown in Figure 3-28. Appendix C provides information on the "Marine Flier" while appendix F provides information on the "David E. Day". The collision angle was set at 51 degrees with a collision location of 10 meters forward of amidships. The initial striking vessel speed was 5.5 knots, while the struck vessel speed was approximately 7 knots. The FEM results are 5.09 meters or 16.7 ft of penetration and 10 meters or 32.8 ft of damage length. The FEM results are non-conservative by approximately 1.8% in penetration and 6.3% in damage length compared to Minorsky's [9] reported penetration and damage length values.

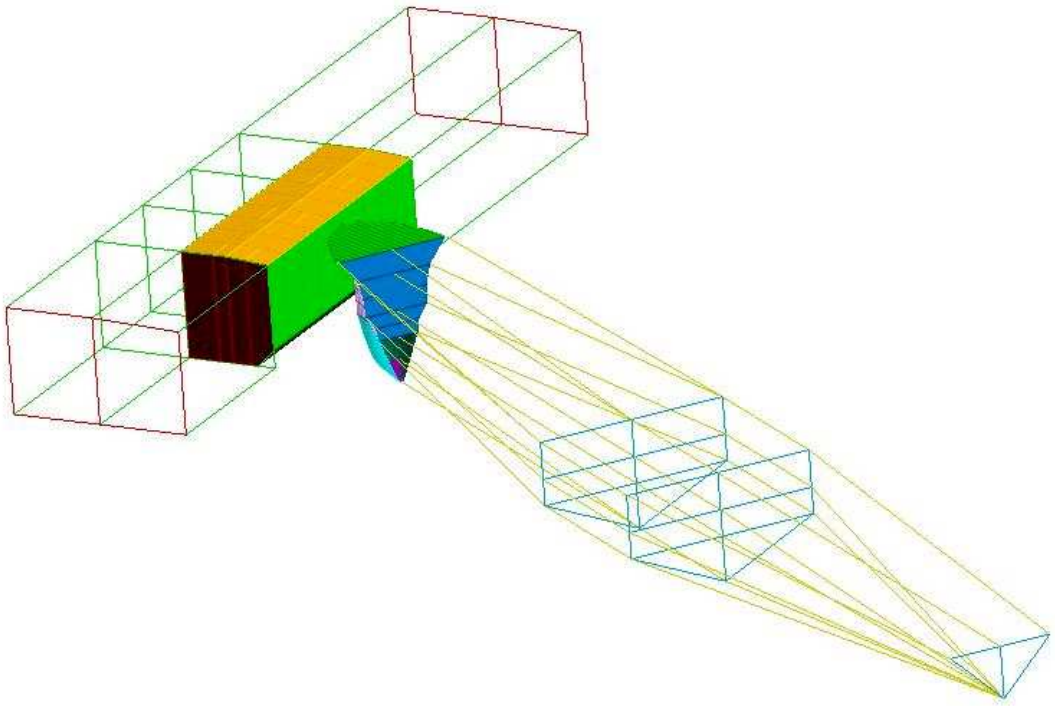

Figure 3-28 David E. Day - Marine Flier Collision Analysis FEA Model

Figure 3-29 through Figure 3-52 provide a visual record of the David E. Day – Marine Flier collision at half-second intervals until the end of the collision event occurring at 4 seconds. The sustained damage within the finite element analysis is representative of the textual description of the damage reported in [84].

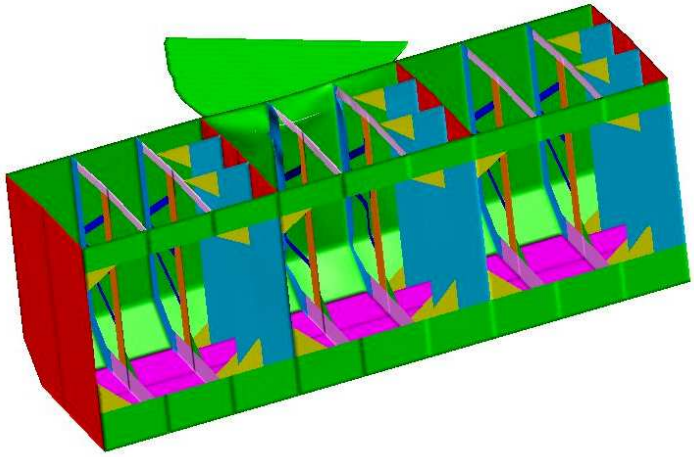

Figure 3-29 David E. Day Marine Flier FEA Damage at 0.5 Seconds

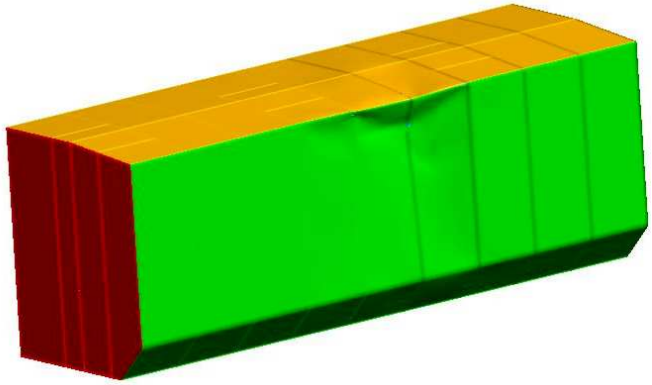

Figure 3-30 David E. Day FEA Hull Damage at 0.5 Seconds

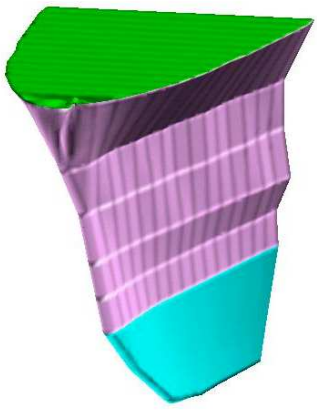

Figure 3-31 Marine Flier FEA Bow Damage at 0.5 Seconds

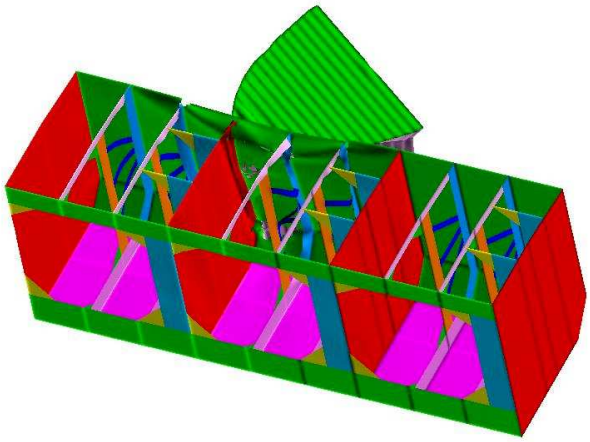

Figure 3-32 David E. Day - Marine Flier Damage at 1.0 Seconds

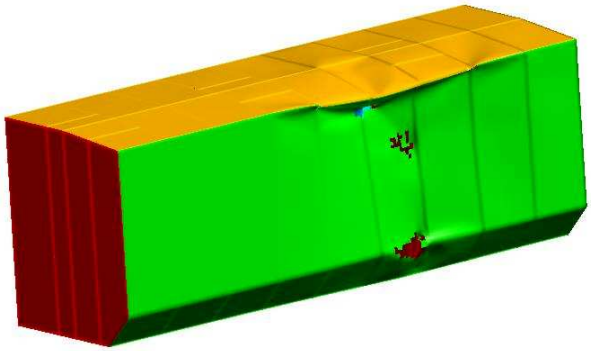

Figure 3-33 David E. Day FEA Hull Damage at 1.0 Seconds

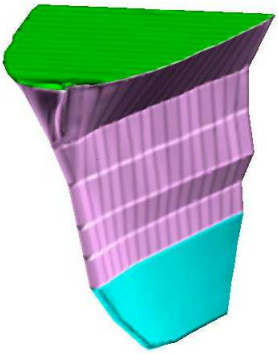

Figure 3-34 Marine Flier FEA Bow Damage at 1.0 Seconds

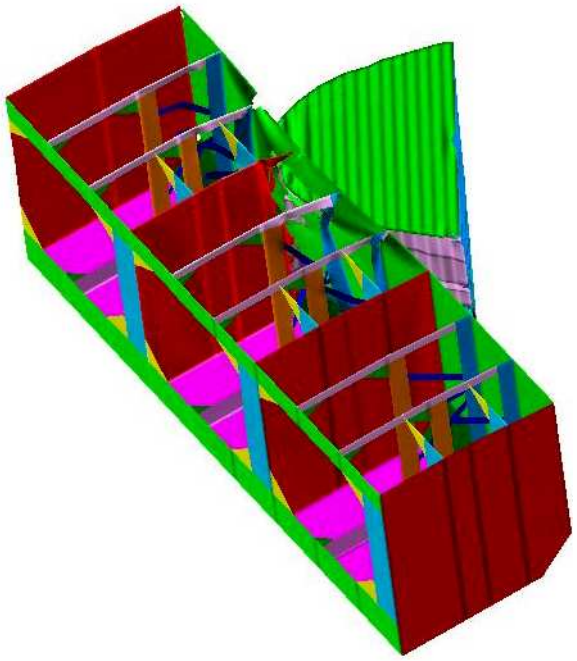

Figure 3-35 David E. Day - Marine Flier FEA Damage at 1.5 Seconds

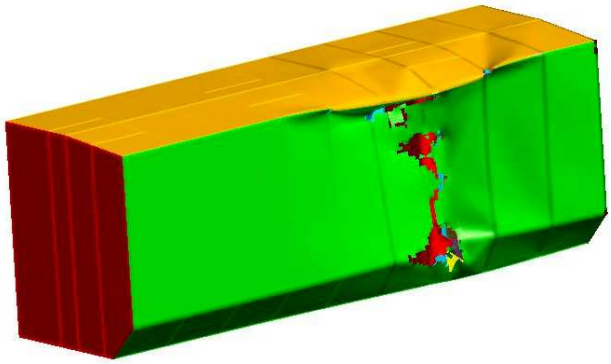

Figure 3-36 David E. Day FEA Hull Damage at 1.5 Seconds

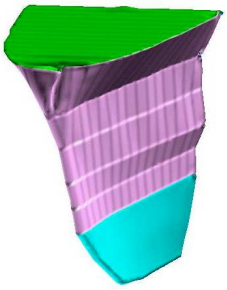

Figure 3-37 Marine Flier FEA Bow Damage at 1.5 Seconds

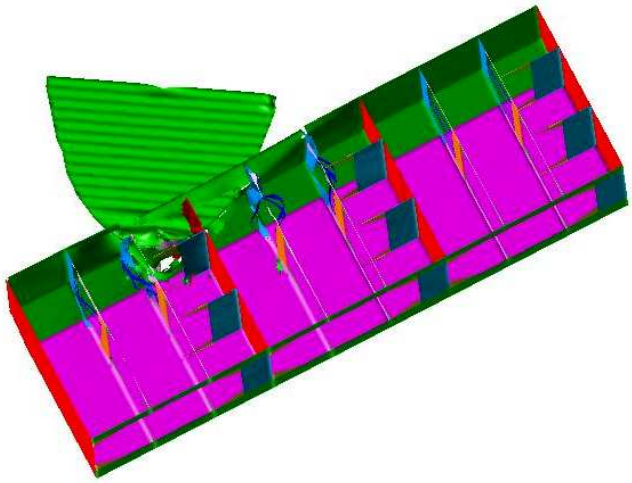

Figure 3-38 David E. Day - Marine Flier FEA Damage at 2.0 seconds

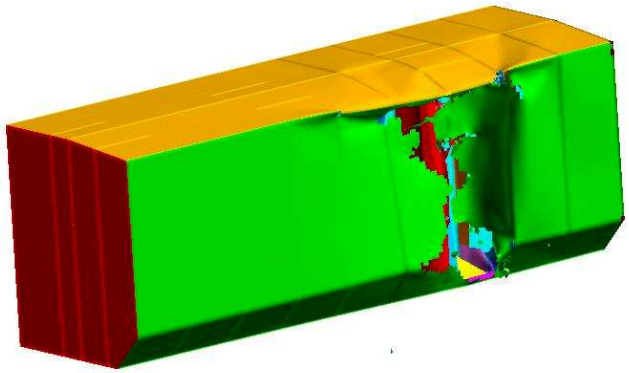

Figure 3-39 David E. Day FEA Hull Damage at 2.0 seconds

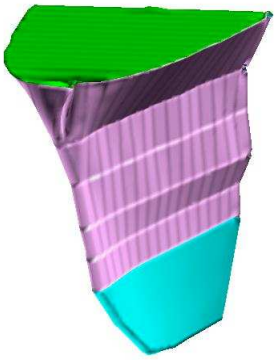

Figure 3-40 Marine Flier FEA Bow Damage at 2.0 Seconds

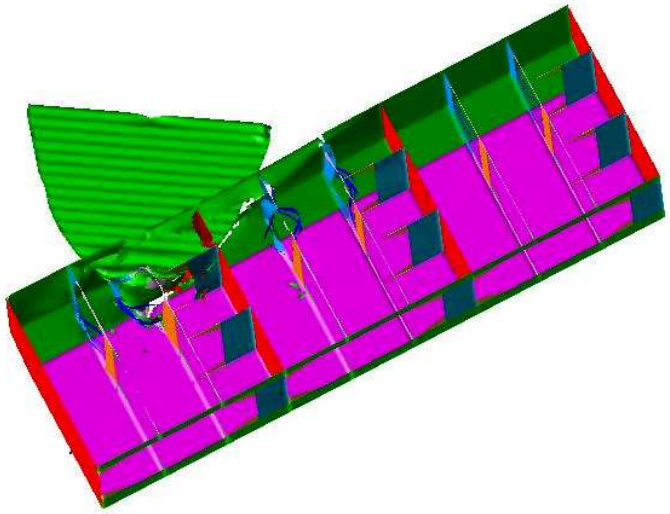

Figure 3-41 David E. Day - Marine Flier FEA Damage at 2.5 Seconds

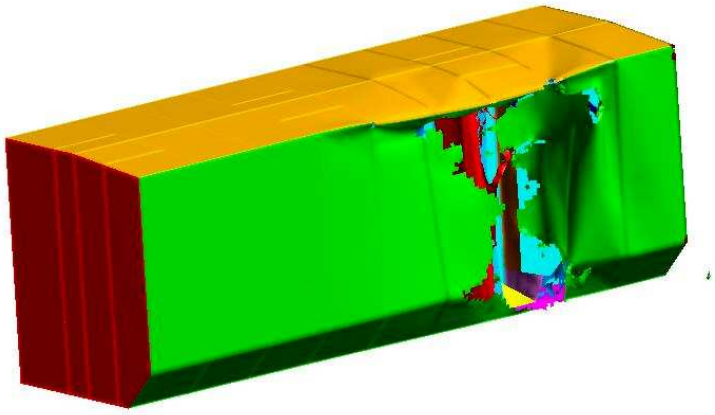

Figure 3-42 David E. Day FEA Hull Damage at 2.5 Seconds

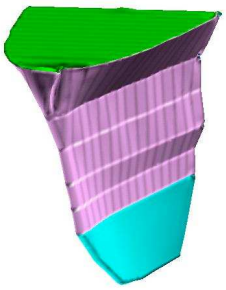

Figure 3-43 Marine Flier FEA Bow Damage at 2.5 Seconds

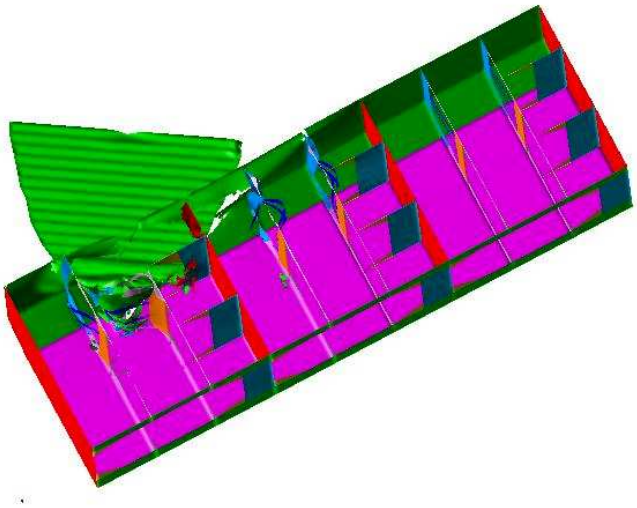

Figure 3-44 David E. Day - Marine Flier FEA Damage at 3.0 Seconds

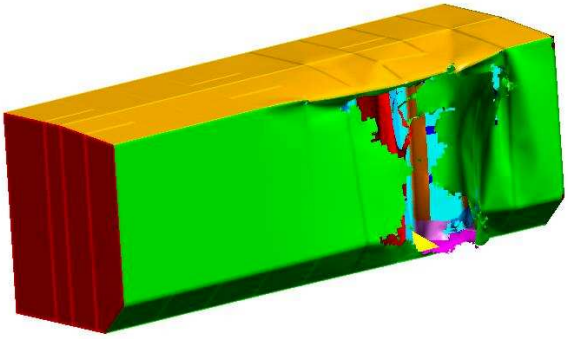

Figure 3-45 David E. Day FEA Hull Damage at 3.5 Seconds

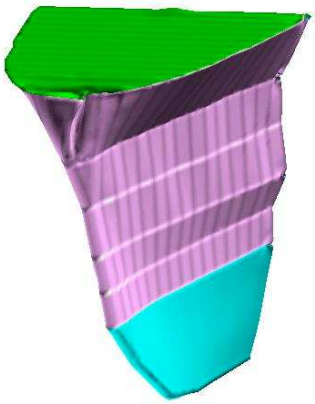

Figure 3-46 Marine Flier FEA Bow Damage at 3.0 Seconds

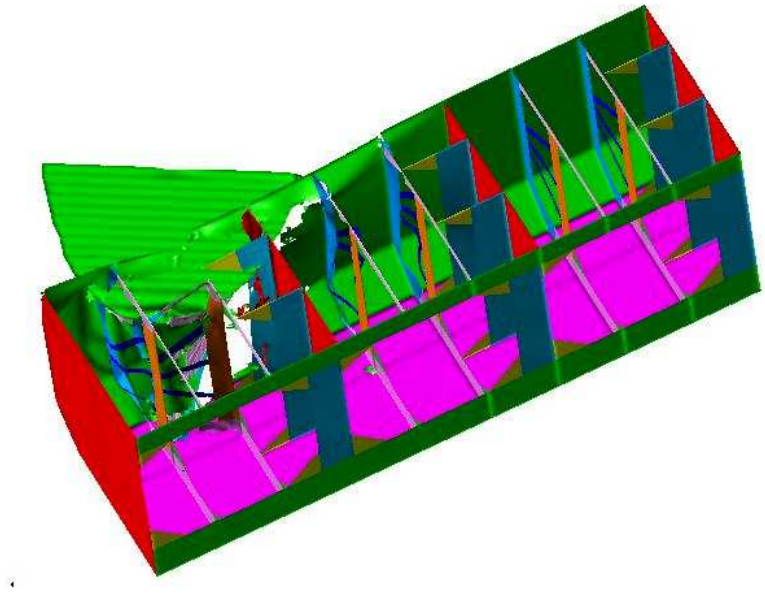

Figure 3-47 David E. Day - Marine Flier FEA Damage at 3.5 Seconds

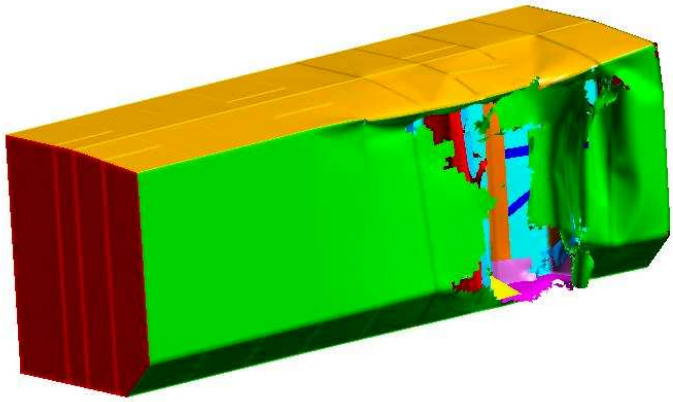

Figure 3-48 David E. Day FEA Hull Damage at 3.5 Seconds

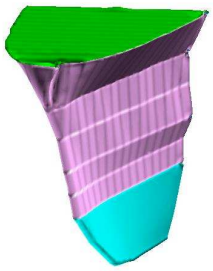

Figure 3-49 Marine Flier FEA Bow Damage at 3.5 Seconds

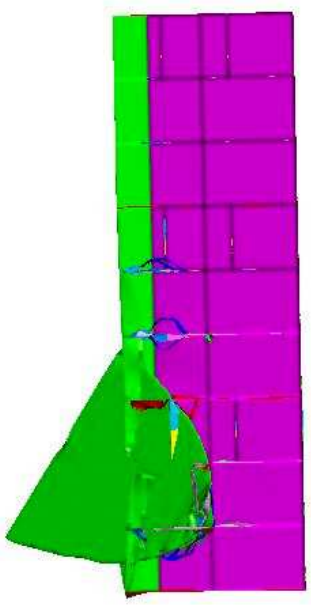

Figure 3-50 David E. Day - Marine Flier FEA Damage at 4.0 Seconds

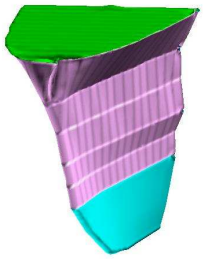

Figure 3-51 Marine Flier FEA Bow Damage at 4.0 Seconds

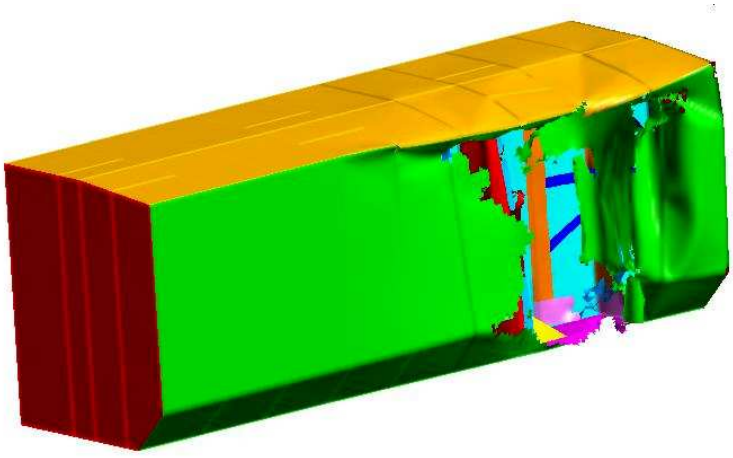

Figure 3-52 David E. Day FEA Hull Damage at 4.0 Seconds

3.9 Summary of Finite Element Analysis in Ship-to-Ship Collisions

While the methods of finite element analysis discussed above seem to provide reasonable and validatable results as shown in Section 3.8.1, the use of finite element analysis for design optimization or the development of variable response surfaces is currently impractical due to the computational requirements of the finite element methods. A practical example is the use of a small Monte Carlo optimization [35] scheme where 1000 analysis are used varying a set number of design parameters for a single collision scenario. Being conservative and using only one fourth of the average ship-to-ship finite element analysis time on a Pentium IV desktop yields a single analysis time of 22 hours. Thus, 1000 analysis requires at minimum 22000 hours or precisely 2 ½ years. If four collision scenarios are examined, then a full decade of computational time is required.

Obviously, the speed at which computer technology improves will reduce the decade wait, but with the increased power of the computer, the wish to improve the detail of the finite element collision model will also occur thus continuously placing the ability of finite element analysis for the use in ship-to-ship collision analysis always one step behind. As such, the use of finite element analysis used within the remaining of this report is relegated to the application of a virtual laboratory assisting in the development and proof of theories and arguments as discussed in later Chapters. An example LSDYNA finite element input file for the David E. Day – Marine Flier collision is presented in appendix I.

4 Simplified Methods

With the high computational cost of finite element analysis, other methods of determining the damage sustained during ship-to-ship collisions were evaluated. Many authors and institutions have investigated aspects of ship-to-ship collisions. A short summary of the methods is provided in the following section with the more applicable methods to this dissertation being discussed in detail in Sections 4.3 through 4.5.

4.1 Timeline and Summary

In 1959 Minorsky developed an empirical methodology to determine the energy absorbed by a ships side structure when struck by another vessel. In 1974 McDermott developed a method of analysis for minor ship collision energy absorption prior to rupture through a membrane strain and web collapse formulation. In 1975, Rosenblatt & Sons, Inc. combined the work of Minorsky and McDermott to yield a method of analysis for ship collision energy analysis through hull rupture. In 1979 Woison proposed modifications to Minorsky's method based on model tests and proposed the idea of a soft bow to absorb energy in the ship-to-ship collision event. Prior to Woison, work with ship-to-ship collisions considered a rigid bow approach. In 1982 Amdahl, based on Woison's idea of a soft bow, developed a method of analyzing the crushing force of a bow based on Wierzbicki's formulations for the crushing of cruciforms, angles and T-sections. Hutchinson, in 1986, developed a probabilistic method for predicting hull damage to ships based upon Minorsky's method as extended by Jones and van Matter (1980). In 1988 Yang and Caldwell modified Amdahl's work on the collision energy absorption of ships' bow structures and in 1993 Pederson proposed an empirical method for predicting the energy absorption of ships bows in collision. From 1993 to 1999 the MIT-Joint Industry Research Project produced the program DAMAGE that determines the absorbed energy of struck ships in collisions and groundings through methods developed by Wierzbicki and Simonsen. From 1995 to 2004 Brown and students developed SIMCOL a probabilistic approach to ship collisions assessing damage and oil outflow based on the work of Minorsky, Rosenblatt and Hutchinson. Both DAMAGE and SIMCOL consider a rigid striking bow. Finally, In 2001 Denmark Technical University (DTU) released a collision model similar to DAMAGE that incorporates a deformable bow model based upon the work of Amdahl and Pederson. Prior to detailed discussion of the methodologies of the varying treatments of ship-to-ship collisions, a list of important or necessary characteristics (summarized from previous Chapters

and presented in section 4.2) of any ship-to-ship evaluation tool is provided for the convenience of model comparisons.

4.2 Important Characteristics of a Ship-to-Ship Collision Model

From details of Chapters 1 through 3 the following list of characteristics necessary for any analytical ship-to-ship collision method is provided. This list can be used to determine the completeness of any method and provides a way to compare each of the methods referenced in Section 4.1 and discussed in Sections 4.3 through 4.5.

- Post Collision Momentum – Any collision analysis method should include the determination of each of the energy components of Equation 2.2 including the energy remaining in the system as kinetic energy due to the post collision motion of the combined vessels as occurs in inelastic collisions.
- Struck Ship Forward Velocity – The collision analysis method must consider struck ship forward velocity and its contribution to the initial kinetic energy of the system.
- Oblique Angle Collisions – The collision analysis method must consider collisions which are not ninety degree T-bone collisions, but occur at varying oblique angles. Few actual collisions occur at exactly a ninety-degree collision angle.
- Determination of Energy from Eight Energy Absorbing Structures – The collision analysis method must consider the energy absorbed from the eight critical energy absorbing structures as found in Chapter 2.
- Deformable Bow – The collision analysis method should consider a deformable or energy absorbing striking ship bow structure as some bow structures may not properly be treated as rigid as discussed in Section 2.4.
- Longitudinal Extent of Damage – The collision analysis method must consider not only the penetration of the striking ship into the struck ship, but also the length of damage along the struck ship known as the longitudinal extent of damage for the determination of the full extent of damage which occurs to the vessel during the collision.
- Low Computational Cost – As discussed in Section 3.9, the collision analysis method must encompass a low computational cost while maintaining high solution fidelity. The method

must allow for the implementation within an optimization scheme or be used to create response surface curves for use within vessel design phases.

- Coupling of Internal Mechanics and External Dynamics – The collision analysis must consider the effect of the interaction between the global behavior of the vessels and the local deformation and resulting forces.

4.3 Methods for Determining Energy Absorbed by the Struck Ship

4.3.1 Minorsky (Energy Coefficient) Method

Minorsky's correlation between the volume of ship structure damaged within a collision and the collisions kinetic energy is based upon the following three assumptions:

- Only the component of the striking ship speed normal to the course of the struck ship contributes to the kinetic energy available to cause damage;
- The mass of the water entrained during the collision in the sway of the struck ship is equal to forty percent of the displacement of the struck ship;
- The collision is an inelastic event.

Using these assumptions the kinetic energy absorbed in damaging the ship structures during the collision is given by Equation 4.1.

$$\Delta KE = \frac{1}{2}\cdot\left[\frac{M_{sis}\cdot\left(M_{sus} + c_{m22}\cdot M_{sus}\right)}{M_{sis} + M_{sus} + c_{m22}\cdot M_{sus}}\right]\cdot\left(V_{sis}\cdot\sin(\theta)\right)^2 \tag{4.1}$$

Where:

ΔKE is the energy absorbed due to damaging structure in the collision

M_{sis} is the displaced mass of the striking ship

M_{sus} is the displaced mass of the struck ship

c_{m22} is the added mass coefficient in sway

V_{sis} is the velocity of the striking ship

θ is the collision angle

By plotting the kinetic energy absorbed in damaging the ship structures during the collision verses the volume of damaged steel material within each collision for several collisions as reported by Minorsky [9] and fitting the data points through a linear least squares fit the correlation between the kinetic energy and the damaged volume is given by Equation 4.2.

$$\Delta KE = 47.2 \cdot R_T + 32.7 \tag{4.2}$$

Where R_T is the volume of damaged steel, the coefficient multiplying R_T is the energy coefficient and the intercept term represents the energy absorbed in puncturing and tearing through the shell of the struck ship (membrane energy). Reardon and Sprung [15] reevaluated Minorsky's correlation adding new collision cases after Minorsky's original 1959 data and estimated the intercept term based upon the average of shell damage energy from seven collisions. Based upon the new data, Reardon and Sprung [15] reported an updated Minorsky correlation given by Equation 4.3.

$$\Delta KE = 47.1 \cdot R_T + 28.4 \tag{4.3}$$

Minorsky's assumptions are conservative, not considering the energy due to the motion of the struck vessel and only considering a forty percent increase of the mass of the struck vessel in sway motion. Paik, Choe and Thayamballi [28] neglect Minorsky's first assumption and allowed the kinetic energy available within the collision to be a function of the relative velocity between the two ships, the ΔKE function reported is:

$$\Delta KE = \tfrac{1}{2} \cdot \frac{(1+c_{a1}) \cdot (1+c_{a2}) \cdot M_1 \cdot M_2}{(1+c_{a1}) \cdot M_1 + (1+c_{a2}) \cdot M_2} \cdot V_r^{\,2} \tag{4.4}$$

Where c_{a1} and c_{a2} are the added mass coefficients for the striking and struck ships in surge and sway respectively, M_1 and M_2 are the displaced masses of the striking and struck ships respectively, and V_r is the relative velocity between the two vessels as given by Equation 4.5.

$$V_r = V_1 + V_2 \cdot \cos(\theta) \tag{4.5}$$

V_1 and V_2 are the forward velocities of the striking and struck ships respectively. Applying Equation 4.4 to the collision data of Reardon and Sprung yields an empirical relation for ΔKE as given by Equation 4.6.

$$\Delta KE = 33 \times R_T + 28.4 \qquad (4.6)$$

The results of Reardon and Sprung, and Paik, Choe, and Thayamballi's empirical approximations are shown Figure 4-1 and Figure 4-2. The high scatter of the results in Paik, Choe, and Thayamballi's empirical approximations becomes more prominent with the use of additional data points.

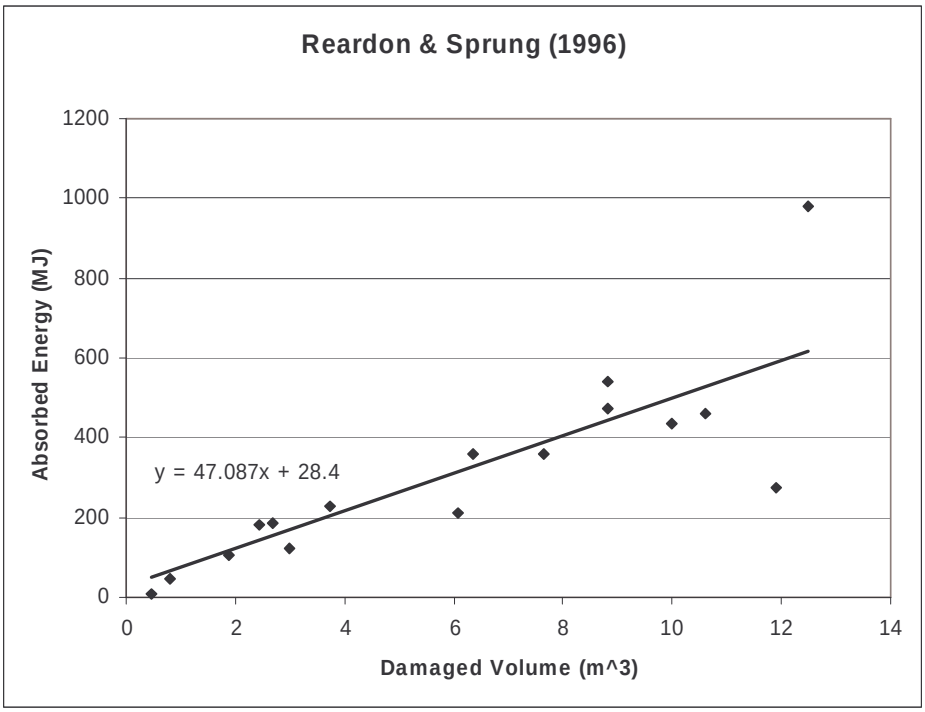

Figure 4-1 Reardon and Sprung Absorbed Energy vs. Damaged Volume

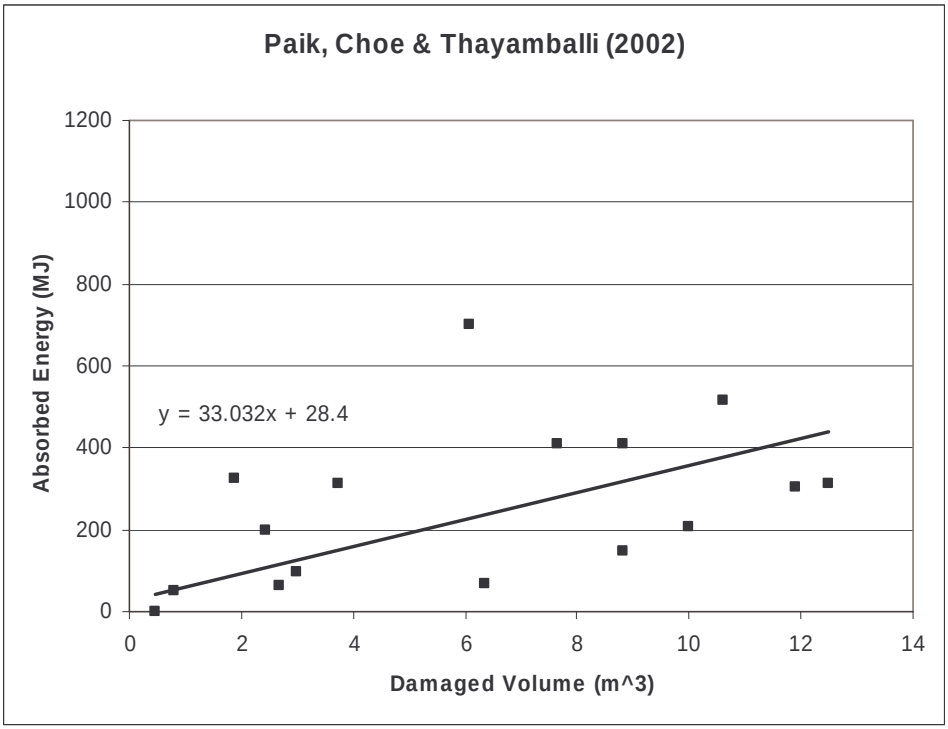

Figure 4-2 Paik, Choe and Thayamballi Absobed Energy vs. Damaged Volume

Several authors have investigated the Minorsky energy coefficient attempting to determine a less empirical approach to the value. Of these, Pedersen and Zhang [14] and Paik and Pedersen [29] approaches are discussed here.

4.3.2 Pederesen and Zhang Energy Coefficient

Pedersen and Zhang developed a relation for the energy absorbed per volume of damaged steel material from the work of Amdahl [23] and Wierzbicki and Abromowicz [87]. The method is based on the crushing, folding and denting modes of L, T or X shaped cross sections. The developed formulation of the Energy Coefficient (E_{coef}) is given by Equation 4.7. Where K is a coefficient that depends on the geometrical shape of the crushed structure, the authors proposed an average value of 3.5 for K.

$$E_{coef} = K \cdot \sigma_o \cdot (\frac{t}{b})^{\frac{2}{3}} \quad (4.7)$$

σ_o is the flow stress, t is the average thickness and b is the span of the crushed material. Figure 4-3 shows the comparison of a fitted line (Minorsky approach) to data points evaluated using Pedersen and Zhangs method of Equation 4.7 on Minorky's original data [9].

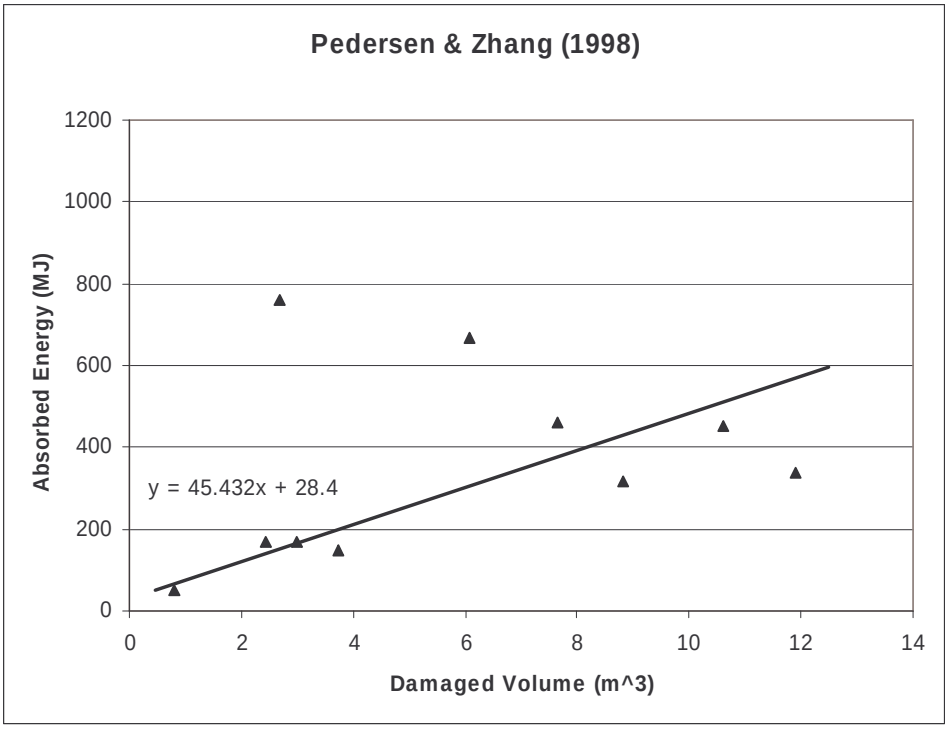

Figure 4-3 Pedersen and Zhang Absorbed Energy vs. Damaged Volume

Pedersen and Zhang also developed a relation for the cutting and tearing of bare plate that is given by Equation 4.8. Γ is the width of the tearing object (often rigid wedge width) if steady state tearing has been reached otherwise Γ is the torn length of the plate.

$$E_{coef} = 3.21 \cdot \sigma_o \cdot (\frac{t}{\Gamma})^{0.6} \quad (4.8)$$

4.3.3 Paik and Pedersen Energy Coefficient

Paik and Pedersen developed two relations for the energy coefficient based on the crushing and folding cutting and tearing damage modes of plated structures (with, and without, material strain rate effects). These formulations are derived from Amdahl [23] and are well formulated within [29]. Equation 4.9 is the formulation of E_{coef} without strain rate effects and Equation 4.10 includes the effect of strain rate.

$$E_{coef} = (1.9514 \cdot (\tfrac{t}{b})^{0.5} + 0.3661 \cdot \tfrac{t}{b}) \cdot \sigma_o \tag{4.9}$$

$$E_{coef} = (1 + (\tfrac{V_m}{1.1026 \cdot 40.4 \cdot \sqrt{b \cdot t}})^{0.2}) \cdot (1.9514 \cdot (\tfrac{t}{b})^{0.5} + 0.3661 \cdot \tfrac{t}{b}) \cdot \sigma_o \tag{4.10}$$

V_m is the mean impact speed that is determined by Equation 4.11.

$$V_m = \frac{\partial \delta}{\partial t} \tag{4.11}$$

Where $\delta(t)$ is the relative motion between the striking and struck vessels.

4.3.4 ALPS/SCOL

ALPS/SCOL is a coarse-mesh 3-D non-linear finite element code using super-elements based on the Idealized Structural Unit Method (ISUM) [28,29]. The geometry of the striking and the struck ships is described in a global (three-dimensional) rectangular coordinate system. The stress in an ISUM unit is described in a local element coordinate system. ALPS/SCOL considers sway and yaw of the struck ship with the following assumptions:

- The added masses of the striking and the struck ships are calculated based on ships of similar type and size using a linear strip theory-based computer program.
- The striking ship is assumed to be rigid.
- The analysis of the external and the internal dynamics is undertaken separately.
- The longitudinal velocity of the struck ship is not considered.

Since ALPS/SCOL is based on a simplified 3-D nonlinear finite element approach, damage in three directions (penetration, vertical and horizontal damage) is considered.
The geometry of the striking ship bow shape is described by gap/contact elements. One cargo hold of the struck ship is taken as the extent of the struck ship analysis. ISUM stiffened panel units are used to model the struck vessel structure.

The geometry of the struck ship is described using rectangular or triangular ISUM units. If the deformation of the struck ship is symmetric, the total degrees of freedom in the numerical model are reduced by half. Each node has 3 degrees of freedom. Figure 4-4 shows damage calculated in a typical ALPS/SCOL simulation.

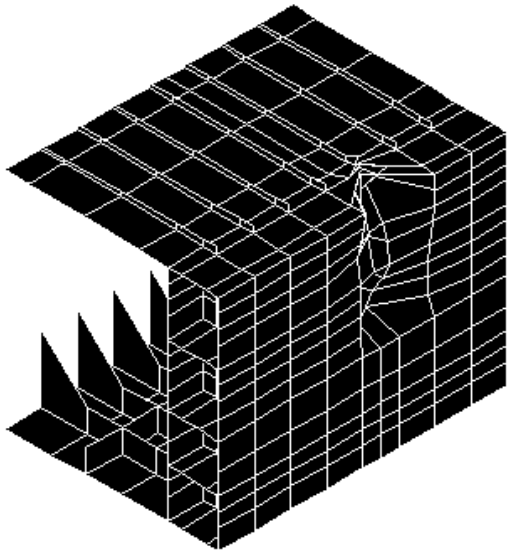

Figure 4-4 Damage from ALPS/SCOL Simulation

Design data required for the striking ship includes a detailed bow geometry description, length, beam, depth, draft and displacement. Design data for the struck ship includes, length, beam, depth, draft and displacement, transverse bulkhead location, COG, and detailed structural design and scantlings. Scenario data required includes striking ship velocity and longitudinal location of impact in the struck ship.

4.3.5 DAMAGE

DAMAGE [10] is a two-degree of freedom (DOF) model developed at MIT. Both sway and yaw are allowed motions of the struck ship, however the striking ship is only allowed one DOF, surge. DAMAGE is based upon the following assumptions:

- The collision angle is ninety degrees
- The struck ship has zero initial energy
- The kinetic energy parallel to the struck ship centerline is negligible
- The collision is totally inelastic

The final speeds of both the striking and struck ships are found using the conservation of linear and angular momentum. From DAMAGE, the total kinetic energy absorbed within the collision (AE) is given by Equation 4.12.

$$AE = \frac{M_{1y} \cdot Vf_1^2 + M_{2x} \cdot Vf_2^2 + I_{1z} \cdot \omega f_1^2 - M_{2x} \cdot Vi_2^2}{2} \qquad (4.12)$$

M_{1y} is the virtual mass of the struck ship including the added mass in sway, M_{2x} is the virtual mass of the striking ship including the added mass in surge and I_{1z} is the virtual moment of inertia in yaw of the struck ship including the yaw added mass (moment of inertia). Vf_1, Vf_2 and ωf_1 are the final velocities of the struck (1) and striking (2) ships, and Vi_2 is the initial velocity of the striking ship.

4.4 Methods for Determining Energy Absorbed by the Striking Ship Bow

4.4.1 Amdahl's Method

Amdahl's model for the energy absorption of a striking ship bow is based on theoretical considerations and is correlated against model test results [23]. The model considers the energy dissipated during plastic deformation of basic structural elements such as angles, T-sections and cruciforms. The total crushing load of a specific structure is obtained by adding up all basic

element crushing-loads. Amdahl's method leads to the following equation for average crushing length.

$$\sigma_c(\sigma_0, n_{AT}, \tau, DA, n_C, n_T) := 2.42 \cdot \sigma_0 \cdot \left(\frac{n_{AT} \cdot \tau^2}{DA}\right)^{\frac{2}{3}} \cdot \left[0.87 + 1.27 \cdot \frac{n_C + 0.31 \cdot n_T}{n_{AT}} \cdot \left[\frac{DA}{(n_C + 0.31 \cdot n_T) \cdot \tau^2}\right]^{\frac{1}{4}}\right]^{\frac{2}{3}} \quad (4.13)$$

The total crushing load is then found by Equation 4.14.

$$P_{AV}(DA, \sigma_c) := DA \cdot \sigma_c \quad (4.14)$$

Where:

σ_c is the average crushing strength of the bow;

σ_0 is the ultimate strength of steel;

τ is the average thickness of the cross section under consideration;

DA is the cross sectional area of the deformed steel material;

n_c is the number of cruciforms in the cross section;

n_T is the number of T-sections in the cross section;

n_{AT} is the number of angle and T-sections in the cross section.

Appendix G provides a detailed calculation using Amdahl's method for the 150K DWT Bulk Carrier Bow Model described in Appendix A.

4.4.2 Pedersen's Method

Pederson [22] proposed a simplified method that consists of an empirical expression to estimate the maximum bow collision load. The maximum bow collision load is given by Equation 4.15.

$$P_{bow} := \begin{cases} \left[P_0 \cdot L_{bar} \cdot \left[E_{bar} + (5 - L_{bar}) \cdot L_{bar}^{1.6}\right]^{0.5}\right] & \text{if } E_{bar} \geq L_{bar}^{2.6} \\ \left[2.24 \cdot P_0 \cdot (E_{bar} \cdot L_{bar})^{0.5}\right] & \text{otherwise} \end{cases} \quad (4.15)$$

Where:

P_{bow} is the maximum bow collision load in MN;

P_0 is Pederson's reference load equal to 210 MN;

L_{bar} is non-dimensional length given as LBP/275;

E_{bar} is the non-dimensional energy given as the initial energy divided by 1425 MN-m.

The total penetration or crush length of the bow of the striking vessel is given by Equation 4.16 and the total duration of the impact is given by Equation 4.17.

$$s_{max} := \frac{\pi}{2} \cdot \frac{E_0}{P_{bow}} \tag{4.16}$$

$$T_0 := 1.67 \cdot \frac{s_{max}}{V_s} \tag{4.17}$$

Where:

E_0 is the initial kinetic energy of the striking ship;

s_{max} is the total crush distance of the bow;

V_s is the maximum service speed of the striking ship.

Appendix H provides a detailed calculation using Pedersens method for the 150K DWT Bulk Carrier Bow Model described in Appendix A.

4.5 Methods for Determining Energy Absorbed by Both the Striking and Struck Ships

4.5.1 DTU Collision Model

The Technical University of Denmark (DTU) ship collision model solves the external ship dynamics problem uncoupled from the internal mechanics problem and applies the calculated absorbed energy to plastic deformation of the struck ship. Solution of the external dynamics is

accomplished based on an analytical method developed by Pederson and Zhang. [14] This method separately estimates the fraction of the kinetic energy that is available for deformation of the ship structure in the transverse and longitudinal directions. Where the largest assumption of the method is that the ratio of the energy dissipation in the longitudinal direction to the transverse direction is constant over the entire collision. The energy loss for dissipation by structural deformation is expressed in closed form expressions. The procedure is based on a rigid body mechanism, where it is assumed that there is negligible strain energy for deformation outside the contact region, and that the contact region is local and small. This implies that the collision can be considered instantaneous as each body is assumed to exert an impulsive force on the other at the point of contact. The model includes friction between the impacting surfaces so those situations with glancing blows can be identified. Both ships have three degrees of freedom: surge, sway and yaw. The interaction between the ships and the surrounding water is approximated by simple added mass coefficients, which are assumed to remain constant during the collision. The loss in kinetic energy by the method is determined in two directions, perpendicular and parallel to the side of the struck ship. Both the right and oblique angle collisions are considered and both vessels may have velocity before the collision. The model for the internal mechanics is based on a set of super-elements, where each element represents a structural component. The calculation method is based on the principle that the area of the struck vessel affected by the collision is restricted to the area touched by the striking vessel. The super-elements and mechanisms are:

- Lateral plate deflection and rupture. Large deflections are assumed; this implies that the bending resistance can be neglected
- Crushing of structure intersection elements (Cruciform or T-Section elements)
- In plane crushing and tearing of plates
- Beam deflection and rupture

The design data for the struck vessel includes length, beam, depth, draft, displacement, center of gravity (COG) and detailed structural design and scantlings. The bow of the striking vessel is assumed to be deformable through Amdahl's [23] approach for longitudinally stiffened bows or Lehmann and Yu [46] for transversely stiffened bows however, only the striking ship bow or the struck ship side structure may deform in any one time-step. By a comparison of the crushing energies for the bow and side of the struck vessel it can be determined which structure deforms during the considered time step. If the striking vessel is equipped with a bulbous bow, the analysis

of the crushing forces is separated into a bulb analysis and an analysis of the top of the bow above the bulb. The design data for the striking vessel includes stem angle, breadth, bow height, and structural details and scantlings. If the bow is equipped with a bulb, this is assumed to have the form of an elliptic parabola. Scenario data required includes striking and struck ship velocity, collision angle and longitudinal location of impact at the struck vessel. Further details on DTU's collision model can be found in [88].

4.5.2 SIMCOL Version 2.1

SIMCOL Version 0.0 was developed as part of the work of SNAME Ad Hoc Panel #3 [2,11] where a probabilistic approach to the determination of damage extents was employed. Based on further research, test runs and the need to make the model sensitive to a broader range of design and scenario variables, improvements were progressively made at Virginia Tech [35]. A sweeping segment method was added to the model in SIMCOL Version 1.0 to improve the calculation of damage volume and the direction of damage forces. Models from Rosenblatt [16,18] were applied in Version 1.1 assuming rigid web frames. In Version 2.0, the lateral deformation of web frames was included. In Version 2.1, the vertical extent of the striking ship bow is considered. Version 2.1 is described in this section.

SIMCOL uses a forward difference time-domain simultaneous solution of external ship dynamics and internal deformation mechanics similar to that originally proposed by Hutchison [12].

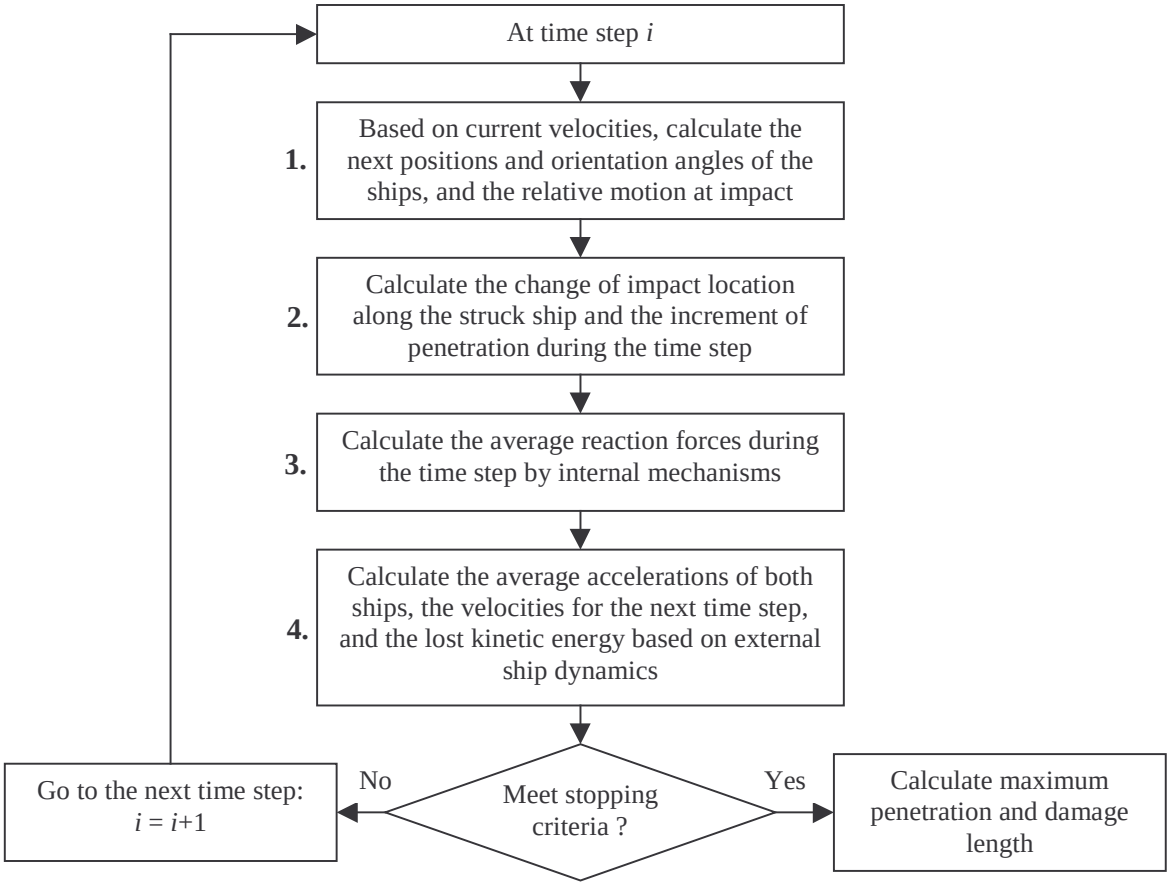

Figure 4-5 SIMCOL Simulation Process

Figure 4-5 shows the SIMCOL simulation process. The Internal Sub-Model performs Steps 2 and 3 in this process. It calculates internal deformation due to the relative motion of the two ships and the internal reaction forces resulting from this deformation. The External Sub-Model performs Steps 1 and 4 in this process. It applies the internal forces to the global motion of the two ships and calculates the resulting accelerations, velocities and motions of the two ships during a time step.

4.5.2.1 SIMCOL Version 2.1 External Dynamics Sub-Model

The External Dynamics Sub-Model uses a global coordinate system shown in Figure 4-6. Its origin is at the initial (time of strike) center of gravity of the struck ship with the *x*-axis towards the bow of the struck ship. The initial locations and orientations of the struck and striking ships in the global coordinate system are:

$$x_{1,0} = 0 \qquad y_{1,0} = 0 \qquad \theta_{1,0} = 0$$
$$x_{2,0} = -l_0 + \frac{L_{BP2}}{2}\cos\phi_0$$
$$y_{2,0} = \frac{B_1}{2} + \frac{L_{BP2}}{2}\sin\phi_0 \qquad (4.18)$$
$$\theta_{2,0} = \phi_0 - \pi$$

where:

x_1, y_1 center of gravity of the struck ship (m), assumed at amidships;

θ_1 heading of the struck ship;

x_2, y_2 center of gravity of the striking ship (m), assumed at amidships;

θ_2 heading of the striking ship;

LBP_2 length between perpendiculars of the striking ship (m);

B_1 breadth of the struck ship (m); and

ϕ collision angle.

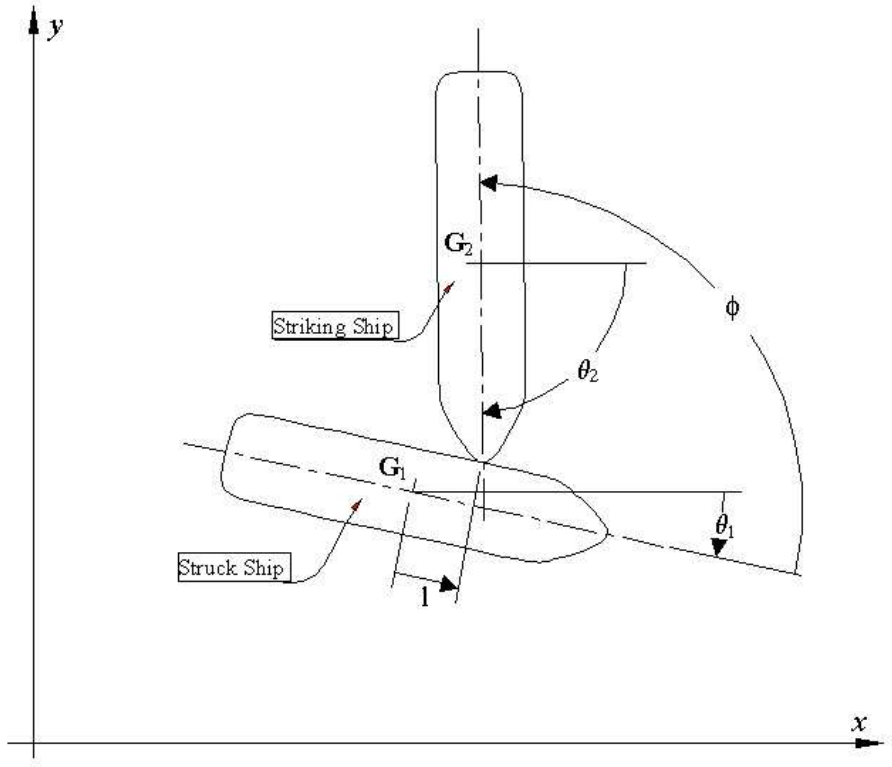

Figure 4-6 SIMCOL External Ship Dynamics

A local damage coordinate system, ξ-η, is established on the struck ship to calculate relative movement and collision forces. The origin of this system is set at amidships on the shell plate of the damaged side of the struck ship. Axes ξ and η point aft and inboard relative to the struck ship. Local coordinate systems are also established at the centers of gravity of both struck and striking ships. Forces and moments in the local systems are transformed to the global *x*-*y* system for solution of the ship dynamics. In the local ship systems, the hydrodynamic added mass for each ship is a tensor in the form:

$$\mathbf{A} = \begin{bmatrix} a_{11} & a_{12} & a_{13} \\ a_{21} & a_{22} & a_{23} \\ a_{31} & a_{32} & a_{33} \end{bmatrix} \tag{4.19}$$

Considering the approximate symmetry of the ships, and with the center of gravity of the ships assumed to be at amidships, the off-diagonal terms of the added mass tensor for each ship are zeros:

$$\mathbf{A}_s = \begin{bmatrix} a_{11} & 0 & 0 \\ 0 & a_{22} & 0 \\ 0 & 0 & a_{33} \end{bmatrix} \tag{4.20}$$

Where:

a_{11} added mass in the surge direction (kg);

a_{22} added mass in the sway direction (kg); and

a_{33} added mass in the yaw direction (kg-m^2).

The added mass tensor is transformed in accordance with the orientation of each ship to the global coordinate system. The transformed tensor, $\mathbf{A}_\theta$, for each ship is:

$$\mathbf{A}_\theta = \begin{bmatrix} a_{11}\cos^2\theta + a_{22}\sin^2\theta & (a_{11}-a_{22})\cos\theta\sin\theta & 0 \\ (a_{11}-a_{22})\cos\theta\sin\theta & a_{11}\sin^2\theta + a_{22}\cos^2\theta & 0 \\ 0 & 0 & a_{33} \end{bmatrix} \quad (4.21)$$

The added mass in surge is approximated by the added mass of a circumscribed cylinder [12]. The added mass in surge, a_{11}, for each ship is:

$$a_{11} = \frac{4}{3}\rho\pi\left(\frac{BT}{\pi}\right)^{\frac{3}{2}} = 0.75225\rho(BT)^{\frac{3}{2}} \quad (4.22)$$

Where:

ρ density of sea water, 1025 kg/m^3;

B breadth of the ship (m); and

T draft of the ship (m).

The added mass in sway is approximated assuming that the cross sections of ships are rectangular [12]. The added mass in sway, a_{22}, for each ship is:

$$a_{22} = 1.189\rho T^2 L_{BP} \quad (4.23)$$

Similarly, by assuming that the water planes are rectangular, the added mass in yaw, a_{33}, is [12]:

$$a_{33} = \frac{2.378\rho T^2 {L_{BP}}^3}{24} = 0.0991\rho T^2 {L_{BP}}^3 \quad (4.24)$$

Instead of calculating added mass directly, added mass coefficients may be used where:

$$\begin{aligned} a_{11} &= c_{11} m_s \\ a_{22} &= c_{22} m_s \\ a_{33} &= c_{33} I_{s33} \end{aligned} \quad (4.25)$$

Coefficients are used in this report to standardize results when compared to other models. Assumed added mass coefficients are 0.05 in surge (c_{11}), 0.85 in sway (c_{22}) and 0.21 in yaw (c_{33}).

The actual mass for each ship is also represented by a tensor:

$$\mathbf{M}_{ship} = \begin{bmatrix} m_s & 0 & 0 \\ 0 & m_s & 0 \\ 0 & 0 & I_{s33} \end{bmatrix} \tag{4.26}$$

where:

m_s ship mass (kg); and

I_{s33} mass moment of inertia about the yaw axes of each ship (kg-m^2).

The virtual mass, $\mathbf{M}_V$, for each ship is then:

$$\mathbf{M}_{V\theta} = \mathbf{M}_{ship} + \mathbf{A}_\theta = \begin{bmatrix} m_{V11} & m_{V12} & 0 \\ m_{V21} & m_{V22} & 0 \\ 0 & 0 & I_{V33} \end{bmatrix}$$
$$= \begin{bmatrix} m_s + a_{11}\cos^2\theta + a_{22}\sin^2\theta & (a_{11} - a_{22})\cos\theta\sin\theta & 0 \\ (a_{11} - a_{22})\cos\theta\sin\theta & m_s + a_{11}\sin^2\theta + a_{22}\cos^2\theta & 0 \\ 0 & 0 & I_{s33} + a_{33} \end{bmatrix} \tag{4.27}$$

In Steps 2 and 3 of Figure 4-5, the Internal Model calculates the resulting deformation, and the average forces and moments generated by this deformation over the time step as discussed in Section 4.5.2.2. In Step 4 of Figure 4-5, these forces and moments are applied to each ship. The new acceleration for each ship is:

$$\mathbf{V_s}' = \frac{\mathbf{F}}{\mathbf{M}_{V\vartheta}} \tag{4.28}$$

or:

$$u' = \frac{F_x m_{V22} - F_y m_{V12}}{m_{V11} m_{V22} - m_{V12}^2}$$
$$v' = \frac{F_y m_{V11} - F_x m_{V12}}{m_{V11} m_{V22} - m_{V12}^2} \qquad (4.29)$$
$$\omega' = \frac{M}{I_{V33}}$$

Where:

F forces exerted on each ship in the global system, $\mathbf{F} = \{Fx, Fy, M\}^T$;

F_x force in the *X* direction in the global coordinate system (N);

F_y force in the *Y* direction in the global coordinate system (N);

M moment about the center of gravity of each ship (N-m);

$\mathbf{V}_s'$ ship acceleration, $\mathbf{V}_s' = \{u', v', \omega'\}^T$;

u' acceleration in the *X* direction in the global coordinate system (m/s^2);

v' acceleration in the *Y* direction in the global coordinate system (m/s^2); and

ω' angular acceleration of each ship in yaw ($degree/s^2$).

The new velocities for each ship at the end of the time step are:

$$\mathbf{V}_{s,n+1} = \mathbf{V}_{s,n} + \mathbf{V}_s' \tau \qquad (4.30)$$

Where:

n time step number; and

τ length of the time step (second).

Referring to Figure 4-5, step 1, the velocities from the previous time step are applied to the ships to calculate their positions at the end of the current time step:

$$\mathbf{X}_{n+1} = \mathbf{X}_n + \mathbf{V}_{sn} \tau \qquad (4.31)$$

Where:

X location and orientation of each ship in the global system, $\mathbf{X} = \{x, y, \theta\}^T$.

4.5.2.2 SIMCOL Version 2.1 Internal Sub-Module

Referring to Figure 4-5, Steps 2 and 3, the Internal Sub-Model calculates the struck ship deformation resulting from the ships' relative motion, and the average internal forces and moments generated by this deformation over the time step. The Internal Sub-Model determines reacting forces from side and bulkhead (vertical) structures using detailed mechanisms adapted from Rosenblatt [16,18] and discussed in detail within this section. It determines absorbed energy and forces from the crushing and tearing of decks, bottoms and stringers (horizontal structures) using the Minorsky correlation [9] as modified by Reardon and Sprung [15], Equation 4.3. Total forces are the sum of these two mechanisms. In SIMCOL Version 2.1, the striking ship bow is assumed to be wedge-shaped with upper and lower extents determined by the bow height of the striking ship and the relative drafts of the two ships. Deformation is only considered in the struck ship. The striking ship is assumed to be rigid.

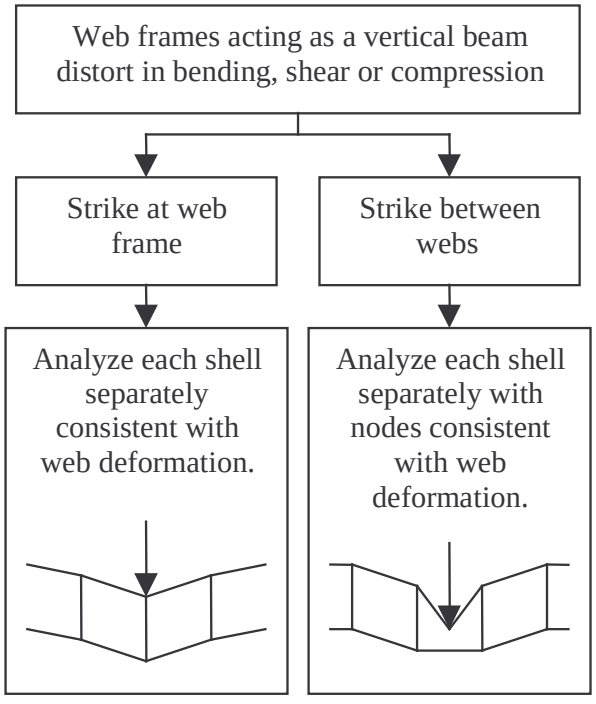

Figure 4-7 Web Deformation in SIMCOL

Penetration of the struck ship begins with the side shell plating and webs (vertical structures). Figure 4-7 illustrates the two basic types of strike determined by the strike location relative to the webs. The following assumptions are made consistent with Rosenblatt [18]:

- Plastic bending of shell plating is not considered - The contribution of plastic bending in the transverse deformation of longitudinally stiffened hull plates is negligible. The sample calculation sheets in Rosenblatt [18] support this argument. In six test cases, the energy absorbed in plastic bending never exceeds 0.55% of the total absorbed energy when the cargo boundary is ruptured. It is a good assumption that the plastic membrane tension phase starts from the beginning of collision penetration and is the primary shell energy-absorption mechanism.
- Rupture of stiffened hull plates starting in the stiffeners is not considered - As suggested in McDermott [16], this mechanism is unlikely for most structures except for flat-bar stiffened plates. It is a standard practice to use angles instead of flat bar for longitudinal stiffeners of side shell and longitudinal bulkheads, therefore, this option is not considered in SIMCOL.
- Web frames do not yield or buckle before plates load in membrane tension - McDermott demonstrates that this mechanism is unlikely and does not contribute significantly to absorbed energy in any case. This mechanism requires very weak web frames that would not be sufficient to satisfy normal sea and operational loads.

SIMCOL Version 1.1 assumes that flanking web frames are rigid. Version 2.0 and subsequent versions consider the transverse deformation of webs.

In a right-angle collision case, Equation 4.32 gives the total plastic energy absorbed in membrane tension in time step *n*. This assumes that the plate is not ruptured, that flanking webs do not deflect in the longitudinal direction, and that compression in the side shell caused by longitudinal bending of ship hull girder is small.

$$E_n = T_m \, e_{tn}$$
$$T_m = \sigma_m \, t \, B_e \qquad (4.32)$$

Where:

E_n plastic energy absorbed by side shell or longitudinal bulkhead (J);

T_m membrane tension (N);

σ_m yield stress of side shell or bulkhead adjusted for strain rate (Pa);

e_{tn} total elongation of shell or bulkhead structure within the web spacing;

t smeared thickness of side shell or bulkhead (m);

B_e effective breadth (height) of side shell or bulkhead (m);

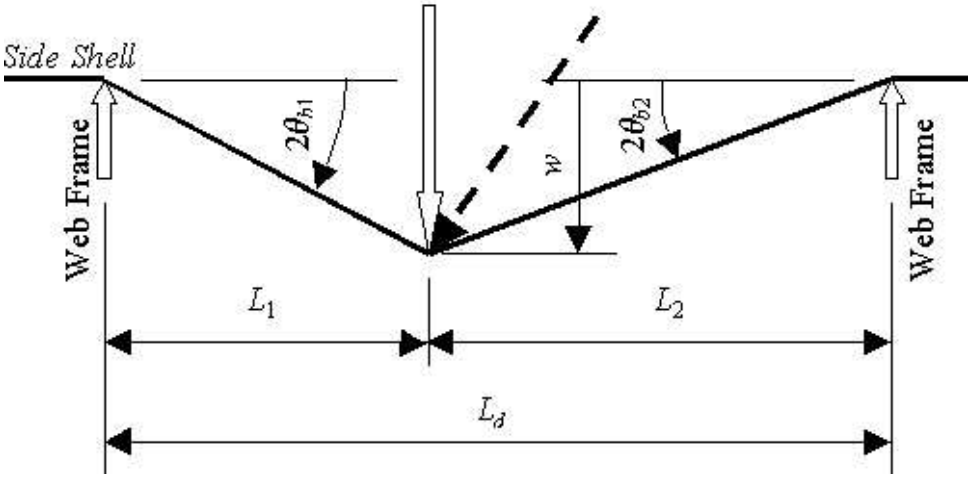

Figure 4-8 Membrane Geometry

Figure 4-8 illustrates the membrane geometry for calculation of elongation where e_1 and e_2 are the elongation of legs L_1 and L_2 respectively:

$$e_i = \sqrt{L_i^2 + w^2} - L_i \cong \frac{w^2}{2L_i}$$
$$e_t = e_1 + e_2 = \frac{L_d}{2L_1L_2} w^2 \qquad (4.33)$$

Where:

L_d damage length, or distance between adjacent webs (m)

w_n deflection of side shell or bulkhead at time step n (m)

Side shell rupture due to membrane tension is determined using the following criteria:

- The strain in the side shell reaches the rupture strain, ε_r, which is taken as 10% in ABS steel;
- The bending angle at a support reaches the critical value as defined in Equation 4.34 [18]:

$$\varepsilon_m = \frac{4}{3}\frac{\sigma_m}{\sigma_u - \sigma_m \cos\theta_c}\sin\theta_c \tan\theta_c = 1.5D \tag{4.34}$$

Where:

ε_m maximum bending and membrane-tension strain at hull rupture;

σ_m in-plate stress under membrane-tension (MPa);

σ_u ultimate stress of the plate (MPa);

θ_c critical bending angle; and

D tension test ductility in a 2-in gage length, 32% for ABS steel.

The criteria for rupture is then:

$$\varepsilon_i = \frac{e_i}{L_i} \le \varepsilon_r$$
$$\theta_{bi} = \frac{1}{2}\arctan\frac{w}{L_i} \cong \frac{w}{2L_i} \le \theta_c \tag{4.35}$$

where:

ε_i strain in leg i; and

θ_{bi} bending angle at flanking web frames of leg i.

Since the striking bow normally has a generous radius, the bending angle at the impact location is not considered in the rupture criteria. From these equations, it can be seen that only the strain and bending angle in the shorter leg need be considered for right angle collisions. Based on material properties of ABS steel, the critical bending angle θ_c from Equation 4.35 is 19.896, 17.318 or

16.812 degrees for ABS grade B (mild steel), AH32 or AH36 grades respectively. Once either of the rupture criteria is reached, the side shell or longitudinal bulkhead is considered ruptured and does not continue to contribute to the reacting force.

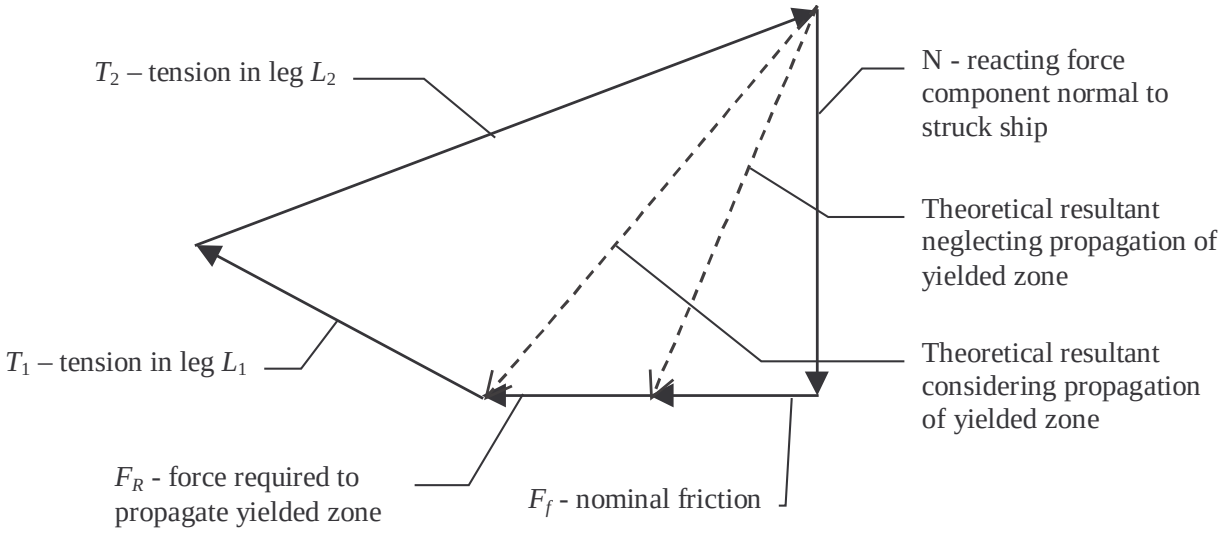

Figure 4-9 Force Diagram for an Oblique Angle Collision

For collisions at an oblique angle, the membrane tension is only fully developed in the leg behind the strike, L_2 in Figure 4-8. This is demonstrated in the force diagram shown in Figure 4-9, where T_1 is much smaller than T_2. It is also assumed that all the plastic strain developed from membrane tension is behind the striking point.

The first rupture criterion in Equation 4.35 becomes:

$$\varepsilon_b = \frac{e_t}{L_b} \leq \varepsilon_r \qquad (4.36)$$

Where ε_b and L_b represent the strain and length of the leg behind the strike.

In SIMCOL Version 2.0 and later, transverse deformation of web frames is also considered. Web failure modes include bending, shear, and compression. Web frames are allowed transverse deformation while keeping their longitudinal locations. The resisting force is assumed constant

(plastic) at a distorted flanking web frame, and the transverse deformation of the web frame is assumed uniform from top to bottom. The magnitude of this force is its maximum elastic capacity. From Figure 4-8, the applied force on a rigid flanking web frame is:

$$P_i = T_i \frac{w}{L_i} \tag{4.37}$$

Where P_i and T_i are referred to the particular leg L_i. If the applied force, P_i, is greater than the maximum elastic capacity of the flanking web, P_{wf}, the particular web frame is deformed as in Figure 4-10. The change of angle, γ_c, at the distorted web is:

$$\gamma_{ci} \cong \frac{P_{wf}}{T_i} \tag{4.38}$$

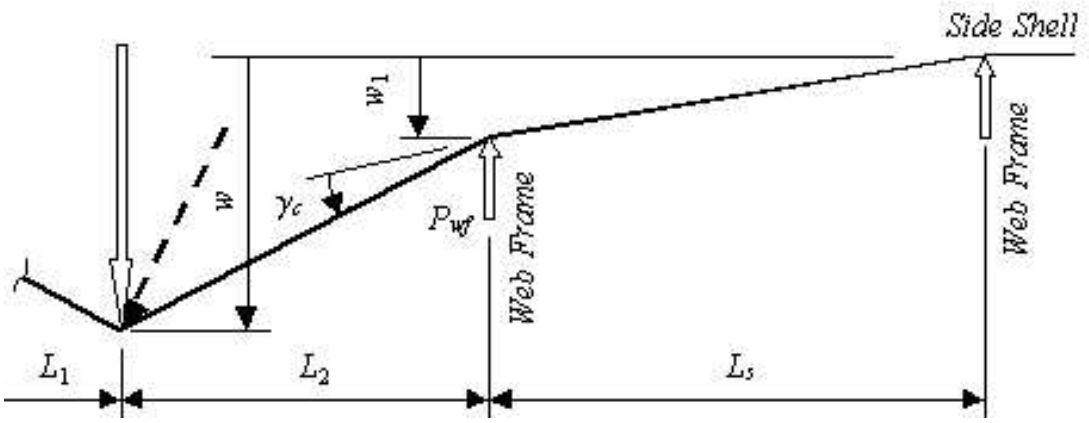

Figure 4-10 Deflection and Forces in Distorted Web Frames

Rosenblatt [18] proposes an approach to determine whether *Pi* exceeds the capacity P_{wf}, and to estimate the value of P_{wf}. First, the allowable bending moment and shear force of the web frame at each support, the crushing load of the web, and the buckling force of supporting struts are calculated. Then, the load, P_i, is applied to the web frame, and the induced moments, shear forces and compression of the web frame and struts are calculated, considering the web frame as a beam with clamped ends. The ratios of the induced loads to the allowable loads are determined using

Equation 4.39. If the maximum ratio, R_m, is greater than unity, the load, P, exceeds the capacity, and the web frame deforms.

$$R_m = \frac{P}{P_{wf}} \tag{4.39}$$

The deflection at the outermost distorted web frame is:

$$w_n = \frac{L_s}{L_i + nL_s}\{w - \gamma_{c2}[nL_i + \frac{1}{2}(n-1)nL_s]\} \tag{4.40}$$

Where:

n total number of deformed web frames on the Li side; and

L_s web frame spacing (m).

The deflection at other deformed web frames is:

$$w_j = (n - j + 1)w_n + \frac{1}{2}(n - j)(n - j + 1)\gamma_{c2}L_s \tag{4.41}$$

Where j is the number of web frames counted from the striking point. The elongation in adjacent webs is:

$$e_j = \sqrt{(w_j - w_{j+1})^2 + L_s^2} - L_s \tag{4.42}$$

And the elongation in the struck web is:

$$e_{0i} = \sqrt{(w - w_1)^2 + L_i^2} - L_i \tag{4.43}$$

With these elongation and deformation results, the same rupture criteria given in equations 4.42 and 4.43 are applied to all deformed webs. The total elongation on the L_i side is:

$$e_{ti} = e_{0i} + \sum_{j=1}^{n} e_{ji} \tag{4.44}$$

And the energy absorbed in membrane tension and web deformation is:

$$E_i = T_i e_{ti} + P_{wf} \sum_{j=1}^{n} w_{ji} \tag{4.45}$$

For right angle collisions, T_i always equals T_m as calculated in Equation 4.32. In oblique angle collisions, T_i equals T_m if L_i is on the side behind the strike. Based on experimental data, Rosenblatt [18] suggests using ½ T_m ahead of the strike and this is used in SIMCOL 2.1.

For double hull ships, if the web frames are distorted because of bending, shearing and buckling of supporting struts, the deformed web frames push the inner skin into membrane tension as shown in Figure 4-7, and the right angle collision mechanism is applied to the inner hull. Inner skin integrity is checked using Equations 4.35 and 4.36, and the energy absorbed in inner skin membrane tension is calculated using Equation 4.32.

In the simulation, the energy absorbed in membrane tension and web deformation during a time step is:

$$\Delta KE_n = (E_{1,n+1} + E_{2,n+1}) - (E_{1n} + E_{2,n}) \tag{4.46}$$

Considering the friction force, F_f, in Figure 4-9, and assuming the dynamic coefficient of friction has a constant value of 0.15, the reacting forces and moments are calculated:

$$\begin{aligned}
\Delta KE_n &= N_n(w_{n+1}-w_n)+F_{fn}\left|l_{n+1}-l_n\right| = N_n\left[(w_{n+1}-w_n)+0.15\left|l_{n+1}-l_n\right|\right] \\
F_{\eta n} &= N_n = \frac{(E_{1,n+1}+E_{2,n+1})-(E_{1n}+E_{2,n})}{(w_{n+1}-w_n)+0.15\left|l_{n+1}-l_n\right|} \\
F_{\xi n} &= F_f\frac{(l_{n+1}-l_n)}{\left|l_{n+1}-l_n\right|} = 0.15F_{\eta n}\frac{(l_{n+1}-l_n)}{\left|l_{n+1}-l_n\right|} \\
M_n &= -F_{\xi n}d_n + F_{\eta n}l_n
\end{aligned} \tag{4.47}$$

Where:

$N_n = F_{\eta n}$ Force on struck ship normal (transverse) to centerline (N)

$F_{\xi n}$ Force on struck ship parallel (longitudinal) to centerline (N)

M_n Yaw moment on struck ship (N m)

d_n Distance of longitudinal line of force from centerline (m)

l_n Distance of transverse line of force from midship (m)

In addition to the friction force, another longitudinal force, F_R, the force to propagate the yielding zone, is considered, as shown in Figure 4-9. McDermott provides an expression for this force [16]:

$$F_R = \frac{\sigma_y d'}{R}\left[d't_w\left(1-\frac{\sigma_y R}{d'E}\right)^2 + t_f(b-t_w)\left(\frac{d'-0.5t_f}{d'}-\frac{\sigma_y R}{d'E}\right)\right] \tag{4.48}$$

Where:

d' depth of side shell longitudinal stiffeners;

R radius of the striking bow;

t_w thickness of side shell stiffener webs;

t_f thickness of side shell stiffener flanges;

b width of side shell stiffener flanges; and

E modulus of elasticity.

Or when simplified:

$$
\begin{aligned}
c_F &= \frac{F_R}{\sigma_y A_{stiff}} \\
c_A &= \frac{A_{stiff}}{A_{total}} \\
F_R &= c_F c_A \sigma_y t B
\end{aligned}
\tag{4.49}
$$

Where:

c_F force coefficient;

c_A ratio of sectional areas;

A_{stiff} sectional area of stiffeners; and

A_{total} total sectional area of stiffeners and their attached plate.

The full implementation of this equation requires structural details that are not appropriate for a simplified analysis. In this study, based on a sampling of typical side shell scantlings, a simplified calculation is used where $c_F c_A$ is assumed to have a constant value of 0.025.

Since F_R also affects membrane tension energy, Equation 4.47 become:

$$
\begin{aligned}
\Delta KE_n &= F_{\eta n}\left[(w_{n+1} - w_n) + 0.15\left|l_{n+1} - l_n\right|\right] + F_R(l_{n+1} - l_n) \\
F_{\eta n} &= \frac{(E_{1,n+1} + E_{2,n+1}) - (E_{1n} + E_{2,n}) - F_R(l_{n+1} - l_n)}{(w_{n+1} - w_n) + 0.15\left|l_{n+1} - l_n\right|} \\
F_{\xi n} &= (F_R + 0.15F_{\eta n})\frac{(l_{n+1} - l_n)}{\left|l_{n+1} - l_n\right|} \\
M_n &= -F_{\xi n} d_n + F_{\eta n} l_n
\end{aligned}
\tag{4.50}
$$

The Internal Sub-Model determines absorbed energy and forces from the crushing and tearing of decks, bottoms and stringers (horizontal structures) in a much more simplified manner using the Minorsky correlation [9] as modified by Reardon and Sprung [15] provided by Equation 4.3.

Step 2, of Figure 4-5, in the SIMCOL collision simulation process calculates damaged area and volume in the struck ship given the relative motion of the two ships calculated in Step 1 by the External Sub-Model. Figure 4-11 illustrates the geometry of the sweeping segment method used for this calculation in SIMCOL Version 2.1.

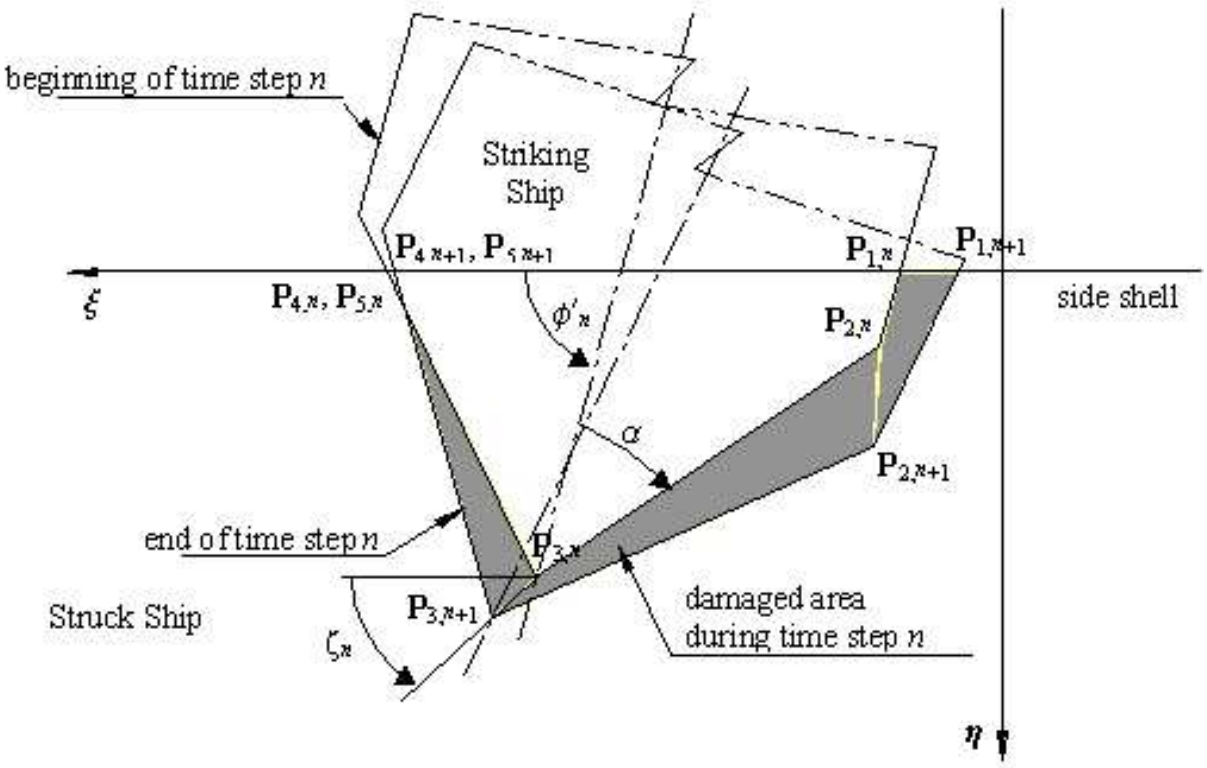

Figure 4-11 Sweeping Segment Method

The intrusion portion of the bow is described with five nodes, as shown in Figure 4-11. The shaded area in Figure 4-11 is the new damaged area of decks and/or bottoms during the time step. Coordinates of the five nodes in the ξ-η system at each time step are derived from the penetration and location of the impact, the collision angle, ϕ, and the half entrance angle, α, of the striking bow.

$\mathbf{P}_3$ is specified by the penetration and location of the striking ship relative to the struck ship:

$$\begin{aligned}&\mathbf{P}_3 = \{\xi_3, \eta_3\} = \{l, d\}\\ &\phi' = \pi - \phi\end{aligned} \tag{4.51}$$

If the parallel body of the striking ship has not penetrated into the struck ship then:

$$\begin{aligned}&\overline{\mathbf{P}_2\mathbf{P}_3} \le \frac{B_2}{2\sin\alpha} \text{ or } \overline{\mathbf{P}_3\mathbf{P}_4} \le \frac{B_2}{2\sin\alpha}, \text{ and}\\ &\mathbf{P}_2 = \{\xi_2, \eta_2\} = \left\{\xi_3 - \frac{\eta_3}{\tan(-\alpha+\phi')}, 0\right\}\\ &\mathbf{P}_1 = \{\xi_1, \eta_1\} = \mathbf{P}_2\\ &\mathbf{P}_4 = \{\xi_4, \eta_4\} = \left\{\xi_3 - \frac{\eta_3}{\tan(\alpha+\phi')}, 0\right\}\\ &\mathbf{P}_5 = \{\xi_5, \eta_5\} = \mathbf{P}_4\end{aligned} \tag{4.52}$$

If the parallel body of the striking ship has penetrated into the struck ship then:

$$\begin{aligned}&\overline{\mathbf{P}_2\mathbf{P}_3} > \frac{B_2}{2\sin\alpha} \text{ or } \overline{\mathbf{P}_3\mathbf{P}_4} > \frac{B_2}{2\sin\alpha}, \text{ and}\\ &\mathbf{P}_2 = \{\xi_2, \eta_2\} = \left\{\xi_3 - \frac{B_2}{2\sin\alpha}\cos(-\alpha+\phi'), \eta_3 - \frac{B_2}{2\sin\alpha}\sin(-\alpha+\phi')\right\}\\ &\mathbf{P}_1 = \{\xi_1, \eta_1\} = \left\{\xi_2 - \frac{\eta_2}{\tan\phi'}, 0\right\}\\ &\mathbf{P}_4 = \{\xi_4, \eta_4\} = \left\{\xi_3 - \frac{B_2}{2\sin\alpha}\cos(\alpha+\phi'), \eta_3 - \frac{B_2}{2\sin\alpha}\sin(\alpha+\phi')\right\}\\ &\mathbf{P}_5 = \{\xi_5, \eta_5\} = \left\{\xi_4 - \frac{\eta_4}{\tan\phi'}, 0\right\}\end{aligned} \tag{4.53}$$

Where:

$\mathbf{P}_i$ node of penetrated bow;

ξ_i, η_i coordinates of node in ξ-η system (m); and

B_2 breadth of the striking ship (m).

Once the node coordinates before and after the time step are calculated, the segment of the bow plan that has caused further damage during the time step and the area swept by a specific segment are determined. In the case of the segment $\mathbf{P}_1\mathbf{P}_2$ in Figure 4-11, the out-sweeping area, A_1, during time step n is calculated as follows:

$$A_{1,n} = \frac{1}{2}\left(\begin{vmatrix} \xi_{2,n} & \xi_{1,n} \\ \eta_{2,n} & \eta_{1,n} \end{vmatrix} + \begin{vmatrix} \xi_{2,n+1} & \xi_{2,n} \\ \eta_{2,n+1} & \eta_{2,n} \end{vmatrix} + \begin{vmatrix} \xi_{1,n+1} & \xi_{2,n+1} \\ \eta_{1,n+1} & \eta_{2,n+1} \end{vmatrix} + \begin{vmatrix} \xi_{1,n} & \xi_{1,n+1} \\ \eta_{1,n} & \eta_{1,n+1} \end{vmatrix} \right) \quad (4.54)$$

The damaged plating thickness t is the sum thickness of deck, stringer and/or bottom structures that are within the upper and lower extents of the striking bow. Given the damaged material volume (area times thickness), the Minorsky force is calculated based on the following assumptions:

- The resistant force acting on each out-sweeping segment is in the opposite direction of the average movement of the segment. The force exerted on the struck ship is in the direction of this average movement.
- The work of the resistant force is done over the distance of this average movement.
- The total force on each segment acts through the geometric center of the sweeping area.

Using the Minorsky relation as modified by Reardon and Sprung, the energy absorbed by the sweeping segment $\mathbf{P}_1\mathbf{P}_2$ is then:

$$\Delta KE_{1,n} = 47.1\times10^6 R_{T1,n} = 47.1\times10^6 A_{1,n}\ t \quad (4.55)$$

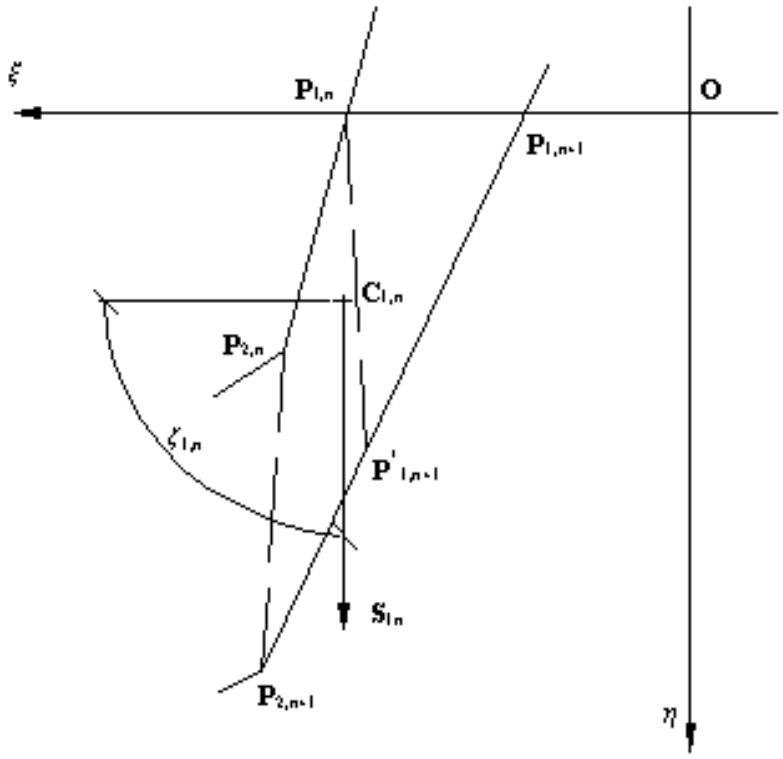

Figure 4-12 Sweeping Segment Geometry

The average motion, $\mathbf{S}_1$, and the geometric center of the sweeping area, $\mathbf{C}_1$, for the segment $\mathbf{P}_1\mathbf{P}_2$ in time step *n* are approximated as follows (Figure 4-11 and Figure 4-12):

Select $\mathbf{P}^*_{1,n+1}$ on $\mathbf{P}_{1,n}$+1$\mathbf{P}_{2,n+1}$, so that $\overline{\mathbf{P}^*_{1,n+1}\mathbf{P}_{2,n+1}} = \overline{\mathbf{P}_{1,n}\mathbf{P}_{2,n}}$

$$\mathbf{S}_{1,n} = \frac{1}{2}(\overrightarrow{\mathbf{P}_{2,n}\mathbf{P}_{2,n+1}} + \overrightarrow{\mathbf{P}_{1,n}\mathbf{P}^*_{1,n+1}})$$

$$= \frac{1}{2}[\mathbf{P}_{2,n+1} - \mathbf{P}_{2,n} + (\mathbf{P}_{2,n+1} - \mathbf{P}_{1,n+1})\frac{\overline{\mathbf{P}_{1,n}\mathbf{P}_{2,n}}}{\overline{\mathbf{P}_{1,n+1}\mathbf{P}_{2,n+1}}} - \mathbf{P}_{1,n}] \qquad (4.56)$$

$$\mathbf{C}_{1,n} = \frac{1}{4}(\mathbf{P}_{1,n} + \mathbf{P}_{2,n} + \mathbf{P}_{1,n+1} + \mathbf{P}_{2,n+1})$$

The force exerted through the segment $\mathbf{P}_1\mathbf{P}_2$ on the struck ship, $\mathbf{F}_{1,n}$, and the moment to the origin of the local coordinate system, $M_{1,n}$, are then:

$$F_{1,n} = \left|\mathbf{F}_{1,n}\right| = \frac{\Delta KE_{1,n}}{s_{1,n}}$$
$$\mathbf{F}_{1,n} = \begin{pmatrix} F_{\xi 1,n} \\ F_{\eta 1,n} \end{pmatrix} = \begin{pmatrix} F_{1,n}\cos\zeta_{1,n} \\ F_{1,n}\sin\zeta_{1,n} \end{pmatrix} \qquad (4.57)$$
$$M_{1,n} = \overrightarrow{\mathbf{OC}_{1,n}} \times \mathbf{F}_{1,n}$$

Where $s_{1,n} = \left|\mathbf{S}_{1,n}\right|$ and $\zeta_{1,n}$ is the direction of $\mathbf{S}_{1,n}$.

Forces and moments acting on other segments are calculated similarly. The total exerted force, $\mathbf{F}_n$, is the sum of the forces and moments on each segment:

$$\mathbf{F}_n = \sum_{i=1}^{4} \left\{ F_{\xi i,n}, F_{\eta i,n}, M_{i,n} \right\} \qquad (4.58)$$

These forces are added to the side shell, bulkhead and web forces.

Internal forces and moments are calculated for the struck ship in the local coordinate system, i.e. the ξ-η system, and converted to the global system. The forces and moments on the striking ship have the same magnitude and the opposite direction from those on the struck ship.

The damage length, L_D, is:

$$L_D = \max(\xi_{i,j}) - \min(\xi_{i,j}) \qquad i = 1, \mathrm{K}\ , 5 \qquad j = 1, \mathrm{K}\ , m \qquad (4.59)$$

Where m is the time step and the penetration is given by:

$$P_D = \max(\eta_{i,j}) \quad i = 1, \ldots, 5 \quad j = 1, \ldots, m \qquad (4.60)$$

Table 4-1 provides a summary of the modeling method used in SIMCOL version 2.1 for each energy absorbing structure discussed in Section 2.4.

Table 4-1 Energy Absorbing Structure Method Summary for SIMCOL

Energy Absorbing Structure	*Modelling Method*
Sideshell	Adapted Rosenblatt Method
Decks	Reardon and Sprung Energy Correlation with Sweeping Segment Method
Stringers	Reardon and Sprung Energy Correlation with Sweeping Segment Method
Longitudinal Bulkheads	Adapted Rosenblatt Method
Transverse Bulkheads	Treated as Rigid
Longitudinal Girders	Reardon and Sprung Energy Correlation
Transverse Girders	Reardon and Sprung Energy Correlation
Webs	Adapted Rosenblatt Method

4.5.2.3 SIMCOL Probabilistic Damage Assessment

SIMCOL calculates probabilistic structural damage using a Monte Carlo simulation [35] with a probabilistic description of the accident scenarios as the primary input. This method uses a simplified collision scenario and striking ship input consistent with available collision scenario and world fleet data. The striking ship is described using a simplified wedge bow geometry [83] shown in Figure 4-11. SIMCOL also calculates a mean value of penetration, longitudinal extent of damage and oil outflow (discussed in Section 4.5.2.4).

4.5.2.4 SIMCOL Simplified Probabilistic Oil Outflow Calculation

Current hypothetical outflow and tank size requirements for oil tankers are found in Regulations 22-24 of Annex I of MARPOL 73/78. Recognizing that these regulations do not actually assess the environmental performance of tankers, IMO instructed its BLG (Bulk Liquids and Gases) Sub-Committee to develop a new accidental oil outflow regulation modeled after the probabilistic methodology contained in the IMO Guidelines [4]. This new regulation will still not consider the crashworthiness of the structural design. One of the primary objectives of the SIMCOL project is to provide a methodology and model that does consider crashworthiness for potential application in future IMO regulations. The IMO Guidelines provide a probabilistic-based procedure for assessing the oil outflow performance of an alternative tanker design. The alternative design is compared to selected reference double hull design based on a pollution prevention index.

The IMO Guidelines present two procedures for evaluating the oil outflow. The “conceptual” method, applicable for conceptual design approval, assumes the ship survives the damage. For

bottom damage, the ship is assumed to rest on the ground at its initial intact drafts, with zero trim and heel. The "survivability" method, applicable to final designs, requires damage stability calculations. For damage cases that fail to satisfy the specified survivability criterion, it is assumed that the ship is lost and 100% of all cargo oil onboard outflows to the sea.

A fully probabilistic evaluation of a specific vessel on a specific route would require development of the following probabilities:

- The probability that the ship will have a grounding or collision accident
- The conditional probability density function for damage location and extent;
- The expected consequences (i.e. quantity of outflow).

The IMO Guidelines do not specifically deal with the probability of whether the ship will have an accident. Rather, it is acknowledged that the risk exists, and it is assumed that the vessel is involved in a grounding or collision event significant enough to breach the outer hull. This is because data for accidents where the outer hull is not breached is rarely recorded. The resulting oil outflow is therefore conditional on an accident significant enough to breach the outer hull. The SIMCOL methodology is conditional only on a collision accident occurring. SIMCOL considers accidents that do not breach the outer hull. This better reflects the true crashworthiness of a structural design.

Rigorous application of the probabilistic oil outflow methodology contained in the IMO Guidelines is a calculation intensive effort based on an empirical description of damage extent and location. SIMCOL follows the basic steps of the IMO methodology, but assembles the damage cases using a Monte Carlo simulation with a probabilistic description of the accident scenarios as the primary input. The following steps are followed in the SIMCOL process:

Step 1: Assemble Damage Cases

For each collision case in the Monte Carlo simulation, SIMCOL calculates damage extent. Once collision damage calculations are completed, SIMCOL determines which cargo tanks have been

penetrated and ruptured by comparing damage extents to cargo tank subdivision boundaries specified in the SIMCOL input. In addition to depth and length of penetration, SIMCOL also flags when a tank boundary is ruptured. It is assumed in side damage that if a tank is penetrated and ruptured, its entire contents are spilled. The volume of oil in each tank is specified in the SIMCOL input. For a specified collision case, SIMCOL sums the outflow from all ruptured tanks to determine the total outflow for the case.

Step 2: Calculate Oil Outflow

Consistent with the IMO analysis approach, 100% outflow for all cargo tanks sustaining side damage is assumed.

Step 3: Calculate Oil Outflow Parameters

- The *probability of zero outflow*, P_0, represents the likelihood that no oil will be released into the environment, given a collision or grounding accident. P_0 equals the cumulative probability of all damage cases without outflow.
- The *mean outflow parameter*, O_M, is the non-dimensionalized mean or expected outflow, and provides an indication of a design's overall effectiveness in limiting oil outflow. The mean outflow equals the sum of the products of each damage case probability and the associated outflow. O_M equals the mean outflow divided by the total quantity of oil onboard the vessel.
- The extreme *outflow parameter*, O_E, is the non-dimensionalized extreme outflow, and provides an indication of the expected oil outflow from particularly severe casualties. The extreme outflow is the weighted average of the upper 10% of all casualties (i.e. all damage cases within the cumulative probability range from 0.9 to 1.0).

Step 4: Compute the Pollution Prevention Index

The Pollution Prevention Index is calculated as in the IMO Guidelines.

Alternative designs are compared to reference double hull designs by substituting the outflow parameters for the reference design and the alternative design into the following formula:

$$E = \frac{(0.5)(P_O)}{P_{OR}} + \frac{(0.4)(0.01 + O_{MR})}{0.01 + O_M} + \frac{(0.1)(0.025 + O_{ER})}{0.025 + O_E} \qquad (4.61)$$

P_0, O_M, and O_E are the oil outflow parameters for the alternative design, and P_{0R}, O_{MR}, and O_{ER} are the oil outflow parameters for the IMO reference ship of equivalent size.

4.6 Summary of Simplified Methods

Table 4-2 provides a summary of the applicability of each simplified method discussed in Chapter 4 with respect to the desired criteria set forth in Section 4.2.

Table 4-2 Simplified Method Summary

	Method	*Energy Coefficient*	*Ahmdahl (cruciform)*	*Pedersen Empiracle*	*DAMAGE*	*DTU*	*SIMCOL version 2.1*
Post Collision Momentum		No	No	No	No	Yes	Yes
Struck Ship Forward Velocity		No	No	No	No	Yes	Yes
Oblque Angle Collisions		No	No	No	No	Yes	Yes
Deformable Bow		No	Yes	Yes	No	Yes	No
Longitudinal Extent of Damage		No	No	No	No	Limited	Limited
Low Computational Cost		Yes	No	Yes	Yes	Yes	Yes
Coupled Internal Mechanics and External Dynamics		No	No	No	No	No	Yes
8 Critical Energy Absorbing Structures	Sideshell	Yes	Yes	Yes	Yes	Yes	Yes
	Longitudinal Bulkheads	Yes	Yes	Yes	Yes	Yes	Yes
	Structural Decks	Yes	Yes	Yes	Yes	Yes	Yes
	Stringers	Yes	Yes	Yes	Yes	Yes	Yes
	Web Frames	Yes	No	No	Yes	Yes	Yes
	Transverse Bulkheads	Yes	No	No	No	No	No
	Longitudinal Girders	Yes	Yes	Yes	Yes	Yes	Yes
	Transverse Girders	Yes	No	No	Yes	Yes	Yes

As Table 4-2 shows, the two most promising simplified analysis methods for ship-to-ship collisions are the DTU model discussed in Section 4.5.1 and SIMCOL version 2.1 discussed in Section 4.5.2. The DTU model is based upon a super element formulation that has the advantages of the cruciform approximations and experiments performed by Amdahl [23] and Wierzbicki [20]. However, the internal mechanics and the external dynamics of the analysis are uncoupled and the formulation of the structural input does not allow for an easy manipulation of the method for use within optimization or response surface generation, as does SIMCOL.

SIMCOL, as it is in version 2.1, is limited in its application necessitating several updates and corrections in order to achieve the desired level of performance as set out in Section 4.2 or as required to fulfill the objectives of the IMO as discussed in Chapter 1. These improvements include a complete method of determining the longitudinal extent of damage through bulkheads and transverse structure and a method for evaluating a deformable bow. Chapter 5 discusses these improvements and inclusions within SIMCOL while creating SIMCOL version 3.0.

5 SIMCOL Version 3.0

SIMCOL Version 3.0 has four minor and one major improvement over version 2.1. The minor improvements are as follows and are discussed thoroughly in Sections 5.1 through 5.4. The minor improvements are:

- Modification of the energy coefficient method used for the treatment of structural decks and stringers.
- Treatment of longitudinal crushing of longitudinal bulkheads through the use of an energy coefficient method
- Treatment of transverse crushing of transverse bulkheads through the use of an energy coefficient method
- Inclusion of a deformable wedge bow model through the use of Pedersen's empirical bow crushing model

The major improvement to SIMCOL is the inclusion of a method for the determination of the energy absorbed through the non-uniform longitudinal deflection of transverse bulkheads and webs, which is a necessity whenever the longitudinal extent of damage is to be accurately determined. The method of determining of the energy absorbed through the non-uniform longitudinal deflection of transverse bulkheads and webs is discussed in Section 5.4.

Again, from Section 2.4, the majority of the energy absorbed by damage to structure within a ship-to-ship collision is absorbed by the following eight structural members; side shell, longitudinal bulkheads, decks, stringers, web frames, transverse bulkheads, longitudinal girders and transverse girders. Section 5.1 discusses methods of energy absorption by the decks and stringers and Sections 5.2 and 5.4 discuss methods of energy absorption by the side shell, longitudinal bulkheads, web frames and transverse bulkheads. The energy absorbed by longitudinal and transverse girders is calculated and determined through the methods of SIMCOL 2.1 (Section 4.5.2).

5.1 Energy Coefficient Method for use with Structural Decks ad Stringers

SIMCOL version 2.1 makes use of the Reardon and Sprung [15] energy coefficient as described in Section 4.3 by Equation 4.3. However, the Reardon and Sprung energy coefficient formulation was developed for a T-bone collision with a statistical damage volume method of determining energy absorption. With this method, the mode of damage (i.e. crushing and folding or cutting and tearing) is not important. Thus the energy coefficient of Reardon and Sprung (Equation 4.3) is not sensitive to specific structure or the damage modes of the structure such as crushing shown in Figure 5-1 and combined modes of crushing, folding and tearing as seen to occur with decks and stringers in actual or finite element simulations of collisions (Figure 5-2 through Figure 5-5).

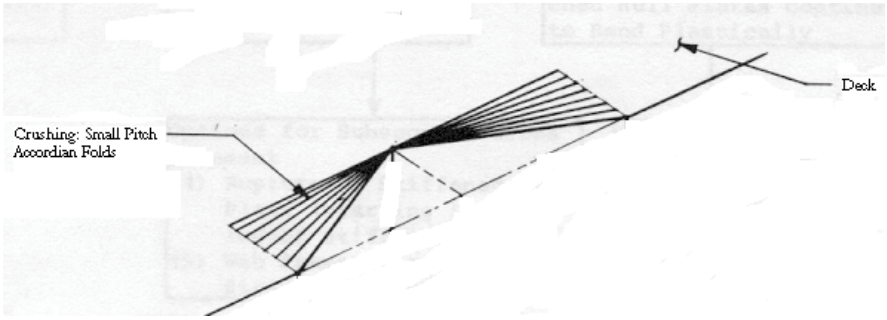

Figure 5-1 Deck Crushing Showing Accordion Folding [21]

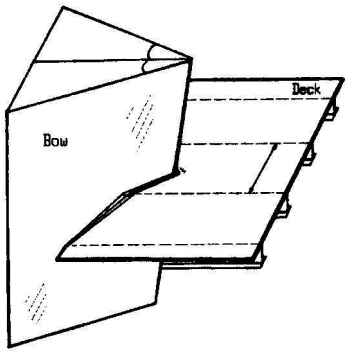

Figure 5-2 Deck Crushing Showing Bow Impingement [21]

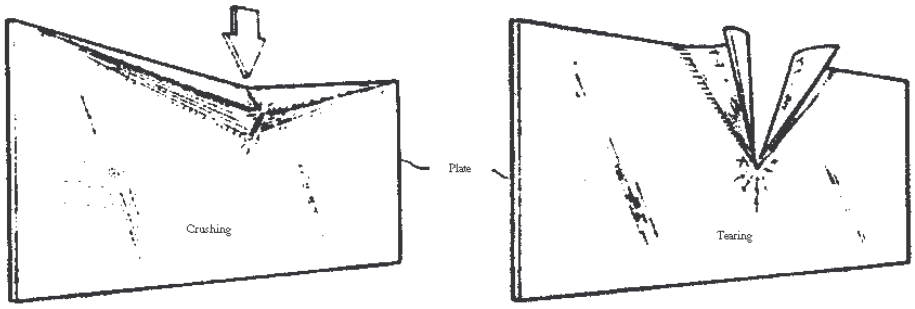

Figure 5-3 Plate Crushing vs. Tearing (Cutting) [21]

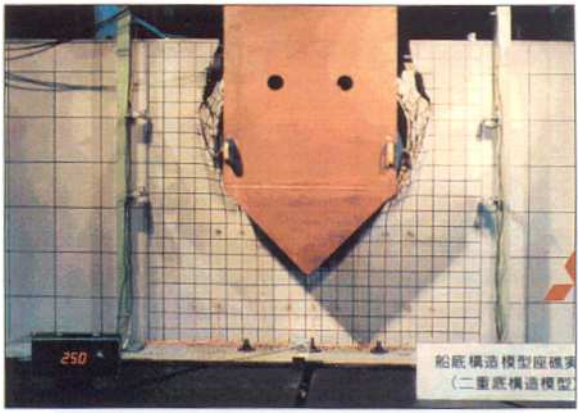

Figure 5-4 Rigid Wedge Cutting and Crushing Deck in Drop Test [89]

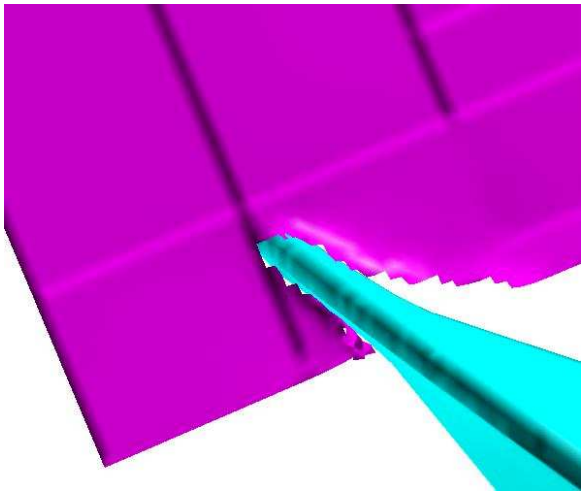

Figure 5-5 FEA Deck Cutting and Crushing

Consequently, an investigation of the energy coefficient methods of Reardon and Sprung and Paik and Pedersen [29], Equations 4.9 and 4.10, is performed to determine which method most accurately captures the energy absorption of decks and stringers when involved in collision. Paik and Pedersen's methods separate the differing types of structure (decks, bulkheads etc.) and modes of damage (crushing, tearing, etc.) and thus may be more applicable for the determination of energy absorption by varying structural designs.

The theory for crushing, folding or tearing of deck structure used within SIMCOL with the methods of Reardon and Sprung and Paik and Pedersen is compared to finite element results of a rigid wedge striking the top deck structure of a 150k dwt double hull oil tanker, where the deck, the supporting transverse deck frames, and longitudinal girders are included as shown in Figure 5-6. The rigid wedge has a mass of 1.0E+06 kg and is given a forward velocity of 5 m/s. The deck structure is described in Table 5-1.

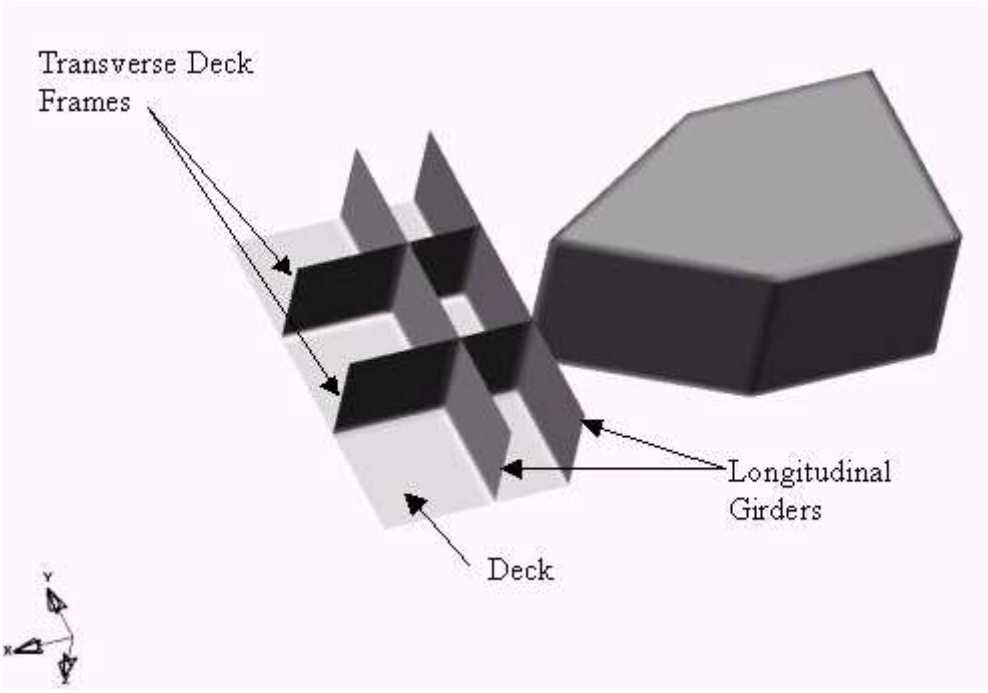

Figure 5-6 FEA Simplified Deck Crushing and Cutting Test Model

Table 5-1 FEA Simplified Deck Crushing and Cutting Test Parameters

Deck Length	9.9 m
Deck Width	5.0 m
Deck Thknss (stiffeners smeared)	31.4 mm
Tr. Deck Frame Depth	3.0 m
Tr. Deck Frame Thknss (flange smeared)	15.0 mm
Outer Long. Girder Depth	3.0 m
Outer Long. Girder Thknss (stiffeners smeared)	23.3 mm
Inner Long. Girder Depth	3.0 m
Inner Long. Girder Thknss (stiffeners smeared)	23.0 mm
Tr. Deck Frame Spacing	3.3 m
Long. Girder Spacing	2.0 m

The forward and aft most edges of the deck structure are simply supported (free only to rotate) while the edge opposite of the impacted edge is clamped (no translation and no rotation). The finite element model is comprised of Belytschko-Tsay shell elements with a uniform mesh size of 250 mm. The material of the deck structure is modeled with a Piecewise Linear Plasticity model for steel representing ABS Gr. B with parameters given in Table 3-4. Analysis with the Finite Element model is performed by substituting nodal constraints on the deck in the z translation and the rotation about the y axis at the intersection for the transverse webs. Additionally, the longitudinal girders are replaced with nodal constraints on the deck in the z translation and rotation about the x axis along the intersection. Replacing the physical structure of the transverse deck frames and longitudinal girders with nodal constraints allows an independent determination of the energy absorbed through the deck plate alone to be evaluated. Thus, the nodal constraints avoid double counting the deformation energy of the webs and longitudinal supports. Friction is assessed through the use of coulomb friction, Equation 3.7 and is representative of mild steel on steel.

The finite element model is run three times, where each iteration consists of a different rigid wedge half entrance angle (HEA) specifically HEA = 30, 45 and 60 degrees. Representative deformation of the deck structure is shown in Figure 5-7 through Figure 5-11 for the analysis with HEA = 30 degrees.

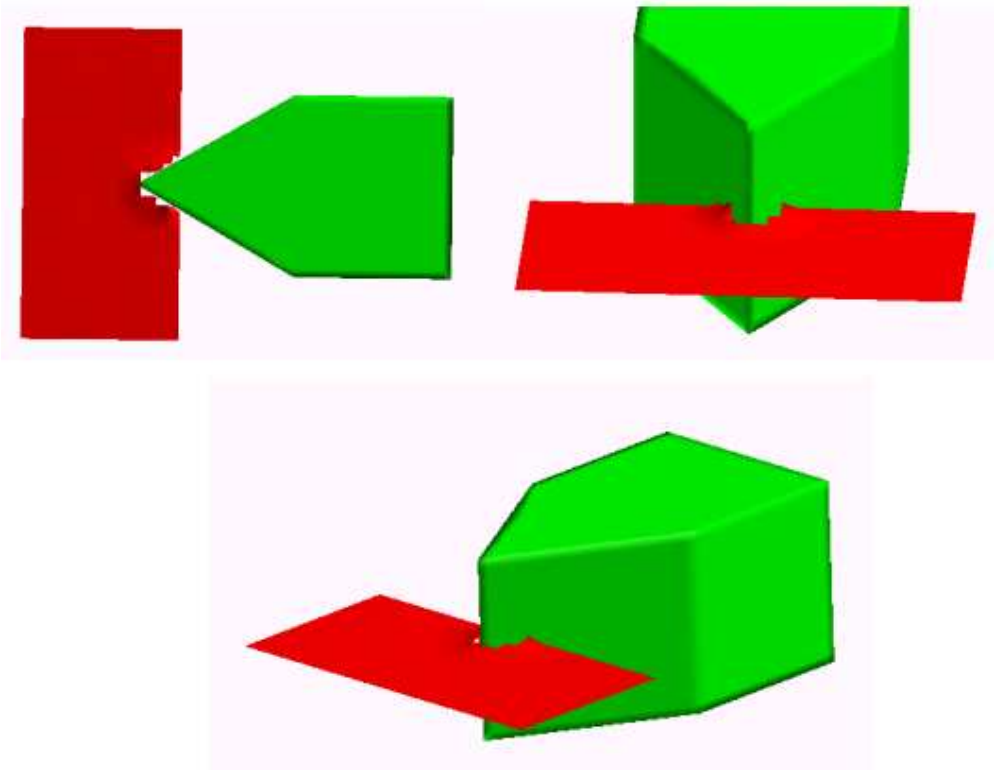

Figure 5-7 FEA Deck Crushing and Tearing with HEA = 30 Degrees at 0.5 Seconds

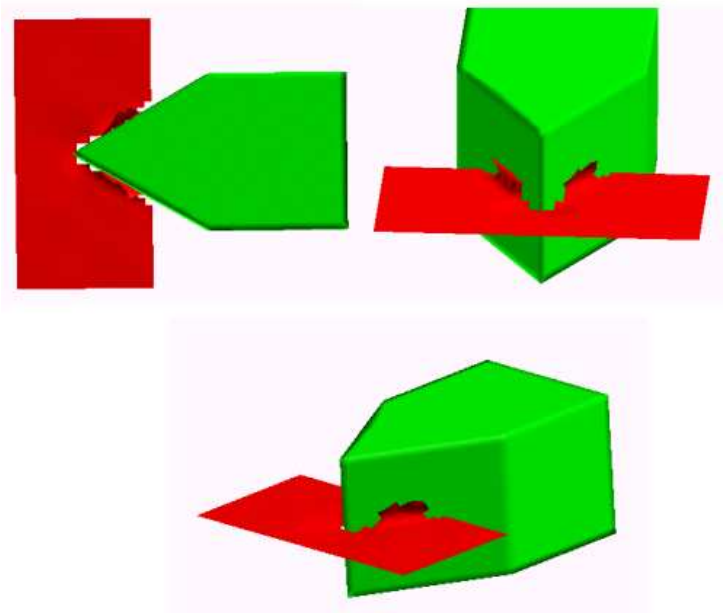

Figure 5-8 Deck Crushing and Tearing with HEA = 30 Degrees at 1.0 Seconds

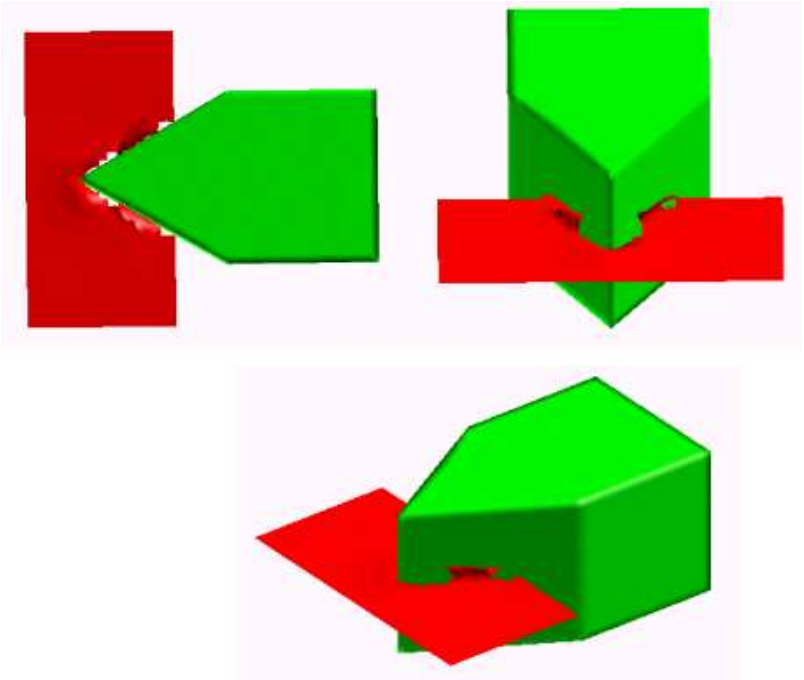

Figure 5-9 Deck Crushing and Tearing with HEA = 30 Degrees at 1.5 Seconds

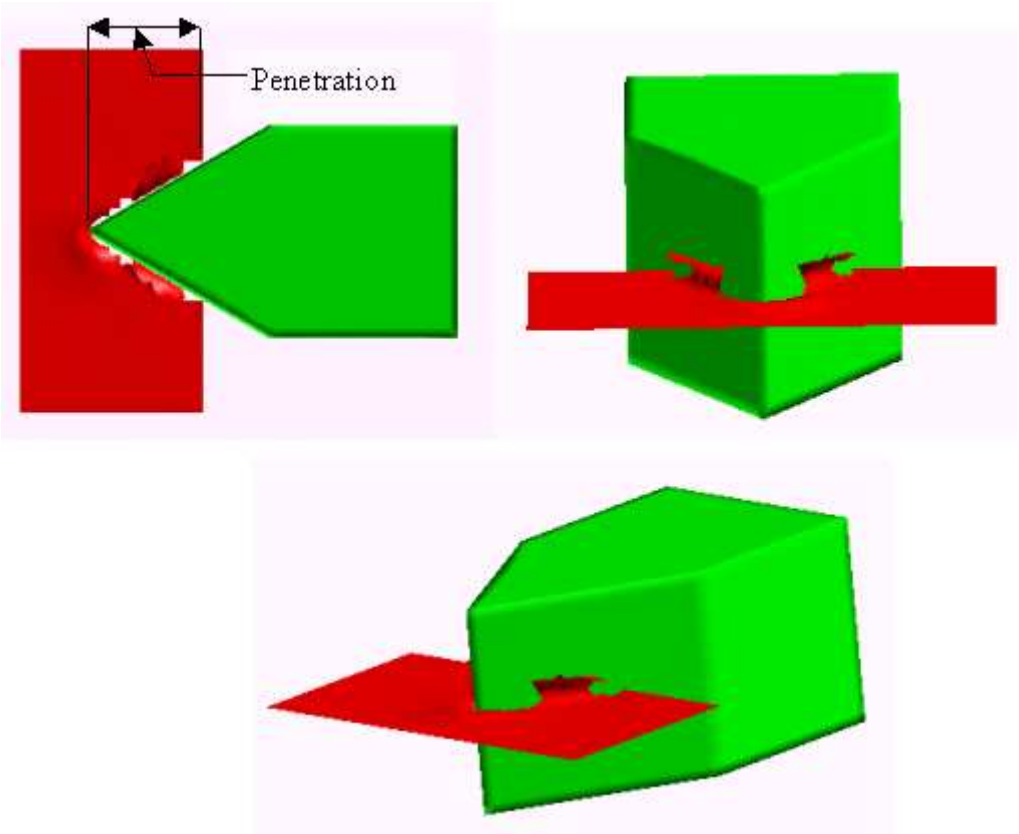

Figure 5-10 Deck Crushing and Tearing with HEA = 30 Degrees at 2.0 Seconds

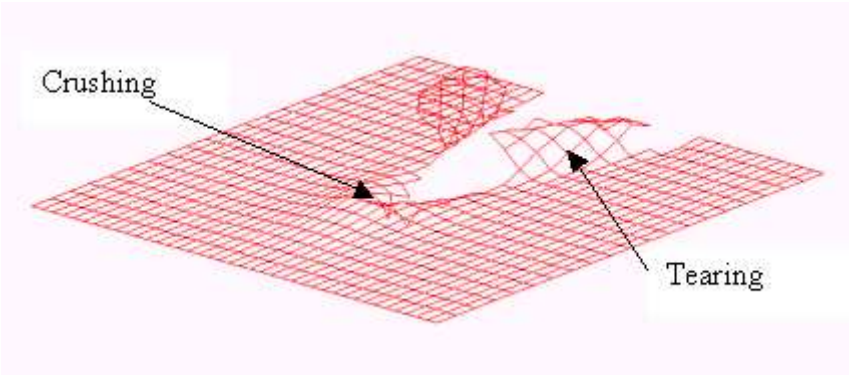

Figure 5-11 FEA Plate Mesh Showing Crushing and Tearing at 2.0 Seconds from HEA = 30 Degrees

Comparative results between the theory for crushing or tearing of deck structure using the Reardon and Sprung formulation (Equation 4.3) and the finite element analysis are provided in Figure 5-12. Comparative results between the theory for crushing or tearing of deck structure using the Paik and Pedersen formulation without strain rate effects (Equation 4.9) and the finite element analysis are provided in Figure 5-12 through Figure 5-14. Finally, comparative results between the theory for crushing or tearing of deck structure using the Paik and Pedersen formulation with strain rate effects (Equation 4.10) and the finite element analysis are again provided in Figure 5-12.

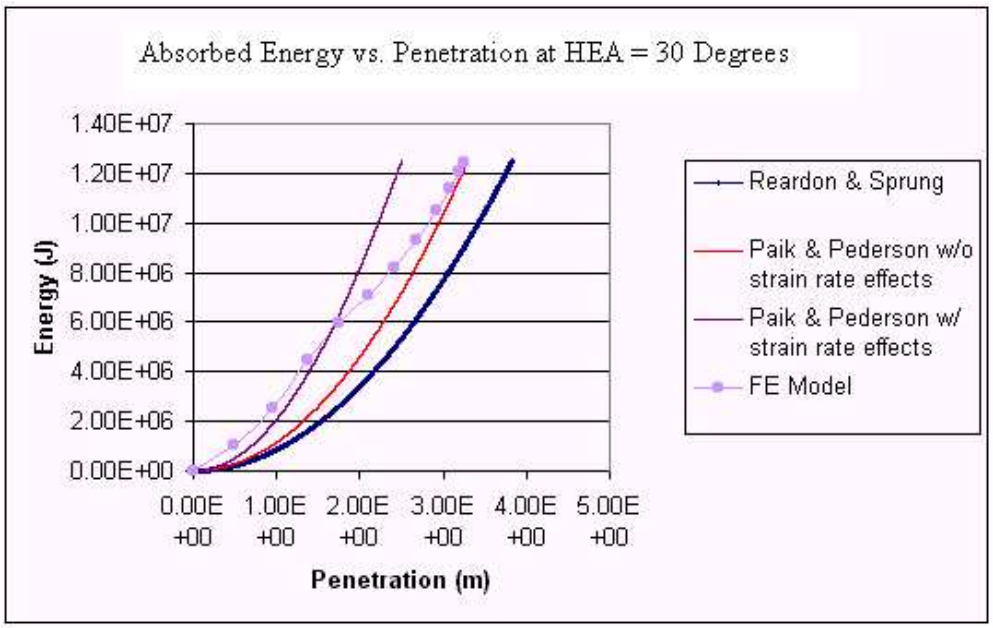

Figure 5-12 Absorbed Energy vs. Penetration at HEA = 30 Degrees

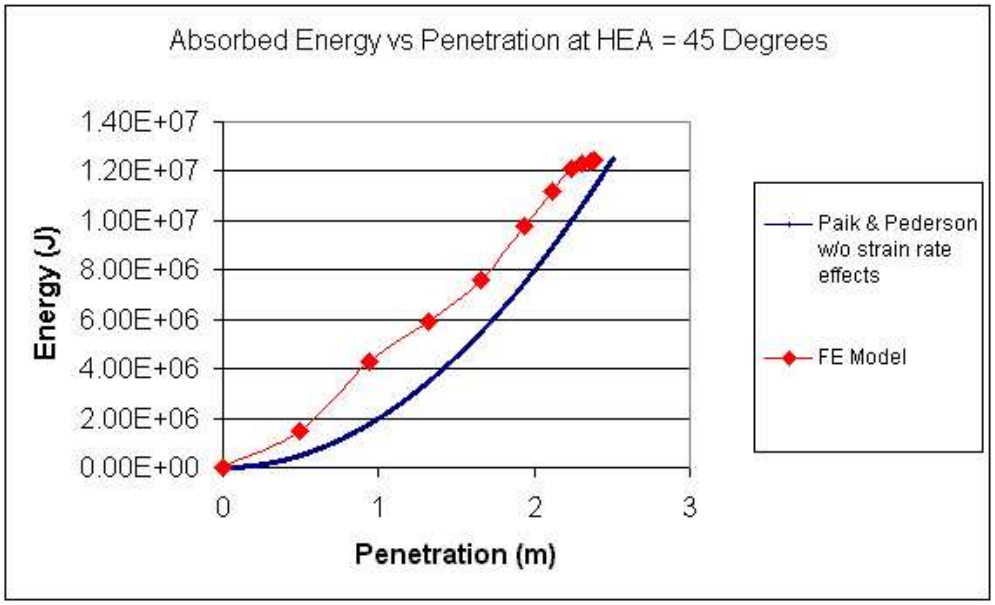

Figure 5-13 Absorbed Energy vs. Penetration at HEA = 45 Degrees

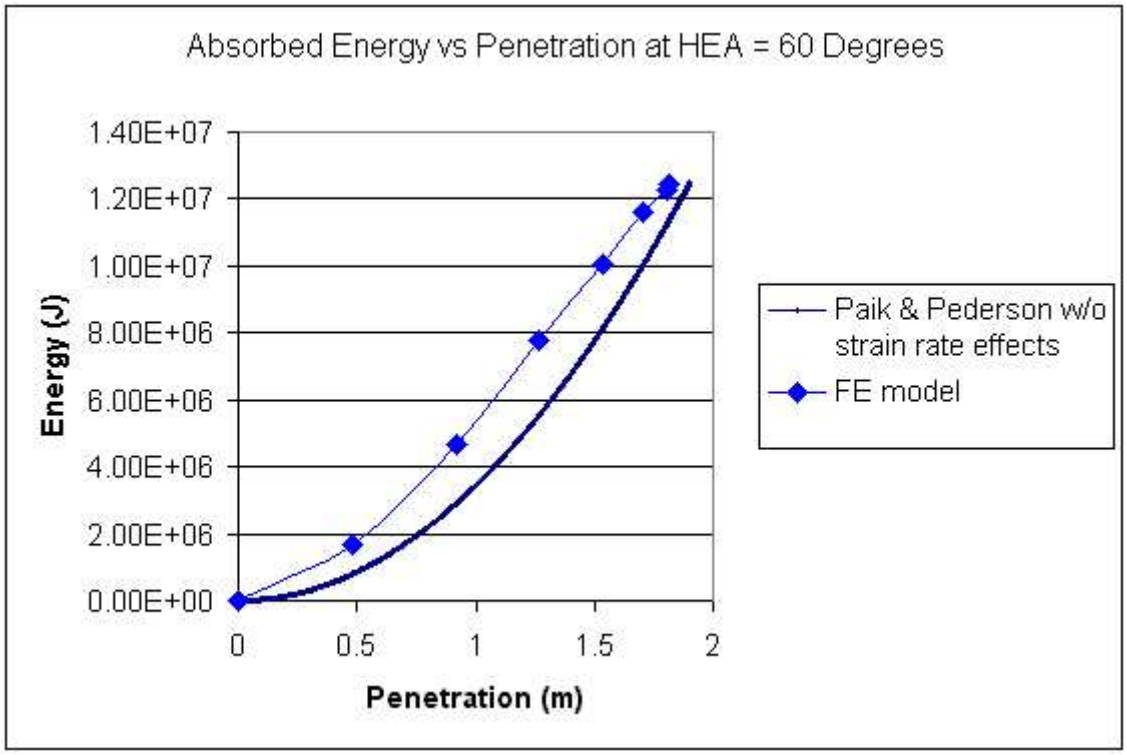

Figure 5-14 Absorbed Energy vs. Penetration at HEA = 60 Degrees

All analyses are run until the initial kinetic energy of the striking rigid bow is absorbed (1.25E+07 Joules). Therefore, the determination of the best method is based on a correlation coefficient between the finite element results and the energy coefficient method. Determination of the correlation coefficient (or average error) is provided in Equation 5.1 where a correlation coefficient of 1 means perfect correlation.

$$R = \frac{\sum_{i=1}^{N} \left(1 - \frac{FE_i - T_i}{FE_i} \right)}{N} \qquad (5.1)$$

Where:

FE_i value of finite element ordinate

T_i value of energy coefficient (or other method) ordinate

N number of abscissa data points

Table 5-2 provides the correlation results of all tests at HEA = 30 degrees.

Table 5-2 Correlation Results of Energy Coefficient Methods to FEA at HEA = 30 Degrees

Method	R (HEA = 30)
Reardon & Sprung	0.683
Paik & Pedersen w/o strain rate effects	0.779
Paik & Pedersen w/ strain rate effects	0.658

At an HEA of 45 and 60 degrees the correlation coefficients for the Paik and Pedersen formulation without strain rate are 0.77 and 0.82 respectively. As shown by Table 5-2 the most appropriate energy coefficient method (of those tested) for use within SIMCOL version 3.0 for the determination of the energy absorbed by structural decks and stingers is Paik and Pedersen's formulation without strain rate effects as given by Equation 4.9. Additionally, Paik and Pedersen's formulation without strain rate effects is more conservative to the Paik and Pedersen's formulation with strain rate effects, however, a combination of the two methods (with and without strain rate effects) may be the best available method but was not tested here.

5.2 Energy Coefficient Method for use with Longitudinal and Transverse Bulkheads and Longitudinal Crushing of Side Shell

Because of the simplicity of the energy coefficient methods, the use of one of these methods for the damage sustained to longitudinal bulkheads subject to an axial or longitudinal force and to transverse bulkheads subject to a transverse force is desired. As shown by Figure 5-15 and Figure 5-16 of actual and finite element simulation damage to transverse and longitudinal bulkheads subjected to an axial (parallel to bulkhead) load the use of a crushing energy coefficient mechanism is most appropriate.

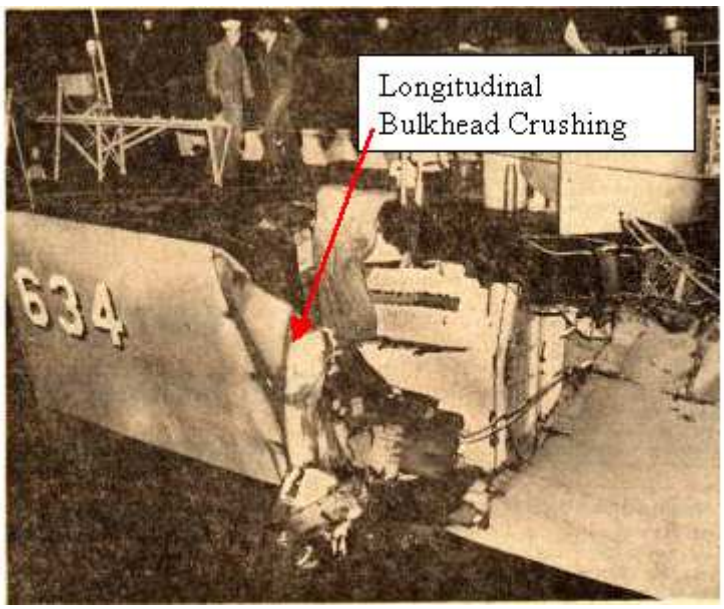

Figure 5-15 Actual Longitudinal Bulkhead Crushing

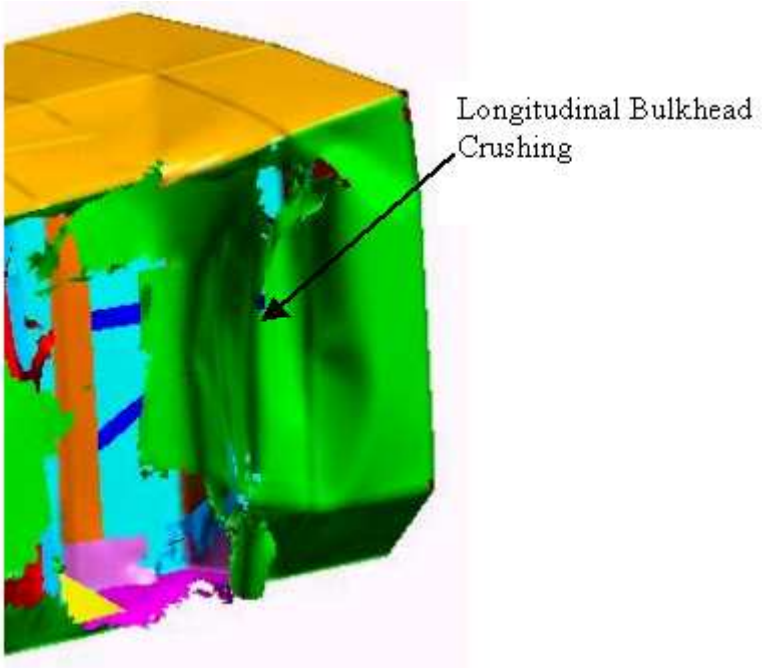

Figure 5-16 FEA Example of Longitudinal Bulkhead Crushing

Consequently, an investigation of the energy coefficient methods of Reardon and Sprung and Pedersen and Zhang [14] is performed to determine which method most accurately captures the energy absorption of crushed bulkheads when involved in collisions.

The theory for crushing of longitudinal and transverse bulkheads as used in SIMCOL is compared to finite element results of a rigid box striking the side shell structure of a 150k dwt double hull oil tanker, where the side shell, the supporting web frames, and stringers are included as shown in Figure 5-17. The rigid box has a mass of 3.0E+06 kg, a height of 17.475 m and is given a forward velocity of 5 m/s. The side shell structure is described in Table 5-3.

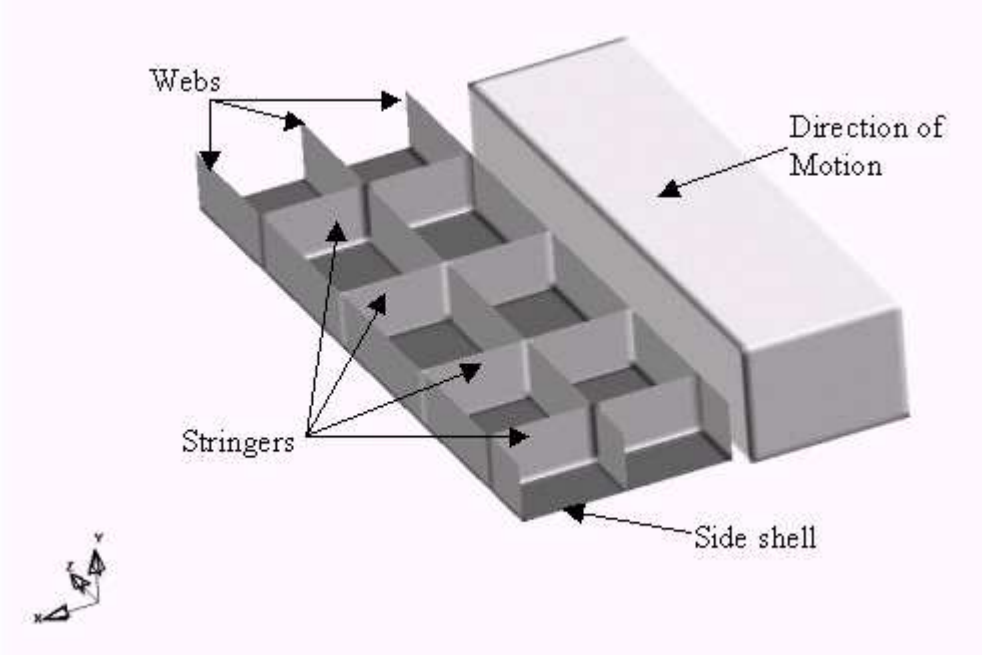

Figure 5-17 Simplified Longitudinal/Transverse Bulkhead Crushing Model

Table 5-3 Simplified Longitudinal/Transverse Crushing Parameters

Sideshell Height	20.50 m
Sideshell Length	6.60 m
Sideshell Thknss (stiffeners smeared)	23.25 mm
Web Frame Depth	2.00 m
Web Frame Thknss	15.00 mm
Stringer Depth	2.00 m
Stringer Thknss	11.70 mm
Web Frame Spacing	3.30 m
First Stringer Height above bottom of Sideshell	1.95 m
Second Stringer Height above bottom of Sideshell	6.20 m
Third Stringer Height above bottom of Sideshell	11.30 m
Fourth Stringer Height above bottom of Sideshell	16.40 m

The upper and lower most edges of the side shell structure are simply supported while the edge opposite of the impacted edge is fixed. The finite element model is comprised of Belytschko-Tsay shell elements with a uniform mesh size of 250 mm. The material of the deck structure is modeled with a Piecewise Linear Plasticity model for steel representing ABS Gr. B with parameters given in Table 3-4. Analysis of the Finite Element model are performed by eliminating the web frames and

substituting the structure with nodal constraints on the sideshell in the y translation and the rotation about the x axis at the intersection. Additionally, the stringers are replaced with nodal constraints on the deck in the y translation and rotation about the z axis along the intersection. Again, the purpose for replacing the physical structure of the webs and stringers is to independantly determine the energy absorbed only through the side shell plate. Friction is assessed through the use of coulomb friction, Equation 3.7 and is representative of mild steel on steel.

The finite element model is run once and representative damage of the analysis is shown in Figure 5-18 through Figure 5-21.

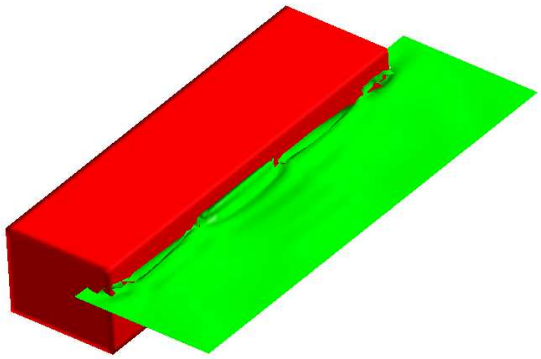

Figure 5-18 Bulkhead Crushing at 0.5 Seconds

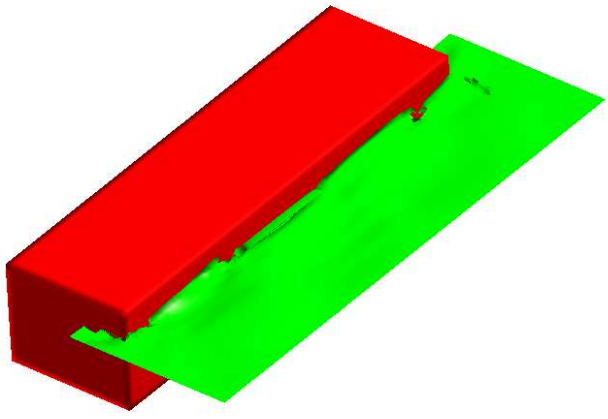

Figure 5-19 Bulkhead Crushing at 1.0 Seconds

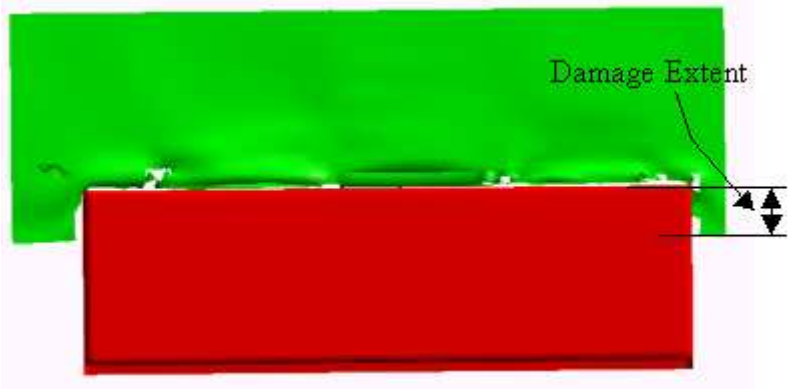

Figure 5-20 Bulkhead Crushing at 1.5 Seconds

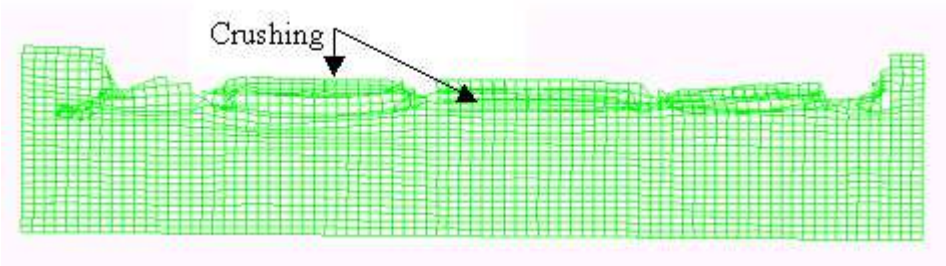

Figure 5-21 Bulkhead Mesh Crushing at 1.5 Seconds

Comparative results between the theory for crushing bulkheads using the Reardon and Sprung formulation (Equation 4.3) and the finite element analysis are provided in Figure 5-22 through Figure 5-24. Comparative results between the theory for crushing bulkheads using the Pedersen and Zhang formulation (Equation 4.7) and the finite element analysis are also provided in Figure 5-22 through Figure 5-24.

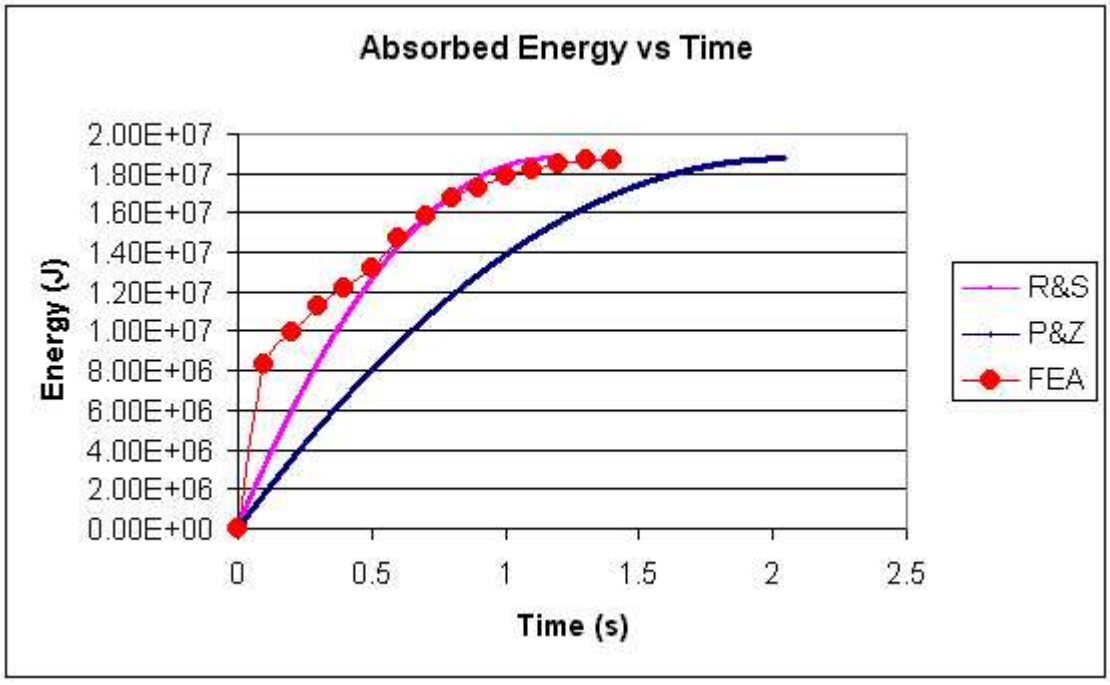

Figure 5-22 Absorbed Energy vs. Time for Crushing of Bulkheads

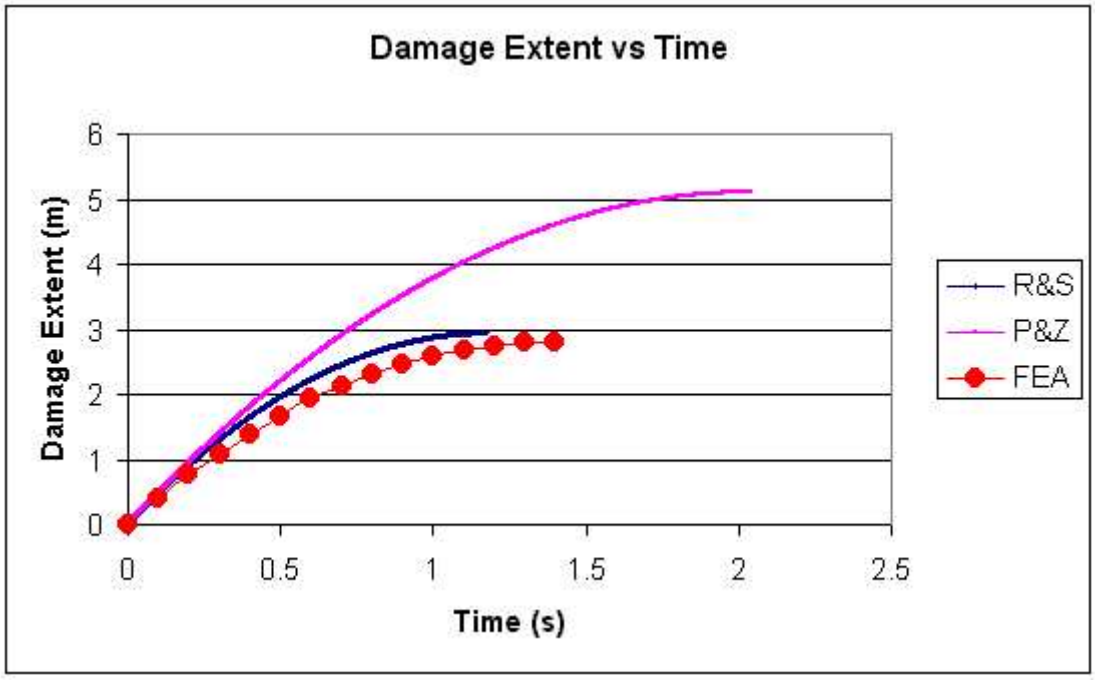

Figure 5-23 Damage Extent vs. Time for Bulkhead Crushing

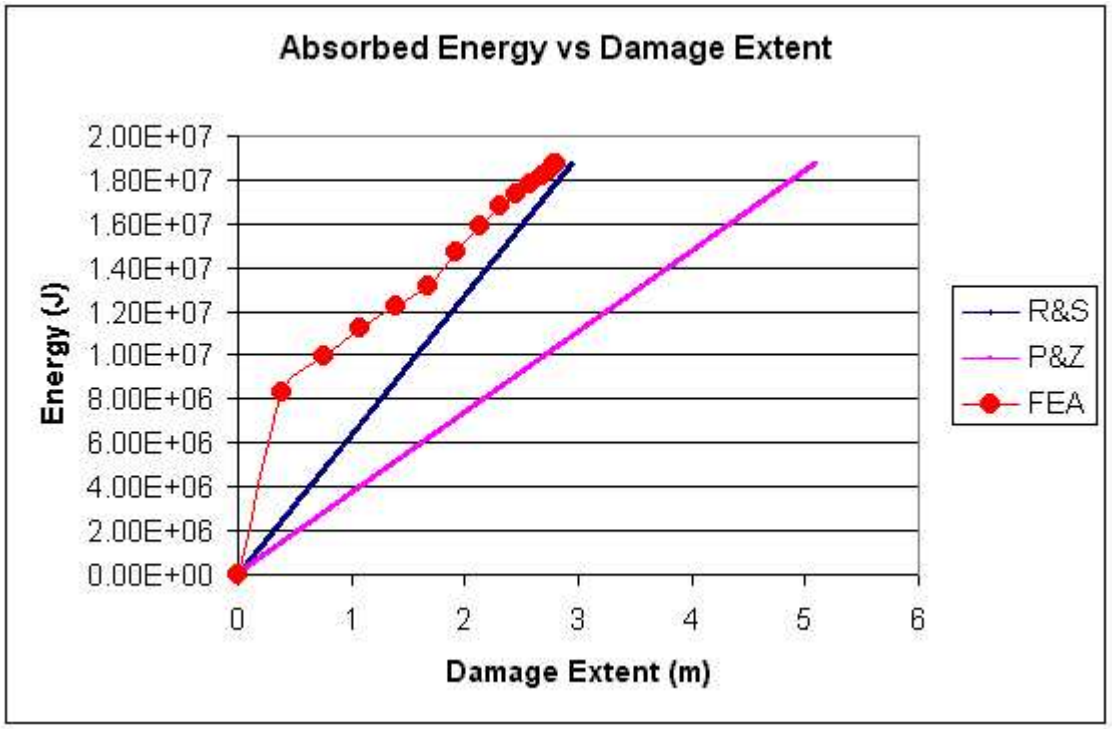

Figure 5-24 Absorbed Energy vs. Damage Extent for Bulkhead Crushing

All analyses are run until the initial kinetic energy of the striking rigid box structure is absorbed (1.91E+07 Joules). Therefore, the determination of the best method is again based upon a correlation coefficient of the absorbed energy between the finite element results and the energy coefficient method. Determination of the correlation coefficient is provided in Equation 5.1. Table 5-4 provides the correlation results of all tests.

Table 5-4 Correlation Results of Energy Coefficient Methods for Bulkhead Crushing

Method	R
Reardon & Sprung	0.869
Pedersen & Zhang	0.459

As shown by Table 5-4 the most appropriate energy coefficient method (of those tested) for use within SIMCOL version 3.0 for the determination of the energy absorbed by crushing longitudinal and transverse bulkheads is the Reardon and Sprung formulation as given by Equation 4.3.

5.3 Deformable Bow Model

SIMCOL version 3.0 incorporates a deformable bow sub-module that is based on a comparative force method. The force required to crush the bow normal to the course of the struck ship is compared to the lateral resistive force (the force normal to the side shell of the struck ship) due to the penetration of the striking ship into the struck ship. The lesser force indicates which vessel will sustain damage in the amount of the relative bow motion within the time step (as discussed in Section 2.4). If the force to crush the bow is less, then the striking ship is not moved or geometrically deformed within the time step, however the force due to crushing the bow is applied to both vessels and the energy due to crushing the bow within the time step is added to the total energy absorbed in the collision. The time step is then cycled. The force required to crush the bow is determined through Pederson's method as discussed in Section 4.4.2 because of its relative simplicity in application while maintaining a reasonable degree of accuracy as shown in Figure 5-25. Figure 5-25 compares Pedersen's method (Appendix H) to that of Amdahl's method (Appendix G) for the bow of a 150k dwt bulk carrier described in Appendix A. The initial kinetic energy of the striking ship (E_0) is given by Equation 5.2. SIMCOL assumes a maximum service vessel speed (V_s) of 16 knots in the Pedersen equation for all striking ships. The crush force per damage length of the bow is given by Equation 5.3 where a simple half sine wave is applied.

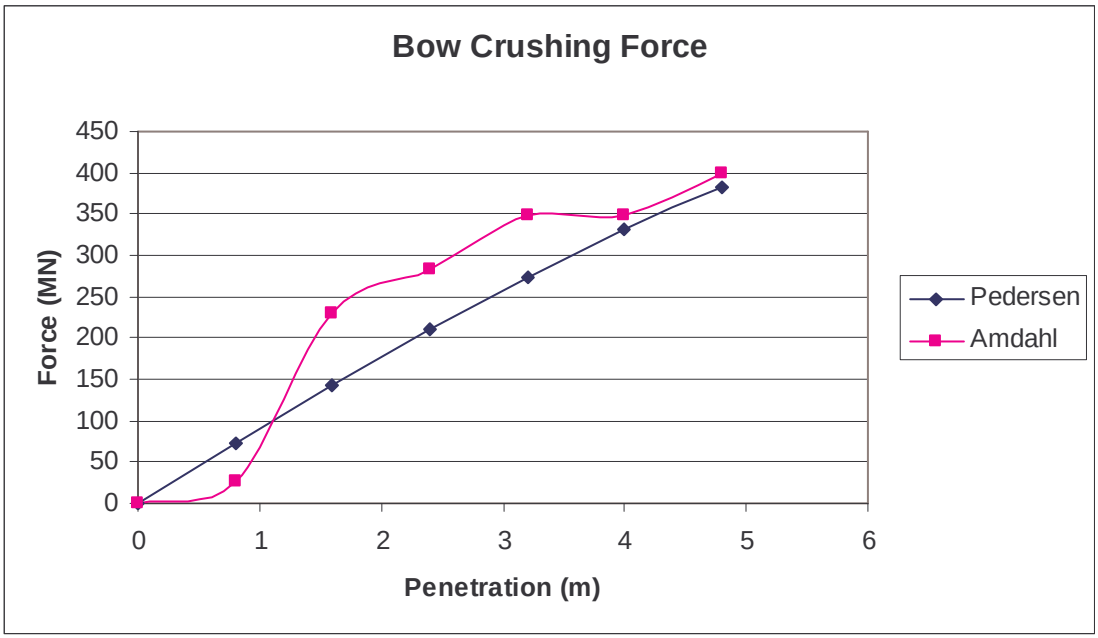

Figure 5-25 Crushing Force vs. Penetration for 150K Bulk Carrier Striking a rigid wall at 90 Degrees

$$E_0 = \frac{1}{2}\cdot\left(1 + c_{11}\right)\cdot M_{sis}\cdot V_s^{\,2} \tag{5.2}$$

$$F_{bow} = \sin\left(\frac{\pi\cdot x}{2\cdot s_{max}}\right)\cdot P_{bow} \tag{5.3}$$

Where:

E_0 is the assumed kinetic energy of the striking ship;

c_{11} is the added mass coefficient in surge (0.05);

M_{sis} is the displaced mass of the striking ship;

V_s is the maximum service speed of the striking vessel (16 knots);

F_{bow} is the crushing force of the bow;

x is the crush distance parallel to the striking ships centerline;

s_{max} is the maximum crush distance of the bow (Equation 4.16);

P_{bow} is the maximum crushing force of the bow (Equation 4.15).

Pederson's method accounts for the effect of strain rate, impact velocity, vessel loading condition, and vessel size for merchant vessels between 500 DWT and 300,000 DWT. Not included within Pederson's method are the effects of eccentric impacts (oblique angle impacts) however, as applied within SIMCOL, only the right angle components of the forces are compared thus retaining the applicability of Pederson's method to the oblique angle cases within SIMCOL.

5.4 Longitudinal Deflection of Transverse Bulkheads and Webs

This section is the most significant and substantial contribution of this dissertation. A definitive theory does not exist for the determination of the energy absorbed through the longitudinal deflection of transverse bulkheads or webs. However, in a ship-to-ship collision, where the struck ship has forward speed or the collision occurs at an oblique angle, the striking ship both penetrates into the struck ship and crushes transverse structure longitudinally, parallel to the struck ship centerline and at a right angle to the transverse structure. This damage along the length of the struck ship increases the longitudinal extent of damage while absorbing additional energy and

providing a resistive force on the striking ship. Within this longitudinal damage the energy is absorbed via two mechanisms; 1) the longitudinal crushing of longitudinal bulkheads as discussed in Section 5.2 and 2) the longitudinal deformation of webs and transverse bulkheads. The non-uniform longitudinal or lateral deflection of transverse bulkheads and webs is best seen in Figure 5-26 through Figure 5-28 where the deformation of the bulkheads and webs is seen to match the geometry of the impinging vessel as was a generality discussed in Section 2.4.

Figure 5-26 Actual Longitudinally Deformed Web [89]

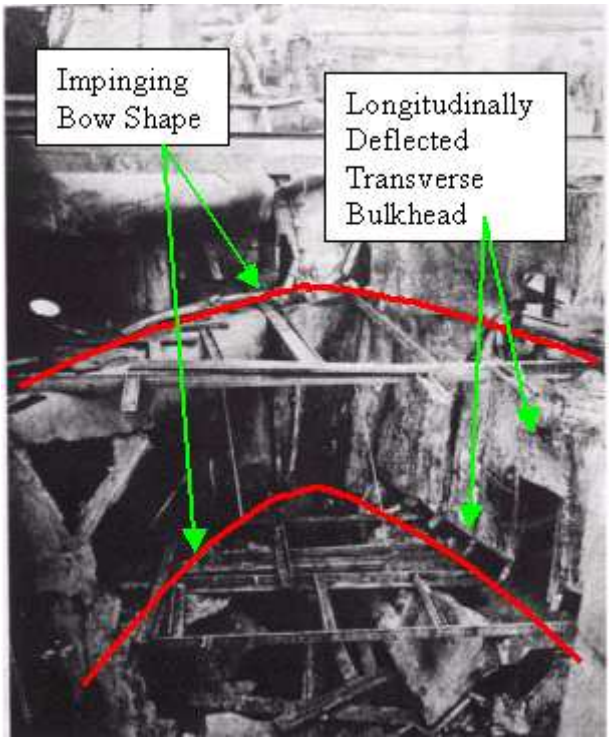

Figure 5-27 Ship Damage Showing Longitudinally Deflected Bulkhead and Impinging Bow Shape

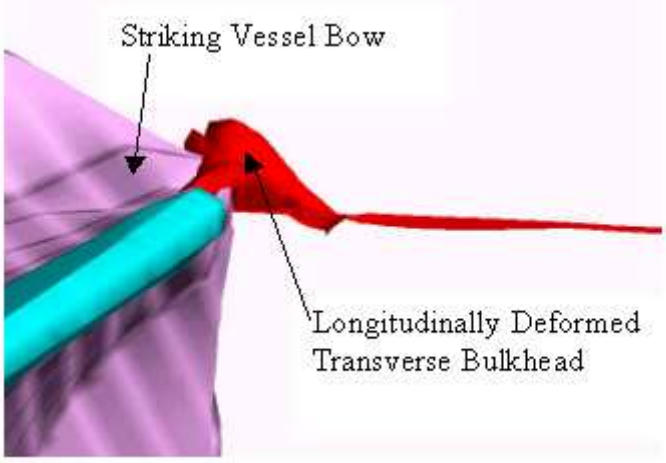

Figure 5-28 FEA Showing Longitudinal Deformation of Transverse Bulkhead

The energy absorbed through the lateral deformation of webs and/or transverse bulkheads is determined using a plastic membrane energy approach that is derived in detail in Sections 5.4.1 through 5.4.5. The following simplified description is provided as an introduction to the method. This simple example assumes that the striking ship does not contact the internal plate boundaries.

Any transverse bulkhead or web (or primary transverse structure such as transverse girders) may be idealized as a plate of uniform properties with the edges bound by some constraints, (simply supported or free) as shown in Figure 5-29. The outboard shell of the ship (RS) is considered a longitudinal bulkhead in this analysis.

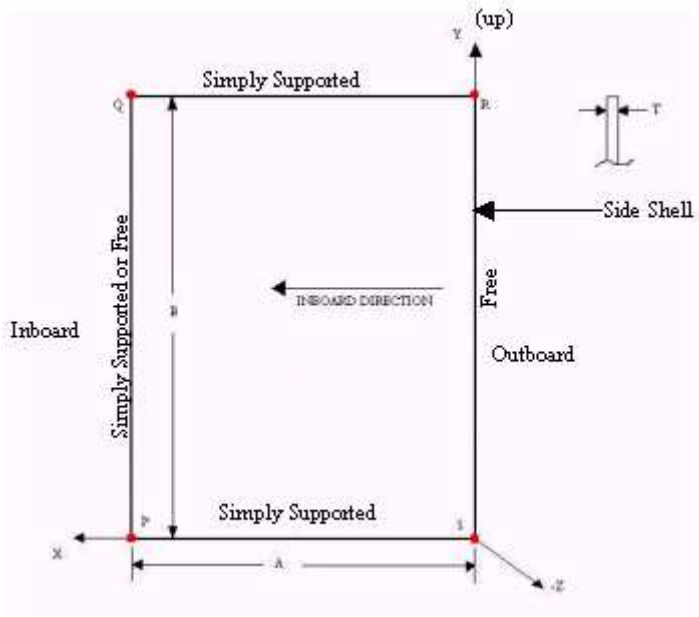

Figure 5-29 Idealized Transverse Plate Model

The span (A) is either the web depth or represents a transverse bulkhead bounded by longitudinal bulkheads and the height (B) is bounded either by decks or by stringers (PS and QR). The upper and lower edges (PS and QR) are thus always simply supported (z = 0) so as to not double count energy absorbed by other mechanisms such as deck or stringer crushing discussed in Section 5.1. PS or QR being the intersection of the bulkhead or web and a deck or stringer the edges are translationaly fixed while rotationally free. The inboard most edge (QP) is free only if the plate is a web not bounded by two longitudinal bulkheads. Otherwise the inboard edge is simply supported being the intersection of the transverse structure (bulkhead or web) and a longitudinal bulkhead. The outboard most edge of the plate (RS) is always considered free, neglecting any interaction with the longitudinal bulkhead supporting this edge by making the assumption that the energy absorbed via the crushing of the longitudinal bulkhead along this edge is considered by the method of

Section 5.2 (i.e. avoids double-counting the energy absorbed in the longitudinal bulkhead at the outer edge).

The transverse plate of Figure 5-29 can then be assumed to absorb energy independent of other contacted structure. Making use of this independence, the plate is laterally deformed by the striking ship represented within SIMCOL as a wedge model shown in Figure 5-30.

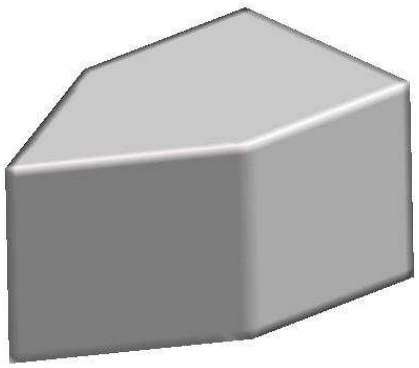

Figure 5-30 SIMCOL Wedge Model

For this derivation the wedge is assumed to be rigid, considering only the energy absorbed in the plate. This wedge model allows for four contact scenarios by which the wedge may strike the plate. These contact scenarios are:

- Contact Scenario 1 - Port or starboard bow section contacts the plate at any angle (φ) less than ninety degrees and greater than zero degrees (illustrated in Figure 5-31 and shown finite element time step progression in Figure 5-32 through Figure 5-35).
- Contact Scenario 2 - Port or starboard bow section contacts the plate at any angle (φ) less than or equal to zero degrees (illustrated in Figure 5-36 and shown finite element time step progression in Figure 5-37 through Figure 5-39).
- Contact Scenario 3 - Port or starboard after body contacts the plate at any angle (α) less than ninety degrees and greater than zero degrees (illustrated in Figure 5-40 and shown finite element time step progression in Figure 5-41 through Figure 5-44).
- Contact Scenario 4 - Port or starboard bow section and after body contact the plate where the angle (φ) is less than ninety degrees and greater than zero degrees and the angle (α) is

less than or equal to zero degrees (illustrated in Figure 5-45 and shown finite element time step progression in Figure 5-46 through Figure 5-48).

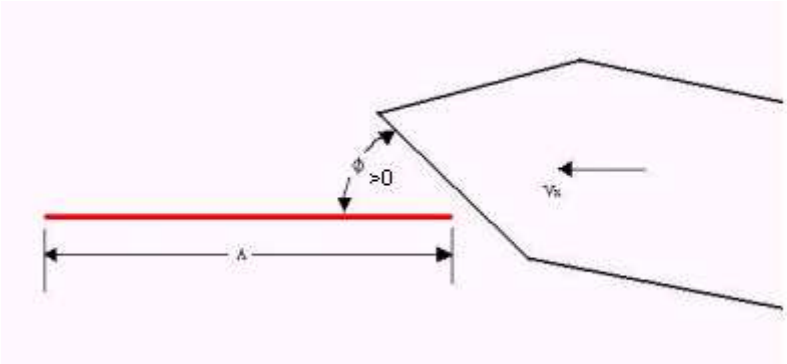

Figure 5-31 Contact Scenario 1 Geometry

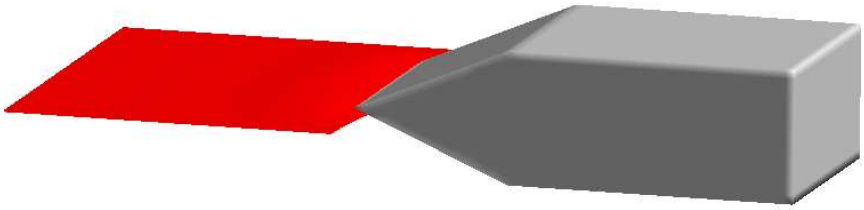

Figure 5-32 Contact Scenario 1 FEA Test Case at 0.1 Seconds

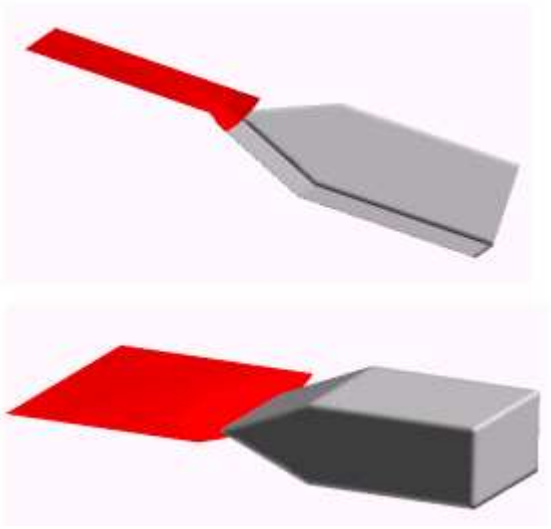

Figure 5-33 Contact Scenario 1 FEA Test Case at 0.2 Seconds

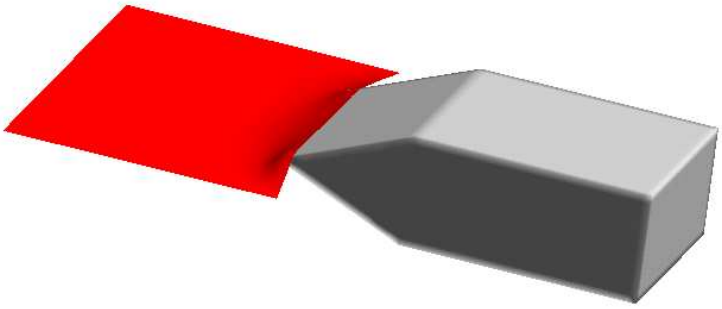

Figure 5-34 Contact Scenario 1 FEA Test Case at 0.3 Seconds

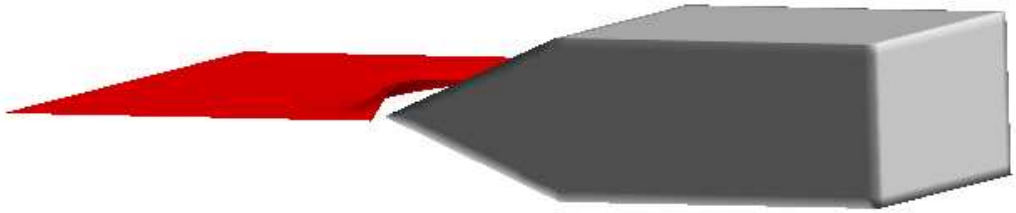

Figure 5-35 Contact Scenario 1 FEA Test Case at 0.8 Seconds

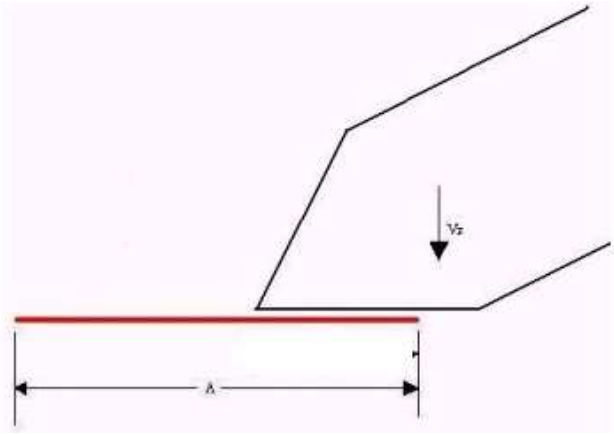

Figure 5-36 Contact Scenario 2 Geometry

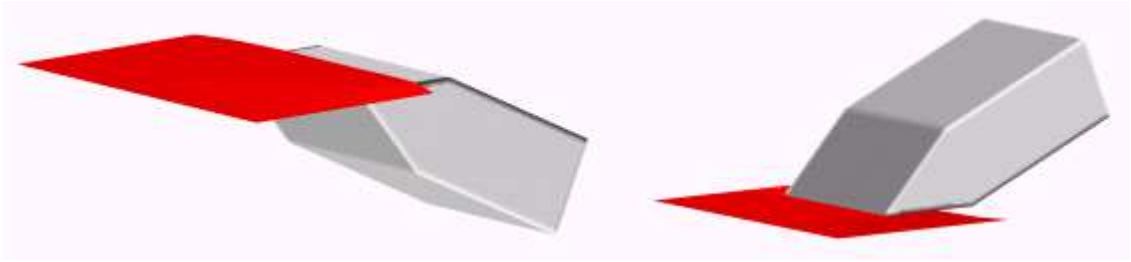

Figure 5-37 Contact Scenario 2 FEA Test Case at 0.2 Seconds

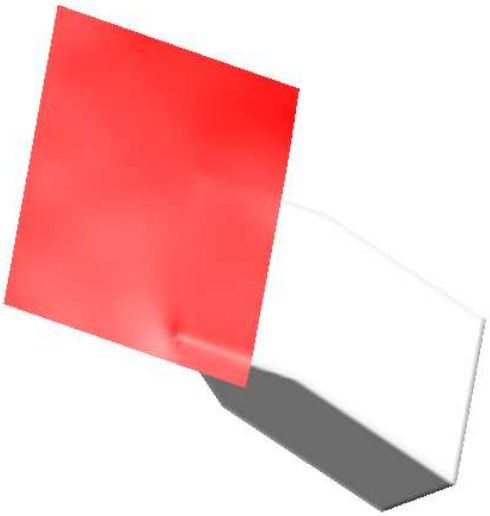

Figure 5-38 Contact Scenario 2 FEA Test Case at 0.25 Seconds

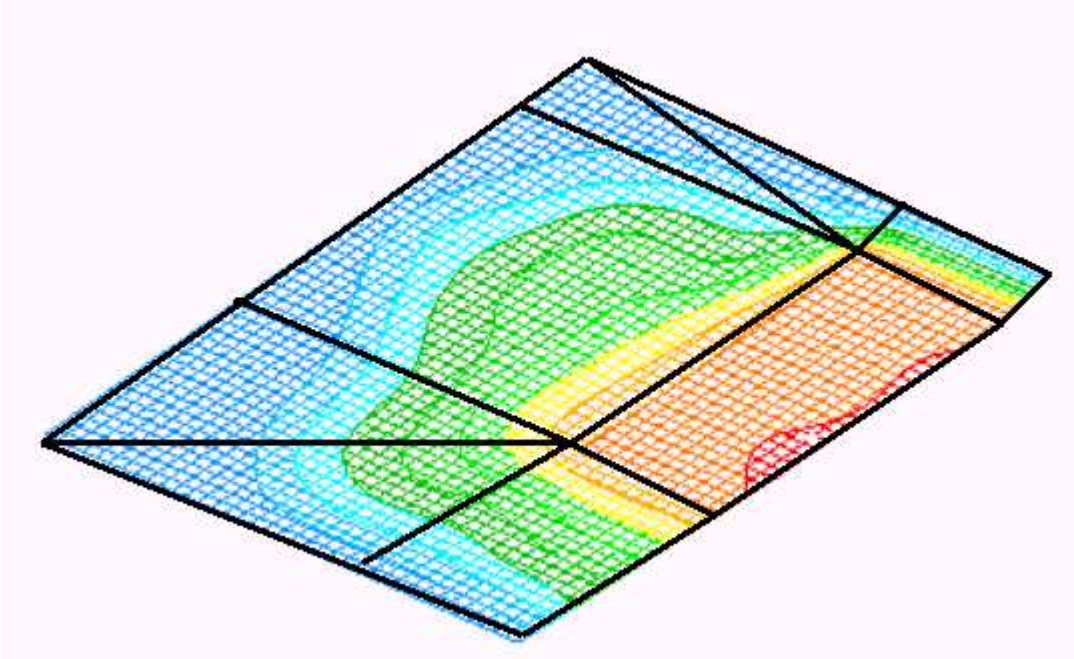

Figure 5-39 Contact Scenario 2 FEA Plate Mesh Deflection at 0.25 Seconds with 8 region model overlay

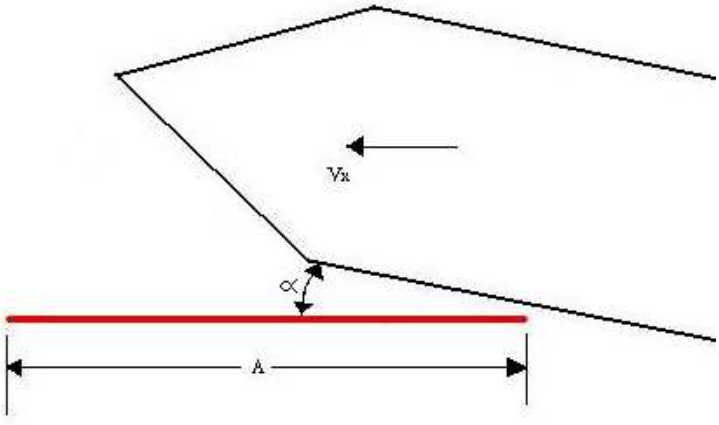

Figure 5-40 Contact Scenario 3 Geometry

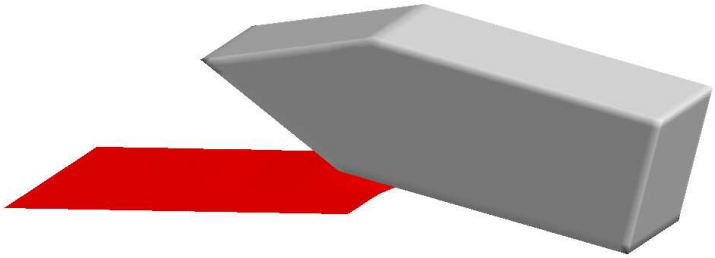

Figure 5-41 Contact Scenario 3 FEA Test Case at 0.1 Seconds

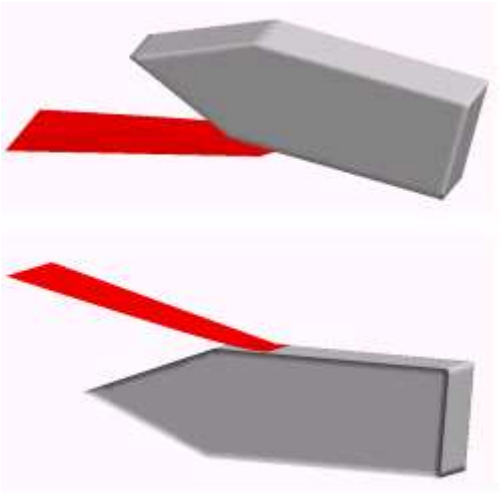

Figure 5-42 Contact Scenario 3 FEA Test Case at 0.2 Seconds

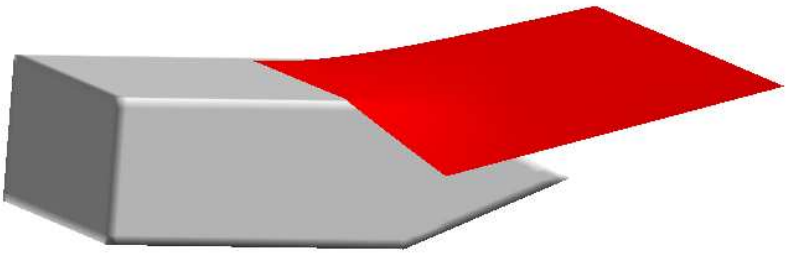

Figure 5-43 Contact Scenario 3 FEA Test Case at 0.3 Seconds

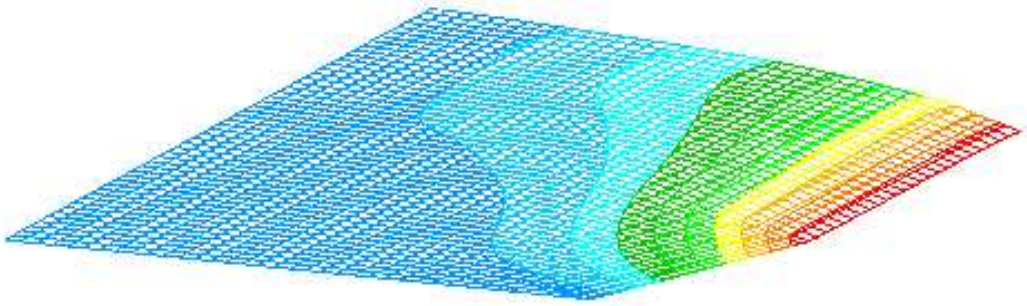

Figure 5-44 Contact Scenario 3 Plate Mesh Deformation at 0.3 Seconds

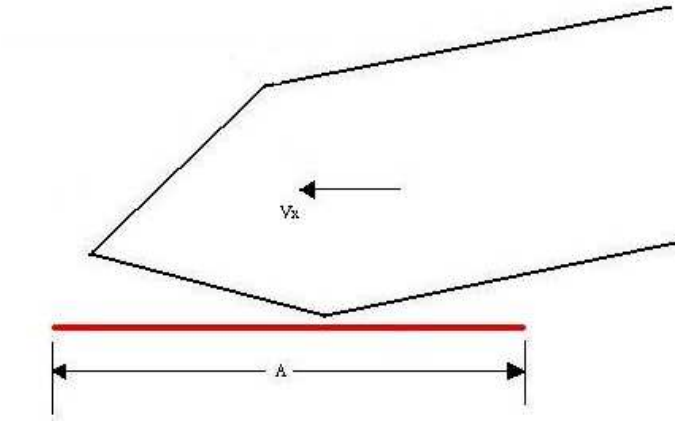

Figure 5-45 Contact Scenario 4 Geometry

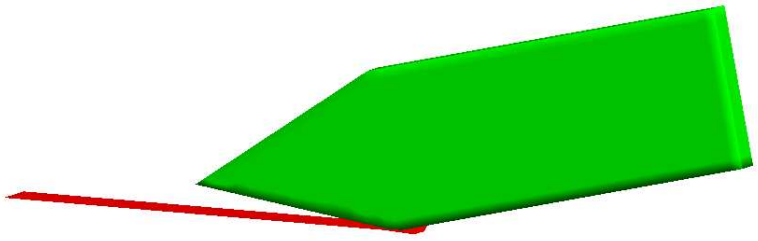

Figure 5-46 Contact Scenario 4 FEA Test Case at 0.1 Seconds

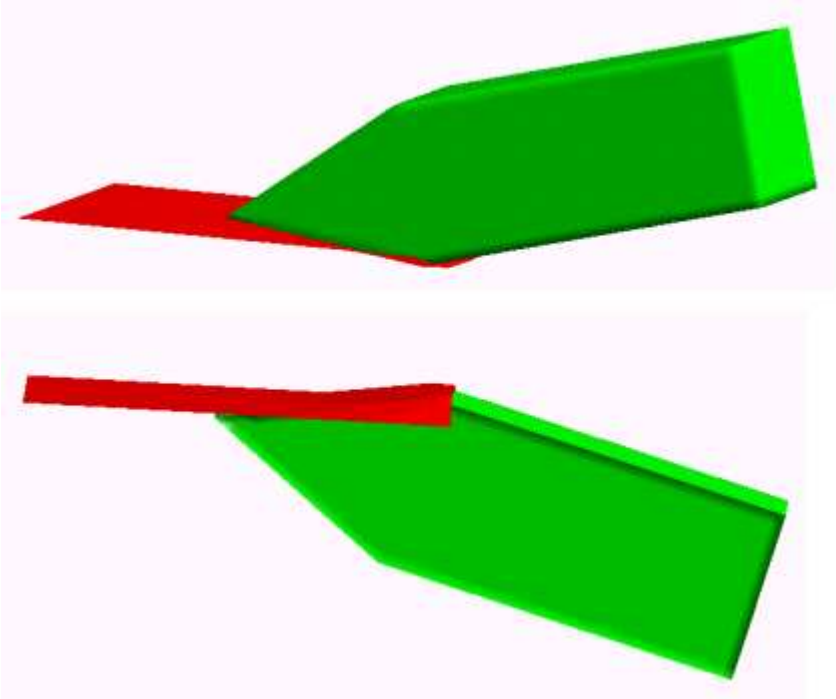

Figure 5-47 Contact Scenario 4 FEA Test Case at 0.2 Seconds

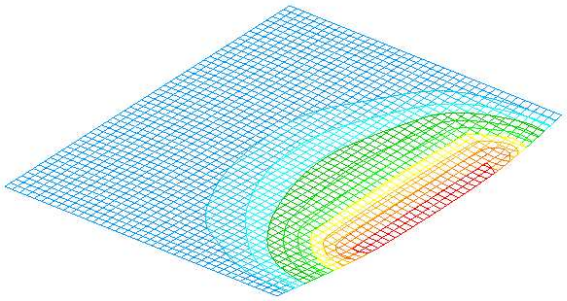

Figure 5-48 Contact Scenario 4 Plate Mesh Deflection at 0.2 Seconds

As an example, suppose that the rigid wedge strikes the plate in contact scenario 2 (Figure 5-36 through Figure 5-39), where the angle (φ) equals zero degrees and the wedge model has the initial component velocity zero m/s in the direction parallel to the plate but greater than zero in the direction normal to the plate as described by Figure 5-49.

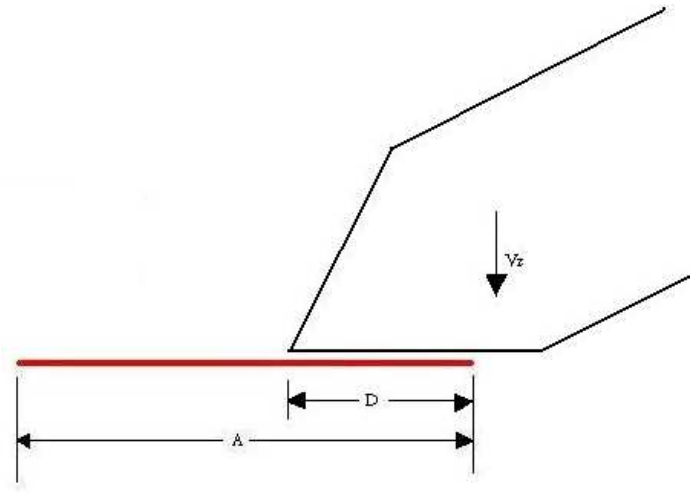

Figure 5-49 Longitudinal Deflection Simplified Argument Example Geometry

Thus the plate is struck by the rigid wedge over the shaded region (DF) of Figure 5-50 in the z direction with an initial velocity V_0 at the time t = 0 seconds (the moment of contact).

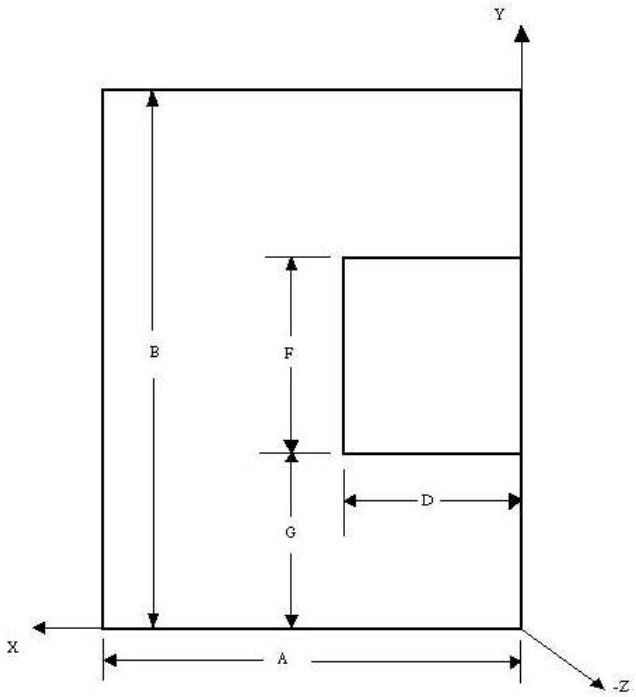

Figure 5-50 Idealized Plate Geometry Definitions for Simplified Argument

In this example, the rigid wedge is required to stay between the upper and lower edges of the plate. Using the nomenclature of Figure 5-50, $G \geq 0$ and $G+F \leq B$. Figure 5-51 through Figure 5-53 show all possible vertical positions of the wedge relative to the plate. These will be considered in the final 25 region model discussed in Section 5.4.5.

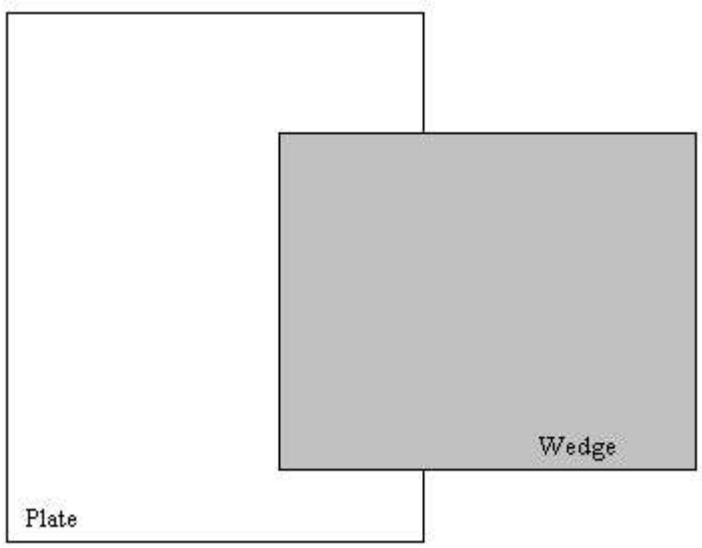

Figure 5-51 Centered Vertical Position of Wedge Striking Plate

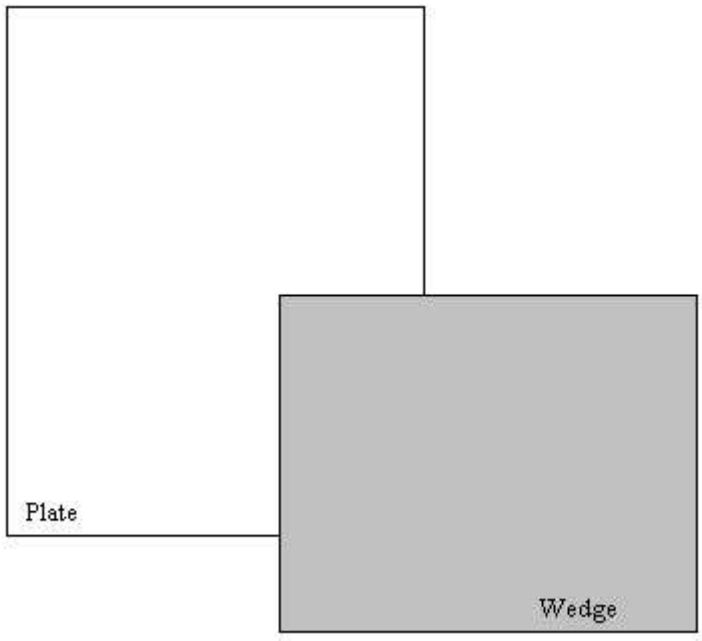

Figure 5-52 Lower Vertical Position of Wedge Striking Plate

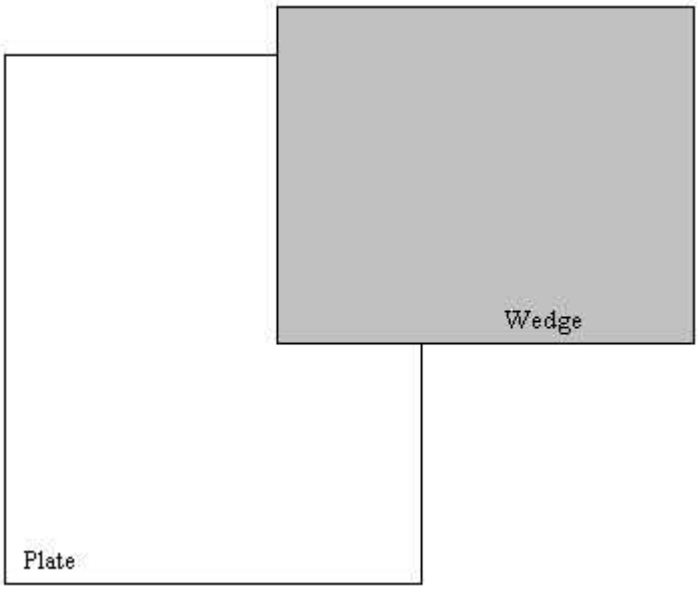

Figure 5-53 Upper Vertical Position of Wedge Striking Plate

For the current contact problem of Figure 5-49, the inboard edge of the plate is assumed simply supported. In contact scenario two with the angle (φ) equal to zero degrees, then the deflections at

(X,Y) = (0,G); (X,Y) = (0,G+F); (X,Y) = (D,G) and (X,Y) = (D,G+F) are equal at any time t. After a small time (τ) a linear form of the deflection of the plate maybe drawn as shown in Figure 5-54. Note that the deformed shape in Figure 5-54 is similar to the deformation of the finite element analysis of contact scenario 2 shown in Figure 5-36 through Figure 5-39 and provided again in Figure 5-54 for side-by-side comparison.

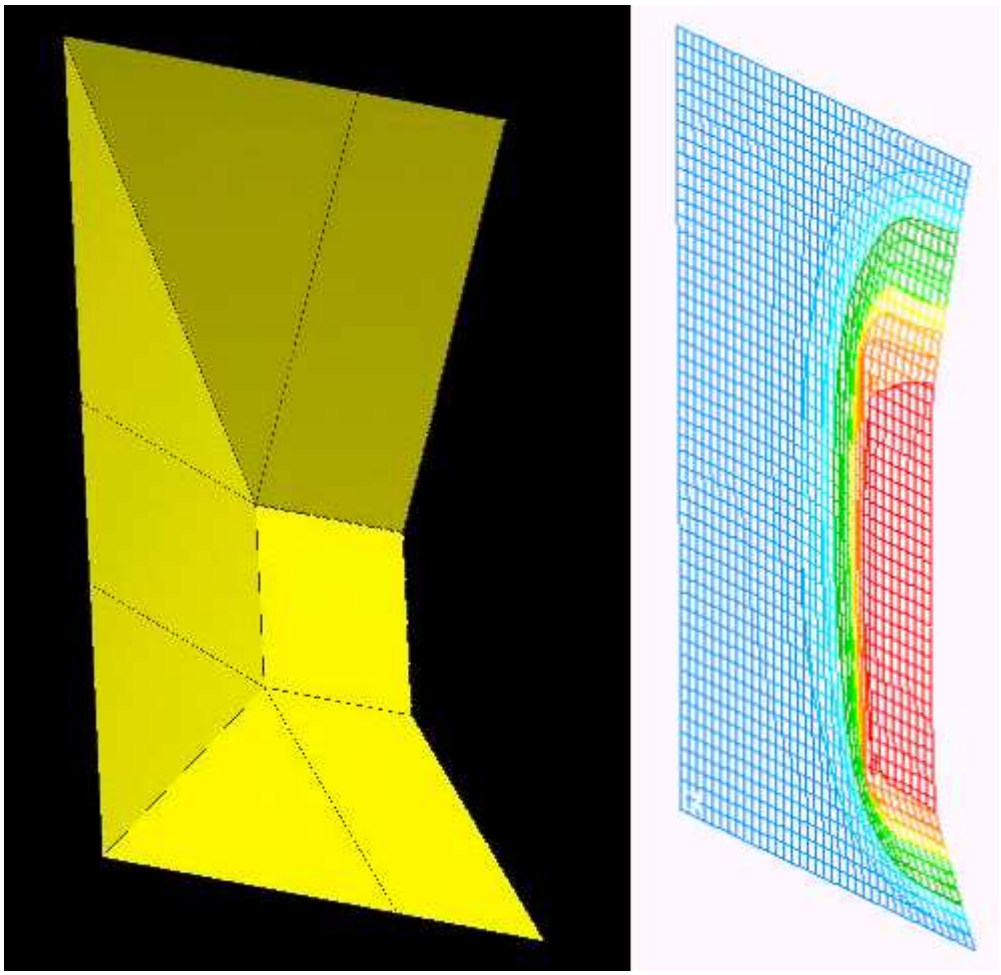

Figure 5-54 Simplified Plate Deflection (left) and Similar FEA Plate Mesh Deflection (right)

The plate is thus divided into eight energy-absorbing regions defined as shown in Figure 5-55.

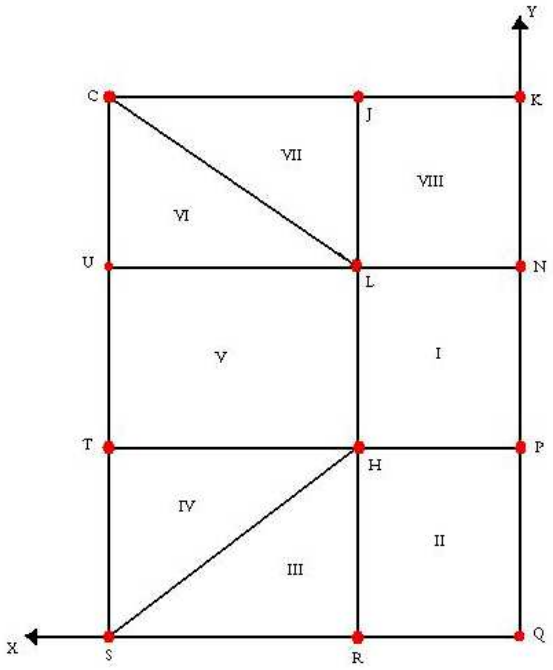

Figure 5-55 Eight Region Plate Model

The energy absorbed through the plastic membrane stretching of each region is calculated over each time step and summed to provide the energy absorbed through the lateral deflection of the plate in each time step. The more complicated but required twenty-five-region plate of Figure 5-60 replaces the simple eight-region plate of Figure 5-55 to properly capture the deformation of the plate using a linear approximation for the more complicated contact scenarios. Development of the energy absorbing rectangular and triangular regions is discussed in Sections 5.4.2 and 5.4.3 while the super positioning and assembly of the full energy absorbed by the plate is discussed in Section 5.4.4.

5.4.1 Flow Theory of Plasticity

Prior to discussion of the energy absorbed by the rectangular and triangular regions presented in Section 5.4.2, a brief review of the flow theory of plasticity is presented. The basic assumptions of flow theory are 1) that the strain of any material may be represented as the sum of an elastic strain and a plastic strain (Equation 5.4) and 2) there exists a loading function (F) at every stage of plastic deformation that prevents the relaxation of the elastic portion of the deformation.

$$\varepsilon_{ij} = \varepsilon_{ij}^{e} + \varepsilon_{ij}^{p} \tag{5.4}$$

The second assumption yields the condition that plastic deformation exists and is definable based upon a yield condition. Making use of Von Misses yield function the yield criterion for plastic deformation is given by Equation 5.5.

$$F = \frac{1}{2} \cdot S_{ij} \cdot S_{ij} - \frac{1}{3} \cdot \sigma_y^{\,2} = 0 \tag{5.5}$$

Where:

$$S_{ij} = \sigma_{ij} - \frac{\sigma_{11} + \sigma_{22} + \sigma_{33}}{3} \cdot \delta_{ij} \tag{5.6}$$

Additionally, by making use of the Drucker Postulates [90]:

- During loading, positive work is performed
- The net work performed through a loading and unloading cycle cannot be negative
- During unloading, the limit of the elastic strain is zero

Then an incremental change in work (positive) is equivalent to an applied stress times an incremental change in the plastic strain ($d\varepsilon_{ij}^{p}$) as shown by Equation 5.7.

$$dE = \sigma_{ij} \cdot d\varepsilon_{ij}^{p} \tag{5.7}$$

For plastic deformation to occur the incremental change in the loading must be positive and the load function must have a positive slope. Assuming that the strain is linearly related to the stress in infinitesimal changes then Equations 5.4 through 5.7 may be written yielding Equation 5.8 known as the associative flow rule.

$$d\varepsilon_{ij} = d\varepsilon_{ij}^{p} = D_{ijkl} \cdot d\sigma_{kl} \tag{5.8}$$

$$d\sigma_{kl} = d\gamma \cdot \frac{d}{d\sigma_{kl}}(F) \tag{5.9}$$

$$d\varepsilon_{ij}^{p} = d\lambda \cdot \frac{d}{d\sigma_{ij}}(F) \tag{5.10}$$

Where $d\lambda$ is the incremental linearity constant which is greater than zero.

The associative flow rule of Equation 5.8 states that the increment of plastic strain is normal to the increment of the yield surface where the strain is in the direction of the applied stress.

Returning to Equation 5.7, the incremental change in work can be written as a function of the effective strain ($d\varepsilon^{p}$) and effective stress (σ) as:

$$dE = \sigma \cdot d\varepsilon^{p} \tag{5.11}$$

Where the effective stress is given through Von Misses yield criterion as:

$$\sigma = \sqrt{\frac{3}{2} \cdot S_{ij} \cdot S_{ij}} \tag{5.12}$$

From the associative flow rule the increment of plastic strain may be written as:

$$d\varepsilon_{ij}^{p} = d\lambda \cdot \frac{3}{2} \cdot \frac{S_{ij}}{\sqrt{\frac{3}{2} \cdot S_{kl} \cdot S_{kl}}} \tag{5.13}$$

Equation 5.13 yields an effective plastic strain increment relation given by:

$$d\varepsilon^{p} = d\lambda \cdot S_{ij} = \sqrt{\frac{2}{3} \cdot d\varepsilon_{ij}^{p} \cdot d\varepsilon_{ij}^{p}} \tag{5.14}$$

Equation 5.14 states that the effective incremental plastic strain is equivalent to the incremental linearity constant times the deviatoric stress, which reaffirms the relation given by Equation 5.8.

Thus, using the associative flow rule, the plastic strain rate may be written as:

$$\frac{d}{dt}\varepsilon_{ij}^{P} = \left(\frac{d}{dt}\lambda\right)\cdot\frac{d}{d\sigma_{ij}}F \tag{5.15}$$

Where the loading function (F) is given by Equation 5.5.

In Equation 5.11 a constant material flow stress (σ) equal to the yield stress is used implying a perfectly plastic material law and allowing the determination of the deviatoric stresses to be neglected. Using the above relations the effective plastic strain rate and the rate of energy absorption are given by Equations 5.16 and 5.17.

$$\varepsilon_{e}^{p} = \sqrt{\frac{2}{3}\cdot\varepsilon_{ij}^{P}\cdot\varepsilon_{ij}^{P}} \tag{5.16}$$

$$E = \sigma\cdot\varepsilon_{e}^{p} \tag{5.17}$$

Finally, the determination of the plastic strain rate ($\dot{\varepsilon}_{ij}^{p}$) is provided through the strain-displacement relation given by Equation 5.18.

$$\varepsilon_{ij}^{p} = \frac{1}{2}\cdot\left(v_{i,j} + v_{j,i}\right) \tag{5.18}$$

Where the velocity flow field vector (υ) describes the vector velocity of any material point at a given time.

The above formulation has the following limitations:

- It is valid for only modest plastic strains (<= 10%)

- It will not predict plastic strains correctly if the principle axes of stress rotate significantly during inelastic deformation

Neither of these limitations provide difficulty with the use of this method as long as the following assumptions are made:

- At plastic strains >=10% the material is assumed to rupture providing no additional energy absorbing capability
- An analysis time step is chosen which limits the rotation of the principle axis of stress for each evaluation

5.4.2 Energy Absorption in Rectangular Region

Given any rectangular region as represented by Figure 5-56, the points Q, R, S and V are only allowed to move in the z direction. The deflections of point Q are equal to the deflections of point R at any time and the deflections of point V are equal to the deflections of point S at any time (i.e. segments QR and VS must always remain parallel to the xy plane). If the deflections of S do not equal the deflections of V, or if the deflections of Q do not equal the deflections of R, then the rectangular region must be evaluated as two triangular regions as discussed in Section 5.4.3.

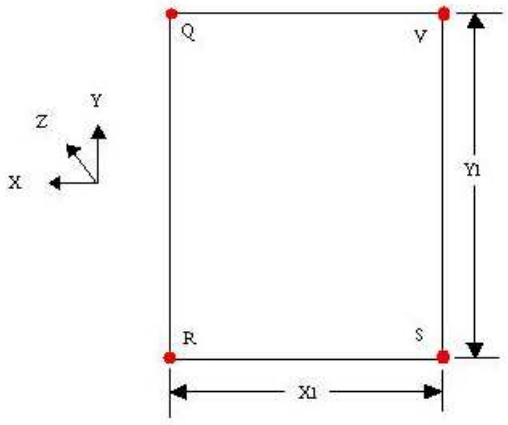

Figure 5-56 Rectangular Region Geometry and Nomenclature

The deflections of points V and Q at time t = i and t = f from the initial V_0 and Q_0 geometry are represented by WV_i, WV_f, WQ_i and WQ_f respectively. Because the deflections of S equal the deflections of V and the deflections of R equal the deflections of Q at any time then:

$$WS_i = WV_i \tag{5.19}$$

$$WS_f = WV_f \tag{5.20}$$

$$WR_i = WQ_i \tag{5.21}$$

$$WR_f = WQ_f \tag{5.22}$$

The segment lengths between points at any time are given by:

$$V_0 \cdot S_0 = V_i \cdot S_i = V_f \cdot S_f = Q_0 \cdot R_0 = Q_i \cdot R_i = Q_f \cdot R_f = Y_1 \tag{5.23}$$

$$Q_0 \cdot V_0 = R_0 \cdot S_0 = X_1 \tag{5.24}$$

$$Q_i \cdot V_i = R_i \cdot S_i = \left[X_1^{\,2} + \left(WV_i - WQ_i \right)^2 \right]^{\frac{1}{2}} \tag{5.25}$$

$$Q_f \cdot V_f = R_f \cdot S_f = \left[X_1^{\,2} + \left(WV_f - WS_f \right)^2 \right]^{\frac{1}{2}} \tag{5.26}$$

Assuming small displacements, then the velocity field vector of any point P bounded by the rectangular region QRSV may be approximated by Equation 5.27.

$$\nu = \frac{P_f - P_i}{\tau} = \frac{f(x,y)}{\tau}\eta + \frac{g(x,y)}{\tau}\xi + \frac{h(x,y)}{\tau}\kappa \tag{5.27}$$

Where the time step (τ) is defined by Equation 5.28.

$$\tau = t_f - t_i \tag{5.28}$$

The unit vector (η) is parallel to the segment SR at any time, (ξ) is parallel to the segment SV at any time and (κ) is orthogonal to both (η) and (ξ) at any time. The extension of any point P, bounded by the region QRSV in the (η) direction over the time step (τ), and assuming small motions can be approximated using Equation 5.29.

$$f(x,y) = \max\left[0, \left(1 - \frac{x}{X_1}\right) \cdot \left(Q_f \cdot V_f - Q_i \cdot V_i\right)\right] \tag{5.29}$$

Where X is defined as less than or equal to X_1 and greater or equal to 0. Similarly, the extension of any point P in the (ξ) can be given by Equation 5.30, and assuming only membrane deflections then the extension in the (κ) direction is given by Equation 5.31.

$$g(x,y) = 0 \tag{5.30}$$

$$h(x,y) = 0 \tag{5.31}$$

Substitution of Equations 5.25 and 5.26 into Equation 5.29 yields:

$$f(x,y) = \max\left[0, \left(1 - \frac{x}{X_1}\right) \cdot \left[\left[X_1^2 + \left(WV_f - WQ_f\right)^2\right]^{\frac{1}{2}} - \left[X_1^2 + \left(WV_i - WQ_i\right)^2\right]^{\frac{1}{2}}\right]\right] \tag{5.32}$$

Substitution of Equations 5.30, 5.31 and 5.32 into Equation 5.27 yields the velocity flow field for the rectangular region QRSV given by Equation 5.33.

$$v = V_1 \cdot \eta \tag{5.33}$$

$$V_1 = \frac{\alpha_1}{\tau} \cdot \left(1 - \frac{x}{X_1}\right) \tag{5.34}$$

$$\alpha_1 = \max\left[0, \left[\left[X_1^2 + \left(WV_f - WQ_f\right)^2\right]^{\frac{1}{2}} - \left[X_1^2 + \left(WV_i - WQ_i\right)^2\right]^{\frac{1}{2}}\right]\right] \tag{5.35}$$

Using Equations 5.16 and 5.17 then the effective plastic strain rate and rate of energy dissipation over the time step are given by Equations 5.36 and 5.37 respectively.

$$\varepsilon_e = \left(\frac{2}{3}\right)^{\frac{1}{2}} \cdot \left(\frac{\alpha_1}{X_1 \cdot \tau}\right) \tag{5.36}$$

$$E = \sigma_y \cdot \int \varepsilon_e \, dv \tag{5.37}$$

Integrating Equation 5.37 over the time step (τ) yields the energy absorbed by the deflection of the rectangular region over the time step as given by Equation 5.38 where T is the uniform thickness of region QRSV.

$$E = \sigma_y \cdot T \cdot Y_1 \cdot \alpha_1 \cdot \sqrt{\frac{2}{3}} \tag{5.38}$$

To determine when the rectangular region QRSV fails (ruptures) and no longer absorbs energy, a rupture criterion is developed based upon Equation 5.5. Assume that rupture occurs when the total effective strain (insert symbol) is greater than some value of failure (rupture) strain (Φ = 10%) at any point P within the region QRSV. The total effective strain (the strain of the region from time t = 0 to t = f) can be given by Equation 5.39 derived in a similar method to Equation 5.36.

$$\varepsilon_{eff} = \left(\frac{1}{X_1}\right) \cdot \left[\left[X_1^2 + \left(WV_f - WQ_f\right)^2\right]^{\frac{1}{2}} - X_1\right] \cdot \sqrt{\frac{2}{3}} \tag{5.39}$$

Thus, for the rectangular region QRSV, the conditional statement of Equation 5.40 gives the energy dissipation over the time step.

$$E = \begin{cases} \sigma_y \cdot T \cdot Y_1 \cdot \alpha_1 \cdot \sqrt{\frac{2}{3}} & \text{if } \varepsilon_e < \psi \\ 0 & \text{otherwise} \end{cases} \tag{5.40}$$

5.4.3 Energy Absorption in Triangular Region

Similar to the development of the rectangular region energy absorption discussed in Section 5.4.2, the energy absorbed in the triangular region shown in Figure 5-57 is derived here. For the triangular region NRV of Figure 5-57, Point N is pinned and points R and V are only allowed movement in the z direction.

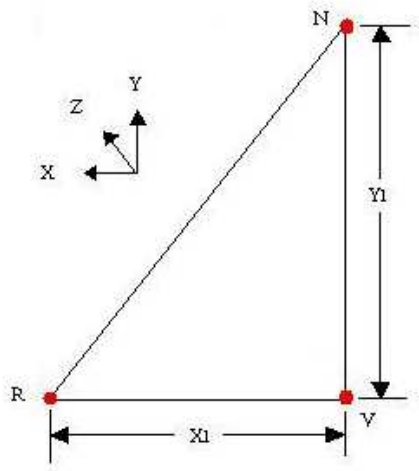

Figure 5-57 Triangular Region Geometry and Nomenclature

Again, the deflections of points V and R at time t = i and t = f from the initial V_0 and R_0 geometry are represented by WV_i, WV_f, WR_i and WR_f respectively, and the segment lengths between points at any time are given by:

$$R_0 \cdot V_0 = X_1 \tag{5.41}$$

$$N \cdot V_0 = Y_1 \tag{5.42}$$

$$N \cdot R_0 = \sqrt{X_1^2 + Y_1^2} \tag{5.43}$$

$$N\cdot R_i = \sqrt{WR_i^{\,2} + X_1^{\,2} + Y_1^{\,2}} \tag{5.44}$$

$$R_i\cdot V_i = \sqrt{X_1^{\,2} + \left(WV_i - WR_i\right)^2} \tag{5.45}$$

$$N\cdot V_i = \sqrt{WV_i^{\,2} + Y_1^{\,2}} \tag{5.46}$$

$$N\cdot R_f = \sqrt{WR_f^{\,2} + X_1^{\,2} + Y_1^{\,2}} \tag{5.47}$$

$$R_f\cdot V_f = \sqrt{X_1^{\,2} + \left(WV_f - WR_f\right)^2} \tag{5.48}$$

$$N\cdot V_f = \sqrt{WV_f^{\,2} + Y_1^{\,2}} \tag{5.49}$$

Again the vector velocity field may be approximated using Equation 5.27 where here the unit vector (η) is parallel to the segment RV at any time, (ξ) is parallel to the segment VN at any time and (κ) is orthogonal to both (η) and (ξ) at any time. The extension of any point P, bounded by the region NRV in the (η) direction over the time step (τ), and assuming small motions can be approximated using Equation 5.50.

$$f(x,y) = \left(1 - \frac{y}{Y_1}\right)\cdot\left(\frac{x}{X_1}\right)\cdot\max\left[0, \left(R_f\cdot V_f - R_i\cdot V_i\right)\right] \tag{5.50}$$

Similarly, the extension of any point P in the (ξ) direction can be given by Equation 5.51, and assuming only membrane deflections then the extension in the (κ) direction is given by Equation 5.54.

$$g(x,y) = \left(1 - \frac{y}{Y_1}\right)\cdot\left(\frac{x}{X_1}\right)\cdot\max\left[0, \left[\sqrt{\left(R_f\cdot V_f\right)^2 + \left(\Omega_1\right)} - \sqrt{\left(R_i\cdot V_i\right)^2 + \left(\Omega_2\right)}\right]\right] \tag{5.51}$$

$$\Omega_1 = \frac{Y_1^{\,2}\cdot\left(R_f\cdot V_f\right)^2}{\left(N\cdot R_0\right)^2\cdot\left(R_f\cdot V_f\right)^2 - \left[\left(R_f\cdot V_f\right)^2 - WV_f\cdot\left(WV_f - WR_f\right)\right]^2} \tag{5.52}$$

$$\Omega_2 = \frac{Y_1^{\,2}\cdot\left(R_i\cdot V_i\right)^2}{\left(N\cdot R_0\right)^2\cdot\left(R_i\cdot V_i\right)^2 - \left[\left(R_i\cdot V_i\right)^2 - WV_i\cdot\left(WV_i - WR_i\right)\right]^2} \tag{5.53}$$

$$h(x,y) = 0 \tag{5.54}$$

Substitution of Equations 5.50, 5.51 and 5.54 into Equation 5.27 yields the velocity flow field for the triangular region NRV given by Equations 5.55 through 5.61.

$$\nu = V_1 \cdot \eta + V_2 \cdot \xi \tag{5.55}$$

$$V_1 = \frac{\alpha_1}{\tau} \cdot \left(\frac{x}{X_1} \right) \cdot \left(1 - \frac{y}{Y_1} \right) \tag{5.56}$$

$$V_2 = \frac{\alpha_2}{\tau} \cdot \left(\frac{x}{X_1} \right) \cdot \left(1 - \frac{y}{Y_1} \right) \tag{5.57}$$

$$\alpha_1 = \max\left[0, \left[\sqrt{X_1^{\,2} + \left(WV_f - WR_f \right)^2} - \sqrt{X_1^{\,2} + \left(WV_i - WR_i \right)^2} \right] \right] \tag{5.58}$$

$$\alpha_2 = \max\left[0, \left[\sqrt{X_1^{\,2} + \left(WV_f - WR_f \right)^2 + \Psi_1} - \sqrt{X_1^{\,2} + \left(WV_i - WR_i \right)^2 + \Psi_2} \right] \right] \tag{5.59}$$

$$\Psi_1 = \frac{Y_1^{\,2} \cdot \left[X_1^{\,2} + \left(WV_f - WR_f \right)^2 \right]}{\left(Y_1^{\,2} + X_1^{\,2} \right) \cdot \left[X_1^{\,2} + \left(WV_f - WR_f \right)^2 \right] - \left[\left[X_1^{\,2} + \left(WV_f - WR_f \right)^2 \right] - WV_f \cdot \left(WV_f - WR_f \right) \right]^2} \tag{5.60}$$

$$\Psi_2 = \frac{Y_1^{\,2} \cdot \left[X_1^{\,2} + \left(WV_i - WR_i \right)^2 \right]}{\left(Y_1^{\,2} + X_1^{\,2} \right) \cdot \left[X_1^{\,2} + \left(WV_i - WR_i \right)^2 \right] - \left[\left[X_1^{\,2} + \left(WV_i - WR_i \right)^2 \right] - WV_i \cdot \left(WV_i - WR_i \right) \right]^2} \tag{5.61}$$

To reduce the number of independent variables in Equations 5.56 and 5.57, the independent variable X is replaced with the constant X_{ave} given by Equation 5.62.

$$X_{ave} = \frac{1}{Y_1} \cdot \int_0^{Y_1} \left(\frac{1}{X_1} \cdot \int_0^{X_1} x \, dx \right) dy = \frac{X_1}{4} \tag{5.62}$$

Using Equation 5.62 then Equations 5.56 and 5.57 simplify to:

$$V_1 = \frac{\alpha_1}{4\cdot\tau}\cdot\left(1 - \frac{y}{Y_1}\right) \tag{5.63}$$

$$V_2 = \frac{\alpha_2}{4\cdot\tau}\cdot\left(1 - \frac{y}{Y_1}\right) \tag{5.64}$$

Using Equations 5.16 and 5.17 then the effective plastic strain rate and rate of energy dissipation over the time step are given by Equations 5.65 and 5.66 respectively.

$$\varepsilon_e = \frac{1}{4\cdot\tau\cdot Y_1}\cdot\sqrt{\frac{2}{3}\cdot\left(\alpha_2^{\,2} + \frac{\alpha_1^{\,2}}{2}\right)} \tag{5.65}$$

$$E = \frac{\sigma_y\cdot T\cdot X_1}{8\cdot\tau}\cdot\sqrt{\frac{2}{3}\cdot\left(\alpha_2^{\,2} + \frac{\alpha_1^{\,2}}{2}\right)} \tag{5.66}$$

Integrating Equation 5.66 over the time step (τ) yields the energy absorbed by the deflection of the rectangular region over the time step as given by Equation 5.67.

$$E = \frac{\sigma_y\cdot T\cdot X_1}{8}\cdot\sqrt{\frac{2}{3}\cdot\left(\alpha_2^{\,2} + \frac{\alpha_1^{\,2}}{2}\right)} \tag{5.67}$$

To determine when the triangular region NRV fails (ruptures) and no longer absorbs energy, a rupture criterion is developed based upon Equation 5.5. Again, assume that rupture occurs when the total effective strain (ε_{eff}) is greater than some value of failure (rupture) strain ($\Phi = 10\%$) at any point P within the region NRV. The total effective strain (the strain of the region from time t = 0 to t = f) can be given by Equation 5.68 derived in a similar method to Equation 5.65.

$$\varepsilon_{eff} = \frac{1}{4 \cdot Y_1} \cdot \sqrt{\frac{2}{3} \cdot \left(\Gamma_2^{\,2} + \frac{\Gamma_1^{\,2}}{2} \right)} \tag{5.68}$$

$$\Gamma_1 = \left[\left(WV_f - WR_f \right)^2 + X_1^{\,2} \right]^{\frac{1}{2}} - X_1 \tag{5.69}$$

$$\Gamma_2 = \sqrt{X_1^{\,2} + \left(WV_f - WR_f \right)^2 + \Psi_1} - \sqrt{X_1^{\,2} + 1} \tag{5.70}$$

Thus, for the triangular region NRV, the conditional statement of Equation 5.71 gives the energy dissipation over the time step.

$$E = \begin{cases} \dfrac{\sigma_y \cdot T \cdot X_1}{8} \cdot \sqrt{\dfrac{2}{3} \left(\alpha_2^{\,2} + \dfrac{\alpha_1^{\,2}}{2} \right)} & \text{if } \varepsilon_{eff} < \Psi \\ 0 \quad \text{otherwise} \end{cases} \tag{5.71}$$

5.4.4 The Energy Absorbed from an Eight-Region Plate

Returning the example of Section 5.4 relating to Figure 5-55, the eight-region plate, and using the derivations of the energy absorbed in rectangular and triangular regions in Sections 5.4.2 and 5.4.3 respectively, then the energy absorbed by the plate of Figure 5-55 over the time step (τ) is given by Equation 5.72.

$$E_{P\tau} = E_I + E_{II} + E_{III} + E_{IV} + E_V + E_{VI} + E_{VII} + E_{VIII} \tag{5.72}$$

Examination of the plate of Figure 5-55 the following conditional statements as to the strength of the plate are expressed in Equation 5.73.

$$E_{P\tau} = \begin{cases} 0 \text{ if } \lambda_I = 0 \\ \frac{E_I}{2} + E_{IV} + E_V + E_{VI} + E_{VII} + E_{VIII} \text{ if } \lambda_{II} = 0 \\ \frac{E_I}{2} + E_{IV} + E_V + E_{VI} + E_{VII} + E_{VIII} \text{ if } \lambda_{III} = 0 \\ E_I + E_{II} + E_{III} + E_{VII} + E_{VIII} \text{ if } \lambda_{IV} = 0 \\ E_I + E_{II} + E_{III} + E_{VII} + E_{VIII} \text{ if } \lambda_V = 0 \\ E_I + E_{II} + E_{III} + E_{VII} + E_{VIII} \text{ if } \lambda_{VI} = 0 \\ \frac{E_I}{2} + E_{II} + E_{III} + E_{IV} + E_V + E_{VI} \text{ if } \lambda_{VII} = 0 \\ \frac{E_I}{2} + E_{II} + E_{III} + E_{IV} + E_V + E_{VI} \text{ if } \lambda_{VIII} = 0 \end{cases} \quad (5.73)$$

Where (λ_i) is a rupture indicator for each region (i = I, II, III, IV, V, VI, VII and VIII) expressed by Equation 5.74.

$$\lambda_i = \begin{cases} 1 \text{ if } \varepsilon_{eff} < \Psi \\ 0 \text{ otherwise} \end{cases} \quad (5.74)$$

Using the conditional statements of Equation 5.73 then:

$$\lambda_{II} = \lambda_{III} \quad (5.75)$$

$$\lambda_{IV} = \lambda_V = \lambda_{VI} \quad (5.76)$$

$$\lambda_{VII} = \lambda_{VIII} \quad (5.77)$$

Using the four independent rupture indicators (λ_I, λ_{II}, λ_{IV} and λ_{VII}) and the conditional statements of Equation 5.73 then the energy absorbed by the eight-region plate of Figure 5-55 over the time step (τ) is:

$$E_{P\tau} = \lambda_I \cdot \left[\frac{\lambda_{II} \cdot \lambda_{III} + \lambda_{VII} \cdot \lambda_{VIII}}{2} \cdot E_I + \lambda_{II} \cdot \lambda_{III} \cdot (E_{II} + E_{III}) + \lambda_{IV} \cdot \lambda_V \cdot \lambda_{VI} \cdot (E_{IV} + E_V + E_{VI}) + \lambda_{VII} \cdot \lambda_{VIII} (E_{VII} + E_{VIII}) \right] \ldots$$

$$\ldots \min\left[1, (\lambda_{II} \cdot \lambda_{III} + \lambda_{IV} \cdot \lambda_V \cdot \lambda_{VI}) \cdot (\lambda_{II} \cdot \lambda_{III} + \lambda_{VII} \cdot \lambda_{VIII}) \cdot (\lambda_{VII} \cdot \lambda_{VIII} + \lambda_{IV} \cdot \lambda_V \cdot \lambda_{VI})\right] \quad (5.78)$$

Summation of the energy absorbed per time step over all time steps between time equal to zero seconds to some time (T) seconds yields the total absorbed energy at any time given by Equation 5.79.

$$E_T = \sum_{\tau=1}^{T} E_{P\tau} \quad (5.79)$$

Using the external dynamics model of SIMCOL and using initial conditions from Table 5-5, Figure 5-58 provides results for the eight-region plate model as compared to a finite element solution of the same plate subject to the same boundary conditions using an element mesh size of 250 mm.

Table 5-5 Eight Region Plate Analysis Initial Conditions

Initial Conditions		
Variable	**Value**	**Unit**
Initial Velocity in Z Direction	3	m/s
Analysis Time Step	0.0001	s
Rigid Wedge Mass	50228.4	kg
A	7.5	m
B	10	m
F	5.5	m
G	1.5	m
D	0.75	m

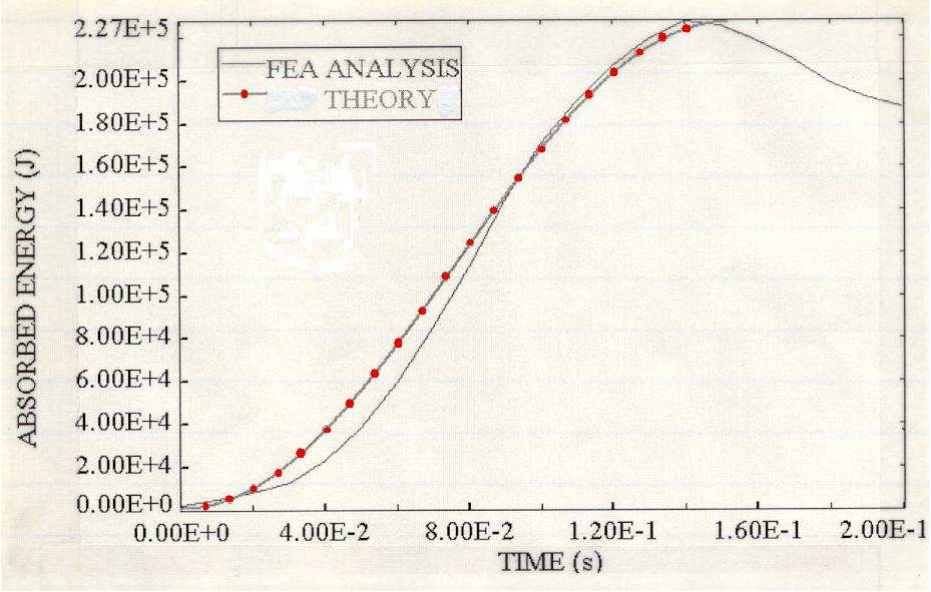

Figure 5-58 Eight Region Plate Absorbed Energy vs. Time Comparison to FEA

The results of the analysis in Figure 5-58 compare well with the finite element solution having a correlation coefficient as calculated by Equation 5.1 of 0.893. The largest difference in the results occurs between t = 0.02 and t = 0.085 seconds due to elastic bending of the plate in the finite element method which is not accounted for in the simplified theory.

While the preceding eight region plate example shows the applicability of the plastic membrane approach to the determination of the energy absorbed from the lateral deflection of transverse bulkheads and plates, to properly use the theory in SIMCOL a new formulation of Equation 5.78 based on twenty five regions is required to accommodate all the possible contact scenarios and an initial velocity vector V_0 which has components both parallel and orthogonal to the plate.

5.4.5 The Energy Absorbed from a Twenty-Five-Region Plate

The eight-panel model of Figure 5-55 is not applicable for contact scenarios 1, 3 or 4 or for contact scenario 2 with both V_X and V_Z initial velocity. For these scenarios a minimum of twenty-five regions is necessary to accurately capture the deformation patterns shown in Figure 5-32 through Figure 5-35, Figure 5-41 through Figure 5-44, Figure 5-46 through Figure 5-48 or Figure 5-59 where the twenty five regions overlay Figure 5-59.

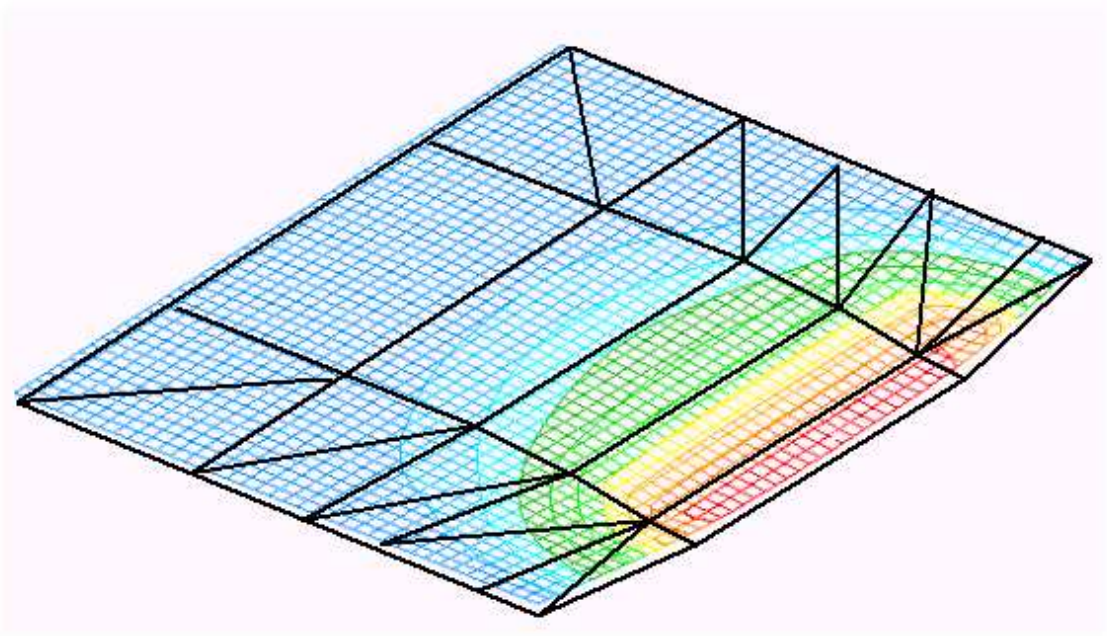

Figure 5-59 Twenty-five Region Plate Overlaying FEA Plate Mesh Deformation

To simplify the task of developing a general Equation for the determination of the total energy absorbed over a time step (τ) the following two additional assumptions are made for convenience:

- For contact scenario 2, the angle (φ) always equals zero degrees, i.e. if the angle (φ) is less than zero degrees then treat the analysis as if (φ) equals zero degrees.
- For contact scenario 4, the angle (α) always equals zero degrees, i.e. if the angle (α) is less than zero degrees then treat the analysis as if (α) equals zero degrees.

Using these two assumptions, the deflections at the outboard edge of the plate of Figure 5-60 (segment HP) will always be equal to the maximum deflection of the plate. Accounting for all four contact scenarios, then after a small time step, a linear form of the deflection of the plate of Figure 5-29 may be represented with twenty five regions as shown in Figure 5-60.

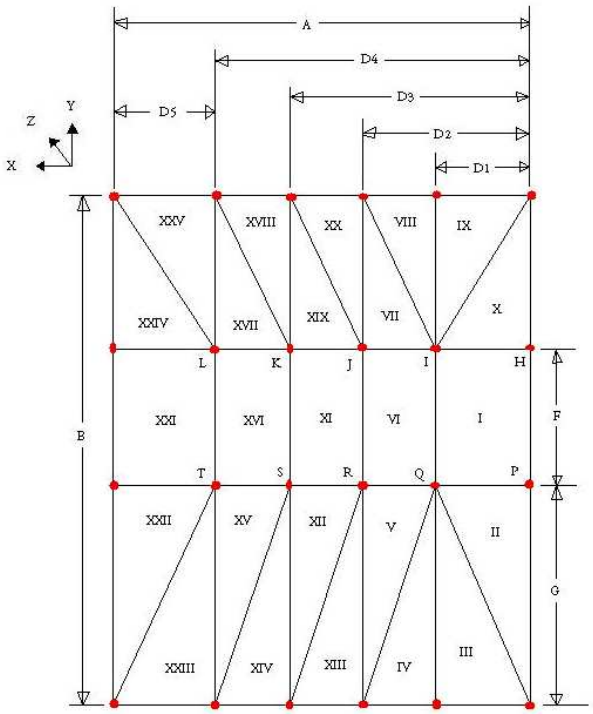

Figure 5-60 Twenty-five Region Plate Geometry

In Figure 5-60, regions I, VI and XI represent the initial contact area between the plate and the striking wedge at time t = i and the deflections of points H, I, J, K and L are equal to the deflections of points P, Q, R, S and T respectively at any time.

With the plate formulation of Figure 5-60, then the total energy absorbed by the plate over a time step may be written as the sum of the energy absorbed due to the translation in the z direction and the energy absorbed due to the motion of the hinge lines in the x direction as is given by Equation 5.80.

$$E_{P\tau} = E_{Z\tau} + E_{X\tau} \qquad (5.80)$$

Equation 5.80 effectively decouples the energy absorbed by the plate such that the motion of the rigid wedge over a small time step may be characterized as either an incremental step in the z direction followed by an incremental step in the x direction or as an increment al step in the x direction followed by an incremental step in the z direction. The choice of the initial step direction

(x or z) is based on the greater of the available kinetic energy in either the x or z directions, which simplifies to the greater velocity component in the x or z direction. Thus if the component of the velocity in the x direction (V_x) is greater than the component of the velocity in the z direction (V_z) then the incremental step in the x direction is followed by an incremental step in the z direction. If, however, V_z is greater than V_x then the incremental step in the z direction is followed by an incremental step in the x direction. The total energy absorbed by the plate of Figure 5-60 is much more complicated than the plate of Figure 5-55 as previously determined in Section 5.4.4, however, the same method as used in Section 5.4.4 applies to the twenty five region plate of Figure 5-60.

Using the method of rupture indicators, as discussed in Section 5.4.4, the following conditional statements for the twenty-five-region plate can be made:

$$E_{Z\tau} = E_{X\tau} = \begin{cases} \sum_{i=III}^{IX} E_i + \sum_{i=XI}^{XXV} E_i \ \text{ if } \lambda_I = 0 \\ \frac{E_I}{2} + E_{III} + \sum_{i=IV}^{XXV} E_i \ \text{ if } \lambda_{II} = 0 \\ E_I + E_{II} + \sum_{i=V}^{XXV} E_i \ \text{ if } \lambda_{III} = 0 \\ E_I + E_{II} + \sum_{i=V}^{XXV} E_i \ \text{ if } \lambda_{IV} = 0 \\ \sum_{i=I}^{IV} E_i + \sum_{i=VI}^{XXV} E_i \ \text{ if } \lambda_V = 0 \\ \sum_{i=I}^{IV} E_i + \sum_{i=VIII}^{XXV} E_i \ \text{ if } \lambda_{VI} = 0 \\ \sum_{i=I}^{VI} E_i + \sum_{i=VIII}^{XXV} E_i \ \text{ if } \lambda_{VII} = 0 \\ \sum_{i=I}^{VII} E_i + \sum_{i=X}^{XXV} E_i \ \text{ if } \lambda_{VIII} = 0 \\ \sum_{i=I}^{VII} E_i + \sum_{i=X}^{XXV} E_i \ \text{ if } \lambda_{IX} = 0 \\ \frac{E_I}{2} + \sum_{i=II}^{IX} E_i + \sum_{i=XI}^{XXV} E_i \ \text{ if } \lambda_X = 0 \\ \sum_{i=I}^{X} E_i + \sum_{i=XIII}^{XVIII} E_i + \sum_{i=XX}^{XXV} E_i \ \text{ if } \lambda_{XI} = 0 \\ \sum_{i=I}^{XI} E_i + \sum_{i=XIII}^{XXV} E_i \ \text{ if } \lambda_{XII} = 0 \\ \sum_{i=I}^{IV} E_i + \sum_{i=VI}^{XII} E_i + \sum_{i=XIV}^{XXV} E_i \ \text{ if } \lambda_{XIII} = 0 \\ \sum_{i=I}^{XI} E_i + E_{XIII} + \sum_{i=XV}^{XXV} E_i \ \text{ if } \lambda_{XIV} = 0 \\ \sum_{i=I}^{XIV} E_i + \sum_{i=XVI}^{XXV} E_i \ \text{ if } \lambda_{XV} = 0 \\ \sum_{i=I}^{XIV} E_i + \sum_{i=XVIII}^{XXV} E_i \ \text{ if } \lambda_{XVI} = 0 \\ \sum_{i=I}^{XVI} E_i + \sum_{i=XVIII}^{XXV} E_i \ \text{ if } \lambda_{XVII} = 0 \\ \sum_{i=I}^{XVII} E_i + \sum_{i=XX}^{XXV} E_i \ \text{ if } \lambda_{XVIII} = 0 \\ \sum_{i=I}^{XVIII} E_i + \sum_{i=XX}^{XXV} E_i \ \text{ if } \lambda_{XIX} = 0 \\ \sum_{i=I}^{VI} E_i + \sum_{i=VIII}^{XIX} E_i + \sum_{i=XXI}^{XXV} E_i \ \text{ if } \lambda_{XX} = 0 \\ E_{XXIII} + E_{XXV} + \sum_{i=I}^{VI} E_i \ \text{ if } \lambda_{XXI} = 0 \\ \sum_{i=I}^{XXI} E_i + \sum_{i=XXIII}^{XXV} E_i \ \text{ if } \lambda_{XXII} = 0 \\ E_{XXIV} + E_{XXV} + \sum_{i=I}^{XIV} E_i + \sum_{i=XVI}^{XXII} E_i \ \text{ if } \lambda_{XXIII} = 0 \\ E_{XXV} + \sum_{i=I}^{XXIII} E_i \ \text{ if } \lambda_{XIV} = 0 \\ \sum_{i=I}^{XVI} E_i + \sum_{i=XVIII}^{XXIV} E_i \ \text{ if } \lambda_{XV} = 0 \end{cases} \tag{5.81}$$

Using the conditional statements of Equation 5.81 then the relations of Equations 5.82 and 5.83 are true.

$$\lambda_{III} = \lambda_{IV} \tag{5.82}$$

$$\lambda_{VIII} = \lambda_{IX} \tag{5.83}$$

Additionally, critical combinations of the rupture indicators lead to the following additional conditional statements:

$$\left(\lambda_{IV} = 0\right) \text{ if } \lambda_{III} = 0 \tag{5.84}$$

$$\left(\lambda_{III} = 0\right) \text{ if } \lambda_{IV} = 0 \tag{5.85}$$

$$\left(\lambda_{IX} = 0\right) \text{ if } \lambda_{VIII} = 0 \tag{5.86}$$

$$\left(\lambda_{VIII} = 0\right) \text{ if } \lambda_{IX} = 0 \tag{5.87}$$

$$\left(\lambda_{II} = \lambda_{X} = 0\right) \text{ if } \lambda_{I} = 0 \tag{5.88}$$

$$\left(\lambda_{VII} = \lambda_{V} = 0\right) \text{ if } \lambda_{VI} = 0 \tag{5.89}$$

$$\left(\lambda_{XII} = \lambda_{XIX} = 0\right) \text{ if } \lambda_{XI} = 0 \tag{5.90}$$

$$\left(\lambda_{XVII} = \lambda_{XV} = 0\right) \text{ if } \lambda_{XVI} = 0 \tag{5.91}$$

$$\left(\lambda_{XXII} = \lambda_{XXIV} = 0\right) \text{ if } \lambda_{XXI} = 0 \tag{5.92}$$

$$\left(\lambda_{V} = 0\right) \text{ if } \lambda_{XIII} = 0 \tag{5.93}$$

$$\left(\lambda_{XII} = 0\right) \text{ if } \lambda_{XIV} = 0 \tag{5.94}$$

$$\left(\lambda_{XV} = 0\right) \text{ if } \lambda_{XXIII} = 0 \tag{5.95}$$

$$(\lambda_{VII} = 0) \text{ if } \lambda_{XX} = 0 \tag{5.96}$$

$$(\lambda_{XIX} = 0) \text{ if } \lambda_{XVIII} = 0 \tag{5.97}$$

$$(\lambda_{XVII} = 0) \text{ if } \lambda_{XXV} = 0 \tag{5.98}$$

$$(\lambda_{VI} = \lambda_{VII} = 0) \text{ if } \begin{vmatrix} \lambda_{V} = 0 \\ \lambda_{XIII} = 1 \end{vmatrix} \tag{5.99}$$

$$(\lambda_{XI} = \lambda_{XIX} = 0) \text{ if } \begin{vmatrix} \lambda_{XII} = 0 \\ \lambda_{XIV} = 1 \end{vmatrix} \tag{5.100}$$

$$(\lambda_{XVI} = \lambda_{XVII} = 0) \text{ if } \begin{vmatrix} \lambda_{XV} = 0 \\ \lambda_{XXIII} = 1 \end{vmatrix} \tag{5.101}$$

$$(\lambda_{VI} = \lambda_{V} = 0) \text{ if } \begin{vmatrix} \lambda_{VII} = 0 \\ \lambda_{XX} = 1 \end{vmatrix} \tag{5.102}$$

$$(\lambda_{XI} = \lambda_{XII} = 0) \text{ if } \begin{vmatrix} \lambda_{XIX} = 0 \\ \lambda_{XVIII} = 1 \end{vmatrix} \tag{5.103}$$

$$(\lambda_{XV} = \lambda_{XVI} = 0) \text{ if } \begin{vmatrix} \lambda_{XVII} = 0 \\ \lambda_{XXV} = 1 \end{vmatrix} \tag{5.104}$$

Using all the above conditional statements, Equations 5.84 through 5.104, then for each region the following conditional equations apply.

$$E_I = \begin{cases} 0 \text{ if } \begin{cases} \lambda_I = 0 \\ \text{or}(\lambda_{II} = \lambda_X = 0) \\ \text{or}(\lambda_{II} = \lambda_{III} = \lambda_{VI} = 0) \\ \text{or}(\lambda_X = \lambda_{IX} = \lambda_{VI} = 0) \\ \text{or}(\lambda_{II} = \lambda_{III} = \lambda_{XIII} = \lambda_{XI} = 0) \\ \text{or}(\lambda_X = \lambda_{IX} = \lambda_{XX} = \lambda_{XI} = 0) \\ \text{or}(\lambda_{II} = \lambda_{III} = \lambda_V = 0) \text{ and } (\lambda_{XIII} = 1) \\ \text{or}(\lambda_X = \lambda_{IX} = \lambda_{VII} = 0) \text{ and } (\lambda_{XX} = 1) \\ \text{or}(\lambda_{II} = \lambda_{III} = \lambda_{XIII} = \lambda_{XIV} = \lambda_{XVI} = 0) \\ \text{or}(\lambda_X = \lambda_{IX} = \lambda_{XX} = \lambda_{XVIII} = \lambda_{XVI} = 0) \\ \text{or}(\lambda_{II} = \lambda_{III} = \lambda_{XIII} = \lambda_{XII} = 0) \text{ and } (\lambda_{XIV} = 1) \\ \text{or}(\lambda_X = \lambda_{IX} = \lambda_{XX} = \lambda_{XIX} = 0) \text{ and } (\lambda_{XVIII} = 1) \\ \text{or}(\lambda_{II} = \lambda_{III} = \lambda_{XIII} = \lambda_{XIV} = \lambda_{XV} = 0) \text{ and } (\lambda_{XXIII} = 1) \\ \text{or}(\lambda_X = \lambda_{IX} = \lambda_{XX} = \lambda_{XVIII} = \lambda_{XVII} = 0) \text{ and } (\lambda_{XXV} = 1) \\ \text{or}(\lambda_{II} = \lambda_{III} = \lambda_{XIII} = \lambda_{XIV} = \lambda_{XXIII} = \lambda_{XXI} = 0) \\ \text{or}(\lambda_X = \lambda_{IX} = \lambda_{XX} = \lambda_{XVIII} = \lambda_{XXV} = \lambda_{XXI} = 0) \end{cases} \\ \frac{E_I}{2} \text{ if } \begin{cases} \lambda_X = 0 \\ \text{or}(\lambda_{II} = 0) \end{cases} \end{cases} \tag{5.105}$$

$$E_{II} = 0 \text{ if } \begin{cases} \lambda_{II} = 0 \\ \text{or}(\lambda_X = 0) \end{cases} \tag{5.106}$$

$$E_{III} = 0 \text{ if } \begin{cases} \lambda_{III} = 0 \\ \text{or}(\lambda_{IV} = 0) \end{cases} \tag{5.107}$$

$$E_{IV} = 0 \text{ if } \begin{cases} \lambda_{IV} = 0 \\ \text{or}(\lambda_{III} = 0) \end{cases} \tag{5.108}$$

$$E_V = 0 \text{ if } \begin{cases} \lambda_V = 0 \\ \text{or}(\lambda_{VI} = 0) \\ \text{or}(\lambda_{XIII} = 0) \end{cases} \tag{5.109}$$

$$
E_{VI} = \begin{cases} 0 \text{ if } \begin{cases} \lambda_{VI} = 0 \\ \text{or}\left(\lambda_{V} = 0\right) \text{and} \left(\lambda_{XIII} = 1\right) \\ \text{or}\left(\lambda_{VII} = 0\right) \text{and} \left(\lambda_{XX} = 1\right) \\ \text{or}\left(\lambda_{II} = \lambda_{III} = \lambda_{XIII} = \lambda_{XI} = 0\right) \\ \text{or}\left(\lambda_{X} = \lambda_{IX} = \lambda_{XX} = \lambda_{XI} = 0\right) \\ \text{or}\left(\lambda_{II} = \lambda_{III} = \lambda_{XIII} = \lambda_{XIV} = \lambda_{XVI} = 0\right) \\ \text{or}\left(\lambda_{X} = \lambda_{IX} = \lambda_{XX} = \lambda_{XVIII} = \lambda_{XVI} = 0\right) \\ \text{or}\left(\lambda_{X} = \lambda_{IX} = \lambda_{VII} = 0\right) \text{and} \left(\lambda_{XX} = 1\right) \\ \text{or}\left(\lambda_{II} = \lambda_{III} = \lambda_{XIII} = \lambda_{XII} = 0\right) \text{and} \left(\lambda_{XIV} = 1\right) \\ \text{or}\left(\lambda_{X} = \lambda_{IX} = \lambda_{XX} = \lambda_{XIX} = 0\right) \text{and} \left(\lambda_{XVIII} = 1\right) \\ \text{or}\left(\lambda_{II} = \lambda_{III} = \lambda_{XIII} = \lambda_{XIV} = \lambda_{XV} = 0\right) \text{and} \left(\lambda_{XXIII} = 1\right) \\ \text{or}\left(\lambda_{X} = \lambda_{IX} = \lambda_{XX} = \lambda_{XVIII} = \lambda_{XVII} = 0\right) \text{and} \left(\lambda_{XXV} = 1\right) \\ \text{or}\left(\lambda_{II} = \lambda_{III} = \lambda_{XIII} = \lambda_{XIV} = \lambda_{XXIII} = \lambda_{XXI} = 0\right) \\ \text{or}\left(\lambda_{X} = \lambda_{IX} = \lambda_{XX} = \lambda_{XVIII} = \lambda_{XXV} = \lambda_{XXI} = 0\right) \end{cases} \\ \frac{E_{VI}}{2} \text{ if } \begin{cases} \lambda_{I} = \lambda_{III} = \lambda_{XX} = 0 \\ \text{or}\left(\lambda_{I} = \lambda_{IX} = \lambda_{XX} = 0\right) \\ \text{or}\left(\lambda_{XX} = \lambda_{XI} = 0\right) \\ \text{or}\left(\lambda_{XIII} = \lambda_{XI} = 0\right) \end{cases} \end{cases} \tag{5.110}
$$

$$
E_{VII} = 0 \text{ if } \begin{cases} \lambda_{VII} = 0 \\ \text{or}\left(\lambda_{XX} = 0\right) \\ \text{or}\left(\lambda_{VI} = 0\right) \end{cases} \tag{5.111}
$$

$$
E_{VIII} = 0 \text{ if } \begin{cases} \lambda_{VIII} = 0 \\ \text{or}\left(\lambda_{IX} = 0\right) \end{cases} \tag{5.112}
$$

$$
E_{IX} = 0 \text{ if } \begin{cases} \lambda_{IX} = 0 \\ \text{or}\left(\lambda_{VIII} = 0\right) \end{cases} \tag{5.113}
$$

$$E_X = 0 \text{ if } \begin{cases} \lambda_X = 0 \\ \text{or}\left(\lambda_I = 0\right) \end{cases} \tag{5.114}$$

$$E_{XI} = \begin{cases} 0 \text{ if } \begin{cases} \lambda_{XI} = 0 \\ \text{or}\left(\lambda_{XII} = 0\right) \text{and}\left(\lambda_{XIV} = 1\right) \\ \text{or}\left(\lambda_{XIX} = 0\right) \text{and}\left(\lambda_{XVIII} = 1\right) \\ \text{or}\left(\lambda_{II} = \lambda_{III} = \lambda_{XIII} = \lambda_{XIV} = \lambda_{XVI} = 0\right) \\ \text{or}\left(\lambda_X = \lambda_{IX} = \lambda_{XX} = \lambda_{XVIII} = \lambda_{XVI} = 0\right) \\ \text{or}\left(\lambda_{II} = \lambda_{III} = \lambda_{XIII} = \lambda_{XIV} = \lambda_{XV} = 0\right) \text{and}\left(\lambda_{XXIII} = 1\right) \\ \text{or}\left(\lambda_X = \lambda_{IX} = \lambda_{XX} = \lambda_{XVIII} = \lambda_{XVII} = 0\right) \text{and}\left(\lambda_{XXV} = 1\right) \\ \text{or}\left(\lambda_{II} = \lambda_{III} = \lambda_{XIII} = \lambda_{XIV} = \lambda_{XXIII} = \lambda_{XXI} = 0\right) \\ \text{or}\left(\lambda_X = \lambda_{IX} = \lambda_{XX} = \lambda_{XVIII} = \lambda_{XXV} = \lambda_{XXI} = 0\right) \end{cases} \\ \frac{E_{XI}}{2} \text{ if } \begin{cases} \lambda_I = \lambda_{III} = \lambda_{VI} = \lambda_{XIII} = \lambda_{XIV} = 0 \\ \text{or}\left(\lambda_I = \lambda_{IX} = \lambda_{VI} = \lambda_{XX} = \lambda_{XVIII} = 0\right) \\ \text{or}\left(\lambda_{XVIII} = \lambda_{XVI} = 0\right) \\ \text{or}\left(\lambda_{XIV} = \lambda_{XVI} = 0\right) \end{cases} \end{cases} \tag{5.115}$$

$$E_{XII} = 0 \text{ if } \begin{cases} \lambda_{XII} = 0 \\ \text{or}\left(\lambda_{XI} = 0\right) \\ \text{or}\left(\lambda_{XIV} = 0\right) \end{cases} \tag{5.116}$$

$$E_{XIII} = 0 \text{ if } \lambda_{XIII} = 0 \tag{5.117}$$

$$E_{XIV} = 0 \text{ if } \lambda_{XIV} = 0 \tag{5.118}$$

$$E_{XV} = 0 \text{ if } \begin{cases} \lambda_{XV} = 0 \\ \text{or}\left(\lambda_{XXIII} = 0\right) \\ \text{or}\left(\lambda_{XVI} = 0\right) \end{cases} \tag{5.119}$$

$$E_{XVI} = \begin{cases} 0 \text{ if } \begin{cases} \lambda_{XVI} = 0 \\ \text{or}\left(\lambda_{XV} = 0\right) \text{and} \left(\lambda_{XXIII} = 1\right) \\ \text{or}\left(\lambda_{XVII} = 0\right) \text{and} \left(\lambda_{XXV} = 1\right) \\ \text{or}\left(\lambda_{II} = \lambda_{III} = \lambda_{XIII} = \lambda_{XIV} = \lambda_{XXIII} = \lambda_{XXI} = 0\right) \\ \text{or}\left(\lambda_{X} = \lambda_{IX} = \lambda_{XX} = \lambda_{XVIII} = \lambda_{XXV} = \lambda_{XXI} = 0\right) \end{cases} \\ \dfrac{E_{XVI}}{2} \text{ if } \begin{cases} \lambda_{I} = \lambda_{III} = \lambda_{VI} = \lambda_{XI} = \lambda_{XIV} = \lambda_{XXIII} = 0 \\ \text{or}\left(\lambda_{I} = \lambda_{III} = \lambda_{VI} = \lambda_{XI} = \lambda_{XVIII} = \lambda_{XXV} = 0\right) \\ \text{or}\left(\lambda_{XXI} = \lambda_{XXV} = 0\right) \\ \text{or}\left(\lambda_{XXI} = \lambda_{XXIII} = 0\right) \end{cases} \end{cases} \tag{5.120}$$

$$E_{XVII} = 0 \text{ if } \begin{cases} \lambda_{XVII} = 0 \\ \text{or}\left(\lambda_{XVI} = 0\right) \\ \text{or}\left(\lambda_{XXV} = 0\right) \end{cases} \tag{5.121}$$

$$E_{XVIII} = 0 \text{ if } \lambda_{XVIII} = 0 \tag{5.122}$$

$$E_{XIX} = 0 \text{ if } \begin{cases} \lambda_{XIX} = 0 \\ \text{or}\left(\lambda_{XVIII} = 0\right) \\ \text{or}\left(\lambda_{XI} = 0\right) \end{cases} \tag{5.123}$$

$$E_{XX} = 0 \text{ if } \lambda_{XX} = 0 \tag{5.124}$$

$$E_{XXI} = 0 \text{ if } \lambda_{XXI} = 0 \tag{5.125}$$

$$E_{XXII} = 0 \text{ if } \begin{cases} \lambda_{XXII} = 0 \\ \text{or}\left(\lambda_{XXI} = 0\right) \end{cases} \tag{5.126}$$

$$E_{XXIII} = 0 \text{ if } \lambda_{XXIII} = 0 \tag{5.127}$$

$$E_{XXIV} = 0 \quad \text{if} \quad \begin{cases} \lambda_{XXIV} = 0 \\ \text{or}\left(\lambda_{XXI} = 0\right) \end{cases} \tag{5.128}$$

$$E_{XXV} = 0 \quad \text{if} \quad \lambda_{XXV} = 0 \tag{5.129}$$

Using Equations 5.105 through 5.129 then the formulation of ($E_{x\tau}$) or ($E_{z\tau}$) may be given by Equation 5.130.

$$\begin{aligned} E_{X\tau} = E_{Z\tau} = {} & \lambda_0 \cdot \left(\lambda_1 \cdot E_I + \lambda_6 \cdot E_{VI} + \lambda_{11} \cdot E_{XI} + \lambda_{16} \cdot E_{XVI} + \lambda_{21} \cdot E_{XXI}\right) + ... \\ .... + {} & \lambda_0 \cdot \lambda_{YL} \cdot \left(\lambda_2 \cdot E_{II} + \lambda_3 \cdot E_{III} + \lambda_4 \cdot E_{IV} + \lambda_5 \cdot E_V + \lambda_{13} \cdot E_{XIII}\right) + ... \\ .... + {} & \lambda_0 \cdot \lambda_{YL} \cdot \left(\lambda_{12} \cdot E_{XII} + \lambda_{14} \cdot E_{XIV} + \lambda_{15} \cdot E_{XV} + \lambda_{23} \cdot E_{XXIII} + \lambda_{22} \cdot E_{XXII}\right) + ... \\ .... + {} & \lambda_0 \cdot \lambda_{YU} \cdot \left(\lambda_{10} \cdot E_X + \lambda_9 \cdot E_{IX} + \lambda_8 \cdot E_{VIII} + \lambda_7 \cdot E_{VII} + \lambda_{20} \cdot E_{XX}\right) + ... \\ .... + {} & \lambda_0 \cdot \lambda_{YU} \cdot \left(\lambda_{19} \cdot E_{XIX} + \lambda_{18} \cdot E_{XVIII} + \lambda_{17} \cdot E_{XVII} + \lambda_{25} \cdot E_{XXV} + \lambda_{24} \cdot E_{XXIV}\right) \end{aligned} \tag{5.130}$$

All of the rupture indicator terms of Equation 5.130 are defined by Equations 5.131 through 5.187.

$$\lambda_I = \left(\frac{\lambda_{II} + \lambda_X}{2}\right) \cdot \min\left[1, \lambda_1 \cdot \lambda_A \cdot \left[\left(\lambda_{II} + \lambda_{III} + \lambda_{VI}\right) \cdot \left(\lambda_X + \lambda_{VI} + \lambda_{IX}\right) \cdot \left(\lambda_{II} + \lambda_{III} + \lambda_{XIII} + \lambda_{XI}\right) \cdot \lambda_{Z1}\right]\right] \tag{5.131}$$

$$\lambda_{ZI} = \left(\lambda_X + \lambda_{IX} + \lambda_{XX} + \lambda_{XI}\right)\left(\lambda_{II} + \lambda_{III} + \lambda_{XIII} + \lambda_{XIV} + \lambda_{XVI}\right)\left(\lambda_X + \lambda_{IX} + \lambda_{XX} + \lambda_{XVIII} + \lambda_{XVI}\right)\left(\lambda_{Z2}\right) \tag{5.132}$$

$$\lambda_{Z2} = \left(\lambda_{II} + \lambda_{III} + \lambda_{XIII} + \lambda_{XIV} + \lambda_{XXIII} + \lambda_{XXI}\right) \cdot \left(\lambda_X + \lambda_{IX} + \lambda_{XX} + \lambda_{XVIII} + \lambda_{XXV} + \lambda_{XXI}\right) \tag{5.133}$$

$$\lambda_A = \left[\lambda_{II} + \lambda_{III} + \lambda_V + \left(1 - \lambda_{XIII}\right)\right]\left[\lambda_X + \lambda_{IX} + \lambda_{VII} + \left(1 - \lambda_{XX}\right)\right]\left[\lambda_{II} + \lambda_{III} + \lambda_{XIII} + \lambda_{XII} + \left(1 - \lambda_{XIV}\right)\right] \cdot \lambda_{Z3} \tag{5.134}$$

$$\lambda_{Z3} = \left[\lambda_X + \lambda_{IX} + \lambda_{XX} + \lambda_{XIX} + \left(1 - \lambda_{XVIII}\right)\right]\left[\lambda_{II} + \lambda_{III} + \lambda_{XIII} + \lambda_{XIV} + \lambda_{XV} + \left(1 - \lambda_{XXIII}\right)\right]\left(\lambda_{Z4}\right) \tag{5.135}$$

$$\lambda_{Z4} = \lambda_X + \lambda_{IX} + \lambda_{XX} + \lambda_{XVIII} + \lambda_{XVII} + \left(1 - \lambda_{XXV}\right) \tag{5.136}$$

$$\lambda_2 = \lambda_I \cdot \lambda_{II} \tag{5.137}$$

$$\lambda_3 = \lambda_{III} \cdot \lambda_{IV} \tag{5.138}$$

$$\lambda_4 = \lambda_3 \tag{5.139}$$

$$\lambda_5 = \lambda_V \cdot \lambda_{VI} \cdot \lambda_{XIII} \tag{5.140}$$

$$\lambda_6 = \lambda_B \cdot \min\left[1, \lambda_{VI} \cdot \lambda_C \cdot \left(\lambda_{II} + \lambda_{III} + \lambda_{XIII} + \lambda_{XI}\right)\left(\lambda_X + \lambda_{IX} + \lambda_{XX} + \lambda_{XI}\right)\left(\lambda_{II} + \lambda_{III} + \lambda_{XIII} + \lambda_{XIV} + \lambda_{XVI}\right) \cdot \lambda_{Z5}\right] \tag{5.141}$$

$$\lambda_{Z5} = \left(\lambda_X + \lambda_{IX} + \lambda_{XX} + \lambda_{XVIII} + \lambda_{XVI}\right)\left(\lambda_{II} + \lambda_{III} + \lambda_{XIII} + \lambda_{XIV} + \lambda_{XXIII} + \lambda_{XXI}\right)\left(\lambda_{Z6}\right) \tag{5.142}$$

$$\lambda_{Z6} = \lambda_X + \lambda_{IX} + \lambda_{XX} + \lambda_{XVIII} + \lambda_{XXV} + \lambda_{XXI} \tag{5.143}$$

$$\lambda_D = \min\left[1, \left(\lambda_1 + \lambda_{III} + \lambda_{XIII}\right)\right] \tag{5.144}$$

$$\lambda_E = \min\left[1, \left(\lambda_I + \lambda_{IX} + \lambda_{XX}\right)\right] \tag{5.145}$$

$$\lambda_F = \min\left[1, \left(\lambda_{XX} + \lambda_{XI}\right)\right] \tag{5.146}$$

$$\lambda_G = \min\left[1, \left(\lambda_{XIII} + \lambda_{XI}\right)\right] \tag{5.147}$$

$$\lambda_B = 8 \cdot \left(\frac{\lambda_D + \lambda_E \cdot \lambda_F \cdot \lambda_G}{2}\right)\left(\frac{\lambda_E + \lambda_D \cdot \lambda_F \cdot \lambda_G}{2}\right)\left(\frac{\lambda_F + \lambda_E \cdot \lambda_D \cdot \lambda_G}{2}\right)\left(\frac{\lambda_G + \lambda_E \cdot \lambda_F \cdot \lambda_D}{2}\right) \tag{5.148}$$

$$\lambda_C = \left[\lambda_V + \left(1 - \lambda_{XIII}\right)\right]\left[\lambda_{VII} + \left(1 - \lambda_{XX}\right)\right]\left[\lambda_{II} + \lambda_{III} + \lambda_{XIII} + \lambda_{XII} + \left(1 - \lambda_{XIV}\right)\right]\left(\lambda_{Z7}\right) \tag{5.149}$$

$$\lambda_{Z7} = \left[\lambda_X + \lambda_{IX} + \lambda_{XX} + \lambda_{XIX} + \left(1 - \lambda_{XVIII}\right)\right]\left[\lambda_{II} + \lambda_{III} + \lambda_{XIII} + \lambda_{XIV} + \lambda_{XV} + \left(1 - \lambda_{XXIII}\right)\right]\left(\lambda_{Z8}\right) \tag{5.150}$$

$$\lambda_{Z8} = \lambda_X + \lambda_{IX} + \lambda_{XX} + \lambda_{XVIII} + \lambda_{XVII} + \left(1 - \lambda_{XXV}\right) \tag{5.151}$$

$$\lambda_7 = \lambda_{VII} \cdot \lambda_{XX} \cdot \lambda_{VI} \tag{5.152}$$

$$\lambda_8 = \lambda_{VIII} \cdot \lambda_{IX} \tag{5.153}$$

$$\lambda_9 = \lambda_8 \tag{5.154}$$

$$\lambda_{10} = \lambda_I \cdot \lambda_X \tag{5.155}$$

$$\lambda_{11} = \lambda_H \cdot \min\left[1, \lambda_{XI} \cdot \lambda_J \cdot \left[\left(\lambda_{II} + \lambda_{III} + \lambda_{XIII} + \lambda_{XIV} + \lambda_{XVI}\right)\left(\lambda_X + \lambda_{IX} + \lambda_{XX} + \lambda_{XVIII} + \lambda_{XVI}\right)\left(\lambda_{Z9}\right)\right]\right] \tag{5.156}$$

$$\lambda_{Z9} = \left(\lambda_{II} + \lambda_{III} + \lambda_{XIII} + \lambda_{XIV} + \lambda_{XXIII} + \lambda_{XXI}\right)\left(\lambda_X + \lambda_{IX} + \lambda_{XX} + \lambda_{XVIII} + \lambda_{XXV} + \lambda_{XXI}\right) \tag{5.157}$$

$$\lambda_K = \min\left[1, \left(\lambda_I + \lambda_{III} + \lambda_{VI} + \lambda_{XIII} + \lambda_{XIV}\right)\right] \tag{5.158}$$

$$\lambda_L = \min\left[1, \left(\lambda_I + \lambda_{IX} + \lambda_{VI} + \lambda_{XX} + \lambda_{XVIII}\right)\right] \tag{5.159}$$

$$\lambda_M = \min\left[1, \left(\lambda_{XVIII} + \lambda_{XVI}\right)\right] \tag{5.160}$$

$$\lambda_N = \min\left[1, \left(\lambda_{XIV} + \lambda_{XVI}\right)\right] \tag{5.161}$$

$$\lambda_H = 8 \cdot \left(\frac{\lambda_K + \lambda_L \cdot \lambda_M \cdot \lambda_N}{2}\right)\left(\frac{\lambda_L + \lambda_K \cdot \lambda_M \cdot \lambda_N}{2}\right)\left(\frac{\lambda_M + \lambda_L \cdot \lambda_K \cdot \lambda_N}{2}\right)\left(\frac{\lambda_N + \lambda_L \cdot \lambda_M \cdot \lambda_K}{2}\right) \tag{5.162}$$

$$\lambda_J = \left[\lambda_{XII} + \left(1 - \lambda_{XIV}\right)\right]\left[\lambda_{XIX} + \left(1 - \lambda_{XVIII}\right)\right]\left[\lambda_{II} + \lambda_{III} + \lambda_{XIII} + \lambda_{XIV} + \lambda_{XV} + \left(1 - \lambda_{XXIII}\right)\right]\left(\lambda_{Z10}\right) \tag{5.163}$$

$$\lambda_{Z10} = \lambda_X + \lambda_{IX} + \lambda_{XX} + \lambda_{XVIII} + \lambda_{XVII} + \left(1 - \lambda_{XXV}\right) \tag{5.164}$$

$$\lambda_{12} = \lambda_{XII} \cdot \lambda_{XI} \cdot \lambda_{XIV} \tag{5.165}$$

$$\lambda_{13} = \lambda_{XIII} \tag{5.166}$$

$$\lambda_{14} = \lambda_{XIV} \tag{5.167}$$

$$\lambda_{15} = \lambda_{XV} \cdot \lambda_{XXIII} \cdot \lambda_{XVI} \tag{5.168}$$

$$\lambda_{16} = \lambda_{P} \cdot \min\left[1, \lambda_{XVI}\left[\left(\lambda_{II} + \lambda_{III} + \lambda_{XIII} + \lambda_{XIV} + \lambda_{XXIII} + \lambda_{XXI}\right)\left[\lambda_{XV} + \left(1 - \lambda_{XXII}\right)\right]\left(\lambda_{Z11}\right)\right]\right] \tag{5.169}$$

$$\lambda_{Z11} = \left[\lambda_{XVII} + \left(1 - \lambda_{XXV}\right)\right] \cdot \left(\lambda_{X} + \lambda_{IX} + \lambda_{XX} + \lambda_{XVIII} + \lambda_{XXV} + \lambda_{XXI}\right) \tag{5.170}$$

$$\lambda_{Q} = \min\left[1, \left(\lambda_{I} + \lambda_{III} + \lambda_{VI} + \lambda_{XI} + \lambda_{XIV} + \lambda_{XXIII}\right)\right] \tag{5.171}$$

$$\lambda_{R} = \min\left[1, \left(\lambda_{I} + \lambda_{IX} + \lambda_{VI} + \lambda_{XI} + \lambda_{XVIII} + \lambda_{XXV}\right)\right] \tag{5.172}$$

$$\lambda_{S} = \min\left[1, \left(\lambda_{XXI} + \lambda_{XXV}\right)\right] \tag{5.173}$$

$$\lambda_{T} = \min\left[1, \left(\lambda_{XXI} + \lambda_{XXIII}\right)\right] \tag{5.174}$$

$$\lambda_{P} = 8 \cdot \left(\frac{\lambda_{Q} + \lambda_{R} \cdot \lambda_{S} \cdot \lambda_{T}}{2}\right)\left(\frac{\lambda_{R} + \lambda_{Q} \cdot \lambda_{S} \cdot \lambda_{T}}{2}\right)\left(\frac{\lambda_{S} + \lambda_{R} \cdot \lambda_{Q} \cdot \lambda_{T}}{2}\right)\left(\frac{\lambda_{T} + \lambda_{R} \cdot \lambda_{S} \cdot \lambda_{Q}}{2}\right) \tag{5.175}$$

$$\lambda_{17} = \lambda_{XVII} \cdot \lambda_{XVI} \cdot \lambda_{XXV} \tag{5.176}$$

$$\lambda_{18} = \lambda_{XVIII} \tag{5.177}$$

$$\lambda_{19} = \lambda_{XIX} \cdot \lambda_{XVIII} \cdot \lambda_{XI} \tag{5.178}$$

$$\lambda_{20} = \lambda_{XX} \tag{5.179}$$

$$\lambda_{21} = \lambda_{XXI} \tag{5.180}$$

$$\lambda_{22} = \lambda_{XXI} \cdot \lambda_{XXII} \tag{5.181}$$

$$\lambda_{23} = \lambda_{XXIII} \tag{5.182}$$

$$\lambda_{24} = \lambda_{XXI} \cdot \lambda_{XXIV} \tag{5.183}$$

$$\lambda_{25} = \lambda_{XXV} \tag{5.184}$$

$$\lambda_{YL} = \begin{cases} 1 & \text{if } G > 0 \\ 0 & \text{otherwise} \end{cases} \tag{5.185}$$

$$\lambda_{YU} = \begin{cases} 1 & \text{if } B - (G + F) > 0 \\ 0 & \text{otherwise} \end{cases} \tag{5.186}$$

$$\lambda_0 = \min\left[1, \left(\lambda_{YL} + \lambda_{YU}\right)\right] \tag{5.187}$$

To enable the treatment of transverse bulkheads and webs between double hulls to be similar to the treatment of single hull webs, where the inboard edge is free, the assumption that the inboard edge is simply supported until contacted by the rigid wedge is necessary. The assumption is only practical because a flange located on the free edge stiffens most free webs. Thus, with this assumption there is no mathematical difference in the treatment of either transverse bulkheads or webs.

In an analysis where V_x is greater than zero then the points I, Q, J, R, K, S, L and T of Figure 5-60 will move from time step to time step in the x direction and thus D_1, D_2, D_3 and D_4 will increase in magnitude while D_5 will decrease. At some time D_5 will equal zero and D_4 will equal the span (A). At later times the D_3 will equal (A) followed by D_2 and then D_1, should the analysis permit. Noting that D_1, D_2, D_3 and D_4 must always be less than or equal to the plate span, and that the energy absorbed within each region is dependant upon having some x dimension, then Equation 5.130 becomes:

$$\begin{aligned} E_{X\tau} = E_{Z\tau} = {} & \lambda_0 \cdot \left(\lambda_1 \cdot E_I + \lambda_{D1} \cdot \lambda_6 \cdot E_{VI} + \lambda_{D2} \cdot \lambda_{11} \cdot E_{XI} + \lambda_{D3} \cdot \lambda_{16} \cdot E_{XVI} + \lambda_{D4} \cdot \lambda_{21} \cdot E_{XXI}\right) + ... \\ .... + {} & \lambda_0 \cdot \lambda_{YL} \cdot \left[\lambda_2 \cdot E_{II} + \lambda_3 \cdot E_{III} + \lambda_{D1} \cdot \left(\lambda_4 \cdot E_{IV} + \lambda_5 \cdot E_V\right) + \lambda_{D2} \cdot \left(\lambda_{12} \cdot E_{XII} + \lambda_{13} \cdot E_{XIII}\right)\right] + ... \\ .... + {} & \lambda_0 \cdot \lambda_{YL} \cdot \left[\lambda_{D3}\left(\lambda_{14} \cdot E_{XIV} + \lambda_{15} \cdot E_{XV}\right) + \lambda_{D4} \cdot \left(\lambda_{22} \cdot E_{XXII} + \lambda_{23} \cdot E_{XXIII}\right)\right] + ... \\ .... + {} & \lambda_0 \cdot \lambda_{YU} \cdot \left[\lambda_9 \cdot E_{IX} + \lambda_{10} \cdot E_X + \lambda_{D1} \cdot \left(\lambda_7 \cdot E_{VII} + \lambda_8 \cdot E_{VIII}\right) + \lambda_{D2} \cdot \left(\lambda_{19} \cdot E_{XIX} + \lambda_{20} \cdot E_{XX}\right)\right] + ... \\ .... + {} & \lambda_0 \cdot \lambda_{YU} \cdot \left[\lambda_{D3}\left(\lambda_{17} \cdot E_{XVII} + \lambda_{18} \cdot E_{XVIII}\right) + \lambda_{D4} \cdot \left(\lambda_{25} \cdot E_{XXV} + \lambda_{24} \cdot E_{XXIV}\right)\right] \end{aligned} \tag{5.188}$$

Where the new rupture indicators of Equation 5.188 (λ_{D1}, λ_{D2}, λ_{D3} and λ_{D4}) are given by Equations 5.189 through 5.192.

$$\lambda_{D1} = \begin{cases} 1 & \text{if } D_1 < A \\ 0 & \text{otherwise} \end{cases} \quad (5.189)$$

$$\lambda_{D2} = \begin{cases} 1 & \text{if } D_2 < A \\ 0 & \text{otherwise} \end{cases} \quad (5.190)$$

$$\lambda_{D3} = \begin{cases} 1 & \text{if } D_3 < A \\ 0 & \text{otherwise} \end{cases} \quad (5.191)$$

$$\lambda_{D4} = \begin{cases} 1 & \text{if } D_4 < A \\ 0 & \text{otherwise} \end{cases} \quad (5.192)$$

For each contact scenario the deflections in the z direction of points P, Q, R, S, and T may differ and will definitely change depending upon which motion (x or z) is the initial incremental step direction. A similar statement may also be made for the values of D_1, D_2, D_3 and D_4. To continue the analysis and to enable the determination of the points P, Q, R, S and T, the initial position (relative to the plate) and the geometry of the striking wedge model must be known. To accomplish this, the x, y and z coordinates of the point B_P (on Figure 5-61) must be defined at time t = 0 seconds. Additionally the striking wedge length (L_{RW}), beam (B_{RW}) and half entrance angle (HEA) must also be known. Finally, the angle between the centerline of the striking wedge and a line orthogonal to the plate, where the positive angle is to the positive z-axis, must also be known as shown in Figure 5-62.

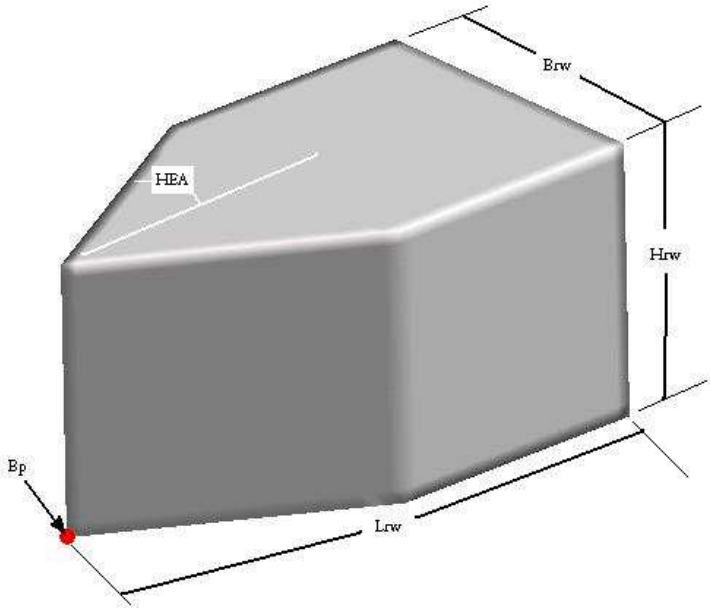

Figure 5-61 Striking Wedge Variable Definitions

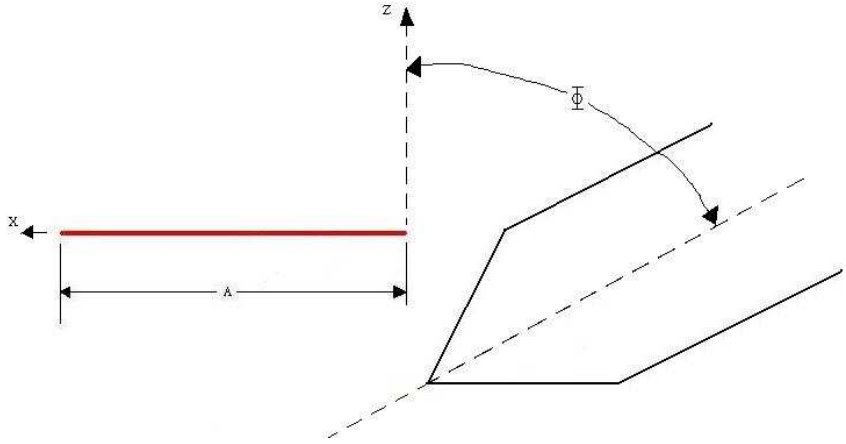

Figure 5-62 Collision Angle Definition

Using the definitions prescribed in Figure 5-61 and Figure 5-62, then the values of G and F in Figure 5-60 may be calculated using Equations 5.193 and 5.194, and the contact scenario (CS) may be defined mathematically through the conditional statement of Equation 5.195.

$$G = \max\left(0, B_{Py}\right) \tag{5.193}$$

$$F = H_{RW} + B_{Py} - G \tag{5.194}$$

$$CS = \begin{cases} 1 \text{ if } \begin{cases} B_{PZ} < 0 \wedge P_{XS} < 0 \wedge P_{ZS} > B_{PZ} \\ \text{or}\left(B_{PZ} > 0 \wedge P_{XP} < 0 \wedge P_{ZP} < B_{PZ}\right) \end{cases} \\ 2 \text{ if } \begin{cases} B_{PZ} > 0 \wedge P_{ZP} \geq B_{PZ} \\ \text{or}\left(B_{PZ} > 0 \wedge P_{ZS} \leq B_{PZ}\right) \end{cases} \\ 3 \text{ if } \begin{cases} P_{ZP} \geq 0 \wedge P_{XP} \geq 0 \wedge \Phi > 90 \\ \text{or}\left(P_{ZP} \leq 0 \wedge P_{XS} \geq 0 \wedge \Phi < 90\right) \end{cases} \\ 4 \text{ if } \begin{cases} P_{ZP} \geq 0 \wedge P_{XP} \geq 0 \wedge \Phi \leq 90 \\ \text{or}\left(P_{ZP} \leq 0 \wedge P_{XS} \geq 0 \wedge \Phi \geq 90\right) \end{cases} \\ \text{unhandled} \quad \text{otherwise} \end{cases} \tag{5.195}$$

Where the terms (P_{XS}, P_{XP}, P_{ZS} and P_{ZP}) are defined by Equations 5.196 through 5.200.

$$L = \frac{B_{RW}}{2 \cdot \text{Tan}(HEA)} \tag{5.196}$$

$$P_{XS} = B_{PX} - \left(L^2 + \frac{B_{RW}^2}{4}\right)^{\frac{1}{2}} \cdot \text{Sin}(\Phi - HEA) \tag{5.197}$$

$$P_{XP} = B_{PX} - \left(L^2 + \frac{B_{RW}^2}{4}\right)^{\frac{1}{2}} \cdot \text{Sin}(\Phi + HEA) \tag{5.198}$$

$$P_{ZS} = B_{PZ} + \left(L^2 + \frac{B_{RW}^2}{4}\right)^{\frac{1}{2}} \cdot \text{Cos}(\Phi - HEA) \tag{5.199}$$

$$P_{ZP} = B_{PZ} + \left(L^2 + \frac{B_{RW}^2}{4}\right)^{\frac{1}{2}} \cdot \text{Cos}(\Phi + HEA) \tag{5.200}$$

In addition to the mathematical determination of the contact scenario (CS) the variables defined by Figure 5-61 and Figure 5-62 allow the determination of the deflections of the points P, Q, R, S, and

T over the time step (τ) along with the change in the lengths D_1, D_2, D_3 and D_4. As previously discussed, for each contact scenario the deflections may differ and will definitely change depending on the initial step direction. By defining the deflections of P, Q, R, S and T at the initial time (prior to the time step) as WP_0, WQ_0, WR_0, WS_0 and WT_0 respectively, and after the initial step (either x or z) as WP_1, WQ_1, WR_1, WS_1 and WT_1 respectively, and at the end of the time step (after both the x and z motions) as WP_2, WQ_2, WR_2, WS_2 and WT_2 respectively, then for each possible contact formulation the following procedures as outlined in Sections 5.4.5.1 through 5.4.5.8 may be followed. Note that in the following sections the right superscript $^{<0>}$ refers to the value of the variable at time t = 0 zero seconds, odd values of the left superscript ($^{<1>,<3>,<5>\cdots}$) refer to the variable value after the initial step direction within a time step and even values of the left superscript ($^{<2>,<4>,<6>\cdots}$) refer to the variable value at the end of the previous time step or at the beginning of the next time step.

5.4.5.1 Determination of Deflections in CS 1 with a Z-Direction Initial Step

Beginning with the initial deflections:

$$WP^{\langle 0\rangle} = WQ^{\langle 0\rangle} = WR^{\langle 0\rangle} = WS^{\langle 0\rangle} = WT^{\langle 0\rangle} = 0$$

$$B_{PZ}{}^{\langle 0\rangle} = \text{Given}$$

$$B_{PX}{}^{\langle 0\rangle} = \text{Given}$$

$$\Phi = \text{Given}$$

$$HEA = \text{Given}$$

$$B_{RW} = \text{Given}$$

$$L_{RW} = \text{Given}$$

$$B_{PY} = \text{Given} \qquad (5.201)$$

$$L = \frac{B_{RW}}{2 \cdot \text{Tan}(HEA)} \qquad (5.202)$$

$$P_{XS}^{\langle 0\rangle} = B_{PX}^{\langle 0\rangle} - \left(L^2 + \frac{B_{RW}^{\ 2}}{4}\right)^{\frac{1}{2}} \cdot \mathrm{Sin}(\Phi - HEA) \tag{5.203}$$

$$P_{XP}^{\langle 0\rangle} = B_{PX}^{\langle 0\rangle} - \left(L^2 + \frac{B_{RW}^{\ 2}}{4}\right)^{\frac{1}{2}} \cdot \mathrm{Sin}(\Phi + HEA) \tag{5.204}$$

$$P_{ZS}^{\langle 0\rangle} = B_{PZ}^{\langle 0\rangle} + \left(L^2 + \frac{B_{RW}^{\ 2}}{4}\right)^{\frac{1}{2}} \cdot \mathrm{Cos}(\Phi - HEA) \tag{5.205}$$

$$P_{ZP}^{\langle 0\rangle} = B_{PZ}^{\langle 0\rangle} + \left(L^2 + \frac{B_{RW}^{\ 2}}{4}\right)^{\frac{1}{2}} \cdot \mathrm{Cos}(\Phi + HEA) \tag{5.206}$$

$$CS = 1 \tag{5.207}$$

$$S_{LP} = \begin{cases} \dfrac{B_{PZ}^{\langle 0\rangle} - P_{ZP}^{\langle 0\rangle}}{B_{PX}^{\langle 0\rangle} - P_{PX}^{\langle 0\rangle}} & \text{if } \Phi \geq 90 \wedge B_{PZ}^{\langle 0\rangle} > 0 \\ \dfrac{B_{PZ}^{\langle 0\rangle} - P_{ZS}^{\langle 0\rangle}}{B_{PX}^{\langle 0\rangle} - P_{XS}^{\langle 0\rangle}} & \text{if } \Phi < 90 \wedge B_{PZ}^{\langle 0\rangle} < 0 \\ 0 & \text{otherwise} \end{cases} \tag{5.208}$$

$$B_{PZ}^{\langle 1\rangle} = B_{PZ}^{\langle 0\rangle} + V_Z^{\langle 0\rangle} \cdot \tau \tag{5.209}$$

$$B_{PX}^{\langle 1\rangle} = B_{PX}^{\langle 0\rangle} \tag{5.210}$$

$$P_{XS}^{\langle 1\rangle} = P_{XS}^{\langle 0\rangle} \tag{5.211}$$

$$P_{XP}^{\langle 1\rangle} = P_{XP}^{\langle 0\rangle} \tag{5.212}$$

$$P_{ZS}^{\langle 1\rangle} = P_{ZS}^{\langle 0\rangle} + V_Z^{\langle 0\rangle} \cdot \tau \tag{5.213}$$

$$P_{ZP}^{\langle 1\rangle} = P_{ZP}^{\langle 0\rangle} + V_Z^{\langle 0\rangle} \cdot \tau \tag{5.214}$$

$$D_2 = \max\left(0, D_3 - V_x^{\langle 0\rangle} \cdot \tau, \frac{D_3}{2}\right) \tag{5.215}$$

$$D_3 = \max\left[0, \left(B_{PX}^{\langle 1\rangle} - \frac{B_{PZ}^{\langle 1\rangle}}{S_{LP}}\right)\right] \tag{5.216}$$

$$D_1 = \max\left(0, D_3 - 2\cdot V_X^{\langle 0\rangle}\cdot\tau, \frac{D_2}{2}\right) \tag{5.217}$$

$$\text{CONTYPE} = \begin{cases} 0 & \text{if } B_{PZ}^{\langle 0\rangle} > 0 \wedge P_{XP}^{\langle 0\rangle} < 0 \wedge P_{ZP}^{\langle 0\rangle} < B_{PZ}^{\langle 0\rangle} \\ 1 & \text{if } B_{PZ}^{\langle 0\rangle} < 0 \wedge P_{XS}^{\langle 0\rangle} < 0 \wedge P_{ZS}^{\langle 0\rangle} > B_{PZ}^{\langle 0\rangle} \end{cases} \tag{5.218}$$

$$WS^{\langle 1\rangle} = \begin{cases} \min\left(0, B_{PZ}^{\langle 1\rangle}\right) & \text{if CONTYPE} = 0 \\ \max\left(0, B_{PZ}^{\langle 1\rangle}\right) & \text{if CONTYPE} = 1 \end{cases} \tag{5.219}$$

$$WP^{\langle 1\rangle} = WS^{\langle 1\rangle} - S_{LP}\cdot D_3 \tag{5.220}$$

$$WR^{\langle 1\rangle} = WS^{\langle 1\rangle} - S_{LP}\cdot\left(D_3 - D_2\right) \tag{5.221}$$

$$WQ^{\langle 1\rangle} = WS^{\langle 1\rangle} - S_{LP}\left(D_3 - D_1\right) \tag{5.222}$$

$$D_4 = D_3 + V_X^{\langle 0\rangle}\cdot\tau \tag{5.223}$$

$$AS_{LP} = \frac{WS^{\langle 1\rangle}}{A - D_3} \tag{5.224}$$

$$WT^{\langle 1\rangle} = AS_{LP}\cdot\left(A - D_4\right) \tag{5.225}$$

$$WT^{\langle 2\rangle} = WS^{\langle 1\rangle} \tag{5.226}$$

$$WS^{\langle 2\rangle} = WT^{\langle 2\rangle} - S_{LP}\cdot\left(D_4 - D_3\right) \tag{5.227}$$

$$WR^{\langle 2\rangle} = WT^{\langle 2\rangle} - S_{LP}\cdot\left(D_4 - D_2\right) \tag{5.228}$$

$$WQ^{\langle 2\rangle} = WT^{\langle 2\rangle} - S_{LP}\left(D_4 - D_1\right) \tag{5.229}$$

$$WP^{\langle 2\rangle} = WT^{\langle 2\rangle} - S_{LP}\cdot D_4 \tag{5.230}$$

The results of Equations 5.201 through 5.230 are used to determine the energies ($E_{x\tau}$) and ($E_{z\tau}$) using Equation 5.188. Thus the total energy absorbed by the plate in either the x or z directions is given by Equations 5.231 and 5.232 respectively.

$$TE_{X\tau} = \sum_{i=0}^{\frac{t}{\tau}} \sum_{j=0}^{\frac{t}{\tau}} E_{X\tau}^{\langle j \rangle} \cdot \delta_{ij} \tag{5.231}$$

$$TE_{Z\tau} = \sum_{i=0}^{\frac{t}{\tau}} \sum_{j=0}^{\frac{t}{\tau}} E_{Z\tau}^{\langle j \rangle} \cdot \delta_{ij} \tag{5.232}$$

Using Equations 5.231 and 5.232 the total energy absorbed by the plate at time (T) is given by Equation 5.233 and the updated velocity components for the rigid wedge (assuming for convenience no induced moments) are given by Equations 5.234 and 5.235.

$$TE_{\tau} = TE_{X\tau} + TE_{Z\tau} \tag{5.233}$$

$$V_X^{\langle 2 \rangle} = \sqrt{\max\left[0, \left(V_X^{\,2}\right)^{\langle 0 \rangle} - \frac{2 \cdot TE_{X\tau}}{M}\right]} \tag{5.234}$$

$$V_Z^{\langle 2 \rangle} = \sqrt{\max\left[0, \left(V_Z^{\,2}\right)^{\langle 0 \rangle} - \frac{2 \cdot TE_{Z\tau}}{M}\right]} \tag{5.235}$$

Cycling the system of equations yields:

$$D_1 = D_2 \tag{5.236}$$

$$D_2 = D_3 \tag{5.237}$$

$$D_3 = \max\left(0, B_{Px}^{\langle 3 \rangle} - \frac{B_{PX}^{\langle 3 \rangle}}{S_{LP}}\right) \tag{5.238}$$

$$D_4 = D_3 + V_X^{\langle 2 \rangle} \cdot \tau \tag{5.239}$$

$$B_{PZ}^{\langle 2 \rangle} = B_{PZ}^{\langle 1 \rangle} \tag{5.240}$$

$$B_{PX}^{\langle 2 \rangle} = B_{PX}^{\langle 1 \rangle} + V_X^{\langle 0 \rangle} \cdot \tau \tag{5.241}$$

$$B_{PZ}^{\langle 3 \rangle} = B_{PZ}^{\langle 2 \rangle} + V_Z^{\langle 2 \rangle} \cdot \tau \tag{5.242}$$

$$B_{PX}^{\langle 3 \rangle} = B_{PX}^{\langle 2 \rangle} \tag{5.243}$$

$$B_{PZ}^{\langle 4 \rangle} = B_{PZ}^{\langle 3 \rangle} \tag{5.244}$$

$$B_{PX}^{\langle 4 \rangle} = B_{PX}^{\langle 3 \rangle} + V_X^{\langle 2 \rangle} \cdot \tau \tag{5.245}$$

$$WP^{\langle 3 \rangle} = WS^{\langle 3 \rangle} - S_{LP} \cdot D_3 \tag{5.246}$$

$$WR^{\langle 3 \rangle} = WS^{\langle 3 \rangle} - S_{LP} \cdot \left(D_3 - D_2 \right) \tag{5.247}$$

$$WQ^{\langle 3 \rangle} = WS^{\langle 3 \rangle} - S_{LP} \left(D_3 - D_1 \right) \tag{5.248}$$

$$AS_{LP} = \frac{WS^{\langle 3 \rangle}}{A - D_3} \tag{5.249}$$

$$WT^{\langle 3 \rangle} = AS_{LP} \cdot \left(A - D_4 \right) \tag{5.250}$$

$$WT^{\langle 4 \rangle} = WS^{\langle 3 \rangle} \tag{5.251}$$

$$WS^{\langle 4 \rangle} = WT^{\langle 4 \rangle} - S_{LP} \cdot \left(D_4 - D_3 \right) \tag{5.252}$$

$$WR^{\langle 4 \rangle} = WT^{\langle 4 \rangle} - S_{LP} \cdot \left(D_4 - D_2 \right) \tag{5.253}$$

$$WQ^{\langle 4 \rangle} = WT^{\langle 4 \rangle} - S_{LP} \left(D_4 - D_1 \right) \tag{5.254}$$

$$WP^{\langle 4 \rangle} = WT^{\langle 4 \rangle} - S_{LP} \cdot D_4 \tag{5.255}$$

Where the cycle continues to repeat for each time step.

5.4.5.2 Determination of Deflections in CS 1 with a X-Direction Initial Step

Beginning with the initial deflections of Equation 5.201 through 5.206, and making use of Equations 5.208 and 5.218, then:

$$CS = 1 \tag{5.256}$$

$$B_{PX}^{\langle 1 \rangle} = B_{PX}^{\langle 0 \rangle} + V_X^{\langle 0 \rangle} \cdot \tau \tag{5.257}$$

$$B_{PX}^{\langle 2 \rangle} = B_{PX}^{\langle 1 \rangle} \tag{5.258}$$

$$B_{PZ}^{\langle 1 \rangle} = B_{PZ}^{\langle 0 \rangle} \tag{5.259}$$

$$B_{PZ}^{\langle 2 \rangle} = B_{PZ}^{\langle 1 \rangle} + V_Z^{\langle 0 \rangle} \cdot \tau \tag{5.260}$$

$$D_3 = \max\left[0, \left(B_{PX}^{\langle 1 \rangle} - \frac{B_{PZ}^{\langle 1 \rangle}}{S_{LP}}\right)\right] \tag{5.261}$$

$$D_2 = \max\left(0, D_3 - V_x^{\langle 0 \rangle} \cdot \tau, \frac{D_3}{2}\right) \tag{5.262}$$

$$D_1 = \max\left(0, D_2 - V_X^{\langle 0 \rangle} \cdot \tau, \frac{D_2}{2}\right) \tag{5.263}$$

$$WS^{\langle 1 \rangle} = \begin{cases} \min\left(0, B_{PZ}^{\langle 1 \rangle}\right) & \text{if CONTYPE} = 0 \\ \max\left(0, B_{PZ}^{\langle 1 \rangle}\right) & \text{if CONTYPE} = 1 \end{cases} \tag{5.264}$$

$$WP^{\langle 1 \rangle} = WS^{\langle 1 \rangle} - S_{LP} \cdot D_3 \tag{5.265}$$

$$WR^{\langle 1 \rangle} = WS^{\langle 1 \rangle} - S_{LP} \cdot \left(D_3 - D_2\right) \tag{5.266}$$

$$WQ^{\langle 1 \rangle} = WS^{\langle 1 \rangle} - S_{LP}\left(D_3 - D_1\right) \tag{5.267}$$

$$AS_{LP} = \frac{WS^{\langle 1 \rangle}}{A - D_3} \tag{5.268}$$

$$D_4 = \max\left(0, B_{PX}^{\langle 2 \rangle} - \frac{B_{PZ}^{\langle 2 \rangle}}{S_{LP}}\right) \tag{5.269}$$

$$WT^{\langle 1 \rangle} = AS_{LP} \cdot \left(A - D_4\right) \tag{5.270}$$

$$WT^{\langle 2\rangle} = \begin{cases} \min\left(0, B_{PZ}^{\langle 2\rangle}\right) & \text{if CONTYPE} = 0 \\ \max\left(0, B_{PZ}^{\langle 2\rangle}\right) & \text{if CONTYPE} = 1 \end{cases} \tag{5.271}$$

$$WS^{\langle 2\rangle} = WT^{\langle 2\rangle} - S_{LP} \cdot \left(D_4 - D_3\right) \tag{5.272}$$

$$WR^{\langle 2\rangle} = WT^{\langle 2\rangle} - S_{LP} \cdot \left(D_4 - D_2\right) \tag{5.273}$$

$$WQ^{\langle 2\rangle} = WT^{\langle 2\rangle} - S_{LP}\left(D_4 - D_1\right) \tag{5.274}$$

$$WP^{\langle 2\rangle} = WT^{\langle 2\rangle} - S_{LP} \cdot D_4 \tag{5.275}$$

Using Equations 5.231 through 5.235 and cycling the system yields:

$$D_1 = D_2 \tag{5.276}$$

$$D_2 = D_3 \tag{5.277}$$

$$B_{PX}^{\langle 3\rangle} = B_{PX}^{\langle 2\rangle} + V_X^{\langle 2\rangle} \cdot \tau \tag{5.278}$$

$$B_{PX}^{\langle 4\rangle} = B_{PX}^{\langle 3\rangle} \tag{5.279}$$

$$B_{PZ}^{\langle 3\rangle} = B_{PZ}^{\langle 2\rangle} \tag{5.280}$$

$$B_{PZ}^{\langle 4\rangle} = B_{PZ}^{\langle 3\rangle} + V_Z^{\langle 2\rangle} \cdot \tau \tag{5.281}$$

$$D_3 = \max\left(0, B_{Px}^{\langle 3\rangle} - \frac{B_{PZ}^{\langle 3\rangle}}{S_{LP}}\right) \tag{5.282}$$

$$D_4 = \max\left(0, B_{Px}^{\langle 4\rangle} - \frac{B_{PZ}^{\langle 4\rangle}}{S_{LP}}\right) \tag{5.283}$$

$$WS^{\langle 3\rangle} = \begin{cases} \min\left(0, B_{PZ}^{\langle 3\rangle}\right) & \text{if CONTYPE} = 0 \\ \max\left(0, B_{PZ}^{\langle 3\rangle}\right) & \text{if CONTYPE} = 1 \end{cases} \tag{5.284}$$

$$WP^{\langle 3\rangle} = WS^{\langle 3\rangle} - S_{LP} \cdot D_3 \tag{5.285}$$

$$WR^{\langle 3\rangle} = WS^{\langle 3\rangle} - S_{LP}\cdot\left(D_3 - D_2\right) \tag{5.286}$$

$$WQ^{\langle 3\rangle} = WS^{\langle 3\rangle} - S_{LP}\left(D_3 - D_1\right) \tag{5.287}$$

$$AS_{LP} = \frac{WS^{\langle 3\rangle}}{A - D_3} \tag{5.288}$$

$$WT^{\langle 3\rangle} = AS_{LP}\cdot\left(A - D_4\right) \tag{5.289}$$

$$WT^{\langle 4\rangle} = \begin{cases} \min\left(0, B_{PZ}{}^{\langle 4\rangle}\right) & \text{if CONTYPE} = 0 \\ \max\left(0, B_{PZ}{}^{\langle 4\rangle}\right) & \text{if CONTYPE} = 1 \end{cases} \tag{5.290}$$

$$WS^{\langle 4\rangle} = WT^{\langle 4\rangle} - S_{LP}\cdot\left(D_4 - D_3\right) \tag{5.291}$$

$$WR^{\langle 4\rangle} = WT^{\langle 4\rangle} - S_{LP}\cdot\left(D_4 - D_2\right) \tag{5.292}$$

$$WQ^{\langle 4\rangle} = WT^{\langle 4\rangle} - S_{LP}\left(D_4 - D_1\right) \tag{5.293}$$

$$WP^{\langle 4\rangle} = WT^{\langle 4\rangle} - S_{LP}\cdot D_4 \tag{5.294}$$

Where the cycle continues to repeat for each time step.

5.4.5.3 Determination of Deflections in CS 2 with a Z-Direction Initial Step

Beginning with the initial deflections of Equations 5.201 through 5.206 then:

$$CS = 2 \tag{5.295}$$

$$\text{CONTYPE} = \begin{cases} 0 & \text{if } B_{PZ}{}^{\langle 0\rangle} > 0 \\ 1 & \text{if } B_{PZ}{}^{\langle 0\rangle} < 0 \end{cases} \tag{5.296}$$

$$B_{PZ}{}^{\langle 1\rangle} = B_{PZ}{}^{\langle 0\rangle} + V_Z{}^{\langle 0\rangle}\cdot\tau \tag{5.297}$$

$$B_{PX}{}^{\langle 1\rangle} = B_{PX}{}^{\langle 0\rangle} \tag{5.298}$$

$$B_{PZ}{}^{\langle 2\rangle} = B_{PZ}{}^{\langle 1\rangle} \tag{5.299}$$

$$B_{PX}{}^{\langle 2\rangle} = B_{PX}{}^{\langle 1\rangle} + V_X{}^{\langle 0\rangle}\cdot\tau \tag{5.300}$$

$$D_3 = B_{PX}^{\langle 0 \rangle} \tag{5.301}$$

$$D_4 = B_{PX}^{\langle 2 \rangle} \tag{5.302}$$

$$D_2 = \max\left(0, D_3 - V_X^{\langle 0 \rangle} \cdot \tau, \frac{D_3}{2}\right) \tag{5.303}$$

$$D_1 = \max\left(0, D_2 - V_X^{\langle 0 \rangle} \cdot \tau, \frac{D_2}{2}\right) \tag{5.304}$$

$$WP^{\langle 1 \rangle} = WS^{\langle 1 \rangle} = WR^{\langle 1 \rangle} = WQ^{\langle 1 \rangle} = B_{PZ}^{\langle 1 \rangle} \tag{5.305}$$

$$AS_{LP} = \frac{WS^{\langle 1 \rangle}}{A - D3} \tag{5.306}$$

$$WT^{\langle 1 \rangle} = AS_{LP} \cdot \left(A - D_4\right) \tag{5.307}$$

$$WT^{\langle 2 \rangle} = WS^{\langle 2 \rangle} = WR^{\langle 2 \rangle} = WQ^{\langle 2 \rangle} = WP^{\langle 2 \rangle} = WS^{\langle 1 \rangle} \tag{5.308}$$

Using Equations 5.231 through 5.235 and cycling the system yields:

$$D_1 = D_2 \tag{5.309}$$

$$D_2 = D_3 \tag{5.310}$$

$$D_3 = D_4 \tag{5.311}$$

$$D_4 = D_3 + V_x^{\langle 2 \rangle} \cdot \tau \tag{5.312}$$

$$B_{PZ}^{\langle 3 \rangle} = B_{PZ}^{\langle 2 \rangle} + V_Z^{\langle 2 \rangle} \cdot \tau \tag{5.313}$$

$$B_{PX}^{\langle 3 \rangle} = B_{PX}^{\langle 2 \rangle} \tag{5.314}$$

$$B_{PZ}^{\langle 4 \rangle} = B_{PZ}^{\langle 3 \rangle} \tag{5.315}$$

$$B_{PX}^{\langle 4 \rangle} = D_4 \tag{5.316}$$

$$WP^{\langle 3 \rangle} = WS^{\langle 3 \rangle} = WR^{\langle 3 \rangle} = WQ^{\langle 3 \rangle} = B_{PZ}^{\langle 3 \rangle} \tag{5.317}$$

$$AS_{LP} = \frac{WS^{\langle 3 \rangle}}{A - D3} \tag{5.318}$$

$$WT^{\langle 3 \rangle} = AS_{LP} \cdot (A - D_4) \tag{5.319}$$

$$WT^{\langle 4 \rangle} = WS^{\langle 4 \rangle} = WR^{\langle 4 \rangle} = WQ^{\langle 4 \rangle} = WP^{\langle 4 \rangle} = WS^{\langle 3 \rangle} \tag{5.320}$$

Where the cycle continues to repeat for each time step.

5.4.5.4 Determination of Deflections in CS 2 with a X-Direction Initial Step

Beginning with the initial deflections of Equations 5.201 through 5.206, and making use of Equations 5.295 and 5.306, then:

$$B_{PX}{}^{\langle 1 \rangle} = B_{PX}{}^{\langle 0 \rangle} + V_X{}^{\langle 0 \rangle} \cdot \tau \tag{5.321}$$

$$B_{PX}{}^{\langle 2 \rangle} = B_{PX}{}^{\langle 1 \rangle} \tag{5.322}$$

$$B_{PZ}{}^{\langle 1 \rangle} = B_{PZ}{}^{\langle 0 \rangle} \tag{5.324}$$

$$B_{PZ}{}^{\langle 2 \rangle} = B_{PZ}{}^{\langle 1 \rangle} + V_Z{}^{\langle 0 \rangle} \cdot \tau \tag{5.325}$$

$$D_2 = B_{PX}{}^{\langle 0 \rangle} \tag{5.326}$$

$$D_3 = B_{PX}{}^{\langle 1 \rangle} \tag{5.327}$$

$$D_4 = D_3 + V_X{}^{\langle 0 \rangle} \cdot \tau \tag{5.328}$$

$$D_1 = \max\left(0, D_2 - V_X{}^{\langle 0 \rangle} \cdot \tau, \frac{D_2}{2}\right) \tag{5.329}$$

$$WP^{\langle 1 \rangle} = WS^{\langle 1 \rangle} = WR^{\langle 1 \rangle} = WQ^{\langle 1 \rangle} = WT^{\langle 1 \rangle} = 0 \tag{5.330}$$

$$WS^{\langle 2 \rangle} = WR^{\langle 2 \rangle} = WQ^{\langle 2 \rangle} = WP^{\langle 2 \rangle} = B_{PZ}{}^{\langle 2 \rangle} \tag{5.331}$$

$$AS_{LP} = \frac{WS^{\langle 2 \rangle}}{A - D3} \tag{5.332}$$

$$WT^{\langle 2 \rangle} = AS_{LP} \cdot (A - D_4) \tag{5.333}$$

Using Equations 5.231 through 5.235 and cycling the system yields:

$$D_1 = D_2 \tag{5.334}$$

$$D_2 = D_3 \tag{5.335}$$

$$D_3 = D_4 \tag{5.336}$$

$$D_4 = D_3 + V_x^{\langle 2 \rangle} \cdot \tau \tag{5.337}$$

$$B_{PX}^{\langle 3 \rangle} = D_3 \tag{5.338}$$

$$B_{PX}^{\langle 4 \rangle} = B_{PX}^{\langle 3 \rangle} \tag{5.339}$$

$$B_{PZ}^{\langle 3 \rangle} = B_{PZ}^{\langle 2 \rangle} \tag{5.340}$$

$$B_{PZ}^{\langle 4 \rangle} = B_{PZ}^{\langle 3 \rangle} + V_Z^{\langle 2 \rangle} \cdot \tau \tag{5.341}$$

$$WS^{\langle 2 \rangle} = WT^{\langle 2 \rangle} \tag{5.342}$$

$$WP^{\langle 3 \rangle} = WS^{\langle 3 \rangle} = WR^{\langle 3 \rangle} = WQ^{\langle 3 \rangle} = B_{PZ}^{\langle 2 \rangle} \tag{5.343}$$

$$AS_{LP} = \frac{WS^{\langle 3 \rangle}}{A - D3} \tag{5.344}$$

$$WT^{\langle 3 \rangle} = AS_{LP} \cdot (A - D_4) \tag{5.345}$$

$$WS^{\langle 4 \rangle} = WR^{\langle 4 \rangle} = WQ^{\langle 4 \rangle} = WP^{\langle 4 \rangle} = B_{PZ}^{\langle 4 \rangle} \tag{5.346}$$

$$AS_{LP} = \frac{WS^{\langle 4 \rangle}}{A - D3} \tag{5.347}$$

$$WT^{\langle 4 \rangle} = AS_{LP} \cdot (A - D_4) \tag{5.348}$$

Where the cycle continues to repeat for each time step.

5.4.5.5 Determination of Deflections in CS 3 with a Z-Direction Initial Step

Beginning with the initial deflections of Equations 5.201 through 5.206 then:

$$CS = 3 \tag{5.349}$$

$$CONTYPE = \begin{cases} 0 \text{ if } P_{ZP}^{\langle 0 \rangle} \geq 0 \wedge P_{XP}^{\langle 0 \rangle} \geq 0 \wedge \Phi > 90 \\ 1 \text{ if } P_{ZP}^{\langle 0 \rangle} \leq 0 \wedge P_{XP}^{\langle 0 \rangle} \geq 0 \wedge \Phi < 90 \end{cases} \tag{5.350}$$

$$B_{PZ}^{\langle 1 \rangle} = B_{PZ}^{\langle 0 \rangle} + V_Z^{\langle 0 \rangle} \cdot \tau \tag{5.351}$$

$$B_{PZ}^{\langle 2 \rangle} = B_{PZ}^{\langle 1 \rangle} \tag{5.352}$$

$$B_{PX}^{\langle 1 \rangle} = B_{PX}^{\langle 0 \rangle} \tag{5.353}$$

$$B_{PX}^{\langle 2 \rangle} = B_{PX}^{\langle 1 \rangle} + V_X^{\langle 0 \rangle} \cdot \tau \tag{5.354}$$

$$P_{XS}^{\langle 1 \rangle} = P_{XS}^{\langle 0 \rangle} \tag{5.355}$$

$$P_{XS}^{\langle 2 \rangle} = P_{XS}^{\langle 1 \rangle} + V_X^{\langle 0 \rangle} \cdot \tau \tag{5.356}$$

$$P_{XP}^{\langle 1 \rangle} = P_{XP}^{\langle 0 \rangle} \tag{5.357}$$

$$P_{XP}^{\langle 2 \rangle} = P_{XP}^{\langle 1 \rangle} + V_X^{\langle 0 \rangle} \cdot \tau \tag{5.358}$$

$$P_{ZS}^{\langle 2 \rangle} = P_{ZS}^{\langle 1 \rangle} \tag{5.359}$$

$$P_{ZS}^{\langle 1 \rangle} = P_{ZS}^{\langle 0 \rangle} + V_Z^{\langle 0 \rangle} \cdot \tau \tag{5.360}$$

$$P_{ZP}^{\langle 2 \rangle} = P_{ZP}^{\langle 1 \rangle} \tag{5.361}$$

$$P_{ZP}^{\langle 1 \rangle} = P_{ZP}^{\langle 0 \rangle} + V_Z^{\langle 0 \rangle} \cdot \tau \tag{5.362}$$

$$AP_{XP}^{\langle 0\rangle} = P_{XP}^{\langle 0\rangle} - (L_{RW} - L)\mathrm{Sin}(\Phi) \tag{5.363}$$

$$AP_{XS}^{\langle 0\rangle} = P_{XS}^{\langle 0\rangle} - (L_{RW} - L)\mathrm{Sin}(\Phi) \tag{5.364}$$

$$AP_{ZP}^{\langle 0\rangle} = P_{ZP}^{\langle 0\rangle} + (L_{RW} - L)\mathrm{Cos}(\Phi) \tag{5.365}$$

$$AP_{ZS}^{\langle 0\rangle} = P_{ZS}^{\langle 0\rangle} + (L_{RW} - L)\mathrm{Cos}(\Phi) \tag{5.366}$$

$$AP_{XP}^{\langle 1\rangle} = AP_{XP}^{\langle 0\rangle} \tag{5.367}$$

$$AP_{XP}^{\langle 2\rangle} = AP_{XP}^{\langle 1\rangle} + V_X^{\langle 0\rangle}\cdot\tau \tag{5.368}$$

$$AP_{XS}^{\langle 1\rangle} = AP_{XS}^{\langle 0\rangle} \tag{5.369}$$

$$AP_{XS}^{\langle 2\rangle} = AP_{XS}^{\langle 1\rangle} + V_X^{\langle 0\rangle}\cdot\tau \tag{5.370}$$

$$AP_{ZP}^{\langle 2\rangle} = AP_{ZP}^{\langle 1\rangle} = AP_{ZP}^{\langle 0\rangle} + V_Z^{\langle 0\rangle}\cdot\tau \tag{5.371}$$

$$AP_{ZS}^{\langle 2\rangle} = AP_{ZS}^{\langle 1\rangle} = AP_{ZS}^{\langle 0\rangle} + V_Z^{\langle 0\rangle}\cdot\tau \tag{5.372}$$

$$S_{LP} = \begin{cases} \dfrac{B_{PZ}^{\langle 0\rangle} - P_{ZP}^{\langle 0\rangle}}{B_{PX}^{\langle 0\rangle} - P_{XP}^{\langle 0\rangle}} & \text{if } CONTYPE = 0 \\ \dfrac{B_{PZ}^{\langle 0\rangle} - P_{ZS}^{\langle 0\rangle}}{B_{PX}^{\langle 0\rangle} - P_{XS}^{\langle 0\rangle}} & \text{if } CONTYPE = 1 \end{cases} \tag{5.373}$$

$$BS_{LP} = \begin{cases} \dfrac{P_{ZP}^{\langle 0\rangle} - AP_{ZP}^{\langle 0\rangle}}{P_{XP}^{\langle 0\rangle} - AP_{XP}^{\langle 0\rangle}} & \text{if } CONTYPE = 0 \\ \dfrac{P_{ZS}^{\langle 0\rangle} - AP_{ZS}^{\langle 0\rangle}}{P_{XS}^{\langle 0\rangle} - AP_{XS}^{\langle 0\rangle}} & \text{if } CONTYPE = 1 \end{cases} \tag{5.374}$$

$$D_2 = \begin{cases} \max\left(0, B_{PX}^{\langle 1\rangle} - \dfrac{B_{PZ}^{\langle 1\rangle}}{S_{LP}}\right) & \text{if } \begin{cases} CONTYPE = 0 \wedge P_{ZP}^{\langle 1\rangle} \le 0 \\ \mathrm{or}\left(CONTYPE = 1 \wedge P_{ZS}^{\langle 1\rangle} \ge 0\right) \end{cases} \\ \max\left(0, P_{XP}^{\langle 1\rangle} - \dfrac{P_{ZP}^{\langle 1\rangle}}{BS_{LP}}\right) & \text{if } CONTYPE = 0 \wedge P_{ZP}^{\langle 1\rangle} > 0 \\ \max\left(0, P_{XS}^{\langle 1\rangle} - \dfrac{P_{ZS}^{\langle 1\rangle}}{BS_{LP}}\right) & \text{if } CONTYPE = 1 \wedge P_{ZS}^{\langle 1\rangle} < 0 \end{cases} \tag{5.375}$$

$$D_1 = \begin{cases} P_{XP}^{\langle 1 \rangle} & \text{if } CONTYPE = 0 \wedge P_{ZP}^{\langle 1 \rangle} \le 0 \\ P_{XS}^{\langle 1 \rangle} & \text{if } CONTYPE = 1 \wedge P_{ZS}^{\langle 1 \rangle} \ge 0 \\ \max\left(0, D_2 - V_X^{\langle 0 \rangle} \cdot \tau, \frac{D_2}{2}\right) & \text{otherwise} \end{cases} \tag{5.376}$$

$$D_4 = D_2 + V_X^{\langle 0 \rangle} \cdot \tau \tag{5.377}$$

$$D_5 = D_1 + V_X^{\langle 0 \rangle} \cdot \tau \tag{5.378}$$

$$ORDER = \begin{cases} 0 & \text{if } D_5 \ge D_2 \\ 1 & \text{otherwise} \end{cases} \tag{5.379}$$

$$D_3 = \begin{cases} D_2 & \text{if } ORDER = 1 \\ D_5 & \text{otherwise} \end{cases} \tag{5.380}$$

$$D_2 = \begin{cases} D_2 & \text{if } ORDER = 0 \\ D_5 & \text{otherwise} \end{cases} \tag{5.381}$$

$$W^{\langle 1 \rangle} = \begin{cases} \min\left(0, B_{PZ}^{\langle 1 \rangle}\right) & \text{if } CONTYPE = 0 \\ \max\left(0, B_{PZ}^{\langle 1 \rangle}\right) & \text{if } CONTYPE = 1 \end{cases} \tag{5.382}$$

$$WR^{\langle 1 \rangle} = W^{\langle 1 \rangle} \quad \text{if } ORDER = 0 \tag{5.383}$$

$$WS^{\langle 1 \rangle} = W^{\langle 1 \rangle} \quad \text{if } ORDER = 1 \tag{5.384}$$

$$WR^{\langle 1 \rangle} = \begin{cases} WR^{\langle 1 \rangle} & \text{if } ORDER = 0 \\ \left[WS^{\langle 1 \rangle} - S_{LP} \cdot (D_3 - D_2) \right] & \text{if } \begin{cases} CONTYPE = 0 \wedge P_{ZP}^{\langle 1 \rangle} \le 0 \\ \text{or}\left(CONTYPE = 1 \wedge P_{ZS}^{\langle 1 \rangle} \ge 0\right) \end{cases} \\ \left[WS^{\langle 1 \rangle} - BS_{LP} \cdot (D_3 - D_2) \right] & \text{otherwise} \end{cases} \tag{5.385}$$

$$WS^{\langle 1 \rangle} = \begin{cases} WS^{\langle 1 \rangle} & \text{if } ORDER = 1 \\ \left[\frac{WR^{\langle 1 \rangle}}{A - D_2} \cdot (A - D_3) \right] & \text{otherwise} \end{cases} \tag{5.386}$$

$$WQ^{\langle 1\rangle} = \begin{cases} P_{ZP}^{\langle 1\rangle} & \text{if } CONTYPE = 0 \wedge P_{ZP}^{\langle 1\rangle} \le 0 \\ P_{ZS}^{\langle 1\rangle} & \text{if } CONTYPE = 1 \wedge P_{ZS}^{\langle 1\rangle} \ge 0 \\ \left[WR^{\langle 1\rangle} - BS_{LP} \cdot (D_2 - D_1) \right] & \text{otherwise} \end{cases} \tag{5.387}$$

$$WP^{\langle 1\rangle} = WQ^{\langle 1\rangle} - BS_{LP} \cdot D_1 \tag{5.388}$$

$$AS_{LP} = \frac{WS^{\langle 1\rangle}}{A - D_3} \tag{5.389}$$

$$WT^{\langle 1\rangle} = AS_{LP} \cdot (A - D_4) \tag{5.390}$$

$$WT^{\langle 2\rangle} = WS^{\langle 1\rangle} \tag{5.391}$$

$$WS^{\langle 2\rangle} = \begin{cases} \left[WT^{\langle 2\rangle} - S_{LP} \cdot (D_4 - D_3) \right] & \text{if } \begin{cases} CONTYPE = 0 \wedge P_{ZP}^{\langle 1\rangle} \le 0 \\ \text{or}\left(CONTYPE = 1 \wedge P_{ZS}^{\langle 1\rangle} \ge 0\right) \end{cases} \\ \left(WT^{\langle 2\rangle} - BS_{LP}(D_4 - D_3) \right) & \text{otherwise} \end{cases} \tag{5.392}$$

$$WR^{\langle 2\rangle} = \begin{cases} P_{ZP}^{\langle 1\rangle} & \text{if } CONTYPE = 0 \wedge P_{ZP}^{\langle 1\rangle} \le 0 \\ P_{ZS}^{\langle 1\rangle} & \text{if } CONTYPE = 1 \wedge P_{ZS}^{\langle 1\rangle} \ge 0 \\ WS^{\langle 1\rangle} - BS_{LP} \cdot (D_3 - D_2) & \text{otherwise} \end{cases} \tag{5.393}$$

$$WQ^{\langle 2\rangle} = WR^{\langle 2\rangle} - BS_{LP} \cdot (D_2 - D_1) \tag{5.394}$$

$$WP^{\langle 2\rangle} = WQ^{\langle 2\rangle} - BS_{LP} \cdot D_1 \tag{5.395}$$

Using Equations 5.231 through 5.235 and cycling the system yields:

$$D_1 = D_2 \tag{5.396}$$

$$D_2 = D_3 \tag{5.397}$$

$$D_4 = D_2 + V_x^{\langle 2\rangle} \cdot \tau \tag{5.398}$$

$$ORDER = \begin{cases} 0 & \text{if } D_5 \ge D_2 \\ 1 & \text{otherwise} \end{cases} \tag{5.399}$$

$$D_3 = \begin{cases} D_2 & \text{if ORDER} = 1 \\ D_5 & \text{otherwise} \end{cases} \tag{5.400}$$

$$D_2 = \begin{cases} D_2 & \text{if ORDER} = 0 \\ D_5 & \text{otherwise} \end{cases} \tag{5.401}$$

$$B_{PZ}^{\langle 3 \rangle} = B_{PZ}^{\langle 2 \rangle} + V_Z^{\langle 2 \rangle} \cdot \tau \tag{5.402}$$

$$B_{PZ}^{\langle 4 \rangle} = B_{PZ}^{\langle 3 \rangle} \tag{5.403}$$

$$B_{PX}^{\langle 3 \rangle} = B_{PX}^{\langle 2 \rangle} \tag{5.404}$$

$$B_{PX}^{\langle 4 \rangle} = B_{PX}^{\langle 3 \rangle} + V_X^{\langle 2 \rangle} \cdot \tau \tag{5.405}$$

Where repeating Equations 5.355 through 5.395 with the superscript ^{1} replaced with ^{3} and ^{2} replaced with ^{4} is sufficient to show how the cycle continues to repeat for each time step.

5.4.5.6 Determination of Deflections in CS 3 with a X-Direction Initial Step

Beginning with the initial deflections of Equations 5.201 through 5.206, and making use of Equations 5.349, 5.350 and 5.363 through 5.366 then:

$$B_{PZ}^{\langle 1 \rangle} = B_{PZ}^{\langle 0 \rangle} \tag{5.406}$$

$$B_{PZ}^{\langle 2 \rangle} = B_{PZ}^{\langle 1 \rangle} + V_Z^{\langle 0 \rangle} \cdot \tau \tag{5.407}$$

$$B_{PX}^{\langle 1 \rangle} = B_{PX}^{\langle 0 \rangle} + V_X^{\langle 0 \rangle} \cdot \tau \tag{5.408}$$

$$B_{PX}^{\langle 2 \rangle} = B_{PX}^{\langle 1 \rangle} \tag{5.409}$$

$$P_{XS}^{\langle 2 \rangle} = P_{XS}^{\langle 1 \rangle} = P_{XS}^{\langle 0 \rangle} + V_X^{\langle 0 \rangle} \cdot \tau \tag{5.410}$$

$$P_{XP}^{\langle 2 \rangle} = P_{XP}^{\langle 1 \rangle} = P_{XP}^{\langle 0 \rangle} + V_X^{\langle 0 \rangle} \cdot \tau \tag{5.411}$$

$$P_{ZP}^{\langle 1 \rangle} = P_{ZP}^{\langle 0 \rangle} \tag{5.412}$$

$$P_{ZP}^{\langle 2 \rangle} = P_{ZP}^{\langle 1 \rangle} + V_Z^{\langle 0 \rangle} \cdot \tau \tag{5.413}$$

$$P_{ZS}^{\langle 1\rangle} = P_{ZS}^{\langle 0\rangle} \tag{5.414}$$

$$P_{ZS}^{\langle 2\rangle} = P_{ZS}^{\langle 1\rangle} + V_Z^{\langle 0\rangle}\cdot\tau \tag{5.415}$$

$$AP_{ZP}^{\langle 1\rangle} = AP_{ZP}^{\langle 0\rangle} \tag{5.416}$$

$$AP_{ZP}^{\langle 2\rangle} = AP_{ZP}^{\langle 1\rangle} + V_Z^{\langle 0\rangle}\cdot\tau \tag{5.417}$$

$$AP_{ZS}^{\langle 1\rangle} = AP_{ZS}^{\langle 0\rangle} \tag{5.418}$$

$$AP_{ZS}^{\langle 2\rangle} = AP_{ZS}^{\langle 1\rangle} + V_Z^{\langle 0\rangle}\cdot\tau \tag{5.419}$$

$$AP_{XS}^{\langle 2\rangle} = AP_{XS}^{\langle 1\rangle} = AP_{XS}^{\langle 0\rangle} + V_X^{\langle 0\rangle}\cdot\tau \tag{5.420}$$

$$AP_{XP}^{\langle 2\rangle} = AP_{XP}^{\langle 1\rangle} = AP_{XP}^{\langle 0\rangle} + V_X^{\langle 0\rangle}\cdot\tau \tag{5.421}$$

Using Equations 5.373 and 5.374 to define S_{LP} and BS_{LP} respectively yields:

$$D_2 = \begin{cases} \max\left(0, P_{XP}^{\langle 1\rangle} - \dfrac{P_{ZP}^{\langle 1\rangle}}{BS_{LP}}\right) & \text{if } CONTYPE = 0 \\ \max\left(0, P_{XS}^{\langle 1\rangle} - \dfrac{P_{ZS}^{\langle 1\rangle}}{BS_{LP}}\right) & \text{if } CONTYPE = 1 \end{cases} \tag{5.422}$$

$$D_1 = \max\left(0, D_2 - V_X^{\langle 0\rangle}\cdot\tau, \frac{D_2}{2}\right) \tag{5.423}$$

$$D_3 = \begin{cases} \max\left(0, P_{XP}^{\langle 2\rangle} - \dfrac{P_{ZP}^{\langle 2\rangle}}{BS_{LP}}\right) & \text{if } CONTYPE = 0 \wedge P_{ZP}^{\langle 2\rangle} > 0 \\ \max\left(0, P_{XS}^{\langle 2\rangle} - \dfrac{P_{ZS}^{\langle 2\rangle}}{BS_{LP}}\right) & \text{if } CONTYPE = 1 \wedge P_{ZS}^{\langle 2\rangle} < 0 \\ P_{XP}^{\langle 2\rangle} & \text{if } CONTYPE = 0 \wedge P_{ZP}^{\langle 2\rangle} \le 0 \\ P_{XS}^{\langle 2\rangle} & \text{if } CONTYPE = 1 \wedge P_{ZS}^{\langle 2\rangle} \ge 0 \end{cases} \tag{5.424}$$

$$D_4 = \begin{cases} \max\left(0, B_{PX}^{\langle 2\rangle} - \dfrac{B_{PZ}^{\langle 2\rangle}}{S_{LP}}\right) & \text{if } \begin{cases} \text{CONTYPE} = 0 \wedge P_{ZP}^{\langle 2\rangle} \le 0 \\ \text{or}\left(\text{CONTYPE} = 1 \wedge P_{ZS}^{\langle 2\rangle} \ge 0\right) \end{cases} \\ D_3 \quad \text{otherwise} \end{cases} \tag{5.425}$$

$$\text{ORDER} = \begin{cases} 1 \quad \text{if } D_3 = D_4 \\ 0 \quad \text{otherwise} \end{cases} \tag{5.426}$$

$$D_3 = \begin{cases} \left(D_2 + \dfrac{D_4 - D_2}{2}\right) & \text{if ORDER} = 1 \\ D_3 \quad \text{otherwise} \end{cases} \tag{5.427}$$

$$WS^{\langle 1\rangle} = WT^{\langle 1\rangle} = WR^{\langle 1\rangle} = 0 \tag{5.428}$$

$$WQ^{\langle 1\rangle} = WR^{\langle 1\rangle} - BS_{LP} \cdot \left(D_2 - D_1\right) \tag{5.429}$$

$$WP^{\langle 1\rangle} = WQ^{\langle 1\rangle} - BS_{LP} \cdot D_1 \tag{5.430}$$

$$WS^{\langle 2\rangle} = \begin{cases} P_{ZP}^{\langle 2\rangle} & \text{if ORDER} = 0 \wedge \text{CONTYPE} = 0 \\ P_{ZS}^{\langle 2\rangle} & \text{if ORDER} = 0 \wedge \text{CONTYPE} = 1 \\ \left[-BS_{LP} \cdot \left(D_4 - D_3\right)\right] & \text{otherwise} \end{cases} \tag{5.431}$$

$$WT^{\langle 2\rangle} = 0 \tag{5.432}$$

$$WR^{\langle 2\rangle} = WS^{\langle 2\rangle} - BS_{LP} \cdot \left(D_3 - D_2\right) \tag{5.433}$$

$$WQ^{\langle 2\rangle} = WQ^{\langle 1\rangle} + V_Z^{\langle 0\rangle} \cdot \tau \tag{5.434}$$

$$WP^{\langle 2\rangle} = WP^{\langle 1\rangle} + V_Z^{\langle 0\rangle} \cdot \tau \tag{5.435}$$

Using Equations 5.231 through 5.235 and cycling the system yields:

$$B_{PZ}^{\langle 3\rangle} = B_{PZ}^{\langle 2\rangle} \tag{5.436}$$

$$B_{PZ}^{\langle 4\rangle} = B_{PZ}^{\langle 3\rangle} + V_Z^{\langle 2\rangle} \cdot \tau \tag{5.437}$$

$$B_{PX}^{\langle 3 \rangle} = B_{PX}^{\langle 2 \rangle} + V_X^{\langle 2 \rangle} \cdot \tau \tag{5.438}$$

$$B_{PX}^{\langle 4 \rangle} = B_{PX}^{\langle 3 \rangle} \tag{5.439}$$

$$P_{XS}^{\langle 4 \rangle} = P_{XS}^{\langle 3 \rangle} = P_{XS}^{\langle 2 \rangle} + V_X^{\langle 2 \rangle} \cdot \tau \tag{5.440}$$

$$P_{XP}^{\langle 4 \rangle} = P_{XP}^{\langle 3 \rangle} = P_{XP}^{\langle 2 \rangle} + V_X^{\langle 2 \rangle} \cdot \tau \tag{5.441}$$

$$P_{ZP}^{\langle 3 \rangle} = P_{ZP}^{\langle 2 \rangle} \tag{5.442}$$

$$P_{ZP}^{\langle 4 \rangle} = P_{ZP}^{\langle 3 \rangle} + V_Z^{\langle 2 \rangle} \cdot \tau \tag{5.443}$$

$$P_{ZS}^{\langle 3 \rangle} = P_{ZS}^{\langle 2 \rangle} \tag{5.444}$$

$$P_{ZS}^{\langle 4 \rangle} = P_{ZS}^{\langle 3 \rangle} + V_Z^{\langle 2 \rangle} \cdot \tau \tag{5.445}$$

$$AP_{ZP}^{\langle 3 \rangle} = AP_{ZP}^{\langle 2 \rangle} \tag{5.446}$$

$$AP_{ZP}^{\langle 4 \rangle} = AP_{ZP}^{\langle 3 \rangle} + V_Z^{\langle 2 \rangle} \cdot \tau \tag{5.447}$$

$$AP_{XS}^{\langle 4 \rangle} = AP_{XS}^{\langle 3 \rangle} = AP_{XS}^{\langle 2 \rangle} + V_X^{\langle 2 \rangle} \cdot \tau \tag{5.448}$$

$$AP_{XP}^{\langle 4 \rangle} = AP_{XP}^{\langle 3 \rangle} = AP_{XP}^{\langle 2 \rangle} + V_X^{\langle 2 \rangle} \cdot \tau \tag{5.449}$$

$$AP_{ZS}^{\langle 3 \rangle} = AP_{ZS}^{\langle 2 \rangle} \tag{5.450}$$

$$AP_{ZS}^{\langle 4 \rangle} = AP_{ZS}^{\langle 3 \rangle} + V_Z^{\langle 2 \rangle} \cdot \tau \tag{5.451}$$

$$D_1 = \begin{cases} D_4 & \text{if } ORDER = 1 \\ D_3 & \text{if } ORDER = 0 \end{cases} \tag{5.452}$$

$$D_2 = \begin{cases} \left(D_1 + V_X^{\langle 2 \rangle} \cdot \tau\right) & \text{if } ORDER = 1 \\ \min\left(D_4, D_1 + V_X^{\langle 2 \rangle} \cdot \tau\right) & \text{if } ORDER = 0 \end{cases} \tag{5.453}$$

$$D_3 = \begin{cases} \max\left(D_4, D_1 + V_X^{\langle 2 \rangle} \cdot \tau\right) & \text{if } ORDER = 0 \\ \max\left(0, P_{XP}^{\langle 4 \rangle} - \dfrac{P_{ZP}^{\langle 4 \rangle}}{BS_{LP}}\right) & \text{if } ORDER = 1 \wedge CONTYPE = 0 \wedge P_{ZP}^{\langle 4 \rangle} > 0 \\ \max\left(0, P_{XS}^{\langle 4 \rangle} - \dfrac{P_{ZS}^{\langle 4 \rangle}}{BS_{LP}}\right) & \text{if } ORDER = 1 \wedge CONTYPE = 1 \wedge P_{ZS}^{\langle 4 \rangle} < 0 \\ P_{XP}^{\langle 4 \rangle} & \text{if } ORDER = 1 \wedge CONTYPE = 0 \wedge P_{ZP}^{\langle 4 \rangle} \le 0 \\ P_{XS}^{\langle 4 \rangle} & \text{if } ORDER = 1 \wedge CONTYPE = 1 \wedge P_{ZS}^{\langle 4 \rangle} \ge 0 \end{cases} \tag{5.454}$$

$$ORDER_A = \begin{cases} 1 & \text{if } D_3 = D_4 \\ 0 & \text{otherwise} \end{cases} \tag{5.455}$$

$$D_3 = \begin{cases} \left(D_2 + \dfrac{D_4 - D_2}{2}\right) & \text{if } ORDER_A = 1 \\ D_3 & \text{otherwise} \end{cases} \tag{5.456}$$

$$WR^{\langle 3 \rangle} = \begin{cases} 0 & \text{if } ORDER = 1 \\ P_{ZP}^{\langle 3 \rangle} & \text{if } ORDER = 0 \wedge D_2 = D_1 + V_X^{\langle 2 \rangle} \cdot \tau \wedge CONTYPE = 0 \\ P_{ZS}^{\langle 3 \rangle} & \text{if } ORDER = 0 \wedge D_2 = D_1 + V_X^{\langle 2 \rangle} \cdot \tau \wedge CONTYPE = 1 \\ P_{ZP}^{\langle 3 \rangle} - BS_{LP}\left(D_3 - D_2\right) & \text{if } ORDER = 0 \wedge D_2 < D_1 + V_X^{\langle 2 \rangle} \cdot \tau \wedge CONTYPE = 0 \\ P_{ZS}^{\langle 3 \rangle} - BS_{LP} \cdot \left(D_3 - D_2\right) & \text{if } ORDER = 0 \wedge D_2 < D_1 + V_X^{\langle 2 \rangle} \cdot \tau \wedge CONTYPE = 1 \end{cases} \tag{5.457}$$

$$WS^{\langle 3 \rangle} = \begin{cases} 0 & \text{if } ORDER = 1 \\ P_{ZP}^{\langle 3 \rangle} & \text{if } ORDER = 0 \wedge D_2 < D_1 + V_X^{\langle 2 \rangle} \cdot \tau \wedge CONTYPE = 0 \\ P_{ZS}^{\langle 3 \rangle} & \text{if } ORDER = 0 \wedge D_2 < D_1 + V_X^{\langle 2 \rangle} \cdot \tau \wedge CONTYPE = 1 \\ \left[WT^{\langle 3 \rangle} - S_{LP} \cdot \left(D_4 - D_3\right)\right] & \text{if } ORDER = 0 \wedge D_2 = D_1 + V_X^{\langle 2 \rangle} \cdot \tau \end{cases} \tag{5.458}$$

$$WT^{\langle 3 \rangle} = \begin{cases} 0 & \text{if } ORDER = 1 \\ \min\left(B_{PZ}^{\langle 3 \rangle}, 0\right) & \text{if } CONTYPE = 0 \wedge ORDER = 0 \\ \max\left(B_{PZ}^{\langle 3 \rangle}, 0\right) & \text{if } CONTYPE = 1 \wedge ORDER = 0 \end{cases} \tag{5.459}$$

$$WQ^{\langle 3 \rangle} = WR^{\langle 3 \rangle} - BS_{LP} \cdot \left(D_2 - D_1\right) \tag{5.460}$$

$$WP^{\langle 3 \rangle} = WQ^{\langle 3 \rangle} - BS_{LP} \cdot D_1 \tag{5.461}$$

$$D_1 = \begin{cases} D_1 & \text{if } ORDER = 1 \\ D_2 & \text{if } ORDER = 0 \wedge D_2 = D_1 + V_X^{\langle 2 \rangle} \cdot \tau \\ D_3 & \text{if } ORDER = 0 \wedge D_2 < D_1 + V_X^{\langle 2 \rangle} \cdot \tau \end{cases} \tag{5.462}$$

$$D_2 = \begin{cases} D_2 & \text{if } ORDER = 1 \\ D_3 & \text{if } ORDER = 0 \wedge D_2 = D_1 + V_X^{\langle 2 \rangle} \cdot \tau \\ D_3 + \dfrac{D_4 - D_3}{2} & \text{if } ORDER = 0 \wedge D_2 < D_1 + V_X^{\langle 2 \rangle} \cdot \tau \end{cases} \tag{5.463}$$

$$D_3 = \begin{cases} D_3 & \text{if } ORDER = 1 \\ D_4 & \text{if } ORDER = 0 \end{cases} \tag{5.464}$$

$$D_4 = \begin{cases} D_4 & \text{if } ORDER = 1 \\ \min\left(B_{PX}^{\langle 4 \rangle}, B_{PX}^{\langle 4 \rangle} - \dfrac{B_{PZ}^{\langle 4 \rangle}}{S_{LP}} \right) & \text{if } ORDER = 0 \end{cases} \tag{5.465}$$

$$WQ^{\langle 3 \rangle} = \begin{cases} WQ^{\langle 3 \rangle} & \text{if } ORDER = 1 \\ P_{ZP}^{\langle 3 \rangle} & \text{if } CONTYPE = 0 \wedge ORDER = 0 \\ P_{ZS}^{\langle 3 \rangle} & \text{if } CONTYPE = 1 \wedge ORDER = 0 \end{cases} \tag{5.466}$$

$$WS^{\langle 3 \rangle} = \begin{cases} WS^{\langle 3 \rangle} & \text{if } ORDER = 1 \\ WT^{\langle 3 \rangle} & \text{if } ORDER = 0 \end{cases} \tag{5.467}$$

$$WT^{\langle 3 \rangle} = \begin{cases} WT^{\langle 3 \rangle} & \text{if } ORDER = 1 \\ \left[\dfrac{WT^{\langle 3 \rangle}}{A - D_3} \cdot (A - D_4) \right] & \text{if } ORDER = 0 \end{cases} \tag{5.468}$$

$$WR^{\langle 3 \rangle} = \begin{cases} WR^{\langle 3 \rangle} & \text{if } ORDER = 1 \\ \left[WS^{\langle 3 \rangle} - S_{LP} \cdot (D_3 - D_2) \right] & \text{if } ORDER = 0 \end{cases} \tag{5.469}$$

$$WQ^{\langle 4 \rangle} = WQ^{\langle 3 \rangle} + V_Z^{\langle 2 \rangle} \cdot \tau \tag{5.470}$$

$$WP^{\langle 4 \rangle} = WP^{\langle 3 \rangle} + V_Z^{\langle 2 \rangle} \cdot \tau \tag{5.471}$$

$$WT^{\langle 4\rangle} = \begin{cases} 0 \text{ if } ORDER = 1 \\ \min\left(B_{PZ}^{\langle 4\rangle}, 0\right) \text{ if } CONTYPE = 0 \wedge ORDER = 0 \\ \max\left(B_{PZ}^{\langle 4\rangle}, 0\right) \text{ if } CONTYPE = 1 \wedge ORDER = 0 \end{cases} \tag{5.472}$$

$$WS^{\langle 4\rangle} = \begin{cases} P_{ZP}^{\langle 4\rangle} \text{ if } ORDER = 1 \wedge ORDER_A = 0 \wedge CONTYPE = 0 \\ P_{ZS}^{\langle 4\rangle} \text{ if } ORDER = 1 \wedge ORDER_A = 0 \wedge CONTYPE = 1 \\ \left[-BS_{LP} \cdot \left(D_4 - D_3\right)\right] \text{ if } ORDER = 1 \wedge ORDER_A = 1 \\ \left[WT^{\langle 4\rangle} - S_{LP} \cdot \left(D_4 - D_3\right)\right] \text{ if } ORDER = 0 \end{cases} \tag{5.473}$$

$$WR^{\langle 4\rangle} = \begin{cases} \left[WS^{\langle 4\rangle} - BS_{LP} \cdot \left(D_3 - D_2\right)\right] \text{ if } ORDER = 1 \\ \left[WS^{\langle 4\rangle} - S_{LP} \cdot \left(D_3 - D_2\right)\right] \text{ if } ORDER = 0 \end{cases} \tag{5.474}$$

Where the cycle continues to repeat for each time step starting with Equation 5.475.

$$ORDER = ORDER_A \tag{5.475}$$

5.4.5.7 Determination of Deflections in CS 4 with a Z-Direction Initial Step

Beginning with the initial deflections of Equations 5.201 through 5.206 and making use of Equations 5.351 through 5.374 then:

$$CS = 4 \tag{5.476}$$

$$CONTYPE = \begin{cases} 0 \text{ if } P_{ZP}^{\langle 0\rangle} \geq 0 \wedge P_{XP}^{\langle 0\rangle} \geq 0 \wedge \Phi \leq 90 \\ 1 \text{ if } P_{ZP}^{\langle 0\rangle} \leq 0 \wedge P_{XS}^{\langle 0\rangle} \geq 0 \wedge \Phi \geq 90 \end{cases} \tag{5.477}$$

$$D_1 = \begin{cases} P_{XP}^{\langle 1\rangle} \text{ if } CONTYPE = 0 \\ P_{XS}^{\langle 1\rangle} \text{ if } CONTYPE = 1 \end{cases} \tag{5.478}$$

$$D_2 = \min\left(B_{PX}^{\langle 2\rangle}, B_{PX}^{\langle 2\rangle} - \frac{B_{PZ}^{\langle 2\rangle}}{S_{LP}}, D_1 + V_X^{\langle 0\rangle} \cdot \tau\right) \tag{5.479}$$

$$D_3 = \max\left(D_1 + V_X^{\langle 0\rangle}\cdot\tau, \min\left(B_{PX}^{\langle 2\rangle}, B_{PX}^{\langle 2\rangle} - \frac{B_{PZ}^{\langle 2\rangle}}{S_{LP}}\right)\right) \tag{5.480}$$

$$D_4 = D_3 + V_X^{\langle 0\rangle}\cdot\tau \tag{5.481}$$

$$WP^{\langle 1\rangle} = WQ^{\langle 1\rangle} = \begin{cases} P_{ZP}^{\langle 1\rangle} & \text{if CONTYPE} = 0 \\ P_{ZS}^{\langle 1\rangle} & \text{if CONTYPE} = 1 \end{cases} \tag{5.482}$$

$$WR^{\langle 1\rangle} = \begin{cases} \min\left[0, WQ^{\langle 1\rangle} + S_{LP}\cdot(D_2 - D_1)\right] & \text{if CONTYE} = 0 \\ \max\left[0, WQ^{\langle 1\rangle} + S_{LP}\cdot(D_2 - D_1)\right] & \text{if CONTYE} = 1 \end{cases} \tag{5.483}$$

$$WS^{\langle 1\rangle} = \frac{WR^{\langle 1\rangle}}{A - D_2}\cdot(A - D_3) \tag{5.484}$$

$$WT^{\langle 1\rangle} = \frac{WR^{\langle 1\rangle}}{A - D_2}\cdot(A - D_4) \tag{5.485}$$

$$WP^{\langle 2\rangle} = WQ^{\langle 2\rangle} = WR^{\langle 2\rangle} = WP^{\langle 1\rangle} \tag{5.486}$$

$$WS^{\langle 2\rangle} = \begin{cases} WP^{\langle 1\rangle} & \text{if } D_3 = D_1 + V_X^{\langle 0\rangle}\cdot\tau \\ \min\left[0, WR^{\langle 2\rangle} + S_{LP}\cdot(D_4 - D_3)\right] & \text{if CONTYPE} = 0 \wedge D_3 > D_1 + V_X^{\langle 0\rangle}\cdot\tau \\ \max\left[0, WR^{\langle 2\rangle} + S_{LP}\cdot(D_4 - D_3)\right] & \text{if CONTYPE} = 1 \wedge D_3 > D_1 + V_X^{\langle 0\rangle}\cdot\tau \end{cases} \tag{5.487}$$

$$WT^{\langle 2\rangle} = \frac{WS^{\langle 2\rangle}}{A - D_3}\cdot(A - D_4) \tag{5.488}$$

Using Equations 5.231 through5.235 and cycling the system yields the exact procedure as starting from Equation 5.478 with the superscript ^{1} replaced with ^{3} and ^{2} replaced with ^{4}.

5.4.5.8 Determination of Deflections in CS 4 with a X-Direction Initial Step

Beginning with the initial deflections of Equations 5.201 through 5.206, and making use of Equations 5.476, 5.477 and 5.406 through 5.420 then:

$$D_1 = \begin{cases} P_{XP}^{\langle 0 \rangle} & \text{if CONTYPE} = 0 \\ P_{XS}^{\langle 0 \rangle} & \text{if CONTYPE} = 1 \end{cases} \tag{5.489}$$

$$D_2 = D_1 + V_X^{\langle 0 \rangle} \cdot \tau \tag{5.490}$$

$$WP^{\langle 1 \rangle} = WQ^{\langle 1 \rangle} = WR^{\langle 1 \rangle} = WS^{\langle 1 \rangle} = WT^{\langle 1 \rangle} = 0 \tag{5.491}$$

$$WP^{\langle 2 \rangle} = WQ^{\langle 2 \rangle} = WR^{\langle 2 \rangle} = \begin{cases} P_{ZP}^{\langle 1 \rangle} & \text{if CONTYPE} = 0 \\ P_{ZS}^{\langle 1 \rangle} & \text{if CONTYPE} = 1 \end{cases} \tag{5.492}$$

$$WT^{\langle 2 \rangle} = \begin{cases} \max\left(0, B_{PZ}^{\langle 2 \rangle}\right) & \text{if CONTYPE} = 1 \\ \min\left(0, B_{PZ}^{\langle 2 \rangle}\right) & \text{if CONTYPE} = 0 \end{cases} \tag{5.493}$$

$$D_4 = \min\left(B_{PX}^{\langle 2 \rangle}, B_{PX}^{\langle 2 \rangle} - \frac{B_{PZ}^{\langle 2 \rangle}}{S_{LP}} \right) \tag{5.494}$$

$$D_3 = D_2 + \frac{D_4 - D_2}{2} \tag{5.495}$$

$$WS = WT - S_{LP} \cdot \left(D_4 - D_3\right) \tag{5.496}$$

Using Equations 5.231 through 5.235 then cycling the system yields:

$$D_1 = D_2 \tag{5.497}$$

$$D_2 = \min\left(D_4, D_1 + V_X^{\langle 2 \rangle} \cdot \tau\right) \tag{5.498}$$

$$D_3 = \max\left(D_4, D_1 + V_X^{\langle 2 \rangle} \cdot \tau\right) \tag{5.499}$$

$$D_4 = \min\left(B_{PX}^{\langle 3 \rangle}, B_{PX}^{\langle 3 \rangle} - \frac{B_{PZ}^{\langle 3 \rangle}}{S_{LP}} \right) \tag{5.500}$$

$$WP^{\langle 3 \rangle} = WQ^{\langle 3 \rangle} = WR^{\langle 3 \rangle} = WP^{\langle 2 \rangle} \tag{5.501}$$

$$WT^{\langle 3 \rangle} = WT^{\langle 2 \rangle} \tag{5.502}$$

$$WS^{\langle 3 \rangle} = WT^{\langle 3 \rangle} - S_{LP} \cdot (D_4 - D_3) \tag{5.503}$$

$$D_1 = \begin{cases} D_2 & \text{if } D_2 = D_1 + V_X^{\langle 2 \rangle} \cdot \tau \\ D_3 & \text{otherwise} \end{cases} \tag{5.504}$$

$$D_2 = \begin{cases} D_3 & \text{if } D_2 = D_1 + V_X^{\langle 2 \rangle} \cdot \tau \\ \left(D_3 + \frac{D_4 - D_3}{2} \right) & \text{otherwise} \end{cases} \tag{5.505}$$

$$D_3 = D_4 \tag{5.506}$$

$$D_4 = \min\left(B_{PX}^{\langle 4 \rangle}, B_{PX}^{\langle 4 \rangle} - \frac{B_{PZ}^{\langle 4 \rangle}}{S_{LP}} \right) \tag{5.507}$$

$$WR^{\langle 3 \rangle} = WQ^{\langle 3 \rangle} + S_{LP} \cdot (D_2 - D_1) \tag{5.508}$$

$$WS^{\langle 3 \rangle} = WT^{\langle 3 \rangle} \tag{5.509}$$

$$WT^{\langle 3 \rangle} = \frac{WS^{\langle 3 \rangle}}{A - D_3} \cdot (A - D_4) \tag{5.510}$$

$$WT^{\langle 4 \rangle} = WT^{\langle 3 \rangle} + V_Z^{\langle 2 \rangle} \cdot \tau \tag{5.511}$$

$$WS^{\langle 4 \rangle} = WS^{\langle 3 \rangle} + V_Z^{\langle 2 \rangle} \cdot \tau \tag{5.512}$$

$$WR^{\langle 4 \rangle} = WR^{\langle 3 \rangle} + V_Z^{\langle 2 \rangle} \cdot \tau \tag{5.513}$$

$$WQ^{\langle 4 \rangle} = WP^{\langle 4 \rangle} = WP^{\langle 3 \rangle} + V_Z^{\langle 2 \rangle} \cdot \tau \tag{5.514}$$

Using Equations 5.232 and 5.235 the cycle continues to repeat for each time step starting with Equation 5.515.

$$D_1 = D_1 \tag{5.515}$$

$$D_2 = \min(D_4, D_1 + V_X^{\langle 4 \rangle} \cdot \tau) \tag{5.516}$$

$$D_3 = \max\left(D_4, D_1 + V_X^{\langle 4\rangle}\cdot\tau\right) \tag{5.517}$$

$$D_4 = D_4 + V_X^{\langle 4\rangle}\cdot\tau \tag{5.518}$$

$$WP^{\langle 4\rangle} = WQ^{\langle 4\rangle} = WR^{\langle 4\rangle} = \begin{cases} P_{ZP}^{\langle 4\rangle} & \text{if CONTYPE} = 0 \\ P_{ZS}^{\langle 4\rangle} & \text{if CONTYPE} = 1 \end{cases} \tag{5.519}$$

$$WT^{\langle 4\rangle} = WT^{\langle 4\rangle} \tag{5.520}$$

$$WS^{\langle 4\rangle} = WT^{\langle 4\rangle} - S_{LP}\cdot\left(D_4 - D_3\right) \tag{5.521}$$

Where the cycle continues to repeat for each time step.

The complexity of the equations of Sections 5.4.5.1 through 5.4.5.8 is simplified as much as possible by the flow chart of appendix J detailing the energy absorption procedure from a plate of Figure 5-60.

5.4.6 Validation of Energy Absorption of Twenty-Five-Region Plate

To validate the proposed twenty-five-region plate plastic membrane theory for the determination of the energy absorbed through the non-uniform longitudinal deflection of transverse bulkheads and webs, the method is compared to finite element analysis for 20 separate cases as outlined by Table 5-7. For each case the initial conditions are provided in Table 5-6.

Table 5-6 Constant Parameters for Twenty-Five Region Plate Test Cases

Case Costants		
Variable	***Value***	***Units***
Rigid Wedge Mass	50228.4	Kg
Failure Strain	0.1	--
HEA	23.2	Degrees
A	7.5	m
B	10	m
Analysis Time Step	0.001	s
Plate Yield Stress	2.35E+08	Pa
Rigid Wedge Height	5.5	m
Rigid Wedge Beam	3	m
Rigid Wedge Length	10	m

Table 5-7 Twenty-Five Region Plate Test Case Variable Values

	Variable							
Case	*CS*	*Collision Angle (degrees)*	*Initial X Component Velocity (m/s)*	*Initial Z Component Velocity (m/s)*	*Plate Thickness (mm)*	*Bpx (m)*	*Bpy (m)*	*Bpz (m)*
1	1	90	3	5	20	0	1.5	0.5
2	1	75	5	3	20	0	1.5	0.5
3	1-4	90	3	3	20	3	-0.5	1.5
4	1-3	105	4	5	20	2	-0.5	2.5
5	2	66.8	2	4	20	2	0.75	0.5
6	2	66.8	4	1	20	2	0.75	0.5
7	2	66.8	2	4	20	2	-0.75	0.5
8	2	66.8	5	3	20	2	-0.75	0.5
9	3	105	4	2	20	4	-0.5	3
10	3	105	2	4	20	4	-0.5	3
11	3	115	5	2	20	4	1	4
12	3	115	2	5	20	4	1	4
13	4	75	5	1	20	4	1.5	1
14	4	75	1	5	20	4	1.5	1
15	4	90	5	2	20	5	-2	1.75
16	4	75	2	5	20	5	-2	2.75
17	1	90	3	5	8	0	1.5	0.5
18	1	90	3	5	31	0	1.5	0.5
19	3	115	2	5	16	4	1	4
20	3	115	2	5	25	4	1	4

Figure 5-63 through Figure 5-71 show a comparison of the resultant deformation from both the finite element analysis and twenty-five-region plate theory for case 4 of Table 5-7.

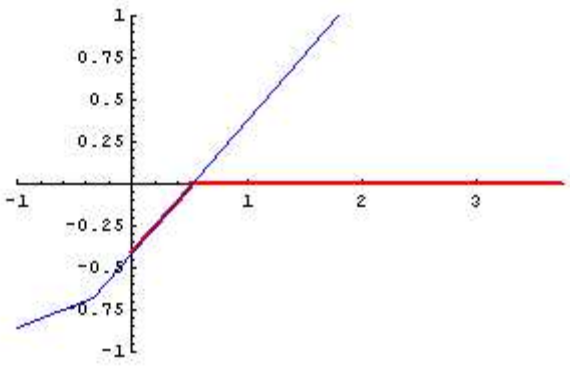

Figure 5-63 Test Case 4 Twenty-Five Region Plate Deflection at 0.1 Seconds

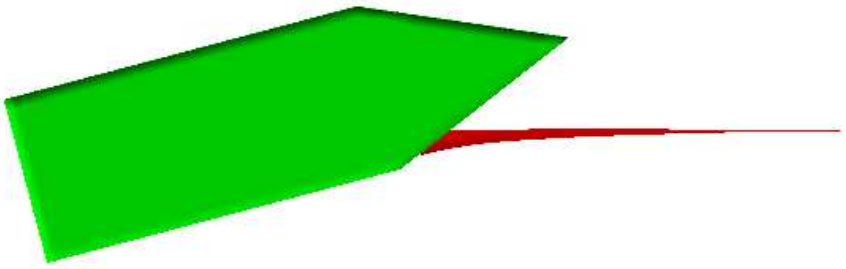

Figure 5-64 Test Case 4 FEA Deflection at 0.1 Seconds

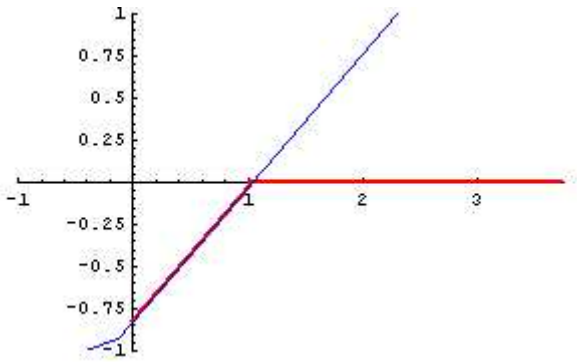

Figure 5-65 Test Case 4 Twenty-Five Region Plate Deflection at 0.2 Seconds

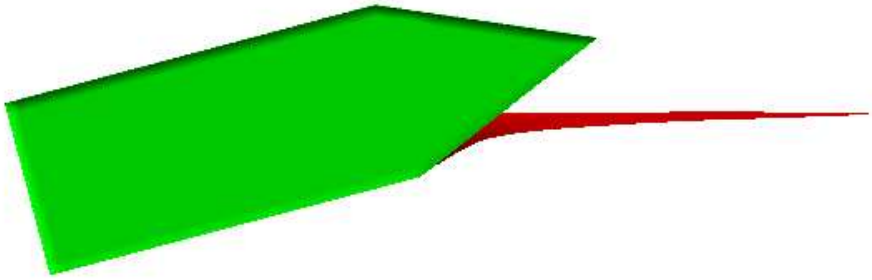

Figure 5-66 Test Case 4 FEA Deflection at 0.2 Seconds

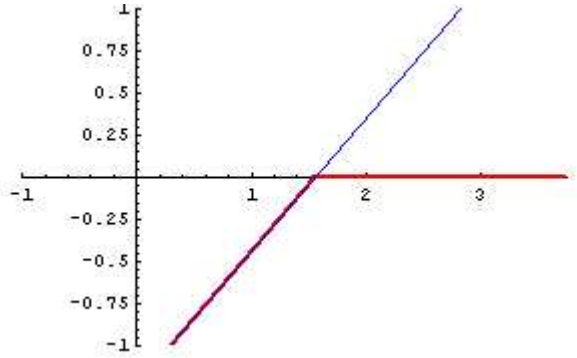

Figure 5-67 Test Case 4 Twenty-Five Region Plate Deflection at 0.3 Seconds

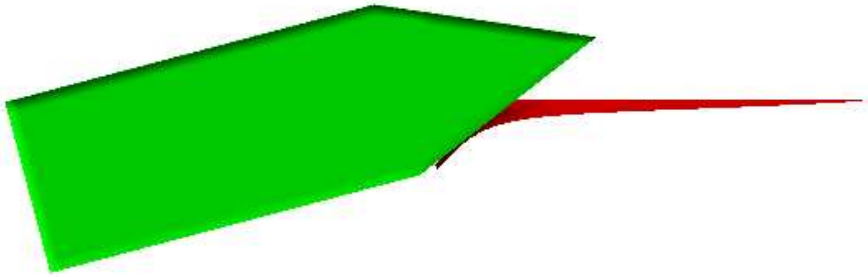

Figure 5-68 Test Case 4 FEA Deflection at 0.3 Seconds

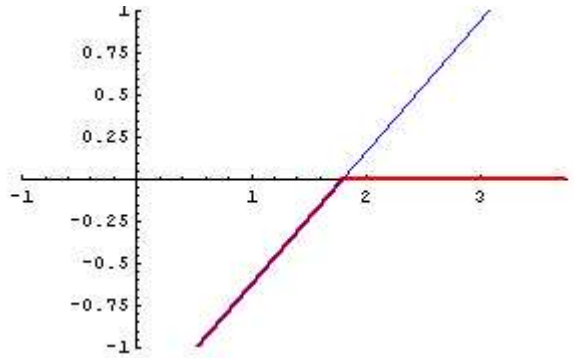

Figure 5-69 Test Case 4 Twenty-Five Region Plate Deflection at 0.35 Seconds

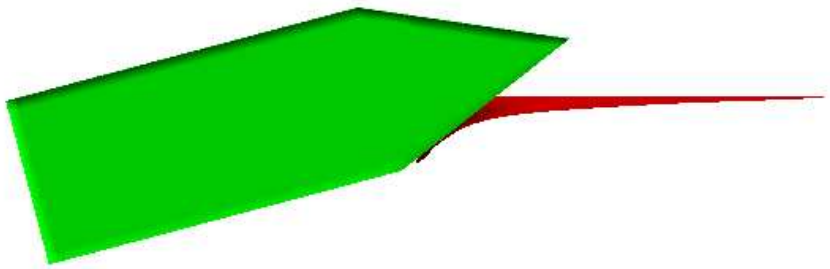

Figure 5-70 Test Case 4 FEA Deflection at 0.35 Seconds

Figure 5-71 Test Case 4 FEA Plate Mesh Deflection at 0.35 Seconds

Figure 5-72 through Figure 5-91 provide the comparison of the energy verses time response for each case of Table 5-7.

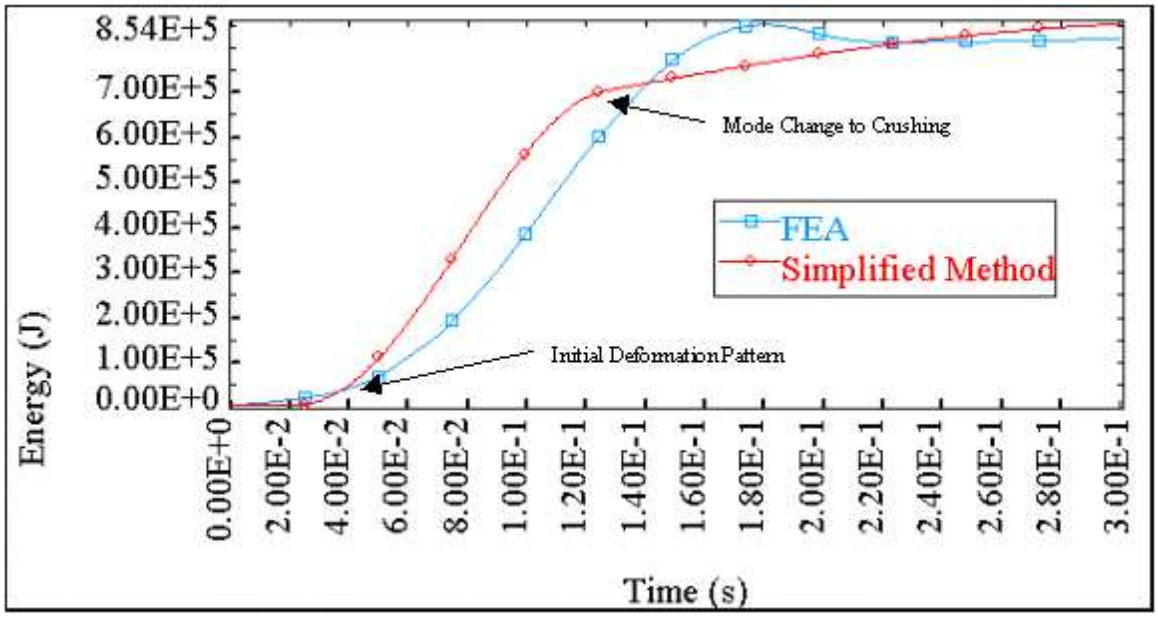

Figure 5-72 Case 1 Simplified Method and FEA Absorbed Energy vs. Time Comparison

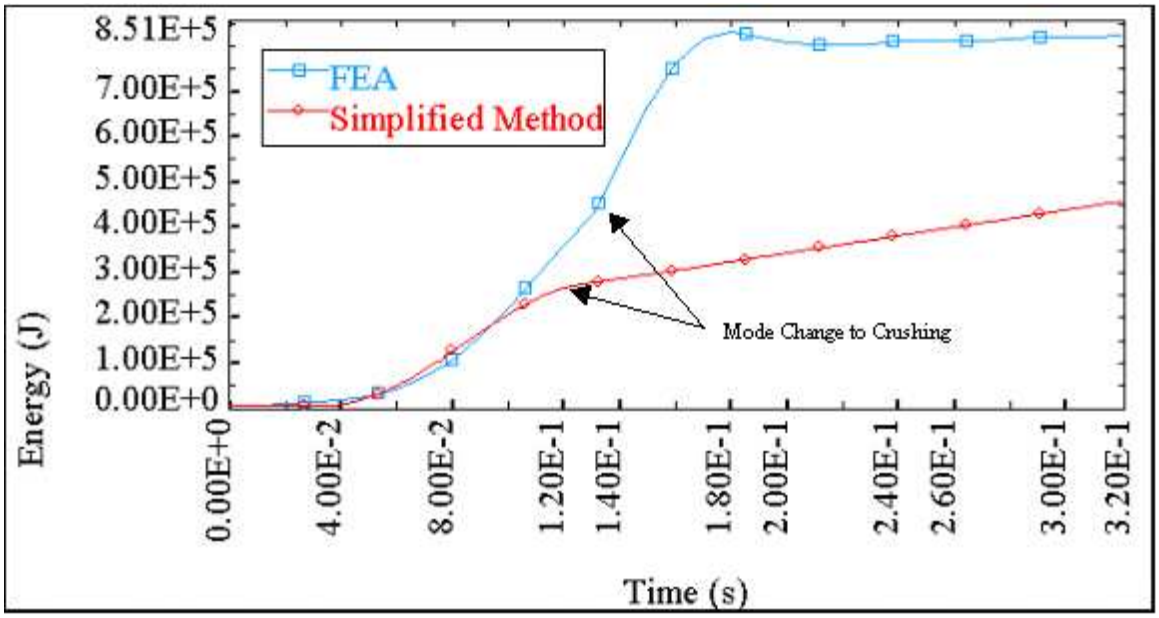

Figure 5-73 Case 2 Simplified Method and FEA Absorbed Energy vs. Time Comparison

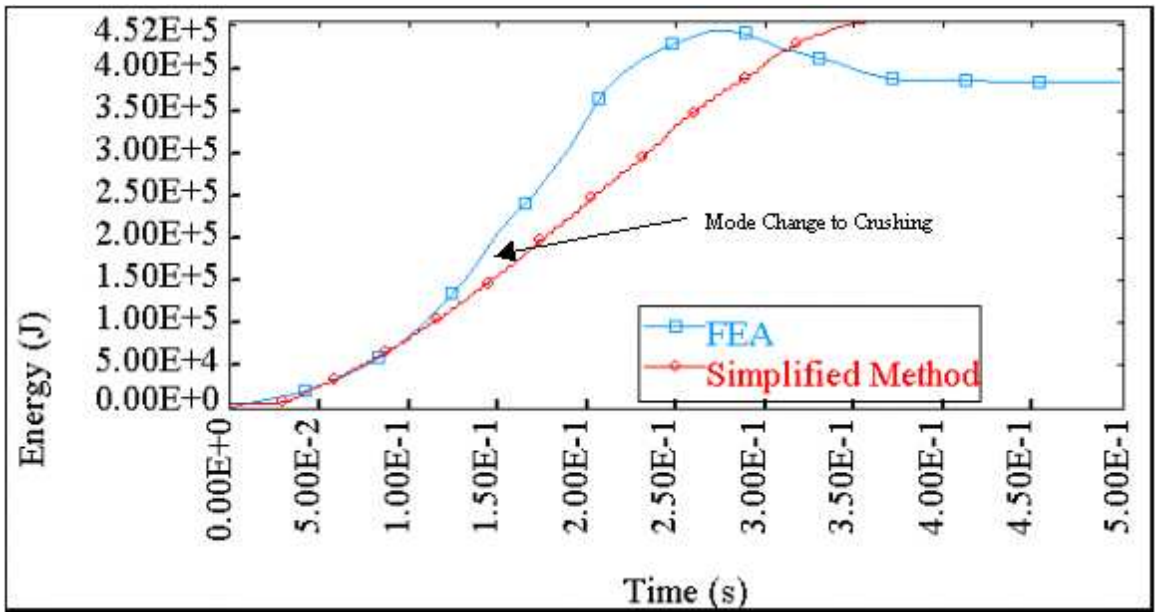

Figure 5-74 Case 3 Simplified Method and FEA Absorbed Energy vs. Time Comparison

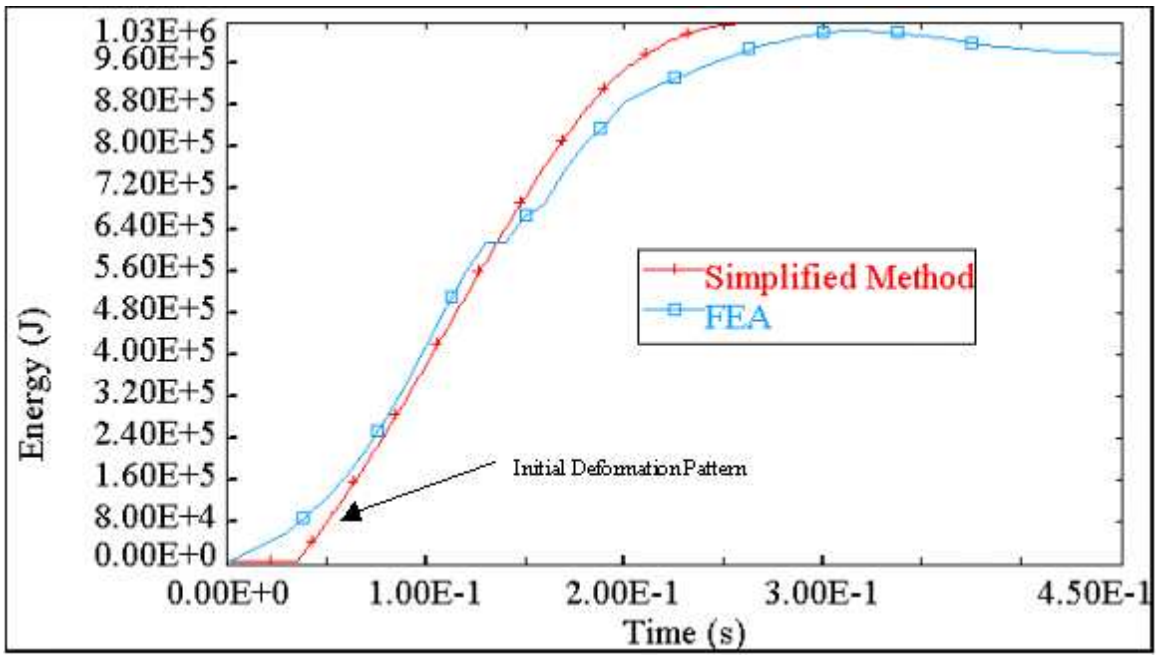

Figure 5-75 Case 4 Simplified Method and FEA Absorbed Energy vs. Time Comparison

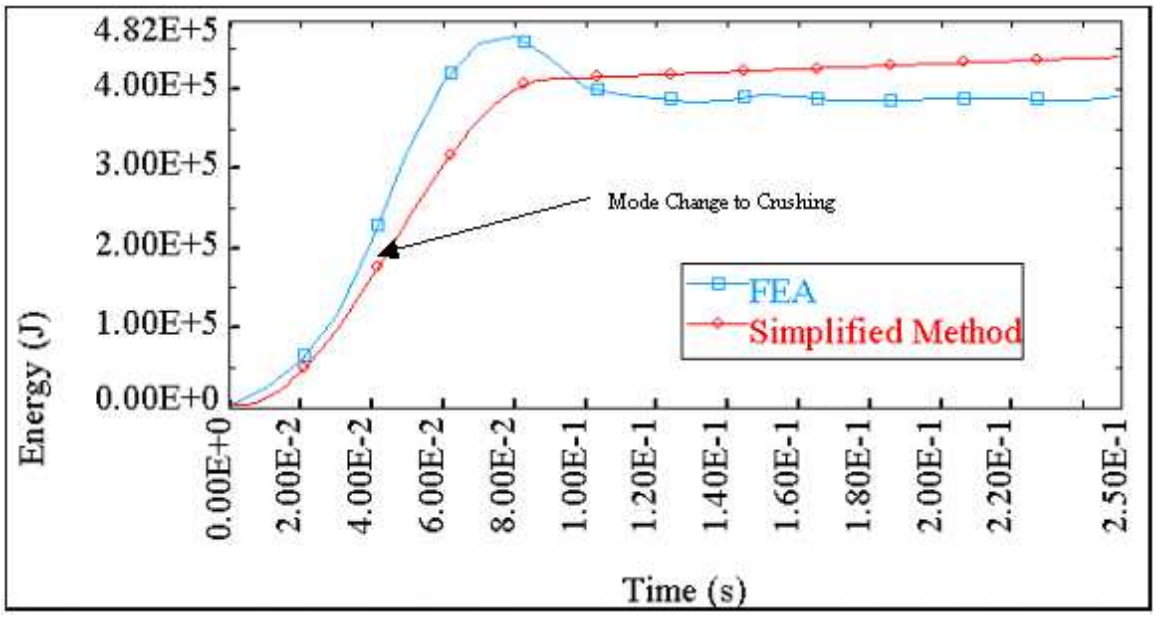

Figure 5-76 Case 5 Simplified Method and FEA Absorbed Energy vs. Time Comparison

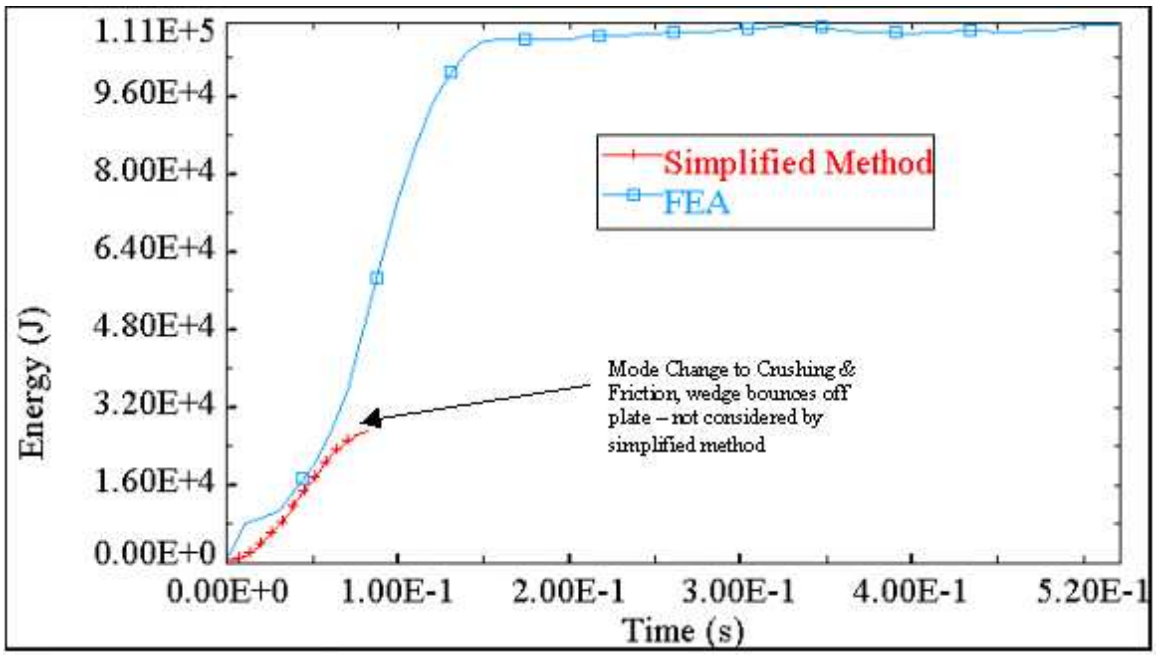

Figure 5-77 Case 6 Simplified Method and FEA Absorbed Energy vs. Time Comparison

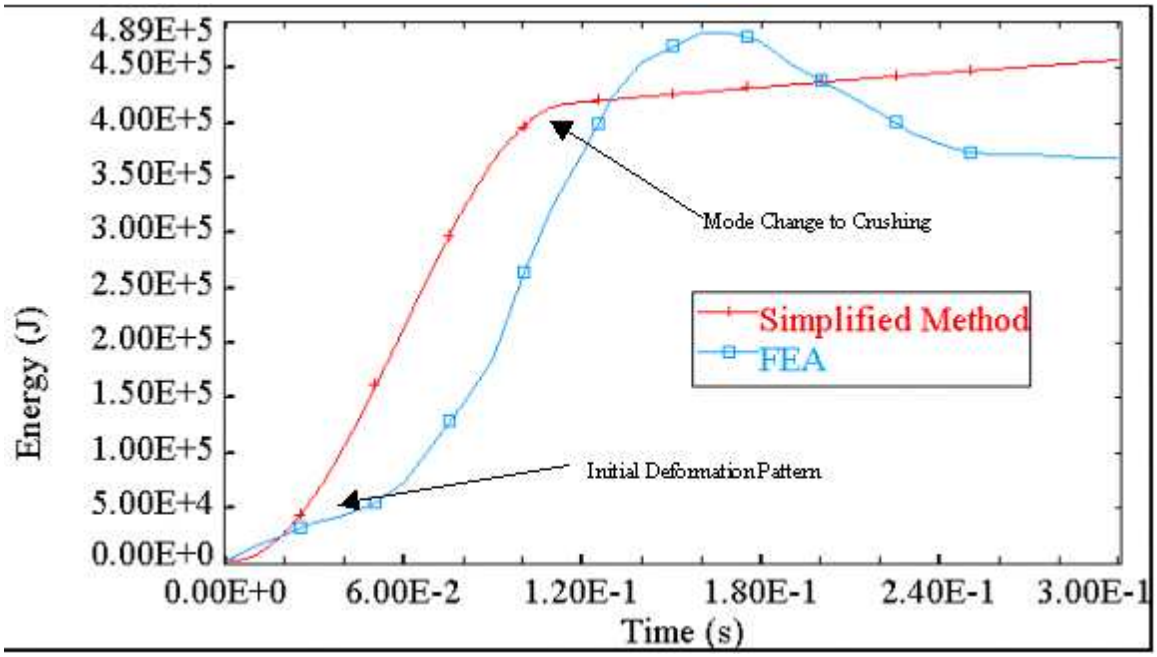

Figure 5-78 Case 7 Simplified Method and FEA Absorbed Energy vs. Time Comparison

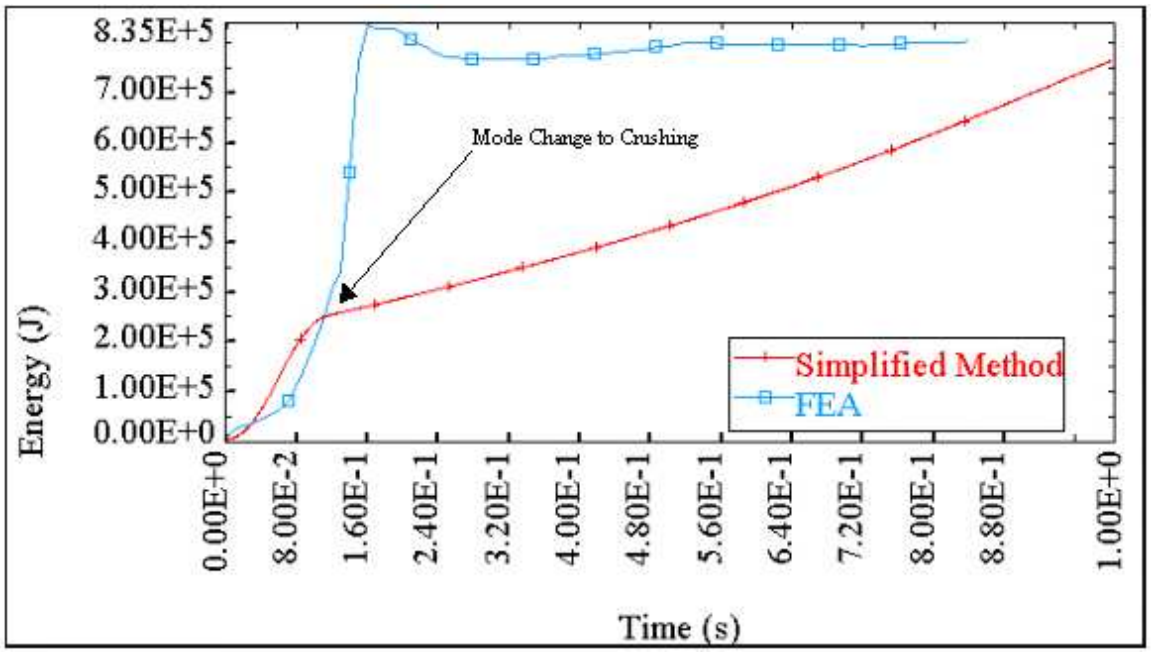

Figure 5-79 Case 8 Simplified Method and FEA Absorbed Energy vs. Time Comparison

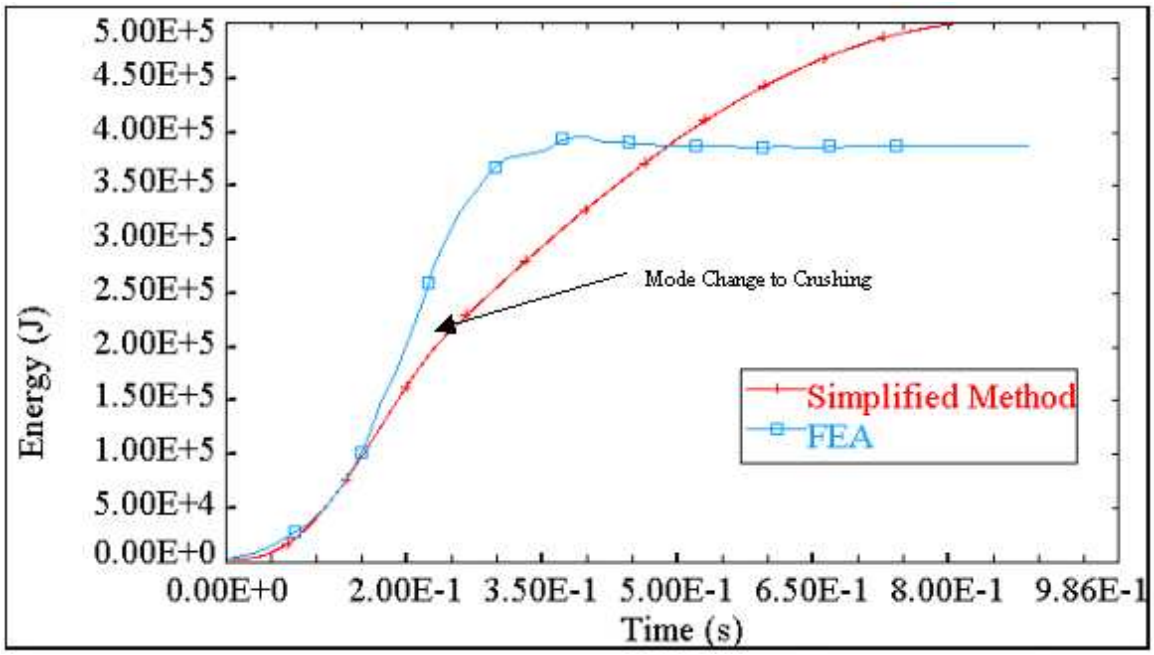

Figure 5-80 Case 9 Simplified Method and FEA Absorbed Energy vs. Time Comparison

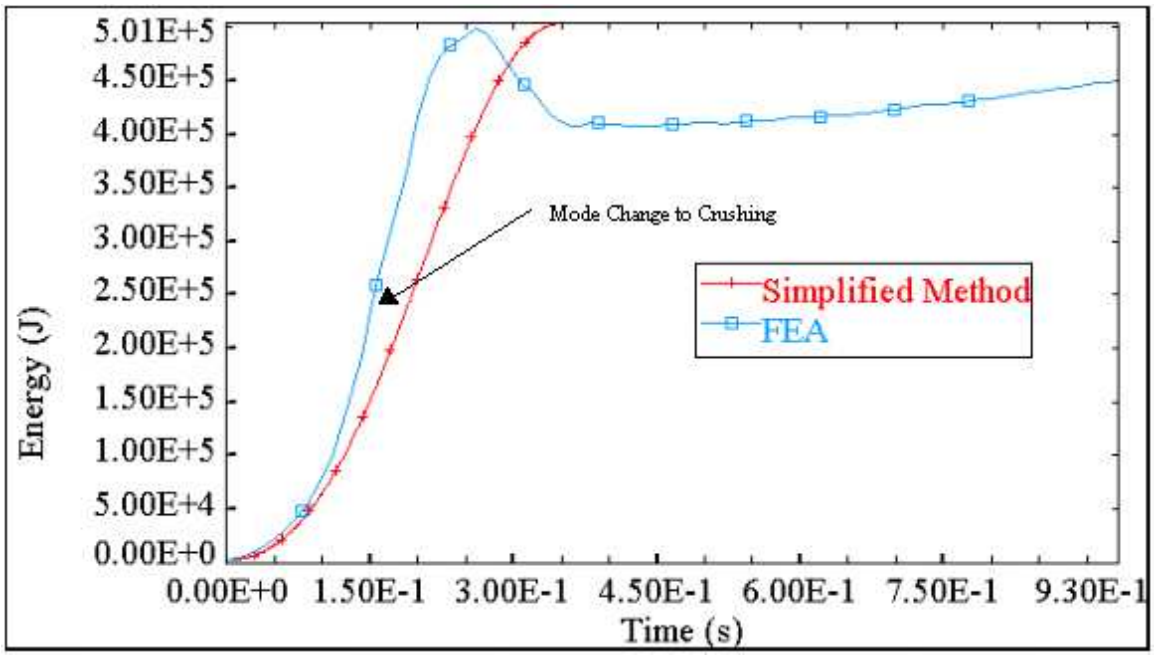

Figure 5-81 Case 10 Simplified Method and FEA Absorbed Energy vs. Time Comparison

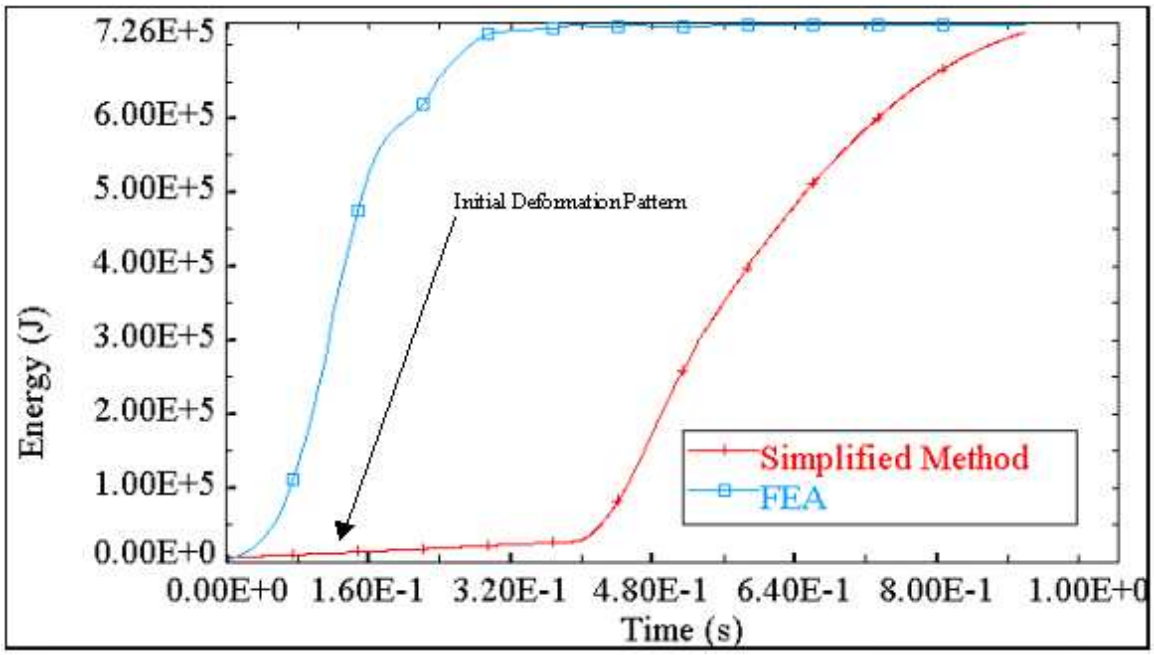

Figure 5-82 Case 11 Simplified Method and FEA Absorbed Energy vs. Time Comparison

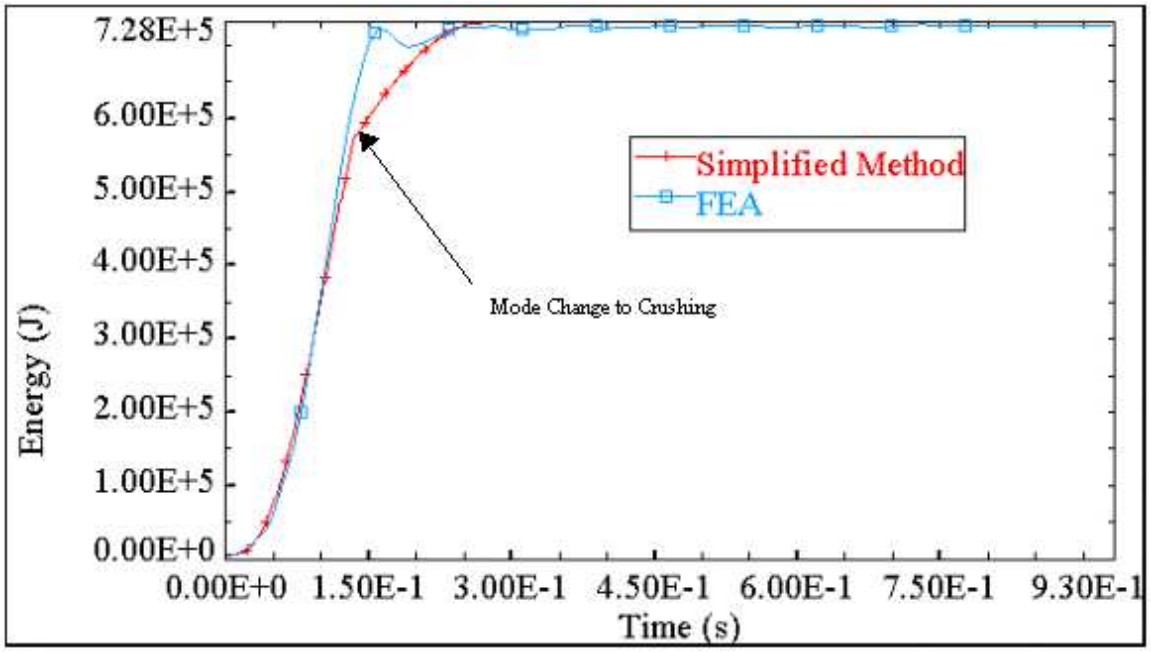

Figure 5-83 Case 12 Simplified Method and FEA Absorbed Energy vs. Time Comparison

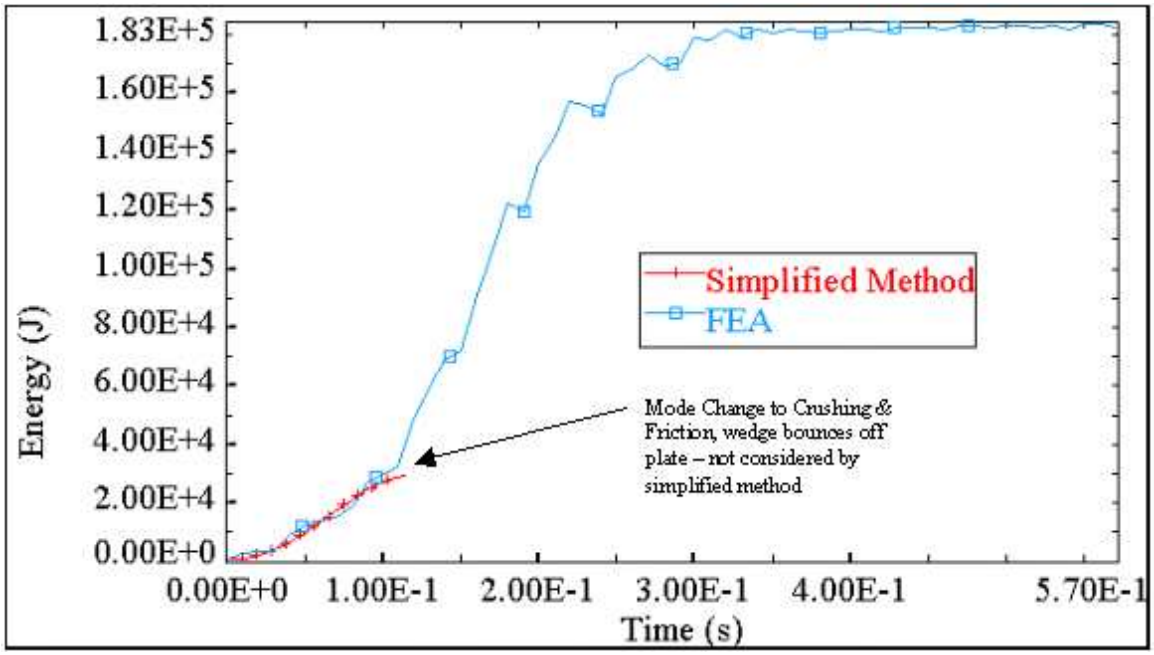

Figure 5-84 Case 13 Simplified Method and FEA Absorbed Energy vs. Time Comparison

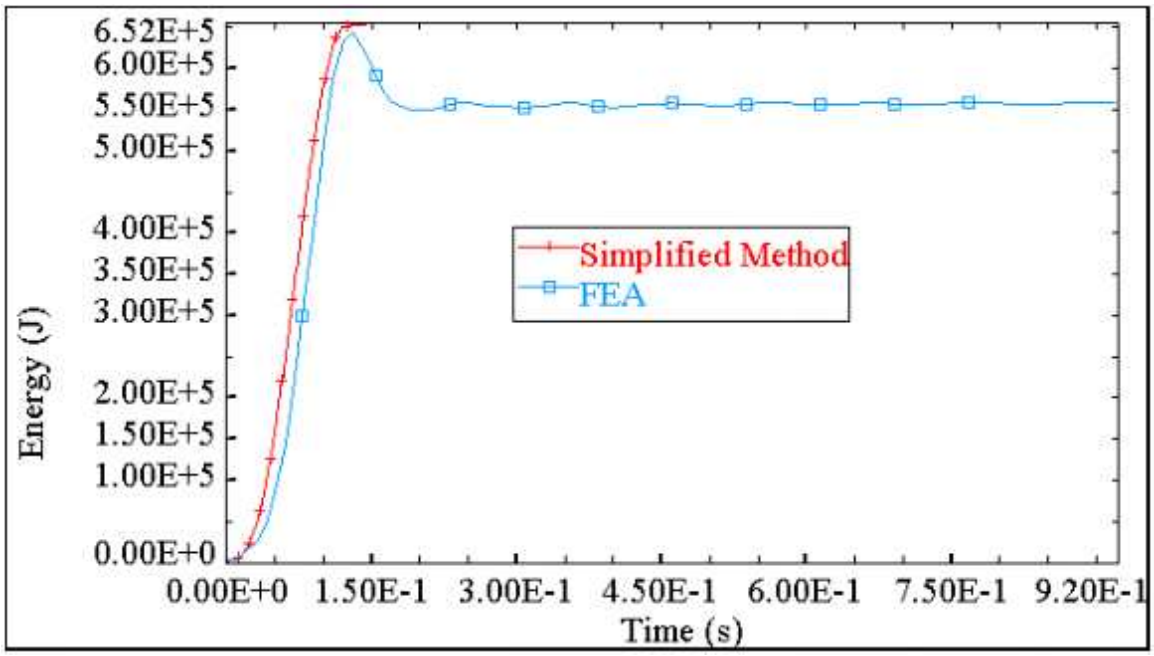

Figure 5-85 Case 14 Simplified Method and FEA Absorbed Energy vs. Time Comparison

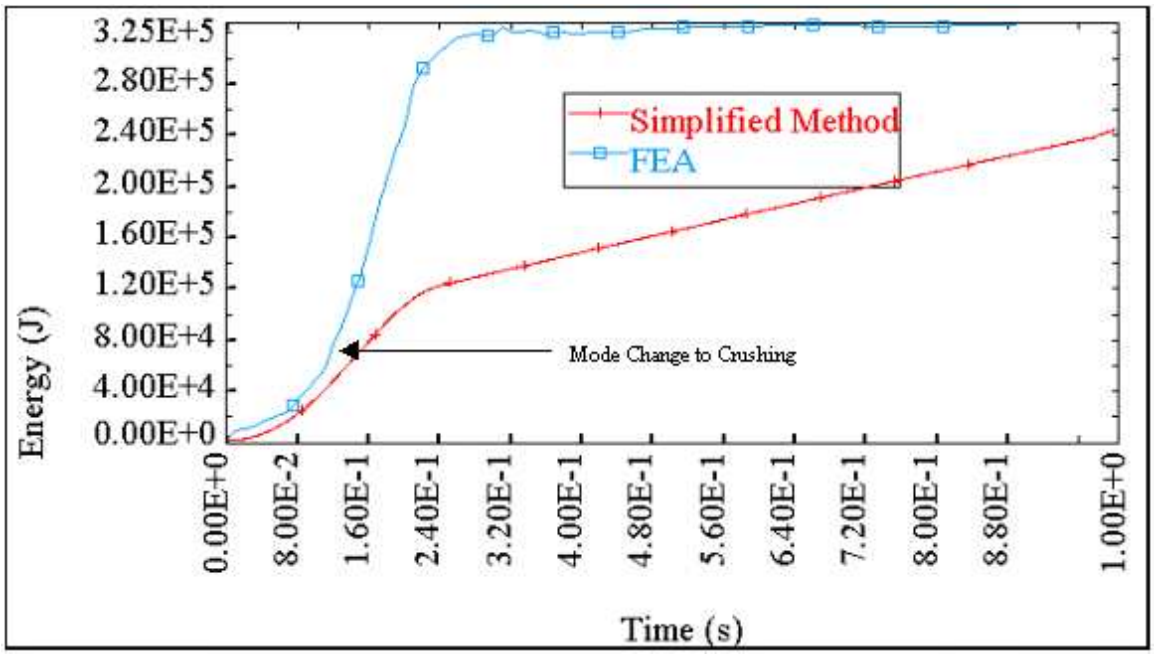

Figure 5-86 Case 15 Simplified Method and FEA Absorbed Energy vs. Time Comparison

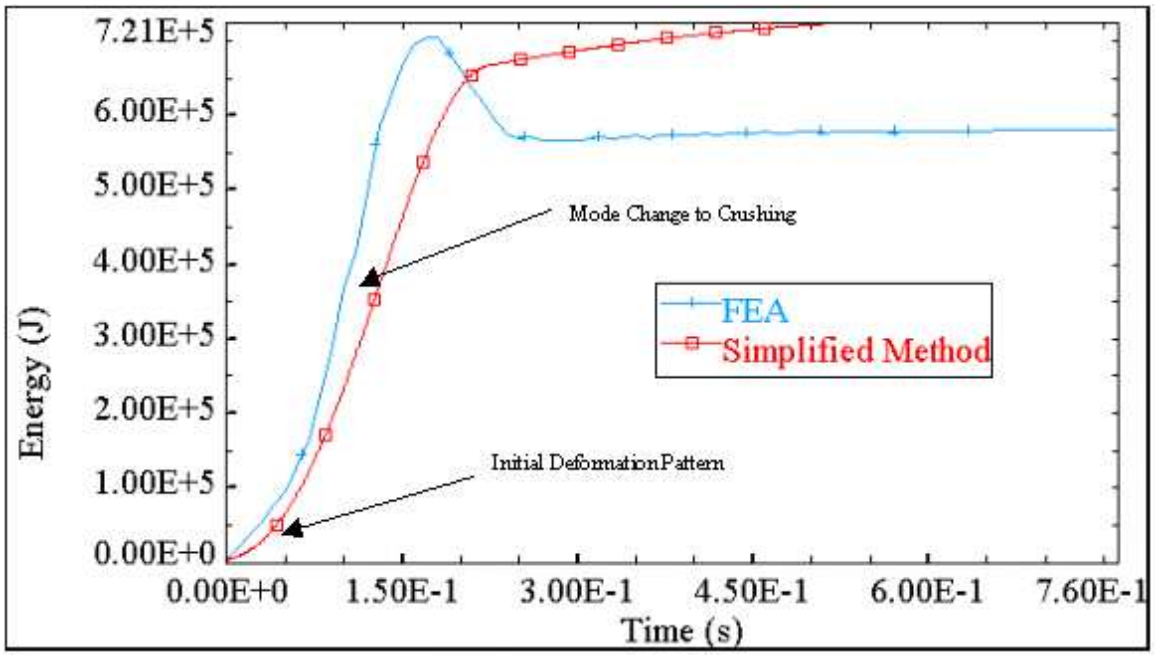

Figure 5-87 Case 16 Simplified Method and FEA Absorbed Energy vs. Time Comparison

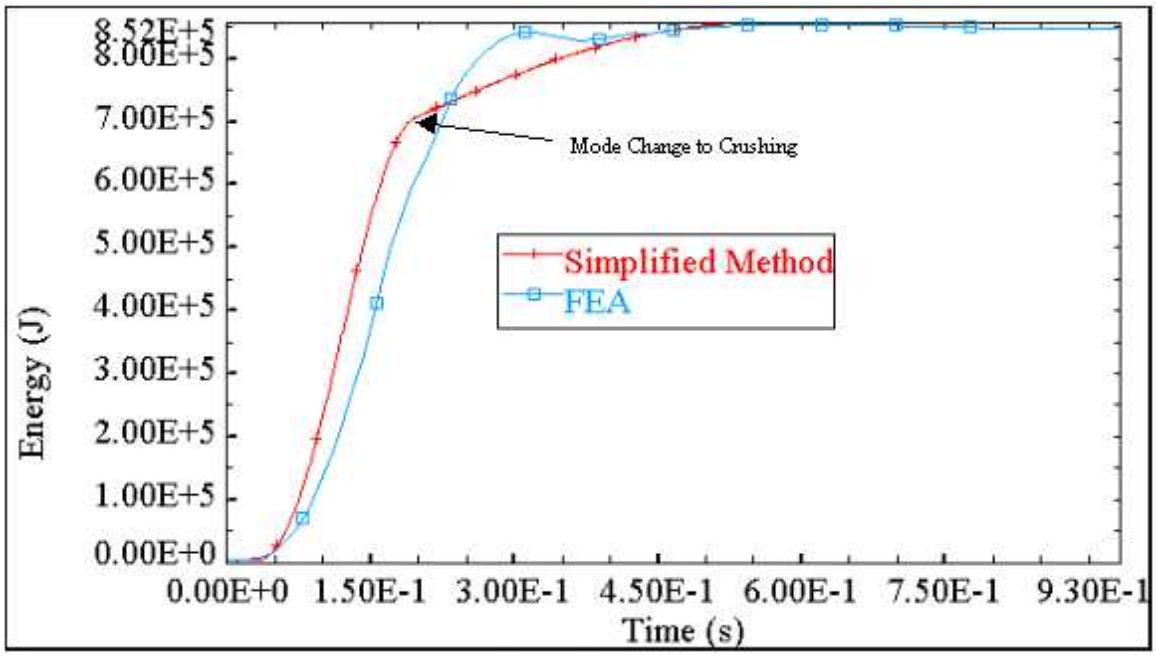

Figure 5-88 Case 17 Simplified Method and FEA Absorbed Energy vs. Time Comparison

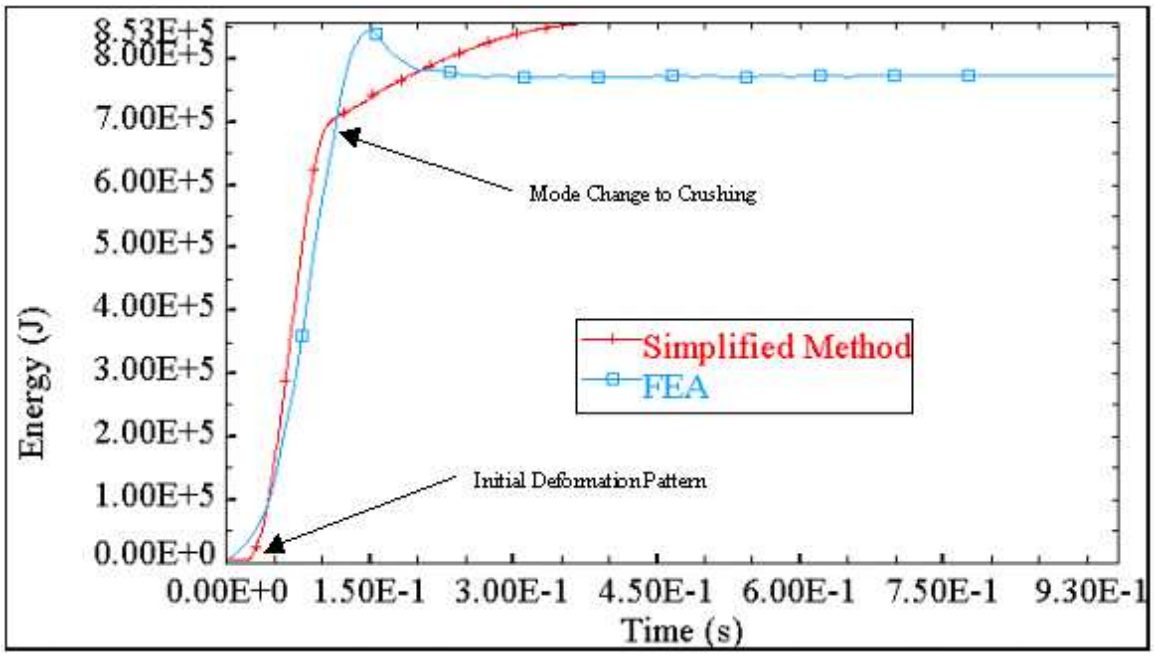

Figure 5-89 Case 18 Simplified Method and FEA Absorbed Energy vs. Time Comparison

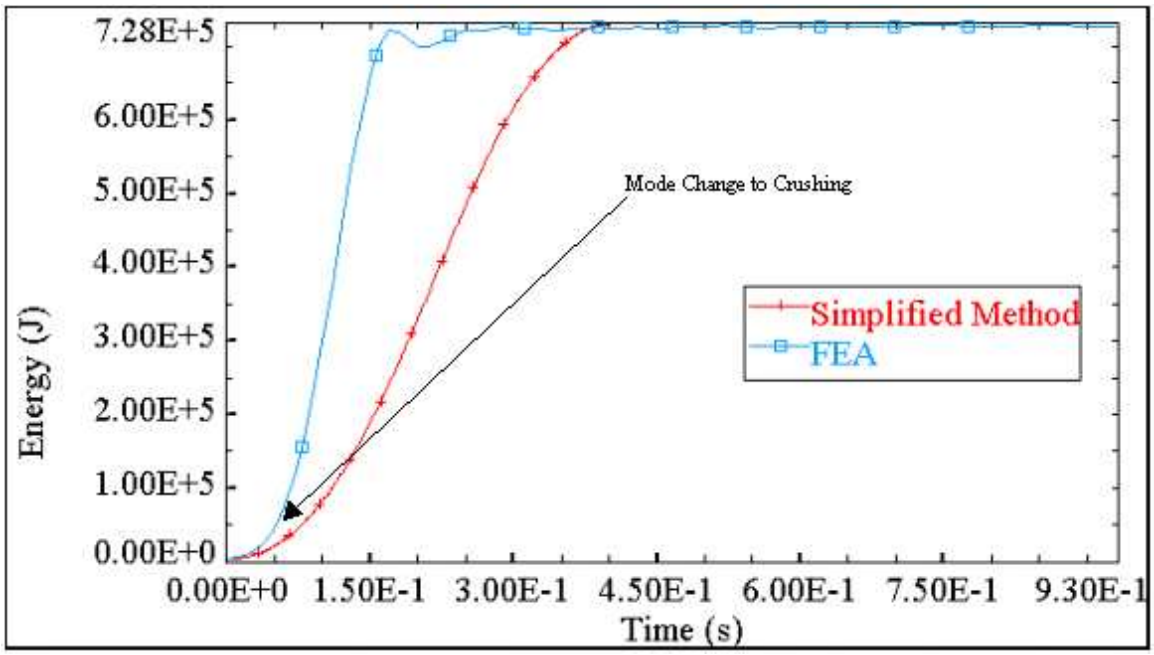

Figure 5-90 Case 19 Simplified Method and FEA Absorbed Energy vs. Time Comparison

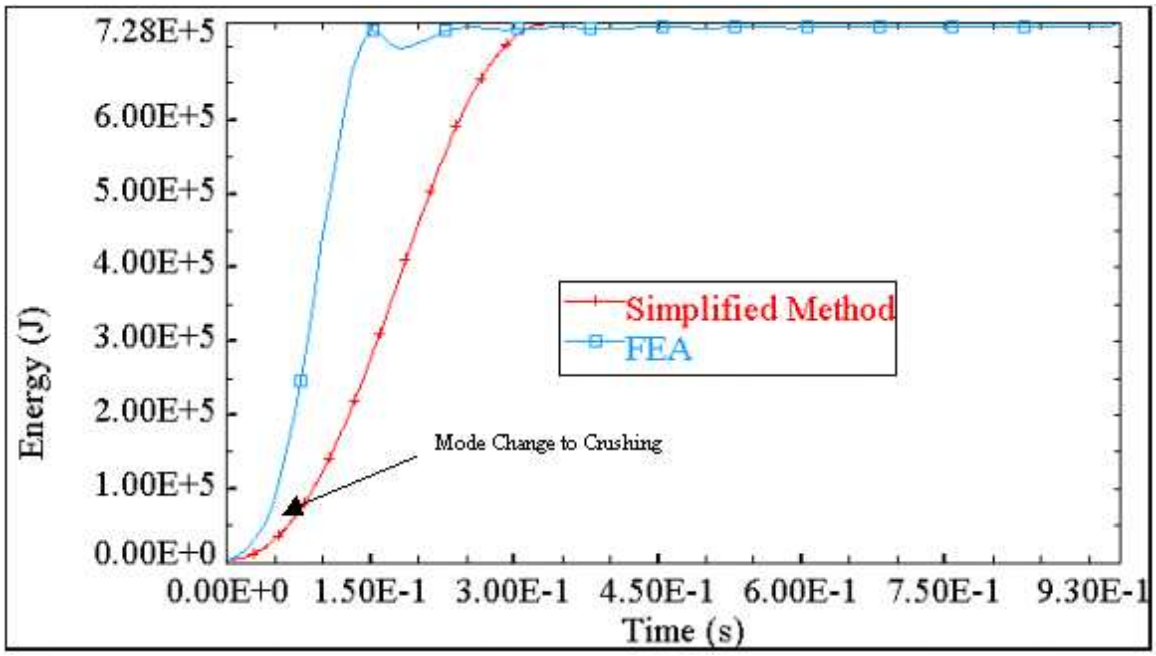

Figure 5-91 Case 20 Simplified Method and FEA Absorbed Energy vs. Time Comparison

As shown in Figure 5-72 through Figure 5-91, there are two differences between the theoretical prediction and the finite element results. These are 1) elastic/plastic bending as indicated by the notation of "Initial Deformation Pattern" and 2) combination deflection and crushing or pure crushing as indicated by the notation "Mode Change to Crushing". Figure 5-92 shows crushing in the finite element analysis of case 6 in Table 5-7 while the same case analyzed by the twenty-five-region simplified method does not consider this crushing.

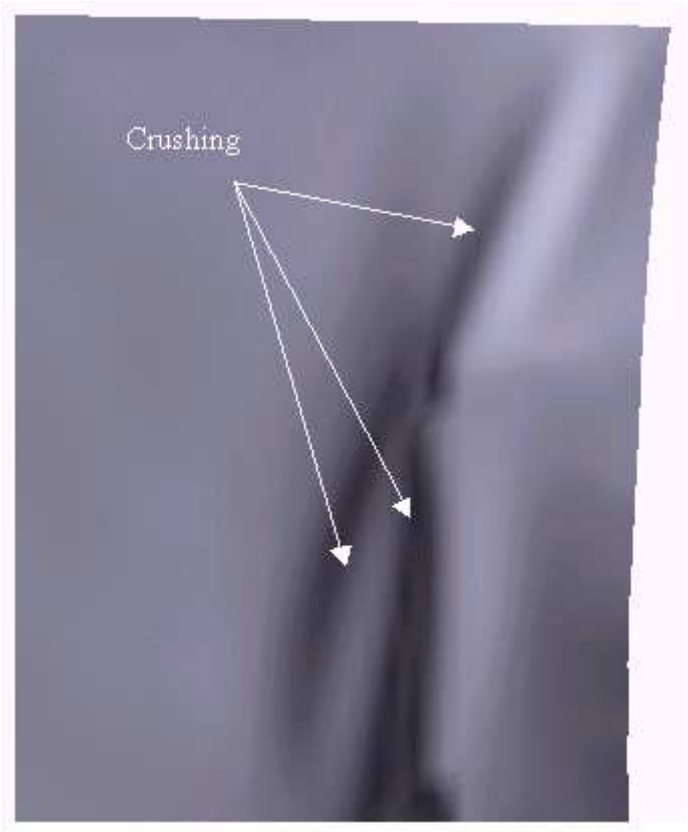

Figure 5-92 FEA Plate Crushing

As discussed in Section 5.4.1 the theory for the energy absorbed by the plate using the flow theory of plasticity is limited to a perfectly plastic material law that does not account for the energy absorbed in initial elastic bending. Additionally, the simplified method strictly assumes that the deformation of the plate is exactly the shape of the impinging rigid wedge, consequently, plastic bending occurring in the finite element model is not accounted for in the simplified method. The difference between the initial bending deformation in the finite element model and the simplified method is highlighted in Figure 5-93 and the effects of this difference are seen in cases 4 and 11 (Figure 5-75 and Figure 5-82) where for case 11 the component of the velocity in the x direction is greater than the component in the z direction and the collision angle is highly oblique forcing more energy to be absorbed in the initial bending of the plate in the finite element model.

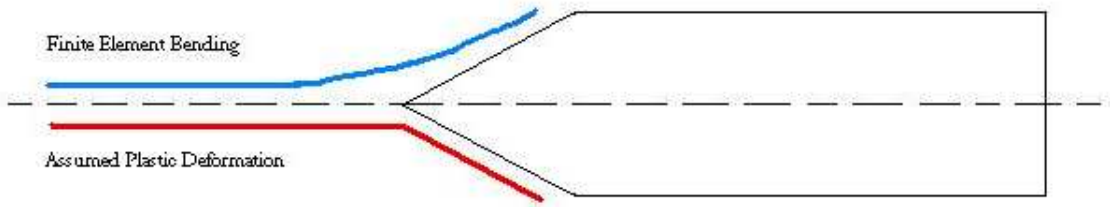

Figure 5-93 FEA Bending vs. Simplified Method Deformation

The second difference in Figure 5-72 through Figure 5-91 is due to the change in the deformation mode of the plate from lateral deflection to that of crushing as treated by the method of Section 5.2 but not shown in these figures. As the plate is laterally deformed, a high amount of velocity in the x direction will tend to push against the plate instigating an axial stress on the plate and causing a change in the deformation mode to crushing. To overcome this variation in the above test cases, the theory of Section 5.2 is incorporated into the flow theory such that if the energy to crush the plate is less than the energy required to laterally deform the plate then the method of Section 5.2 is used to determine the energy absorbed during the time step, if however the energy to laterally deform the plate is the lesser then that energy and deformation mode is used for the time step. Figure 5-94 through Figure 5-100 present the results of this combination of method analysis for cases 2, 7, 8, 12, 15, 18 and 19 of Table 5-7.

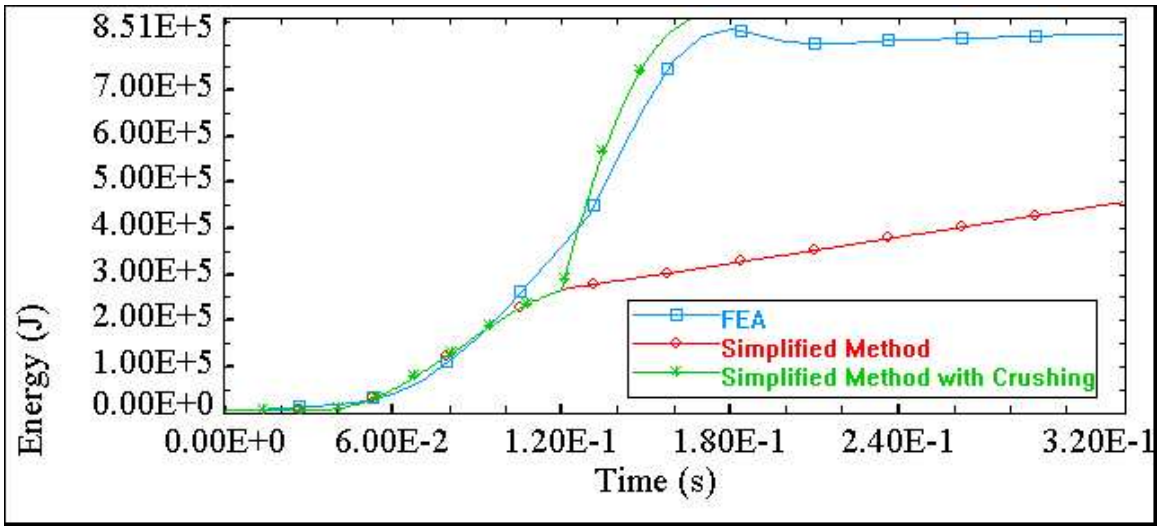

Figure 5-94 Case 2 Simplified Method (With and Without Crushing) and FEA Comparison

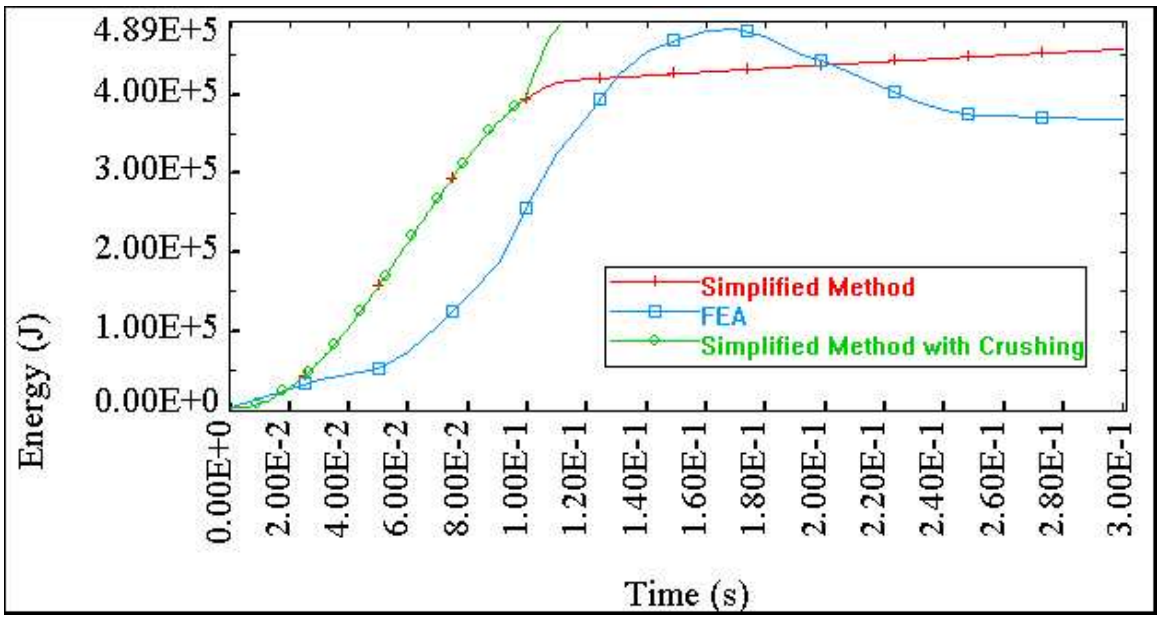

Figure 5-95 Case 7 Simplified Method (With and Without Crushing) and FEA Comparison

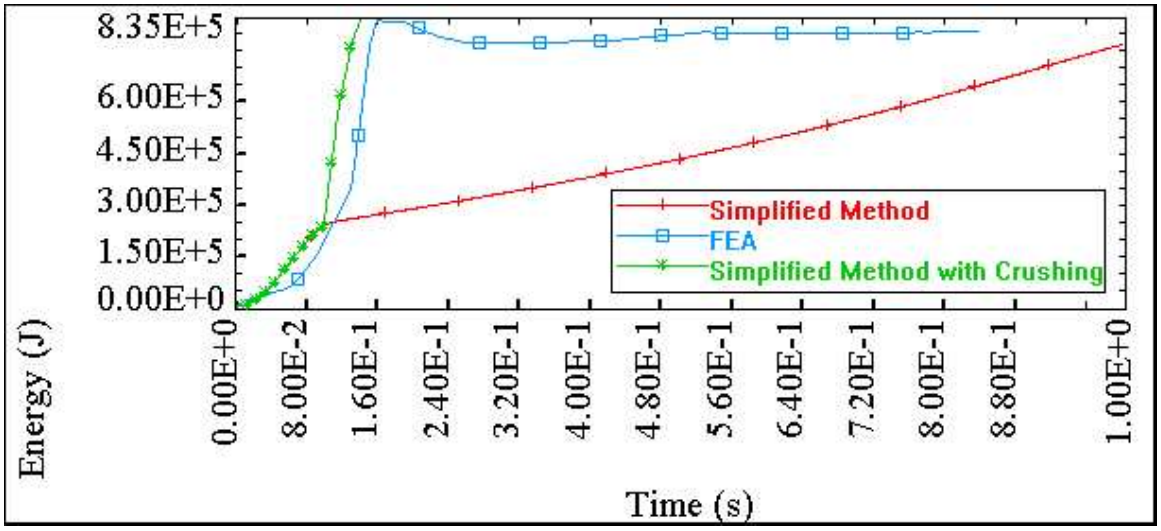

Figure 5-96 Case 8 Simplified Method (With and Without Crushing) and FEA Comparison

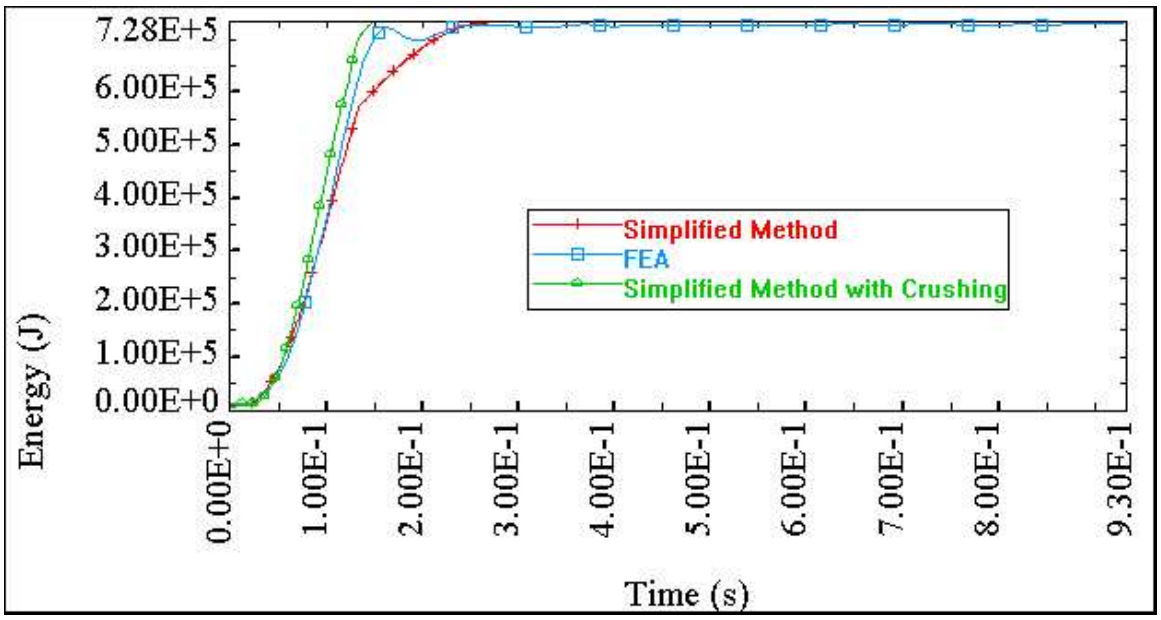

Figure 5-97 Case 12 Simplified Method (With and Without Crushing) and FEA Comparison

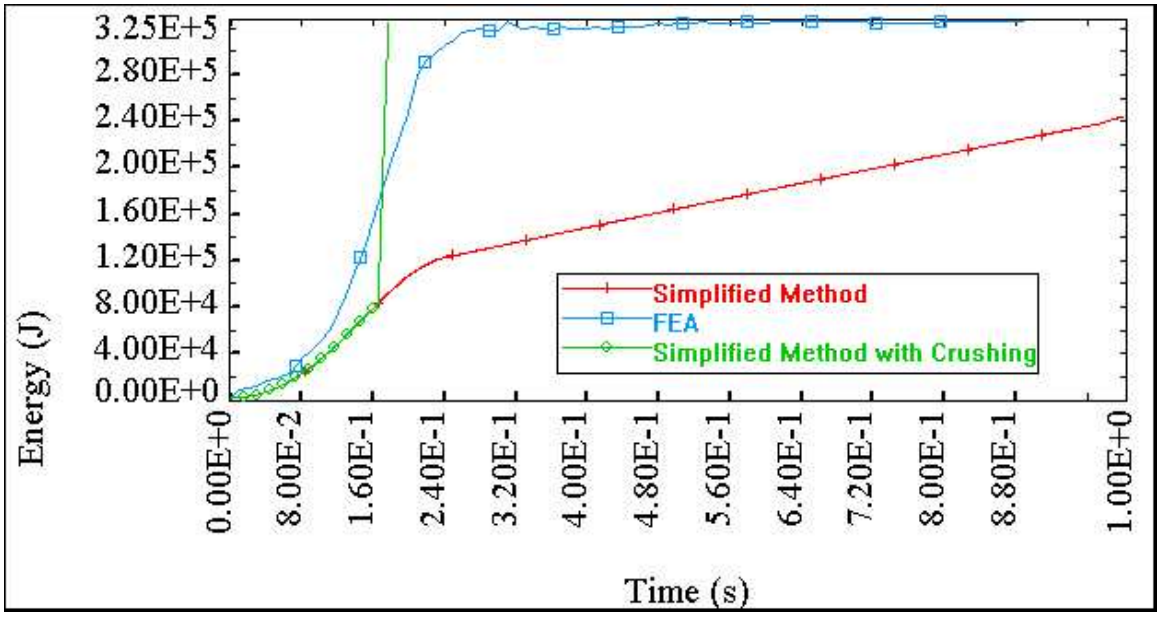

Figure 5-98 Case 15 Simplified Method (With and Without Crushing) and FEA Comparison

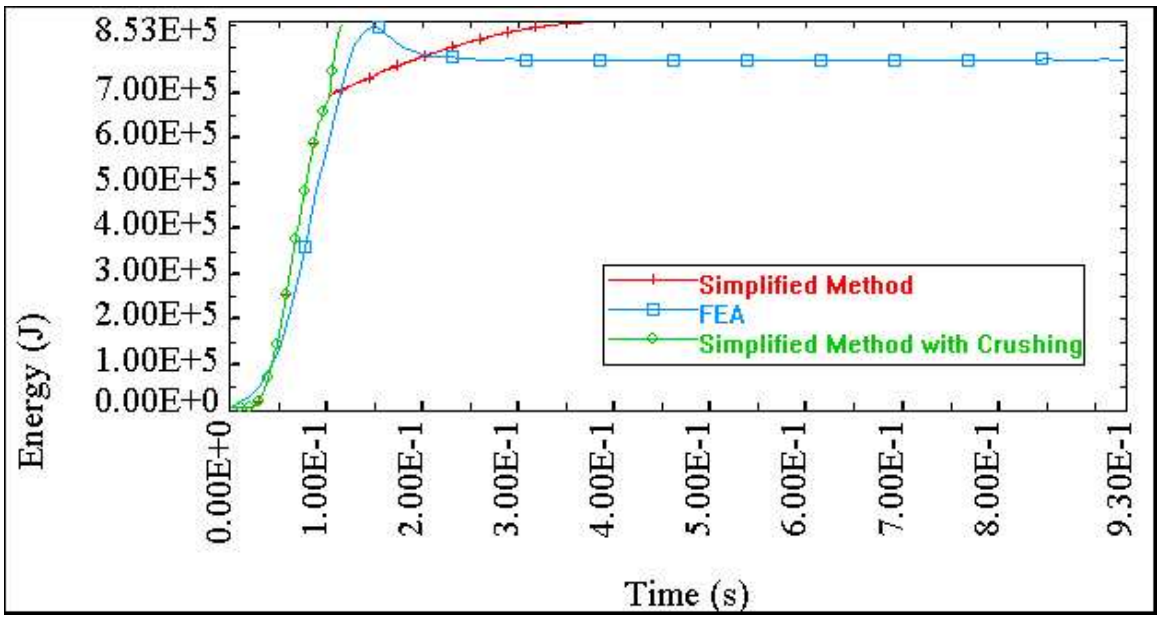

Figure 5-99 Case 18 Simplified Method (With and Without Crushing) and FEA Comparison

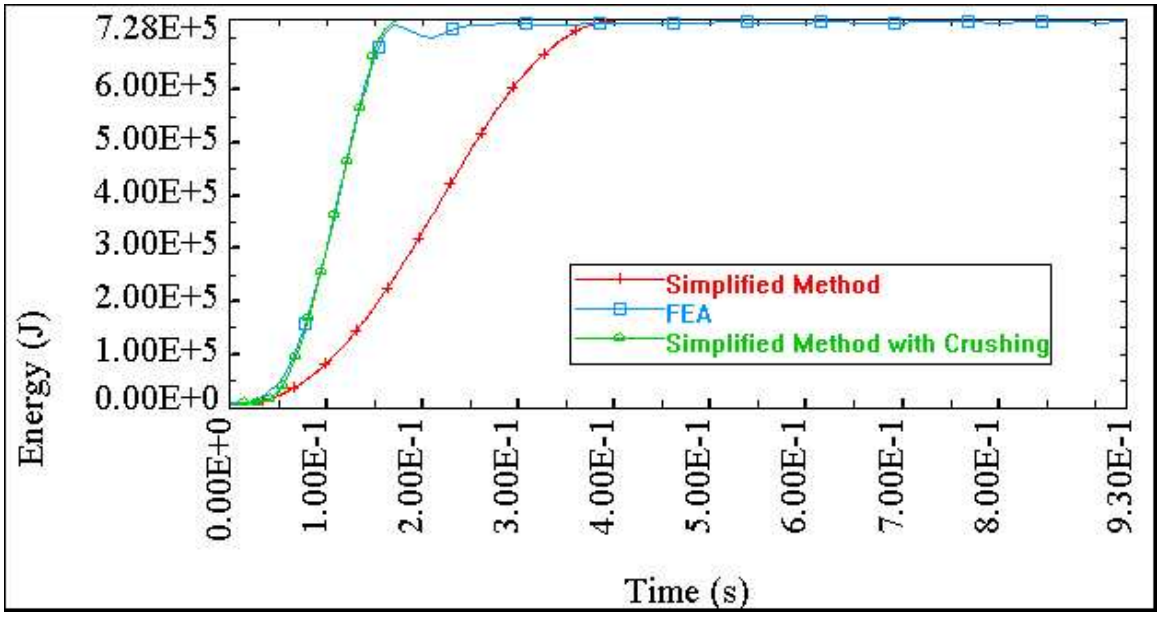

Figure 5-100 Case 19 Simplified Method (With and Without Crushing) and FEA Comparison

As shown in Figure 5-94 through Figure 5-100 the combination mode provides a better representation of the energy absorbed by the plate when subjected to a lateral and axial load. The correlation coefficients for these cases are provided in Table 5-8 as calculated using Equation 5.1.

SIMCOL version 3.0 is adapted to use this combination mode for the energy absorbed by transverse bulkheads and webs.

Table 5-8 Correlation Coefficient of Simplified Method to FEA Energy vs. Time Curves

Case #	*Correlation Coefficient*
2	0.744
7	0.623
8	0.648
12	0.875
15	0.571
18	0.71
19	0.903

6 Correlation and Validation of SIMCOL

6.1 SIMCOL Correlation

Penetration results of SIMCOL 3.0 with and without the deformable bow model of Section 5.3 for the 150K DWT Bulk Carrier (BC150) striking a 150K DWT Double Hull tanker (DH150) are provided in Figure 6-1 through Figure 6-6 where the ALPS/SCOL, DAMAGE, and DTU collision model results (discussed in Sections 4.3.4, 4.3.5 and 4.5.1 respectively) are also shown. The BC150 and DH150 structural models are discussed in Appendixes A and E.

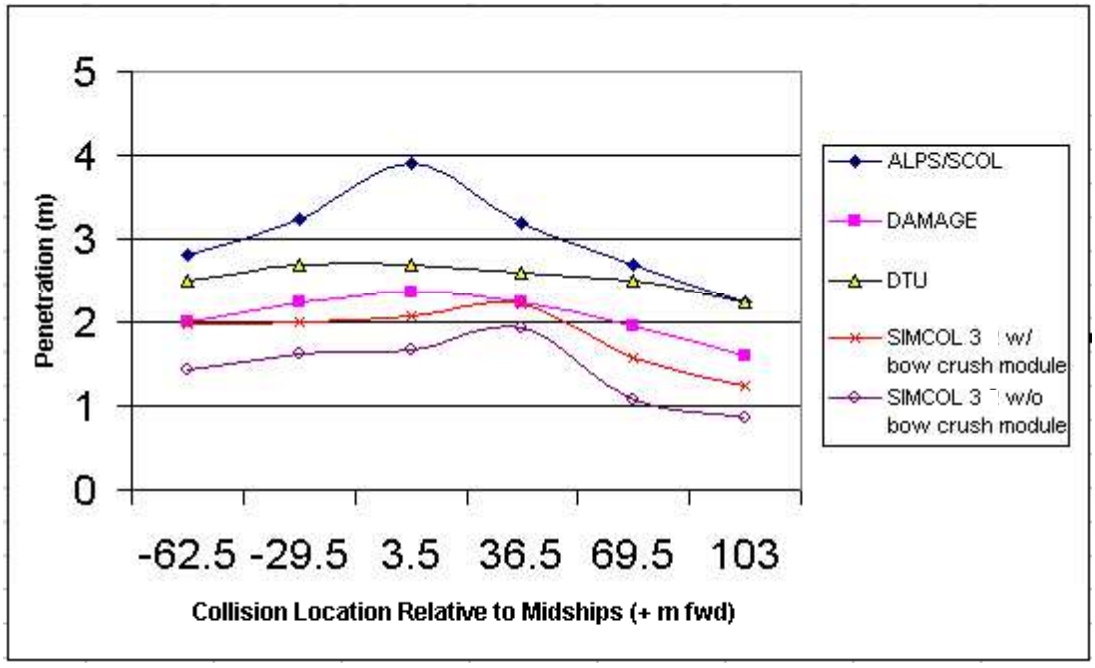

Figure 6-1 Penetration vs. Collision Location for BC150 Striking DH150 at 90 Degrees and 3 knots

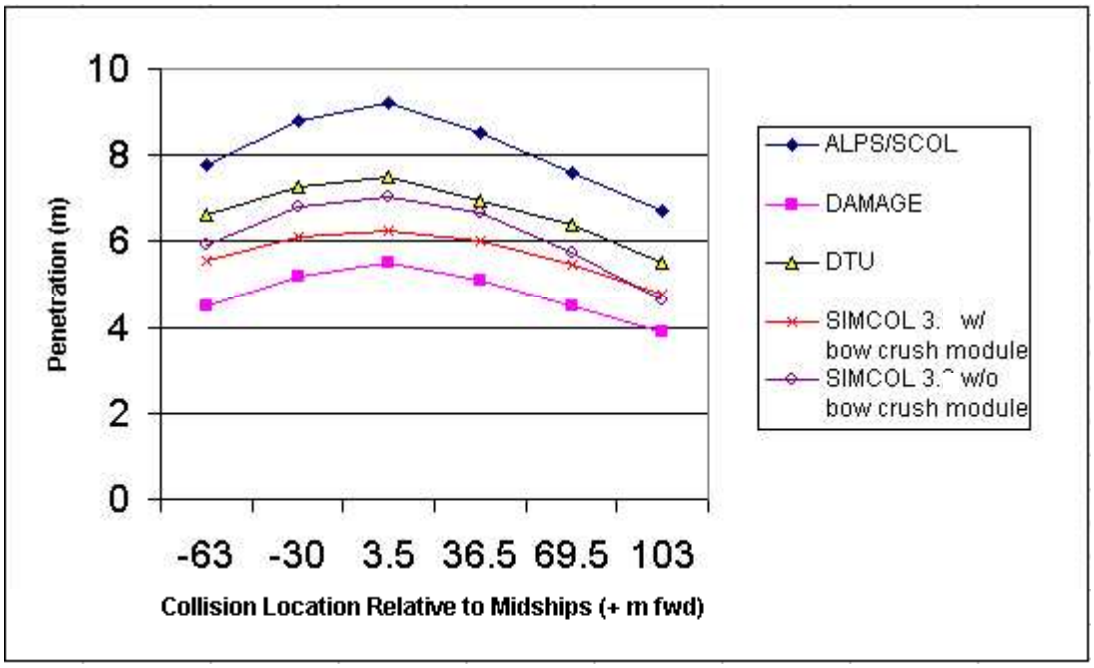

Figure 6-2 Penetration vs. Collision Location for BC150 Striking DH150 at 90 Degrees and 7 knots

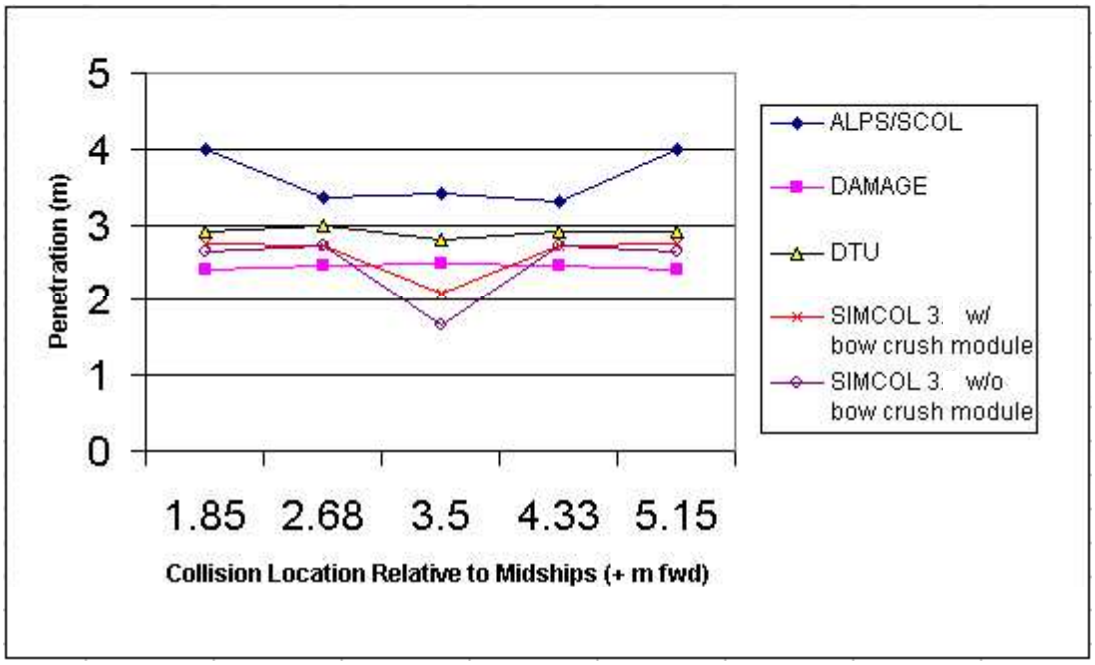

Figure 6-3 Penetration vs. Collision Location for BC150 Striking DH150 at 90 Degrees and 3 knots

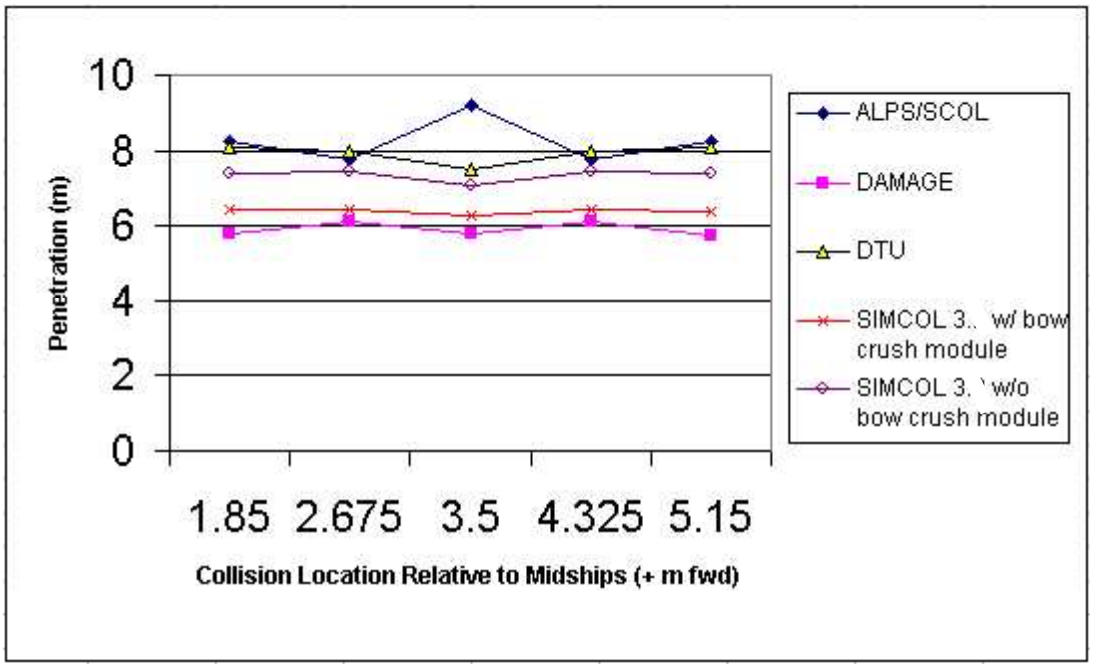

Figure 6-4 Penetration vs. Collision Location for BC150 Striking DH150 at 90 Degrees and 7 knots

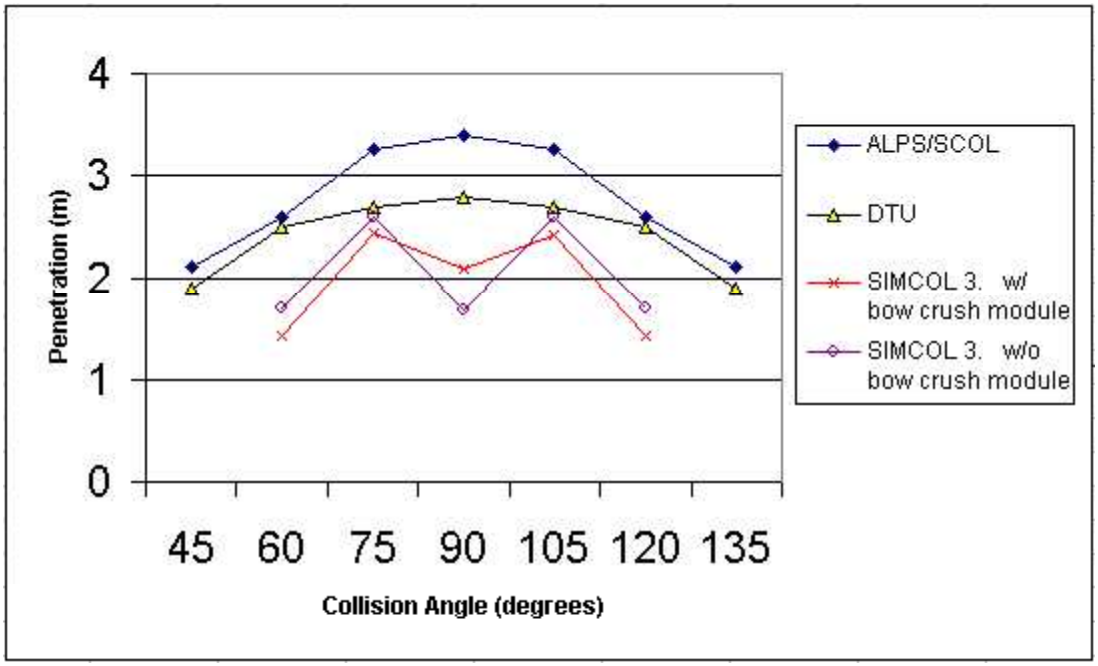

Figure 6-5 Penetration vs. Collision Angle for BC150 - DH150 at 3.5 m fwd Amidships and 3 knots

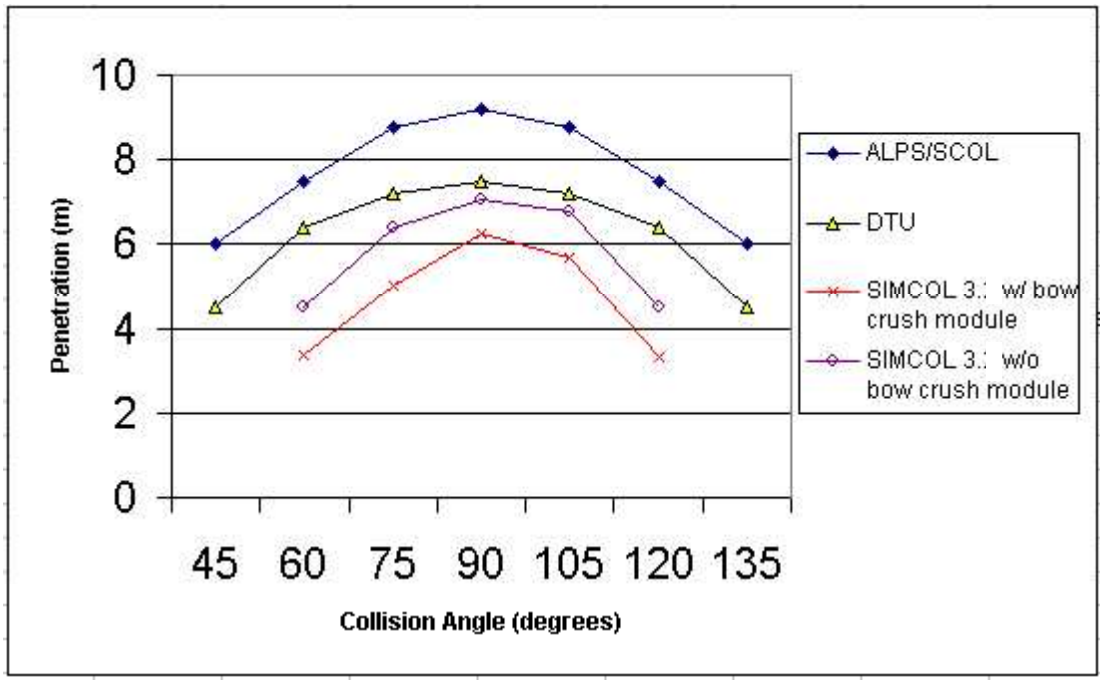

Figure 6-6 Penetration vs. Collision Angle for BC150 - DH150 at 3.5 m fwd Amidships and 7 knots

In most cases the SIMCOL penetration results are less than that predicted by the DTU, ALPS/SCOL or DAMAGE models. The predominant cause of the lower prediction of penetration is that other methods do not properly consider the energy absorbed in longitudinal extent of damage (DTU method considers fixed penetration to longitudinal extent of damage energy ratio) leaving additional energy to be absorbed in additional penetration. Furthermore, DAMAGE, ALPS/SCOL and the DTU model do not consider yaw (and in some cases sway) motions of the struck ships providing a fixed rigid target that must absorb all energy through structural deformation vice imparting kinetic energy to the vessel which would produce a lower penetration.

Additionally, in some cases the SIMCOL results with the inclusion of Pedersen's bow crush model are lower than the penetration results without the inclusion of Pedersen's bow crush model. Though counterintuitive, this phenomenon occurs when the energy required to crush the bow structure is much less than the energy required to crush the structure of the struck ship for the same penetration. Thus, more initial energy is available for the following time step and enables the analysis to produce more penetration.

The hump in the SIMCOL results on Figure 6-1 where the collision location is 36.5 meters forward of amidships and the collision speed is three knots is caused because the collision provides enough moment to the struck ship to move the contact point from “on the web” to “off the web” thus increasing the penetration. Not enough moment however, is provided to the struck ship to decrease the penetration as seen in collision location cases of 69.5 and 102.5 meters forward of amidships. As seen by comparing Figure 6-1 to Figure 6-2 and Figure 6-3 to Figure 6-4 the increase of striking ship velocity reduces the effect of striking “on the web” or “off the web”. The full effect of striking “on a web” is seen in Figure 6-5 and Figure 6-6 where the energy required to laterally deform the web is added to the total lost energy of the system yielding less energy available to cause more penetration. Finally, the asymmetry in the SIMCOL results of Figure 6-6 is due to the collision location being offset 3.5 meters forward from amidships. Therefore oblique collision angles less than 90 degrees would show a decrease in penetration over the collision angles that are greater than 90 degrees due to the difference in moments caused on the struck ship.

Comparative results for the longitudinal extent of damage, like the results of penetration in Figure 6-1 through Figure 6-6 are desirable, however no results for the longitudinal extent of damage for any comparative collision cases are available.

6.2 SIMCOL Validation

SIMCOL is validated using two collision events described by Minorsky’s [9] original data and updated with additional library research. The first validation case is the collision between the David E. Day and the Marine Flier in the Pacific Ocean on May 17, 1952. The second validation case is the collision between the P&T Adventurer and the Tullahoma in the North Pacific on August 4, 1951.

6.2.1 David E. Day Marine Flier Collision

On May 17, 1952 the C4 cargo vessel “Marine Flier” struck the T2 tanker “David E. Day” at a reported 55-degree collision angle between frames 59 and 62 of the David E. Day, approximately 9 meters forward of amidships. The reported vessel speeds at the time of the collision were 16.3 knots for the David E. Day and 16.5 knots for the Marine Flier causing a reported 17 ft of penetration and 35 ft of damage length. However, extensive examination of documents related to

the collision reveal that the actual speeds of the Marine Flier and David E. Day at the time of the collision were closer to 5 to 7 knots and the collision angle was in actuality between 50 and 55 degrees. In part these changes are due to last minute “Full Astern” and “Hard Right Rudder” orders given by the masters of each vessel in the effort to avoid the collision.

Structural drawings for both ships were obtained through the National Archives and Records Administration and specific data was used in SIMCOL version 3.0. Appendix C provides information on the “Marine Flier” while appendix F provides information on the “David E. Day”. In the SIMCOL analysis the collision angle was set at 51 degrees with a collision location of 10 meters forward of amidships. The initial striking vessel speed was set at 5.5 knots, and the struck vessel speed was retained at 7 knots. The SIMCOL results are 5.289 meters or 17.35 ft of penetration and 10.787 meters or 35.39 ft of damage length. The SIMCOL results are conservative by approximately 2% in penetration and 1% in damage length compared to Minorsky’s (1959) reported penetration and damage length values. The variation from SIMCOL version 3.0 to the validation of the finite element analysis of the same case is shown in Table 6-1.

Table 6-1 FEA - SIMCOL Validation Percent Difference

Validation with Marine Flier - David E. Day Collision		
Method	Penetration (ft)	L.E.D. (ft)
SIMCOL	17.35	35.39
FEA	16.7	32.8
% Difference	3.75%	7.32%
Reported	17	35
% Difference	2.06%	1.11%

6.2.2 P&T Adventurer Tullahoma Collision

On August 4, 1951 the Victory cargo vessel “P&T Adventurer” struck the T2 tanker “Tullahoma” at a reported 90-degree collision angle between frames 41 and 45 on the Tullahoma, approximately 44.5 meters aft of amidships. The reported vessel speeds at the time of the collision were 10 knots for the Tullahoma and 14 knots for the Adventurer causing a reported 25 ft of penetration and 20 ft of damage length. However, extensive examination of documents related to the collision reveal that the actual speed of the Adventurer at the time of the collision was closer to 9.5 knots and the actual

speed of the Tullahoma was approximately 8 knots. Again, these changes are due to last minute orders given by the masters of each vessel in the effort to avoid the collision.

Structural drawings for both ships were obtained through the National Archives and Records Administration and specific data was used within SIMCOL version 3.0. Appendix D provides information on the "P&T Adventurer" while appendix F provides information on the "Tullahoma". In the SIMCOL analysis the collision angle was set at 90 degrees with a collision location of 44.5 meters aft of amidships. The initial striking vessel speed was set at 9.5 knots, with the struck vessel speed set at 8 knots. The SIMCOL results are 7.694 meters or 25.24 ft of penetration and 6.34 meters or 20.8 ft of damage length. The SIMCOL results are conservative by approximately 1% in penetration and 4% in damage length compared to Minorsky's (1959) reported penetration and damage length values. The variation from SIMCOL version 3.0 resultant damage to the reported damage is presented in Table 6-2.

Table 6-2: SIMCOL Validation Percent Difference

Validation with Tullahoma - P&T Adventurer Collision		
Method	Penetration (ft)	L.E.D. (ft)
SIMCOL	25.24	20.8
Reported	25	20
% Difference	0.96%	4.00%

6.3 SIMCOL Probabilistic Validation

The probabilistic validation of SIMCOL version 3.0 is performed by comparison of MARPOL 73/78 probabilistic damage extents reported in Annex 1 [4] and the HARDER project [133] reported damage extent database to SIMCOL analysis of a 100k dwt single hull tanker (SH100) and a 150k dwt double hull tanker (DH150) using 10000 probabilistic striking ship contact scenarios [100]. The structure and design of both the SH100 and DH150 are provided in appendix K and appendix E respectively.

Figure 6-7 and Figure 6-8 show the comparison of the non-dimensional results of the penetration for the SH100 and DH150 respectively.

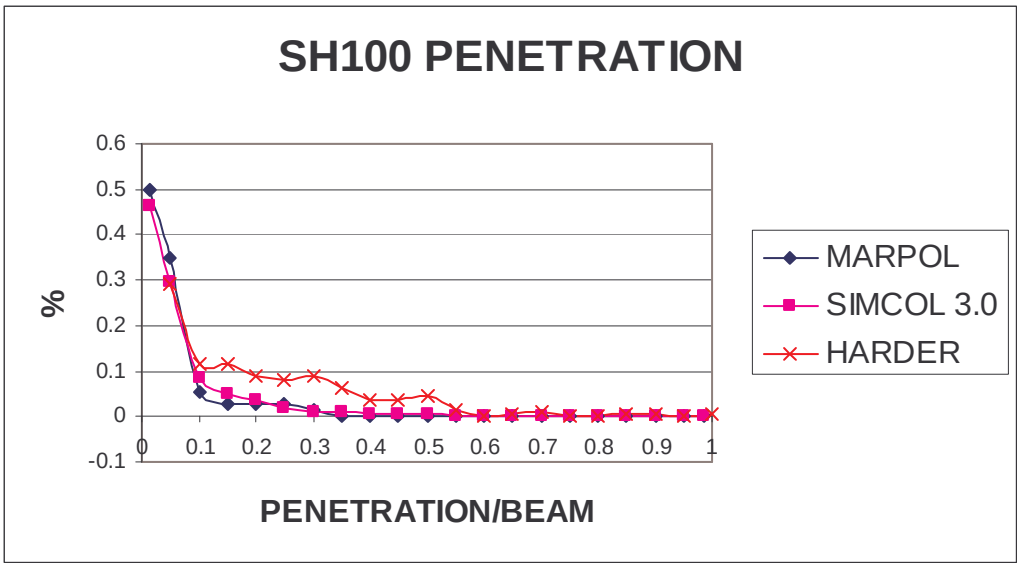

Figure 6-7: SIMCOL, MARPOL & HARDER SH100 Penetration Comparison

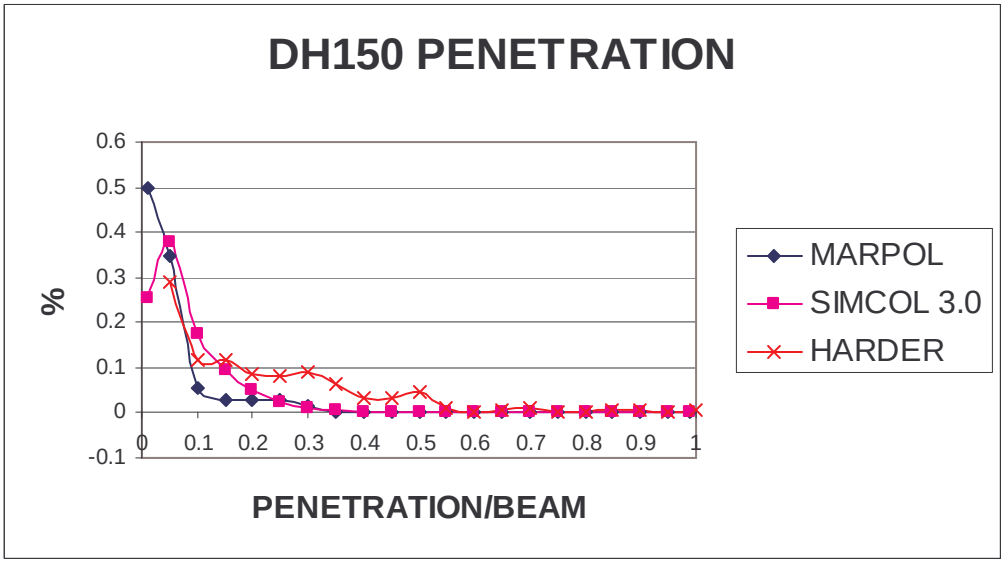

Figure 6-8: SIMCOL, MARPOL & HARDER DH150 Penetration Comparison

The SIMCOL version 3.0 results compare well to the trends of both the MARPOL and HARDER data where the SH100 SIMCOL analysis results better match the data of MARPOL, which was compiled using older single hull vessels [100]. The DH150 results fall between the MARPOL and HARDER data where the HARDER data contains the original MARPOL data and a collection of more recent collision events involving both single and double hull vessels.

Figure 6-9 and Figure 6-10 show the comparison of the non-dimensional results of the longitudinal extent of damage (LED) for the SH100 and DH150 respectively.

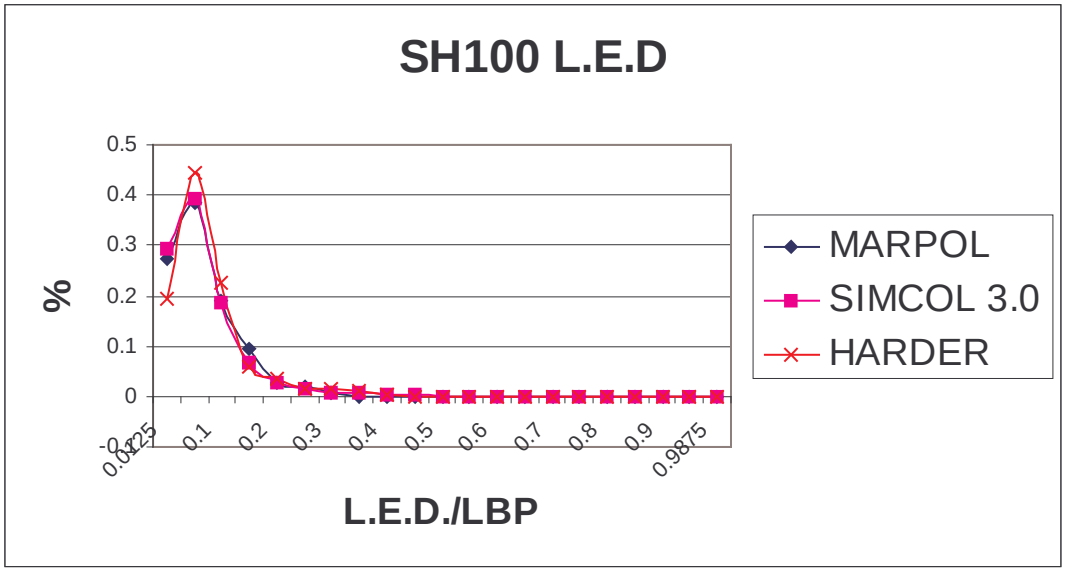

Figure 6-9: SIMCOL, MARPOL & HARDER SH100 LED Comparison

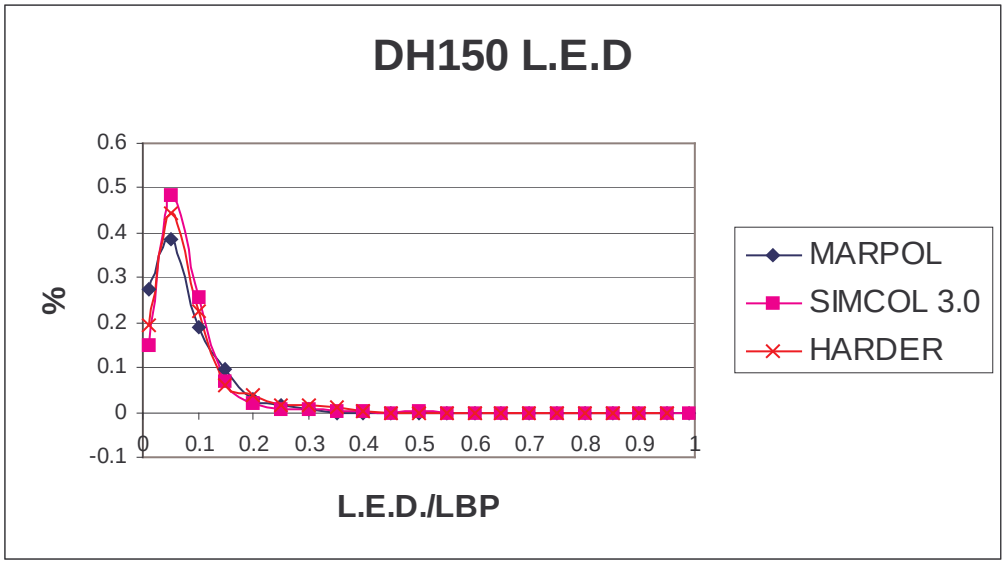

Figure 6-10: SIMCOL, MARPOL & HARDER DH150 LED Comparison

Because of the geometry of the striking ship used within SIMCOL as shown in Figure 5-30, the standard calculation of LED using the distance between the forward most and aft most contact of the striking ship to the struck ship hull will be low compared to the actual results for collisions where the collision angle is less oblique and penetration is low. This is because the LED is determined on the geometry of the striking ship; specifically for less oblique low penetration collisions the LED is most sensitive to the half entrance angle (HEA). However, the defined SIMCOL HEA input is for the striking ship waterline but in actual less oblique low penetration collisions the LED is predominantly a function of the HEA at the forecastle deck or the at the bulb, both of which are often greater than the HEA at the waterline. To overcome the deficiency in the LED calculation SIMCOL version 3.0 uses the following calculation of LED.

$$\frac{LED}{LBP1} = \begin{cases} \frac{LOC\_AFT - LOC\_FOR}{LBP1} & \text{if } PEN < B2 \wedge \frac{LOC\_AFT - LOC\_FOR}{LBP1} < B4 \\ \left[\frac{LOC\_AFT - LOC\_FOR}{LBP1} \cdot \frac{B1}{B2} \cdot (B3 - PEN)\right] & \text{otherwise} \end{cases} \tag{6.1}$$

Where:

PEN – penetration of striking ship into the struck ship divided by the struck ship beam

LBP1 – struck ship length between perpendiculars

LOC_FOR – forward most point on struck ship that striking ship hull contacts

LOC_AFT – aft most point on struck ship that striking ship hull contacts

B1 = 1/B2

B2 = 0.25 or other fitted value

B3 = 0.3125 or other fitted value

B4 = 0.2

A restriction on B1, B2, B3 and B4 is required such that $B4 \leq B2/(B3 \times B1)$. Additionally, a second restriction on B2 is required such that $B2 \leq 0.25$. This method considers only the less oblique cases where penetration and longitudinal extent of damage are minimal as occurs in all less oblique low penetration collisions.

As with the penetration results of Figure 6-7 and Figure 6-8 the SIMCOL LED results of Figure 6-9 and Figure 6-10 compare well to the data of both MARPOL and HARDER where the maximum variation between any of the data is less than 10%.

7 Conclusions

A simplified model for the prediction of damage in ship collisions is presented. SIMCOL uses a time-domain simultaneous solution of external ship dynamics and internal deformation mechanics. Reacting forces for deformation in side and bulkhead (vertical) structures are determined using specific component deformation mechanisms including: bow crushing; membrane tension; shell rupture; web frame bending; shear and compression; force required to propagate the yielded zone; force induced through longitudinal deflection of webs and transverse bulkheads; and friction. Absorbed energy and forces from the crushing and tearing of decks, bottoms, stringers, longitudinal and transverse bulkheads are determined using the modified Minorsky correlation with a careful calculation of changes in struck-ship damaged volume.

SIMCOL is validated using two separate collision cases providing a good correlation to observed penetration and longitudinal extent of damage values. The difficulty in obtaining exact and probabilistic values of the vessel speeds and collision angle along with initial contact location is discussed, relying heavily upon engineering assessment of all available documentation of the collision event.

Further validation of SIMCOL has been performed using the intended probabilistic functionality of SIMCOL and compared to the data collection of both MARPOL and the HARDER project. Good agreement between the probabilistic damage extent from SIMCOL to both data collection has been obtained.

Efforts are on going with the US Coast Guard to collect more recent collision data sufficient for additional physical validation of SIMCOL. This data is difficult to obtain and frequently incomplete in some aspect.

8 Future Work

Future work includes the following:

1) Incorporation of additional struck vessel structural geometries, such as passenger vessels, bulk carriers and containerships into the SIMCOL program.
2) Incorporation of a cargo energy-absorbing module into the SIMCOL program.
3) Investigation into the fracture and failure of ship material and structures to better understand and predict element and material failure strain for use in both FEA and SIMCOL.
4) Development of a raked bow (with and without bulb) model for SIMCOL to enable a higher degree of accuracy in capturing the striking vessel bow geometry.
5) Application of SIMCOL in a probabilistic optimization framework such as Model Center or ISIGHT.
6) Development of SIMCOL user-friendly front-end interface.
7) Development of SIMCOL users and theoretical manual.
8) Development of SIMCOL graphical output to enable user visualization of analysis.
9) Additional validation of the SIMCOL program to actual collision events.

References

[1] Sirkar, J., Ameer, P., Brown, A.J., Goss, P., Michel, K., Willis, W., "A Framework for Assessing the Environmental Performance of Tankers in Accidental Grounding and Collision", *SNAME Transactions* ***105****, 253-295*, 1997.

[2] Rawson, C., Crake, K. and Brown, A.J., "Assessing the Environmental Performance of Tankers in Accidental Grounding and Collision", *SNAME Transactions* ***106****, 41-58*, 1998.

[3] Brown, A.J. and Amrozowicz, M., "Tanker Environmental Risk - Putting the Pieces Together", SNAME/SNAJ International Conference on Designs and Methodologies for Collision and Grounding Protection of Ships, August 1996.

[4] IMO, "Interim Guidelines for Approval of Alternative Methods of Design and Construction of Oil Tankers under Regulation 13F(5) of Annex I of MARPOL 73/78", Resolution MEPC.66 (37), Adopted September 14, 1995.

[5] Jones, N., "A Literature Survey on the Collision and grounding Protection of Ships", Ship Structure Committee Report No. SSC-283, 1979.

[6] Giannotti, J.G., Jones, N., Genalis, P. and Van Mater, P.R., "Critical Evaluations of Low-Energy Ship Collision - Damage Theories and Design Methodologies, Volume I: Evaluation and Recommendations", Ship Structure Committee Report No. SSC-284, 1979.

[7] Giannotti, J.G., Jones, N., Genalis, P. and Van Mater, P.R., "Critical Evaluations of Low-Energy Ship Collision - Damage Theories and Design Methodologies, Volume II: Literature Search and Review", Ship Structure Committee Report No. SSC-285, 1979.

[8] ISSC, Report by Specialist Panel V.4 – Structural Design Against Collision and Grounding, Proceedings of the 13th International Ship and Offshore Structures Congress 1997, Trondheim, Norway, 1997.

[9] Minorsky, V.V.,"An Analysis of Ship Collisions with Reference to Protection of Nuclear Power Plants," Journal of Ship Research, 1959.

[10] Simonsen, B.C., "Theory and Validation for the DAMAGE Collision Module", Joint MIT-Industry Program on Tanker Safety, Report No. 67, June 1999.

[11] Crake, K., "Probabilistic Evaluations of Tanker Ship Damage in Grounding Events", Naval Engineer Thesis, MIT, 1995.

[12] Hutchison, B.L., “Barge Collisions, Rammings and Groundings - an Engineering Assessment of the Potential for Damage to Radioactive Material Transport Casks”, Report No. SAND85-7165 TTC-05212, 1986.

[13] Zhang, S., “The Mechanics of Ship Collisions”, Ph.D. Thesis, Department of Naval Architecture and Offshore Engineering, technical University of Denmark, Lyngby, 1999.

[14] Pedersen, P.T. and Zhang, S., 1998. “On Impact Mechanics in Ship Collisions”, Marine Structures, Vol. 11, pp. 429-449.

[15] Reardon, P. and Sprung, J.L., “Validation of Minorsky’s Ship Collision Model and Use of the Model to Estimate the Probability of Damaging a Radioactive Material Transportation Cask During a Ship Collision”, *Proceedings of the International Conference on Design and Methodologies for Collision and Grounding Protection of Ships*, San Francisco, August 1996.

[16] McDermott, J.F., Kline, R.G., Jones, E.L., Maniar, N.M., Chiang, W.P., “Tanker Structural Analysis for Minor Collisions”, *SNAME Transactions*, Vol. 82, pp. 382-414, 1974.

[17] Woisin, G., "Design Against Collision", *International Symposium on Advances in Marine Technology*, Trondheim, Norway, June 1979.

[18] Rosenblatt & Son, Inc, “Tanker Structural Analysis for Minor Collision”, USCG Report, CG-D-72-76, 1975.

[19] Reckling, K.A., "Mechanics of Minor Ship Collisions", *International Journal of Impact Engineering*, Vol. 1, No. 3, pp. 281-299, 1983.

[20] Wierzbicki, T., "Crushing Behavior of Plate Intersections", *Structural Crashworthiness*, edited by A. Jones and T. Wierzbicki, Chapter 3, Butterworth and Co., London, 1983.

[21] Paik, J. and Wierzbicki, T., "A Benchmark Study on Crushing and Cutting of Plated Structures", *Journal of Ship Research*, p. 147, June, 1997.

[22] Pedersen, P.T., et al, "Ship Impacts: Bow Collisions", *International Journal of Impact Engineering*, Vol. 13, No. 2, pp. 163-187, 1993.

[23] Amdahl, J., “Energy Absorption in Ship-Platform Impacts”, Dr. Ing. Thesis, Report No. UR-83-84, The Norwegian Institute of Technology, Trondheim, 1983.

[24] Yang, P.D.C. and Caldwell, J.B., "Collision Energy Absorption in Ships Bow Structures", *International Journal of Impact Engineering*, Vol. 7, No. 2, 1988.

[25] Ito, H., et al, "A Simplified Method to Analyze the Strength of Double Hulled Structures in Collision", *Journal of Society of Naval Architects of Japan*, Vol. 156, pp. 283-295, 1984.

[26] Ito, H., et al, "A Simplified Method to Analyze the Strength of Double Hulled Structures in Collision, 2nd Report", *Journal of Society of Naval Architects of Japan*, Vol. 158, pp. 420-434, 1985.

[27] Ito, H., et al, "A Simplified Method to Analyze the Strength of Double Hulled Structures in Collision, 3rd Report", *Journal of Society of Naval Architects of Japan*, Vol. 160, pp. 401-409, 1986.

[28] Paik, J.K., et al, "On Rational Design of Double Hull Tanker Structures against Collision", *1999 SNAME Annual Meeting*, 1999.

[29] Paik, J.K. and Pedersen, P.T., "Modeling of the Internal Mechanics in Ship Collisions", *Ocean Engineering*, Vol. 23, No. 2, pp. 107-142, 1996.

[30] Hallquist, J.O (1998), "LSDYNA Examples Manual", Livermore Software Technology Corporation (LSTC), March 1998.

[31] Hallquist, J.O (1998), "LSDYNA Theoretical Manual", Livermore Software Technology Corporation (LSTC), May 1998.

[32] Hallquist, J.O (1999), "LSDYNA Keyword Users Manual – Nonlinear Dynamic Structural Analysis of Structures", Livermore Software Technology Corporation (LSTC), May 1999.

[33] Lenselink, H., and Thung, K.G., "Numerical Simulations of the Dutch-Japanese Full Scale Ship Collision Tests", Proceedings of Conference on Prediction Methodology of Tanker Structural Failure, ASIS, Tokyo, July 1992.

[34] Wevers, L.J. and Vredeveldt, A.W., "Full Scale Ship Collision Experiments", TNO Report 98-CMC-R0359, 1999.

[35] Chen, D., "Simplified Collision Model (SIMCOL)", Dept. of Ocean Engineering, Virginia Tech, Master of Science Thesis, May 2000.

[36] Gibbs and Cox, Inc., "Design Criteria and Guide for Design of Nuclear-Powered Merchant Ships", for the US Department of Commerce, MARAD Nuclear Projects Office, January 1960.

[37] Kierkegaard, H., "Ship Collisions with Icebergs", PhD Thesis, DTU, April 1993.

[38] Kitamura, K. and Akita, M., "A Study on Collision by an Elastic Stem to the Side Structure of Ships", Trans. SNAJ, 131, 307-317, 1972.

[39] Hagiwara, K., Takanabe, H. and Kawano, H., "A Proposed Method of Predicting Ship Collision Damage", International Journal of Impact Engineering, No. 1, International Journal of Impact Engineering, No. 1, 1983.

[40] Kim, J.Y., “Crushing of a Bow: Theory vs. Scale Model Tests”, Joint MIT-Industry Program on Tanker Safety, Report No. 69, June 1999.

[41] Kim, J.Y., “Analysis of a Dropped Bow Collision Model”, Joint MIT-Industry Program on Tanker Safety, Report No. 72, May 2000.

[42] Gooding, Peter W. (1999), “Collision with a Crushable Bow”, MIT Thesis, 1999

[43] Gerard, G., ""The Crippling Strength of Compression Elements", *Journal of Aeronautical Science*, 1958.

[44] Amdahl, J. and Kavlie, D., “Experimental and Numerical Simulation of Double Hull Stranding”, Proceedings of the DNV-MIT Workshop on “Mechanics of Ship Collision and Grounding”, Oslo, 1992.

[45] Amdahl, J. and Kavlie, D., “Design of Tankers for Grounding and Collision”, MARIENV ’95, 1995.

[46] Lehmann, E. and Yu, X., “Progressive Folding of Bulbous Bows”, The Sixth International Symposium on Practical Design of Ships and Mobile Units (PRADS), September, 1995.

[47] Lutzen, M., Simonsen, B.C. and Pedersen, P.T., "Rapid Prediction of Damage to Struck and Striking Vessels in a Collision Event", Ship Structure Symposium 2000, Washington D.C., 2000.

[48] Kierkegaard, H., Ship Bow Response in High Energy Collision", Marine Structures, Vol. 6, pp. 359-376, 1993.

[49] Arita, K., “A Probabilistic Assessment on Protective Structures in Ship Collisions”, 63 General Meeting of Ship Research Institute, 1994.

[50] Valsgard, S. and Pettersen, E., "Simplified Non-Linear Analysis of Ship/Ship Collisions", Norwegian Maritime Research, No. 3, pp. 2-17, 1982.

[51] Bach-Gansmo, O. and Valsgard S., “Simplified stiffness evaluation of a bulbous ship bow”, Progress report No. 1, DnV, Report No. 81-0437 (Rev. no. 1 of 17.02.82), 1981.

[52] Chang, P.Y., Seibold, F. and Thasantorn, C., “A Rational Methodology for the Prediction of Structural Response due to Collision of Ships.”, Paper No. 6, SNAME Annual Meeting, New York, NY, Nov. 13-15, 1980.

[53] Wang, G., Katsuyuki, S., Ohtsubo, H. (1995), "Predicting Collision Strength of Bow Structure", Marienv 95

[54] Suzuki, K., Ohtsubo, H. (1995), "Crushing Strength of Ship Bow Structure - Calculation of Absorbed Energy and Optimal Design", Marienv95

[55] Vakkalanka, Suryanarayana, “Simplified Bow Model for a Striking Ship in Collision”, Dept. of Ocean Engineering, Virginia Tech, Master of Science Thesis, July 2000.

[56] Xia, Jianjun, “Finite Element Analysis of Ship Collisions”, Department of Ocean Engineering, Virginia Tech, Master of Science Thesis, May 2001.

[57] Kitamura, O., “FEM Approach to the Simulation of Collision and Grounding Damage”, 2nd International Conference on Collision and Grounding of Ships, Copenhagen, Denmark, July, 2001.

[58] Gu, Y. and Wang, Z.L., “An Inertia Equivalent Model for Numerical Simulation of Ship-Ship Collisions”, 2nd International Conference on Collision and Grounding of Ships, Copenhagen, Denmark, July, 2001.

[59] Lemmen, P.P.M. and Vredeveldt, A.W., "Application of Explicit Finite Element Method in Ship Collision Analysis", TNO Report 93-CMC-R1153, 1 December 1993.

[60] Servis, D. et. al., “The Implementation of Finite Element Codes for the Simulation of Ship-Ship Collision”, 2nd International Conference on Collision and Grounding of Ships, Copenhagen, Denmark, July, 2001.

[61] Naar, H. et. al., “Comparison of the Crashworthiness of Various Bottom and Side Structures”, 2nd International Conference on Collision and Grounding of Ships, Copenhagen, Denmark, July, 2001.

[62] Sinmao, M. & Abramowicz, W. “Joint MIT-Industry Report #66.” MIT Department of Ocean Engineering, 1999.

[63] Tikka, K.K. & Chen, Y.J. “Prediction of Structural Response in Grounding”, Ship Structure Symposium 2000, Washington D.C., 2000.

[64] Simonsen, B.C. “Ship Grounding on Rock – I.”, Marine Structures, 10, pp. 519-562, 1997.

[65] Kitamura, O. “Buffer Bow Design for the Improved Safety of Ships”, Ship Structure Symposium 2000, Washington D.C., 2000.

[66] “Machinery’s Handbook 25, Twenty Fifth Edition.” Industrial Press Inc., 1996.

[67] Simonsen, B.C. & Wierzbicki, T. “Joint MIT-Industry Report #59.” MIT Department of Ocean Engineering, 1999.

[68] Shibue, T., Abe, A. and Fujita, K. “The Effect of the Strut Arrangement on the Energy Absorption of Side Structure in Collision”, 2nd International Conference on Collision and Grounding of Ships, Copenhagen, Denmark, July, 2001.

[69] Lehmann, E. & Peschmann, J. “Energy Absorption by the Steel Structure of Ships in the Event of Collisions”, 2nd International Conference on Collision and Grounding of Ships, Copenhagen, Denmark, July, 2001.

[70] Wisniewski, K., Kolakowski, P., Rozmarynowski, B. & Gierlinski, J.T. “Dynamic FE simulation of damage in ships collision”, 2nd International Conference on Collision and Grounding of Ships, Copenhagen, Denmark, July, 2001.

[71] “LSDYNA USER’S MANUAL”, Livermore Software Technology Corporation, 2001.

[72] Lemmen, P.M., Vredeveldt, A.W., and Pinkster, J.A., “Design Analysis for Grounding Experiments”, SNAME/SNAJ International Conference on Designs and Methodologies for Collision and Grounding Protection of Ships, San Francisco, August 1996.

[73] Simonsen and Lauridsen. “Energy Absorption and Ductile Failure in Metal Sheets Under Lateral Indentation by a Sphere.”

[74] Kitamura, O., “Comparative Study on Collision Resistance of Side Structure”, Marine Technology, Vol. 34, No. 4, pp.293-308, October 1997.

[75] Servis, D.P., and Samuelides, M., “Ship Collision Analysis Using Finite Elements”, Safer Euroro Spring Meeting, Nantes Greece, 28 April 1999.

[76] Francis, P.H., Cook, T.S., and Nagy, A., Ship Structure Committee Report Number 276 (SSC-276), 1978.

[77] R.L. Rothman & R.E. Monroe, Ship Structure Committee Report Number 235 (SSC-235), 1973.

[78] Sandia National Laboratories, *Data and Methods for the Assessment of the Risks Associated with the Maritime Transport of Radioactive Materials Results of the SeaRAM Program Studies*, SAND98-1171/2, Albuquerque, NM, May 1998.

[79] Lloyds Worldwide Ship data, provided by MARAD, 1993.

[80] ORI, *Hazardous Environment Experienced by Radioactive Material Packages Transported by Water*, Silver Spring, MD, October 1980.

[81] ORI, *Accident Severities Experienced by Radioactive Material Packages Transported by Water*, Silver Spring, MD, November 1981.

[82] USCG Ship Casualty Data, 1982-1990.

[83] Brown, A.J., Ship Structure Committee Report Number 422 (SSC-422), 2002.

[84] MVI, *SS P&T ADVENTURER-SS TULLAHOMA Collision Off Destruction Island*, Chief, Merchant Vessel Inspection Division, March 1952

[85] Hughes, Ship Structural Design, SNAME, 1988

[86] Sanford, Principles of Fracture Mechanics, Prentice Hall, 2003

[87] Wierzbicki and Abromowicz, *On the Crushing Mechanics of Thin-Walled Structures*, ASME Winter Annual Meeting, Presented 1983

[88] Lutzen, Marie, "Ship Collision Damages", Department of Mechanical Engineering, Technical University of Denmark, Doctoral Thesis, December 2001.

[89] ASIS, *Research on the Methodology for the Prediction of Accidental Damage to Tanker Structure in Case of Collision and Grounding and Development of New Hull Design with Improved Crashworthiness*, March 1998

[90] Bower, A.F., 1999, Lecture Notes – Advanced Mechanics of Solids

[91] USCG, *Decision and Final Order of the Commandant in the Matter of License No. 124294*, May 1952

[92] Brown, A.J., Sajdak, J.A.W., *Floating Production, Storage and Offloading Vessel Collision Study*, Report for Herbert Engineering SSSE 01-4, April 2002

[93] Brown, A.J., Chen, D., *Probabilistic Method for Predicting Ship Collision Damage*, Oceanic Engineering International, V.6 No. 1, 2002

[94] Glykas, Das & Barltrop, *Application of Failure and Fracture Criteria During a Tanker Head-on Collision*, Ocean Engineering V.28, 2001

[95] Paik & Thayamballi, *A Concise Introduction to the Idealized Structural Unit MethodforNonlinear Analysis of Large Plated Structures and its Application*, Thin Walled Structures, V.41, 2003

[96] Glykas & Das, *Energy Conservation During a Tanker Collision*, Ocean Engineering, V.28, 2001

[97] Egge & Bckenhauer, *Calculation of the Collisin Resistance of Ships and its Assessment for Classification Purposes*, Nuclear Engineering and Design, V.150, 1994

[98] Carlebur, *Full-Scale Collision Tests*, Safety Science, V.19, 1995

[99] Ishiyama, Nishimura & Tsuchiya, *Impact Response of Thin Walled Plane Frame Strucures*, Journal of Impact Engineering, V.1, No. 3, 1983

[100] Brown, A.J., *Collision Scenarios and Probabilistic Collision Damage*, Marine Structures, V.15, 2002

[101] Wang, G., *Some Recent Studies on Plastic Behavior of Plates Subjected to Large Impact Loads*, Journal of Offshore Mechanics and Arctic Engineering, V.124, August 2002

[102] Zhu & Faulkner, *Dynamic Inelastic Behavior of Plates in Minor Ship Collisions*, Journal of Impact Engineering, V.15, No. 2, 1994

[103] Ziliotto et al., *Comparison of Different Finite Element Analyses of the Transverse Frame of a 350000 TDW Tanker*, Marine Structures, V.4, 1991

[104] Zheng & Wierzbicki, *A Theoretical Study of Steady-State Wedge Cutting Through Metal Plates*, International Journal of Fracture, V.78, 1996

[105] Wierzbicki, Bao and Werner, *Ductile Fracture: Theory, Calibration and Applications*, EuroPAM, 2002

[106] Wierzbicki & Driscoll, *Crushing Damage of Web Girders Under Localized Static Loads*, Journal of Construction Steel Research, V.33, 1995

[107] Ueda, Rashed & Paik, *Buckling and Ultimate Strength Interation in Plates and Stiffened Panels Under Combined Inplane Biaxial and Shearing Forces*, Marine Structures, V.8, 1995

[108] Hu & Jiang, *A Finite Element Simulation of the test Procedure of Stiffened Panels*, Marine Structures, V.11, 1998

[109] Jones & Jouri, *A Study of Plate Tearing for Ship Collision and Grounding Damage*, Journal of Ship Research, V.31, No. 4, December 1987

[110] Johnson & Katcharian, *Several Recent Rammings Investigated by the National Transportation Safety Board*, Marine Technology, V.28, No. 6, November 1991

[111] Huang, Chen & Zhang, *Pseudo-Shakedown in the Collision Mechanics of Ships*, International Journal of Impact Engineering, V.24, 2000

[112] Kuroiwa, Kawamoto, Kusuba & Stillman, (1995), *Numerical Simulation of Collision and Grounding of Ships*, Marienv95

[113] Daidola, *Tanker Structure Behavior During Collision and Grounding*, Marine Technology, V.32, No. 1, January 1995

[114] Paik & Pedersen, *Ultimate and Crushing Strength of Plated Structures*, Journal of Ship Research, V.39, No. 3, September 1995

[115] Paik, Chung & Chun, *On Quasi-Static Crushing of a Stiffened Square Tube*, Journal of Ship Research, V.40, No. 3, September 1996
[116] Pedersen, (1995), *Collision and Grounding Mechanics*, WEMT 95 – Ship Safety and the Protection of the Environment
[117] Paik & Pedersen, *On Design of Double Hull Tankers Against Collisions*, Sixth International Symposium on Practical Design of Ships and Mobile Units, PRADS95, September 1995
[118] Hayduk & Wierzbicki, *Extensional Collapse Modes of Structural Members*, Computers & Structures, V.18, No. 3, 1984
[119] Dand, *Hydrodynamic Aspects of Shallow Water Collisions*, RINA Meeting, London, April 1976
[120] Paik & Wierzbicki, *A Benchmark Study on Crushing and Cutting of Plate Structures*, Journal of Ship Research, V.41, No. 2, June 1997
[121] Paik, Thayamballi & Yang, *Residual Strength Assessment of Ships after Collision and Grounding*, Marine Technology, January 1998
[122] Pedersen & Zhang, *Collision Analysis for MS DEXTRA*, SAFER EURORO Spring Meeting, April 1999
[123] Pedersen & Zhang, *Effect of Ship Structure and Size on Grounding and Collision Damage Distributions*, Ocean Engineering, V.27, 2000
[124] Pedersen & Zhang, *Absorbed Energy in Ship Collisions and Grounding – Revising Minorsky's Empirical Method*, Journal of Ship Research, June 2000
[125] Petersen, *Dynamics of Ship Collisions*, Ocean Engineering, V.9, No. 4, 1982
[126] Paik, Choe & Thayamballi, *Predicting Resistance of Spherical-Type LNG Carrier Structures to Ship Collisions*, Marine Technology, V.39, No. 2, April 2002
[127] Sano, et al., (1995), *A Study on the Strength of Double Hull Side Structure of VLCC in Collision*, Marienv95
[128] Sano, et al., *Strength Analysis f a New Double Hull Structure for VLCC in Collision*, SNAME/SNAJ Conference, August 1996
[129] Simonsen & Ocakli, *Experiments and Theory on Deck and Girder Crushing*, Thin-Walled Structures, V.34, 1999
[130] Simonsen & Wierzbicki, *Plasticity, Fracture and Friction in Steady-State Plate Cutting*, Interational Journal of Impact Engineering, V.19, No. 8, 1997

[131] Arita & Shoji, (1995), *Expected Effectiveness of Double Side Structures in Ship Collisions*, Marienv95

[132] Akita, Ando, Fujita & Kitamura, *Studies on Collision-Protective Structures in Nuclear Powered Ships*, Nuclear Engineering and Design, V.19, 1972

[133] Mains, C., *Updated Damage Statistics on Collision and Grounding*, Germanischer Lloyd, 1-11-D-2001-01-1, July 2001

Appendix A: 150K dwt Bulk Carrier Bow Structural Data

150,000 DWT Bulk Carrier

Ship Particulars

LBP	: 274 m
Breadth moulded	: 47.0 m
Depth molded	: 21.6 m
Depth to forecastle deck	: 26.0 m
Max. Draft	: 15.96 m
Displacement	: 174850 tons
Max. service speed	: 7.7 m/s (15.00 knots)

The bow is stiffened longitudinally. The transverse frames supporting the longitudinals have a spacing of 3.2 m. The most important structural data for the bow are:

Material

Yield Stress for plates and stiffeners (σ_Y)	: 315 Mpa
Ratio between ultimate and Yield stress (σ_u/σ_Y)	: 1.6

Bottom

plate thickness	: 18.0 mm
longitudinals, spacing	: L450 x 150 x 12/16
CL-Girder	: L2500 x 400 x 15/25

Side shell

Plate thickness, side shell up to 8.1 m abl	: 18.0 mm
Plate thickness, side shell between 8.1 and 17.0 m abl	: 33.0 mm
Plate thickness, side shell between 17.0 and 26.0 m abl	: 16.0 mm
Longitudinals between 1.2 and 6.8 m abl, spacing 0.8 m	: L450 x 150 x 12/16
Longitudinals between 8.4 and 16.2 m abl, spacing 0.6 m	: L400 x 100 x 19/19

Longitudinals between 17.4 and 24.8 m abl, spacing 0.8 m : L350 x 100 x 12/17

Forecastle deck, 26.0 m abl

Plate thickness	: 13.0 mm
Longitudinals, spacing	: L250 x 90 x 12/16
CL-girder	: L1400 x 250 x 12/25

Tank top, 20.0 m abl

Plate thickness	: 13.0 mm
Longitudinals, spacing	: L250 x 90 x 12/16
CL-girder	: L1400 x 250 x 12/25

Deck (not water-tight), 7.7 m abl

Plate thickness	: 13.0 mm
Longitudinals, spacing	: L250 x 90 x 12/16
CL-girder	: L1400 x 250 x 12/25

Breast hooks

Number of breast hooks	: 32
Cross-section	: 1200 x 15
Length	: 3000 mm
CL-girder along stem line cross-section	: T1400 x 250 x 12/25
CL-bulkhead in bulb fwd F.P (plate thickness)	: 12mm
Vertical stiffening spacing	: 0.8 m

Appendix B: 40K dwt Container Ship Bow Structural Data

40,000 DWT Containership

Principal dimensions:

LBP	**: 211.50 m**
Breadth moulded	**: 32.20 m**
Depth mld to main deck	**: 21.00 m**
Depth to shelter deck	**: 24.00 m**
Max. Draft	**: 11.90 m**
Displacement (Loaded)	**: 54,000 tons**
Max. Service Speed	**: 11.3 m/s (21.97 knots)**

The bulbous bow is stiffened longitudinally. The transverse frames supporting the longitudinals have a spacing of 2.4 m. The most important structural data for the bow are:

Bottom:

Plate thickness	**: 19.0**
Longitudinals, spacing 0.8 m	**: L 250 X 90 X 12 / 16**
CL-Girder	**: L 1900 X 250 X 15 / 25**

Side shell

Plate thickness, side shell up to 6.1 m abl	**: 17.0 mm**
Plate thickness, side shell between 6.1 and 12.3 m abl	**: 35.0 mm**
Plate thickness, side shell between 12.3 and 21.0 m abl	**: 16.0 mm**
Plate thickness, side shell above 21.0 m abl	**: 14.0 mm**
Longitudinals below 5.2 m abl and above 13.6 m abl (spacing 0.8 m)	**: L250 x 90 x 10/15**
Longitudinals between 6.6 and 12.0 m abl, spacing 0.6 m	**: L250 x 90 x 12/16**

Forecastle deck, 24.0 m at

Plate thickness	: 15.0 mm
Longitudinals, spacing 0.8 m	: L150 x 100 x 9
CL-girder	: L700 x 150 x 12/12

Main deck,21.0 m abl

Plate thickness	: 11.0 mm
Longitudinals, spacing 0.8 m	: L150 x 100 x 9
CL-girder	: L700 x 150 x 12/12

Deck 17.6 m abl

Plate thickness	: 11.0 mm
Longitudinals, spacing 0.8 m	: L150 x 100 x 9
CL-girder	: L700 x 150 x 12/12

Deck 12.8 m abl

Plate thickness	: 15.0 mm
Longitudinals, spacing 0.8 m	: L200 x 90 x 9/14
CL-girder	: L700 x 150 x 12/12

Deck (not water-tight), 6 m abl

Plate thickness	: 11.0 mm
Longitudinals, spacing 0.8 m	: Fl. 150 x 12

Appendix C: C4 Cargo Ship Bow Structural Data

The scantlings and dimensions of the C4 cargo vessel used are the same as the Victory Cargo ship of appendix D multiplied by a factor of 1.149. All thicknesses used are exactly those of the VC2-S-AP3 of appendix D.

Appendix D: Victory Cargo Ship Bow Structural Data

VC2-S-AP3 (Victory Cargo)

Ship Particulars:

LBP	: 436.5 ft
LWL	: 444.0 ft
Length Overall	: 455.25 ft
Moulded beam	: 62.0 ft
Moulded depth	: 38.0 ft
Moulded Draft at DWL	: 28.0 ft
Displacement (loaded)	: 14,832 tons
Max. Service Speed	: 16.0 knots

The bow is stiffened transversely. The transverse stiffener spacing is 2.0 ft. The most important structural data for the bow are:

Material:

Yield Stress for plates and stiffeners	: 235 Mpa
Ratio between ultimate and Yield stress	: 1.4

Bottom:

Plate thickness	: 27.0 mm
CL-Girder	: 19.5 mm

Sideshell:

Plate thickness, side shell up to 18 ft abl	: 27.0 mm
Plate thickness, side shell between 18 ft and 51 ft abl	: 21.25 mm

Forecastle deck, 51 ft abl:

Plate thickness : 10.5 mm

CL-Girder : 27 in x 19.5 mm

Main deck, 42 ft abl:

Plate thickness : 10.5 mm

CL-Girder : 28 in x 19.5 mm

Second deck, 28 ft abl:

Plate thickness : 10.5 mm

CL-Girder : 24 in x 19.5 mm

Stringer deck 3 (not watertight), 35 ft abl:

Plate thickness : 10.5 mm

Stringer deck 2 (not watertight), 23 ft abl:

Plate thickness : 10.5 mm

Stringer deck 1 (not watertight), 18 ft abl:

Plate thickness : 10.5 mm

Breast hooks:

Number of breast hooks : 14

Thickness : 10.0 mm

The following are graphical representations of the VC2-S-AP3 bow:

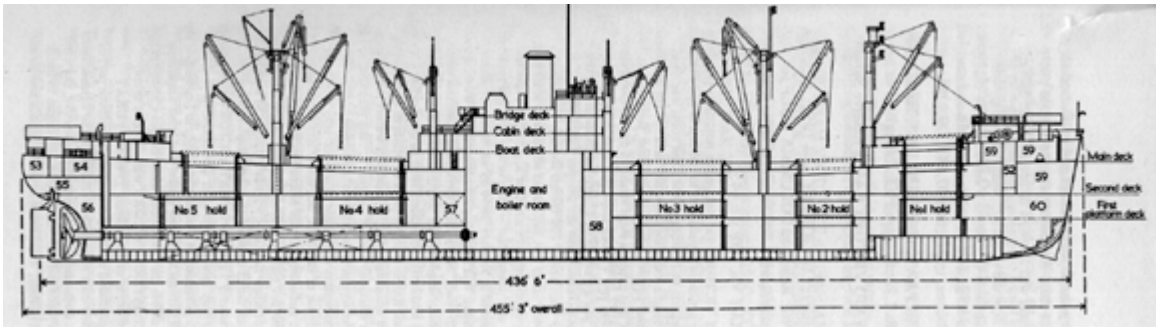

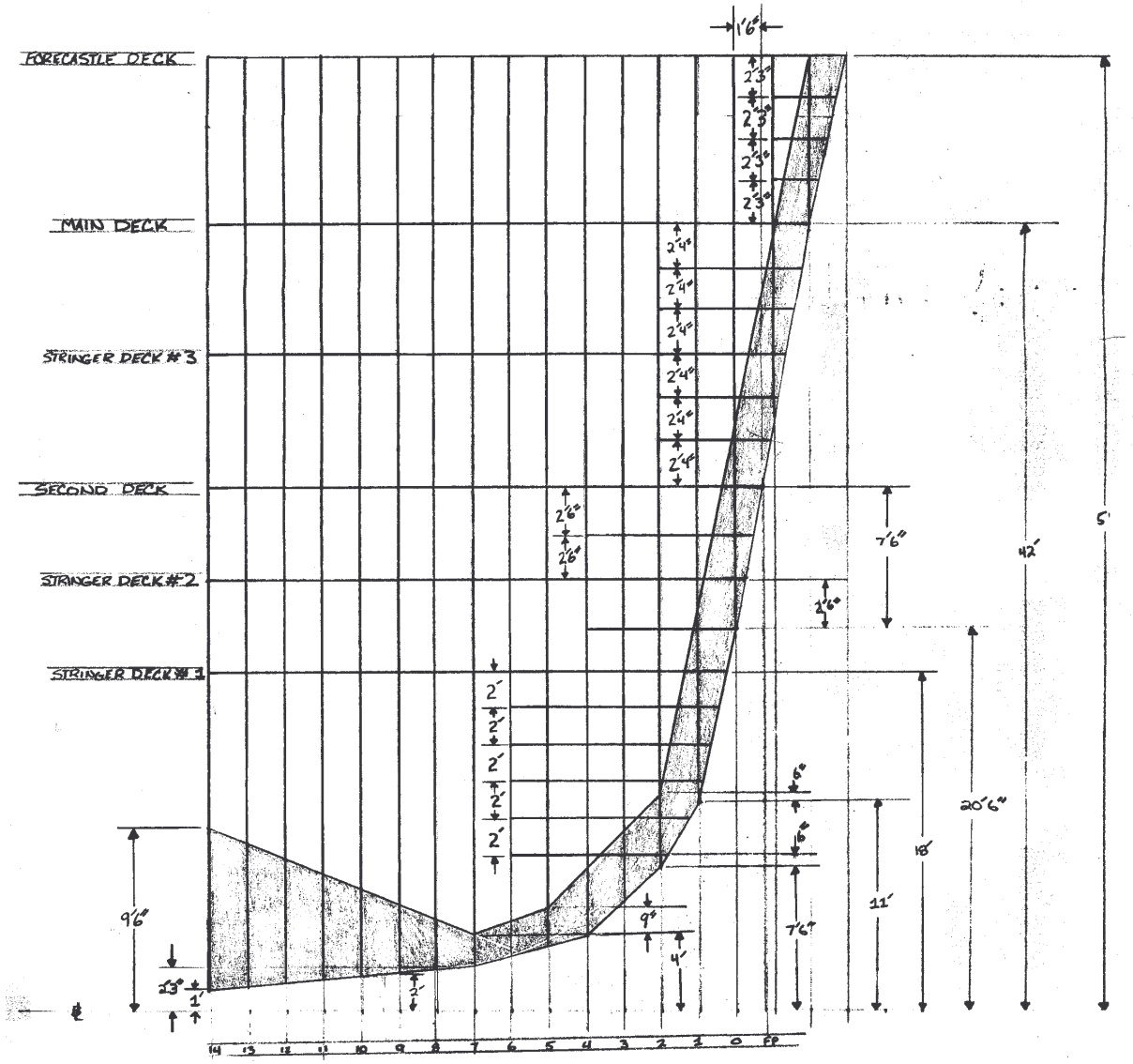
FORECASTLE DECK
MAIN DECK
STRINGER DECK #3
SECOND DECK
STRINGER DECK #2
STRINGER DECK #1
1'6"
2'3"
2'4"
2'6"
2'
7'6"
42'
6"
16"
18'
20'6"
11'
9'6"
9"
4"
23"
1'
14 13 12 11 10 9 8 7 6 5 4 3 2 1 0 FP

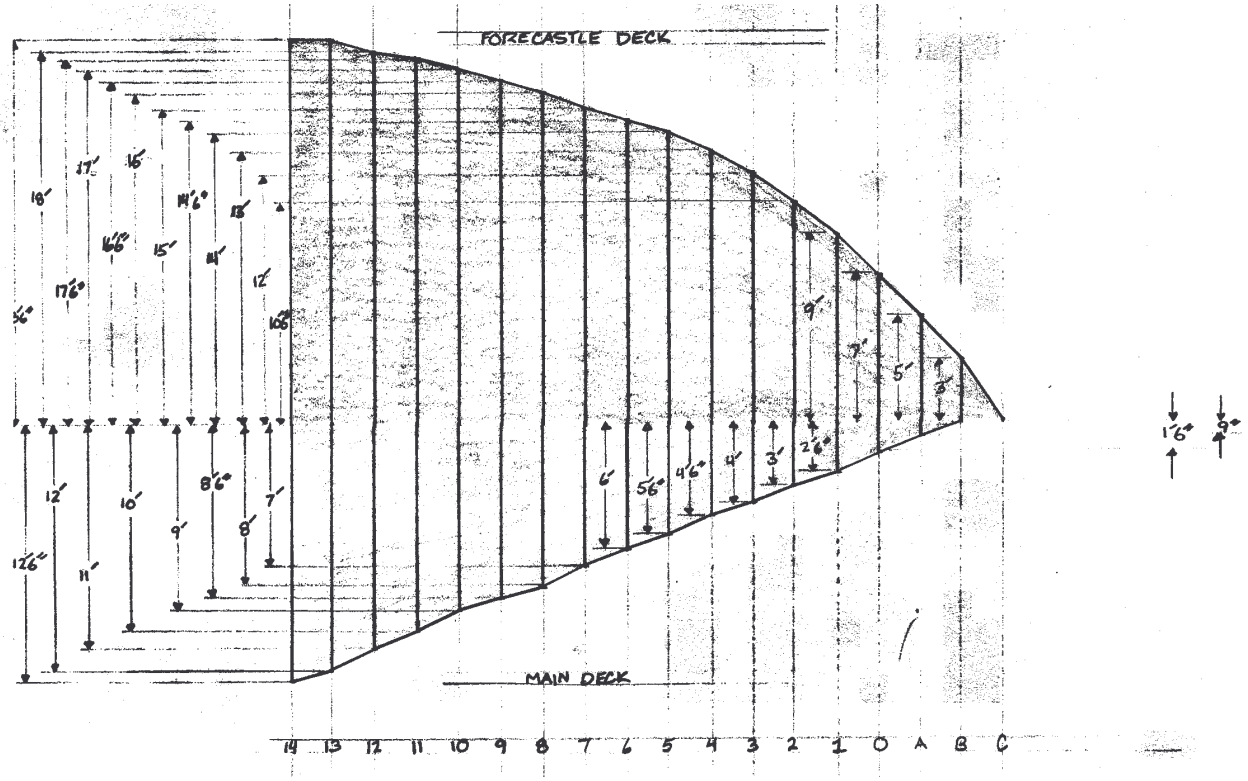
FORECASTLE DECK
MAIN DECK
14 13 12 11 10 9 8 7 6 5 4 3 2 1 0 A B C

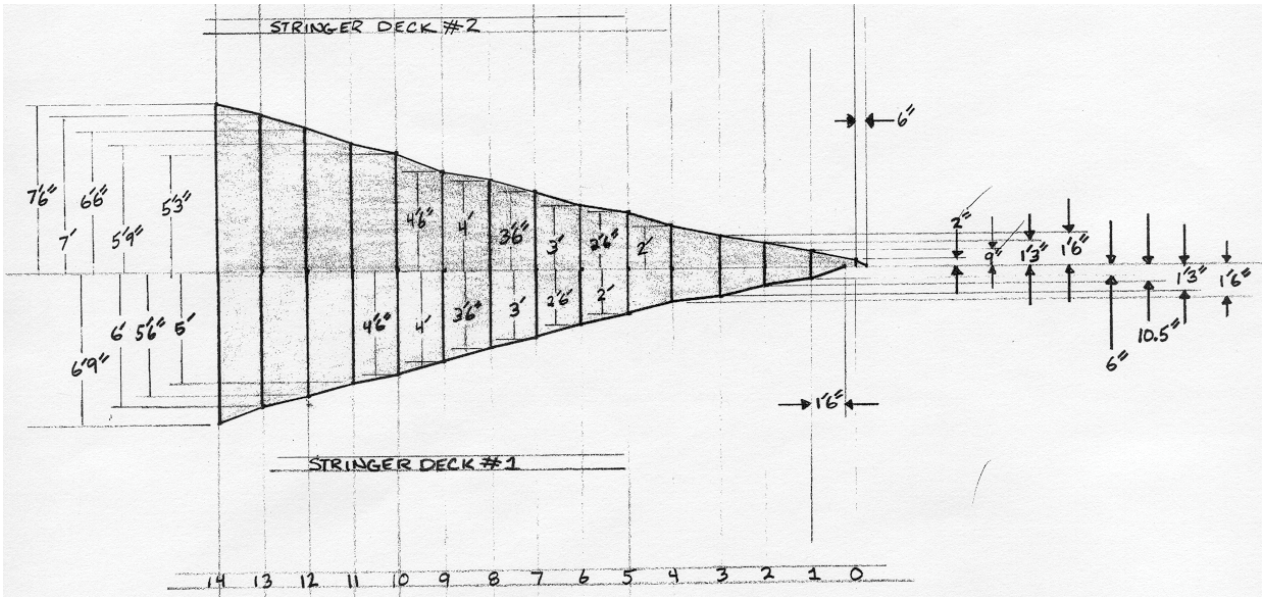
STRINGER DECK #2
STRINGER DECK #1
6"
1'6"
14 13 12 11 10 9 8 7 6 5 4 3 2 1 0

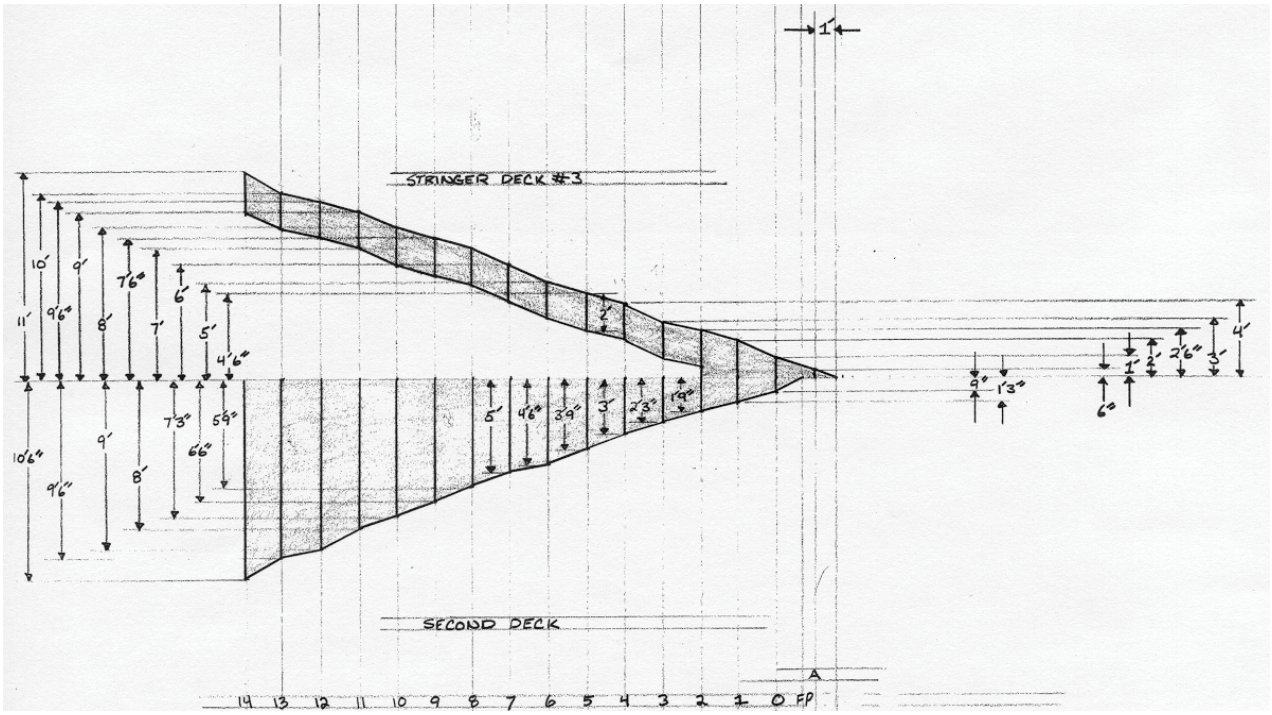
1'
STRINGER DECK #3
11'
10'
9'6"
9'
8'
7'6"
7'
6'
5'
4'6"
2'
5'
4'6"
3'9"
3'
2'3"
1'9"
9"
1'3"
6"
1'
2'
2'6"
3'
4'
10'6"
9'6"
9'
8'
7'3"
6'6"
5'9"
SECOND DECK
A
14 13 12 11 10 9 8 7 6 5 4 3 2 1 0 FP

Appendix E: 150K dwt Double Hull Tanker Cargo Section Structural Data

IMO 150k dwt Double Hull Reference Tanker

Information Book For

Grounding and Collision Analysis

UPDATE: OCTOBER 15, 1999

A. J. Brown

Naval Architecture

L = 264 m B = 48 m D = 24 m T = 16.8 m Δ = 178867 MT

Profile and Plan

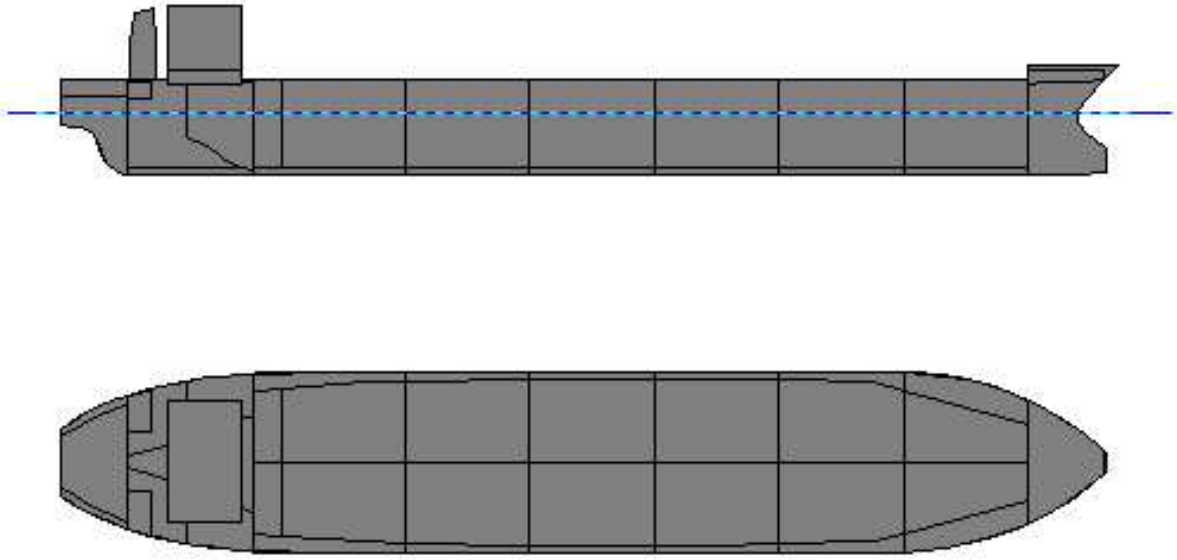

Weights and Stability

Full Load Departure

Item	Weight MT	VCG m	LCG m-MS	TCG m-CL	FSMom m-MT
Light Ship	22,849	12.960	1.380F	0.000	----
Constant	673	20.740	10.013A	0.000	----
Cargo Oil	150,056	13.523	12.767F	0.000S	254,794
Fuel Oil	4,328	17.069	93.920A	0.004S	3,395
Diesel Oil	334	17.986	106.941A	0.392P	88
Lube Oil	129	16.661	101.003A	7.355P	41
Fresh Water	498	22.596	116.193A	0.000	0
SW Ballast	0	----	----	----	----
Misc.	0	----	----	----	----
Misc. Weights	0	----	----	----	----
Displacement	178,867	13.600	7.980F	0.006P	258,318

Stability Calculation			Trim Calculation		
KMt	19.676	m	LCF Draft	16.800	m
VCG	13.600	m	LCB (even keel)	7.981F	m-MS
GMt (Solid)	6.076	m	LCF	0.217A	m-MS
FSc	1.444	m	MT1cm	2,111	m-MT
GMt (Corrected)	4.632	m	Trim	0.000	m
			List	0.1S	deg

Primary Subdivision

Double Bottom: h_{DB} = 2.32 meters

Double Side: w = 2 meters

	Compartment	Mir	# Sta	Aft m-MS	Fwd m-MS
1	FOREPEAK	N	7	119.000F	139.400F
2	FOCSLE DECK	N	5	119.000F	139.000F
3	NO.1 WBT S	Y	13	86.000F	119.000F
4	NO.1 COT S	N	13	86.000F	119.000F
5	NO.1 WBT P	N	13	86.000F	119.000F
6	NO.1 COT P	N	13	86.000F	119.000F
7	NO.2 WBT S	Y	9	53.000F	86.000F
8	NO.2 COT S	Y	9	53.000F	86.000F
9	NO.2 WBT P	N	9	53.000F	86.000F
10	NO.2 COT P	N	9	53.000F	86.000F
11	NO.3 WBT S	Y	7	20.000F	53.000F
12	NO.3 COT S	Y	7	20.000F	53.000F
13	NO.3 WBT P	N	7	20.000F	53.000F
14	NO.3 COT P	N	7	20.000F	53.000F
15	NO.4 WBT S	Y	9	13.000A	20.000F
16	NO.4 COT S	Y	9	13.000A	20.000F
17	NO.4 WBT P	N	9	13.000A	20.000F
18	NO.4 COT P	N	9	13.000A	20.000F
19	NO.5 WBT S	Y	7	46.000A	13.000A
20	NO.5 COT S	Y	7	46.000A	13.000A
21	NO.5 WBT P	N	7	46.000A	13.000A
22	NO.5 COT P	N	7	46.000A	13.000A
23	NO.6 WBT S	Y	11	86.500A	46.000A
24	NO.6 COT S	Y	9	79.000A	46.000A
25	NO.6 WBT P	N	11	86.500A	46.000A
26	NO.6 COT P	N	9	79.000A	46.000A
27	SLOP TANK S	Y	5	86.500A	79.000A
28	SLOP TANK P	N	5	86.500A	79.000A

Full Load cargo

Full Load Departure

Cargo Oil Tank Name	Weight MT	% Full	Capacity MT	VCG m-BL	LCG m-MS	TCG m-CL	FSmom m-MT	Density MT/m3	Volume m3
NO.1 COT P	8,462	98.0	8,635	13.876	100.607F	7.268P	8,506	0.8550	9,897
NO.1 COT S	8,462	98.0	8,635	13.876	100.607F	7.268S	8,506	0.8550	9,897
NO.2 COT P	12,677	98.0	12,935	13.418	69.217F	10.388P	21,834	0.8550	14,827
NO.2 COT S	12,677	98.0	12,935	13.418	69.217F	10.388S	21,835	0.8550	14,827
NO.3 COT P	13,309	98.0	13,580	13.316	36.449F	10.891P	24,454	0.8550	15,566
NO.3 COT S	13,309	98.0	13,580	13.316	36.449F	10.891S	24,454	0.8550	15,566
NO.4 COT P	13,382	98.0	13,655	13.302	3.504F	10.950P	24,757	0.8550	15,652
NO.4 COT S	13,382	98.0	13,655	13.302	3.504F	10.950S	24,757	0.8550	15,652
NO.5 COT P	13,105	98.0	13,373	13.357	29.387A	10.727P	23,627	0.8550	15,328
NO.5 COT S	13,105	98.0	13,373	13.357	29.387A	10.727S	23,627	0.8550	15,328
NO.6 COT P	11,875	98.0	12,117	13.802	61.844A	9.877P	20,440	0.8550	13,889
NO.6 COT S	11,875	98.0	12,117	13.802	61.844A	9.877S	20,440	0.8550	13,889
SLOP TANK P	2,218	98.0	2,263	14.826	82.680A	8.458P	3,778	0.8550	2,594
SLOP TANK S	2,218	98.0	2,263	14.826	82.680A	8.458S	3,778	0.8550	2,594
Totals	150,056	98.0	153,118	13.523	12.767F	0.000S	254,794		175,504

Structural Design

Ship Dimensions

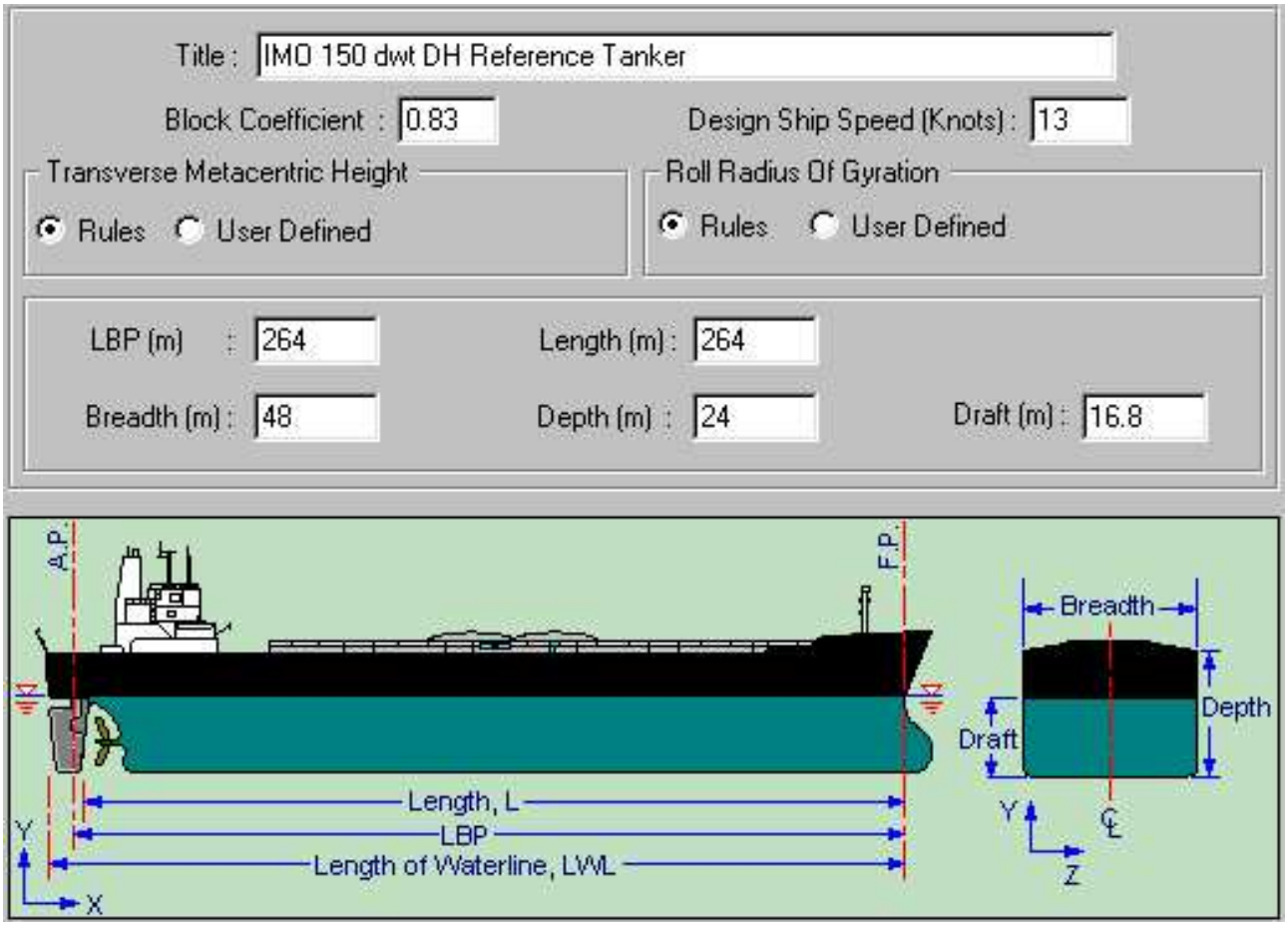

HULL TYPE

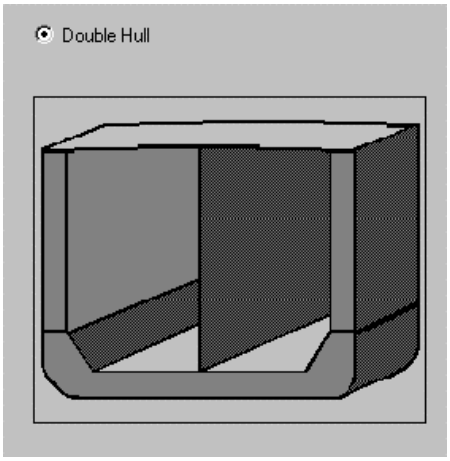

MIDSHIP GEOMETRY

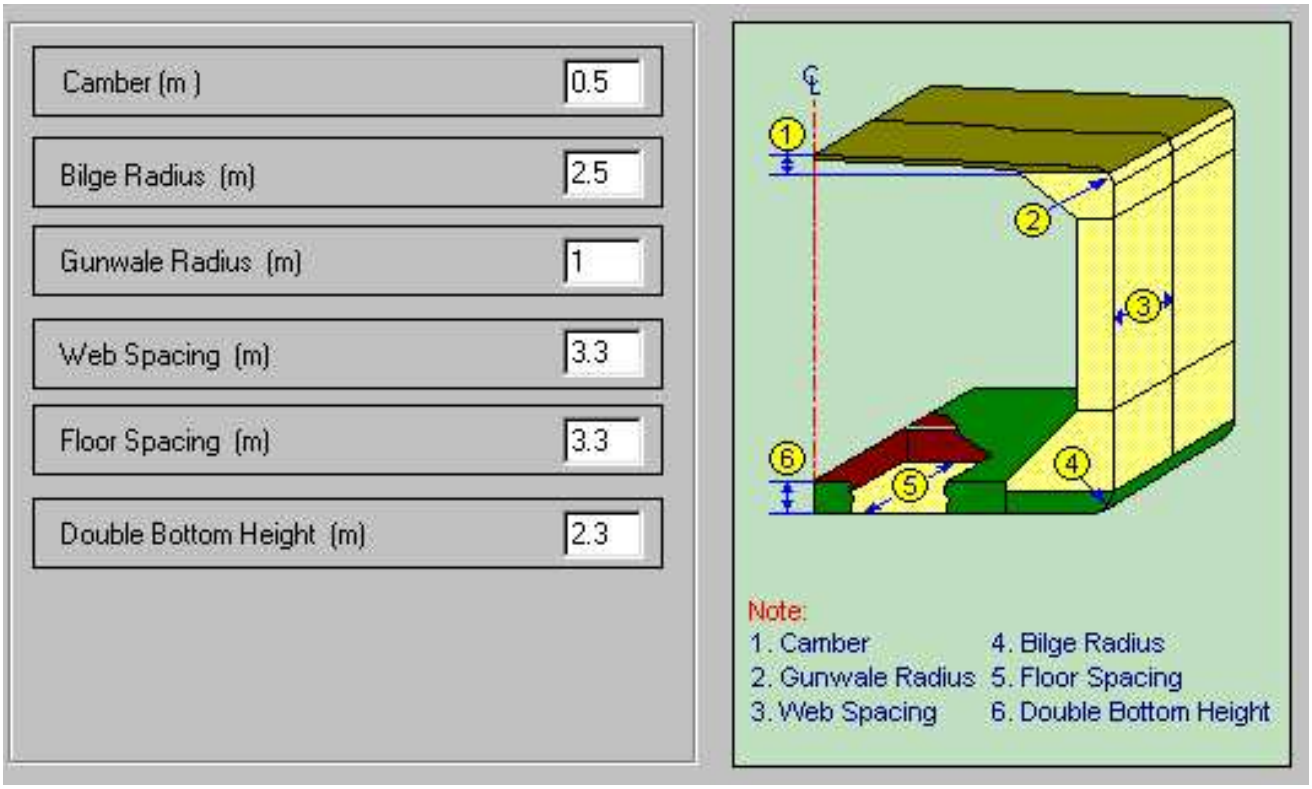

TANK DEFINITION

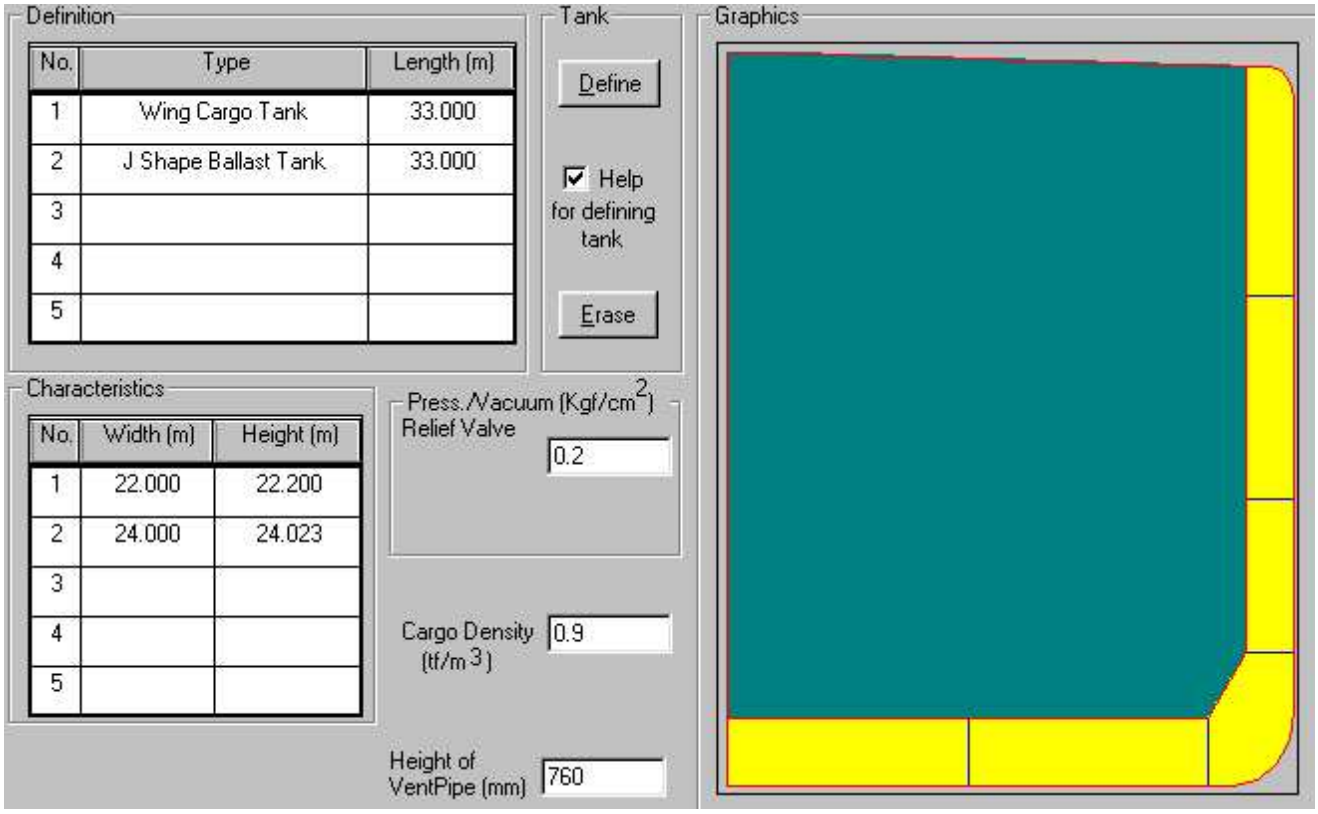

TRANSVERSE MEMBERS

Web Configuration

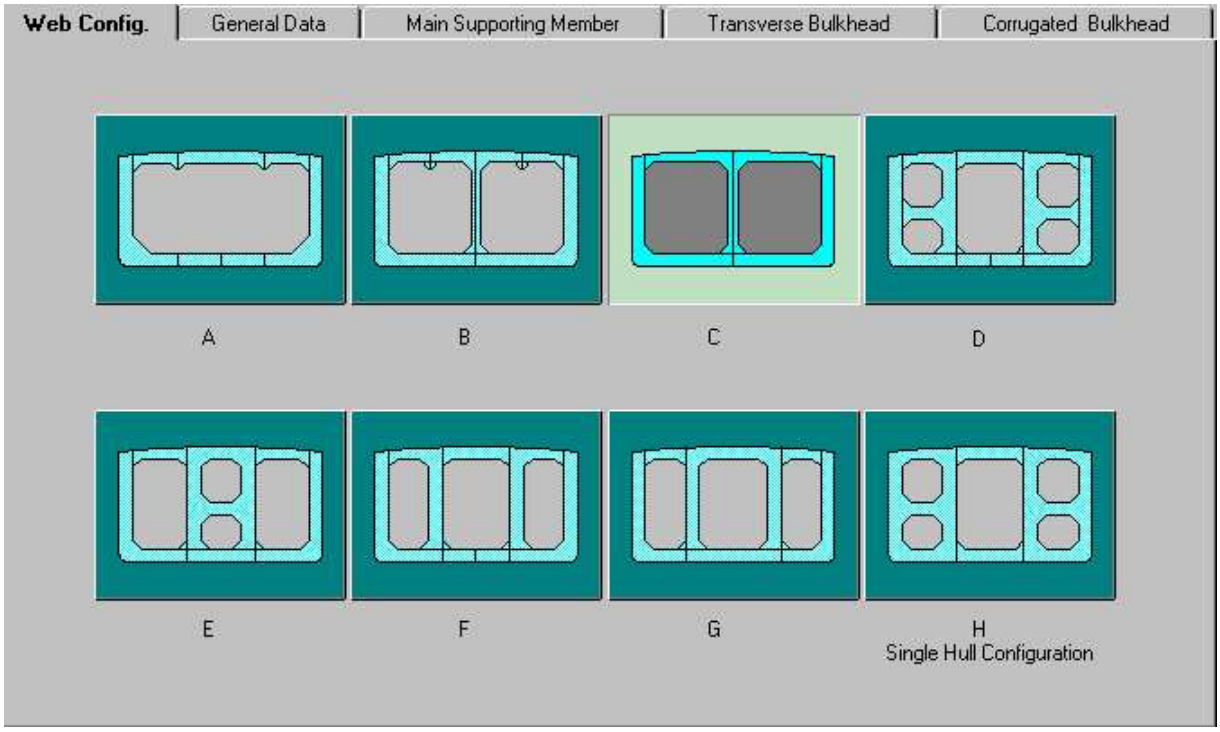
Web Config.
General Data
Main Supporting Member
Transverse Bulkhead
Corrugated Bulkhead
A
B
C
D
E
F
G
H
Single Hull Configuration


Spacing
Side Transverse (m) :
3.300
Deck Transverse (m) :
3.300
Vertical Web On Longitudinal Bulkhead (m) :
3.300

Main Supporting Members – Side Transverse (Web)

Transverse Member Description :

Side Transverse

No.	Bw(m)	Bh(m)	Mat.	Lib.ID	Cont
1L	1.600	2.150	MILD	25	
1U	2.500	2.500	MILD	24	

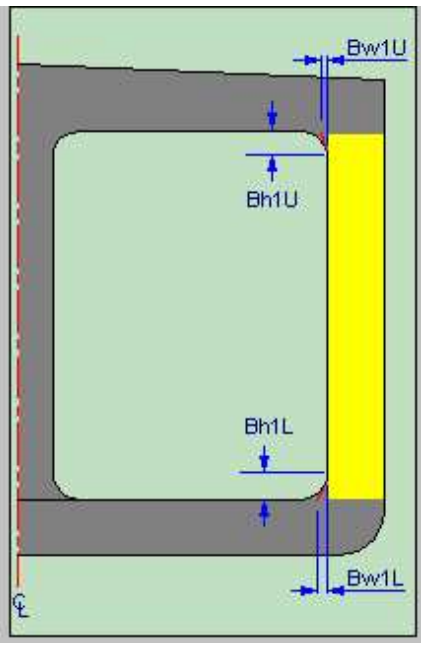

Web thickness upper = 12 mm
Web thickness lower = 18 mm
Main Supporting Members – Deck Transverse

Transverse Member Description :

Deck Transverse

No.	Bw(m)	Bh(m)	Mat.	Lib.ID	Width(mm)	Thick(mm)	Cont
2O	2.500	2.500	MILD	26	500.000	24.000	✖
2I	2.500	2.500	MILD	26	500.000	24.000	✖

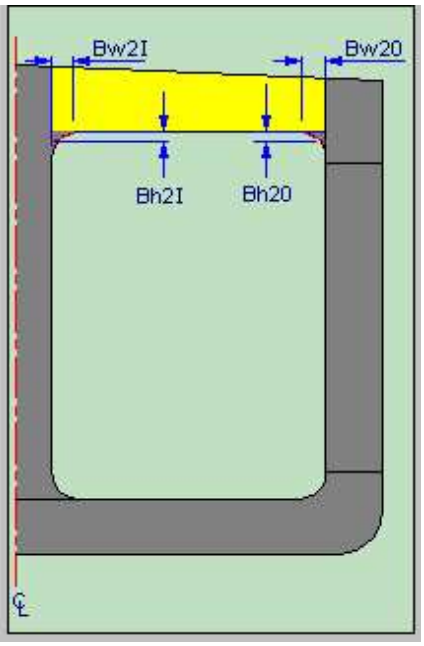

Deck Transverse Web thickness = 15 mm; Depth = 2.5 m

Main Supporting Members – Vertical Web on Longitudinal Bulkhead

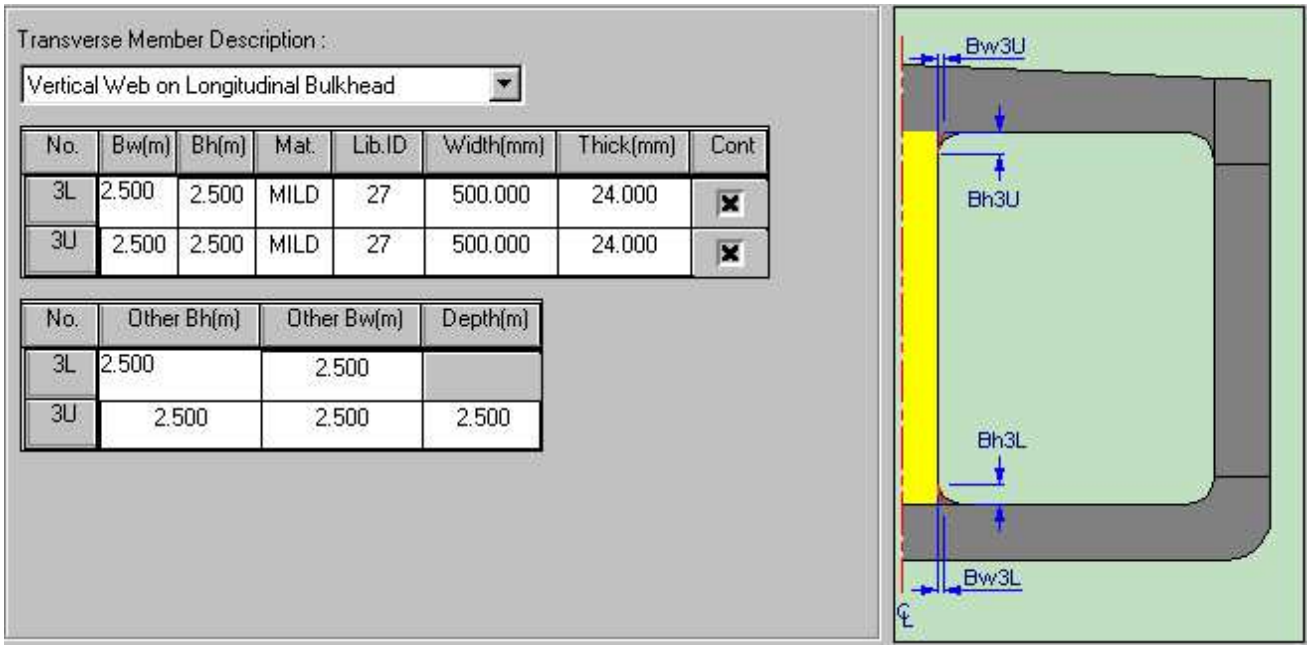

CL Bulkhead Vertical Web thickness = 14 mm; Depth = 2.0 m

Double Bottom Floor / Girder Properties

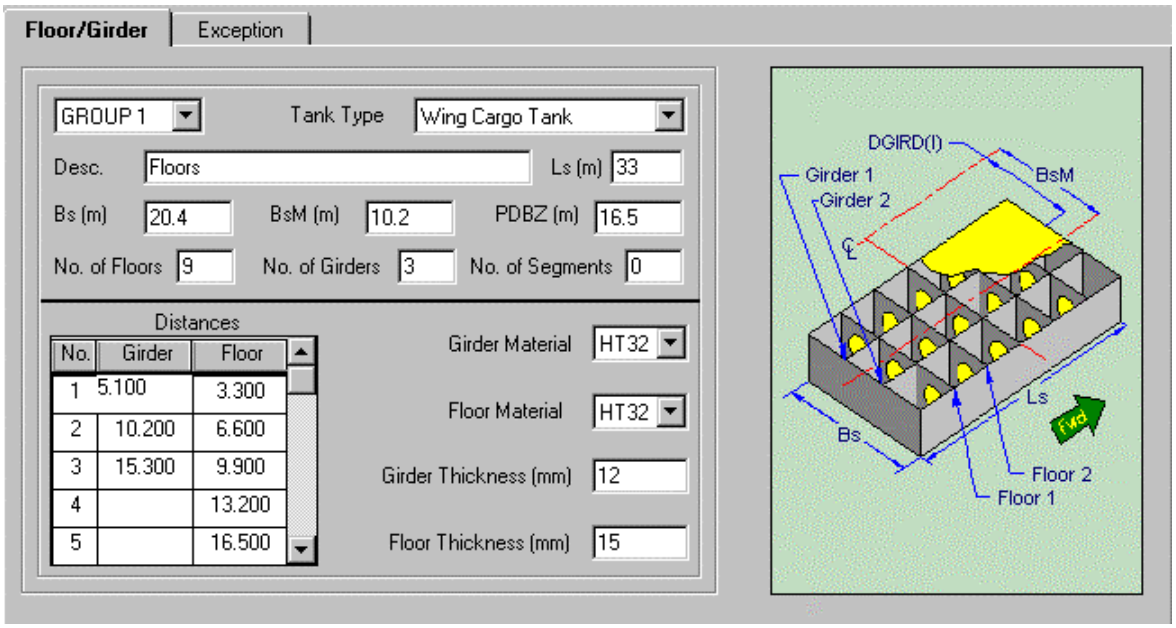

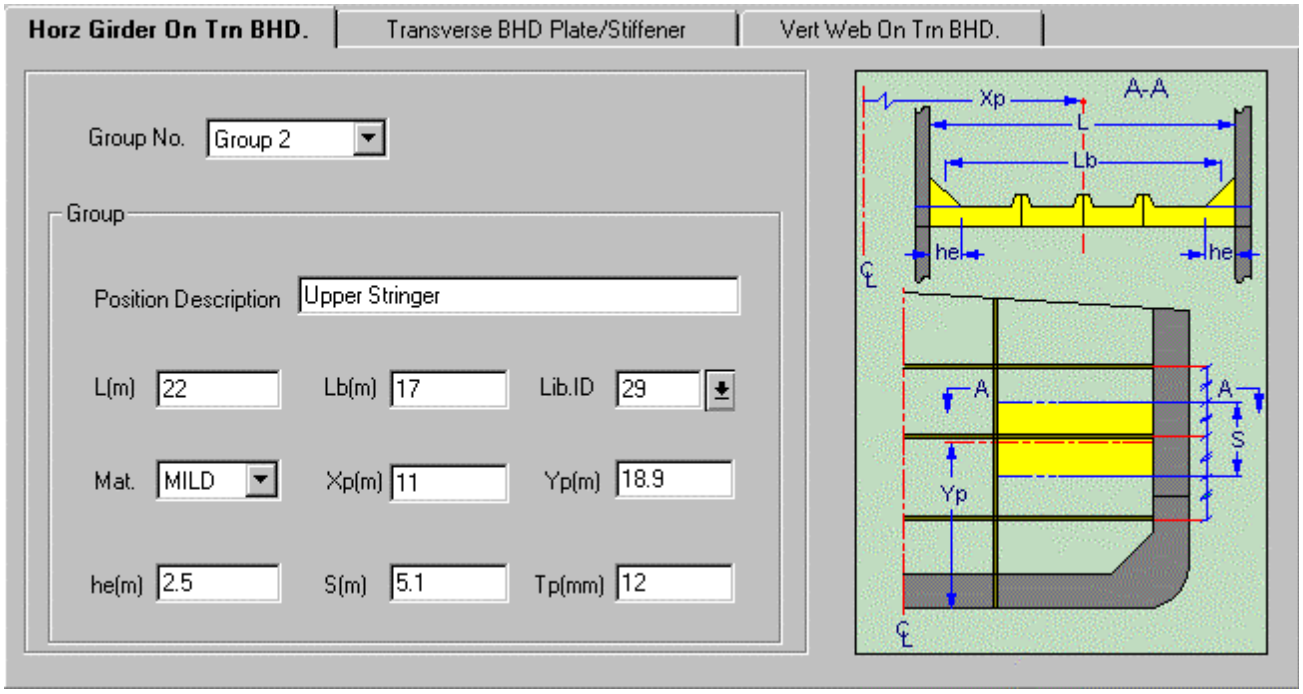
Horz Girder On Trn BHD.
Transverse BHD Plate/Stiffener
Vert Web On Trn BHD.
Group No.
Group 2
Group
Position Description
Upper Stringer
L(m)
22
Lb(m)
17
Lib.ID
29
Mat.
MILD
Xp(m)
11
Yp(m)
18.9
he(m)
2.5
S(m)
5.1
Tp(mm)
12
A-A
Xp
L
Lb
he
he
A
A
S
Yp

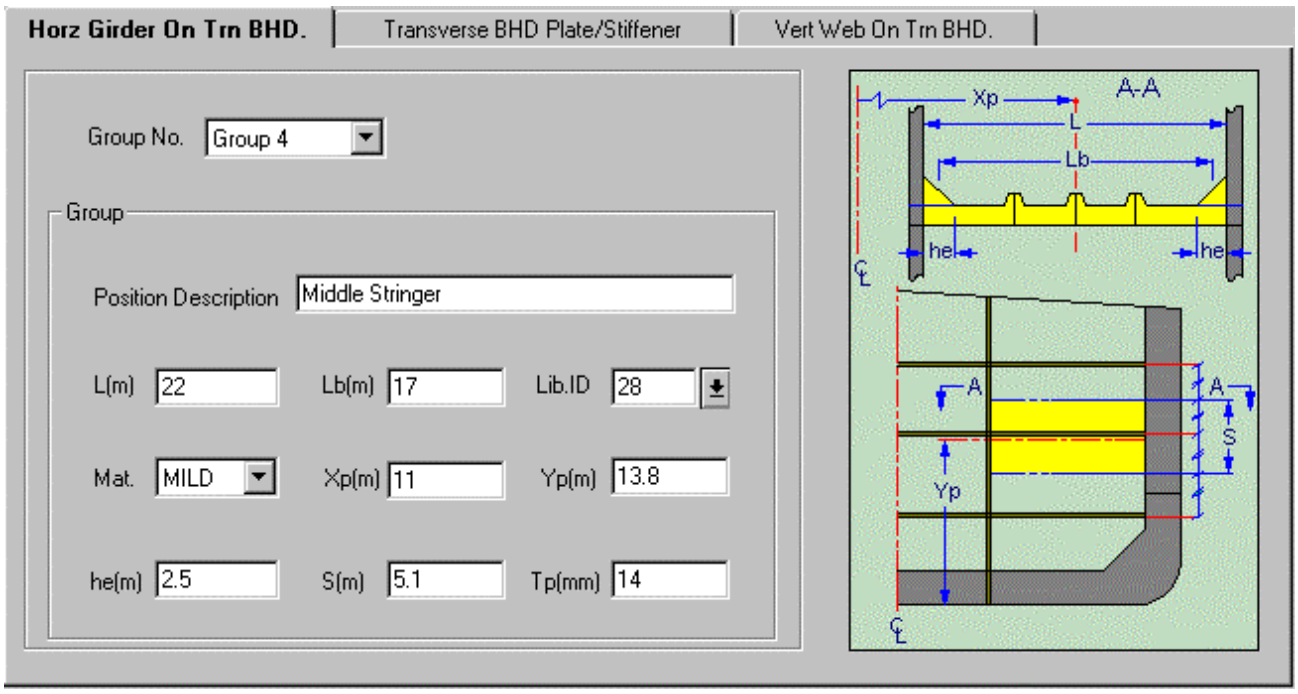
Horz Girder On Trn BHD.
Transverse BHD Plate/Stiffener
Vert Web On Trn BHD.
Group No.
Group 4
Group
Position Description
Middle Stringer
L(m)
22
Lb(m)
17
Lib.ID
28
Mat.
MILD
Xp(m)
11
Yp(m)
13.8
he(m)
2.5
S(m)
5.1
Tp(mm)
14
A-A
Xp
L
Lb
he
he
A
A
S
Yp

Horz Girder On Trn BHD. | Transverse BHD Plate/Stiffener | Vert Web On Trn BHD.

Group No. Group 1

Group

Position Description: Lower Stringer

L(m)	22	Lb(m)	17	Lib.ID	28
Mat.	MILD	Xp(m)	11	Yp(m)	8.7
he(m)	2.5	S(m)	4.675	Tp(mm)	18

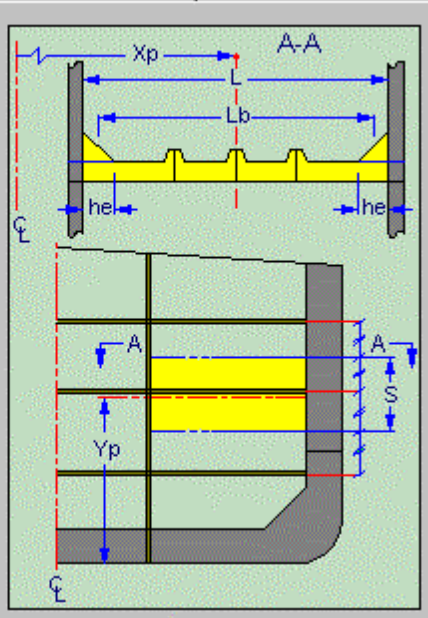

Horz Girder On Trn BHD. | Transverse BHD Plate/Stiffener | Vert Web On Trn BHD.

Group No. Group 3

Group

Position Description: Stool Level

L(m)	22	Lb(m)	17	Lib.ID	28
Mat.	MILD	Xp(m)	11	Yp(m)	4.45
he(m)	2.5	S(m)	3.2	Tp(mm)	18

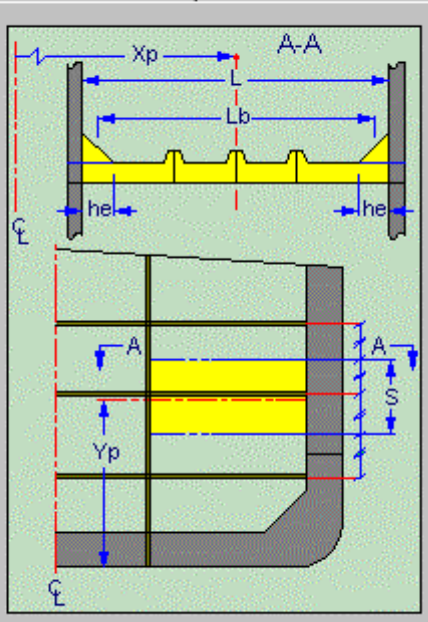

Horz Girder On Trn BHD. | **Transverse BHD Plate/Stiffener** | Vert Web On Trn BHD.

TB Group 1 | Tank Type: Wing Cargo Tank

Description: Upper | Xap (m): 152

Plate

Group: Plate 1 | Zp (m): 11 | SMax (mm): 850 | Yp (m): 18.9

Description: TB Upper | Thick.(mm): 12 | Mat: MILD

Stiffener

No.	Type	Sp(mm)	Sl(m)	ZStfp(m)	YStfp(m)	Lib.ID	Mat.
1	1	850.00	5.100	11.000	21.450	11	MILD
2							
3							
4							
5							

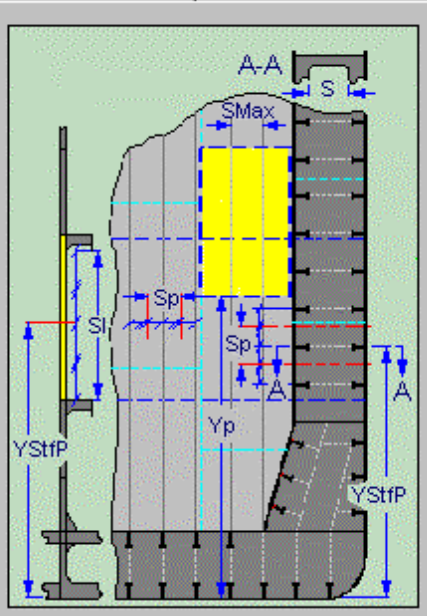

Horz Girder On Trn BHD. | **Transverse BHD Plate/Stiffener** | Vert Web On Trn BHD.

TB Group 2 | Tank Type: Wing Cargo Tank

Description: Middle | Xap (m): 152

Plate

Group: Plate 1 | Zp (m): 11 | SMax (mm): 850 | Yp (m): 13.8

Description: TB Middle | Thick.(mm): 14 | Mat: MILD

Stiffener

No.	Type	Sp(mm)	Sl(m)	ZStfp(m)	YStfp(m)	Lib.ID	Mat.
1	1	850.00	5.100	11.000	16.350	16	MILD
2							
3							
4							
5							

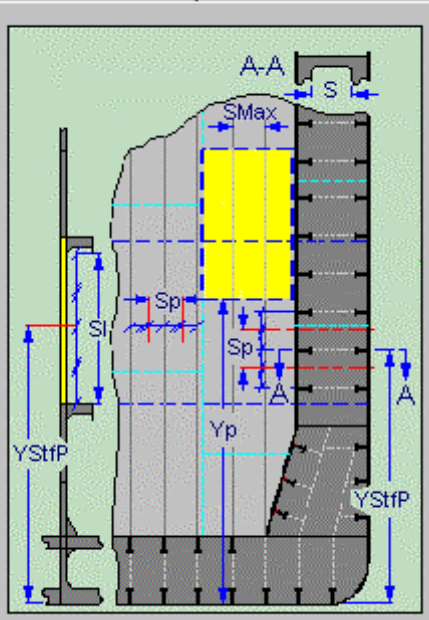

Horz Girder On Trn BHD. | **Transverse BHD Plate/Stiffener** | Vert Web On Trn BHD.

TB Group 3 | Tank Type: Wing Cargo Tank

Description: Lower | Xap (m): 152

Plate

Group: Plate 1 | Zp (m): 11 | SMax (mm): 850 | Yp (m): 8.7

Description: TB Lower | Thick.(mm): 16 | Mat: MILD

Stiffener

No.	Type	Sp(mm)	Sl(m)	ZStfp(m)	YStfp(m)	Lib.ID	Mat.
1	1	850.00	5.100	11.000	11.250	20	MILD
2							
3							
4							
5							

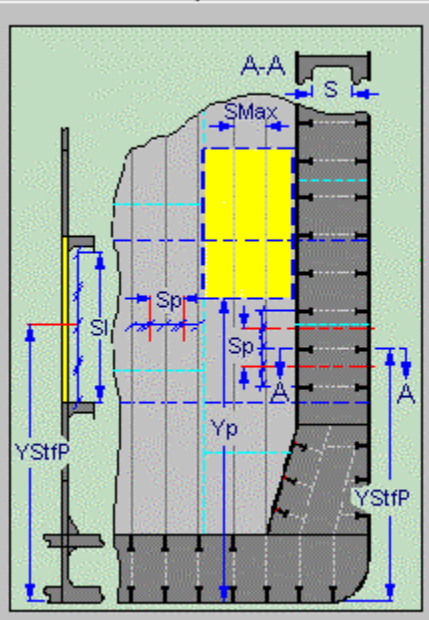

Horz Girder On Trn BHD. | **Transverse BHD Plate/Stiffener** | Vert Web On Trn BHD.

TB Group 4 | Tank Type: Wing Cargo Tank

Description: Stool | Xap (m): 152

Plate

Group: Plate 1 | Zp (m): 11 | SMax (mm): 850 | Yp (m): 4.45

Description: TB Stool | Thick.(mm): 18 | Mat: MILD

Stiffener

No.	Type	Sp(mm)	Sl(m)	ZStfp(m)	YStfp(m)	Lib.ID	Mat.
1	1	850.00	4.250	11.000	6.575	18	MILD
2							
3							
4							
5							

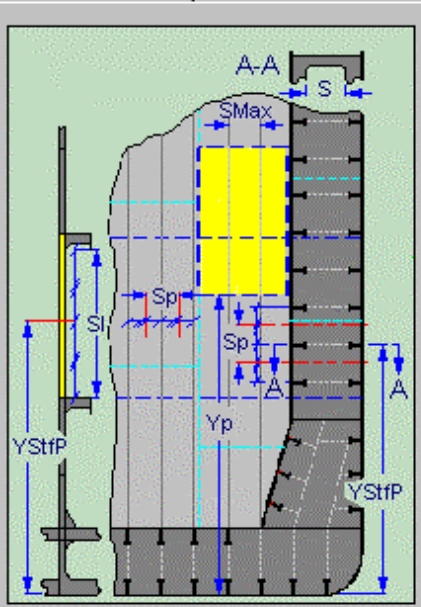

Horz Girder On Trn BHD. | **Transverse BHD Plate/Stiffener** | Vert Web On Trn BHD.

TB Group 8 | Tank Type: Wing Cargo Tank

Description: Bottom | Xap (m): 152

Plate

Group: Plate 1 | Zp (m): 11 | SMax (mm): 850 | Yp (m): 2.3

Description: TB Bottom | Thick.(mm): 18 | Mat: MILD

Stiffener

No.	Type	Sp(mm)	Sl(m)	ZStfp(m)	YStfp(m)	Lib.ID	Mat.
1	1	850.00	2.150	11.000	3.375	8	MILD
2							
3							
4							
5							

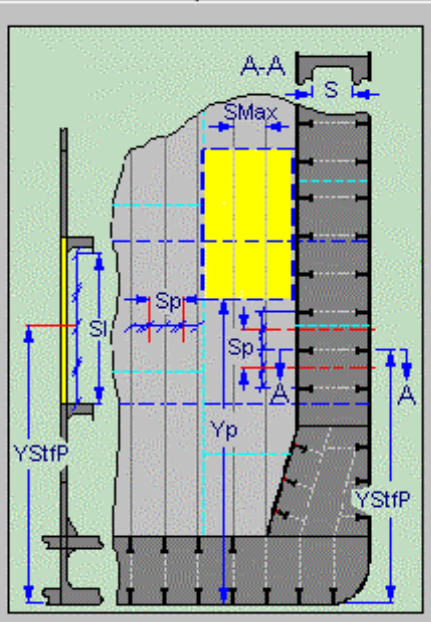

Horz Girder On Trn BHD. | **Transverse BHD Plate/Stiffener** | Vert Web On Trn BHD.

TB Group 5 | Tank Type: J Shape Ballast Tank

Description: Upper | Xap (m): 152

Plate

Group: Plate 1 | Zp (m): 23 | SMax (mm): 668 | Yp (m): 18.9

Description: J Tank TB Upper | Thick.(mm): 12 | Mat: MILD

Stiffener

No.	Type	Sp(mm)	Sl(m)	ZStfp(m)	YStfp(m)	Lib.ID	Mat.
1	1	668.00	5.100	23.000	21.450	10	MILD
2							
3							
4							
5							

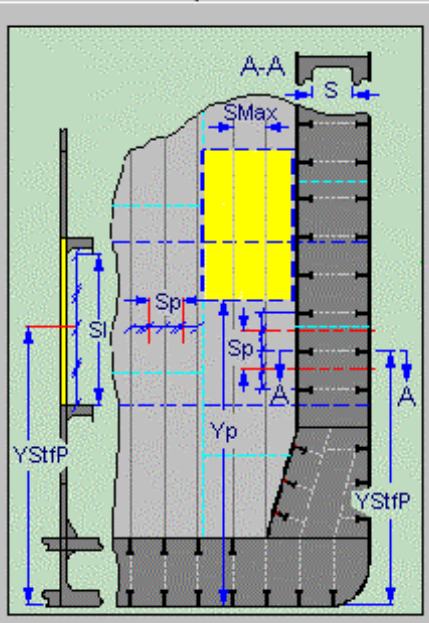

Horz Girder On Trn BHD. | **Transverse BHD Plate/Stiffener** | Vert Web On Trn BHD.

TB Group 6 | Tank Type: J Shape Ballast Tank

Description: Middle | Xap (m): 152

Plate

Group: Plate 1 | Zp (m): 23 | SMax (mm): 668 | Yp (m): 13.8

Description: J Tank TB Middle | Thick.(mm): 12 | Mat: MILD

Stiffener

No.	Type	Sp(mm)	Sl(m)	ZStfp(m)	YStfp(m)	Lib.ID	Mat.
1	1	668.00	5.100	11.000	16.350	14	MILD
2							
3							
4							
5							

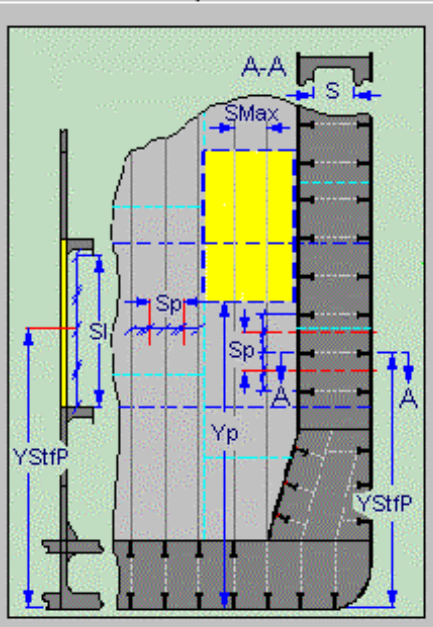

Horz Girder On Trn BHD. | **Transverse BHD Plate/Stiffener** | Vert Web On Trn BHD.

TB Group 7 | Tank Type: J Shape Ballast Tank

Description: Lower | Xap (m): 152

Plate

Group: Plate 1 | Zp (m): 23 | SMax (mm): 668 | Yp (m): 8.7

Description: J Tank TB Lower | Thick.(mm): 14 | Mat: MILD

Stiffener

No.	Type	Sp(mm)	Sl(m)	ZStfp(m)	YStfp(m)	Lib.ID	Mat.
1	1	668.00	5.100	23.000	11.250	17	MILD
2							
3							
4							
5							

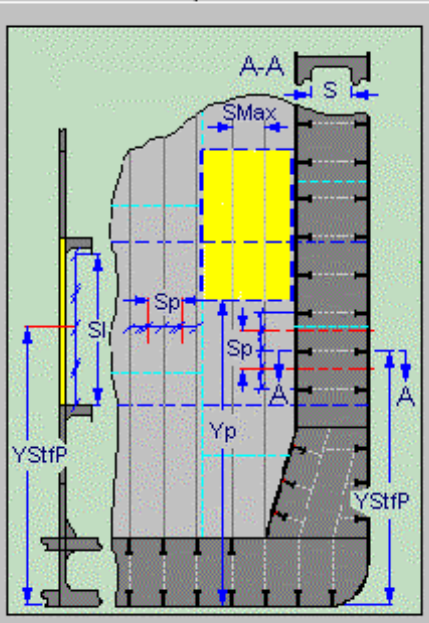

Horz Girder On Trn BHD. | **Transverse BHD Plate/Stiffener** | Vert Web On Trn BHD.

TB Group 9 | Tank Type: J Shape Ballast Tank

Description: Stool | Xap (m): 152

Plate

Group: Plate 1 | Zp (m): 23 | SMax (mm): 668 | Yp (m): 4.45

Description: J tank TB Stool | Thick.(mm): 14 | Mat: MILD

Stiffener

No.	Type	Sp(mm)	Sl(m)	ZStfp(m)	YStfp(m)	Lib.ID	Mat.
1	1	668.00	4.250	23.000	6.575	16	MILD
2							
3							
4							
5							

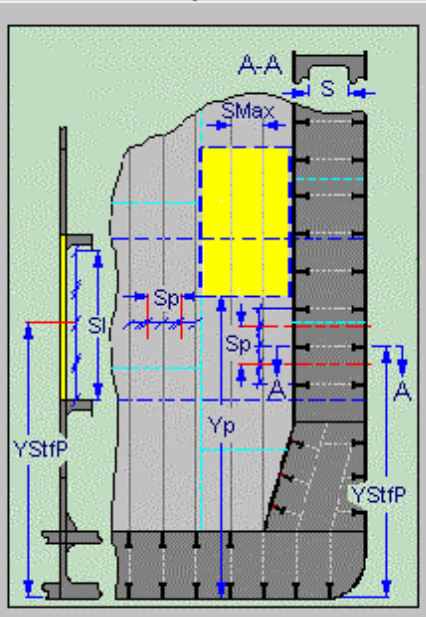

Horz Girder On Trn BHD. | **Transverse BHD Plate/Stiffener** | Vert Web On Trn BHD.

TB Group 10 | Tank Type: J Shape Ballast Tank

Description: IB | Xap (m): 152

Plate

Group: Plate 1 | Zp (m): 12 | SMax (mm): 850 | Yp (m): 0

Description: TB IB | Thick.(mm): 20 | Mat: MILD

Stiffener

No.	Type	Sp(mm)	Sl(m)	ZStfp(m)	YStfp(m)	Lib.ID	Mat.
1	1	850.00	2.300	12.000	1.150	9	MILD
2							
3							
4							
5							

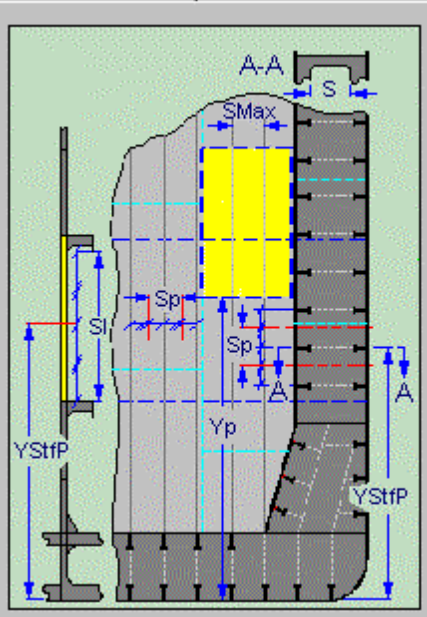

Material

Material Zones:

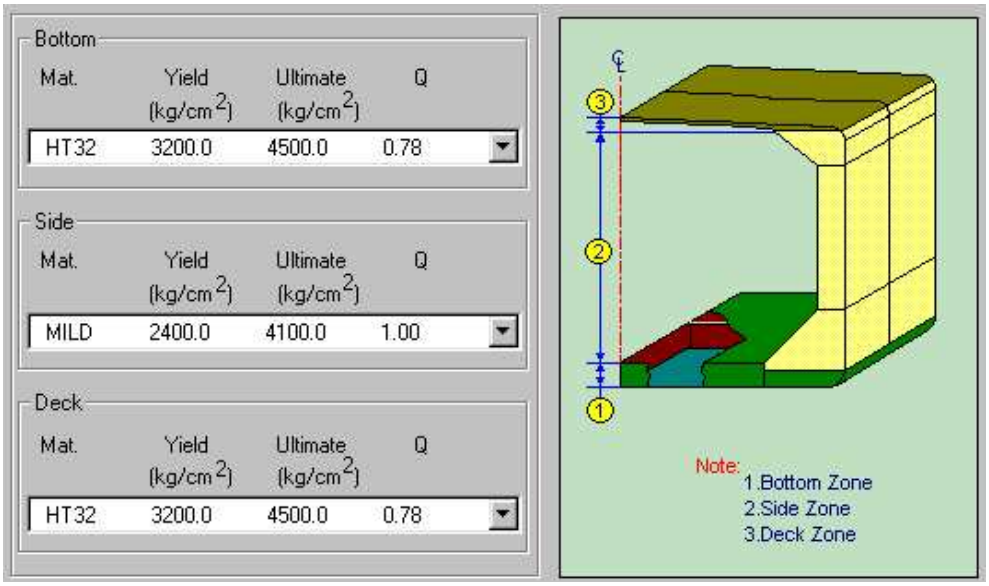

MATERIAL TABLE

==========

MAT #	MAT ID	YIELD STRESS	ULT STRESS	Q-FAC	Sm
(kgf/cm2)	(kgf/cm2)				
1	MILD	2400.	4100.	1.000	1.0
2	HT32	3200.	4500.	.780	.950
3	HT36	3600.	5000.	.720	.908
4	HT40	4000.	5200.	.680	.875

Stiffener Library:

#ID#	TYPE	ABS ID	DESCRIPTION	VAR 1	VAR 2	VAR 3	VAR 4	VAR 5	VAR 6
#(dimensions)				(mm)	(mm)	(mm)	(mm)	(mm)	(mm)
1	LANG	ILA200A	200x90x9x12 LIA	200.00	90.00	9.00	12.00	7.50	15.00
2	LANG	ILA225A	225x90x9x12 LIA	225.00	90.00	9.00	12.00	7.50	15.00
3	LANG	ILA250A	250x90x9x13 LIA	250.00	90.00	9.00	13.00	7.50	15.00
4	LANG	ILA250B	250x90x10.5x15 LIA	250.00	90.00	10.50	15.00	7.50	15.00
5	LANG	ILA250C	250x90x11.5x16 LIA	250.00	90.00	11.50	16.00	7.50	15.00
6	LANG	ILA275A	250x100x10.5x14 LIA	275.00	100.00	10.50	14.00	7.50	15.00
7	LANG	ILA300A	300x100x10.5x15 LIA	300.00	100.00	10.50	15.00	7.50	15.00
8	LANG	ILA300B	300x100x11.5x16 LIA	300.00	100.00	11.50	16.00	7.50	15.00
9	LANG	ILA325A	325x120x10.5x14 LIA	325.00	120.00	10.50	14.00	10.00	20.00
10	LANG	ILA325B	325x120x11.5x15 LIA	325.00	120.00	11.50	15.00	10.00	20.00
11	LANG	ILA350A	350x120x10.5x16 LIA	350.00	120.00	10.50	16.00	10.00	20.00

```
12    LANG ILA350B  350x120x11.5x18 LIA             350.00   120.00    11.50    18.00    10.00
20.00
13    LANG ILA375A  375x120x10.5x18 LIA             375.00   120.00    10.50    18.00    10.00
20.00
14    LANG ILA375B  375x120x11.5x20 LIA             375.00   120.00    11.50    20.00    10.00
20.00
15    LANG ILA400A  400x120x11.5x23 LIA             400.00   120.00    11.50    23.00    10.00
20.00
16    LANG ILA425A  425x120x11.5x24 LIA             425.00   120.00    11.50    24.00    10.00
20.00
17    LANG ILA450A  450x120x11.5x25 LIA             450.00   120.00    11.50    25.00    10.00
20.00
18    LANG ILA475A  475x120x11.5x28 LIA             475.00   120.00    11.50    28.00    10.00
20.00
19    LANG ILA475B  475x120x12.5x30 LIA             475.00   120.00    12.50    30.00    10.00
20.00
20    LANG ILA500A  500x120x12.5x33 LIA             500.00   120.00    12.50    33.00    10.00
20.00
21    LANG ILA500B  500x120x13.5x35 LIA             500.00   120.00    13.50    35.00    10.00
20.00
22    FLAT USER-DEF FB 400x28                      400.00    28.00
23    UANG IUA150G  150X90X15 UIA                  150.00    90.00    15.00    15.00     6.00
12.00
24    FLAT USER-DEF FB2000X12                     2000.00    12.00
25    FLAT USER-DEF FB2000X18                     2000.00    18.00
26    MSTF USER-DEF DECK WEB                            3
27    MSTF USER-DEF LBHD WEB                            7
28    MSTF USER-DEF BHD L STR                           4
29    MSTF USER-DEF BHD U STR                           4
```

User-Defined Shapes / Webs:

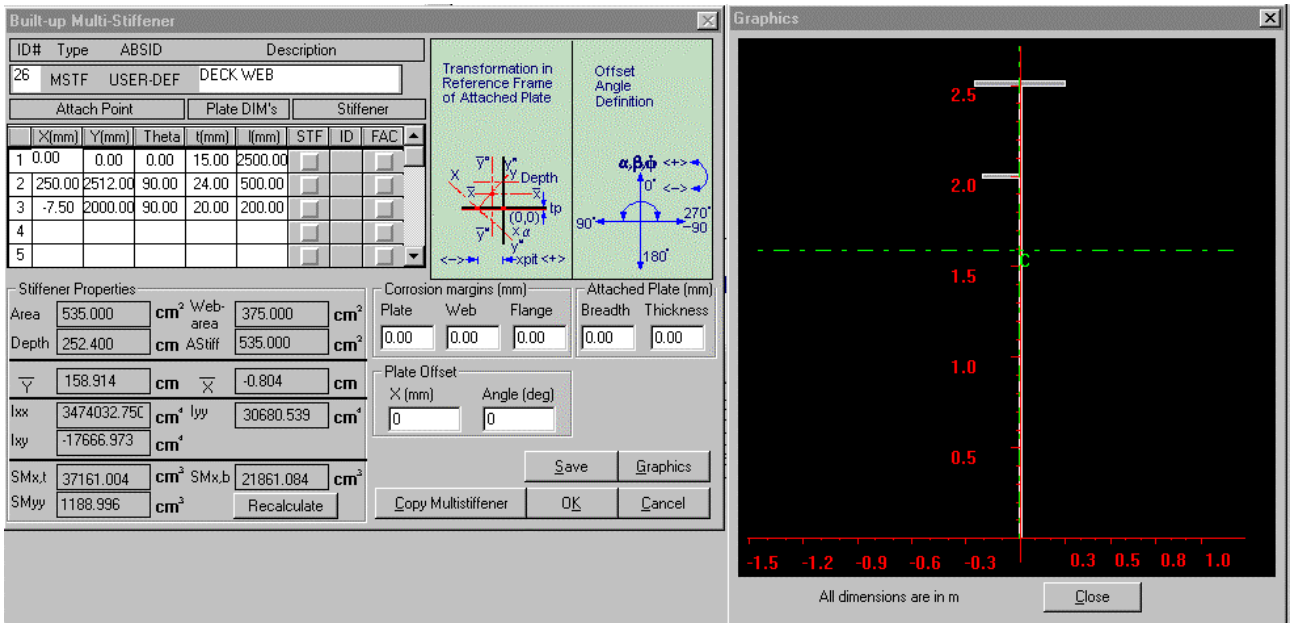

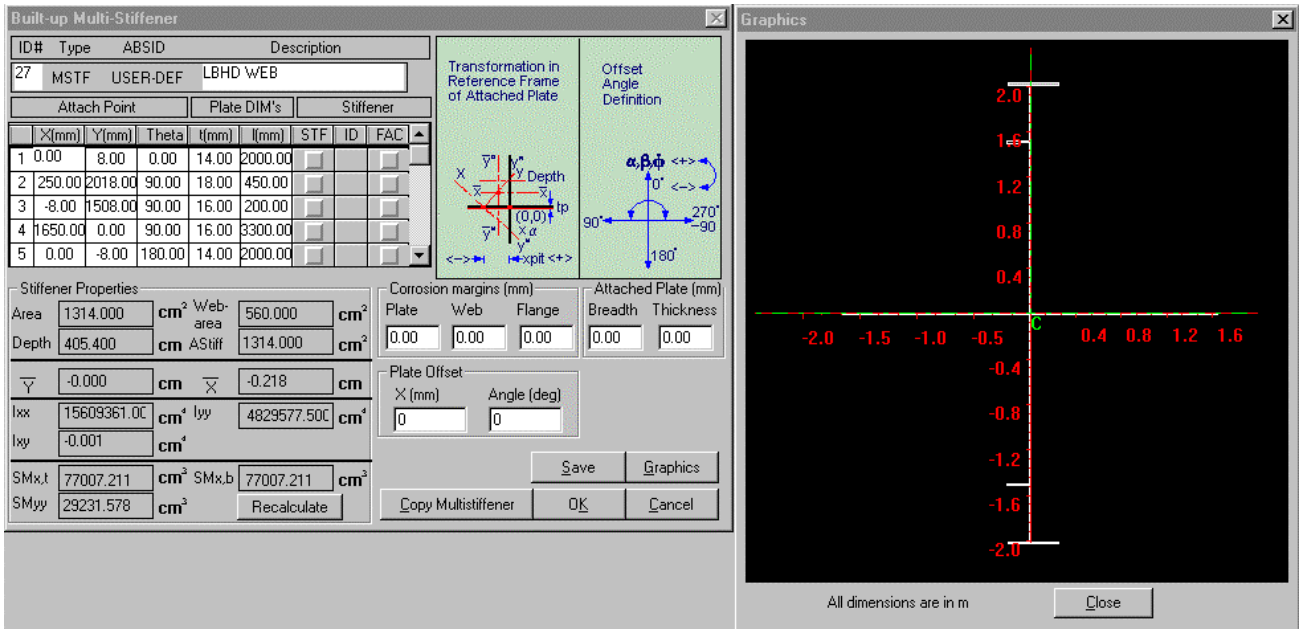

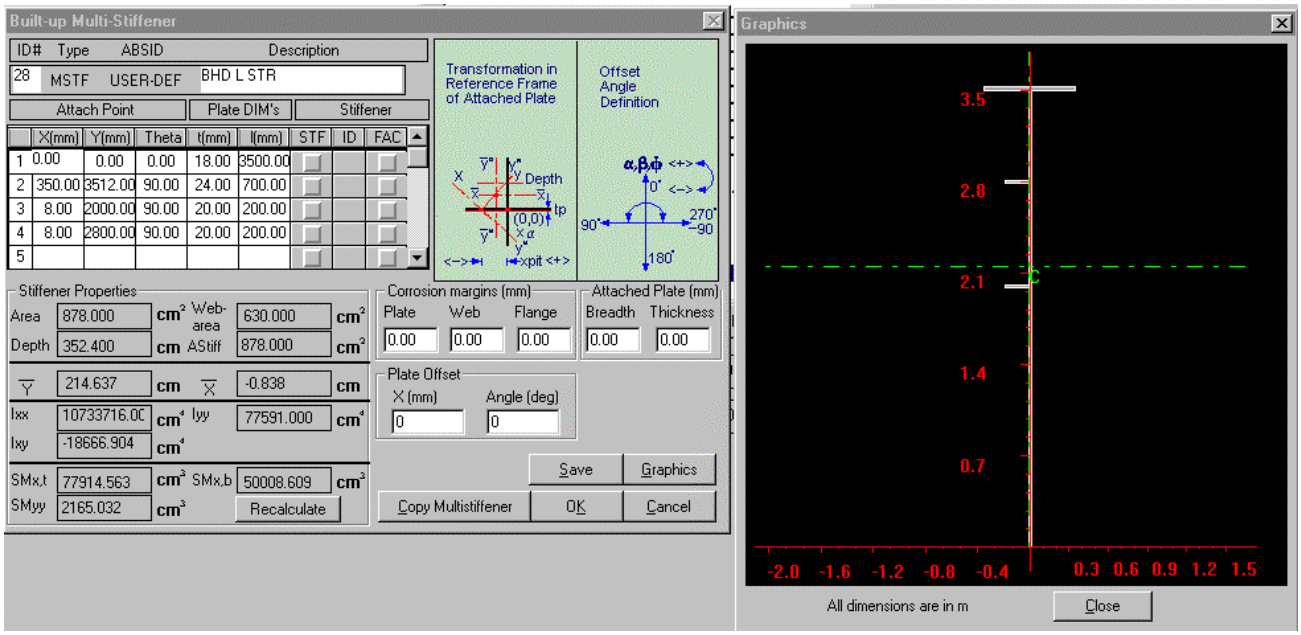
Built-up Multi-Stiffener
ID# Type ABSID Description
28 MSTF USER-DEF BHD L STR
Attach Point
Plate DIM's
Stiffener
X(mm) Y(mm) Theta t(mm) l(mm) STF ID FAC
1 0.00 0.00 0.00 18.00 3500.00
2 350.00 3512.00 90.00 24.00 700.00
3 8.00 2000.00 90.00 20.00 200.00
4 8.00 2800.00 90.00 20.00 200.00
5
Transformation in Reference Frame of Attached Plate
Offset Angle Definition
Depth
tp
(0,0)
xpit
α,β,ϕ
0°
90°
270°
-90
180°
Stiffener Properties
Area 878.000 cm² Web-area 630.000 cm²
Depth 352.400 cm AStiff 878.000 cm²
214.637 cm -0.838 cm
Ixx 10733716.00 cm⁴ Iyy 77591.000 cm⁴
Ixy -18666.904 cm⁴
SMx,t 77914.563 cm³ SMx,b 50008.609 cm³
SMyy 2165.032 cm³
Recalculate
Corrosion margins (mm)
Plate Web Flange
0.00 0.00 0.00
Attached Plate (mm)
Breadth Thickness
0.00 0.00
Plate Offset
X (mm) Angle (deg)
0 0
Save Graphics
Copy Multistiffener OK Cancel
Graphics
3.5
2.8
2.1
1.4
0.7
-2.0 -1.6 -1.2 -0.8 -0.4
0.3 0.6 0.9 1.2 1.5
All dimensions are in m
Close

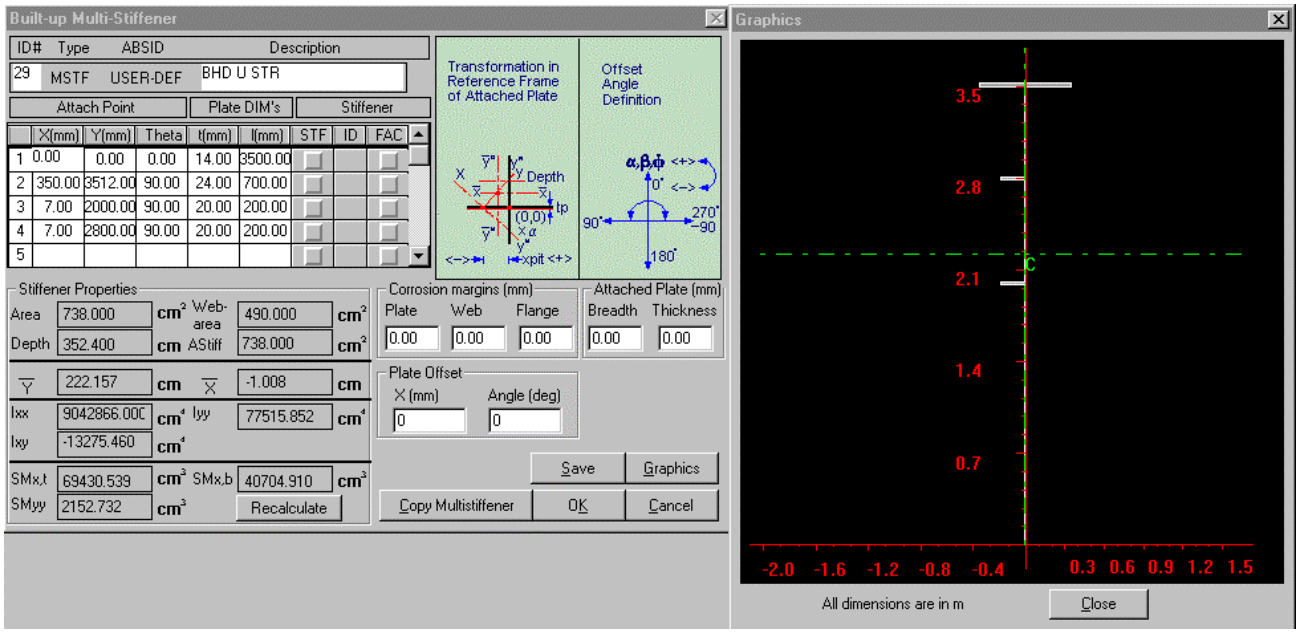
Built-up Multi-Stiffener
ID# Type ABSID Description
29 MSTF USER-DEF BHD U STR
Attach Point
Plate DIM's
Stiffener
X(mm) Y(mm) Theta t(mm) l(mm) STF ID FAC
1 0.00 0.00 0.00 14.00 3500.00
2 350.00 3512.00 90.00 24.00 700.00
3 7.00 2000.00 90.00 20.00 200.00
4 7.00 2800.00 90.00 20.00 200.00
5
Transformation in Reference Frame of Attached Plate
Offset Angle Definition
Depth
tp
(0,0)
xpit
α,β,ϕ
0°
90°
270°
-90
180°
Stiffener Properties
Area 738.000 cm² Web-area 490.000 cm²
Depth 352.400 cm AStiff 738.000 cm²
222.157 cm -1.008 cm
Ixx 9042866.000 cm⁴ Iyy 77515.852 cm⁴
Ixy -13275.460 cm⁴
SMx,t 69430.539 cm³ SMx,b 40704.910 cm³
SMyy 2152.732 cm³
Recalculate
Corrosion margins (mm)
Plate Web Flange
0.00 0.00 0.00
Attached Plate (mm)
Breadth Thickness
0.00 0.00
Plate Offset
X (mm) Angle (deg)
0 0
Save Graphics
Copy Multistiffener OK Cancel
Graphics
3.5
2.8
2.1
1.4
0.7
-2.0 -1.6 -1.2 -0.8 -0.4
0.3 0.6 0.9 1.2 1.5
All dimensions are in m
Close

Longitudinal Plate and Stiffener Elements

Local Plate IDs:

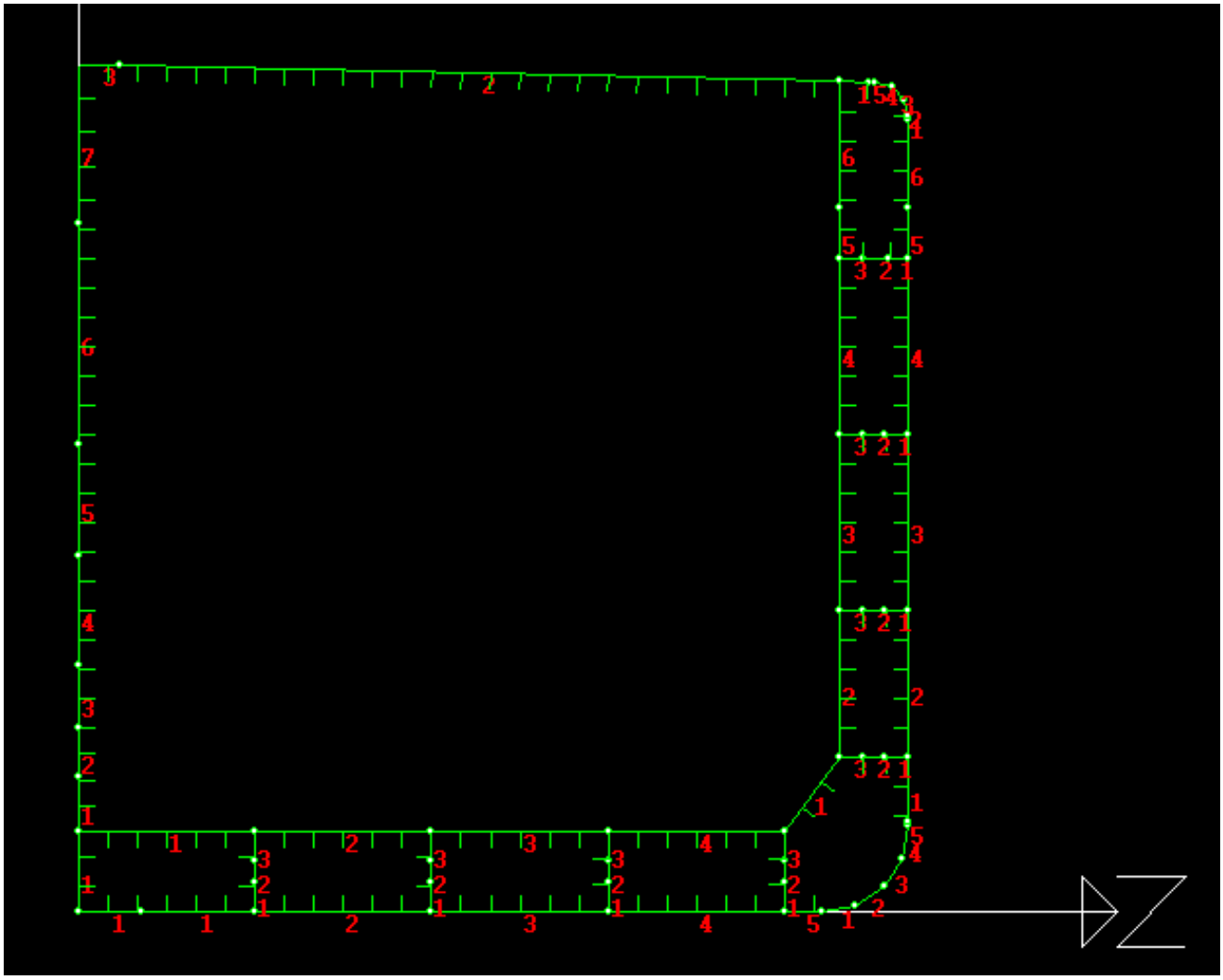

Global Plate Ids:

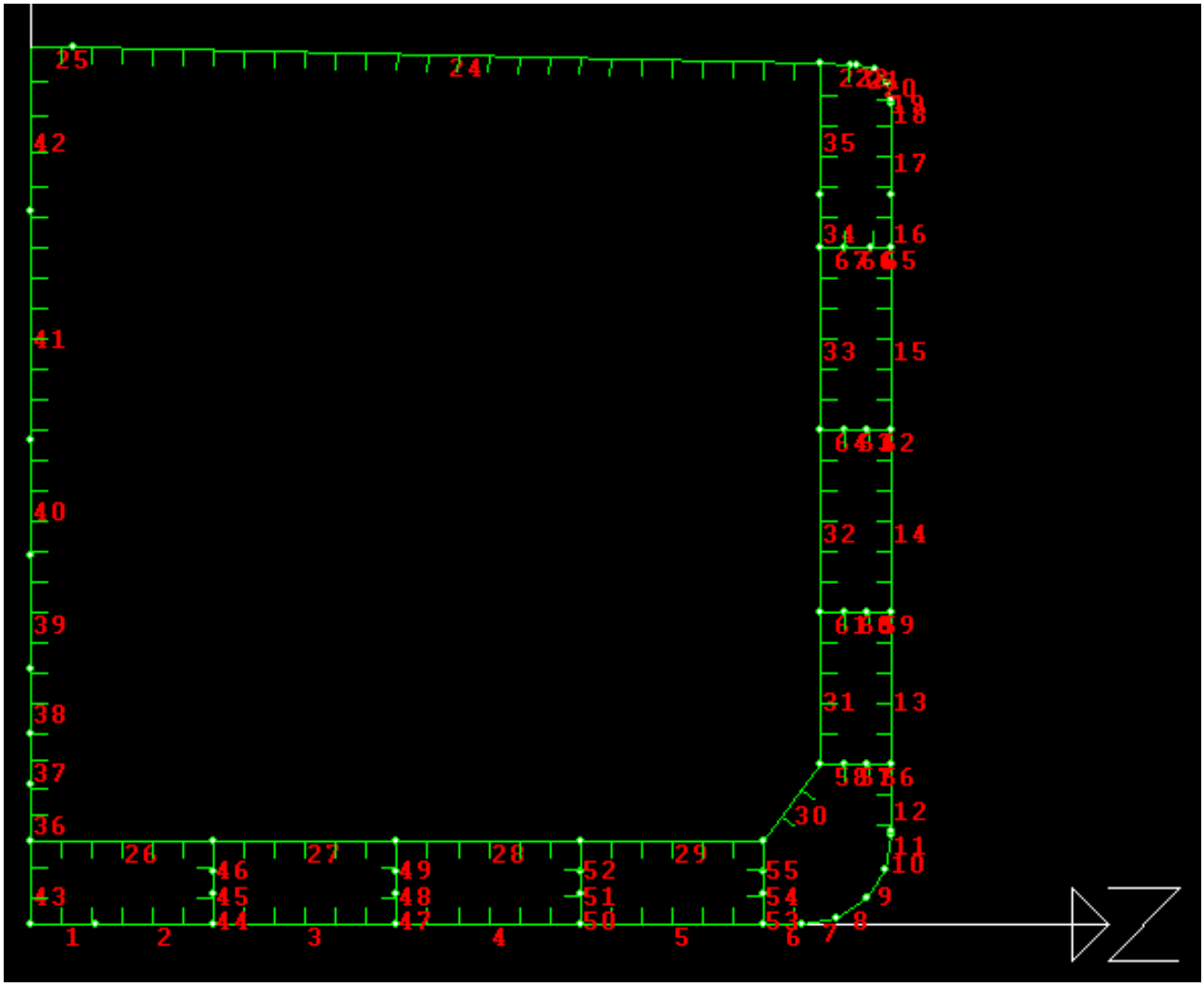

Plate:

SEQ NO	ID	DESCRIPTION	B m	THK cm	CORROSION (mm)	A cm2	SPACING (m)	MATID	START X-COORD (METER)	NODE Y-COORD (METER)	END NODE X-COORD (METER)	Y-COORD (METER)
1	KPL-01	KEEL PLATE	1.8	1.9	1	342	0.85	2	0	0	1.8	0
2	BTM-01	BOTTOM	3.3	1.7	1	561	0.85	2	1.8	0	5.1	0
3	BTM-02	BOTTOM	5.1	1.7	1	867	0.85	2	5.1	0	10.2	0
4	BTM-03	BOTTOM	5.1	1.7	1	867	0.85	2	10.2	0	15.3	0
5	BTM-04	BOTTOM	5.1	1.7	1	867	0.85	2	15.3	0	20.4	0
6	BTM-05	BOTTOM	1.1	1.7	1	187	0.85	2	20.4	0	21.5	0
7	BLG-01	BILGE	0.976	1.7	1	165.87	2.201	2	21.5	0	22.457	0.19
8	BLG-02	BILGE	0.975	1.7	1	165.82	2.927	2	22.457	0.19	23.268	0.732
9	BLG-03	BILGE	0.975	1.7	1	165.82	2.927	2	23.268	0.732	23.81	1.543
10	BLG-04	BILGE	0.976	1.7	1	165.87	2.201	2	23.81	1.543	24	2.5
11	BLG-05	BILGE	0.1	1.7	1	17	1.226	2	24	2.5	24	2.6
12	SHL-01	SIDE	1.85	1.7	1.5	314.5	0.85	2	24	2.6	24	4.45
13	SHL-02	SIDE	4.25	1.8	1.5	765	0.85	1	24	4.45	24	8.7
14	SHL-03	SIDE	5.1	1.8	1.5	918	0.85	1	24	8.7	24	13.8
15	SHL-04	SIDE	5.1	1.8	1.5	918	0.85	1	24	13.8	24	18.9
16	SHL-05	SIDE	1.45	1.8	1.5	261	0.85	1	24	18.9	24	20.35
17	SHL-06	SIDE	2.55	2	1.5	510	0.85	2	24	20.35	24	22.9
18	GWR-01	GUNWALE	0.1	2	2	20	0.7	2	24	22.9	24	23
19	GWR-02	GUNWALE	0.518	2	2	103.53	0.518	2	24	23	23.866	23.5
20	GWR-03	GUNWALE	0.518	2	2	103.52	0.518	2	23.866	23.5	23.5	23.866
21	GWR-04	GUNWALE	0.518	2	2	103.53	0.718	2	23.5	23.866	23	24
22	GWR-05	GUNWALE	0.15	2	2	30.01	0.718	2	23	24	22.85	24.003
23	DEC-01	UPPER DECK	0.85	2	2	170.05	0.8	2	22.85	24.003	22	24.023
24	DEC-02	UPPER DECK	20.805	1.9	1	3953.04	0.855	2	22	24.023	1.2	24.5
25	DEC-03	UPPER DECK	1.2	1.9	1	228	0.855	2	1.2	24.5	0	24.5
26	INB-01	INNER BOTTOM	5.1	1.7	1.5	867	0.85	2	0	2.3	5.1	2.3
27	INB-02	INNER BOTTOM	5.1	1.7	1.5	867	0.85	2	5.1	2.3	10.2	2.3
28	INB-03	INNER BOTTOM	5.1	1.7	1.5	867	0.85	2	10.2	2.3	15.3	2.3
29	INB-04	INNER BOTTOM	5.1	1.7	1.5	867	0.85	2	15.3	2.3	20.4	2.3
30	INS-01	I.S. BULKHEAD	2.68	2	1.5	536	0.9	2	20.4	2.3	22	4.45
31	INS-02	I.S. BULKHEAD	4.25	1.8	1.5	765	0.85	2	22	4.45	22	8.7
32	INS-03	I.S. BULKHEAD	5.1	1.9	1.5	969	0.85	1	22	8.7	22	13.8
33	INS-04	I.S. BULKHEAD	5.1	1.6	1.5	816	0.85	1	22	13.8	22	18.9
34	INS-05	I.S. BULKHEAD	1.45	1.65	1.5	239.25	0.85	1	22	18.9	22	20.35
35	INS-06	I.S. BULKHEAD	3.673	1.8	1.5	661.14	0.873	2	22	20.35	22	24.023
36	CTR-01	C.L. BULKHEAD	1.6	1.6	1	128	0.75	2	0	2.3	0	3.9
37	CTR-02	C.L. BULKHEAD	1.4	1.65	1	115.5	0.75	1	0	3.9	0	5.3
38	CTR-03	C.L. BULKHEAD	1.8	1.65	1	148.5	0.85	1	0	5.3	0	7.1
39	CTR-04	C.L. BULKHEAD	3.2	1.6	1	256	0.85	1	0	7.1	0	10.3
40	CTR-05	C.L. BULKHEAD	3.2	1.5	1	240	0.85	1	0	10.3	0	13.5
41	CTR-06	C.L. BULKHEAD	6.4	1.5	1	480	0.85	1	0	13.5	0	19.9
42	CTR-07	C.L. BULKHEAD	4.6	1.8	1	414	0.975	2	0	19.9	0	24.5
43	BGR-01	W.T.BTM.GIRDER	2.3	1.8	2	207	0.8	2	0	0	0	2.3
44	NBG-01	N-TIGHT B. GDR	0.85	1.4	2	119	0.8	2	5.1	0	5.1	0.85
45	NBG-02	N-TIGHT B. GDR	0.6	0	2	0	0.8	2	5.1	0.85	5.1	1.45
46	NBG-03	N-TIGHT B. GDR	0.85	1.4	2	119	0.8	2	5.1	1.45	5.1	2.3
47	NBG-04	N-TIGHT B. GDR	0.85	1.4	2	119	0.8	2	10.2	0	10.2	0.85

48	NBG-05	N-TIGHT B. GDR	0.6	0	2	0	0.8	2	10.2	0.85	10.2	1.45
49	NBG-06	N-TIGHT B. GDR	0.85	1.4	2	119	0.8	2	10.2	1.45	10.2	2.3
50	NBG-07	N-TIGHT B. GDR	0.85	1.5	2	127.5	0.8	2	15.3	0	15.3	0.85
51	NBG-08	N-TIGHT B. GDR	0.6	0	2	0	0.7	2	15.3	0.85	15.3	1.45
52	NBG-09	N-TIGHT B. GDR	0.85	1.5	2	127.5	0.8	2	15.3	1.45	15.3	2.3
53	NBG-10	N-TIGHT B. GDR	0.85	1.5	2	127.5	0.8	2	20.4	0	20.4	0.85
54	NBG-11	N-TIGHT B. GDR	0.6	0	2	0	0.7	2	20.4	0.85	20.4	1.45
55	NBG-12	N-TIGHT B. GDR	0.85	1.5	2	127.5	0.8	2	20.4	1.45	20.4	2.3
56	NTS-01	NON-TIGHT STR	0.7	1.2	2	84	0.7	1	24	4.45	23.3	4.45
57	NTS-02	NON-TIGHT STR	0.6	0	2	0	0.7	1	23.3	4.45	22.7	4.45
58	NTS-03	NON-TIGHT STR	0.7	1.2	2	84	0.7	1	22.7	4.45	22	4.45
59	NTS-04	NON-TIGHT STR	0.7	1.2	2	84	0.7	1	24	8.7	23.3	8.7
60	NTS-05	NON-TIGHT STR	0.6	0	2	0	0.7	1	23.3	8.7	22.7	8.7
61	NTS-06	NON-TIGHT STR	0.7	1.2	2	84	0.7	1	22.7	8.7	22	8.7
62	NTS-07	NON-TIGHT STR	0.7	1.2	2	84	0.7	1	24	13.8	23.3	13.8
63	NTS-08	NON-TIGHT STR	0.6	0	2	0	0.7	1	23.3	13.8	22.7	13.8
64	NTS-09	NON-TIGHT STR	0.7	1.2	2	84	0.7	1	22.7	13.8	22	13.8
65	NTS-10	NON-TIGHT STR	0.6	1.2	2	72	0.8	1	24	18.9	23.4	18.9
66	NTS-11	NON-TIGHT STR	0.7	0	2	0	0.8	1	23.4	18.9	22.7	18.9
67	NTS-12	NON-TIGHT STR	0.7	1.2	2	84	0.8	1	22.7	18.9	22	18.9

Local Stiffener Ids:

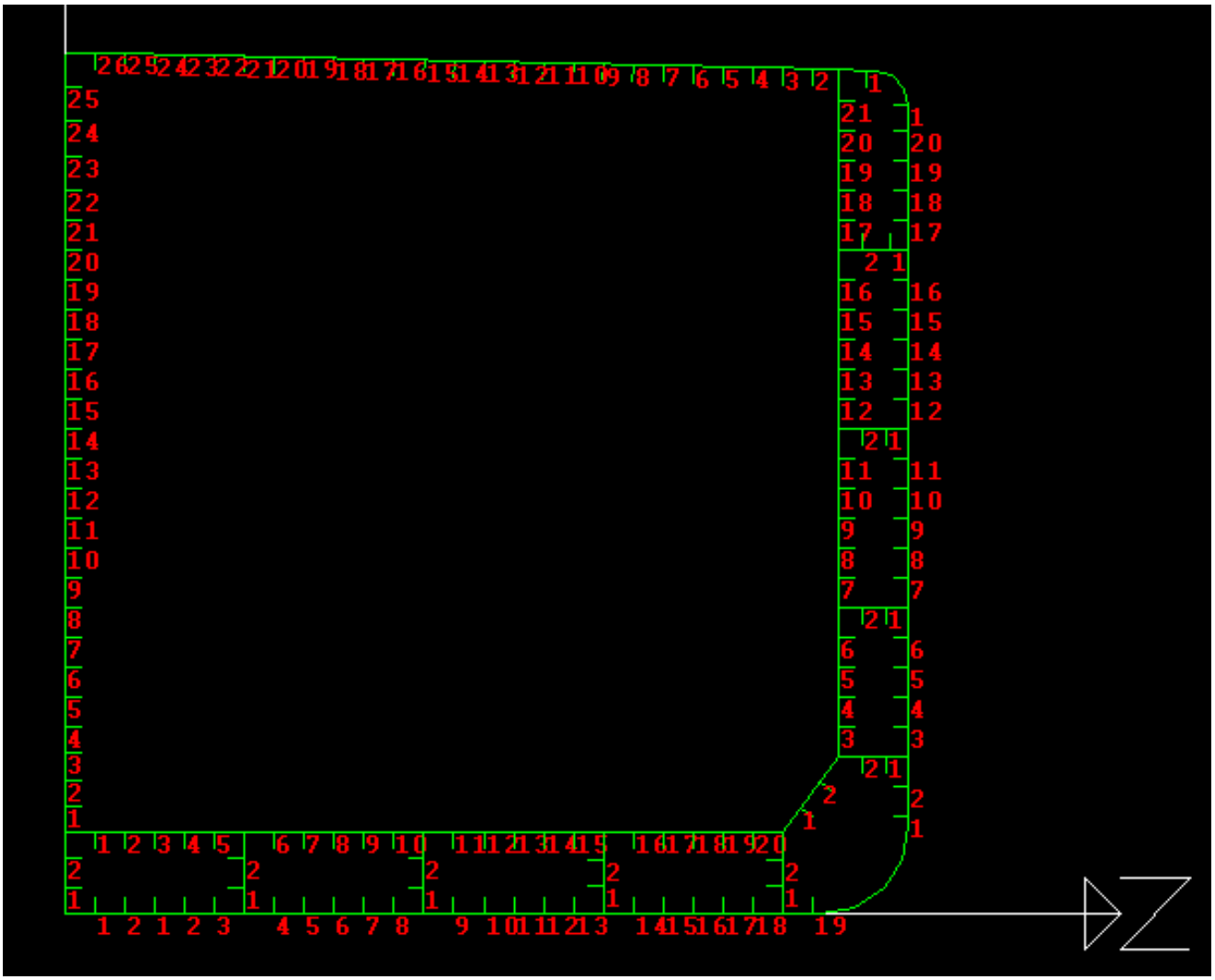

Global Stiffener IDs:

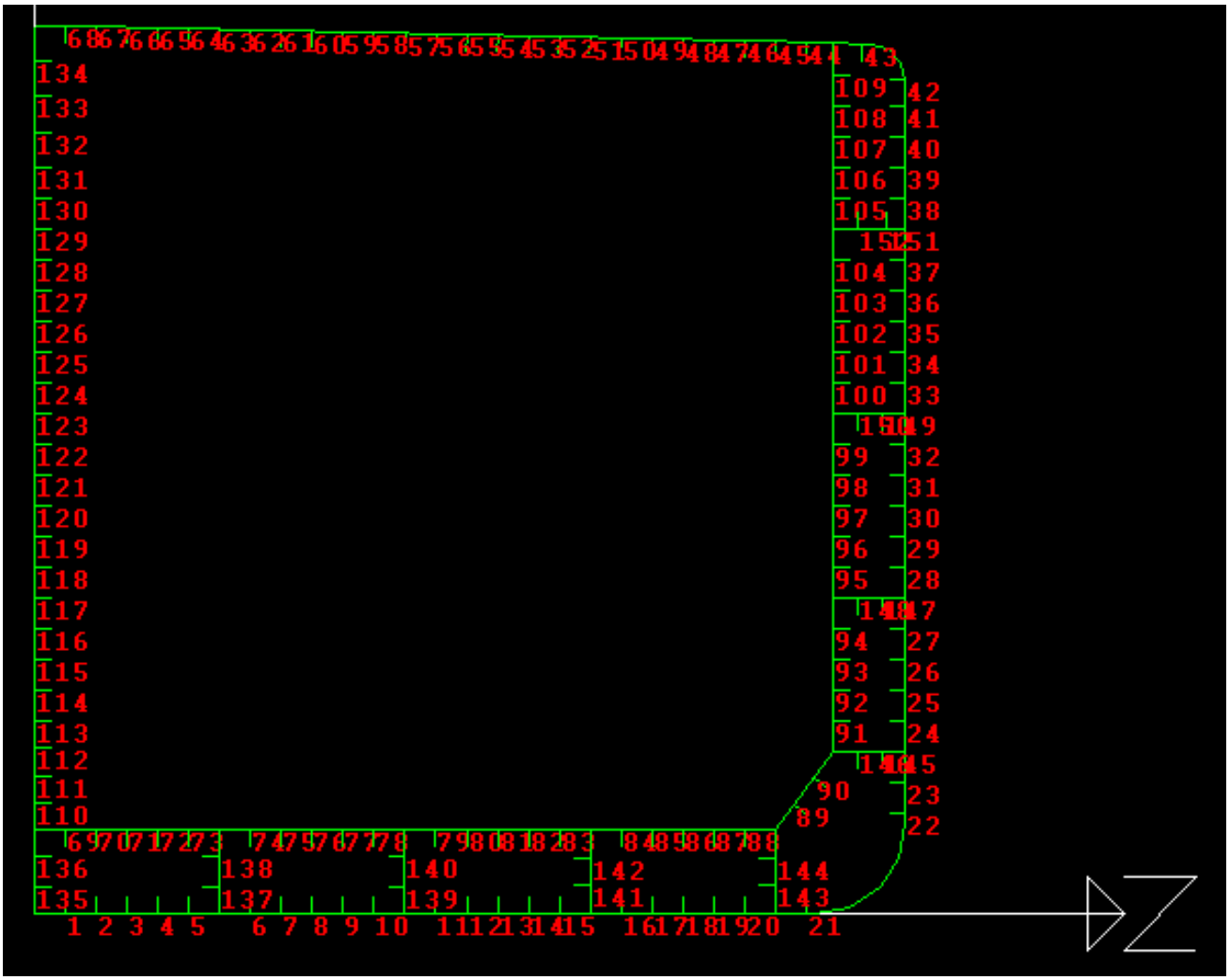

Stiffeners:

ID	SID	XLB	A	STFSP	MATID
			cm2	(m)	
KPL- 101	15	400x120x11.5x23 LIA	71.6	0.85	2
KPL- 102	15	400x120x11.5x23 LIA	71.6	0.85	2
BTM- 101	15	400x120x11.5x23 LIA	71.6	0.85	2
BTM- 102	15	400x120x11.5x23 LIA	71.6	0.85	2
BTM- 103	15	400x120x11.5x23 LIA	71.6	0.85	2
BTM- 204	15	400x120x11.5x23 LIA	71.6	0.85	2
BTM- 205	15	400x120x11.5x23 LIA	71.6	0.85	2
BTM- 206	15	400x120x11.5x23 LIA	71.6	0.85	2
BTM- 207	15	400x120x11.5x23 LIA	71.6	0.85	2
BTM- 208	15	400x120x11.5x23 LIA	71.6	0.85	2
BTM- 309	15	400x120x11.5x23 LIA	71.6	0.85	2
BTM- 310	15	400x120x11.5x23 LIA	71.6	0.85	2
BTM- 311	15	400x120x11.5x23 LIA	71.6	0.85	2
BTM- 312	15	400x120x11.5x23 LIA	71.6	0.85	2
BTM- 313	15	400x120x11.5x23 LIA	71.6	0.85	2
BTM- 414	15	400x120x11.5x23 LIA	71.6	0.85	2
BTM- 415	15	400x120x11.5x23 LIA	71.6	0.85	2
BTM- 416	15	400x120x11.5x23 LIA	71.6	0.85	2
BTM- 417	15	400x120x11.5x23 LIA	71.6	0.85	2
BTM- 418	15	400x120x11.5x23 LIA	71.6	0.85	2
BTM- 519	15	400x120x11.5x23 LIA	71.6	0.85	2
SHL- 101	12	350x120x11.5x18 LIA	60.42	0.85	2
SHL- 102	12	350x120x11.5x18 LIA	60.42	0.85	2
SHL- 203	12	350x120x11.5x18 LIA	60.42	0.85	2
SHL- 204	12	350x120x11.5x18 LIA	60.42	0.85	2
SHL- 205	12	350x120x11.5x18 LIA	60.42	0.85	1
SHL- 206	11	350x120x10.5x16 LIA	54.91	0.85	1
SHL- 307	11	350x120x10.5x16 LIA	54.91	0.85	1
SHL- 308	9	325x120x10.5x14 LIA	50.1	0.85	1
SHL- 309	9	325x120x10.5x14 LIA	50.1	0.85	1
SHL- 310	9	325x120x10.5x14 LIA	50.1	0.85	1
SHL- 311	9	325x120x10.5x14 LIA	50.1	0.85	1
SHL- 412	7	300x100x10.5x15 LIA	45.29	0.85	1
SHL- 413	7	300x100x10.5x15 LIA	45.29	0.85	1
SHL- 414	7	300x100x10.5x15 LIA	45.29	0.85	1
SHL- 415	7	300x100x10.5x15 LIA	45.29	0.85	1
SHL- 416	7	300x100x10.5x15 LIA	45.29	0.85	1
SHL- 517	7	300x100x10.5x15 LIA	45.29	0.85	1
SHL- 618	7	300x100x10.5x15 LIA	45.29	0.85	1
SHL- 619	5	250x90x11.5x16 LIA	41.67	0.85	2
SHL- 620	5	250x90x11.5x16 LIA	41.67	0.85	2
GWR- 101	5	250x90x11.5x16 LIA	41.67	0.05	2
DEC- 101	22	FB 400x28	112	0.425	2
DEC- 202	22	FB 400x28	112	0.8	2
DEC- 203	22	FB 400x28	112	0.85	2
DEC- 204	22	FB 400x28	112	0.85	2
DEC- 205	22	FB 400x28	112	0.85	2
DEC- 206	22	FB 400x28	112	0.85	2
DEC- 207	22	FB 400x28	112	0.85	2
DEC- 208	22	FB 400x28	112	0.85	2
DEC- 209	22	FB 400x28	112	0.85	2
DEC- 210	22	FB 400x28	112	0.85	2

DEC- 211	22	FB 400x28	112	0.85	2
DEC- 212	22	FB 400x28	112	0.85	2
DEC- 213	22	FB 400x28	112	0.85	2
DEC- 214	22	FB 400x28	112	0.85	2
DEC- 215	22	FB 400x28	112	0.85	2
DEC- 216	22	FB 400x28	112	0.85	2
DEC- 217	22	FB 400x28	112	0.85	2
DEC- 218	22	FB 400x28	112	0.85	2
DEC- 219	22	FB 400x28	112	0.85	2
DEC- 220	22	FB 400x28	112	0.85	2
DEC- 221	22	FB 400x28	112	0.85	2
DEC- 222	22	FB 400x28	112	0.85	2
DEC- 223	22	FB 400x28	112	0.85	2
DEC- 224	22	FB 400x28	112	0.85	2
DEC- 225	22	FB 400x28	112	1.103	2
DEC- 326	22	FB 400x28	112	0.6	2
INB- 101	15	400x120x11.5x23 LIA	71.6	0.85	2
INB- 102	15	400x120x11.5x23 LIA	71.6	0.85	2
INB- 103	15	400x120x11.5x23 LIA	71.6	0.85	2
INB- 104	15	400x120x11.5x23 LIA	71.6	0.85	2
INB- 105	15	400x120x11.5x23 LIA	71.6	0.85	2
INB- 206	15	400x120x11.5x23 LIA	71.6	0.85	2
INB- 207	15	400x120x11.5x23 LIA	71.6	0.85	2
INB- 208	15	400x120x11.5x23 LIA	71.6	0.85	2
INB- 209	15	400x120x11.5x23 LIA	71.6	0.85	2
INB- 210	15	400x120x11.5x23 LIA	71.6	0.85	2
INB- 311	15	400x120x11.5x23 LIA	71.6	0.85	2
INB- 312	15	400x120x11.5x23 LIA	71.6	0.85	2
INB- 313	15	400x120x11.5x23 LIA	71.6	0.85	2
INB- 314	15	400x120x11.5x23 LIA	71.6	0.85	2
INB- 315	15	400x120x11.5x23 LIA	71.6	0.85	2
INB- 416	15	400x120x11.5x23 LIA	71.6	0.85	2
INB- 417	15	400x120x11.5x23 LIA	71.6	0.85	2
INB- 418	15	400x120x11.5x23 LIA	71.6	0.85	2
INB- 419	15	400x120x11.5x23 LIA	71.6	0.85	2
INB- 420	15	400x120x11.5x23 LIA	71.6	0.85	2
INS- 101	13	375x120x10.5x18 LIA	59.73	0.895	2
INS- 102	13	375x120x10.5x18 LIA	59.73	0.895	2
INS- 203	13	375x120x10.5x18 LIA	59.73	0.85	2
INS- 204	13	375x120x10.5x18 LIA	59.73	0.85	2
INS- 205	12	350x120x11.5x18 LIA	60.42	0.85	1
INS- 206	12	350x120x11.5x18 LIA	60.42	0.85	1
INS- 307	11	350x120x10.5x16 LIA	54.91	0.85	1
INS- 308	11	350x120x10.5x16 LIA	54.91	0.85	1
INS- 309	11	350x120x10.5x16 LIA	54.91	0.85	1
INS- 310	11	350x120x10.5x16 LIA	54.91	0.85	1
INS- 311	11	350x120x10.5x16 LIA	54.91	0.85	1
INS- 412	11	350x120x10.5x16 LIA	54.91	0.85	1
INS- 413	11	350x120x10.5x16 LIA	54.91	0.85	1
INS- 414	7	300x100x10.5x15 LIA	45.29	0.85	1
INS- 415	7	300x100x10.5x15 LIA	45.29	0.85	1
INS- 416	7	300x100x10.5x15 LIA	45.29	0.85	1
INS- 517	7	300x100x10.5x15 LIA	45.29	0.85	1
INS- 618	7	300x100x10.5x15 LIA	45.29	0.85	1
INS- 619	7	300x100x10.5x15 LIA	45.29	0.85	1
INS- 620	7	300x100x10.5x15 LIA	45.29	0.85	1
INS- 621	7	300x100x10.5x15 LIA	45.29	0.862	1

CTR- 101	**11**	**350x120x10.5x16 LIA**	**27.46**	**0.75**	**2**
CTR- 102	**11**	**350x120x10.5x16 LIA**	**27.46**	**0.75**	**2**
CTR- 203	**11**	**350x120x10.5x16 LIA**	**27.46**	**0.75**	**1**
CTR- 204	**11**	**350x120x10.5x16 LIA**	**27.46**	**0.8**	**1**
CTR- 305	**11**	**350x120x10.5x16 LIA**	**27.46**	**0.85**	**1**
CTR- 306	**11**	**350x120x10.5x16 LIA**	**27.46**	**0.85**	**1**
CTR- 407	**11**	**350x120x10.5x16 LIA**	**27.46**	**0.85**	**1**
CTR- 408	**11**	**350x120x10.5x16 LIA**	**27.46**	**0.85**	**1**
CTR- 409	**11**	**350x120x10.5x16 LIA**	**27.46**	**0.85**	**1**
CTR- 510	**11**	**350x120x10.5x16 LIA**	**27.46**	**0.85**	**1**
CTR- 511	**9**	**325x120x10.5x14 LIA**	**25.05**	**0.85**	**1**
CTR- 512	**9**	**325x120x10.5x14 LIA**	**25.05**	**0.85**	**1**
CTR- 513	**9**	**325x120x10.5x14 LIA**	**25.05**	**0.85**	**1**
CTR- 614	**9**	**325x120x10.5x14 LIA**	**25.05**	**0.85**	**1**
CTR- 615	**9**	**325x120x10.5x14 LIA**	**25.05**	**0.85**	**1**
CTR- 616	**9**	**325x120x10.5x14 LIA**	**25.05**	**0.85**	**1**
CTR- 617	**9**	**325x120x10.5x14 LIA**	**25.05**	**0.85**	**1**
CTR- 618	**9**	**325x120x10.5x14 LIA**	**25.05**	**0.85**	**1**
CTR- 619	**9**	**325x120x10.5x14 LIA**	**25.05**	**0.85**	**1**
CTR- 620	**5**	**250x90x11.5x16 LIA**	**20.84**	**0.85**	**1**
CTR- 621	**5**	**250x90x11.5x16 LIA**	**20.84**	**0.85**	**1**
CTR- 722	**5**	**250x90x11.5x16 LIA**	**20.84**	**0.912**	**1**
CTR- 723	**5**	**250x90x11.5x16 LIA**	**20.84**	**0.975**	**2**
CTR- 724	**5**	**250x90x11.5x16 LIA**	**20.84**	**0.975**	**2**
CTR- 725	**5**	**250x90x11.5x16 LIA**	**20.84**	**0.975**	**2**
BGR- 101	**13**	**375x120x10.5x18 LIA**	**29.86**	**0.775**	**2**
BGR- 102	**12**	**350x120x11.5x18 LIA**	**30.21**	**0.775**	**2**
NBG- 101	**3**	**250x90x9x13 LIA**	**33.39**	**1.1**	**2**
NBG- 302	**3**	**250x90x9x13 LIA**	**33.39**	**0.425**	**2**
NBG- 403	**3**	**250x90x9x13 LIA**	**33.39**	**1.1**	**2**
NBG- 604	**3**	**250x90x9x13 LIA**	**33.39**	**0.425**	**2**
NBG- 705	**3**	**250x90x9x13 LIA**	**33.39**	**0.75**	**2**
NBG- 906	**3**	**250x90x9x13 LIA**	**33.39**	**0.75**	**2**
NBG-1007	**3**	**250x90x9x13 LIA**	**33.39**	**0.75**	**2**
NBG-1208	**3**	**250x90x9x13 LIA**	**33.39**	**0.75**	**2**
NTS- 101	**3**	**250x90x9x13 LIA**	**33.39**	**0.975**	**1**
NTS- 302	**3**	**250x90x9x13 LIA**	**33.39**	**0.35**	**1**
NTS- 403	**3**	**250x90x9x13 LIA**	**33.39**	**0.975**	**1**
NTS- 604	**3**	**250x90x9x13 LIA**	**33.39**	**0.35**	**1**
NTS- 705	**3**	**250x90x9x13 LIA**	**33.39**	**0.975**	**1**
NTS- 906	**3**	**250x90x9x13 LIA**	**33.39**	**0.35**	**1**
NTS-1007	**0**	**250x90x9x13 LIA**	**33.39**	**0.975**	**1**
NTS-1208	**0**	**250x90x9x13 LIA**	**33.39**	**0.35**	**1**

Appendix F: T2 Tanker Cargo Section Structural Data

T2-SE-A1 Single Hull Tanker

Ship Dimensions:

Length Overall	: 523.5 ft
LBP	: 503.0 ft
Moulded beam	: 68.0 ft
Moulded depth	: 39.25 ft
Draft loaded	: 30.25 ft
Displacement (loaded)	: 16,613 tons
Max. Service Speed	: 14.5 knots

Material:

Yield Stress for plates and stiffeners	: 235 MPa
Ratio between ultimate and Yield stress	: 1.4

Hull Type: Single Hull

Midship Geometry:

Camber	: 1.5 ft
Bilge Radius	: 6.0 ft
Web Spacing	: 12.167 ft

The following are graphical representations of the T2-SE-A1:

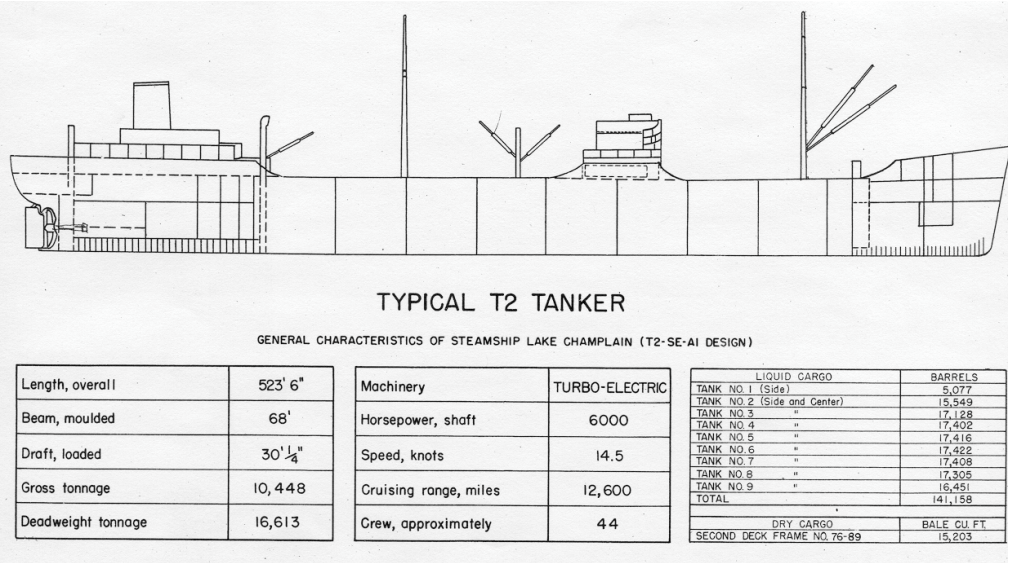

TYPICAL T2 TANKER

GENERAL CHARACTERISTICS OF STEAMSHIP LAKE CHAMPLAIN (T2-SE-A1 DESIGN)

Length, overall	523' 6"
Beam, moulded	68'
Draft, loaded	30' 1/4"
Gross tonnage	10,448
Deadweight tonnage	16,613

Machinery	TURBO-ELECTRIC
Horsepower, shaft	6000
Speed, knots	14.5
Cruising range, miles	12,600
Crew, approximately	44

LIQUID CARGO	BARRELS
TANK NO. 1 (Side)	5,077
TANK NO. 2 (Side and Center)	15,549
TANK NO. 3 "	17,128
TANK NO. 4 "	17,402
TANK NO. 5 "	17,416
TANK NO. 6 "	17,422
TANK NO. 7 "	17,408
TANK NO. 8 "	17,305
TANK NO. 9 "	16,451
TOTAL	141,158

DRY CARGO	BALE CU. FT.
SECOND DECK FRAME NO. 76-89	15,203

(Typical T2 Tanker Profile)

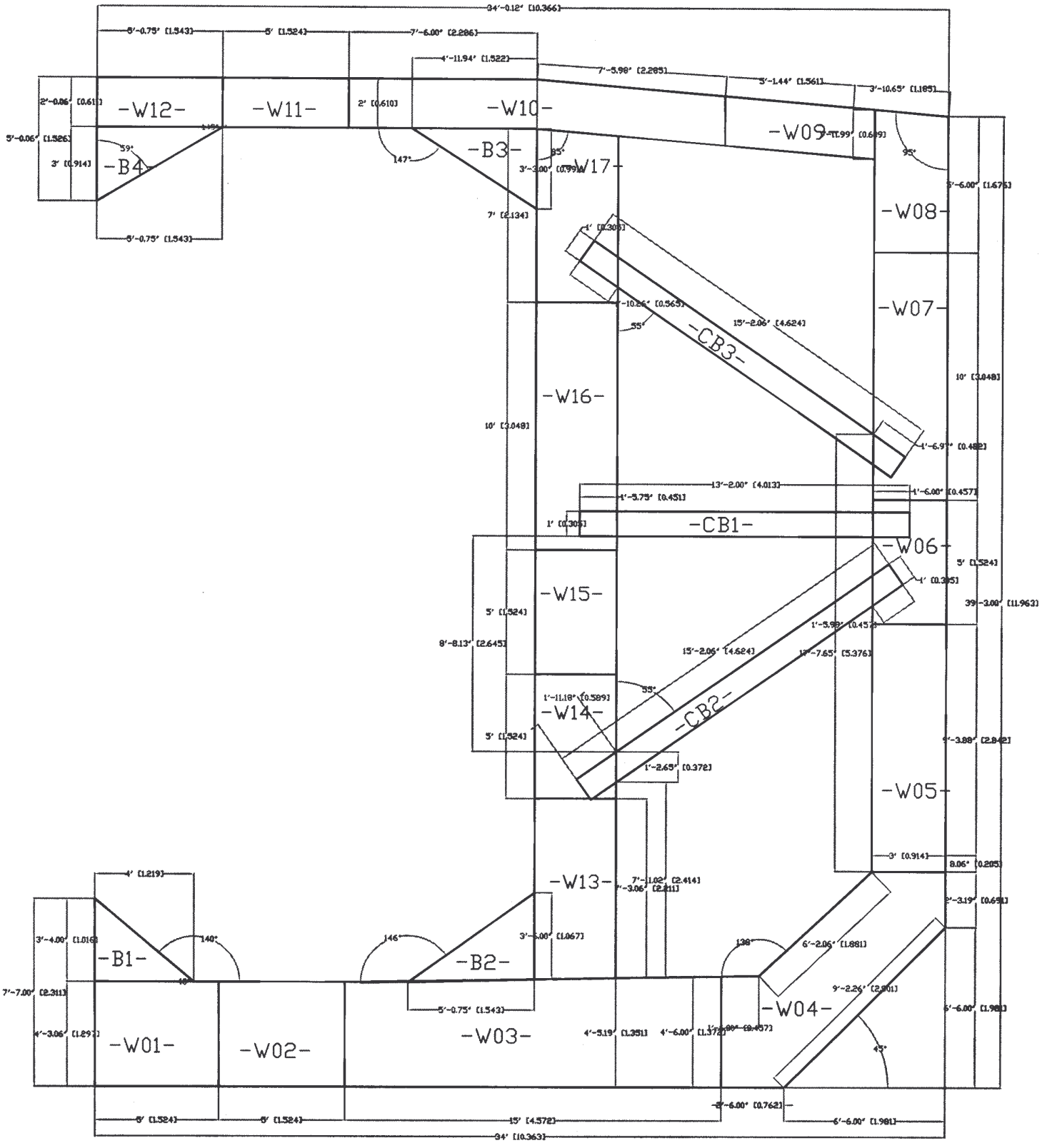

(Midship Section Web and Bracket Drawing)
(note: all dimensions are: feet-inches [meters])

WEB	FLANGE DEPTH (m)	FLANGE THICKNESS (m)	PLATE THICKNESS (#)
W01	0.1778	0.0127	20
W02	0.1778	0.0127	20
W03	0.1778	0.0127	20
W04	0.1778	0.0127	20
W05	0.127	0.0127	20
W06	0.127	0.0127	20
W07	0.127	0.0127	20
W08	0.127	0.0127	20
W09	0.127	0.0127	20
W10	0.127	0.0127	20
W11	0.127	0.0127	20
W12	0.127	0.0127	20
W13	0.127	0.0127	20
W14	0.127	0.0127	20
W15	0.127	0.0127	20
W16	0.127	0.0127	20
W17	0.127	0.0127	20
BRACKET			
B1	0.1778	0.0127	20
B2	0.1778	0.0127	20
B3	0.127	0.0127	20
B4	0.127	0.0127	20
CENTER BRACE			
CB1	N/A	N/A	64
CB2	N/A	N/A	53
CB3	N/A	N/A	53

(Flange Details and Plate Weight for Midship Section Web and Bracket Drawing)

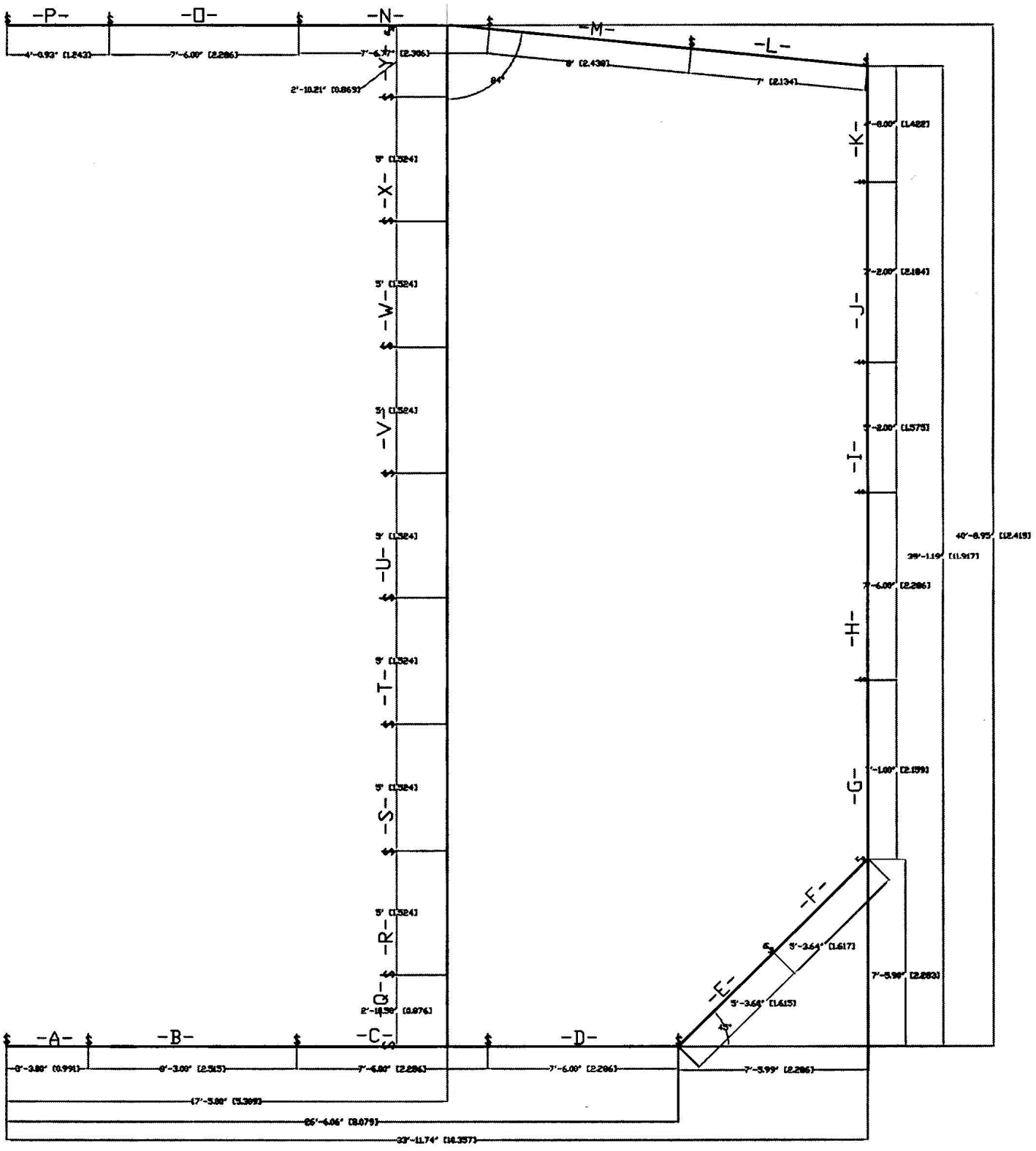

(Midship Section Shell Plating Drawing]

Plate	location	thickness (m)
A	bottom shell	0.015748
B	bottom shell	0.019304
C	bottom shell	0.019304
D	bottom shell	0.019304
E	bilge shell	0.016764
F	bilge shell	0.016764
G	side shell	0.014478
H	side shell	0.014478
I	side shell	0.014478
J	side shell	0.014478
K	side shell	0.022098
L	upper deck shell	0.023876
M	upper deck shell	0.020828
N	upper deck shell	0.020828
O	upper deck shell	0.020828
P	upper deck shell	0.020828
Q	verticle web shell	0.015748
R	verticle web shell	0.014732
S	verticle web shell	0.013716
T	verticle web shell	0.012192
U	verticle web shell	0.011176
V	verticle web shell	0.010668
W	verticle web shell	0.010668
X	verticle web shell	0.0127
Y	verticle web shell	0.0127

(Plate Thickness Table)

Plate	Stiffener	Stiffener Spacing (m)	Stiffener Dimensions (m)
A	L26	0.762 from CL	0.4826 x 0.1524 x 0.0127
B	L25	0.762	0.4826 x 0.1524 x 0.0128
	L24	0.762	0.4826 x 0.1524 x 0.0129
	L23	0.762	0.4826 x 0.1524 x 0.0130
C	L22	0.762	0.4826 x 0.1524 x 0.0131
	L21	0.762	0.4826 x 0.1524 x 0.0132
	L20	0.762	0.4826 x 0.1524 x 0.0133
D	L19	0.762	0.4826 x 0.1524 x 0.0134
	L18	0.762	0.4826 x 0.1524 x 0.0135
	L17	0.762	0.4826 x 0.1524 x 0.0136
E	L16	0.762	0.4826 x 0.1524 x 0.0137
	L15	0.9144	0.4826 x 0.1524 x 0.0138
F	L14	0.9144	0.4826 x 0.1524 x 0.0139
	L13	0.9144	0.4826 x 0.1524 x 0.0140
G	L12	0.9144	0.381 x 0.1524 x 0.0127
	L11	0.762	0.381 x 0.1524 x 0.0128
	L10	0.762	0.381 x 0.1524 x 0.0129
H	L9	0.762	0.381 x 0.1524 x 0.0130
	L8	0.762	0.381 x 0.1524 x 0.0131
	L7	0.762	0.254 x 0.1016 x 0.0127
I	L6	0.762	0.254 x 0.1016 x 0.0128
	L5	0.762	0.254 x 0.1016 x 0.0129
J	L4	0.762	0.254 x 0.1016 x 0.0130
	L3	0.762	0.254 x 0.1016 x 0.0131
	L2	0.762	0.254 x 0.1016 x 0.0132
K	L1	0.762	0.254 x 0.1016 x 0.0133
		0.9144 to mld line of upper deck	
L	L27	0.9144 from side	0.2032 x 0.1016 x 0.0112
	L28	0.9144	0.2032 x 0.1016 x 0.0113
M	L29	0.9144	0.2032 x 0.1016 x 0.0114
	L30	0.762	0.2032 x 0.1016 x 0.0115
	L31	0.762	0.2032 x 0.1016 x 0.0116
N	L32	0.762	0.2032 x 0.1016 x 0.0117
	L33	0.762	0.2032 x 0.1016 x 0.0118
O	L34	0.762	0.2032 x 0.1016 x 0.0119
	L35	0.762	0.2032 x 0.1016 x 0.0120
	L36	0.762	0.2032 x 0.1016 x 0.0121
P	L37	0.762	0.2032 x 0.1016 x 0.0122

(Stiffener Detail Table)

(note: Longitudinal L26 spacing measured from center line)

(note: all other longitudinals measured from previous longitudinal position)

Appendix G: Amdahl Calculation of Energy Absorbed by Bow Damage

The following is a complete analysis of the 150k dwt bulk carrier bow using the method of Amdahl and starting with a geometric description of the vessel bow and transverse sections.

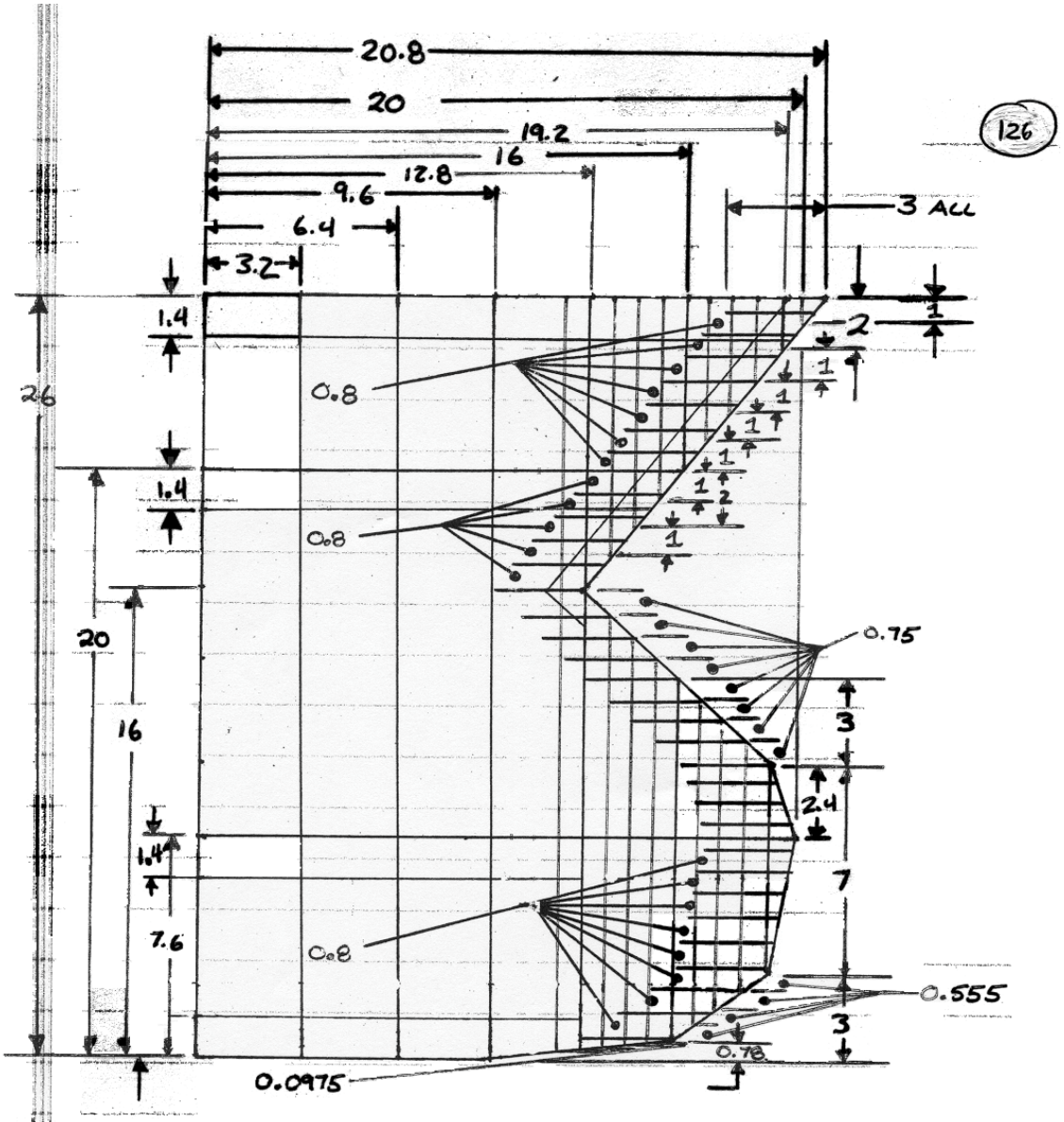

BOW PLAN 150K DWT BULK CARRIER SCALE 1:200

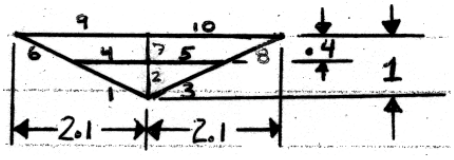

SECTION 1 150K DWT BULK CARRIER SCALE 1:100

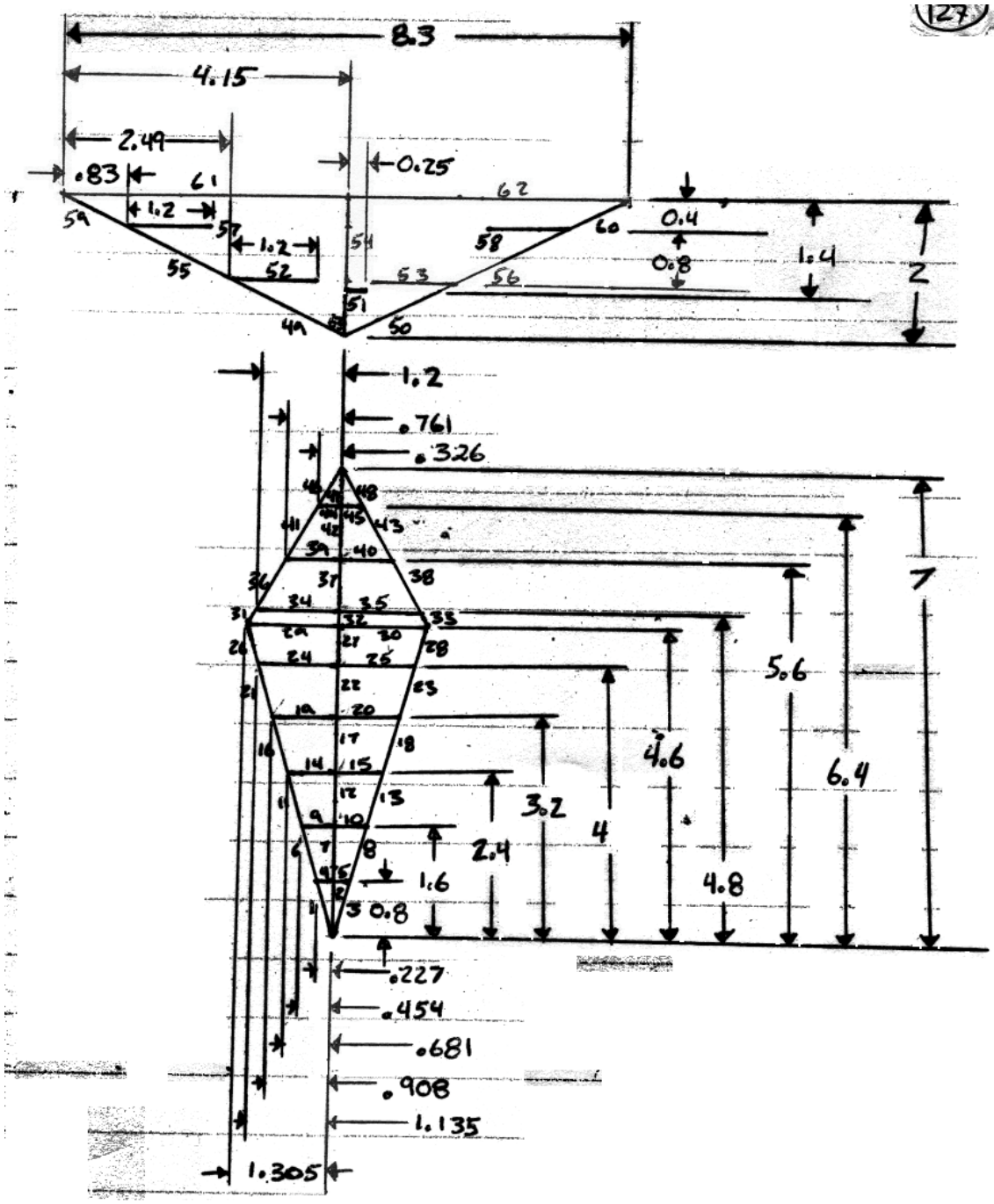

SECTION 2 150K DWT BULK CARRIER SCALE 1:100

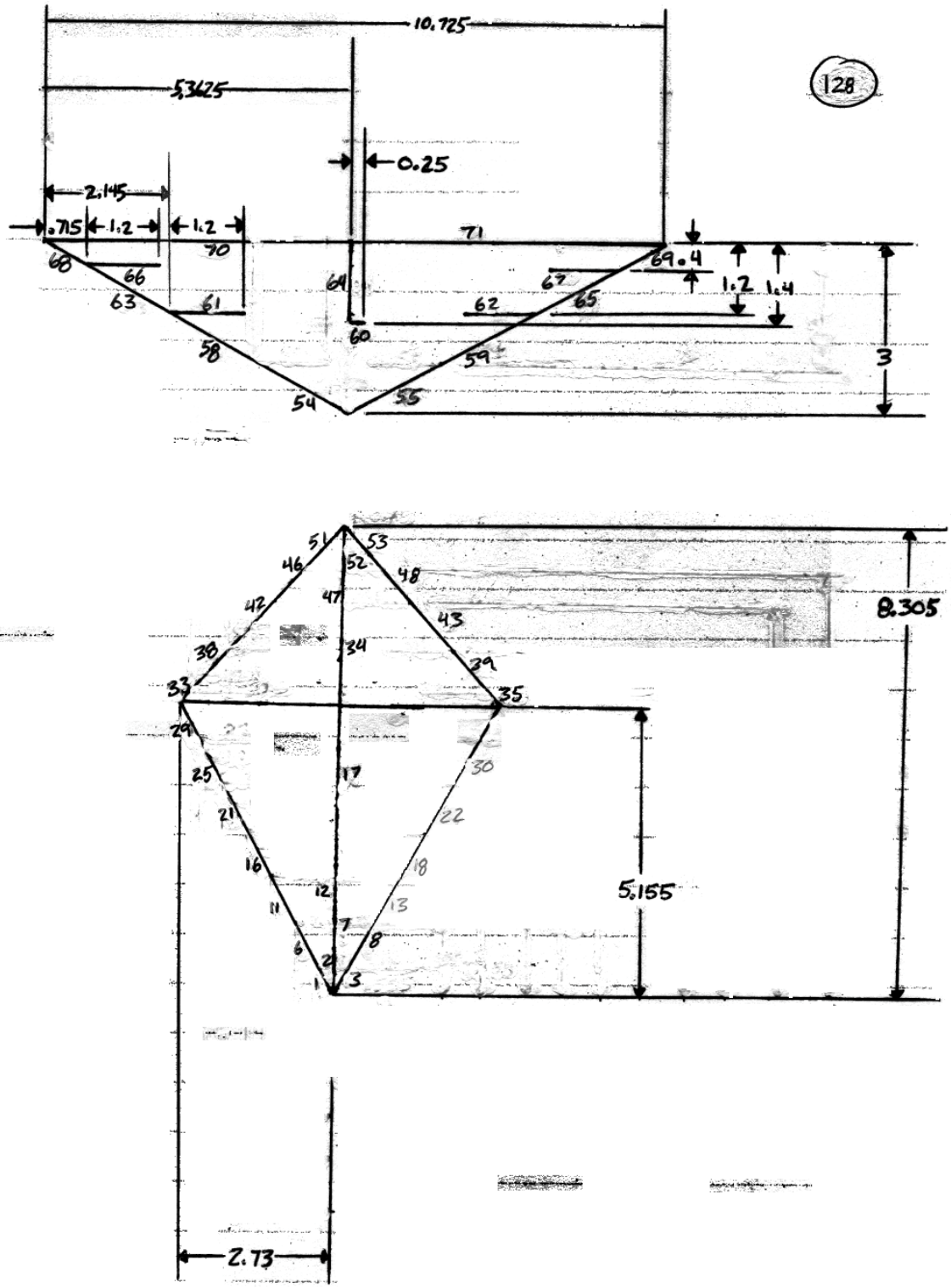

SECTION 3 150K DWT BULK CARRIER SCALE 1:100

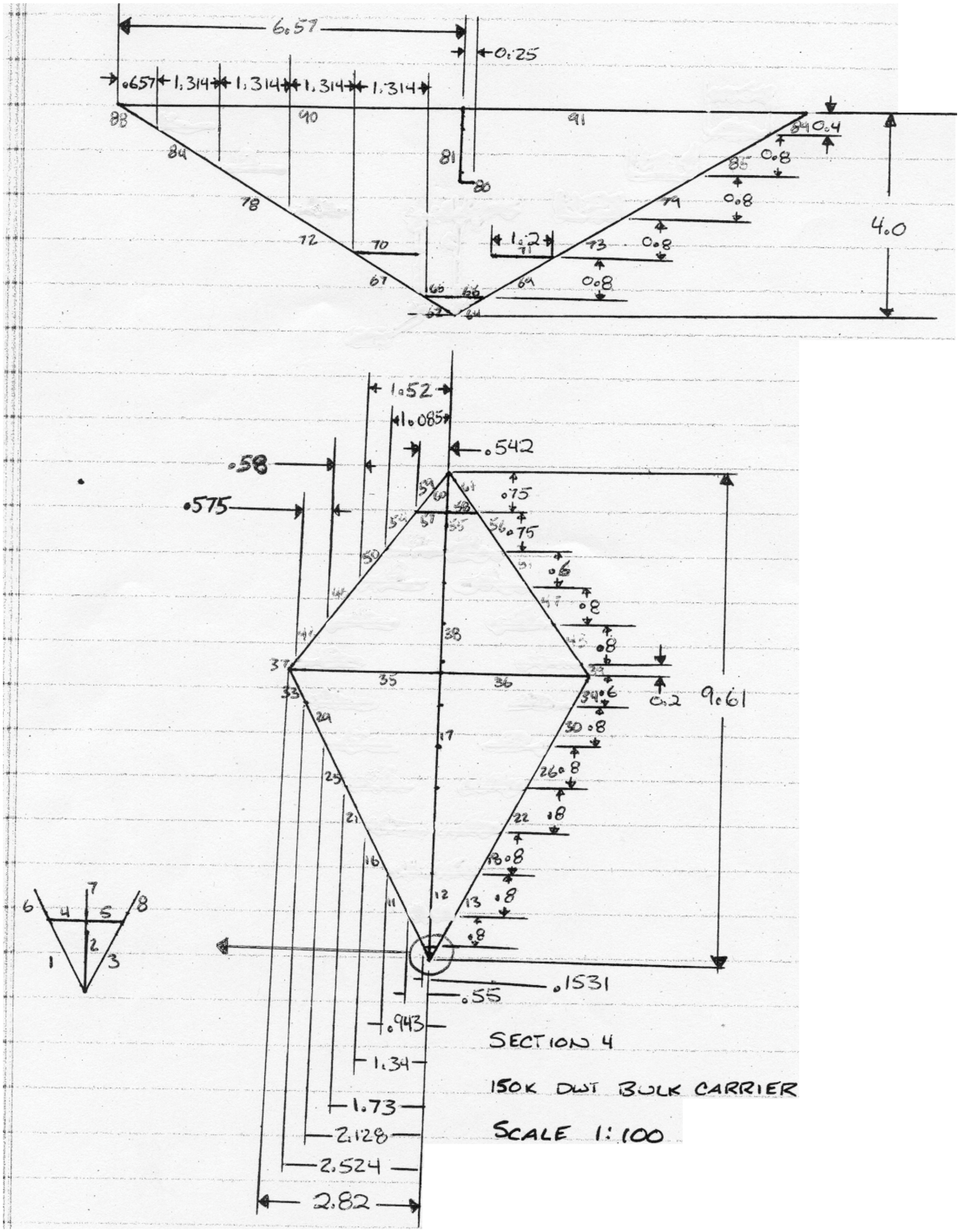
6.57
0.25
.657
1.314
1.314
1.314
1.314
0.4
0.8
0.8
0.8
0.8
1.2
4.0
1.52
1.085
.542
.58
.575
.75
.75
.6
.8
.8
0.2
9.61
.6
.8
.8
.8
.8
.8
.8
.1531
.55
.943
1.34
1.73
2.128
2.524
2.82
SECTION 4
150K DWT BULK CARRIER
SCALE 1:100

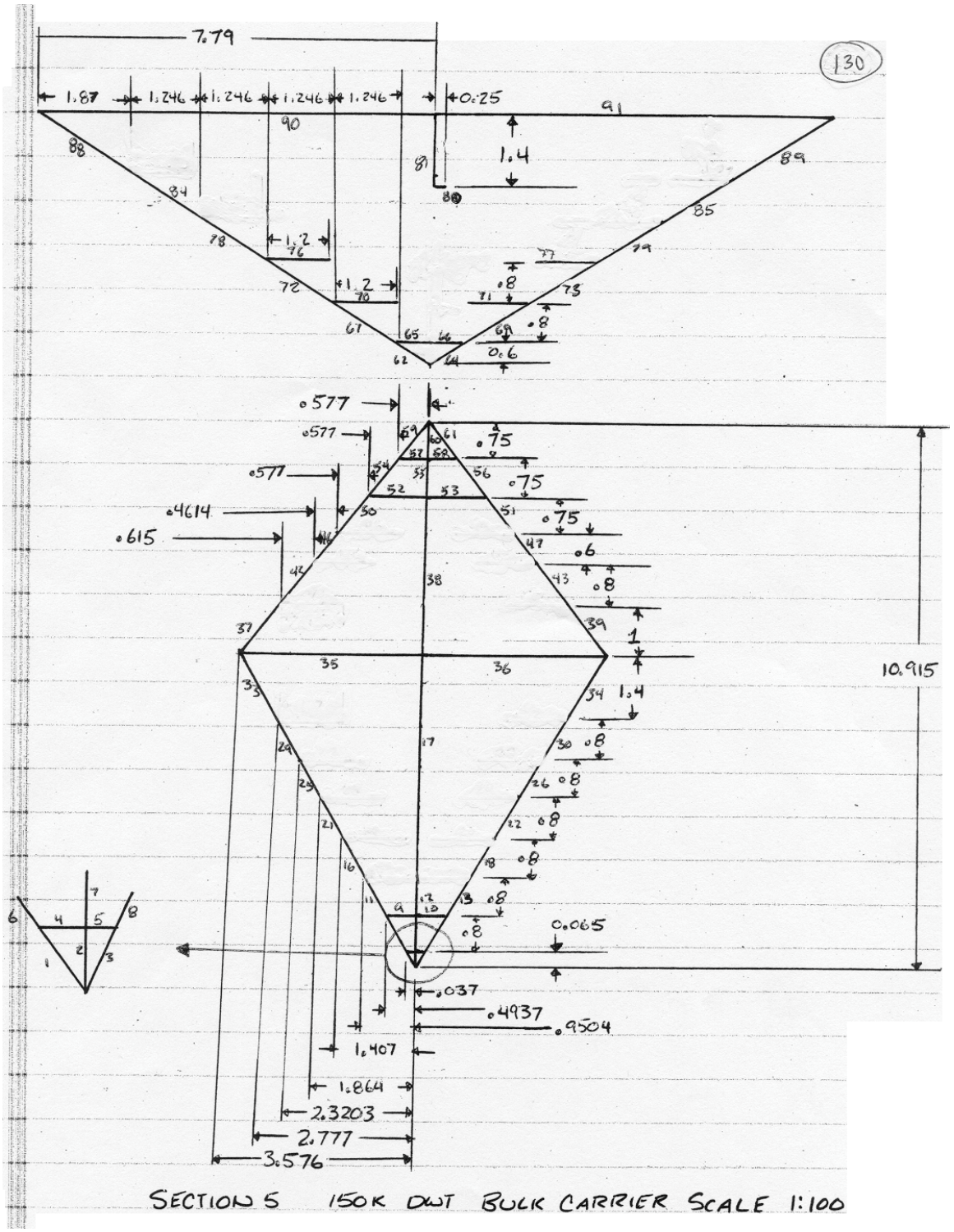

SECTION 5 150K DWT BULK CARRIER SCALE 1:100

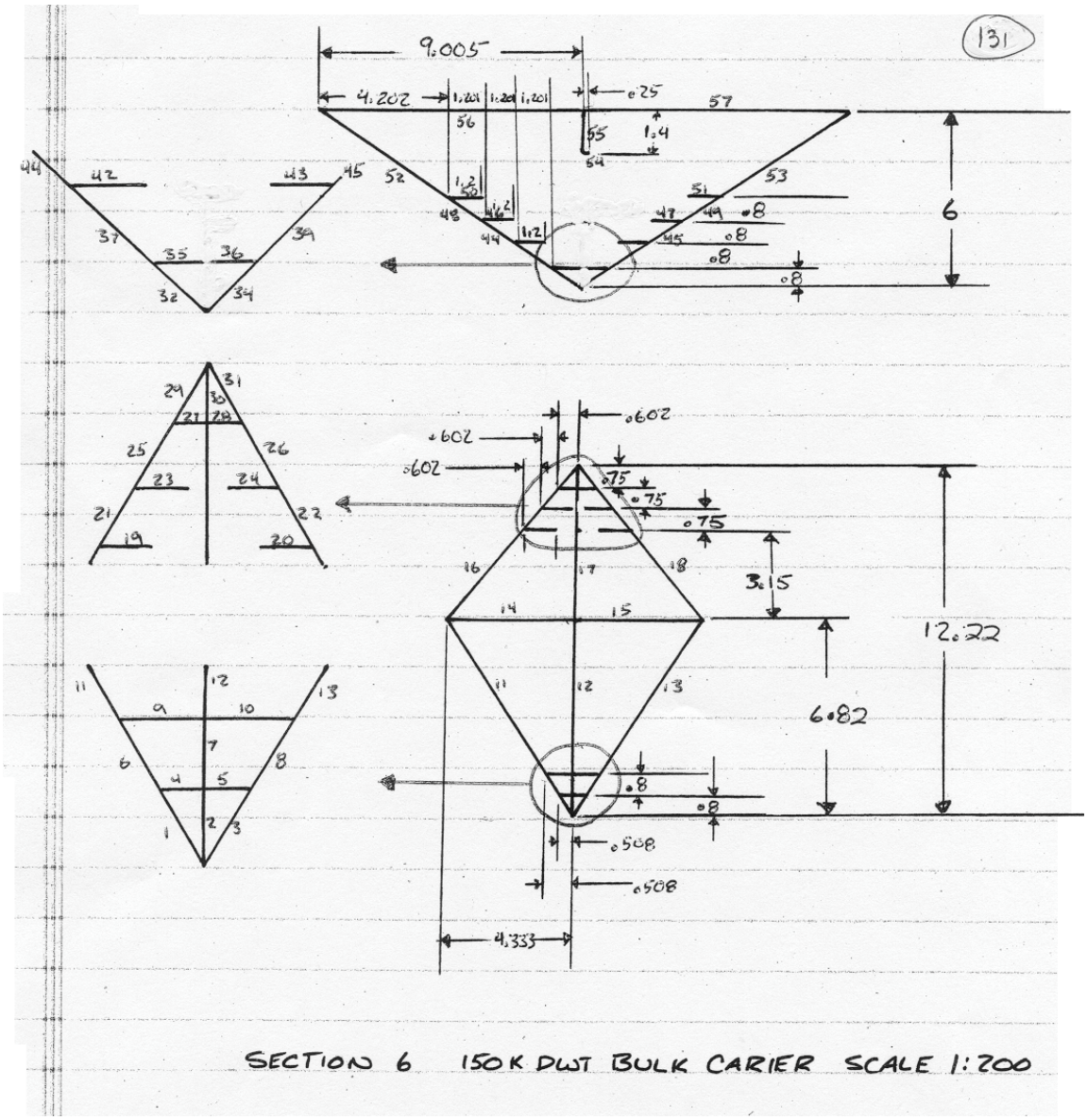

Following are the properties for each element used within the Amdahl analysis along with the smeared thickness, average thickness, and damaged area calculations for each illustrated section above.

The neccessary units and functions for the analysis of the 150k dwt Bulk Carrier using Amdahls method with Pedersons Modifications are given as follows, the below calculation considers no longitudinal stiffener intersections, does not include the stem and only considers those breasthooks which span the complete distance between frames (not sections):

$MPa := 10^6 Pa$ Mega Pascal Definition

$$t_s(h_w, t_w, h_f, t_f, s_s, E_t) := \left[\frac{(h_w \cdot t_w + h_f \cdot t_f)}{s_s} + E_t\right]$$ Smeared Plate Thickness Formula

$MN := 10^6 N$ Mega Newton Definition

Crushing Stress Formula:

$$\sigma_c(\sigma_0, n_{AT}, \tau, DA, n_C, n_T) := 2.42 \cdot \sigma_0 \cdot \left(\frac{n_{AT} \cdot \tau^2}{DA}\right)^{\frac{2}{3}} \cdot \left[0.87 + 1.27 \cdot \frac{n_C + 0.31 \cdot n_T}{\left[\frac{DA}{(n_C + 0.31 \cdot n_T) \cdot \tau^2}\right]^{\frac{1}{4}}}\right]^{\frac{2}{3}}$$

$P_{AV}(DA, \sigma_c) := DA \cdot \sigma_c$ Average Crushing Load Formula

The necessary 150k dwt Bulk Carrier Ship Particulars are defined as shown below.

$\Delta := 174850000 kg$ Displacement

$V_s := 9.3 \frac{m}{s}$ Maximum Service Speed

The material properties for the 150k dwt Bulk Carrier are defined as shown below.

$\sigma_y := 315 MPa$ Mild Steel Yeild Stress

$\sigma_u := 1.6 \cdot \sigma_y$ $\sigma_u = 504\ MPa$ Mild Steel Ultimate Stress

Therefor the Distance between transverse frames is defined as follows:

$D_T := 0.8m$ Distance Between Transverse "Sections" equals 1/4 the distance between transverse frames.

Properties for **Section 1** are given as follows:

$n_{T_1} := 4$ Number of "T" intersections for section 1

$n_{L_1} := 0$ Number of Angle Intersections for section 1

$n_{C_1} := 2$ Number of Cruciform Intersections for section 1

$n_{F_1} := 10$ Number of Elements within Section 1

$n_{AT_1} := n_{T_1} + n_{L_1}$ $n_{AT_1} = 4$ Number of "T" and Angle Intersections for section 1

$$s1b := \begin{pmatrix} 1.3956 \\ .6 \\ 1.3956 \\ 1.26 \\ 1.26 \\ .9304 \\ .4 \\ .9304 \\ 2.1 \\ 2.1 \end{pmatrix} m$$

Element Spans within section 1 for elements 1 through 10

$$s1E_t := \begin{pmatrix} 16 \\ 12 \\ 16 \\ 15 \\ 15 \\ 16 \\ 12 \\ 16 \\ 13 \\ 13 \end{pmatrix} mm$$

Element Plate Thicknesses within section 1 for elements 1 through 10

$$s1h_w := \begin{pmatrix} 0 \\ 0 \\ 0 \\ 0 \\ 0 \\ 0 \\ 0 \\ 0 \\ 250 \\ 250 \end{pmatrix} mm$$

Element Web heights within section 1 on elements 1 through 10

$$s1t_w := \begin{pmatrix} 0 \\ 0 \\ 0 \\ 0 \\ 0 \\ 0 \\ 0 \\ 0 \\ 12 \\ 12 \end{pmatrix} mm$$

Element Web Thicknesses within section 1 on elements 1 through 10

$$s1h_f := \begin{pmatrix} 0 \\ 0 \\ 0 \\ 0 \\ 0 \\ 0 \\ 0 \\ 0 \\ 90 \\ 90 \end{pmatrix} mm$$

Element Flange Span within Section 1 on elements 1 through 10

$$s1t_f := \begin{pmatrix} 0 \\ 0 \\ 0 \\ 0 \\ 0 \\ 0 \\ 0 \\ 0 \\ 16 \\ 16 \end{pmatrix} mm$$

Element Flange Thickness within section 1 elements 1 through 10

$$s1s := \begin{pmatrix} 1 \\ 1 \\ 1 \\ 1 \\ 1 \\ 1 \\ 800 \\ 800 \end{pmatrix} mm$$

Element Stiffener Spacing within section 1 elements 1 through 10

$$:= 1 .. n_{F_1}$$

Iteration Counter

$$s1t_{s_i} := t_s\left(s1h_{w_i}, s1t_{w_i}, s1h_{f_i}, s1t_{f_i}, s1s_i, s1E_{t_i}\right)$$

$$s1t_s = \begin{pmatrix} 0.016 \\ 0.012 \\ 0.016 \\ 0.015 \\ 0.015 \\ 0.016 \\ 0.012 \\ 0.016 \\ 0.019 \\ 0.019 \end{pmatrix} m$$

Element Smeared thicknesses in section 1 for elements 1 through 14

$$\tau_1 := \frac{1}{n_{F_1}}\left(\sum_{i=1}^{n_{F_1}} s1t_{s_i}\right) \qquad \tau_1 = 0.016\,m$$

Section 1 Average Thickness

$$DA_1 := \tau_1 \cdot \sum_{i=1}^{n_{F_1}} s1b_i \qquad DA_1 = 0.192\,m^2$$

Section 1 Damaged Cross Sectional Area

$$DA_{E_1} := \sum_{i=1}^{n_{F_1}} s1b_i \cdot s1t_{s_i} \qquad DA_{E_1} = 0.202\,m^2$$

Section 1 Exact Damaged Cross Sectional Area

Properties for **Section 2** are given as follows:

$n_{T_2} := 27$ Number of "T" intersections for section 2

$n_{L_2} := 0$ Number of Angle Intersections for section 2

$n_{C_2} := 10$ Number of Cruciform Intersections for section 2

$n_{F_2} := 63$ Number of Elements within Section 2

$n_{AT_2} := n_{T_2} + n_{L_2}$ $\quad n_{AT_2} = 27$ Number of "T" and Angle Intersections for section 2

Element Spans within section 2 for elements 1 through 63

$s2b_1 := .8316m$ $\quad s2b_2 := 0.8m$ $\quad s2b_3 := .8316m$ $\quad s2b_4 := .227m$

$s2b_5 := .227m$ $\quad s2b_6 := .8316m$ $\quad s2b_7 := .8m$ $\quad s2b_8 := .8316m$

$s2b_9 := .454m$ $\quad s2b_{10} := .454m$ $\quad s2b_{11} := .8316m$ $\quad s2b_{12} := .8m$

$s2b_{13} := .8316m$ $s2b_{14} := .681m$ $s2b_{15} := .681m$ $s2b_{16} := .8316m$

$s2b_{17} := 0.8m$ $s2b_{18} := .8316m$ $s2b_{19} := .908m$ $s2b_{20} := .908m$

$s2b_{21} := .8316m$ $s2b_{22} := .8m$ $s2b_{23} := .8316m$ $s2b_{24} := 1.135m$

$s2b_{25} := 1.135m$ $s2b_{26} := .6236m$ $s2b_{27} := 0.6m$ $s2b_{28} := .6236m$

$s2b_{29} := 1.305m$ $s2b_{30} := 1.305m$ $s2b_{31} := .2259m$ $s2b_{32} := .2m$

$s2b_{33} := .2259m$ $s2b_{34} := 1.2m$ $s2b_{35} := 1.2m$ $s2b_{36} := .9125m$

$s2b_{37} := .8m$ $s2b_{38} := .9125m$ $s2b_{39} := .761m$ $s2b_{40} := .761m$

$s2b_{41} := .9106m$ $s2b_{42} := .8m$ $s2b_{43} := .9106m$ $s2b_{44} := .326m$

$s2b_{45} := .326m$ $s2b_{46} := .6828m$ $s2b_{47} := .6m$ $s2b_{48} := .6828m$

$s2b_{49} := 1.8427m$ $s2b_{50} := 1.8427m$ $s2b_{51} := .25m$ $s2b_{52} := 1.2m$

$s2b_{53} := 1.2m$ $s2b_{54} := 1.4m$ $s2b_{55} := 1.8427m$ $s2b_{56} := 1.8427m$

$s2b_{57} := 1.2m$ $s2b_{58} := 1.2m$ $s2b_{59} := .9214m$ $s2b_{60} := .9214m$

$s2b_{61} := 4.15m$ $s2b_{62} := 4.15m$ $s2b_{63} := .6m$

Element Plate Thicknesses within section 2 for elements 1 through 63

$s2E_{t_1} := 18mm$ $s2E_{t_2} := 12mm$ $s2E_{t_3} := 18mm$ $s2E_{t_4} := 15mm$

$s2E_{t_5} := 15mm$ $s2E_{t_6} := 18mm$ $s2E_{t_7} := 12mm$ $s2E_{t_8} := 18mm$

$s2E_{t_9} := 15mm$ $s2E_{t_{10}} := 15mm$ $s2E_{t_{11}} := 18mm$ $s2E_{t_{12}} := 12mm$

$s2E_{t_{13}} := 18mm$ $s2E_{t_{14}} := 15mm$ $s2E_{t_{15}} := 15mm$ $s2E_{t_{16}} := 18mm$

$s2E_{t_{17}} := 12mm$ $s2E_{t_{18}} := 18mm$ $s2E_{t_{19}} := 15mm$ $s2E_{t_{20}} := 15mm$

$s2E_{t_{21}} := 18mm$ $s2E_{t_{22}} := 12mm$ $s2E_{t_{23}} := 18mm$ $s2E_{t_{24}} := 15mm$

$s2E_{t_{25}} := 15mm$ $s2E_{t_{26}} := 18mm$ $s2E_{t_{27}} := 12mm$ $s2E_{t_{28}} := 18mm$

$s2E_{t_{29}} := 13mm$ $s2E_{t_{30}} := 13mm$ $s2E_{t_{31}} := 18mm$ $s2E_{t_{32}} := 12mm$

$s2E_{t_{33}} := 18mm$ $s2E_{t_{34}} := 15mm$ $s2E_{t_{35}} := 15mm$ $s2E_{t_{36}} := 33mm$

$s2E_{t_{37}} := 12mm$ $s2E_{t_{38}} := 33mm$ $s2E_{t_{39}} := 15mm$ $s2E_{t_{40}} := 15mm$

$s2E_{t_{41}} := 33mm$ $s2E_{t_{42}} := 12mm$ $s2E_{t_{43}} := 33mm$ $s2E_{t_{44}} := 15mm$

$s2E_{t_{45}} := 15mm$ $s2E_{t_{46}} := 33mm$ $s2E_{t_{47}} := 12mm$ $s2E_{t_{48}} := 33mm$

$s2E_{t_{49}} := 16mm$ $s2E_{t_{50}} := 16mm$ $s2E_{t_{51}} := 25mm$ $s2E_{t_{52}} := 15mm$

$s2E_{t_{53}} := 15mm$ $s2E_{t_{54}} := 12mm$ $s2E_{t_{55}} := 16mm$ $s2E_{t_{56}} := 16mm$

$s2E_{t_{57}} := 15mm$ $s2E_{t_{58}} := 15mm$ $s2E_{t_{59}} := 16mm$ $s2E_{t_{60}} := 16mm$

$s2E_{t_{61}} := 13mm$ $s2E_{t_{62}} := 13mm$ $s2E_{t_{63}} := 12mm$

Element Web heights within section 2 on elements 1 through 63

$s2h_{w_1} := 450mm$ $s2h_{w_2} := 0mm$ $s2h_{w_3} := 450mm$ $s2h_{w_4} := 0mm$

$s2h_{w_5} := 0mm$ $s2h_{w_6} := 450mm$ $s2h_{w_7} := 0mm$ $s2h_{w_8} := 450mm$

$s2h_{w_9} := 0mm$ $s2h_{w_{10}} := 0mm$ $s2h_{w_{11}} := 450mm$ $s2h_{w_{12}} := 0mm$

$s2h_{w_{13}} := 450mm$ $s2h_{w_{14}} := 0mm$ $s2h_{w_{15}} := 0mm$ $s2h_{w_{16}} := 450mm$

$s2h_{w_{17}} := 0mm$ $s2h_{w_{18}} := 450mm$ $s2h_{w_{19}} := 0mm$ $s2h_{w_{20}} := 0mm$

$s2h_{w_{21}} := 450mm$ $s2h_{w_{22}} := 0mm$ $s2h_{w_{23}} := 450mm$ $s2h_{w_{24}} := 0mm$

$s2h_{w_{25}} := 0mm$ $s2h_{w_{26}} := 450mm$ $s2h_{w_{27}} := 0mm$ $s2h_{w_{28}} := 450mm$

$s2h_{w_{29}} := 250mm$ $s2h_{w_{30}} := 250mm$ $s2h_{w_{31}} := 400mm$ $s2h_{w_{32}} := 0mm$

$s2h_{w_{33}} := 400mm$ $s2h_{w_{34}} := 0mm$ $s2h_{w_{35}} := 0mm$ $s2h_{w_{36}} := 400mm$

$s2h_{w_{37}} := 0mm$ $s2h_{w_{38}} := 400mm$ $s2h_{w_{39}} := 0mm$ $s2h_{w_{40}} := 0mm$

$s2h_{w_{41}} := 400mm$ $s2h_{w_{42}} := 0mm$ $s2h_{w_{43}} := 400mm$ $s2h_{w_{44}} := 0mm$

$s2h_{w_{45}} := 0mm$ $s2h_{w_{46}} := 400mm$ $s2h_{w_{47}} := 0mm$ $s2h_{w_{48}} := 400mm$

$s2h_{w_{49}} := 350mm$ $s2h_{w_{50}} := 350mm$ $s2h_{w_{51}} := 0mm$ $s2h_{w_{52}} := 0mm$

$s2h_{w_{53}} := 0mm$ $s2h_{w_{54}} := 0mm$ $s2h_{w_{55}} := 350mm$ $s2h_{w_{56}} := 350mm$

$s2h_{w_{57}} := 0mm$ $s2h_{w_{58}} := 0mm$ $s2h_{w_{59}} := 350mm$ $s2h_{w_{60}} := 350mm$

$s2h_{w_{61}} := 250mm$ $s2h_{w_{62}} := 250mm$ $s2h_{w_{63}} := 0mm$

Element Web heights within section 2 on elements 1 through 63

$s2t_{w_1} := 12mm$ $s2t_{w_2} := 0mm$ $s2t_{w_3} := 12mm$ $s2t_{w_4} := 0mm$

$s2t_{w_5} := 0mm$ $s2t_{w_6} := 12mm$ $s2t_{w_7} := 0mm$ $s2t_{w_8} := 12mm$

$s2t_{w_9} := 0mm$ $s2t_{w_{10}} := 0mm$ $s2t_{w_{11}} := 12mm$ $s2t_{w_{12}} := 0mm$

$s2t_{w_{13}} := 12mm$ $s2t_{w_{14}} := 0mm$ $s2t_{w_{15}} := 0mm$ $s2t_{w_{16}} := 12mm$

$s2t_{w_{17}} := 0mm$ $s2t_{w_{18}} := 12mm$ $s2t_{w_{19}} := 0mm$ $s2t_{w_{20}} := 0mm$

$s2t_{w_{21}} := 12mm$ $s2t_{w_{22}} := 0mm$ $s2t_{w_{23}} := 12mm$ $s2t_{w_{24}} := 0mm$

$s2t_{w_{25}} := 0mm$ $s2t_{w_{26}} := 12mm$ $s2t_{w_{27}} := 0mm$ $s2t_{w_{28}} := 12mm$

$s2t_{w_{29}} := 12mm$ $s2t_{w_{30}} := 12mm$ $s2t_{w_{31}} := 19mm$ $s2t_{w_{32}} := 0mm$

$s2t_{w_{33}} := 19mm$ $s2t_{w_{34}} := 0mm$ $s2t_{w_{35}} := 0mm$ $s2t_{w_{36}} := 19mm$

$s2t_{w_{37}} := 0mm$ $s2t_{w_{38}} := 19mm$ $s2t_{w_{39}} := 0mm$ $s2t_{w_{40}} := 0mm$

$s2t_{w_{41}} := 19mm$ $s2t_{w_{42}} := 0mm$ $s2t_{w_{43}} := 19mm$ $s2t_{w_{44}} := 0mm$

$s2t_{w_{45}} := 0mm$ $s2t_{w_{46}} := 19mm$ $s2t_{w_{47}} := 0mm$ $s2t_{w_{48}} := 19mm$

$s2t_{w_{49}} := 12mm$ $s2t_{w_{50}} := 12mm$ $s2t_{w_{51}} := 0mm$ $s2t_{w_{52}} := 0mm$

$s2t_{w_{53}} := 0mm$ $s2t_{w_{54}} := 0mm$ $s2t_{w_{55}} := 12mm$ $s2t_{w_{56}} := 12mm$

$s2t_{w_{57}} := 0mm$ $s2t_{w_{58}} := 0mm$ $s2t_{w_{59}} := 12mm$ $s2t_{w_{60}} := 12mm$

$s2t_{w_{61}} := 12mm$ $s2t_{w_{62}} := 12mm$ $s2t_{w_{63}} := 0mm$

Element Flange Span within Section 2 on elements 1 through 63

$s2h_{f_1} := 150mm$ $s2h_{f_2} := 0mm$ $s2h_{f_3} := 150mm$ $s2h_{f_4} := 0mm$

$s2h_{f_5} := 0mm$ $s2h_{f_6} := 150mm$ $s2h_{f_7} := 0mm$ $s2h_{f_8} := 150mm$

$s2h_{f_9} := 0mm$ $s2h_{f_{10}} := 0mm$ $s2h_{f_{11}} := 150mm$ $s2h_{f_{12}} := 0mm$

$s2h_{f_{13}} := 150mm$ $s2h_{f_{14}} := 0mm$ $s2h_{f_{15}} := 0mm$ $s2h_{f_{16}} := 150mm$

$s2h_{f_{17}} := 0mm$ $s2h_{f_{18}} := 150mm$ $s2h_{f_{19}} := 0mm$ $s2h_{f_{20}} := 0mm$

$s2h_{f_{21}} := 150mm$ $s2h_{f_{22}} := 0mm$ $s2h_{f_{23}} := 150mm$ $s2h_{f_{24}} := 0mm$

$s2h_{f_{25}} := 0mm$ $s2h_{f_{26}} := 150mm$ $s2h_{f_{27}} := 0mm$ $s2h_{f_{28}} := 150mm$

$s2h_{f_{29}} := 90mm$ $s2h_{f_{30}} := 90mm$ $s2h_{f_{31}} := 100mm$ $s2h_{f_{32}} := 0mm$

$s2h_{f_{33}} := 100mm$ $s2h_{f_{34}} := 0mm$ $s2h_{f_{35}} := 0mm$ $s2h_{f_{36}} := 100mm$

$s2h_{f_{37}} := 0mm$ $s2h_{f_{38}} := 100mm$ $s2h_{f_{39}} := 0mm$ $s2h_{f_{40}} := 0mm$

$s2h_{f_{41}} := 100mm$ $s2h_{f_{42}} := 0mm$ $s2h_{f_{43}} := 100mm$ $s2h_{f_{44}} := 0mm$

$s2h_{f_{45}} := 0mm$ $s2h_{f_{46}} := 100mm$ $s2h_{f_{47}} := 0mm$ $s2h_{f_{48}} := 100mm$

$s2h_{f_{49}} := 100mm$ $s2h_{f_{50}} := 100mm$ $s2h_{f_{51}} := 0mm$ $s2h_{f_{52}} := 0mm$

$s2h_{f_{53}} := 0mm$ $s2h_{f_{54}} := 0mm$ $s2h_{f_{55}} := 100mm$ $s2h_{f_{56}} := 100mm$

$s2h_{f_{57}} := 0mm$ $s2h_{f_{58}} := 0mm$ $s2h_{f_{59}} := 100mm$ $s2h_{f_{60}} := 100mm$

$s2h_{f_{61}} := 90mm$ $s2h_{f_{62}} := 90mm$ $s2h_{f_{63}} := 0mm$

Element Flange Thickness within section 2 elements 1 through 63

$s2t_{f_1} := 16mm$ $s2t_{f_2} := 0mm$ $s2t_{f_3} := 16mm$ $s2t_{f_4} := 0mm$

$s2t_{f_5} := 0mm$ $s2t_{f_6} := 16mm$ $s2t_{f_7} := 0mm$ $s2t_{f_8} := 16mm$

$s2t_{f_9} := 0mm$ $s2t_{f_{10}} := 0mm$ $s2t_{f_{11}} := 16mm$ $s2t_{f_{12}} := 0mm$

$s2t_{f_{13}} := 16mm$ $s2t_{f_{14}} := 0mm$ $s2t_{f_{15}} := 0mm$ $s2t_{f_{16}} := 16mm$

$s2t_{f_{17}} := 0mm$ $s2t_{f_{18}} := 16mm$ $s2t_{f_{19}} := 0mm$ $s2t_{f_{20}} := 0mm$

$s2t_{f_{21}} := 16mm$ $s2t_{f_{22}} := 0mm$ $s2t_{f_{23}} := 16mm$ $s2t_{f_{24}} := 0mm$

$s2t_{f_{25}} := 0mm$ $s2t_{f_{26}} := 16mm$ $s2t_{f_{27}} := 0mm$ $s2t_{f_{28}} := 16mm$

$s2t_{f_{29}} := 16mm$ $s2t_{f_{30}} := 16mm$ $s2t_{f_{31}} := 19mm$ $s2t_{f_{32}} := 0mm$

$s2t_{f_{33}} := 19mm$ $s2t_{f_{34}} := 0mm$ $s2t_{f_{35}} := 0mm$ $s2t_{f_{36}} := 19mm$

$s2t_{f_{37}} := 0mm$ $s2t_{f_{38}} := 19mm$ $s2t_{f_{39}} := 0mm$ $s2t_{f_{40}} := 0mm$

$s2t_{f_{41}} := 19mm$ $s2t_{f_{42}} := 0mm$ $s2t_{f_{43}} := 19mm$ $s2t_{f_{44}} := 0mm$

$s2t_{f_{45}} := 0mm$ $s2t_{f_{46}} := 19mm$ $s2t_{f_{47}} := 0mm$ $s2t_{f_{48}} := 19mm$

$s2t_{f_{49}} := 17mm$ $s2t_{f_{50}} := 17mm$ $s2t_{f_{51}} := 0mm$ $s2t_{f_{52}} := 0mm$

$s2t_{f_{53}} := 0mm$ $s2t_{f_{54}} := 0mm$ $s2t_{f_{55}} := 17mm$ $s2t_{f_{56}} := 17mm$

$s2t_{f_{57}} := 0mm$ $s2t_{f_{58}} := 0mm$ $s2t_{f_{59}} := 17mm$ $s2t_{f_{60}} := 17mm$

$s2t_{f_{61}} := 16mm$ $s2t_{f_{62}} := 16mm$ $s2t_{f_{63}} := 0mm$

Element Stiffener Spacing within section 2 elements 1 through 63

$s2s_1 := 800mm$ $s2s_2 := 0mm$ $s2s_3 := 800mm$ $s2s_4 := 0mm$

$s2s_5 := 0mm$ $s2s_6 := 800mm$ $s2s_7 := 0mm$ $s2s_8 := 800mm$

$s2s_9 := 0mm$ $s2s_{10} := 0mm$ $s2s_{11} := 800mm$ $s2s_{12} := 0mm$

$s2s_{13} := 800mm$ $s2s_{14} := 0mm$ $s2s_{15} := 0mm$ $s2s_{16} := 800mm$

$s2s_{17} := 0mm$ $s2s_{18} := 800mm$ $s2s_{19} := 0mm$ $s2s_{20} := 0mm$

$s2s_{21} := 800mm$ $s2s_{22} := 0mm$ $s2s_{23} := 800mm$ $s2s_{24} := 0mm$

$s2s_{25} := 0mm$ $s2s_{26} := 800mm$ $s2s_{27} := 0mm$ $s2s_{28} := 800mm$

$s2s_{29} := 800mm$ $s2s_{30} := 800mm$ $s2s_{31} := 600mm$ $s2s_{32} := 0mm$

$s2s_{33} := 600mm$ $s2s_{34} := 0mm$ $s2s_{35} := 0mm$ $s2s_{36} := 600mm$

$s2s_{37} := 0mm$ $s2s_{38} := 600mm$ $s2s_{39} := 0mm$ $s2s_{40} := 0mm$

$s2s_{41} := 600mm$ $s2s_{42} := 0mm$ $s2s_{43} := 600mm$ $s2s_{44} := 0mm$

$s2s_{45} := 0mm$ $s2s_{46} := 600mm$ $s2s_{47} := 0mm$ $s2s_{48} := 600mm$

$s2s_{49} := 800mm$ $s2s_{50} := 800mm$ $s2s_{51} := 0mm$ $s2s_{52} := 0mm$

$s2s_{53} := 0mm$ $s2s_{54} := 0mm$ $s2s_{55} := 800mm$ $s2s_{56} := 800mm$

$s2s_{57} := 0mm$ $s2s_{58} := 0mm$ $s2s_{59} := 800mm$ $s2s_{60} := 800mm$

$s2s_{61} := 800mm$ $s2s_{62} := 800mm$ $s2s_{63} := 0mm$

$i := 1 .. n_{F_2}$ Iteration Counter

$s2t_{s_i} := t_s\left(s2h_{w_i}, s2t_{w_i}, s2h_{f_i}, s2t_{f_i}, s2s_i, s2E_{t_i}\right)$ Smeared Thickness Calculation

$\tau_2 := \frac{1}{n_{F_2}}\left(\sum_{i=1}^{n_{F_2}} s2t_{s_i}\right)$ $\tau_2 = 0.022\,m$ Section 2 Average Thickness

$DA_2 := \tau_2 \cdot \sum_{i=1}^{n_{F_2}} s2b_i$ $DA_2 = 1.278\,m^2$ Section 2 Damaged Cross Sectional Area

$DA_{E_2} := \sum_{i=1}^{n_{F_2}} s2b_i \cdot s2t_{s_i}$ $DA_{E_2} = 1.249\,m^2$ Section 2 Exact Damaged Cross Sectional Area

Properties for Section 3 are given as follows:

$n_{T_3} := 31$ Number of "T" intersections for section 3

$n_{L_3} := 4$ Number of Angle Intersections for section 3

$n_{C_3} := 4$ Number of Cruciform Intersections for section 3

$n_{F_3} := 72$ Number of Elements within Section 3

$n_{AT_3} := n_{T_3} + n_L$ $n_{AT_3} = 35$ Number of "T" and Angle Intersections for section 3

Element Spans within section 3 for elements 1 through 72

$s3b_1 := .6281m$ $s3b_2 := .555m$ $s3b_3 := .6281m$ $s3b_4 := .294m$

$s3b_5 := .294m$ $s3b_6 := .9054m$ $s3b_7 := .8m$ $s3b_8 := .9054m$

$s3b_9 := .718m$ $s3b_{10} := .718m$ $s3b_{11} := .9054m$ $s3b_{12} := .8m$

$s3b_{13} := .9054m$ $s3b_{14} := 1.2m$ $s3b_{15} := 1.2m$ $s3b_{16} := .9054m$

$s3b_{17} := 3m$ $s3b_{18} := .9054m$ $s3b_{19} := 1.2m$ $s3b_{20} := 1.2m$

$s3b_{21} := .9054m$ $s3b_{22} := .9054m$ $s3b_{23} := 1.2m$ $s3b_{24} := 1.2m$

$s3b_{25} := .9054m$ $s3b_{26} := .9054m$ $s3b_{27} := 1.2m$ $s3b_{28} := 1.2m$

$s3b_{29} := .679m$ $s3b_{30} := .679m$ $s3b_{31} := 2.73m$ $s3b_{32} := 2.73m$

$s3b_{33} := .2625m$ $s3b_{34} := 1.8m$ $s3b_{35} := .2625m$ $s3b_{36} := 1.2m$

$s3b_{37} := 1.2m$ $s3b_{38} := 1.063m$ $s3b_{39} := 1.063m$ $s3b_{40} := 1.2m$

$s3b_{41} := 1.2m$ $s3b_{42} := 1.056m$ $s3b_{43} := 1.056m$ $s3b_{44} := 1.2m$

$s3b_{45} := 1.2m$ $s3b_{46} := .794m$ $s3b_{47} := .6m$ $s3b_{48} := .794m$

$s3b_{49} := .65m$ $s3b_{50} := .65m$ $s3b_{51} := .9925m$ $s3b_{52} := .75m$

$s3b_{53} := .9925m$ $s3b_{54} := 2.05m$ $s3b_{55} := 2.05m$ $s3b_{56} := 1.2m$

$s3b_{57} := 1.2m$ $s3b_{58} := 1.6385m$ $s3b_{59} := 1.6385m$ $s3b_{60} := .25m$

$s3b_{61} := 1.2m$ $s3b_{62} := 1.2m$ $s3b_{63} := 1.6385m$ $s3b_{64} := 1.4m$

$s3b_{65} := 1.6385m$ $s3b_{66} := 1.2m$ $s3b_{67} := 1.2m$ $s3b_{68} := .82m$

$s3b_{69} := .82m$ $s3b_{70} := 5.3625m$ $s3b_{71} := 5.3625m$ $s3b_{72} := 0m$

Element Plate Thicknesses within section 3 for elements 1 through 72

$s3E_{t_1} := 18mm$ $s3E_{t_2} := 12mm$ $s3E_{t_3} := 18mm$ $s3E_{t_4} := 15mm$

$s3E_{t_5} := 15mm$ $s3E_{t_6} := 18mm$ $s3E_{t_7} := 12mm$ $s3E_{t_8} := 18mm$

$s3E_{t_9} := 15mm$ $s3E_{t_{10}} := 15mm$ $s3E_{t_{11}} := 18mm$ $s3E_{t_{12}} := 12mm$

$s3E_{t_{13}} := 18mm$ $s3E_{t_{14}} := 15mm$ $s3E_{t_{15}} := 15mm$ $s3E_{t_{16}} := 18mm$

$s3E_{t_{17}} := 12mm$ $s3E_{t_{18}} := 18mm$ $s3E_{t_{19}} := 15mm$ $s3E_{t_{20}} := 15mm$

$s3E_{t_{21}} := 18mm$ $s3E_{t_{22}} := 18mm$ $s3E_{t_{23}} := 15mm$ $s3E_{t_{24}} := 15mm$

$s3E_{t_{25}} := 18mm$ $s3E_{t_{26}} := 18mm$ $s3E_{t_{27}} := 15mm$ $s3E_{t_{28}} := 15mm$

$s3E_{t_{29}} := 18mm$ $s3E_{t_{30}} := 18mm$ $s3E_{t_{31}} := 13mm$ $s3E_{t_{32}} := 13mm$

$s3E_{t_{33}} := 18mm$ $s3E_{t_{34}} := 12mm$ $s3E_{t_{35}} := 18mm$ $s3E_{t_{36}} := 15mm$

$s3E_{t_{37}} := 15mm$ $s3E_{t_{38}} := 33mm$ $s3E_{t_{39}} := 33mm$ $s3E_{t_{40}} := 15mm$

$s3E_{t_{41}} := 15mm$ $s3E_{t_{42}} := 33mm$ $s3E_{t_{43}} := 33mm$ $s3E_{t_{44}} := 15mm$

$s3E_{t_{45}} := 15mm$ $s3E_{t_{46}} := 33mm$ $s3E_{t_{47}} := 12mm$ $s3E_{t_{48}} := 33mm$

$s3E_{t_{49}} := 15mm$ $s3E_{t_{50}} := 15mm$ $s3E_{t_{51}} := 33mm$ $s3E_{t_{52}} := 12mm$

$s3E_{t_{53}} := 33mm$ $s3E_{t_{54}} := 16mm$ $s3E_{t_{55}} := 16mm$ $s3E_{t_{56}} := 15mm$

$s3E_{t_{57}} := 15mm$ $s3E_{t_{58}} := 16mm$ $s3E_{t_{59}} := 16mm$ $s3E_{t_{60}} := 25mm$

$s3E_{t_{61}} := 15mm$ $s3E_{t_{62}} := 15mm$ $s3E_{t_{63}} := 16mm$ $s3E_{t_{64}} := 12mm$

$s3E_{t_{65}} := 16mm$ $s3E_{t_{66}} := 15mm$ $s3E_{t_{67}} := 15mm$ $s3E_{t_{68}} := 16mm$

$s3E_{t_{69}} := 16mm$ $s3E_{t_{70}} := 13mm$ $s3E_{t_{71}} := 13mm$ $s3E_{t_{72}} := 12mm$

Element Web heights within section 3 on elements 1 through 72

$s3h_{w_1} := 450mm$ $s3h_{w_2} := 0mm$ $s3h_{w_3} := 450mm$ $s3h_{w_4} := 0mm$

$s3h_{w_5} := 0mm$ $s3h_{w_6} := 450mm$ $s3h_{w_7} := 0mm$ $s3h_{w_8} := 450mm$

$s3h_{w_9} := 0mm$ $s3h_{w_{10}} := 0mm$ $s3h_{w_{11}} := 450mm$ $s3h_{w_{12}} := 0mm$

$s3h_{w_{13}} := 450mm$ $s3h_{w_{14}} := 0mm$ $s3h_{w_{15}} := 0mm$ $s3h_{w_{16}} := 450mm$

$s3h_{w_{17}} := 0mm$ $s3h_{w_{18}} := 450mm$ $s3h_{w_{19}} := 0mm$ $s3h_{w_{20}} := 0mm$

$s3h_{w_{21}} := 450mm$ $s3h_{w_{22}} := 450mm$ $s3h_{w_{23}} := 0mm$ $s3h_{w_{24}} := 0mm$

$s3h_{w_{25}} := 450mm$ $s3h_{w_{26}} := 450mm$ $s3h_{w_{27}} := 0mm$ $s3h_{w_{28}} := 0mm$

$s3h_{w_{29}} := 450mm$ $s3h_{w_{30}} := 450mm$ $s3h_{w_{31}} := 250mm$ $s3h_{w_{32}} := 250mm$

$s3h_{w_{33}} := 400mm$ $s3h_{w_{34}} := 0mm$ $s3h_{w_{35}} := 400mm$ $s3h_{w_{36}} := 0mm$

$s3h_{w_{37}} := 0mm$ $s3h_{w_{38}} := 400mm$ $s3h_{w_{39}} := 400mm$ $s3h_{w_{40}} := 0mm$

$s3h_{w_{41}} := 0mm$ $s3h_{w_{42}} := 400mm$ $s3h_{w_{43}} := 400mm$ $s3h_{w_{44}} := 0mm$

$s3h_{w_{45}} := 0mm$ $s3h_{w_{46}} := 400mm$ $s3h_{w_{47}} := 0mm$ $s3h_{w_{48}} := 400mm$

$s3h_{w_{49}} := 0mm$ $s3h_{w_{50}} := 0mm$ $s3h_{w_{51}} := 400mm$ $s3h_{w_{52}} := 0mm$

$s3h_{w_{53}} := 400mm$ $s3h_{w_{54}} := 350mm$ $s3h_{w_{55}} := 350mm$ $s3h_{w_{56}} := 0mm$

$s3h_{w_{57}} := 0mm$ $s3h_{w_{58}} := 350mm$ $s3h_{w_{59}} := 350mm$ $s3h_{w_{60}} := 0mm$

$s3h_{w_{61}} := 0mm$ $s3h_{w_{62}} := 0mm$ $s3h_{w_{63}} := 350mm$ $s3h_{w_{64}} := 0mm$

$s3h_{w_{65}} := 350mm$ $s3h_{w_{66}} := 0mm$ $s3h_{w_{67}} := 0mm$ $s3h_{w_{68}} := 350mm$

$s3h_{w_{69}} := 350mm$ $s3h_{w_{70}} := 250mm$ $s3h_{w_{71}} := 250mm$ $s3h_{w_{72}} := 0mm$

Element Web heights within section 3 on elements 1 through 72

$s3t_{w_1} := 12mm$ $s3t_{w_2} := 0mm$ $s3t_{w_3} := 12mm$ $s3t_{w_4} := 0mm$

$s3t_{w_5} := 0mm$ $s3t_{w_6} := 12mm$ $s3t_{w_7} := 0mm$ $s3t_{w_8} := 12mm$

$s3t_{w_9} := 0mm$ $s3t_{w_{10}} := 0mm$ $s3t_{w_{11}} := 12mm$ $s3t_{w_{12}} := 0mm$

$s3t_{w_{13}} := 12mm$ $s3t_{w_{14}} := 0mm$ $s3t_{w_{15}} := 0mm$ $s3t_{w_{16}} := 12mm$

$s3t_{w_{17}} := 0mm$ $s3t_{w_{18}} := 12mm$ $s3t_{w_{19}} := 0mm$ $s3t_{w_{20}} := 0mm$

$s3t_{w_{21}} := 12mm$ $s3t_{w_{22}} := 12mm$ $s3t_{w_{23}} := 0mm$ $s3t_{w_{24}} := 0mm$

$s3t_{w_{25}} := 12mm$ $s3t_{w_{26}} := 12mm$ $s3t_{w_{27}} := 0mm$ $s3t_{w_{28}} := 0mm$

$s3t_{w_{29}} := 12mm$ $s3t_{w_{30}} := 12mm$ $s3t_{w_{31}} := 12mm$ $s3t_{w_{32}} := 12mm$

$s3t_{w_{33}} := 19mm$ $s3t_{w_{34}} := 0mm$ $s3t_{w_{35}} := 19mm$ $s3t_{w_{36}} := 0mm$

$s3t_{w_{37}} := 0mm$ $s3t_{w_{38}} := 19mm$ $s3t_{w_{39}} := 19mm$ $s3t_{w_{40}} := 0mm$

$s3t_{w_{41}} := 0mm$ $s3t_{w_{42}} := 19mm$ $s3t_{w_{43}} := 19mm$ $s3t_{w_{44}} := 0mm$

$s3t_{w_{45}} := 0mm$ $s3t_{w_{46}} := 19mm$ $s3t_{w_{47}} := 0mm$ $s3t_{w_{48}} := 19mm$

$s3t_{w_{49}} := 0mm$ $s3t_{w_{50}} := 0mm$ $s3t_{w_{51}} := 19mm$ $s3t_{w_{52}} := 0mm$

$s3t_{w_{53}} := 19mm$ $s3t_{w_{54}} := 12mm$ $s3t_{w_{55}} := 12mm$ $s3t_{w_{56}} := 0mm$

$s3t_{w_{57}} := 0mm$ $s3t_{w_{58}} := 12mm$ $s3t_{w_{59}} := 12mm$ $s3t_{w_{60}} := 0mm$

$s3t_{w_{61}} := 0mm$ $s3t_{w_{62}} := 0mm$ $s3t_{w_{63}} := 12mm$ $s3t_{w_{64}} := 0mm$

$s3t_{w_{65}} := 12mm$ $s3t_{w_{66}} := 0mm$ $s3t_{w_{67}} := 0mm$ $s3t_{w_{68}} := 12mm$

$s3t_{w_{69}} := 12mm$ $s3t_{w_{70}} := 12mm$ $s3t_{w_{71}} := 12mm$ $s3t_{w_{72}} := 0mm$

Element Flange Span within Section 3 on elements 1 through 72

$s3h_{f_1} := 150mm$ $s3h_{f_2} := 0mm$ $s3h_{f_3} := 150mm$ $s3h_{f_4} := 0mm$

$s3h_{f_5} := 0mm$ $s3h_{f_6} := 150mm$ $s3h_{f_7} := 0mm$ $s3h_{f_8} := 150mm$

$s3h_{f_9} := 0mm$ $s3h_{f_{10}} := 0mm$ $s3h_{f_{11}} := 150mm$ $s3h_{f_{12}} := 0mm$

$s3h_{f_{13}} := 150mm$ $s3h_{f_{14}} := 0mm$ $s3h_{f_{15}} := 0mm$ $s3h_{f_{16}} := 150mm$

$s3h_{f_{17}} := 0mm$ $s3h_{f_{18}} := 150mm$ $s3h_{f_{19}} := 0mm$ $s3h_{f_{20}} := 0mm$

$s3h_{f_{21}} := 150mm$ $s3h_{f_{22}} := 150mm$ $s3h_{f_{23}} := 0mm$ $s3h_{f_{24}} := 0mm$

$s3h_{f_{25}} := 150mm$ $s3h_{f_{26}} := 150mm$ $s3h_{f_{27}} := 0mm$ $s3h_{f_{28}} := 0mm$

$s3h_{f_{29}} := 150mm$ $s3h_{f_{30}} := 150mm$ $s3h_{f_{31}} := 90mm$ $s3h_{f_{32}} := 90mm$

$s3h_{f_{33}} := 100mm$ $s3h_{f_{34}} := 0mm$ $s3h_{f_{35}} := 100mm$ $s3h_{f_{36}} := 0mm$

$s3h_{f_{37}} := 0mm$ $s3h_{f_{38}} := 100mm$ $s3h_{f_{39}} := 100mm$ $s3h_{f_{40}} := 0mm$

$s3h_{f_{41}} := 0mm$ $s3h_{f_{42}} := 100mm$ $s3h_{f_{43}} := 100mm$ $s3h_{f_{44}} := 0mm$

$s3h_{f_{45}} := 0mm$ $s3h_{f_{46}} := 100mm$ $s3h_{f_{47}} := 0mm$ $s3h_{f_{48}} := 100mm$

$s3h_{f_{49}} := 0mm$ $s3h_{f_{50}} := 0mm$ $s3h_{f_{51}} := 100mm$ $s3h_{f_{52}} := 0mm$

$s3h_{f_{53}} := 100mm$ $s3h_{f_{54}} := 100mm$ $s3h_{f_{55}} := 100mm$ $s3h_{f_{56}} := 0mm$

$s3h_{f_{57}} := 0mm$ $s3h_{f_{58}} := 100mm$ $s3h_{f_{59}} := 100mm$ $s3h_{f_{60}} := 0mm$

$s3h_{f_{61}} := 0mm$ $s3h_{f_{62}} := 0mm$ $s3h_{f_{63}} := 100mm$ $s3h_{f_{64}} := 0mm$

$s3h_{f_{65}} := 100mm$ $s3h_{f_{66}} := 0mm$ $s3h_{f_{67}} := 0mm$ $s3h_{f_{68}} := 100mm$

$s3h_{f_{69}} := 100mm$ $s3h_{f_{70}} := 90mm$ $s3h_{f_{71}} := 90mm$ $s3h_{f_{72}} := 0mm$

Element Flange Thickness within section 3 elements 1 through 72

$s3t_{f_1} := 16mm$ $s3t_{f_2} := 0mm$ $s3t_{f_3} := 16mm$ $s3t_{f_4} := 0mm$

$s3t_{f_5} := 0mm$ $s3t_{f_6} := 16mm$ $s3t_{f_7} := 0mm$ $s3t_{f_8} := 16mm$

$s3t_{f_9} := 0mm$ $s3t_{f_{10}} := 0mm$ $s3t_{f_{11}} := 16mm$ $s3t_{f_{12}} := 0mm$

$s3t_{f_{13}} := 16mm$ $s3t_{f_{14}} := 0mm$ $s3t_{f_{15}} := 0mm$ $s3t_{f_{16}} := 16mm$

$s3t_{f_{17}} := 0mm$ $s3t_{f_{18}} := 16mm$ $s3t_{f_{19}} := 0mm$ $s3t_{f_{20}} := 0mm$

$s3t_{f_{21}} := 16mm$ $s3t_{f_{22}} := 16mm$ $s3t_{f_{23}} := 0mm$ $s3t_{f_{24}} := 0mm$

$s3t_{f_{25}} := 16mm$ $s3t_{f_{26}} := 16mm$ $s3t_{f_{27}} := 0mm$ $s3t_{f_{28}} := 0mm$

$s3t_{f_{29}} := 16mm$ $s3t_{f_{30}} := 16mm$ $s3t_{f_{31}} := 16mm$ $s3t_{f_{32}} := 16mm$

$s3t_{f_{33}} := 19mm$ $s3t_{f_{34}} := 0mm$ $s3t_{f_{35}} := 19mm$ $s3t_{f_{36}} := 0mm$

$s3t_{f_{37}} := 0mm$ $s3t_{f_{38}} := 19mm$ $s3t_{f_{39}} := 19mm$ $s3t_{f_{40}} := 0mm$

$s3t_{f_{41}} := 0mm$ $s3t_{f_{42}} := 19mm$ $s3t_{f_{43}} := 19mm$ $s3t_{f_{44}} := 0mm$

$s3t_{f_{45}} := 0mm$ $s3t_{f_{46}} := 19mm$ $s3t_{f_{47}} := 0mm$ $s3t_{f_{48}} := 19mm$

$s3t_{f_{49}} := 0mm$ $s3t_{f_{50}} := 0mm$ $s3t_{f_{51}} := 19mm$ $s3t_{f_{52}} := 0mm$

$s3t_{f_{53}} := 19mm$ $s3t_{f_{54}} := 17mm$ $s3t_{f_{55}} := 17mm$ $s3t_{f_{56}} := 0mm$

$s3t_{f_{57}} := 0mm$ $s3t_{f_{58}} := 17mm$ $s3t_{f_{59}} := 17mm$ $s3t_{f_{60}} := 0mm$

$s3t_{f_{61}} := 0mm$ $s3t_{f_{62}} := 0mm$ $s3t_{f_{63}} := 17mm$ $s3t_{f_{64}} := 0mm$

$s3t_{f_{65}} := 17mm$ $s3t_{f_{66}} := 0mm$ $s3t_{f_{67}} := 0mm$ $s3t_{f_{68}} := 17mm$

$s3t_{f_{69}} := 17mm$ $s3t_{f_{70}} := 16mm$ $s3t_{f_{71}} := 16mm$ $s3t_{f_{72}} := 0mm$

Element Stiffener Spacing within section 3 elements 1 through 72

$s3s_1 := 800mm$ $s3s_2 := 1mm$ $s3s_3 := 800mm$ $s3s_4 := 1mm$

$s3s_5 := 1mm$ $s3s_6 := 800mm$ $s3s_7 := 1mm$ $s3s_8 := 800mm$

$s3s_9 := 1mm$ $s3s_{10} := 1mm$ $s3s_{11} := 800mm$ $s3s_{12} := 1mm$

$s3s_{13} := 800mm$ $s3s_{14} := 1mm$ $s3s_{15} := 1mm$ $s3s_{16} := 800mm$

$s3s_{17} := 1mm$ $s3s_{18} := 800mm$ $s3s_{19} := 1mm$ $s3s_{20} := 1mm$

$s3s_{21} := 800mm$ $s3s_{22} := 800mm$ $s3s_{23} := 1mm$ $s3s_{24} := 1mm$

$s3s_{25} := 800mm$ $s3s_{26} := 800mm$ $s3s_{27} := 1mm$ $s3s_{28} := 1mm$

$s3s_{29} := 800mm$ $s3s_{30} := 800mm$ $s3s_{31} := 800mm$ $s3s_{32} := 800mm$

$s3s_{33} := 600mm$ $s3s_{34} := 1mm$ $s3s_{35} := 600mm$ $s3s_{36} := 1mm$

$s3s_{37} := 1mm$ $s3s_{38} := 600mm$ $s3s_{39} := 600mm$ $s3s_{40} := 1mm$

$s3s_{41} := 1mm$ $s3s_{42} := 600mm$ $s3s_{43} := 600mm$ $s3s_{44} := 1mm$

$s3s_{45} := 1mm$ $s3s_{46} := 600mm$ $s3s_{47} := 1mm$ $s3s_{48} := 600mm$

$s3s_{49} := 1mm$ $s3s_{50} := 1mm$ $s3s_{51} := 600mm$ $s3s_{52} := 1mm$

$s3s_{53} := 600mm$ $s3s_{54} := 800mm$ $s3s_{55} := 800mm$ $s3s_{56} := 1mm$

$s3s_{57} := 1mm$ $s3s_{58} := 800mm$ $s3s_{59} := 800mm$ $s3s_{60} := 1mm$

$s3s_{61} := 1mm$ $s3s_{62} := 1mm$ $s3s_{63} := 800mm$ $s3s_{64} := 1mm$

$s3s_{65} := 800mm$ $s3s_{66} := 1mm$ $s3s_{67} := 1mm$ $s3s_{68} := 800mm$

$s3s_{69} := 800mm$ $s3s_{70} := 800mm$ $s3s_{71} := 800mm$ $s3s_{72} := 1mm$

$i := n_F$ Iteration Counter

$s3t_i := t_s\left(s3h_{w_i}, s3t_{w_i}, s3h_{f_i}, s3t_{f_i}, s3s_i, s3E_{t_i}\right)$ Smeared Thickness Calculation

$\tau_3 := \frac{1}{n_{F_3}}\left(\sum_{i=1}^{n_{F_3}} s3t_i\right)$ $\tau_3 = 0.023\,m$ Section 3 Average Thickness

$DA_3 := \tau_3 \cdot \sum_{i=1}^{n_{F_3}} s3b_i$ $DA_3 = 1.902\,m^2$ Section 3 Damaged Cross Sectional Area

$DA_{E_3} := \sum_{i=1}^{n_{F_3}} s3b_i \cdot s3t_i$ $DA_{E_3} = .793\,m^2$ Section 3 Exact Damaged Cross Sectional Area

Properties for Section 4 are given as follows:

$n_{T_4} := 39$ Number of "T" intersections for section 4

$n_{L_4} := 4$ Number of Angle Intersections for section 4

$n_{C_4} := 6$ Number of Cruciform Intersections for section 4

$n_{F_4} := 91$ Number of Elements within Section 4

$n_{AT_4} := n_{T_4} + n_{L_4}$ $n_{AT_4} = 43$ Number of "T" and Angle Intersections for section 4

Element Spans within section 4 for elements 1 through 91

$s4b_1 := .3457m$	$s4b_2 := .31m$	$s4b_3 := .3457m$	$s4b_4 := .1531m$
$s4b_5 := .1531m$	$s4b_6 := .7975m$	$s4b_7 := .8m$	$s4b_8 := .7975m$
$s4b_9 := .55m$	$s4b_{10} := .55m$	$s4b_{11} := .7975m$	$s4b_{12} := .8m$
$s4b_{13} := .7975m$	$s4b_{14} := .943m$	$s4b_{15} := .943m$	$s4b_{16} := .7975m$
$s4b_{17} := 3.8m$	$s4b_{18} := .7975m$	$s4b_{19} := 1.2m$	$s4b_{20} := 1.2m$
$s4b_{21} := .7975m$	$s4b_{22} := .7975m$	$s4b_{23} := 1.2m$	$s4b_{24} := 1.2m$
$s4b_{25} := .7975m$	$s4b_{26} := .7975m$	$s4b_{27} := 1.2m$	$s4b_{28} := 1.2m$
$s4b_{29} := .7975m$	$s4b_{30} := .7975m$	$s4b_{31} := 1.2m$	$s4b_{32} := 1.2m$
$s4b_{33} := .669m$	$s4b_{34} := .669m$	$s4b_{35} := 2.82m$	$s4b_{36} := 2.82m$
$s4b_{37} := .247m$	$s4b_{38} := 2.4m$	$s4b_{39} := .247m$	$s4b_{40} := 1.2m$
$s4b_{41} := 1.2m$	$s4b_{42} := .9852m$	$s4b_{43} := .9852m$	$s4b_{44} := 1.2m$
$s4b_{45} := 1.2m$	$s4b_{46} := .9881m$	$s4b_{47} := .9881m$	$s4b_{48} := 1.2m$
$s4b_{49} := 1.2m$	$s4b_{50} := .7411m$	$s4b_{51} := .7411m$	$s4b_{52} := 1.085m$
$s4b_{53} := 1.085m$	$s4b_{54} := .9259m$	$s4b_{55} := .75m$	$s4b_{56} := .9259m$
$s4b_{57} := .542m$	$s4b_{58} := .542m$	$s4b_{59} := .9253m$	$s4b_{60} := .75m$
$s4b_{61} := .9253m$	$s4b_{62} := .7692m$	$s4b_{63} := 0m$	$s4b_{64} := .7692m$

$s4b_{65} := .657m$ $s4b_{66} := .657m$ $s4b_{67} := 1.538m$ $s4b_{68} := 0m$

$s4b_{69} := 1.538m$ $s4b_{70} := 1.2m$ $s4b_{71} := 1.2m$ $s4b_{72} := 1.538m$

$s4b_{73} := 1.538m$ $s4b_{74} := 0m$ $s4b_{75} := 0m$ $s4b_{76} := 1.2m$

$s4b_{77} := 1.2m$ $s4b_{78} := 1.538m$ $s4b_{79} := 1.538m$ $s4b_{80} := .25m$

$s4b_{81} := 1.4m$ $s4b_{82} := 1.2m$ $s4b_{83} := 1.2m$ $s4b_{84} := 1.538m$

$s4b_{85} := 1.538m$ $s4b_{86} := 1.2m$ $s4b_{87} := 1.2m$ $s4b_{88} := .7692m$

$s4b_{89} := .7692m$ $s4b_{90} := 6.57m$ $s4b_{91} := 6.57m$

Element Plate Thicknesses within section 4 for elements 1 through 91

$s4E_{t_1} := 18mm$ $s4E_{t_2} := 12mm$ $s4E_{t_3} := 18mm$ $s4E_{t_4} := 15mm$

$s4E_{t_5} := 15mm$ $s4E_{t_6} := 18mm$ $s4E_{t_7} := 12mm$ $s4E_{t_8} := 18mm$

$s4E_{t_9} := 15mm$ $s4E_{t_{10}} := 15mm$ $s4E_{t_{11}} := 18mm$ $s4E_{t_{12}} := 12mm$

$s4E_{t_{13}} := 18mm$ $s4E_{t_{14}} := 15mm$ $s4E_{t_{15}} := 15mm$ $s4E_{t_{16}} := 18mm$

$s4E_{t_{17}} := 12mm$ $s4E_{t_{18}} := 18mm$ $s4E_{t_{19}} := 15mm$ $s4E_{t_{20}} := 15mm$

$s4E_{t_{21}} := 18mm$ $s4E_{t_{22}} := 18mm$ $s4E_{t_{23}} := 15mm$ $s4E_{t_{24}} := 15mm$

$s4E_{t_{25}} := 18mm$ $s4E_{t_{26}} := 18mm$ $s4E_{t_{27}} := 15mm$ $s4E_{t_{28}} := 15mm$

$s4E_{t_{29}} := 18mm$ $s4E_{t_{30}} := 18mm$ $s4E_{t_{31}} := 15mm$ $s4E_{t_{32}} := 15mm$

$s4E_{t_{33}} := 18mm$ $s4E_{t_{34}} := 18mm$ $s4E_{t_{35}} := 13mm$ $s4E_{t_{36}} := 13mm$

$s4E_{t_{37}} := 18mm$ $s4E_{t_{38}} := 12mm$ $s4E_{t_{39}} := 18mm$ $s4E_{t_{40}} := 15mm$

$s4E_{t_{41}} := 15mm$ $s4E_{t_{42}} := 33mm$ $s4E_{t_{43}} := 33mm$ $s4E_{t_{44}} := 15mm$

$s4E_{t_{45}} := 15mm$ $s4E_{t_{46}} := 33mm$ $s4E_{t_{47}} := 33mm$ $s4E_{t_{48}} := 15mm$

$s4E_{t_{49}} := 15mm$ $s4E_{t_{50}} := 33mm$ $s4E_{t_{51}} := 33mm$ $s4E_{t_{52}} := 15mm$

$s4E_{t_{53}} := 15mm$ $s4E_{t_{54}} := 33mm$ $s4E_{t_{55}} := 12mm$ $s4E_{t_{56}} := 33mm$

$s4E_{t_{57}} := 15mm$ $s4E_{t_{58}} := 15mm$ $s4E_{t_{59}} := 33mm$ $s4E_{t_{60}} := 12mm$

$s4E_{t_{61}} := 33mm$ $s4E_{t_{62}} := 16mm$ $s4E_{t_{63}} := 12mm$ $s4E_{t_{64}} := 16mm$

$s4E_{t_{65}} := 15mm$ $s4E_{t_{66}} := 15mm$ $s4E_{t_{67}} := 16mm$ $s4E_{t_{68}} := 12mm$

$s4E_{t_{69}} := 16mm$ $s4E_{t_{70}} := 15mm$ $s4E_{t_{71}} := 15mm$ $s4E_{t_{72}} := 16mm$

$s4E_{t_{73}} := 16mm$ $s4E_{t_{74}} := 25mm$ $s4E_{t_{75}} := 25mm$ $s4E_{t_{76}} := 15mm$

$s4E_{t_{77}} := 15mm$ $s4E_{t_{78}} := 16mm$ $s4E_{t_{79}} := 16mm$ $s4E_{t_{80}} := 25mm$

$s4E_{t_{81}} := 12mm$ $s4E_{t_{82}} := 15mm$ $s4E_{t_{83}} := 15mm$ $s4E_{t_{84}} := 16mm$

$s4E_{t_{85}} := 16mm$ $s4E_{t_{86}} := 15mm$ $s4E_{t_{87}} := 15mm$ $s4E_{t_{88}} := 16mm$

$s4E_{t_{89}} := 16mm$ $s4E_{t_{90}} := 13mm$ $s4E_{t_{91}} := 13mm$

Element Web heights within section 4 on elements 1 through 91

$s4h_{w_1} := 450mm$ $s4h_{w_2} := 0mm$ $s4h_{w_3} := 450mm$ $s4h_{w_4} := 0mm$

$s4h_{w_5} := 0mm$ $s4h_{w_6} := 450mm$ $s4h_{w_7} := 0mm$ $s4h_{w_8} := 450mm$

$s4h_w := 0mm$ $s4h_{w_{10}} := 0mm$ $s4h_{w_{11}} := 450mm$ $s4h_{w_{12}} := 0mm$

$s4h_{w_{13}} := 450mm$ $s4h_{w_{14}} := 0mm$ $s4h_{w_{15}} := 0mm$ $s4h_{w_{16}} := 450mm$

$s4h_{w_{17}} := 0mm$ $s4h_{w_{18}} := 450mm$ $s4h_{w_{19}} := 0mm$ $s4h_{w_{20}} := 0mm$

$s4h_{w_{21}} := 450mm$ $s4h_{w_{22}} := 450mm$ $s4h_{w_{23}} := 0mm$ $s4h_{w_{24}} := 0mm$

$s4h_{w_{25}} := 450mm$ $s4h_{w_{26}} := 450mm$ $s4h_{w_{27}} := 0mm$ $s4h_{w_{28}} := 0mm$

$s4h_{w_{29}} := 450mm$ $s4h_{w_{30}} := 450mm$ $s4h_{w_{31}} := 0mm$ $s4h_{w_{32}} := 0mm$

$s4h_{w_{33}} := 450mm$ $s4h_{w_{34}} := 450mm$ $s4h_{w_{35}} := 250mm$ $s4h_{w_{36}} := 250mm$

$s4h_{w_{37}} := 400mm$ $s4h_{w_{38}} := 0mm$ $s4h_{w_{39}} := 400mm$ $s4h_{w_{40}} := 0mm$

$s4h_{w_{41}} := 0mm$ $s4h_{w_{42}} := 400mm$ $s4h_{w_{43}} := 400mm$ $s4h_{w_{44}} := 0mm$

$s4h_{w_{45}} := 0mm$ $s4h_{w_{46}} := 400mm$ $s4h_{w_{47}} := 400mm$ $s4h_{w_{48}} := 0mm$

$s4h_{w_{49}} := 0mm$ $s4h_{w_{50}} := 400mm$ $s4h_{w_{51}} := 400mm$ $s4h_{w_{52}} := 0mm$

$s4h_{w_{53}} := 0mm$ $s4h_{w_{54}} := 400mm$ $s4h_{w_{55}} := 0mm$ $s4h_{w_{56}} := 400mm$

$s4h_{w_{57}} := 0mm$ $s4h_{w_{58}} := 0mm$ $s4h_{w_{59}} := 400mm$ $s4h_{w_{60}} := 0mm$

$s4h_{w_{61}} := 400mm$ $s4h_{w_{62}} := 350mm$ $s4h_{w_{63}} := 0mm$ $s4h_{w_{64}} := 350mm$

$s4h_{w_{65}} := 0mm$ $s4h_{w_{66}} := 0mm$ $s4h_{w_{67}} := 350mm$ $s4h_{w_{68}} := 0mm$

$s4h_{w_{69}} := 350mm$ $s4h_{w_{70}} := 0mm$ $s4h_{w_{71}} := 0mm$ $s4h_{w_{72}} := 350mm$

$s4h_{w_{73}} := 350mm$ $s4h_{w_{74}} := 0mm$ $s4h_{w_{75}} := 0mm$ $s4h_{w_{76}} := 0mm$

$s4h_{w_{77}} := 0mm$ $s4h_{w_{78}} := 350mm$ $s4h_{w_{79}} := 350mm$ $s4h_{w_{80}} := 0mm$

$s4h_{w_{81}} := 0mm$ $s4h_{w_{82}} := 0mm$ $s4h_{w_{83}} := 0mm$ $s4h_{w_{84}} := 350mm$

$s4h_{w_{85}} := 350mm$ $s4h_{w_{86}} := 0mm$ $s4h_{w_{87}} := 0mm$ $s4h_{w_{88}} := 350mm$

$s4h_{w_{89}} := 350mm$ $s4h_{w_{90}} := 250mm$ $s4h_{w_{91}} := 250mm$

Element Web thickness within section 4 on elements 1 through 91

$s4t_{w_1} := 12mm$ $s4t_{w_2} := 0mm$ $s4t_{w_3} := 12mm$ $s4t_{w_4} := 0mm$

$s4t_{w_5} := 0mm$ $s4t_{w_6} := 12mm$ $s4t_{w_7} := 0mm$ $s4t_{w_8} := 12mm$

$s4t_{w_9} := 0mm$ $s4t_{w_{10}} := 0mm$ $s4t_{w_{11}} := 12mm$ $s4t_{w_{12}} := 0mm$

$s4t_{w_{13}} := 12mm$ $s4t_{w_{14}} := 0mm$ $s4t_{w_{15}} := 0mm$ $s4t_{w_{16}} := 12mm$

$s4t_{w_{17}} := 0mm$ $s4t_{w_{18}} := 12mm$ $s4t_{w_{19}} := 0mm$ $s4t_{w_{20}} := 0mm$

$s4t_{w_{21}} := 12mm$ $s4t_{w_{22}} := 12mm$ $s4t_{w_{23}} := 0mm$ $s4t_{w_{24}} := 0mm$

$s4t_{w_{25}} := 12mm$ $s4t_{w_{26}} := 12mm$ $s4t_{w_{27}} := 0mm$ $s4t_{w_{28}} := 0mm$

$s4t_{w_{29}} := 12mm$ $s4t_{w_{30}} := 12mm$ $s4t_{w_{31}} := 0mm$ $s4t_{w_{32}} := 0mm$

$s4t_{w_{33}} := 12mm$ $s4t_{w_{34}} := 12mm$ $s4t_{w_{35}} := 12mm$ $s4t_{w_{36}} := 12mm$

$19mm$ $s4t_{w_{38}} := 0mm$ $s4t_{w_{39}} := 19mm$ $s4t_{w_{40}} := 0mm$

$s4t_{w_{41}} := 0mm$ $s4t_{w_{42}} := 19mm$ $s4t_{w_{43}} := 19mm$ $s4t_{w_{44}} := 0mm$

$s4t_{w_{45}} := 0mm$ $s4t_{w_{46}} := 19mm$ $s4t_{w_{47}} := 19mm$ $s4t_{w_{48}} := 0mm$

$s4t_{w_{49}} := 0mm$ $s4t_{w_{50}} := 19mm$ $s4t_{w_{51}} := 19mm$ $s4t_{w_{52}} := 0mm$

$s4t_{w_{53}} := 0mm$ $s4t_{w_{54}} := 19mm$ $s4t_{w_{55}} := 0mm$ $s4t_{w_{56}} := 19mm$

$s4t_{w_{57}} := 0mm$ $s4t_{w_{58}} := 0mm$ $s4t_{w_{59}} := 19mm$ $s4t_{w_{60}} := 0mm$

$s4t_{w_{61}} := 19mm$ $s4t_{w_{62}} := 12mm$ $s4t_{w_{63}} := 0mm$ $s4t_{w_{64}} := 12mm$

$s4t_{w_{65}} := 0mm$ $s4t_{w_{66}} := 0mm$ $s4t_{w_{67}} := 12mm$ $s4t_{w_{68}} := 0mm$

$s4t_{w_{69}} := 12mm$ $s4t_{w_{70}} := 0mm$ $s4t_{w_{71}} := 0mm$ $s4t_{w_{72}} := 12mm$

$s4t_{w_{73}} := 12mm$ $s4t_{w_{74}} := 0mm$ $s4t_{w_{75}} := 0mm$ $s4t_{w_{76}} := 0mm$

$s4t_{w_{77}} := 0mm$ $s4t_{w_{78}} := 12mm$ $s4t_{w_{79}} := 12mm$ $s4t_{w_{80}} := 0mm$

$s4t_{w_{81}} := 0mm$ $s4t_{w_{82}} := 0mm$ $s4t_{w_{83}} := 0mm$ $s4t_{w_{84}} := 12mm$

$s4t_{w_{85}} := 12mm$ $s4t_{w_{86}} := 0mm$ $s4t_{w_{87}} := 0mm$ $s4t_{w_{88}} := 12mm$

$s4t_{w_{89}} := 12mm$ $s4t_{w_{90}} := 12mm$ $s4t_{w_{91}} := 12mm$

Element Flange Span within Section 4 on elements 1 through 91

$s4h_{f_1} := 150mm$ $s4h_{f_2} := 0mm$ $s4h_{f_3} := 150mm$ $s4h_{f_4} := 0mm$

$s4h_{f_5} := 0mm$ $s4h_{f_6} := 150mm$ $s4h_{f_7} := 0mm$ $s4h_{f_8} := 150mm$

$s4h_{f_9} := 0mm$ $s4h_{f_{10}} := 0mm$ $s4h_{f_{11}} := 150mm$ $s4h_{f_{12}} := 0mm$

$s4h_{f_{13}} := 150mm$ $s4h_{f_{14}} := 0mm$ $s4h_{f_{15}} := 0mm$ $s4h_{f_{16}} := 150mm$

$s4h_{f_{17}} := 0mm$ $s4h_{f_{18}} := 150mm$ $s4h_{f_{19}} := 0mm$ $s4h_{f_{20}} := 0mm$

$s4h_{f_{21}} := 150mm$ $s4h_{f_{22}} := 150mm$ $s4h_{f_{23}} := 0mm$ $s4h_{f_{24}} := 0mm$

$s4h_{f_{25}} := 150mm$ $s4h_{f_{26}} := 150mm$ $s4h_{f_{27}} := 0mm$ $s4h_{f_{28}} := 0mm$

$s4h_{f_{29}} := 150mm$ $s4h_{f_{30}} := 150mm$ $s4h_{f_{31}} := 0mm$ $s4h_{f_{32}} := 0mm$

$s4h_{f_{33}} := 150mm$ $s4h_{f_{34}} := 150mm$ $s4h_{f_{35}} := 90mm$ $s4h_{f_{36}} := 90mm$

$s4h_{f_{37}} := 100mm$ $s4h_{f_{38}} := 0mm$ $s4h_{f_{39}} := 100mm$ $s4h_{f_{40}} := 0mm$

$s4h_{f_{41}} := 0mm$ $s4h_{f_{42}} := 100mm$ $s4h_{f_{43}} := 100mm$ $s4h_{f_{44}} := 0mm$

$s4h_{f_{45}} := 0mm$ $s4h_{f_{46}} := 100mm$ $s4h_{f_{47}} := 100mm$ $s4h_{f_{48}} := 0mm$

$s4h_{f_{49}} := 0mm$ $s4h_{f_{50}} := 100mm$ $s4h_{f_{51}} := 100mm$ $s4h_{f_{52}} := 0mm$

$s4h_{f_{53}} := 0mm$ $s4h_{f_{54}} := 100mm$ $s4h_{f_{55}} := 0mm$ $s4h_{f_{56}} := 100mm$

$s4h_{f_{57}} := 0mm$ $s4h_{f_{58}} := 0mm$ $s4h_{f_{59}} := 100mm$ $s4h_{f_{60}} := 0mm$

$s4h_{f_{61}} := 100mm$ $s4h_{f_{62}} := 100mm$ $s4h_{f_{63}} := 0mm$ $s4h_{f_{64}} := 100mm$

$s4h_{f_{65}} := 0mm$ $s4h_{f_{66}} := 0mm$ $s4h_{f_{67}} := 100mm$ $s4h_{f_{68}} := 0mm$

$s4h_{f_{69}} := 100mm$ $s4h_{f_{70}} := 0mm$ $s4h_{f_{71}} := 0mm$ $s4h_{f_{72}} := 100mm$

$s4h_{f_{73}} := 100mm$ $s4h_{f_{74}} := 0mm$ $s4h_{f_{75}} := 0mm$ $s4h_{f_{76}} := 0mm$

$s4h_{f_{77}} := 0mm$ $s4h_{f_{78}} := 100mm$ $s4h_{f_{79}} := 100mm$ $s4h_{f_{80}} := 0mm$

$s4h_{f_{81}} := 0mm$ $s4h_{f_{82}} := 0mm$ $s4h_{f_{83}} := 0mm$ $s4h_{f_{84}} := 100mm$

$s4h_{f_{85}} := 100mm$ $s4h_{f_{86}} := 0mm$ $s4h_{f_{87}} := 0mm$ $s4h_{f_{88}} := 100mm$

$s4h_{f_{89}} := 100mm$ $s4h_{f_{90}} := 90mm$ $s4h_{f_{91}} := 90mm$

Element Flange Thickness within section 4 elements 1 through 91

$s4t_{f_1} := 16mm$ $s4t_{f_2} := 0mm$ $s4t_{f_3} := 16mm$ $s4t_{f_4} := 0mm$

$s4t_{f_5} := 0mm$ $s4t_{f_6} := 16mm$ $s4t_{f_7} := 0mm$ $s4t_{f_8} := 16mm$

$s4t_{f_9} := 0mm$ $s4t_{f_{10}} := 0mm$ $s4t_{f_{11}} := 16mm$ $s4t_{f_{12}} := 0mm$

$s4t_{f_{13}} := 16mm$ $s4t_{f_{14}} := 0mm$ $s4t_{f_{15}} := 0mm$ $s4t_{f_{16}} := 16mm$

$s4t_{f_{17}} := 0mm$ $s4t_{f_{18}} := 16mm$ $s4t_{f_{19}} := 0mm$ $s4t_{f_{20}} := 0mm$

$s4t_{f_{21}} := 16mm$ $s4t_{f_{22}} := 16mm$ $s4t_{f_{23}} := 0mm$ $s4t_{f_{24}} := 0mm$

$s4t_{f_{25}} := 16mm$ $s4t_{f_{26}} := 16mm$ $s4t_{f_{27}} := 0mm$ $s4t_{f_{28}} := 0mm$

$s4t_{f_{29}} := 16mm$ $s4t_{f_{30}} := 16mm$ $s4t_{f_{31}} := 0mm$ $s4t_{f_{32}} := 0mm$

$s4t_{f_{33}} := 16mm$ $s4t_{f_{34}} := 16mm$ $s4t_{f_{35}} := 16mm$ $s4t_{f_{36}} := 16mm$

$s4t_{f_{37}} := 19mm$ $s4t_{f_{38}} := 0mm$ $s4t_{f_{39}} := 19mm$ $s4t_{f_{40}} := 0mm$

$s4t_{f_{41}} := 0mm$ $s4t_{f_{42}} := 19mm$ $s4t_{f_{43}} := 19mm$ $s4t_{f_{44}} := 0mm$

$s4t_{f_{45}} := 0mm$ $s4t_{f_{46}} := 19mm$ $s4t_{f_{47}} := 19mm$ $s4t_{f_{48}} := 0mm$

$s4t_{f_{49}} := 0mm$ $s4t_{f_{50}} := 19mm$ $s4t_{f_{51}} := 19mm$ $s4t_{f_{52}} := 0mm$

$s4t_{f_{53}} := 0mm$ $s4t_{f_{54}} := 19mm$ $s4t_{f_{55}} := 0mm$ $s4t_{f_{56}} := 19mm$

$s4t_{f_{57}} := 0mm$ $s4t_{f_{58}} := 0mm$ $s4t_{f_{59}} := 19mm$ $s4t_{f_{60}} := 0mm$

$s4t_{f_{61}} := 19mm$ $s4t_{f_{62}} := 17mm$ $s4t_{f_{63}} := 0mm$ $s4t_{f_{64}} := 17mm$

$s4t_{f_{65}} := 0mm$ $s4t_{f_{66}} := 0mm$ $s4t_{f_{67}} := 17mm$ $s4t_{f_{68}} := 0mm$

$s4t_{f_{69}} := 17mm$ $s4t_{f_{70}} := 0mm$ $s4t_{f_{71}} := 0mm$ $s4t_{f_{72}} := 17mm$

$s4t_{f_{73}} := 17mm$ $s4t_{f_{74}} := 0mm$ $s4t_{f_{75}} := 0mm$ $s4t_{f_{76}} := 0mm$

$s4t_{f_{77}} := 0mm$ $s4t_{f_{78}} := 17mm$ $s4t_{f_{79}} := 17mm$ $s4t_{f_{80}} := 0mm$

$s4t_{f_{81}} := 0mm$ $s4t_{f_{82}} := 0mm$ $s4t_{f_{83}} := 0mm$ $s4t_{f_{84}} := 17mm$

$s4t_{f_{85}} := 17mm$ $s4t_{f_{86}} := 0mm$ $s4t_{f_{87}} := 0mm$ $s4t_{f_{88}} := 17mm$

$s4t_{f_{89}} := 17mm$ $s4t_{f_{90}} := 16mm$ $s4t_{f_{91}} := 16mm$

Element Stiffener Spacing within section 4 elements 1 through 91

$s4s_1 := 800mm$ $s4s_2 := 1mm$ $s4s_3 := 800mm$ $s4s_4 := 1mm$

$s4s_5 := 1mm$ $s4s_6 := 800mm$ $s4s_7 := 1mm$ $s4s_8 := 800mm$

$s4s_9 := 1mm$ $s4s_{10} := 1mm$ $s4s_{11} := 800mm$ $s4s_{12} := 1mm$

$s4s_{13} := 800mm$ $s4s_{14} := 1mm$ $s4s_{15} := 1mm$ $s4s_{16} := 800mm$

$s4s_{17} := 1mm$ $s4s_{18} := 800mm$ $s4s_{19} := 1mm$ $s4s_{20} := 1mm$

$s4s_{21} := 800mm$ $s4s_{22} := 800mm$ $s4s_{23} := 1mm$ $s4s_{24} := 1mm$

$s4s_{25} := 800mm$ $s4s_{26} := 800mm$ $s4s_{27} := 1mm$ $s4s_{28} := 1mm$

$s4s_{29} := 800mm$ $s4s_{30} := 800mm$ $s4s_{31} := 1mm$ $s4s_{32} := 1mm$

$s4s_{33} := 800mm$ $s4s_{34} := 800mm$ $s4s_{35} := 800mm$ $s4s_{36} := 800mm$

$s4s_{37} := 600mm$ $s4s_{38} := 1mm$ $s4s_{39} := 600mm$ $s4s_{40} := 1mm$

$s4s_{41} := 1mm$ $s4s_{42} := 600mm$ $s4s_{43} := 600mm$ $s4s_{44} := 1mm$

$s4s_{45} := 1mm$ $s4s_{46} := 600mm$ $s4s_{47} := 600mm$ $s4s_{48} := 1mm$

$s4s_{49} := 1mm$ $s4s_{50} := 600mm$ $s4s_{51} := 600mm$ $s4s_{52} := 1mm$

$s4s_{53} := 1mm$ $s4s_{54} := 600mm$ $s4s_{55} := 1mm$ $s4s_{56} := 600mm$

$s4s_{57} := 1mm$ $s4s_{58} := 1mm$ $s4s_{59} := 600mm$ $s4s_{60} := 1mm$

$s4s_{61} := 600mm$ $s4s_{62} := 800mm$ $s4s_{63} := 1mm$ $s4s_{64} := 800mm$

$s4s_{65} := 1mm$ $s4s_{66} := 1mm$ $s4s_{67} := 800mm$ $s4s_{68} := 1mm$

$s4s_{69} := 800mm$ $s4s_{70} := 1mm$ $s4s_{71} := 1mm$ $s4s_{72} := 800mm$

$s4s_{73} := 800mm$ $s4s_{74} := 1mm$ $s4s_{75} := 1mm$ $s4s_{76} := 1mm$

$s4s_{77} := 1mm$ $s4s_{78} := 800mm$ $s4s_{79} := 800mm$ $s4s_{80} := 1mm$

$s4s_{81} := 1mm$ $s4s_{82} := 1mm$ $s4s_{83} := 1mm$ $s4s_{84} := 800mm$

$s4s_{85} := 800mm$ $s4s_{86} := 1mm$ $s4s_{87} := 1mm$ $s4s_{88} := 800mm$

$s4s_{89} := 800mm$ $s4s_{90} := 800mm$ $s4s_{91} := 800mm$

$i := 1 .. n_{F_4}$ Iteration Counter

$s4t_{s_i} := t_s\left(s4h_{w_i}, s4t_{w_i}, s4h_{f_i}, s4t_{f_i}, s4s_i, s4E_{t_i}\right)$ Smeared Thickness Calculation

$\tau_4 := \frac{1}{n_{F_4}}\left(\sum_{i=1}^{n_{F_4}} s4t_{s_i}\right)$ $\tau_4 = 0.023\,m$ Section 4 Average Thickness

$DA_4 := \tau_4 \cdot \sum_{i=1}^{n_{F_4}} s4b_i$ $DA_4 = 2.248\,m^2$ Section 4 Damaged Cross Sectional Area

$DA_{E_4} := \sum_{i=1}^{n_{F_4}} s4b_i \cdot s4t_{s_i}$ $DA_{E_4} = 2.1\,m^2$ Section 4 Exact Damaged Cross Sectional Area

Properties for **Section 5** are given as follows:

$n_{T_5} := 41$ Number of "T" intersections for section 5

$n_{L_5} := 4$ Number of Angle Intersections for section 5

$n_{C_5} := 3$ Number of Cruciform Intersections for section 5

$n_{F_5} := 91$ Number of Elements within Section 5

$n_{AT_5} := n_{T_5} + n_{L_5}$ $n_{AT_5} = 45$ Number of "T" and Angle Intersections for section 5

Element Spans within section 5 for elements 1 through 91

$s5b_1 := .0748m$ $s5b_2 := .065m$ $s5b_3 := .0748m$ $s5b_4 := 0m$

$s5b_5 := 0m$ $s5b_6 := .9212m$ $s5b_7 := .8m$ $s5b_8 := .9212m$

$s5b_9 := .4937m$ $s5b_{10} := .4937m$ $s5b_{11} := .9212m$ $s5b_{12} := .8m$

$s5b_{13} := .9212m$ $s5b_{14} := 1.2m$ $s5b_{15} := 1.2m$ $s5b_{16} := .9212m$

$s5b_{17} := 4.6m$ $s5b_{18} := .9212m$ $s5b_{19} := 1.2m$ $s5b_{20} := 1.2m$

$s5b_{21} := .9212m$ $s5b_{22} := .9212m$ $s5b_{23} := 1.2m$ $s5b_{24} := 1.2m$

$s5b_{25} := .9212m$ $s5b_{26} := .9212m$ $s5b_{27} := 1.2m$ $s5b_{28} := 1.2m$

$s5b_{29} := .9212m$ $s5b_{30} := .9212m$ $s5b_{31} := 0m$ $s5b_{32} := 0m$

$s5b_{33} := 1.612m$ $s5b_{34} := 1.612m$ $s5b_{35} := 3.567m$ $s5b_{36} := 3.567m$

$s5b_{37} := 1.2612m$ $s5b_{38} := 3.15m$ $s5b_{39} := 1.2612m$ $s5b_{40} := 0m$

$s5b_{41} := 0m$ $s5b_{42} := 1.009m$ $s5b_{43} := 1.009m$ $s5b_{44} := 0m$

$s5b_{45} := 0m$ $s5b_{46} := .7569m$ $s5b_{47} := .7569m$ $s5b_{48} := 1.2m$

$s5b_{49} := 1.2m$ $s5b_{50} := .9463m$ $s5b_{51} := .9463m$ $s5b_{52} := 1.2m$

$s5b_{53} := 1.2m$ $s5b_{54} := .9463m$ $s5b_{55} := .75m$ $s5b_{56} := .9463m$

$s5b_{57} := .577m$ $s5b_{58} := .577m$ $s5b_{59} := .9463m$ $s5b_{60} := .75m$

$s5b_{61} := .9463m$ $s5b_{62} := 1.1118m$ $s5b_{63} := 0m$ $s5b_{64} := 1.1118m$

$s5b_{65} := .936m$ $s5b_{66} := .936m$ $s5b_{67} := 1.4807m$ $s5b_{68} := 0m$

$s5b_{69} := 1.4807m$ $s5b_{70} := 1.2m$ $s5b_{71} := 1.2m$ $s5b_{72} := 1.4807m$

$s5b_{73} := 1.4807m$ $s5b_{74} := 0m$ $s5b_{75} := 0m$ $s5b_{76} := 1.2m$

$s5b_{77} := 1.2m$ $s5b_{78} := 1.4807m$ $s5b_{79} := 1.4807m$ $s5b_{80} := .25m$

$s5b_{81} := 1.4m$ $s5b_{82} := 1.2m$ $s5b_{83} := 1.2m$ $s5b_{84} := 1.4807m$

$s5b_{85} := 1.4807m$ $s5b_{86} := 0m$ $s5b_{87} := 0m$ $s5b_{88} := 2.2219m$

$s5b_{89} := 2.2219m$ $s5b_{90} := 7.79m$ $s5b_{91} := 7.79m$

$i := 1 .. n_{F_5}$ Iteration Counter

Element Plate Thicknesses within section 5 for elements 1 through 91

$s5E_{t_i} := s4E_{t_i}$

Element Web heights within section 5 on elements 1 through 91

$s5h_{w_i} := s4h_{w_i}$

Element Web thickness within section 5 on elements 1 through 91

$s5t_{w_i} := s4t_{w_i}$

Element Flange Span within Section 5 on elements 1 through 91

$s5h_{f_i} := s4h_{f_i}$

Element Flange Thickness within section 5 elements 1 through 91

$s5t_{f_i} := s4t_{f_i}$

Element Stiffener Spacing within section 4 elements 1 through 91

$s5s_i := s4s_i$

$s5t_{s_i} := t_s\left(s5h_{w_i}, s5t_{w_i}, s5h_{f_i}, s5t_{f_i}, s5s_i, s5E_{t_i}\right)$ Smeared Thickness Calculation

$\tau_5 := \frac{1}{n_{F_5}}\left(\sum_{i=1}^{n_{F_5}} s5t_{s_i}\right)$ $\tau_5 = 0.023\,m$ Section 5 Average Thickness

$DA_5 := \tau_5 \cdot \sum_{i=1}^{n_{F_5}} s5b_i$ $DA_5 = 2.348\,m^2$ Section 5 Damaged Cross Sectional Area

$DA_{E_5} := \sum_{i=1}^{n_{F_5}} s5b_i \cdot s5t_{s_i}$ $DA_{E_5} = 2.277\,m^2$ Section 5 Exact Damaged Cross Sectional Area

Properties for **Section 6** are given as follows:

$n_{T_6} := 51$ Number of "T" intersections for section 6

$n_{L_6} := 4$ Number of Angle Intersections for section 6

$n_{C_6} := 3$ Number of Cruciform Intersections for section 6

$n_{F_6} := 57$ Number of Elements within Section 6

$n_{AT_6} := n_{T_6} + n_{L_6}$ $n_{AT_6} = 55$ Number of "T" and Angle Intersections for section 6

Element Spans within section 6 for elements 1 through 57

$s6b_1 := .9477m$	$s6b_2 := 0.8m$	$s6b_3 := .9477m$	$s6b_4 := .508m$
$s6b_5 := .508m$	$s6b_6 := .9477m$	$s6b_7 := .8m$	$s6b_8 := .9477m$
$s6b_9 := 1.2m$	$s6b_{10} := 1.2m$	$s6b_{11} := 6.185m$	$s6b_{12} := 5.22m$
$s6b_{13} := 6.185m$	$s6b_{14} := 4.333m$	$s6b_{15} := 4.333m$	$s6b_{16} := 4.038m$
$s6b_{17} := 3.15m$	$s6b_{18} := 4.038m$	$s6b_{19} := 1.2m$	$s6b_{20} := 1.2m$
$s6b_{21} := .9617m$	$s6b_{22} := .9617m$	$s6b_{23} := 1.2m$	$s6b_{24} := 1.2m$
$s6b_{25} := .9617m$	$s6b_{26} := .9617m$	$s6b_{27} := .602m$	$s6b_{28} := .602m$

$s6b_{29} := .9617m$ $s6b_{30} := .75m$ $s6b_{31} := .9617m$ $s6b_{32} := 1.4422m$

$s6b_{33} := 0m$ $s6b_{34} := 1.4422m$ $s6b_{35} := 1.2m$ $s6b_{36} := 1.2m$

$s6b_{37} := 1.4422m$ $s6b_{38} := 0m$ $s6b_{39} := 1.4422m$ $s6b_{40} := 0m$

$s6b_{41} := 0m$ $s6b_{42} := 1.2m$ $s6b_{43} := 1.2m$ $s6b_{44} := 1.4422m$

$s6b_{45} := 1.4422m$ $s6b_{46} := 1.2m$ $s6b_{47} := 1.2m$ $s6b_{48} := 1.4422m$

$s6b_{49} := 1.4422m$ $s6b_{50} := 2.4m$ $s6b_{51} := 2.4m$ $s6b_{52} := 5.05m$

$s6b_{53} := 5.05m$ $s6b_{54} := .25m$ $s6b_{55} := 1.4m$ $s6b_{56} := 9.005m$

$s6b_{57} := 9.005m$

Element Plate Thicknesses within section 6 for elements 1 through 57

$s6E_{t_1} := 18mm$ $s6E_{t_2} := 12mm$ $s6E_{t_3} := 18mm$ $s6E_{t_4} := 15mm$

$s6E_{t_5} := 15mm$ $s6E_{t_6} := 18mm$ $s6E_{t_7} := 12mm$ $s6E_{t_8} := 18mm$

$s6E_{t_9} := 15mm$ $s6E_{t_{10}} := 15mm$ $s6E_{t_{11}} := 18mm$ $s6E_{t_{12}} := 12mm$

$s6E_{t_{13}} := 18mm$ $s6E_{t_{14}} := 13mm$ $s6E_{t_{15}} := 13mm$ $s6E_{t_{16}} := 33mm$

$s6E_{t_{17}} := 12mm$ $s6E_{t_{18}} := 33mm$ $s6E_{t_{19}} := 15mm$ $s6E_{t_{20}} := 15mm$

$s6E_{t_{21}} := 33mm$ $s6E_{t_{22}} := 33mm$ $s6E_{t_{23}} := 15mm$ $s6E_{t_{24}} := 15mm$

$s6E_{t_{25}} := 33mm$ $s6E_{t_{26}} := 33mm$ $s6E_{t_{27}} := 15mm$ $s6E_{t_{28}} := 15mm$

$s6E_{t_{29}} := 33mm$ $s6E_{t_{30}} := 12mm$ $s6E_{t_{31}} := 33mm$ $s6E_{t_{32}} := 16mm$

$s6E_{t_{33}} := 12mm$ $s6E_{t_{34}} := 16mm$ $s6E_{t_{35}} := 15mm$ $s6E_{t_{36}} := 15mm$

$s6E_{t_{37}} := 16mm$ $s6E_{t_{38}} := 12mm$ $s6E_{t_{39}} := 16mm$ $s6E_{t_{40}} := 25mm$

$s6E_{t_{41}} := 25mm$ $s6E_{t_{42}} := 15mm$ $s6E_{t_{43}} := 15mm$ $s6E_{t_{44}} := 16mm$

$s6E_{t_{45}} := 16mm$ $s6E_{t_{46}} := 15mm$ $s6E_{t_{47}} := 15mm$ $s6E_{t_{48}} := 16mm$

$s6E_{t_{49}} := 16mm$ $s6E_{t_{50}} := 15mm$ $s6E_{t_{51}} := 15mm$ $s6E_{t_{52}} := 16mm$

$s6E_{t_{53}} := 16mm$ $s6E_{t_{54}} := 25mm$ $s6E_{t_{55}} := 12mm$ $s6E_{t_{56}} := 13mm$

$s6E_{t_{57}} := 13mm$

Element Web heights within section 6 on elements 1 through 57

$s6h_{w_1} := 450mm$ $s6h_{w_2} := 0mm$ $s6h_{w_3} := 450mm$ $s6h_{w_4} := 0mm$

$s6h_{w_5} := 0mm$ $s6h_{w_6} := 450mm$ $s6h_{w_7} := 0mm$ $s6h_{w_8} := 450mm$

$s6h_{w_9} := 0mm$ $s6h_{w_{10}} := 0mm$ $s6h_{w_{11}} := 450mm$ $s6h_{w_{12}} := 0mm$

$s6h_{w_{13}} := 450mm$ $s6h_{w_{14}} := 250mm$ $s6h_{w_{15}} := 250mm$ $s6h_{w_{16}} := 400mm$

$s6h_{w_{17}} := 0mm$ $s6h_{w_{18}} := 400mm$ $s6h_{w_{19}} := 0mm$ $s6h_{w_{20}} := 0mm$

$s6h_{w_{21}} := 400mm$ $s6h_{w_{22}} := 400mm$ $s6h_{w_{23}} := 0mm$ $s6h_{w_{24}} := 0mm$

$s6h_{w_{25}} := 400mm$ $s6h_{w_{26}} := 400mm$ $s6h_{w_{27}} := 0mm$ $s6h_{w_{28}} := 0mm$

$s6h_{w_{29}} := 400mm$ $s6h_{w_{30}} := 0mm$ $s6h_{w_{31}} := 400mm$ $s6h_{w_{32}} := 350mm$

$s6h_{w_{33}} := 0mm$ $s6h_{w_{34}} := 350mm$ $s6h_{w_{35}} := 0mm$ $s6h_{w_{36}} := 0mm$

$s6h_{w_{37}} := 350mm$ $s6h_{w_{38}} := 0mm$ $s6h_{w_{39}} := 350mm$ $s6h_{w_{40}} := 0mm$

$s6h_{w_{41}} := 0mm$ $s6h_{w_{42}} := 0mm$ $s6h_{w_{43}} := 0mm$ $s6h_{w_{44}} := 350mm$

$s6h_{w_{45}} := 350mm$ $s6h_{w_{46}} := 0mm$ $s6h_{w_{47}} := 0mm$ $s6h_{w_{48}} := 350mm$

$s6h_{w_{49}} := 350mm$ $s6h_{w_{50}} := 0mm$ $s6h_{w_{51}} := 0mm$ $s6h_{w_{52}} := 350mm$

$s6h_{w_{53}} := 350mm$ $s6h_{w_{54}} := 0mm$ $s6h_{w_{55}} := 0mm$ $s6h_{w_{56}} := 250mm$

$s6h_{w_{57}} := 250mm$

Element Web heights within section 6 on elements 1 through 57

$s6t_{w_1} := 12mm$ $s6t_{w_2} := 0mm$ $s6t_{w_3} := 12mm$ $s6t_{w_4} := 0mm$

$s6t_{w_5} := 0mm$ $s6t_{w_6} := 12mm$ $s6t_{w_7} := 0mm$ $s6t_{w_8} := 12mm$

$s6t_{w_9} := 0mm$ $s6t_{w_{10}} := 0mm$ $s6t_{w_{11}} := 12mm$ $s6t_{w_{12}} := 0mm$

$s6t_{w_{13}} := 12mm$ $s6t_{w_{14}} := 12mm$ $s6t_{w_{15}} := 12mm$ $s6t_{w_{16}} := 19mm$

$s6t_{w_{17}} := 0mm$ $s6t_{w_{18}} := 19mm$ $s6t_{w_{19}} := 0mm$ $s6t_{w_{20}} := 0mm$

$s6t_{w_{21}} := 19mm$ $s6t_{w_{22}} := 19mm$ $s6t_{w_{23}} := 0mm$ $s6t_{w_{24}} := 0mm$

$s6t_{w_{25}} := 19mm$ $s6t_{w_{26}} := 19mm$ $s6t_{w_{27}} := 0mm$ $s6t_{w_{28}} := 0mm$

$s6t_{w_{29}} := 19mm$ $s6t_{w_{30}} := 0mm$ $s6t_{w_{31}} := 19mm$ $s6t_{w_{32}} := 12mm$

$s6t_{w_{33}} := 0mm$ $s6t_{w_{34}} := 12mm$ $s6t_{w_{35}} := 0mm$ $s6t_{w_{36}} := 0mm$

$s6t_{w_{37}} := 12mm$ $s6t_{w_{38}} := 0mm$ $s6t_{w_{39}} := 12mm$ $s6t_{w_{40}} := 0mm$

$s6t_{w_{41}} := 0mm$ $s6t_{w_{42}} := 0mm$ $s6t_{w_{43}} := 0mm$ $s6t_{w_{44}} := 12mm$

$s6t_{w_{45}} := 12mm$ $s6t_{w_{46}} := 0mm$ $s6t_{w_{47}} := 0mm$ $s6t_{w_{48}} := 12mm$

$s6t_{w_{49}} := 12mm$ $s6t_{w_{50}} := 0mm$ $s6t_{w_{51}} := 0mm$ $s6t_{w_{52}} := 12mm$

$s6t_{w_{53}} := 12mm$ $s6t_{w_{54}} := 0mm$ $s6t_{w_{55}} := 0mm$ $s6t_{w_{56}} := 12mm$

$s6t_{w_{57}} := 12mm$

Element Flange Span within Section 6 on elements 1 through 57

$s6h_{f_1} := 150mm$ $s6h_{f_2} := 0mm$ $s6h_{f_3} := 150mm$ $s6h_{f_4} := 0mm$

$s6h_{f_5} := 0mm$ $s6h_{f_6} := 150mm$ $s6h_{f_7} := 0mm$ $s6h_{f_8} := 150mm$

$s6h_{f_9} := 0mm$ $s6h_{f_{10}} := 0mm$ $s6h_{f_{11}} := 150mm$ $s6h_{f_{12}} := 0mm$

$s6h_{f_{13}} := 150mm$ $s6h_{f_{14}} := 90mm$ $s6h_{f_{15}} := 90mm$ $s6h_{f_{16}} := 100mm$

$s6h_{f_{17}} := 0mm$ $s6h_{f_{18}} := 100mm$ $s6h_{f_{19}} := 0mm$ $s6h_{f_{20}} := 0mm$

$s6h_{f_{21}} := 100mm$ $s6h_{f_{22}} := 100mm$ $s6h_{f_{23}} := 0mm$ $s6h_{f_{24}} := 0mm$

$s6h_{f_{25}} := 100mm$ $s6h_{f_{26}} := 100mm$ $s6h_{f_{27}} := 0mm$ $s6h_{f_{28}} := 0mm$

$s6h_{f_{29}} := 100mm$ $s6h_{f_{30}} := 0mm$ $s6h_{f_{31}} := 100mm$ $s6h_{f_{32}} := 100mm$

$s6h_{f_{33}} := 0mm$ $s6h_{f_{34}} := 100mm$ $s6h_{f_{35}} := 0mm$ $s6h_{f_{36}} := 0mm$

$s6h_{f_{37}} := 100mm$ $s6h_{f_{38}} := 0mm$ $s6h_{f_{39}} := 100mm$ $s6h_{f_{40}} := 0mm$

$s6h_{f_{41}} := 0mm$ $s6h_{f_{42}} := 0mm$ $s6h_{f_{43}} := 0mm$ $s6h_{f_{44}} := 100mm$

$s6h_{f_{45}} := 100mm$ $s6h_{f_{46}} := 0mm$ $s6h_{f_{47}} := 0mm$ $s6h_{f_{48}} := 100mm$

$s6h_{f_{49}} := 100mm$ $s6h_{f_{50}} := 0mm$ $s6h_{f_{51}} := 0mm$ $s6h_{f_{52}} := 100mm$

$s6h_{f_{53}} := 100mm$ $s6h_{f_{54}} := 0mm$ $s6h_{f_{55}} := 0mm$ $s6h_{f_{56}} := 90mm$

$s6h_{f_{57}} := 90mm$

Element Flange Thickness within section 6 elements 1 through 57

$s6t_{f_1} := 16mm$ $s6t_{f_2} := 0mm$ $s6t_{f_3} := 16mm$ $s6t_{f_4} := 0mm$

$s6t_{f_5} := 0mm$ $s6t_{f_6} := 16mm$ $s6t_{f_7} := 0mm$ $s6t_{f_8} := 16mm$

$s6t_{f_9} := 0mm$ $s6t_{f_{10}} := 0mm$ $s6t_{f_{11}} := 16mm$ $s6t_{f_{12}} := 0mm$

$s6t_{f_{13}} := 16mm$ $s6t_{f_{14}} := 16mm$ $s6t_{f_{15}} := 16mm$ $s6t_{f_{16}} := 19mm$

$s6t_{f_{17}} := 0mm$ $s6t_{f_{18}} := 19mm$ $s6t_{f_{19}} := 0mm$ $s6t_{f_{20}} := 0mm$

$s6t_{f_{21}} := 19mm$ $s6t_{f_{22}} := 19mm$ $s6t_{f_{23}} := 0mm$ $s6t_{f_{24}} := 0mm$

$s6t_{f_{25}} := 19mm$ $s6t_{f_{26}} := 19mm$ $s6t_{f_{27}} := 0mm$ $s6t_{f_{28}} := 0mm$

$s6t_{f_{29}} := 19mm$ $s6t_{f_{30}} := 0mm$ $s6t_{f_{31}} := 19mm$ $s6t_{f_{32}} := 17mm$

$s6t_{f_{33}} := 0mm$ $s6t_{f_{34}} := 17mm$ $s6t_{f_{35}} := 0mm$ $s6t_{f_{36}} := 0mm$

$s6t_{f_{37}} := 17mm$ $s6t_{f_{38}} := 0mm$ $s6t_{f_{39}} := 17mm$ $s6t_{f_{40}} := 0mm$

$s6t_{f_{41}} := 0mm$ $s6t_{f_{42}} := 0mm$ $s6t_{f_{43}} := 0mm$ $s6t_{f_{44}} := 17mm$

$s6t_{f_{45}} := 17mm$ $s6t_{f_{46}} := 0mm$ $s6t_{f_{47}} := 0mm$ $s6t_{f_{48}} := 17mm$

$s6t_{f_{49}} := 17mm$ $s6t_{f_{50}} := 0mm$ $s6t_{f_{51}} := 0mm$ $s6t_{f_{52}} := 17mm$

$s6t_{f_{53}} := 17mm$ $s6t_{f_{54}} := 0mm$ $s6t_{f_{55}} := 0mm$ $s6t_{f_{56}} := 16mm$

$s6t_{f_{57}} := 16mm$

Element Stiffener Spacing within section 6 elements 1 through 57

$s6s_1 := 800mm$ $s6s_2 := 1mm$ $s6s_3 := 800mm$ $s6s_4 := 1mm$

$s6s_5 := 1mm$ $s6s_6 := 800mm$ $s6s_7 := 1mm$ $s6s_8 := 800mm$

$s6s_9 := 1mm$ $s6s_{10} := 1mm$ $s6s_{11} := 800mm$ $s6s_{12} := 1mm$

$s6s_{13} := 800mm$ $s6s_{14} := 800mm$ $s6s_{15} := 800mm$ $s6s_{16} := 600mm$

$s6s_{17} := 1mm$ $s6s_{18} := 600mm$ $s6s_{19} := 1mm$ $s6s_{20} := 1mm$

$s6s_{21} := 600mm$ $s6s_{22} := 600mm$ $s6s_{23} := 1mm$ $s6s_{24} := 1mm$

$s6s_{25} := 600mm$ $s6s_{26} := 600mm$ $s6s_{27} := 1mm$ $s6s_{28} := 1mm$

$s6s_{29} := 600mm$ $s6s_{30} := 1mm$ $s6s_{31} := 600mm$ $s6s_{32} := 800mm$

$s6s_{33} := 1mm$ $s6s_{34} := 800mm$ $s6s_{35} := 1mm$ $s6s_{36} := 1mm$

$s6s_{37} := 800mm$ $s6s_{38} := 1mm$ $s6s_{39} := 800mm$ $s6s_{40} := 1mm$

$s6s_{41} := 1mm$ $s6s_{42} := 1mm$ $s6s_{43} := 1mm$ $s6s_{44} := 800mm$

$s6s_{45} := 800mm$ $s6s_{46} := 1mm$ $s6s_{47} := 1mm$ $s6s_{48} := 800mm$

$s6s_{49} := 800mm$ $s6s_{50} := 1mm$ $s6s_{51} := 1mm$ $s6s_{52} := 800mm$

$s6s_{53} := 800mm$ $s6s_{54} := 1mm$ $s6s_{55} := 1mm$ $s6s_{56} := 800mm$

$s6s_{57} := 800mm$

$i := 1 .. n_{F_6}$ Iteration Counter

$s6t_{s_i} := t_s\left(s6h_{w_i}, s6t_{w_i}, s6h_{f_i}, s6t_{f_i}, s6s_i, s6E_{t_i}\right)$ Smeared Thickness Calculation

$\tau_6 := \frac{1}{n_{F_6}}\left(\sum_{i=1}^{n_{F_6}} s6t_{s_i}\right)$ $\tau_6 = 0.023\,m$ Section 6 Average Thickness

$DA_6 := \tau_6 \cdot \sum_{i=1}^{n_{F_6}} s6b_i$ $DA_6 = 2.405\,m^2$ Section 6 Damaged Cross Sectional Area

$DA_{E_6} := \sum_{i=1}^{n_{F_6}} s6b_i \cdot s6t_{s_i}$ $DA_{E_6} = 2.4\,m^2$ Section 6 Exact Damaged Cross Sectional Area

Determining the crush force for each indentation step of 0.8 meters is done by the following calculations.

$m_x := \Delta \cdot 1.05$ $m_x = 1.836 \times 10^8\,kg$

$E_0 := \frac{1}{2} \cdot m_x \cdot V_s^2$ $E_0 = 7.939 \times 10^9\,J$

Section 1, from x = 0 to x = 0.8 meters has the following properties

$V_0 := V_s$ $V_0 = 9.3\,\frac{m}{s}$ Ship forward Velocity

$\varepsilon r_0 := \frac{V_0 \cdot s}{0.8m}$ $\varepsilon r_0 = 11.625$ Strain Rate

$\sigma_0 := 1.29 \cdot \sigma_u \cdot \varepsilon r_0^{0.037}$ $\sigma_0 = 7.119 \times 10^8\,Pa$ Dynamic Flow Stress

$s\sigma_{c_1} := \sigma_c\left(\sigma_0, n_{AT_1}, \tau_1, DA_{E_1}, n_{C_1}, n_{T_1}\right)$ $s\sigma_{c_1} = 1.316 \times 10^8\,Pa$ Crushing Stress

$P_{c_1} := P_{AV}\left(DA_{E_1}, s\sigma_{c_1}\right)$ $P_{c_1} = 26.603\,MN$ Crushing Force

$E_1 := \int_{0m}^{(0.8 \cdot 0.75)m} P_{c_1}\,dx$ $E_1 = 1.596 \times 10^7\,J$ Crushing Energy for x = 0 to 0.8 m

$E_{R_1} := E_0 - E_1$ $E_{R_1} = 7.923 \times 10^9\,J$ Remaining Kinetic Energy

Point Velocity at x = 0.8 meters is given below.

$$V_1 := \left(\frac{E_{R_1}}{\frac{1}{2}\cdot m_x}\right)^{\frac{1}{2}} \qquad V_1 = 9.291\,\frac{m}{s}$$

Section 2, from x = 0.8 to x = 1.6 meters has the following properties

$$\varepsilon r_1 := \frac{V_1 \cdot s}{0.8m} \qquad \varepsilon r_1 = 11.613$$

$\sigma_0 := 1.29\cdot\sigma_u\cdot(\varepsilon r_1)^{0.037}$ $\sigma_0 = 7.119 \times 10^8\,Pa$

$s\sigma_{c_2} := \sigma_c(\sigma_0, n_{AT_2}, \tau_2, DA_{E_2}, n_{C_2}, n_{T_2})$ $s\sigma_{c_2} = 1.872 \times 10^8\,Pa$

$P_{c_2} := P_{AV}(DA_{E_2}, s\sigma_{c_2})$ $P_{c_2} = 233.71\,MN$

$E_2 := \int_{(0.8-0.75)m}^{(1.6-0.75)m} P_{c_2}\,dx$ $E_2 = 1.402 \times 10^8\,J$ Crushing Energy for x = 0.8 to 1.6 m

$E_{R_2} := E_{R_1} - E_2$ $E_{R_2} = 7.783 \times 10^9\,J$ Remaining Kinetic Energy

Point Velocity at x = 1.6 meters is given below.

$$V_2 := \left(\frac{E_{R_2}}{\frac{1}{2}\cdot m_x}\right)^{\frac{1}{2}} \qquad V_2 = 9.208\,\frac{m}{s}$$

Section 3, from x = 1.6 to x = 2.4 meters has the following properties

$$\varepsilon r_2 := \frac{V_2 \cdot s}{0.8m} \qquad \varepsilon r_2 = 11.51$$

$\sigma_0 := 1.29\cdot\sigma_u\cdot(\varepsilon r_2)^{0.037}$ $\sigma_0 = 7.117 \times 10^8\,Pa$

$s\sigma_{c_3} := \sigma_c(\sigma_0, n_{AT_3}, \tau_3, DA_{E_3}, n_{C_3}, n_{T_3})$ $s\sigma_{c_3} = 1.608 \times 10^8\,Pa$

$P_{c_3} := P_{AV}(DA_{E_3}, s\sigma_{c_3})$ $P_{c_3} = 288.227\,MN$

$E_3 := \int_{(1.6\cdot 0.75)m}^{(2.4\cdot 0.75)m} P_{c_3}\, dx$ $E_3 = 1.729 \times 10^8\,J$ Crushing Energy for x = 1.6 to 2.4 m

$E_{R_3} := E_{R_2} - E_3$ $E_{R_3} = 7.61 \times 10^9\,J$ Remaining Kinetic Energy

Point Velocity at x = 2.4 meters is given below.

$V_3 := \left(\frac{E_{R_3}}{\frac{1}{2}\cdot m_x}\right)^{\frac{1}{2}}$ $V_3 = 9.105\,\frac{m}{s}$

Section 4, from x = 2.4 to x = 3.2 meters has the following properties

$\varepsilon r_3 := \frac{V_3\cdot s}{0.8m}$ $\varepsilon r_3 = 11.381$

$\sigma_0 := 1.29\cdot\sigma_u\cdot(\varepsilon r_3)^{0.037}$ $\sigma_0 = 7.114 \times 10^8\,Pa$

$s\sigma_{c_4} := \sigma_c(\sigma_0, n_{AT_4}, \tau_4, DA_{E_4}, n_{C_4}, n_{T_4})$ $s\sigma_{c_4} = 1.694 \times 10^8\,Pa$

$P_{c_4} := P_{AV}(DA_{E_4}, s\sigma_{c_4})$ $P_{c_4} = 355.803\,MN$

$E_4 := \int_{(2.4\cdot 0.75)m}^{(3.2\cdot 0.75)m} P_{c_4}\, dx$ $E_4 = 2.135 \times 10^8\,J$ Crushing Energy for x = 2.4 to 3.2 m

$E_{R_4} := E_{R_3} - E_4$ $E_{R_4} = 7.397 \times 10^9\,J$ Remaining Kinetic Energy

Point Velocity at x = 3.2 meters is given below.

$V_4 := \left(\frac{E_{R_4}}{\frac{1}{2}\cdot m_x}\right)^{\frac{1}{2}}$ $V_4 = 8.977\,\frac{m}{s}$

Section 5, from x = 3.2 to x = 4 meters has the following properties

$\varepsilon r_4 := \frac{V_4\cdot s}{0.8m}$ $\varepsilon r_4 = 11.221$

$\sigma_0 := 1.29\cdot\sigma_u\cdot(\varepsilon r_4)^{0.037}$ $\sigma_0 = 7.11 \times 10^8\,Pa$

$s\sigma_{c_5} := \sigma_c(\sigma_0, n_{AT_5}, \tau_5, DA_{E_5}, n_{C_5}, n_{T_5})$ $s\sigma_{c_5} = 1.557 \times 10^8\,Pa$

$P_{c_5} := P_{AV}(DA_{E_5}, s\sigma_{c_5})$ $P_{c_5} = 354.483\,MN$

$E_5 := \int_{(3.2\cdot 0.75)m}^{(4\cdot 0.75)m} P_{c_\epsilon}\, dx$ $E_5 = 2.127 \times 10^8\,J$ Crushing Energy for x = 3.2 to 4 m

$E_{R_\epsilon} := E_{R_4} - E_5$ $E_{R_\epsilon} = 7.184 \times 10^9\,J$ Remaining Kinetic Energy

Point Velocity at x = 4 meters is given below.

$V_5 := \left(\frac{E_{R_5}}{\frac{1}{2}\cdot m_x}\right)^{\frac{1}{2}}$ $V_5 = 8.847\,\frac{m}{s}$

Section 6, from x = 4 to x = 4.8 meters has the following properties

$\epsilon r_5 := \frac{V_5\cdot s}{0.8m}$ $\epsilon r_5 = 11.058$

$\sigma_0 := 1.29\cdot\sigma_u\cdot(\epsilon r_5)^{0.037}$ $\sigma_0 = 7.106 \times 10^8\,Pa$

$s\sigma_{c_6} := \sigma_c(\sigma_0, n_{AT_6}, \tau_6, DA_{E_6}, n_{C_6}, n_{T_6})$ $s\sigma_{c_6} = 1.701 \times 10^8\,Pa$

$P_{c_6} := P_{AV}(DA_{E_6}, s\sigma_{c_6})$ $P_{c_6} = 408.216\,MN$

$E_6 := \int_{(4\cdot 0.75)m}^{(4.8\cdot 0.75)m} P_{c_6}\, dx$ $E_6 = 2.449 \times 10^8\,J$ Crushing Energy for x = 4 to 4.8 m

$E_{R_6} := E_{R_5} - E_6$ $E_{R_6} = 6.939 \times 10^9\,J$ Remaining Kinetic Energy

Point Velocity at x = 4.8 meters is given below.

$V_6 := \left(\frac{E_{R_6}}{\frac{1}{2}\cdot m_x}\right)^{\frac{1}{2}}$ $V_6 = 8.694\,\frac{m}{s}$

The following figure provides a comparison of the above results for sections 1 through 6 to those numerical results extracted from the graph presented by pederson for the 150k dwt Bulk Carrier.

$P_c = \begin{pmatrix} 26.603 \\ 233.71 \\ 288.227 \\ 355.803 \\ 354.483 \\ 408.216 \end{pmatrix} MN$ $P_p := \begin{pmatrix} 25 \\ 205 \\ 280 \\ 333 \\ 320 \\ 410 \end{pmatrix} MN$ $D_c := \begin{pmatrix} 0.8 \\ 1.6 \\ 2.4 \\ 3.2 \\ 4 \\ 4.8 \end{pmatrix} m$ $D_p := 0.75\cdot D_c$ $D_p = \begin{pmatrix} 0.6 \\ 1.2 \\ 1.8 \\ 2.4 \\ 3 \\ 3.6 \end{pmatrix} m$

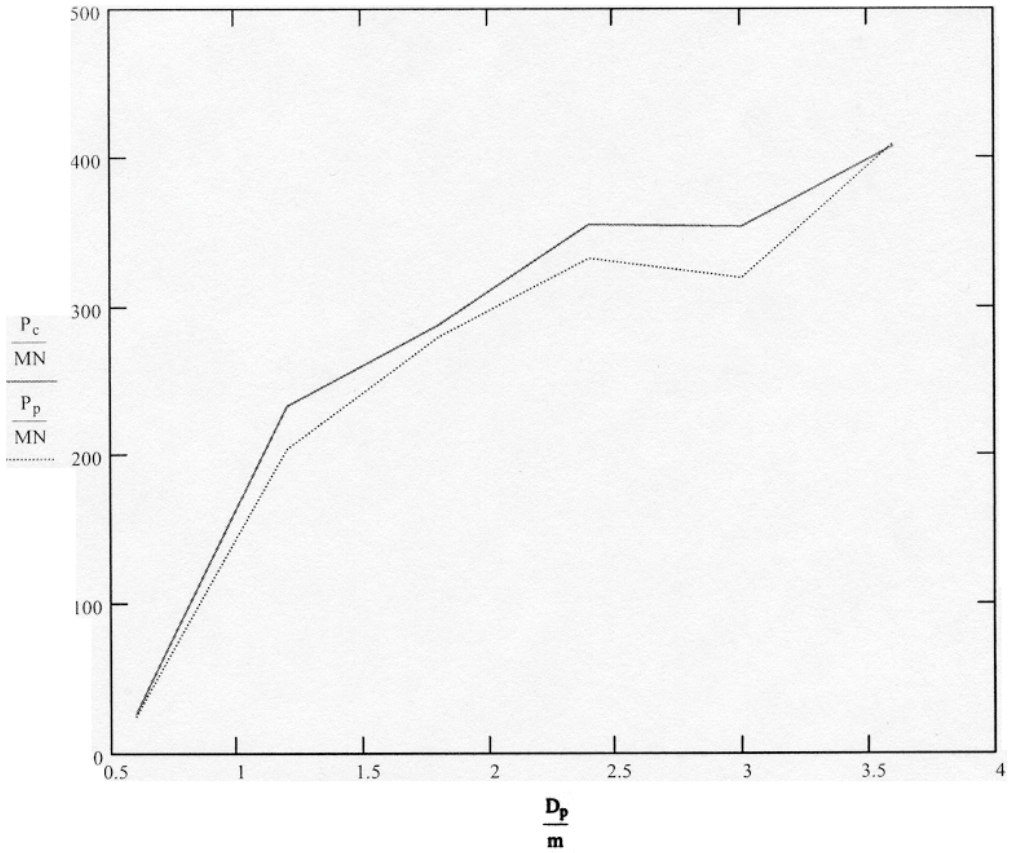

Pp is Pedersons reported results as extracted.

Pc is reanalysis of Amdahls method neglecting Pedersen's cruciform assumption, including stiffener T's formed from longitudinals and side shell.

Appendix H: Pedersen Calculation of Energy Absorbed by Bow Damage

Pedersons proposed simplified method consists of an empirical expression to estimate the maximum bow collision load.

The neccessary units and functions for the analysis of the 150k dwt Bulk Carrier using Pedersons method:

$MN := 10^6 N$ Mega Newton Definition

The 150k dwt Bulk Carrier Ship Particulars are defined as shown below.

$LBP := 274m$ Length Between Perpendiculars

$B := 47m$ Breadth Moulded

$D := 21.6m$ Depth Moulded

$D_F := 26m$ Depth to Forecastle Deck

$T := 15.96m$ Maximum Draft

$\Delta := 174850000kg$ Displacement

$V_s := 1.5433\frac{m}{s}$ Maximum Service Speed

Pedersons Non-Dimensional Length Parameter:

$L_{bar} := \frac{LBP}{275m}$ $L_{bar} = 0.996$

$P_0 := 210MN$ Reference Load

$m_x := \Delta \cdot 1.05$ $m_x = 1.836 \times 10^8 kg$

$E_0 := \frac{1}{2} \cdot m_x \cdot V_s^2$ $E_0 = 2.186 \times 10^8 J$ Initial Energy

$E_{bar} := \frac{E_0}{1425MN \cdot m}$ $E_{bar} = 0.153$ Non-Dimensional Energy

$$P_{bow} := \begin{cases} \left[P_0 \cdot L_{bar} \cdot \left[E_{bar} + \left(5 - L_{bar}\right) \cdot L_{bar}^{1.6} \right]^{0.5} \right] & \text{if } E_{bar} \geq L_{bar}^{2.6} \\ \left[2.24 \cdot P_0 \cdot \left(E_{bar} \cdot L_{bar}\right)^{0.5} \right] & \text{otherwise} \end{cases}$$

$P_{bow} = 183.921MN$ Maximum Bow Collision Load

$s_{max} := \frac{\pi}{2} \cdot \frac{E_0}{P_{bow}}$ $s_{max} = 1.867m$ Total Penetration

$T_0 := 1.67 \cdot \frac{s_{max}}{V_s}$ $T_0 = 2.021s$ Collision Duration

$P_p(x) := \sin\left(\frac{\pi \cdot x}{2s_{max}}\right) \cdot P_{bow}$

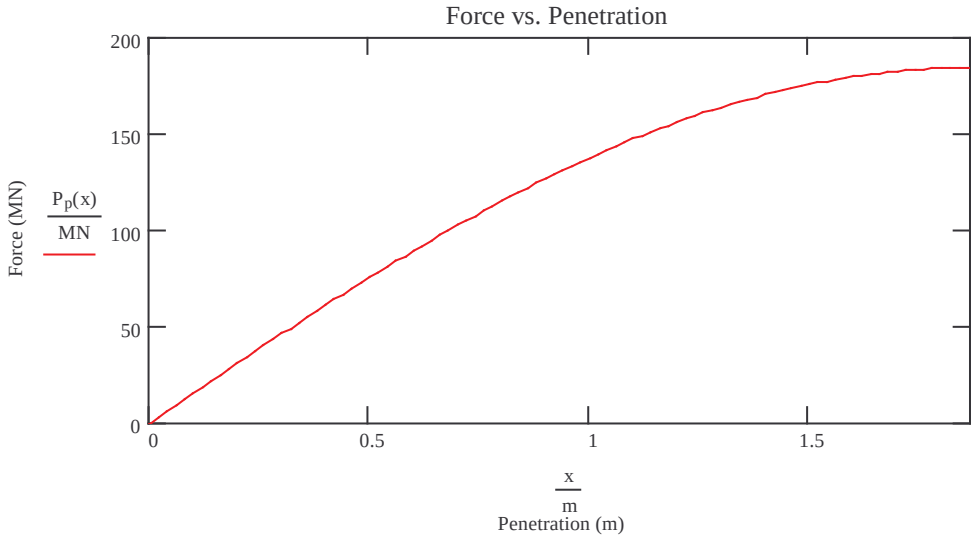

The Assumptions used within the analysis are as follows:

1. Vessel Maximum Service Speed is assumed to be 3 knots.
2. Assume Force vs. Penetration can be approximated with a half sine wave

Appendix I: Example LSDYNA Finite Element Input File

The following is an example LSDYNA keyword input deck file

```
*KEYWORD
$---+----1----+----2----+----3----+----4----+----5----+----6----+----7----+----8
$
$ DYNA3D(936) DECK WAS WRITTEN BY: ETA/FEMB VERSION 26
$ DATE  : Jun 18, 2003 at 12:04:25
$
$---+----1----+----2----+----3----+----4----+----5----+----6----+----7----+----8
$                   (1) TITLE CARD.
$---+----1----+----2----+----3----+----4----+----5----+----6----+----7----+----8
*TITLE
David E Day Marine Flier Collision
$---+----1----+----2----+----3----+----4----+----5----+----6----+----7----+----8
$                   (2) CONTROL CARDS.
$---+----1----+----2----+----3----+----4----+----5----+----6----+----7----+----8
*CONTROL_TERMINATION
$   ENDTIM    ENDCYC     DTMIN    ENDNEG    ENDMAS
  .400E+01         0      .000      .000      .000
*CONTROL_TIMESTEP
$   DTINIT      SCFT      ISDO    TSLIMT      DTMS      LCTM     ERODE     MS1ST
      .000      .900         0
*CONTROL_HOURGLASS
$      IHQ        QH
         1      .100
*CONTROL_BULK_VISCOSITY
$       Q2        Q1
     1.500      .060
*CONTROL_SHELL
$   WRPANG    ITRIST     IRNXX    ISTUPD    THEORY       BWC     MITER
    20.000         2        -1         0         2         2         1
*CONTROL_CONTACT
$   SLSFAC    RWPNAL    ISLCHK    SHLTHK    PENOPT    THKCHG     ORIEN
      .100                 2         1         1
$   USRSTR    USRFAC     NSBCS    INTERM     XPENE
         0         0        10         0     4.000
$    SFRIC     DFRIC       EDC       VFC        TH     TH_SF    PEN_SF

$   IGNORE    FRCENG
         1         1
*CONTROL_ENERGY
$     HGEN      RWEN    SLNTEN     RYLEN
         2         2         2         2
*CONTROL_DAMPING
$   NRCYCK     DRTOL    DRFCTR    DRTERM    TSSFDR    IRELAL     EDTTL    IDRFLG
       250      .001      .995
*CONTROL_OUTPUT
$    NPOPT    NEECHO    NREFUP    IACCOP     OPIFS    IPNINT    IKEDIT
         0         0         0         0      .000         0       100
*CONTROL_ACCURACY
$      OSU       INN    PIDOSU
         0         2
$---+----1----+----2----+----3----+----4----+----5----+----6----+----7----+----8
$                   (3) DATABASE CONTROL CARDS - ASCII HISTORY FILE
$---+----1----+----2----+----3----+----4----+----5----+----6----+----7----+----8
$*DATABASE_HISTORY_OPTION
$      ID1       ID2       ID3       ID4       ID5       ID6       ID7       ID8
$
$OPTION : BEAM    BEAM_SET   NODE   NODE_SET
$         SHELL   SHELL_SET  SOLID  SOLID_SET
$         TSHELL  TSHELL_SET
$---+----1----+----2----+----3----+----4----+----5----+----6----+----7----+----8
$                   (4) DATABASE CONTROL CARDS FOR ASCII FILE
$---+----1----+----2----+----3----+----4----+----5----+----6----+----7----+----8
$---+----1----+----2----+----3----+----4----+----5----+----6----+----7----+----8
$*DATABASE_OPTION
$       DT
$
$OPTION : SECFORC RWFORC NODOUT ELOUT  GLSTAT
$         DEFORC  MATSUM NCFORC RCFORC DEFGEO
$         SPCFORC SWFORC ABSTAT NODFOR BNDOUT
```

```
$         RBDOUT  GCEOUT SLEOUT MPGS   SBTOUT
$         JNTFORC AVSFLT MOVIE
*DATABASE_GLSTAT
  .400E-02
*DATABASE_MATSUM
  .400E-02
*DATABASE_RCFORC
  .400E-02
*DATABASE_SLEOUT
  .400E-02
$---+----1----+----2----+----3----+----4----+----5----+----6----+----7----+----8
$                    (5) DATABASE CONTROL CARDS FOR BINARY FILE
$---+----1----+----2----+----3----+----4----+----5----+----6----+----7----+----8
*DATABASE_BINARY_D3PLOT
$  DT/CYCL      LCDT    NOBEAM
  .100E+00
*DATABASE_BINARY_D3THDT
$  DT/CYCL      LCDT    NOBEAM
  .100E+00
$*DATABASE_BINARY_OPTION
$  DT/CYCL      LCDT    NOBEAM
$
$OPTION : D3DRFL D3DUMP RUNRSF INTFOR
$---+----1----+----2----+----3----+----4----+----5----+----6----+----7----+----8
*DATABASE_EXTENT_BINARY
         0         0         3         0         1         1         1         1
         0         0         0         0         0         0
$---+----1----+----2----+----3----+----4----+----5----+----6----+----7----+----8
$                    (6) DEFINE PARTS CARDS
$---+----1----+----2----+----3----+----4----+----5----+----6----+----7----+----8
*PART
$HEADING
 PART PID =      303 PART NAME :BTMSHELL
$      PID       SID       MID     EOSID      HGID      GRAV    ADPOPT      TMID
       303       503       701
*PART
$HEADING
 PART PID =      304 PART NAME :SIDSHELL
$      PID       SID       MID     EOSID      HGID      GRAV    ADPOPT      TMID
       304       504       701
*PART
$HEADING
 PART PID =      305 PART NAME :MAINDECK
$      PID       SID       MID     EOSID      HGID      GRAV    ADPOPT      TMID
       305       505       701
*PART
$HEADING
 PART PID =      306 PART NAME :INRBLKHD
$      PID       SID       MID     EOSID      HGID      GRAV    ADPOPT      TMID
       306       506       701
*PART
$HEADING
 PART PID =      307 PART NAME :DECKTRAN
$      PID       SID       MID     EOSID      HGID      GRAV    ADPOPT      TMID
       307       507       701
*PART
$HEADING
 PART PID =      308 PART NAME :OUTRWEB
$      PID       SID       MID     EOSID      HGID      GRAV    ADPOPT      TMID
       308       508       701
*PART
$HEADING
 PART PID =      309 PART NAME :INNRWEB
$      PID       SID       MID     EOSID      HGID      GRAV    ADPOPT      TMID
       309       509       701
*PART
$HEADING
 PART PID =      310 PART NAME :BTMTRAN
$      PID       SID       MID     EOSID      HGID      GRAV    ADPOPT      TMID
       310       510       701
*PART
$HEADING
 PART PID =      311 PART NAME :BRACKET
$      PID       SID       MID     EOSID      HGID      GRAV    ADPOPT      TMID
       311       511       701
*PART
$HEADING
```

```
 PART PID =      312 PART NAME :STRUT
$      PID       SID       MID     EOSID      HGID      GRAV    ADPOPT      TMID
       312       512       701
*PART
$HEADING
 PART PID =      313 PART NAME :TRBLKHD
$      PID       SID       MID     EOSID      HGID      GRAV    ADPOPT      TMID
       313       513       701
*PART
$HEADING
 PART PID =      314 PART NAME :CLGIRDER
$      PID       SID       MID     EOSID      HGID      GRAV    ADPOPT      TMID
       314       514       701
*PART
$HEADING
 PART PID =      315 PART NAME :TRBHDWEB
$      PID       SID       MID     EOSID      HGID      GRAV    ADPOPT      TMID
       315       515       701
*PART
$HEADING
 PART PID =      316 PART NAME :TRBRACKT
$      PID       SID       MID     EOSID      HGID      GRAV    ADPOPT      TMID
       316       516       701
*PART
$HEADING
 PART PID =      203 PART NAME :STEM
$      PID       SID       MID     EOSID      HGID      GRAV    ADPOPT      TMID
       203       403       601
*PART
$HEADING
 PART PID =      204 PART NAME :DECK
$      PID       SID       MID     EOSID      HGID      GRAV    ADPOPT      TMID
       204       404       601
*PART
$HEADING
 PART PID =      205 PART NAME :STRINGER
$      PID       SID       MID     EOSID      HGID      GRAV    ADPOPT      TMID
       205       405       601
*PART
$HEADING
 PART PID =      206 PART NAME :LSHELPLT
$      PID       SID       MID     EOSID      HGID      GRAV    ADPOPT      TMID
       206       406       601
*PART
$HEADING
 PART PID =      207 PART NAME :USHELPLT
$      PID       SID       MID     EOSID      HGID      GRAV    ADPOPT      TMID
       207       407       601
*PART
$HEADING
 PART PID =      208 PART NAME :FRAMES
$      PID       SID       MID     EOSID      HGID      GRAV    ADPOPT      TMID
       208       408       601
*PART
$HEADING
 PART PID =      301 PART NAME :MSTRUCK
$      PID       SID       MID     EOSID      HGID      GRAV    ADPOPT      TMID
       301       501       607
*PART
$HEADING
 PART PID =      302 PART NAME :HSTRUCK
$      PID       SID       MID     EOSID      HGID      GRAV    ADPOPT      TMID
       302       502       606
*PART
$HEADING
 PART PID =      201 PART NAME :MSTRIKE
$      PID       SID       MID     EOSID      HGID      GRAV    ADPOPT      TMID
       201       401       605
*PART
$HEADING
 PART PID =      202 PART NAME :HSTRIKE
$      PID       SID       MID     EOSID      HGID      GRAV    ADPOPT      TMID
       202       402       604
$---+----1----+----2----+----3----+----4----+----5----+----6----+----7----+----8
$                   (7) MATERIAL CARDS
*MAT_PIECEWISE_LINEAR_PLASTICITY
$MATERIAL NAME:M24GB
```

```
$      MID        RO         E        PR      SIGY      ETAN      EPPF      TDEL
       701 7.780E+03 1.900E+11 2.810E-01 2.350E+08 3.750E+09 0.725E-01 0.000E+00
$        C         P      LCSS      LCSR        VP
  .404E+02  .500E+01  .000E+00  .000E+00  .100E+01
$     EPS1      EPS2      EPS3      EPS4      EPS5      EPS6      EPS7      EPS8
 0.000E+00 0.000E+00 0.000E+00 0.000E+00 0.000E+00 0.000E+00 0.000E+00 0.000E+00
$      ES1       ES2       ES3       ES4       ES5       ES6       ES7       ES8
 0.000E+00 0.000E+00 0.000E+00 0.000E+00 0.000E+00 0.000E+00 0.000E+00 0.000E+00
*MAT_PLASTIC_KINEMATIC
$MATERIAL NAME:M3GB
$      MID        RO         E        PR      SIGY      ETAN      BETA
       601 7.780E+03 1.900E+11 2.810E-01 2.350E+08 3.750E+09 0.000E+00
$      SRC       SRP        FS        VP
 4.040E+01 5.000E+00 0.000E+00 0.000E+00
*MAT_PLASTIC_KINEMATIC
$MATERIAL NAME:MSTRUCK
$      MID        RO         E        PR      SIGY      ETAN      BETA
       607 1.816E+04 2.100E+11 3.030E-01 3.550E+08 3.220E+09 0.000E+00
$      SRC       SRP        FS        VP
 4.040E+01 5.000E+00 0.000E+00 0.000E+00
*MAT_PLASTIC_KINEMATIC
$MATERIAL NAME:HSTRUCK
$      MID        RO         E        PR      SIGY      ETAN      BETA
       606 1.767E+04 2.100E+11 3.030E-01 3.550E+08 3.220E+09 0.000E+00
$      SRC       SRP        FS        VP
 4.040E+01 5.000E+00 0.000E+00 0.000E+00
*MAT_PLASTIC_KINEMATIC
$MATERIAL NAME:MSTRIKE
$      MID        RO         E        PR      SIGY      ETAN      BETA
       605 2.297E+04 2.100E+11 3.030E-01 3.550E+08 3.220E+09 0.000E+00
$      SRC       SRP        FS        VP
 4.040E+01 5.000E+00 0.000E+00 0.000E+00
*MAT_PLASTIC_KINEMATIC
$MATERIAL NAME:HSTRIKE
$      MID        RO         E        PR      SIGY      ETAN      BETA
       604 9.460E+03 2.100E+11 3.030E-01 3.550E+08 3.220E+09 0.000E+00
$      SRC       SRP        FS        VP
 4.040E+01 5.000E+00 0.000E+00 0.000E+00
$---+----1----+----2----+----3----+----4----+----5----+----6----+----7----+----8
$                   (7.1) SECTION CARDS
$---+----1----+----2----+----3----+----4----+----5----+----6----+----7----+----8
*SECTION_SHELL
$PROPERTY NAME:BTMSHELL
$      SID    ELFORM      SHRF       NIP     PROPT   QR/IRID     ICOMP     SETYP
       503         2  .833E+00         5  .000E+00  .000E+00         0         1
$       T1        T2        T3        T4      NLOC
  .288E-01  .288E-01  .288E-01  .288E-01  .000E+00
*SECTION_SHELL
$PROPERTY NAME:SIDSHELL
$      SID    ELFORM      SHRF       NIP     PROPT   QR/IRID     ICOMP     SETYP
       504         2  .833E+00         5  .000E+00  .000E+00         0         1
$       T1        T2        T3        T4      NLOC
  .225E-01  .225E-01  .225E-01  .225E-01  .000E+00
*SECTION_SHELL
$PROPERTY NAME:MAINDECK
$      SID    ELFORM      SHRF       NIP     PROPT   QR/IRID     ICOMP     SETYP
       505         2  .833E+00         5  .000E+00  .000E+00         0         1
$       T1        T2        T3        T4      NLOC
  .252E-01  .252E-01  .252E-01  .252E-01  .000E+00
*SECTION_SHELL
$PROPERTY NAME:INRBLKHD
$      SID    ELFORM      SHRF       NIP     PROPT   QR/IRID     ICOMP     SETYP
       506         2  .833E+00         5  .000E+00  .000E+00         0         1
$       T1        T2        T3        T4      NLOC
  .125E-01  .125E-01  .125E-01  .125E-01  .000E+00
*SECTION_SHELL
$PROPERTY NAME:DECKTRAN
$      SID    ELFORM      SHRF       NIP     PROPT   QR/IRID     ICOMP     SETYP
       507         2  .833E+00         5  .000E+00  .000E+00         0         1
$       T1        T2        T3        T4      NLOC
  .132E-01  .132E-01  .132E-01  .132E-01  .000E+00
*SECTION_SHELL
$PROPERTY NAME:OUTRWEB
$      SID    ELFORM      SHRF       NIP     PROPT   QR/IRID     ICOMP     SETYP
       508         2  .833E+00         5  .000E+00  .000E+00         0         1
$       T1        T2        T3        T4      NLOC
  .135E-01  .135E-01  .135E-01  .135E-01  .000E+00
```

```
*SECTION_SHELL
$PROPERTY NAME:INNRWEB
$      SID    ELFORM      SHRF       NIP     PROPT   QR/IRID     ICOMP     SETYP
       509         2  .833E+00         5  .000E+00  .000E+00         0         1
$       T1        T2        T3        T4      NLOC
  .135E-01  .135E-01  .135E-01  .135E-01  .000E+00
*SECTION_SHELL
$PROPERTY NAME:BTMTRAN
$      SID    ELFORM      SHRF       NIP     PROPT   QR/IRID     ICOMP     SETYP
       510         2  .833E+00         5  .000E+00  .000E+00         0         1
$       T1        T2        T3        T4      NLOC
  .133E-01  .133E-01  .133E-01  .133E-01  .000E+00
*SECTION_SHELL
$PROPERTY NAME:BRACKET
$      SID    ELFORM      SHRF       NIP     PROPT   QR/IRID     ICOMP     SETYP
       511         2  .833E+00         5  .000E+00  .000E+00         0         1
$       T1        T2        T3        T4      NLOC
  .138E-01  .138E-01  .138E-01  .138E-01  .000E+00
*SECTION_SHELL
$PROPERTY NAME:STRUT
$      SID    ELFORM      SHRF       NIP     PROPT   QR/IRID     ICOMP     SETYP
       512         2  .833E+00         5  .000E+00  .000E+00         0         1
$       T1        T2        T3        T4      NLOC
  .215E-01  .215E-01  .215E-01  .215E-01  .000E+00
*SECTION_SHELL
$PROPERTY NAME:TRBLKHD
$      SID    ELFORM      SHRF       NIP     PROPT   QR/IRID     ICOMP     SETYP
       513         2  .833E+00         5  .000E+00  .000E+00         0         1
$       T1        T2        T3        T4      NLOC
  .118E-01  .118E-01  .118E-01  .118E-01  .000E+00
*SECTION_SHELL
$PROPERTY NAME:CLGIRDER
$      SID    ELFORM      SHRF       NIP     PROPT   QR/IRID     ICOMP     SETYP
       514         2  .833E+00         5  .000E+00  .000E+00         0         1
$       T1        T2        T3        T4      NLOC
  .167E-01  .167E-01  .167E-01  .167E-01  .000E+00
*SECTION_SHELL
$PROPERTY NAME:TRBHDWEB
$      SID    ELFORM      SHRF       NIP     PROPT   QR/IRID     ICOMP     SETYP
       515         2  .833E+00         5  .000E+00  .000E+00         0         1
$       T1        T2        T3        T4      NLOC
  .125E-01  .125E-01  .125E-01  .125E-01  .000E+00
*SECTION_SHELL
$PROPERTY NAME:TRBRACKT
$      SID    ELFORM      SHRF       NIP     PROPT   QR/IRID     ICOMP     SETYP
       516         2  .833E+00         5  .000E+00  .000E+00         0         1
$       T1        T2        T3        T4      NLOC
  .127E-01  .127E-01  .127E-01  .127E-01  .000E+00
*SECTION_SHELL
$PROPERTY NAME:STEM
$      SID    ELFORM      SHRF       NIP     PROPT   QR/IRID     ICOMP     SETYP
       403         2  .833E+00         5  .000E+00  .000E+00         0         1
$       T1        T2        T3        T4      NLOC
  .194E-01  .194E-01  .194E-01  .194E-01  .000E+00
*SECTION_SHELL
$PROPERTY NAME:DECK
$      SID    ELFORM      SHRF       NIP     PROPT   QR/IRID     ICOMP     SETYP
       404         2  .833E+00         5  .000E+00  .000E+00         0         1
$       T1        T2        T3        T4      NLOC
  .105E-01  .105E-01  .105E-01  .105E-01  .000E+00
*SECTION_SHELL
$PROPERTY NAME:STRINGER
$      SID    ELFORM      SHRF       NIP     PROPT   QR/IRID     ICOMP     SETYP
       405         2  .833E+00         5  .000E+00  .000E+00         0         1
$       T1        T2        T3        T4      NLOC
  .105E-01  .105E-01  .105E-01  .105E-01  .000E+00
*SECTION_SHELL
$PROPERTY NAME:LSHELPLT
$      SID    ELFORM      SHRF       NIP     PROPT   QR/IRID     ICOMP     SETYP
       406         2  .833E+00         5  .000E+00  .000E+00         0         1
$       T1        T2        T3        T4      NLOC
  .269E-01  .269E-01  .269E-01  .269E-01  .000E+00
*SECTION_SHELL
$PROPERTY NAME:USHELPLT
$      SID    ELFORM      SHRF       NIP     PROPT   QR/IRID     ICOMP     SETYP
       407         2  .833E+00         5  .000E+00  .000E+00         0         1
$       T1        T2        T3        T4      NLOC
```

```
  .213E-01  .213E-01  .213E-01  .213E-01  .000E+00
*SECTION_SHELL
$PROPERTY NAME:FRAMES
$      SID    ELFORM      SHRF       NIP     PROPT   QR/IRID     ICOMP     SETYP
       408         2  .833E+00         5  .000E+00  .000E+00         0         1
$       T1        T2        T3        T4      NLOC
  .567E-02  .567E-02  .567E-02  .567E-02  .000E+00
*SECTION_BEAM
$PROPERTY NAME:MSTRUCK
$      SID    ELFORM      SHRF   QR/IRID       CST     SCOOR
       501         1  .833E+00  .200E+01  .000E+00  .000E+00
$      TS1       TS2       TT1       TT2     NSLOC     NTLOC
  .100E+01  .100E+01  .100E+01  .100E+01  .000E+00  .000E+00
*SECTION_BEAM
$PROPERTY NAME:HSTRUCK
$      SID    ELFORM      SHRF   QR/IRID       CST     SCOOR
       502         1  .833E+00  .200E+01  .000E+00  .000E+00
$      TS1       TS2       TT1       TT2     NSLOC     NTLOC
  .100E+01  .100E+01  .100E+01  .100E+01  .000E+00  .000E+00
*SECTION_BEAM
$PROPERTY NAME:MSTRIKE
$      SID    ELFORM      SHRF   QR/IRID       CST     SCOOR
       401         1  .833E+00  .200E+01  .000E+00  .000E+00
$      TS1       TS2       TT1       TT2     NSLOC     NTLOC
  .100E+01  .100E+01  .100E+01  .100E+01  .000E+00  .000E+00
*SECTION_BEAM
$PROPERTY NAME:HSTRIKE
$      SID    ELFORM      SHRF   QR/IRID       CST     SCOOR
       402         1  .833E+00  .200E+01  .000E+00  .000E+00
$      TS1       TS2       TT1       TT2     NSLOC     NTLOC
  .100E+01  .100E+01  .100E+01  .100E+01  .000E+00  .000E+00
$---+----1----+----2----+----3----+----4----+----5----+----6----+----7----+----8
$                   (8) NODAL POINT CARDS
$---+----1----+----2----+----3----+----4----+----5----+----6----+----7----+----8
*NODE
$   NODE               X               Y               Z      TC      RC
       1  .209390000E+01  .588140000E+01 -.396240000E+01
       2  .228287600E+01  .588139900E+01 -.396240000E+01
       3  .228440000E+01  .608622600E+01 -.396240000E+01
... ... ... ... ... ... ... ...
  100474     202   96487   68389   96680
  100475     202   96485   67996   96681
$---+----1----+----2----+----3----+----4----+----5----+----6----+----7----+----8
$                   (11) SHELL ELEMENT CARDS
$---+----1----+----2----+----3----+----4----+----5----+----6----+----7----+----8
*ELEMENT_SHELL
$    EID     PID      N1      N2      N3      N4
       1     303       1       2       3       4
       2     303       2       5       6       3
       3     303       5       7       8       6
... ... ... ... ... ... ... ...
  100286     208   83613   83614   83621   83621
  100287     208   82681   73829   82682   82682
$---+----1----+----2----+----3----+----4----+----5----+----6----+----7----+----8
$                   (12) SPRING OR DAMPER ELEMENT CARDS
$---+----1----+----2----+----3----+----4----+----5----+----6----+----7----+----8
*ELEMENT_DISCRETE
$    EID     PID      N1      N2     VID               S      PF
*ELEMENT_MASS
$    EID     NID            MASS
*ELEMENT_INERTIA
$---+----1----+----2----+----3----+----4----+----5----+----6----+----7----+----8
$                   (14) HOURGLASS AND BULK PROPERTIES CARDS
$---+----1----+----2----+----3----+----4----+----5----+----6----+----7----+----8
$*HOURGLASS
$      IHQ        QH      IBQ       Q1        Q2
$
$---+----1----+----2----+----3----+----4----+----5----+----6----+----7----+----8
$                   (15) DEFINE SET CARDS
$---+----1----+----2----+----3----+----4----+----5----+----6----+----7----+----8
$---+----1----+----2----+----3----+----4----+----5----+----6----+----7----+----8
$                   (16) BOUNDARY CONDITION CARDS
$---+----1----+----2----+----3----+----4----+----5----+----6----+----7----+----8
*BOUNDARY_SPC_NODE
$ NID/NSID       CID      DOFX      DOFY      DOFZ     DOFRX     DOFRY     DOFRZ
     64860         0         0         0         1         1         1         0
     64913         0         0         0         1         1         1         0
```

```
     65487         0         0         0         1         1         1         0
... ... ... ... ... ... ... ...
     96492         0         0         0         1         1         1         0
     96493         0         0         0         1         1         1         0
$---+----1----+----2----+----3----+----4----+----5----+----6----+----7----+----8
$                   (17) LOCAL COORDINATE SYSTEM
$---+----1----+----2----+----3----+----4----+----5----+----6----+----7----+----8
$---+----1----+----2----+----3----+----4----+----5----+----6----+----7----+----8
$                   (18) NODAL CONSTRAINT CARDS
$---+----1----+----2----+----3----+----4----+----5----+----6----+----7----+----8
$---+----1----+----2----+----3----+----4----+----5----+----6----+----7----+----8
$                   (19) INITIAL CARDS
$---+----1----+----2----+----3----+----4----+----5----+----6----+----7----+----8
*INITIAL_VELOCITY_NODE
$      NID        VX        VY        VZ       VXR       VYR       VZR
     68252 2.320E+00-1.625E+00 0.000E+00 0.000E+00 0.000E+00 0.000E+00
     68389 2.320E+00-1.625E+00 0.000E+00 0.000E+00 0.000E+00 0.000E+00
     64913 2.320E+00-1.625E+00 0.000E+00 0.000E+00 0.000E+00 0.000E+00
... ... ... ... ... ... ... ...
     86351 2.320E+00-1.625E+00 0.000E+00 0.000E+00 0.000E+00 0.000E+00
     93912 2.320E+00-1.625E+00 0.000E+00 0.000E+00 0.000E+00 0.000E+00
$---+----1----+----2----+----3----+----4----+----5----+----6----+----7----+----8
$                   (22) DEFINE CONTACT SURFACE
$---+----1----+----2----+----3----+----4----+----5----+----6----+----7----+----8
*CONTACT_NODES_TO_SURFACE_TITLE
$      CID      NAME
         1    GLOBAL
$     SSID      MSID     SSTYP     MSTYP    SBOXID    MBOXID       SPR       MPR
         2         3         2         2         0         0         0         0
$       FS        FD        DC         V       VDC    PENCHK        BT        DT
 7.000E-01 3.000E-01 7.000E+00 1.360E+08 0.000E+00         0 0.000E+00 1.000E+20
$      SFS       SFM       SST       MST      SFST      SFMT       FSF       VSF
  .100E+01  .100E+01                     .100E+01  .100E+01  .100E+01  .100E+01
$---+----1----+----2----+----3----+----4----+----5----+----6----+----7----+----8
*SET_PART_LIST
$      SID
         2
$     PID1      PID2      PID3      PID4      PID5      PID6      PID7      PID8
       303       304       305       306       307       308       309       310
       311       312       313       315       316
*SET_PART_LIST
$      SID
         3
$     PID1      PID2      PID3      PID4      PID5      PID6      PID7      PID8
       204       206       207
$---+----1----+----2----+----3----+----4----+----5----+----6----+----7----+----8
*CONTACT_AUTOMATIC_NODES_TO_SURFACE_TITLE
$      CID      NAME
         4    SIDSHL
$     SSID      MSID     SSTYP     MSTYP    SBOXID    MBOXID       SPR       MPR
         5       304         2         3         0         0         0         0
$       FS        FD        DC         V       VDC    PENCHK        BT        DT
 7.000E-01 3.000E-01 7.000E+00 1.360E+08 0.000E+00         0 0.000E+00 1.000E+20
$      SFS       SFM       SST       MST      SFST      SFMT       FSF       VSF
  .100E+01  .100E+01                     .100E+01  .100E+01  .100E+01  .100E+01
$---+----1----+----2----+----3----+----4----+----5----+----6----+----7----+----8
*SET_PART_LIST
$      SID
         5
$     PID1      PID2      PID3      PID4      PID5      PID6      PID7      PID8
       306       307       308       309       310       311       312       313
       315       316
$---+----1----+----2----+----3----+----4----+----5----+----6----+----7----+----8
*CONTACT_AUTOMATIC_NODES_TO_SURFACE_TITLE
$      CID      NAME
         6    MNDECK
$     SSID      MSID     SSTYP     MSTYP    SBOXID    MBOXID       SPR       MPR
         7       305         2         3         0         0         0         0
$       FS        FD        DC         V       VDC    PENCHK        BT        DT
 7.000E-01 3.000E-01 7.000E+00 1.360E+08 0.000E+00         0 0.000E+00 1.000E+20
$      SFS       SFM       SST       MST      SFST      SFMT       FSF       VSF
  .100E+01  .100E+01                     .100E+01  .100E+01  .100E+01  .100E+01
$---+----1----+----2----+----3----+----4----+----5----+----6----+----7----+----8
*SET_PART_LIST
$      SID
         7
$     PID1      PID2      PID3      PID4      PID5      PID6      PID7      PID8
```

```
       307       308       309       312       313       315       316
$---+----1----+----2----+----3----+----4----+----5----+----6----+----7----+----8
*CONTACT_AUTOMATIC_NODES_TO_SURFACE_TITLE
$      CID      NAME
         8    MNDECK
$     SSID      MSID     SSTYP     MSTYP    SBOXID    MBOXID       SPR       MPR
         9       306         2         3         0         0         0         0
$       FS        FD        DC         V       VDC    PENCHK        BT        DT
 7.000E-01 3.000E-01 7.000E+00 1.360E+08 0.000E+00         0 0.000E+00 1.000E+20
$      SFS       SFM       SST       MST      SFST      SFMT       FSF       VSF
  .100E+01  .100E+01                     .100E+01  .100E+01  .100E+01  .100E+01
$---+----1----+----2----+----3----+----4----+----5----+----6----+----7----+----8
*SET_PART_LIST
$      SID
         9
$     PID1      PID2      PID3      PID4      PID5      PID6      PID7      PID8
       308       309       312
$---+----1----+----2----+----3----+----4----+----5----+----6----+----7----+----8
$---+----1----+----2----+----3----+----4----+----5----+----6----+----7----+----8
*CONTACT_AUTOMATIC_NODES_TO_SURFACE_TITLE
$      CID      NAME
        10     STRUT
$     SSID      MSID     SSTYP     MSTYP    SBOXID    MBOXID       SPR       MPR
       309       312         3         3         0         0         0         0
$       FS        FD        DC         V       VDC    PENCHK        BT        DT
 7.000E-01 3.000E-01 7.000E+00 1.360E+08 0.000E+00         0 0.000E+00 1.000E+20
$      SFS       SFM       SST       MST      SFST      SFMT       FSF       VSF
  .100E+01  .100E+01                     .100E+01  .100E+01  .100E+01  .100E+01
$---+----1----+----2----+----3----+----4----+----5----+----6----+----7----+----8
*CONTACT_AUTOMATIC_NODES_TO_SURFACE_TITLE
$      CID      NAME
        11       SIS
$     SSID      MSID     SSTYP     MSTYP    SBOXID    MBOXID       SPR       MPR
        12        13         2         2         0         0         0         0
$       FS        FD        DC         V       VDC    PENCHK        BT        DT
 7.000E-01 3.000E-01 7.000E+00 1.360E+08 0.000E+00         0 0.000E+00 1.000E+20
$      SFS       SFM       SST       MST      SFST      SFMT       FSF       VSF
  .100E+01  .100E+01                     .100E+01  .100E+01  .100E+01  .100E+01
$---+----1----+----2----+----3----+----4----+----5----+----6----+----7----+----8
*SET_PART_LIST
$      SID
        12
$     PID1      PID2      PID3      PID4      PID5      PID6      PID7      PID8
       203       205       208
*SET_PART_LIST
$      SID
        13
$     PID1      PID2      PID3      PID4      PID5      PID6      PID7      PID8
       204       206       207
$---+----1----+----2----+----3----+----4----+----5----+----6----+----7----+----8
*CONTACT_AUTOMATIC_NODES_TO_SURFACE_TITLE
$      CID      NAME
        14      DECK
$     SSID      MSID     SSTYP     MSTYP    SBOXID    MBOXID       SPR       MPR
       204       207         3         3         0         0         0         0
$       FS        FD        DC         V       VDC    PENCHK        BT        DT
 7.000E-01 3.000E-01 7.000E+00 1.360E+08 0.000E+00         0 0.000E+00 1.000E+20
$      SFS       SFM       SST       MST      SFST      SFMT       FSF       VSF
  .100E+01  .100E+01                     .100E+01  .100E+01  .100E+01  .100E+01
$---+----1----+----2----+----3----+----4----+----5----+----6----+----7----+----8
*CONTACT_AUTOMATIC_SINGLE_SURFACE_TITLE
$      CID      NAME
        15    SINGLE
$     SSID      MSID     SSTYP     MSTYP    SBOXID    MBOXID       SPR       MPR
        16                  2                   0         0         0         0
$       FS        FD        DC         V       VDC    PENCHK        BT        DT
 7.000E-01 3.000E-01 7.000E+00 1.360E+08 0.000E+00         0 0.000E+00 1.000E+20
$      SFS       SFM       SST       MST      SFST      SFMT       FSF       VSF
  .100E+01  .100E+01                     .100E+01  .100E+01  .100E+01  .100E+01
$---+----1----+----2----+----3----+----4----+----5----+----6----+----7----+----8
*SET_PART_LIST
$      SID
        16
$     PID1      PID2      PID3      PID4      PID5      PID6      PID7      PID8
       204       206       207       208
$---+----1----+----2----+----3----+----4----+----5----+----6----+----7----+----8
$---+----1----+----2----+----3----+----4----+----5----+----6----+----7----+----8
```

```
$                   (23) DEFINE RIGID WALL
$---+----1----+----2----+----3----+----4----+----5----+----6----+----7----+----8
$                   (24) NODAL RIGID BODY CARDS
$---+----1----+----2----+----3----+----4----+----5----+----6----+----7----+----8
$                   (25) JOINT CARDS
$---+----1----+----2----+----3----+----4----+----5----+----6----+----7----+----8
$---+----1----+----2----+----3----+----4----+----5----+----6----+----7----+----8
$---+----1----+----2----+----3----+----4----+----5----+----6----+----7----+----8
*END
```

Appendix J: Flowchart of Method of Lateral Deformation of Webs and Transverse Bulkheads

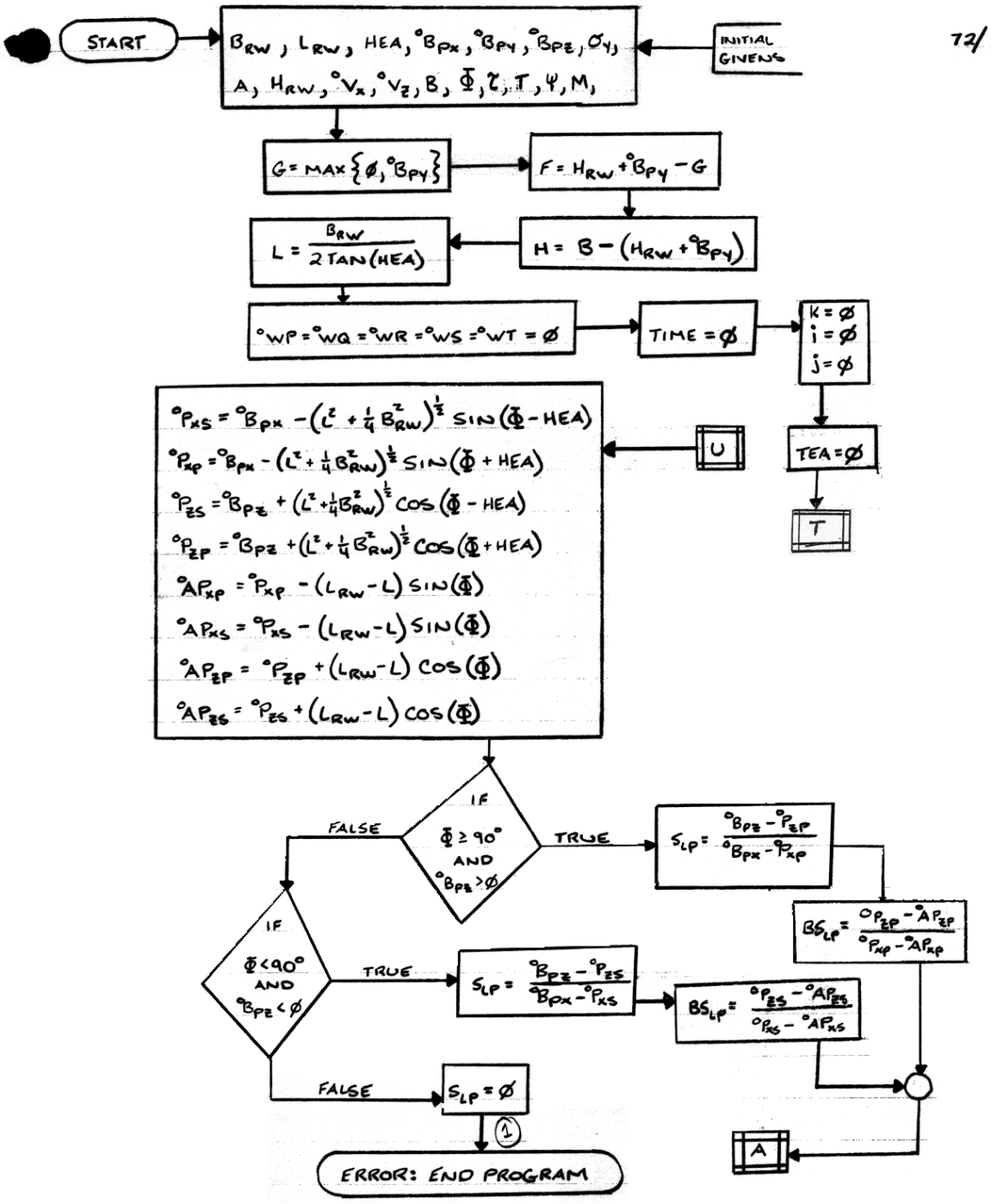

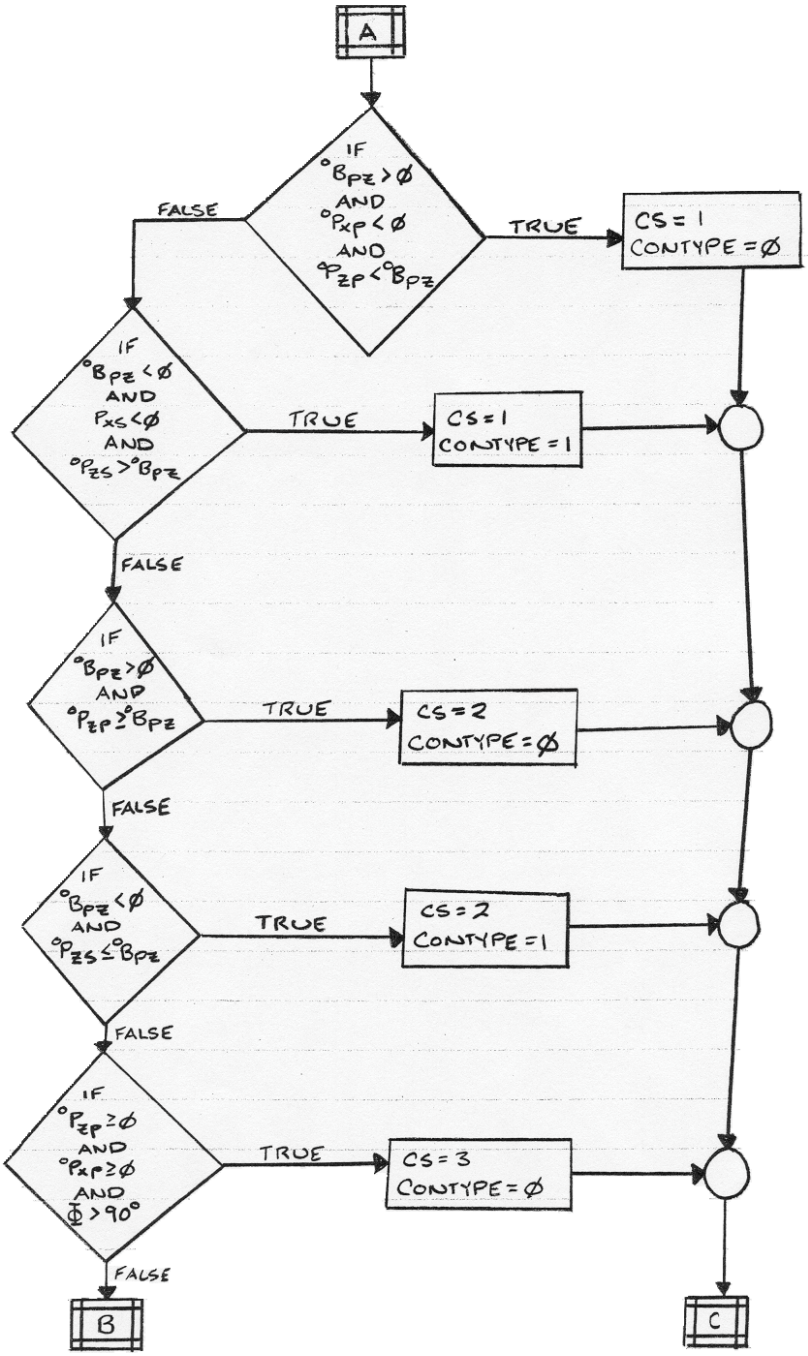
A
IF
°Bpz > ∅
AND
°Pxp < ∅
AND
°Pzp < °Bpz
TRUE
CS = 1
CONTYPE = ∅
FALSE
IF
°Bpz < ∅
AND
Pxs < ∅
AND
°Pzs > °Bpz
TRUE
CS = 1
CONTYPE = 1
FALSE
IF
°Bpz > ∅
AND
°Pzp ≥ °Bpz
TRUE
CS = 2
CONTYPE = ∅
FALSE
IF
°Bpz < ∅
AND
°Pzs ≤ °Bpz
TRUE
CS = 2
CONTYPE = 1
FALSE
IF
°Pzp ≥ ∅
AND
°Pxp ≥ ∅
AND
Φ > 90°
TRUE
CS = 3
CONTYPE = ∅
FALSE
B
C

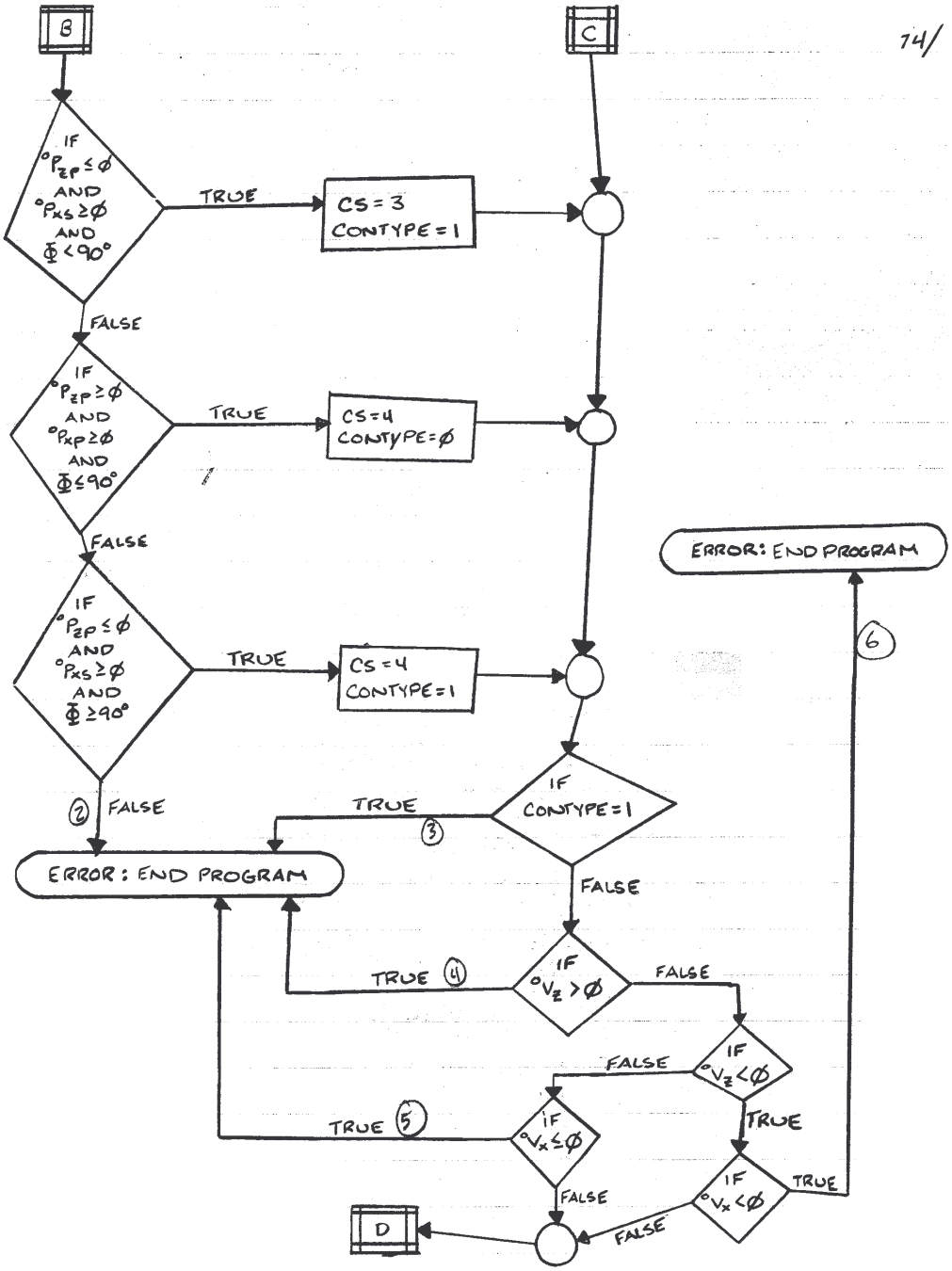
B
C
IF °P_ZP ≤ ∅ AND °P_XS ≥ ∅ AND Φ < 90°
TRUE
CS = 3
CONTYPE = 1
FALSE
IF °P_ZP ≥ ∅ AND °P_XP ≥ ∅ AND Φ ≤ 90°
TRUE
CS = 4
CONTYPE = ∅
FALSE
IF °P_ZP ≤ ∅ AND °P_XS ≥ ∅ AND Φ ≥ 90°
TRUE
CS = 4
CONTYPE = 1
2
FALSE
ERROR: END PROGRAM
IF CONTYPE = 1
TRUE
3
FALSE
IF °V_Z > ∅
TRUE
4
FALSE
IF °V_Z < ∅
FALSE
IF °V_X ≤ ∅
TRUE
5
FALSE
IF °V_X < ∅
TRUE
FALSE
D
ERROR: END PROGRAM
6

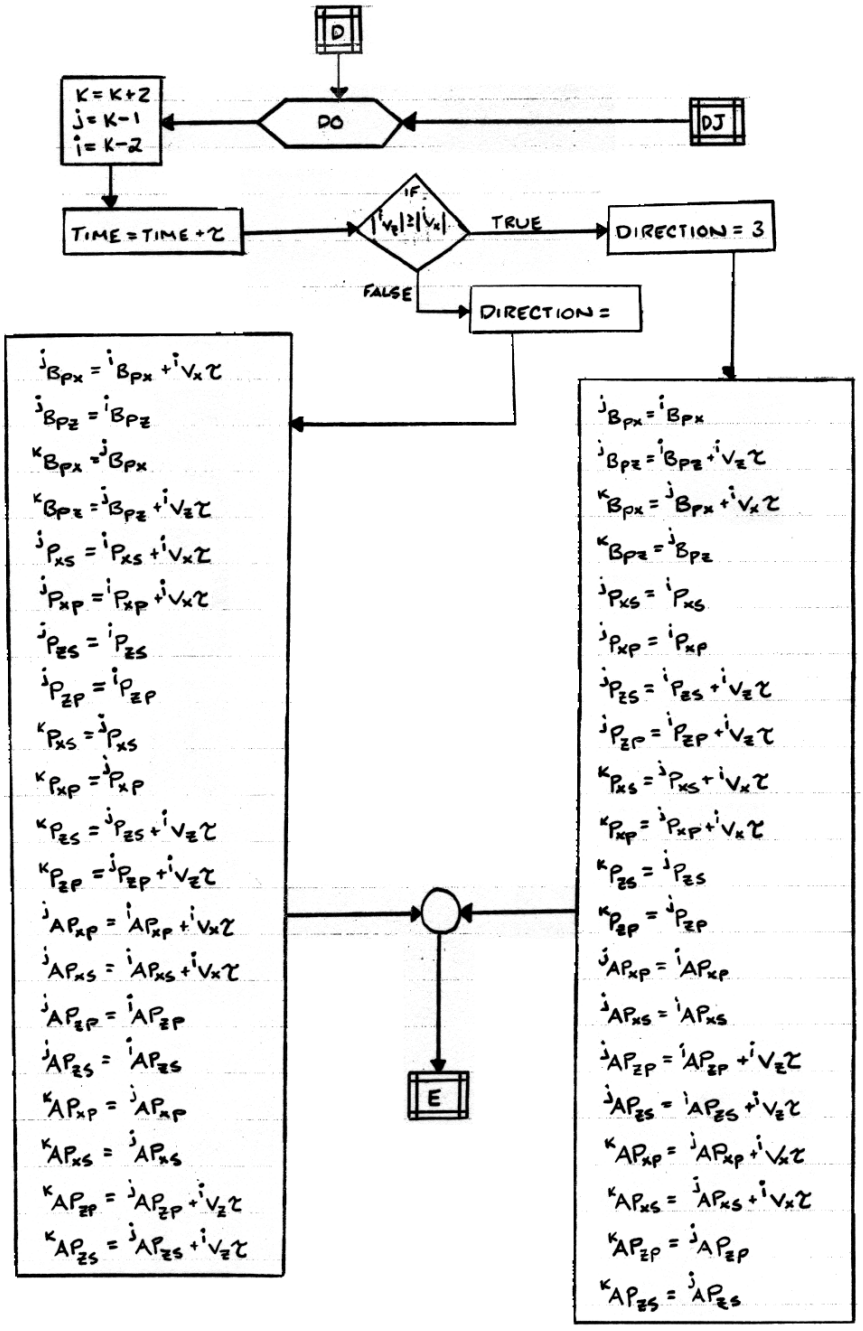
D
K = K+2
j = K-1
i = K-2
DO
DJ
TIME = TIME + τ
IF
$|^iV_z| \geq |^iV_x|$
TRUE
DIRECTION = 3
FALSE
DIRECTION =
$^jB_{px} = {}^iB_{px} + {}^iV_x\tau$
$^jB_{pz} = {}^iB_{pz}$
$^kB_{px} = {}^jB_{px}$
$^kB_{pz} = {}^jB_{pz} + {}^iV_z\tau$
$^jP_{xs} = {}^iP_{xs} + {}^iV_x\tau$
$^jP_{xp} = {}^iP_{xp} + {}^iV_x\tau$
$^jP_{zs} = {}^iP_{zs}$
$^jP_{zp} = {}^iP_{zp}$
$^kP_{xs} = {}^jP_{xs}$
$^kP_{xp} = {}^jP_{xp}$
$^kP_{zs} = {}^jP_{zs} + {}^iV_z\tau$
$^kP_{zp} = {}^jP_{zp} + {}^iV_z\tau$
$^jAP_{xp} = {}^iAP_{xp} + {}^iV_x\tau$
$^jAP_{xs} = {}^iAP_{xs} + {}^iV_x\tau$
$^jAP_{zp} = {}^iAP_{zp}$
$^jAP_{zs} = {}^iAP_{zs}$
$^kAP_{xp} = {}^jAP_{xp}$
$^kAP_{xs} = {}^jAP_{xs}$
$^kAP_{zp} = {}^jAP_{zp} + {}^iV_z\tau$
$^kAP_{zs} = {}^jAP_{zs} + {}^iV_z\tau$
$^jB_{px} = {}^iB_{px}$
$^jB_{pz} = {}^iB_{pz} + {}^iV_z\tau$
$^kB_{px} = {}^jB_{px} + {}^iV_x\tau$
$^kB_{pz} = {}^jB_{pz}$
$^jP_{xs} = {}^iP_{xs}$
$^jP_{xp} = {}^iP_{xp}$
$^jP_{zs} = {}^iP_{zs} + {}^iV_z\tau$
$^jP_{zp} = {}^iP_{zp} + {}^iV_z\tau$
$^kP_{xs} = {}^jP_{xs} + {}^iV_x\tau$
$^kP_{xp} = {}^jP_{xp} + {}^iV_x\tau$
$^kP_{zs} = {}^jP_{zs}$
$^kP_{zp} = {}^jP_{zp}$
$^jAP_{xp} = {}^iAP_{xp}$
$^jAP_{xs} = {}^iAP_{xs}$
$^jAP_{zp} = {}^iAP_{zp} + {}^iV_z\tau$
$^jAP_{zs} = {}^iAP_{zs} + {}^iV_z\tau$
$^kAP_{xp} = {}^jAP_{xp} + {}^iV_x\tau$
$^kAP_{xs} = {}^jAP_{xs} + {}^iV_x\tau$
$^kAP_{zp} = {}^jAP_{zp}$
$^kAP_{zs} = {}^jAP_{zs}$
E

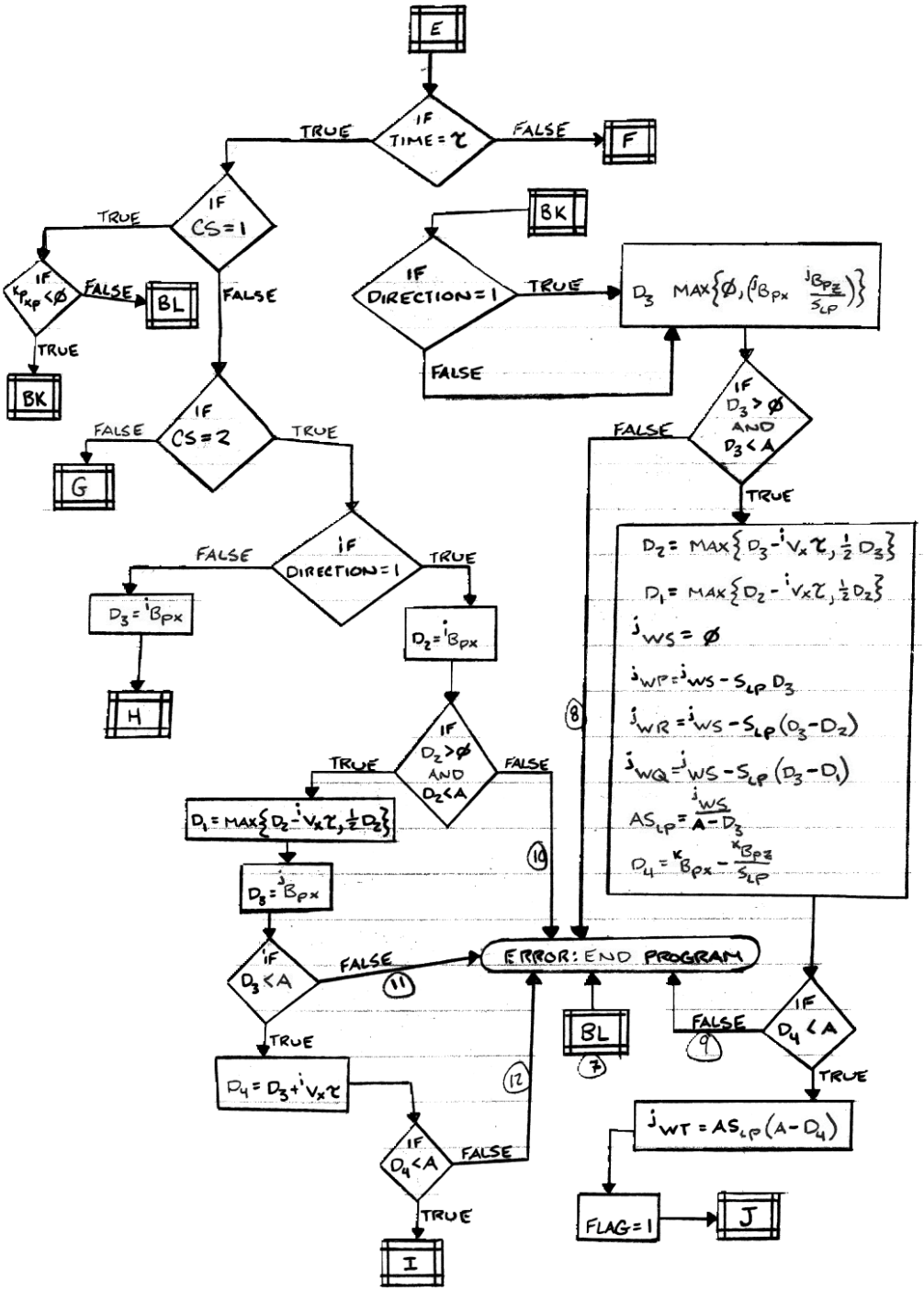
E
IF TIME = τ
TRUE
FALSE
F
IF CS = 1
TRUE
IF κ_Bpx < ∅
FALSE
BL
TRUE
BK
FALSE
IF CS = 2
FALSE
G
TRUE
IF DIRECTION = 1
FALSE
H
TRUE
D3 = iBpx
D2 = iBpx
IF D2 > ∅ AND D2 < A
TRUE
FALSE
D1 = MAX{D2 - iVx τ, ½ D2}
D8 = jBpx
IF D3 < A
FALSE
TRUE
D4 = D3 + iVx τ
IF D4 < A
FALSE
TRUE
I
ERROR: END PROGRAM
BK
IF DIRECTION = 1
TRUE
FALSE
D3 MAX{∅, (κBpx jBpz/sLP)}
IF D3 > ∅ AND D3 < A
FALSE
TRUE
D2 = MAX{D3 - iVx τ, ½ D3}
D1 = MAX{D2 - iVx τ, ½ D2}
jWS = ∅
jWP = jWS - SLP D3
jWR = jWS - SLP (D3 - D2)
jWQ = jWS - SLP (D3 - D1)
ASLP = jWS / (A - D3)
D4 = κBpx - κBpz/sLP
8
10
11
12
BL
7
9
IF D4 < A
TRUE
jWT = ASLP (A - D4)
FLAG = 1
J

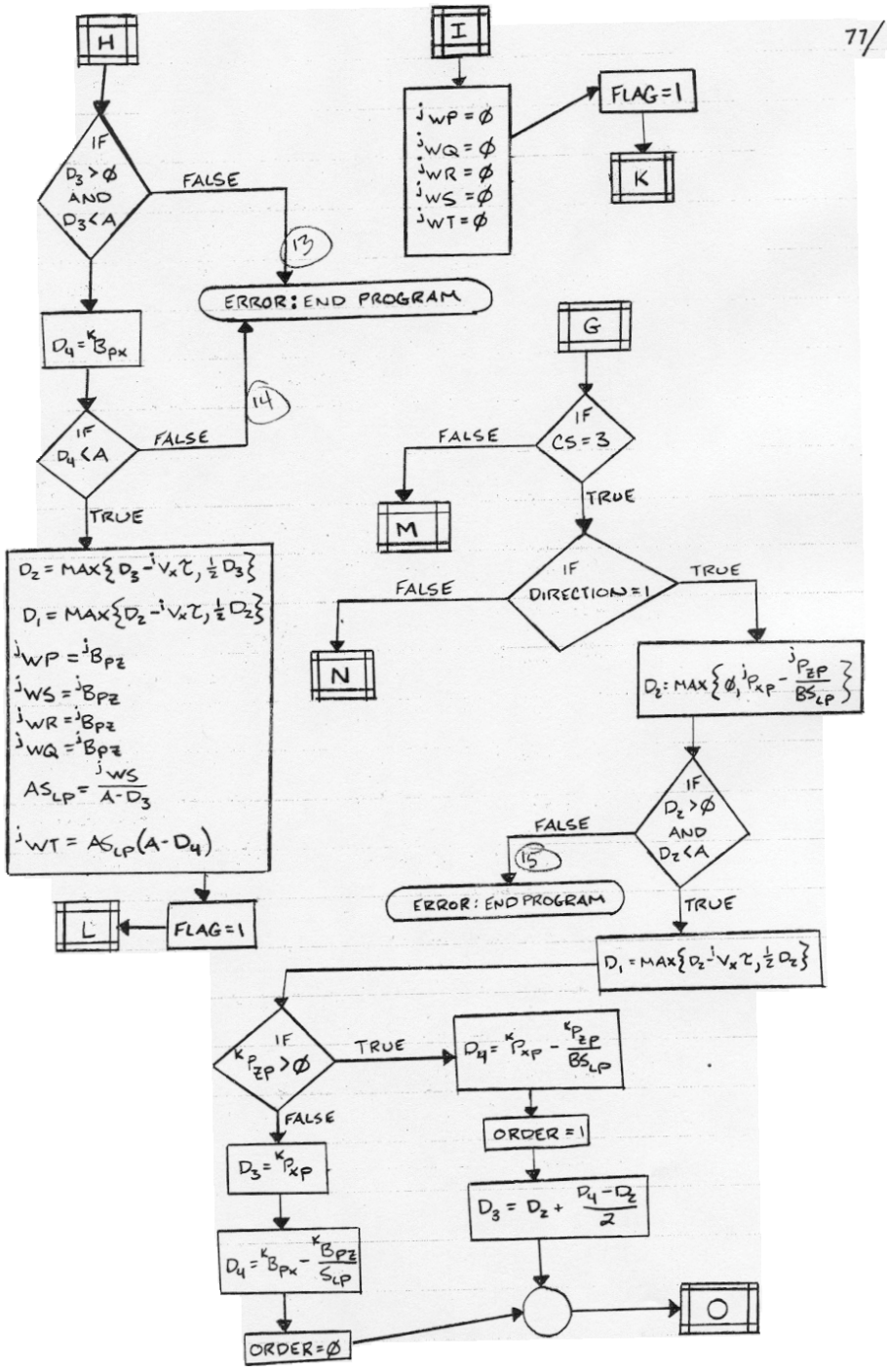
H
IF $D_3 > \emptyset$ AND $D_3 < A$
FALSE
13
ERROR: END PROGRAM
$D_4 = {}^{K}B_{PX}$
IF $D_4 < A$
FALSE
14
TRUE
$D_2 = MAX\{D_3 - {}^{j}V_x\tau, \frac{1}{2}D_3\}$
$D_1 = MAX\{D_2 - {}^{j}V_x\tau, \frac{1}{2}D_2\}$
${}^{j}WP = {}^{j}B_{PZ}$
${}^{j}WS = {}^{j}B_{PZ}$
${}^{j}WR = {}^{j}B_{PZ}$
${}^{j}WQ = {}^{j}B_{PZ}$
$AS_{LP} = \frac{{}^{j}WS}{A - D_3}$
${}^{j}WT = AS_{LP}(A - D_4)$
L
FLAG=1
I
${}^{j}WP = \emptyset$
${}^{j}WQ = \emptyset$
${}^{j}WR = \emptyset$
${}^{j}WS = \emptyset$
${}^{j}WT = \emptyset$
FLAG=1
K
G
IF CS=3
FALSE
TRUE
M
IF DIRECTION=1
FALSE
TRUE
N
$D_2 = MAX\{\emptyset, {}^{j}P_{XP} - \frac{{}^{j}P_{ZP}}{BS_{LP}}\}$
IF $D_2 > \emptyset$ AND $D_2 < A$
FALSE
15
ERROR: END PROGRAM
TRUE
$D_1 = MAX\{D_2 - {}^{j}V_x\tau, \frac{1}{2}D_2\}$
IF ${}^{K}P_{ZP} > \emptyset$
TRUE
$D_4 = {}^{K}P_{XP} - \frac{{}^{K}P_{ZP}}{BS_{LP}}$
ORDER=1
$D_3 = D_2 + \frac{D_4 - D_2}{2}$
FALSE
$D_3 = {}^{K}P_{XP}$
$D_4 = {}^{K}B_{PX} - \frac{{}^{K}B_{PZ}}{S_{LP}}$
ORDER=$\emptyset$
O

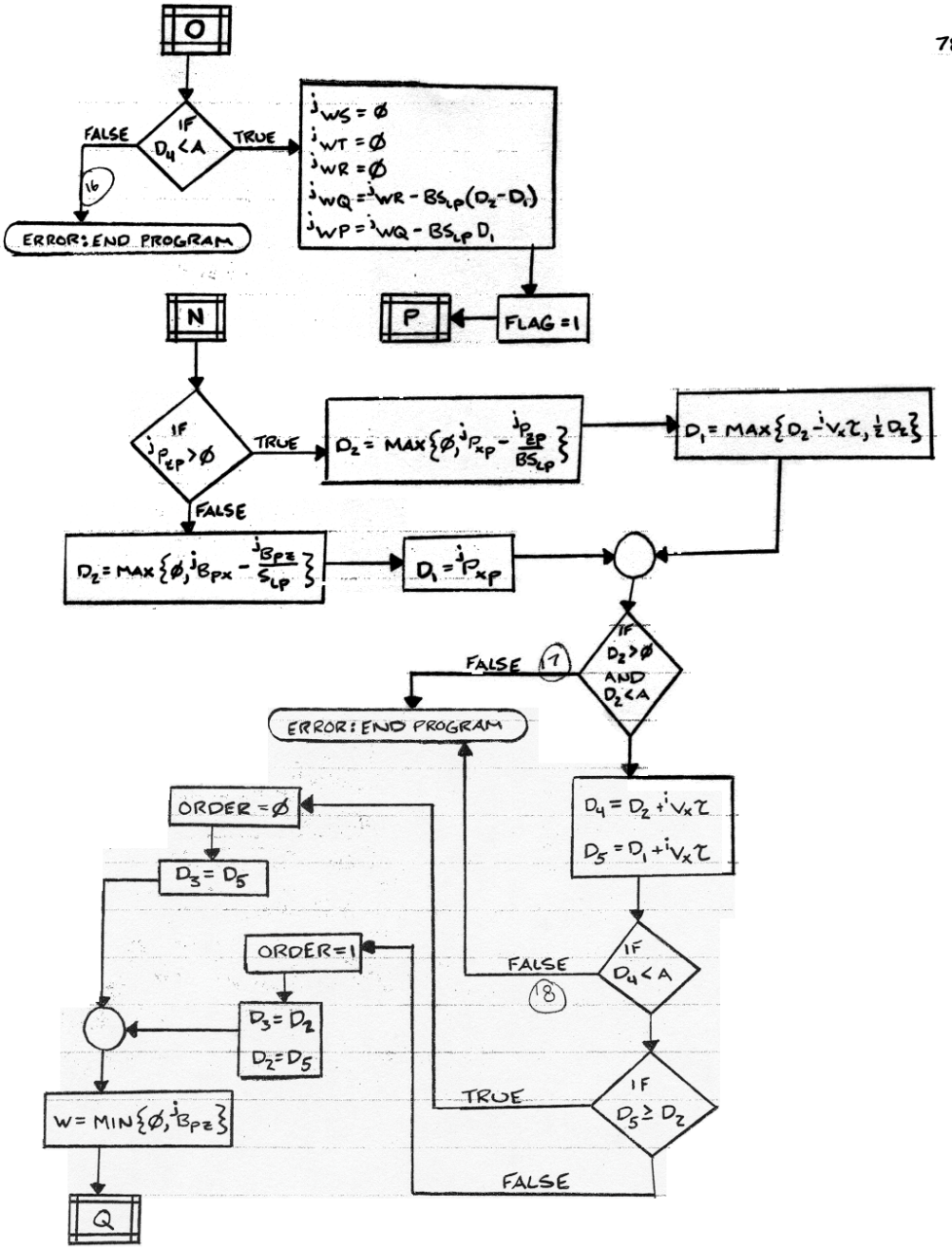
O
IF $D_4 < A$
FALSE
TRUE
16
ERROR: END PROGRAM
$^jW_S = \emptyset$
$^jW_T = \emptyset$
$^jW_R = \emptyset$
$^jW_Q = {}^jW_R - BS_{LP}(D_2 - D_1)$
$^jW_P = {}^jW_Q - BS_{LP} D_1$
P
FLAG = 1
N
IF $^jP_{EP} > \emptyset$
TRUE
$D_2 = MAX\{\emptyset, {}^jP_{XP} - \frac{^jP_{EP}}{BS_{LP}}\}$
$D_1 = MAX\{D_2 - {}^iV_x\tau, \frac{1}{2}D_2\}$
FALSE
$D_2 = MAX\{\emptyset, {}^jB_{PX} - \frac{^jB_{PE}}{S_{LP}}\}$
$D_1 = {}^jP_{XP}$
IF $D_2 > \emptyset$ AND $D_2 < A$
FALSE
17
ERROR: END PROGRAM
$D_4 = D_2 + {}^iV_x\tau$
$D_5 = D_1 + {}^iV_x\tau$
ORDER = $\emptyset$
$D_3 = D_5$
IF $D_4 < A$
FALSE
18
ORDER = 1
$D_3 = D_2$
$D_2 = D_5$
IF $D_5 \geq D_2$
TRUE
FALSE
$W = MIN\{\emptyset, {}^jB_{PE}\}$
Q

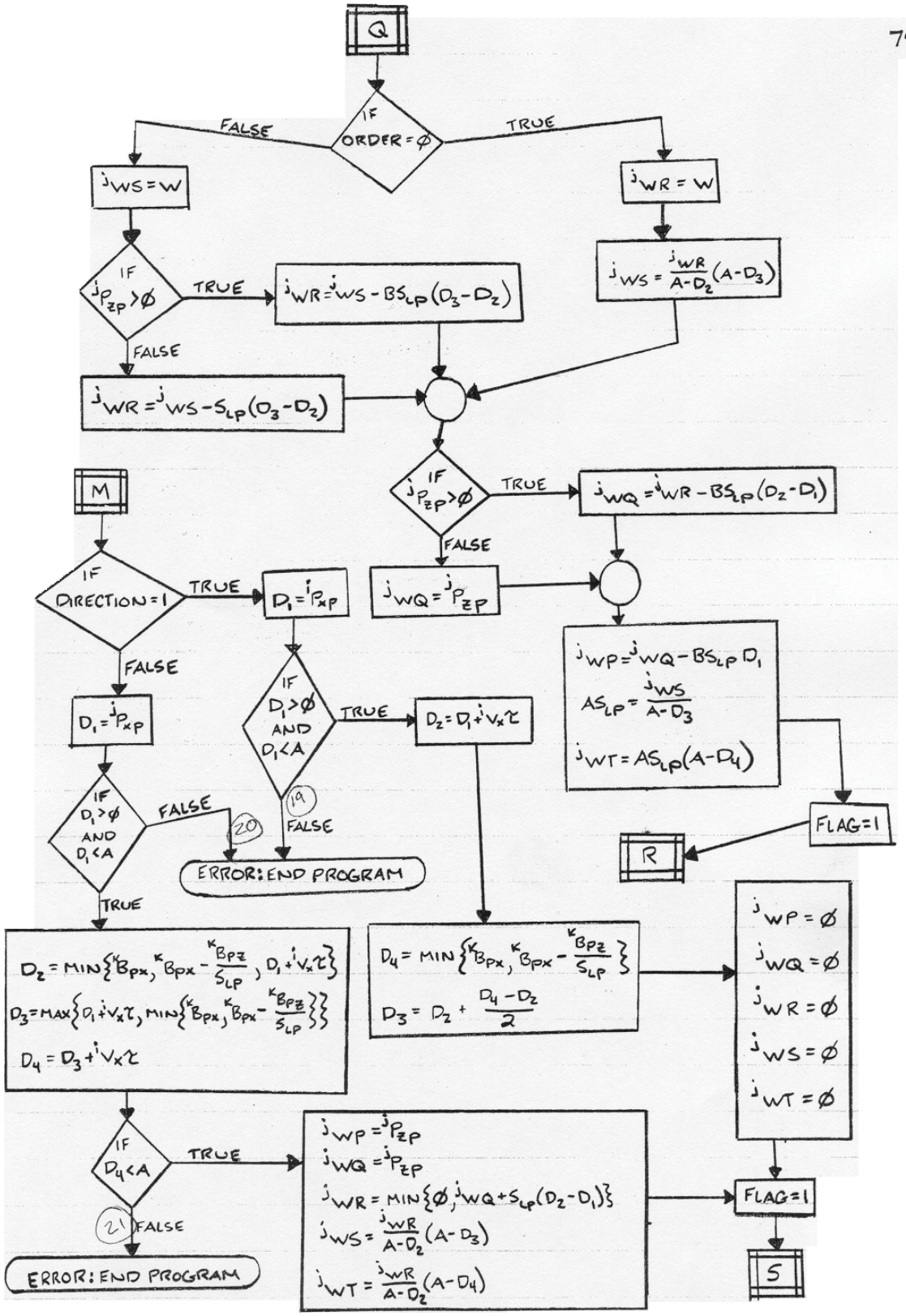
Q
IF ORDER = ∅
FALSE
TRUE
$^{j}W_S = W$
$^{j}W_R = W$
IF $^{j}P_{zP} > ∅$
TRUE
$^{j}W_R = {}^{j}W_S - BS_{LP}(D_3 - D_2)$
$^{j}W_S = \frac{^{j}W_R}{A - D_2}(A - D_3)$
FALSE
$^{j}W_R = {}^{j}W_S - S_{LP}(D_3 - D_2)$
M
IF $^{j}P_{zP} > ∅$
TRUE
$^{j}W_Q = {}^{j}W_R - BS_{LP}(D_2 - D_1)$
FALSE
$^{j}W_Q = {}^{j}P_{zP}$
IF DIRECTION = 1
TRUE
$D_1 = {}^{i}P_{xP}$
FALSE
$D_1 = {}^{j}P_{xP}$
IF $D_1 > ∅$ AND $D_1 < A$
TRUE
$D_2 = D_1 + {}^{i}V_x \tau$
FALSE
19
IF $D_1 > ∅$ AND $D_1 < A$
FALSE
20
ERROR: END PROGRAM
TRUE
$^{j}W_P = {}^{j}W_Q - BS_{LP} D_1$
$AS_{LP} = \frac{^{j}W_S}{A - D_3}$
$^{j}W_T = AS_{LP}(A - D_4)$
FLAG = 1
R
$D_2 = MIN\left\{{}^{K}B_{px}, {}^{K}B_{px} - \frac{{}^{K}B_{pz}}{S_{LP}}, D_1 + {}^{i}V_x \tau\right\}$
$D_3 = MAX\left\{D_1 + {}^{i}V_x \tau, MIN\left\{{}^{K}B_{px}, {}^{K}B_{px} - \frac{{}^{K}B_{pz}}{S_{LP}}\right\}\right\}$
$D_4 = D_3 + {}^{i}V_x \tau$
$D_4 = MIN\left\{{}^{K}B_{px}, {}^{K}B_{px} - \frac{{}^{K}B_{pz}}{S_{LP}}\right\}$
$D_3 = D_2 + \frac{D_4 - D_2}{2}$
$^{j}W_P = ∅$
$^{j}W_Q = ∅$
$^{j}W_R = ∅$
$^{j}W_S = ∅$
$^{j}W_T = ∅$
IF $D_4 < A$
TRUE
21
FALSE
ERROR: END PROGRAM
$^{j}W_P = {}^{j}P_{zP}$
$^{j}W_Q = {}^{j}P_{zP}$
$^{j}W_R = MIN\{∅, {}^{j}W_Q + S_{LP}(D_2 - D_1)\}$
$^{j}W_S = \frac{^{j}W_R}{A - D_2}(A - D_3)$
$^{j}W_T = \frac{^{j}W_R}{A - D_2}(A - D_4)$
FLAG = 1
5

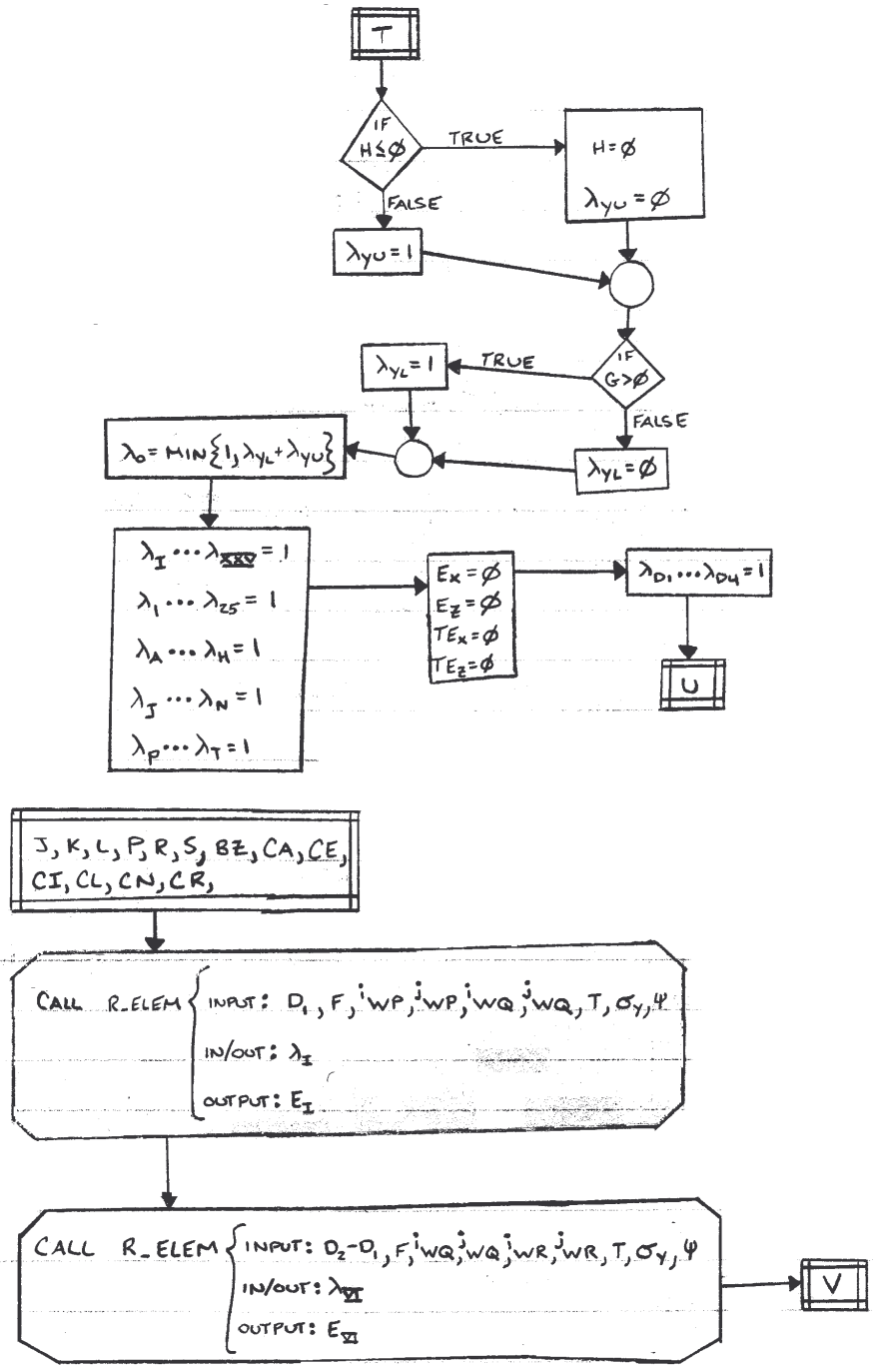
T
IF H≤∅
TRUE
H=∅
λyu=∅
FALSE
λyu=1
λyL=1
TRUE
IF G>∅
FALSE
λo=MIN{1, λyL+λyu}
λyL=∅
λI ... λXXV=1
λ1 ... λ25=1
λA ... λH=1
λJ ... λN=1
λP ... λT=1
Ex=∅
Ez=∅
TEx=∅
TEz=∅
λD1 ... λD4=1
U
J, K, L, P, R, S, BZ, CA, CE, CI, CL, CN, CR,
CALL R_ELEM
INPUT: D1, F, iWP, jWP, iWQ, jWQ, T, σy, ψ
IN/OUT: λI
OUTPUT: EI
CALL R_ELEM
INPUT: D2-D1, F, iWQ, jWQ, iWR, jWR, T, σy, ψ
IN/OUT: λVI
OUTPUT: EVI
V

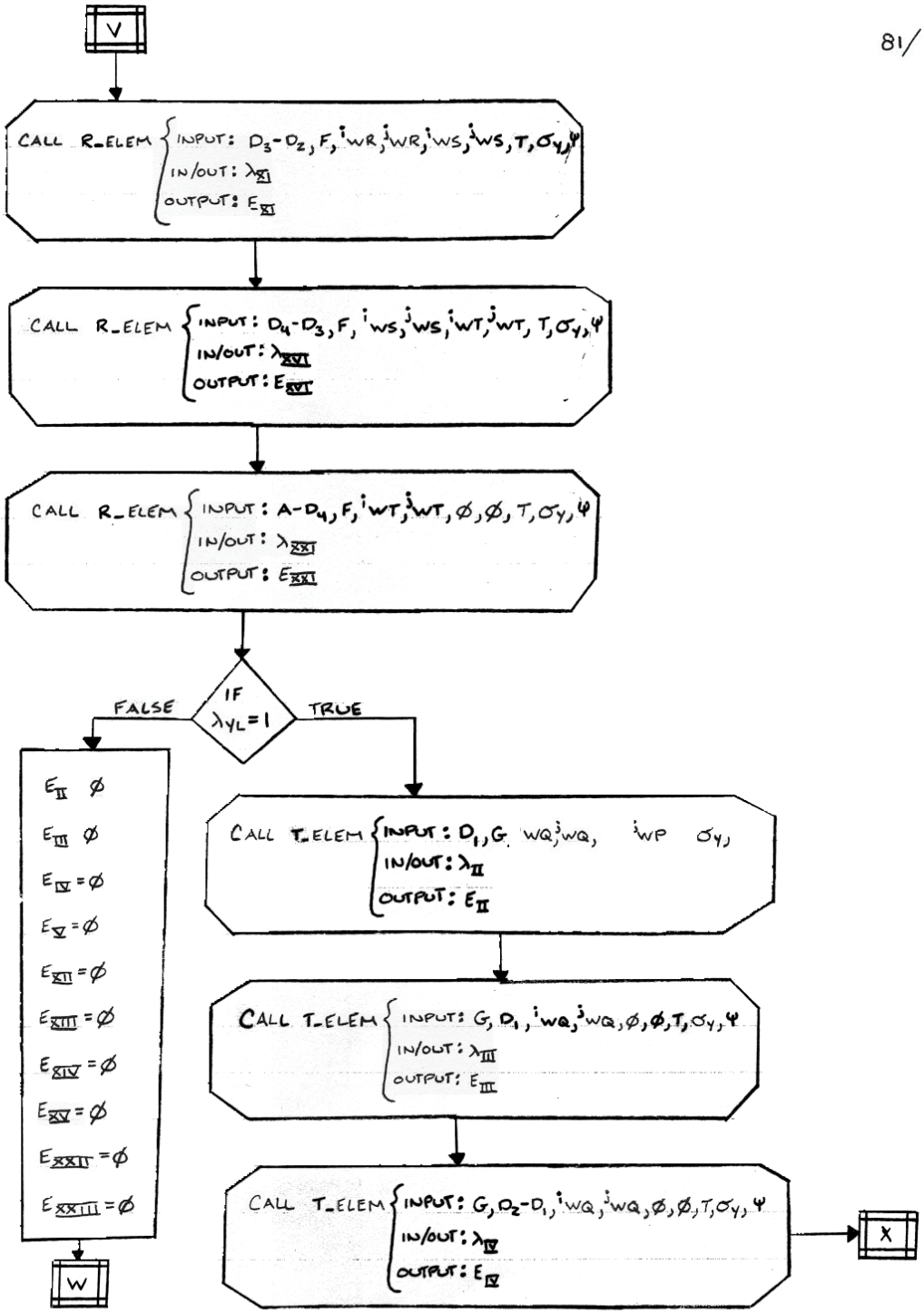
V
CALL R_ELEM
INPUT: $D_3-D_2, F, {}^iWR, {}^jWR, {}^iWS, {}^jWS, T, \sigma_y, \psi$
IN/OUT: λ_{XI}
OUTPUT: E_{XI}
CALL R_ELEM
INPUT: $D_4-D_3, F, {}^iWS, {}^jWS, {}^iWT, {}^jWT, T, \sigma_y, \psi$
IN/OUT: λ_{XVI}
OUTPUT: E_{XVI}
CALL R_ELEM
INPUT: $A-D_4, F, {}^iWT, {}^jWT, \phi, \phi, T, \sigma_y, \psi$
IN/OUT: λ_{XXI}
OUTPUT: E_{XXI}
IF $\lambda_{YL}=1$
FALSE
TRUE
$E_{II} \phi$
$E_{III} \phi$
$E_{IV}=\phi$
$E_{V}=\phi$
$E_{XII}=\phi$
$E_{XIII}=\phi$
$E_{XIV}=\phi$
$E_{XV}=\phi$
$E_{XXII}=\phi$
$E_{XXIII}=\phi$
W
CALL T_ELEM
INPUT: $D_1, G, WQ, {}^jWQ, {}^iWP, \sigma_y$
IN/OUT: λ_{II}
OUTPUT: E_{II}
CALL T_ELEM
INPUT: $G, D_1, {}^iWQ, {}^jWQ, \phi, \phi, T, \sigma_y, \psi$
IN/OUT: λ_{III}
OUTPUT: E_{III}
CALL T_ELEM
INPUT: $G, D_2-D_1, {}^iWQ, {}^jWQ, \phi, \phi, T, \sigma_y, \psi$
IN/OUT: λ_{IV}
OUTPUT: E_{IV}
X

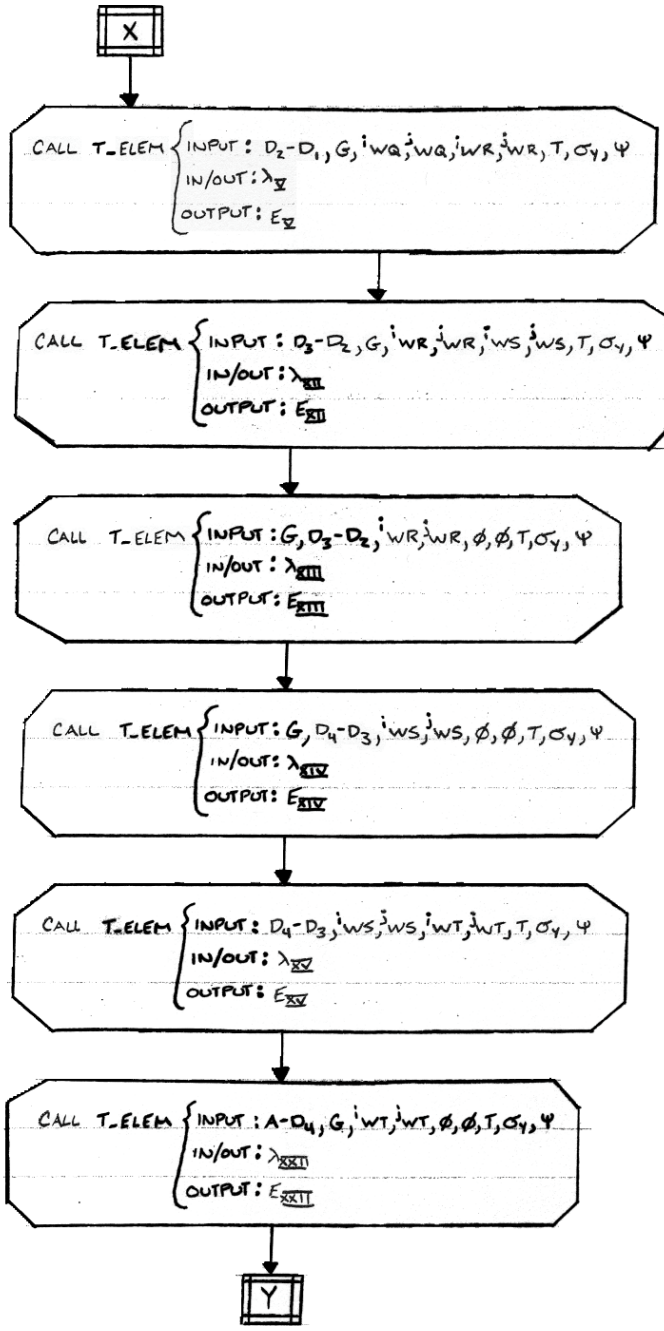
X
CALL T_ELEM
INPUT : $D_2-D_1, G, {}^iWQ, {}^jWQ, {}^iWR, {}^jWR, T, \sigma_y, \Psi$
IN/OUT : λ_V
OUTPUT : E_V
CALL T_ELEM
INPUT : $D_3-D_2, G, {}^iWR, {}^jWR, {}^iWS, {}^jWS, T, \sigma_y, \Psi$
IN/OUT : λ_{VI}
OUTPUT : E_{VI}
CALL T_ELEM
INPUT : $G, D_3-D_2, {}^iWR, {}^jWR, \phi, \phi, T, \sigma_y, \Psi$
IN/OUT : λ_{VII}
OUTPUT : E_{VII}
CALL T_ELEM
INPUT : $G, D_4-D_3, {}^iWS, {}^jWS, \phi, \phi, T, \sigma_y, \Psi$
IN/OUT : λ_{VIII}
OUTPUT : E_{VIII}
CALL T_ELEM
INPUT : $D_4-D_3, {}^iWS, {}^jWS, {}^iWT, {}^jWT, T, \sigma_y, \Psi$
IN/OUT : λ_{IX}
OUTPUT : E_{IX}
CALL T_ELEM
INPUT : $A-D_4, G, {}^iWT, {}^jWT, \phi, \phi, T, \sigma_y, \Psi$
IN/OUT : λ_{XI}
OUTPUT : E_{XI}
Y

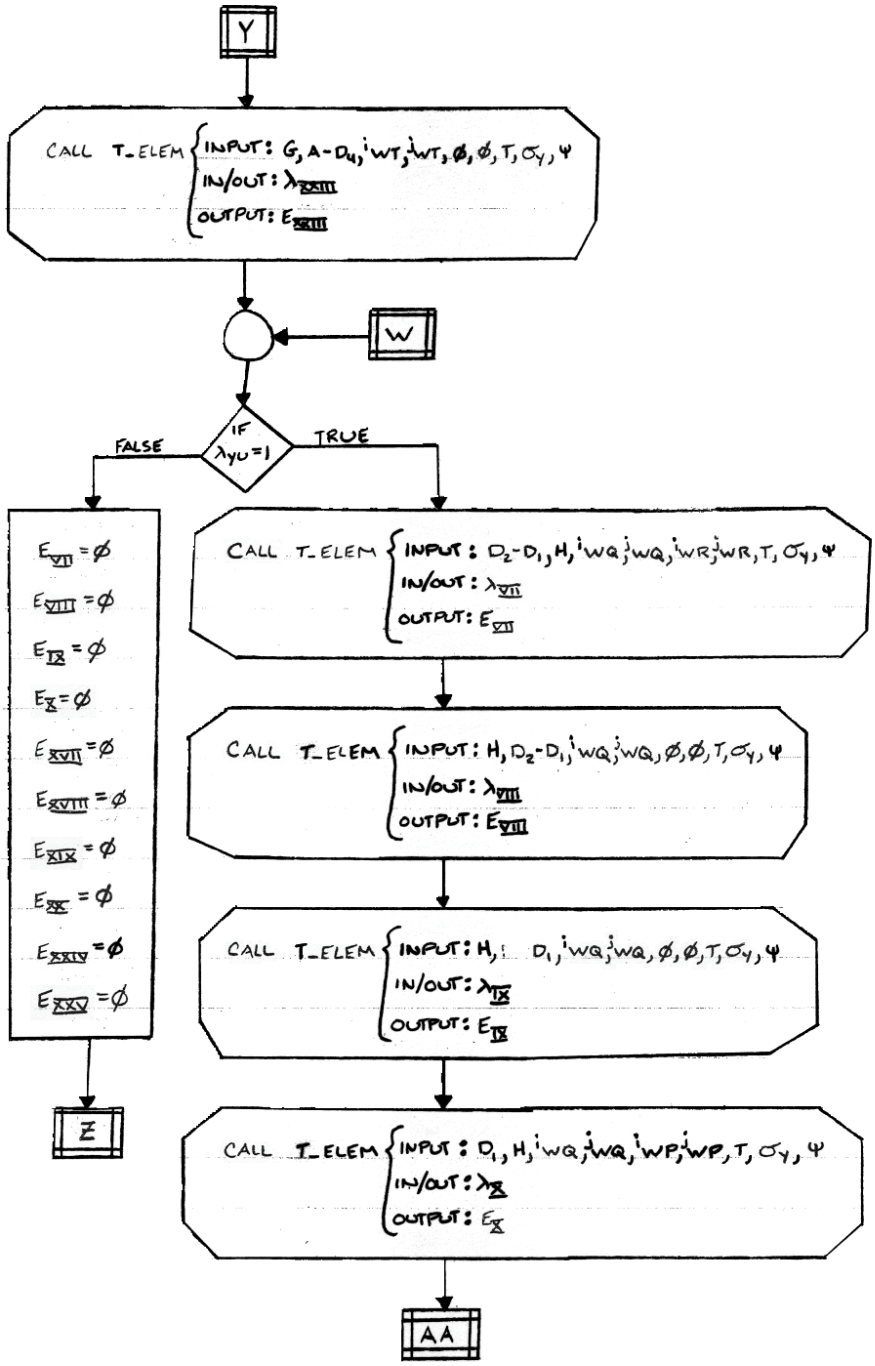
Y
CALL T_ELEM
INPUT: G, A-D4, iWT, jWT, Ø, Ø, T, σy, Ψ
IN/OUT: λXXIII
OUTPUT: EXXIII
W
IF λyu=1
FALSE
TRUE
EVII = Ø
EVIII = Ø
EIX = Ø
EX = Ø
EXVII = Ø
EXVIII = Ø
EXIX = Ø
EXX = Ø
EXXIV = Ø
EXXV = Ø
Z
CALL T_ELEM
INPUT: D2-D1, H, iWQ, jWQ, iWR, jWR, T, σy, Ψ
IN/OUT: λVII
OUTPUT: EVII
CALL T_ELEM
INPUT: H, D2-D1, iWQ, jWQ, Ø, Ø, T, σy, Ψ
IN/OUT: λVIII
OUTPUT: EVIII
CALL T_ELEM
INPUT: H, D1, iWQ, jWQ, Ø, Ø, T, σy, Ψ
IN/OUT: λIX
OUTPUT: EIX
CALL T_ELEM
INPUT: D1, H, iWQ, jWQ, iWP, jWP, T, σy, Ψ
IN/OUT: λX
OUTPUT: EX
AA

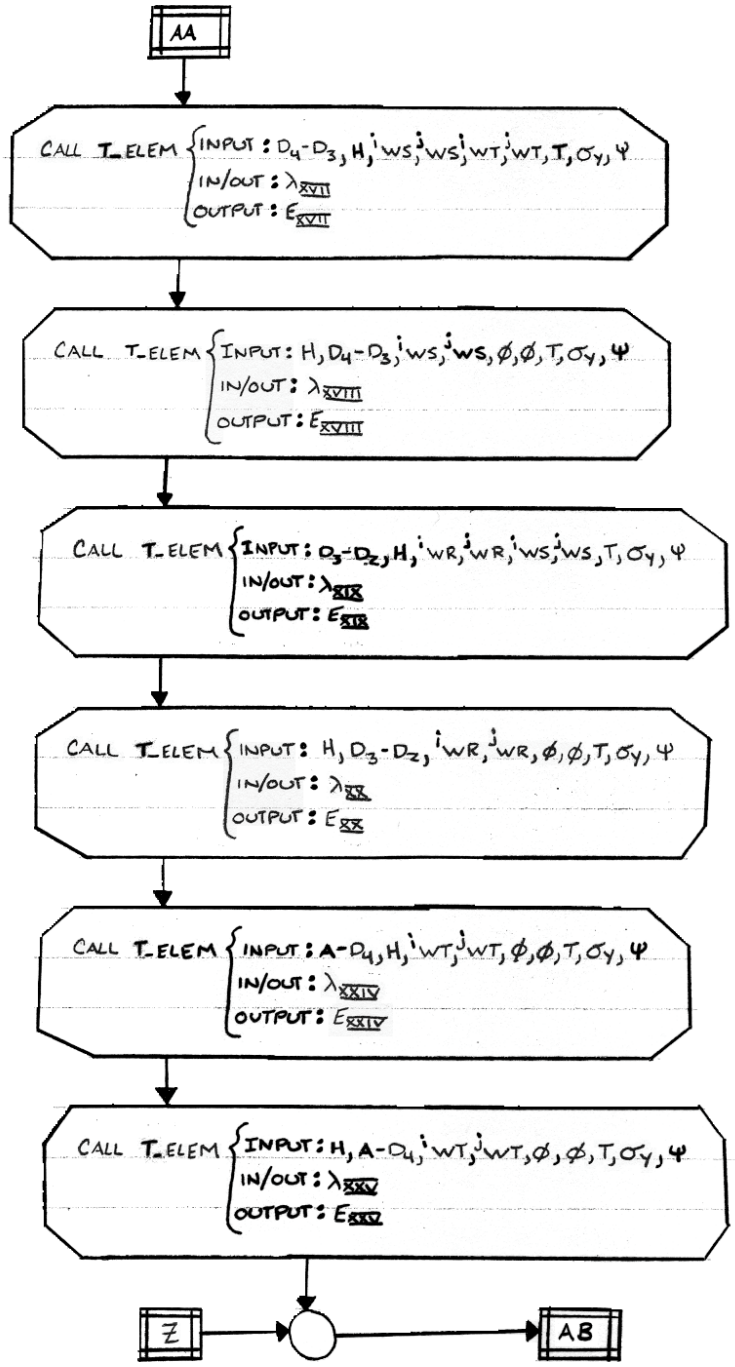
AA
CALL T_ELEM
INPUT : D_4-D_3, H, ^{i}WS, ^{j}WS, ^{i}WT, ^{j}WT, T, σ_y, ψ
IN/OUT : λ_{XVII}
OUTPUT : E_{XVII}
CALL T_ELEM
INPUT : H, D_4-D_3, ^{i}WS, ^{j}WS, ϕ, ϕ, T, σ_y, ψ
IN/OUT : λ_{XVIII}
OUTPUT : E_{XVIII}
CALL T_ELEM
INPUT : D_3-D_2, H, ^{i}WR, ^{j}WR, ^{i}WS, ^{j}WS, T, σ_y, ψ
IN/OUT : λ_{XIX}
OUTPUT : E_{XIX}
CALL T_ELEM
INPUT : H, D_3-D_2, ^{i}WR, ^{j}WR, ϕ, ϕ, T, σ_y, ψ
IN/OUT : λ_{XX}
OUTPUT : E_{XX}
CALL T_ELEM
INPUT : A-D_4, H, ^{i}WT, ^{j}WT, ϕ, ϕ, T, σ_y, ψ
IN/OUT : λ_{XXIV}
OUTPUT : E_{XXIV}
CALL T_ELEM
INPUT : H, A-D_4, ^{i}WT, ^{j}WT, ϕ, ϕ, T, σ_y, ψ
IN/OUT : λ_{XXV}
OUTPUT : E_{XXV}
Z
AB

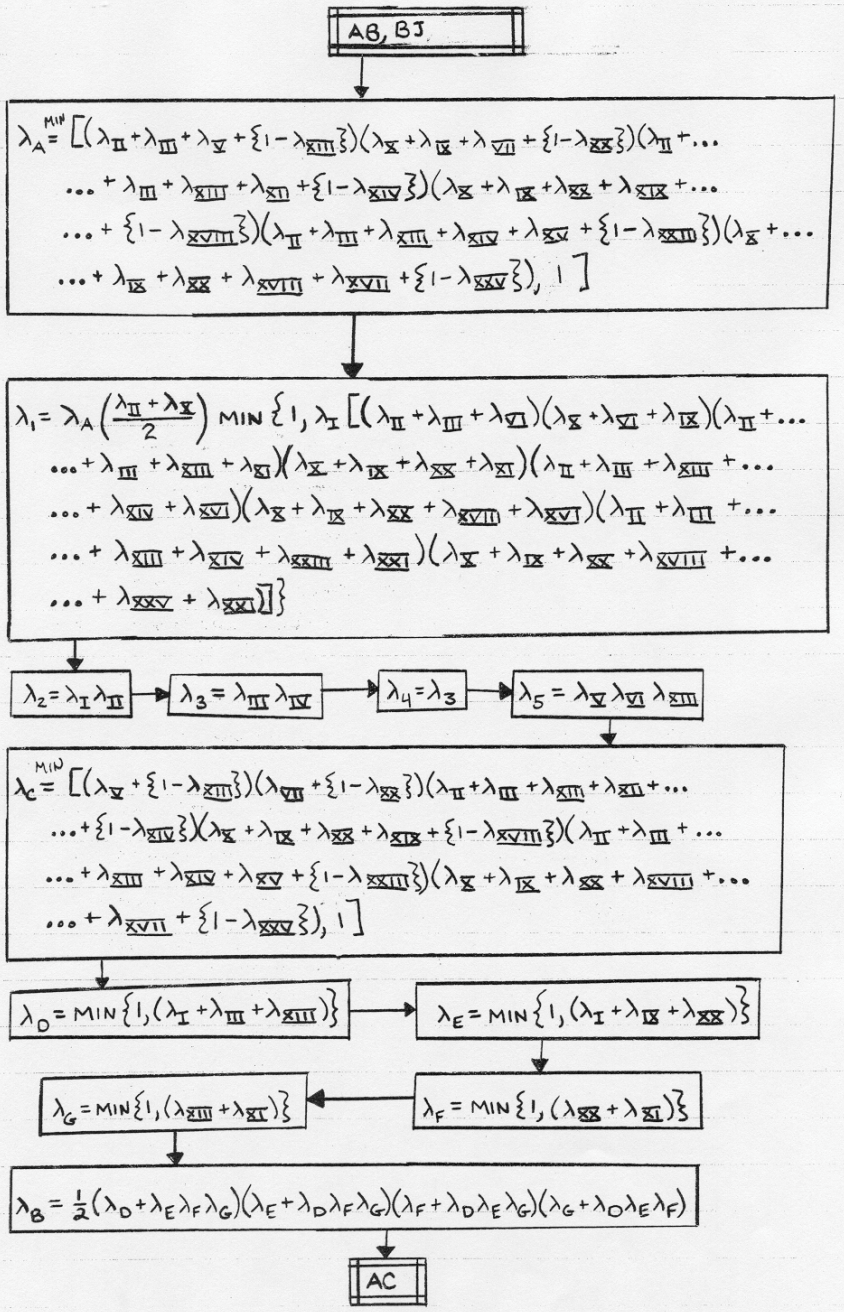
AB, BJ
$\lambda_A = \overset{MIN}{[}(\lambda_{II}+\lambda_{III}+\lambda_V+\{1-\lambda_{XIII}\})(\lambda_X+\lambda_{IX}+\lambda_{VII}+\{1-\lambda_{XX}\})(\lambda_{II}+\ldots$
$\ldots+\lambda_{III}+\lambda_{XIII}+\lambda_{XII}+\{1-\lambda_{XIV}\})(\lambda_X+\lambda_{IX}+\lambda_{XX}+\lambda_{XIX}+\ldots$
$\ldots+\{1-\lambda_{XVIII}\})(\lambda_{II}+\lambda_{III}+\lambda_{XIII}+\lambda_{XIV}+\lambda_{XV}+\{1-\lambda_{XXIII}\})(\lambda_X+\ldots$
$\ldots+\lambda_{IX}+\lambda_{XX}+\lambda_{XVII}+\lambda_{XVII}+\{1-\lambda_{XXV}\}),1]$
$\lambda_1 = \lambda_A\left(\frac{\lambda_{II}+\lambda_X}{2}\right)$ MIN $\{1, \lambda_I[(\lambda_{II}+\lambda_{III}+\lambda_{VI})(\lambda_X+\lambda_{VI}+\lambda_{IX})(\lambda_{II}+\ldots$
$\ldots+\lambda_{III}+\lambda_{XIII}+\lambda_{XI})(\lambda_V+\lambda_{IX}+\lambda_{XX}+\lambda_{XI})(\lambda_{II}+\lambda_{III}+\lambda_{XIII}+\ldots$
$\ldots+\lambda_{XIV}+\lambda_{XVI})(\lambda_X+\lambda_{IX}+\lambda_{XX}+\lambda_{XVII}+\lambda_{XVI})(\lambda_{II}+\lambda_{III}+\ldots$
$\ldots+\lambda_{XIII}+\lambda_{XIV}+\lambda_{XXIII}+\lambda_{XXI})(\lambda_V+\lambda_{IX}+\lambda_{XX}+\lambda_{XVIII}+\ldots$
$\ldots+\lambda_{XXV}+\lambda_{XXI}]]\}$
$\lambda_2 = \lambda_I\lambda_{II}$
$\lambda_3 = \lambda_{III}\lambda_{IV}$
$\lambda_4 = \lambda_3$
$\lambda_5 = \lambda_V\lambda_{VI}\lambda_{XIII}$
$\lambda_C = \overset{MIN}{[}(\lambda_V+\{1-\lambda_{XIII}\})(\lambda_{VII}+\{1-\lambda_{XX}\})(\lambda_{II}+\lambda_{III}+\lambda_{XIII}+\lambda_{XII}+\ldots$
$\ldots+\{1-\lambda_{XIV}\})(\lambda_X+\lambda_{IX}+\lambda_{XX}+\lambda_{XIX}+\{1-\lambda_{XVIII}\})(\lambda_{II}+\lambda_{III}+\ldots$
$\ldots+\lambda_{XIII}+\lambda_{XIV}+\lambda_{XV}+\{1-\lambda_{XXIII}\})(\lambda_X+\lambda_{IX}+\lambda_{XX}+\lambda_{XVIII}+\ldots$
$\ldots+\lambda_{XVII}+\{1-\lambda_{XXV}\}),1]$
$\lambda_D = MIN\{1,(\lambda_I+\lambda_{III}+\lambda_{XIII})\}$
$\lambda_E = MIN\{1,(\lambda_I+\lambda_{IX}+\lambda_{XX})\}$
$\lambda_G = MIN\{1,(\lambda_{XIII}+\lambda_{XI})\}$
$\lambda_F = MIN\{1,(\lambda_{XX}+\lambda_{XI})\}$
$\lambda_B = \frac{1}{2}(\lambda_D+\lambda_E\lambda_F\lambda_G)(\lambda_E+\lambda_D\lambda_F\lambda_G)(\lambda_F+\lambda_D\lambda_E\lambda_G)(\lambda_G+\lambda_D\lambda_E\lambda_F)$
AC

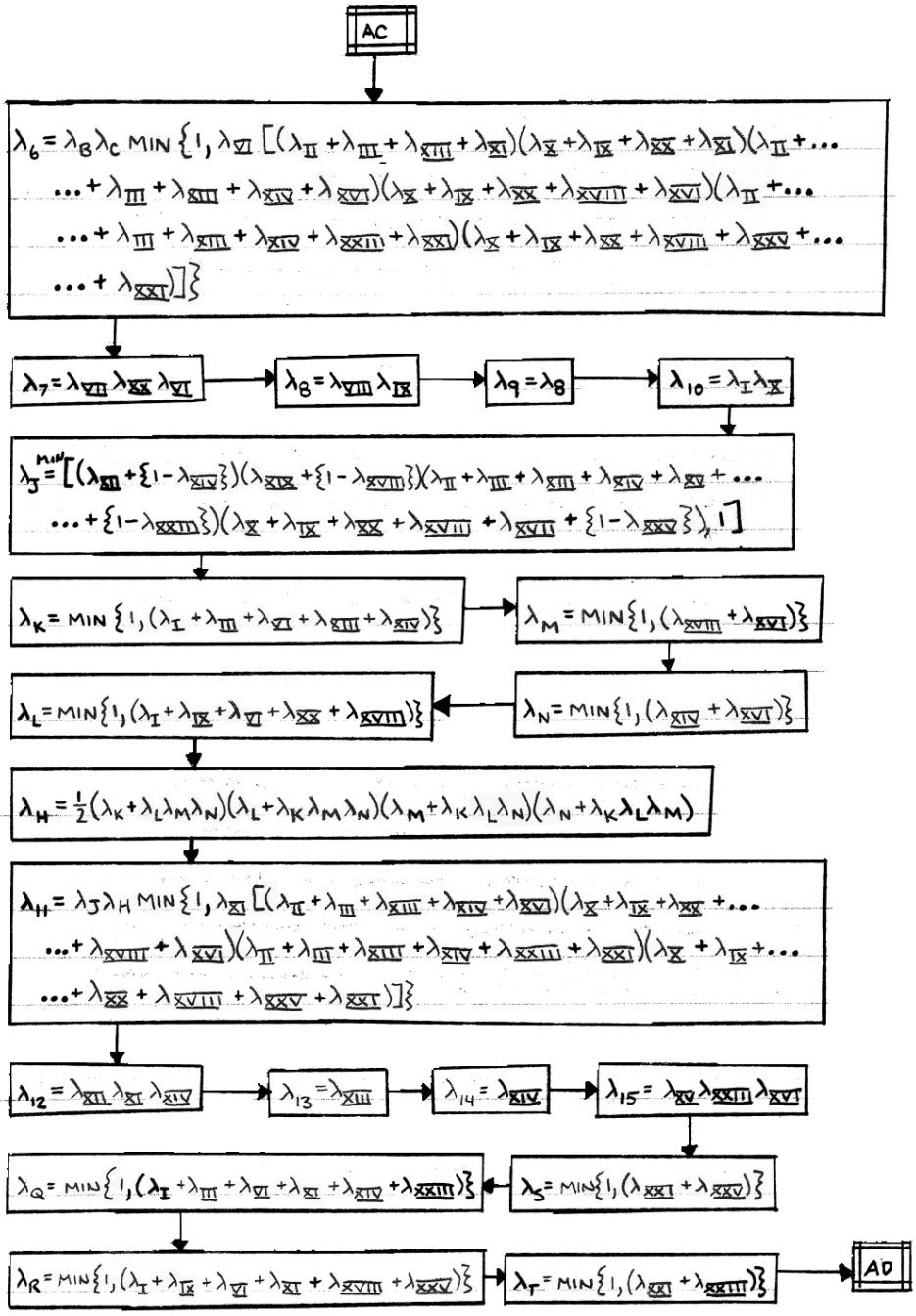
AC
$\lambda_6 = \lambda_B \lambda_C \text{ MIN}\{1, \lambda_{VI}[(\lambda_{II}+\lambda_{III}+\lambda_{XIII}+\lambda_{XI})(\lambda_X+\lambda_{IX}+\lambda_{XX}+\lambda_{XI})(\lambda_{II}+\ldots$
$\ldots+\lambda_{III}+\lambda_{XIII}+\lambda_{XIV}+\lambda_{XVI})(\lambda_X+\lambda_{IX}+\lambda_{XX}+\lambda_{XVIII}+\lambda_{XVI})(\lambda_{II}+\ldots$
$\ldots+\lambda_{III}+\lambda_{XIII}+\lambda_{XIV}+\lambda_{XXIII}+\lambda_{XXI})(\lambda_X+\lambda_{IX}+\lambda_{XX}+\lambda_{XVIII}+\lambda_{XXV}+\ldots$
$\ldots+\lambda_{XXI})]\}$
$\lambda_7 = \lambda_{VII}\lambda_{XX}\lambda_{VI}$
$\lambda_8 = \lambda_{VIII}\lambda_{IX}$
$\lambda_9 = \lambda_8$
$\lambda_{10} = \lambda_I \lambda_X$
$\lambda_J = [(\lambda_{XII}+\{1-\lambda_{XIV}\})(\lambda_{XIX}+\{1-\lambda_{XVIII}\})(\lambda_{II}+\lambda_{III}+\lambda_{XIII}+\lambda_{XIV}+\lambda_{XV}+\ldots$
$\ldots+\{1-\lambda_{XXIII}\})(\lambda_X+\lambda_{IX}+\lambda_{XX}+\lambda_{XVII}+\lambda_{XVIII}+\{1-\lambda_{XXV}\}),1]$
$\lambda_K = \text{MIN}\{1, (\lambda_I+\lambda_{III}+\lambda_{VI}+\lambda_{XIII}+\lambda_{XIV})\}$
$\lambda_M = \text{MIN}\{1, (\lambda_{XVIII}+\lambda_{XVI})\}$
$\lambda_N = \text{MIN}\{1, (\lambda_{XIV}+\lambda_{XVI})\}$
$\lambda_L = \text{MIN}\{1, (\lambda_I+\lambda_{IX}+\lambda_{VI}+\lambda_{XX}+\lambda_{XVIII})\}$
$\lambda_H = \frac{1}{2}(\lambda_K+\lambda_L\lambda_M\lambda_N)(\lambda_L+\lambda_K\lambda_M\lambda_N)(\lambda_M+\lambda_K\lambda_L\lambda_N)(\lambda_N+\lambda_K\lambda_L\lambda_M)$
$\lambda_H = \lambda_J\lambda_H \text{ MIN}\{1, \lambda_{XI}[(\lambda_{II}+\lambda_{III}+\lambda_{XIII}+\lambda_{XIV}+\lambda_{XVI})(\lambda_X+\lambda_{IX}+\lambda_{XX}+\ldots$
$\ldots+\lambda_{XVIII}+\lambda_{XVI})(\lambda_{II}+\lambda_{III}+\lambda_{XIII}+\lambda_{XIV}+\lambda_{XXIII}+\lambda_{XXI})(\lambda_X+\lambda_{IX}+\ldots$
$\ldots+\lambda_{XX}+\lambda_{XVIII}+\lambda_{XXV}+\lambda_{XXI})]\}$
$\lambda_{12} = \lambda_{XII}\lambda_{XI}\lambda_{XIV}$
$\lambda_{13} = \lambda_{XIII}$
$\lambda_{14} = \lambda_{XIV}$
$\lambda_{15} = \lambda_{XV}\lambda_{XXIII}\lambda_{XVI}$
$\lambda_Q = \text{MIN}\{1, (\lambda_I+\lambda_{III}+\lambda_{VI}+\lambda_{XI}+\lambda_{XIV}+\lambda_{XXIII})\}$
$\lambda_S = \text{MIN}\{1, (\lambda_{XXI}+\lambda_{XXV})\}$
$\lambda_R = \text{MIN}\{1, (\lambda_I+\lambda_{IX}+\lambda_{VI}+\lambda_{XI}+\lambda_{XVIII}+\lambda_{XXV})\}$
$\lambda_T = \text{MIN}\{1, (\lambda_{XXI}+\lambda_{XXIII})\}$
AD

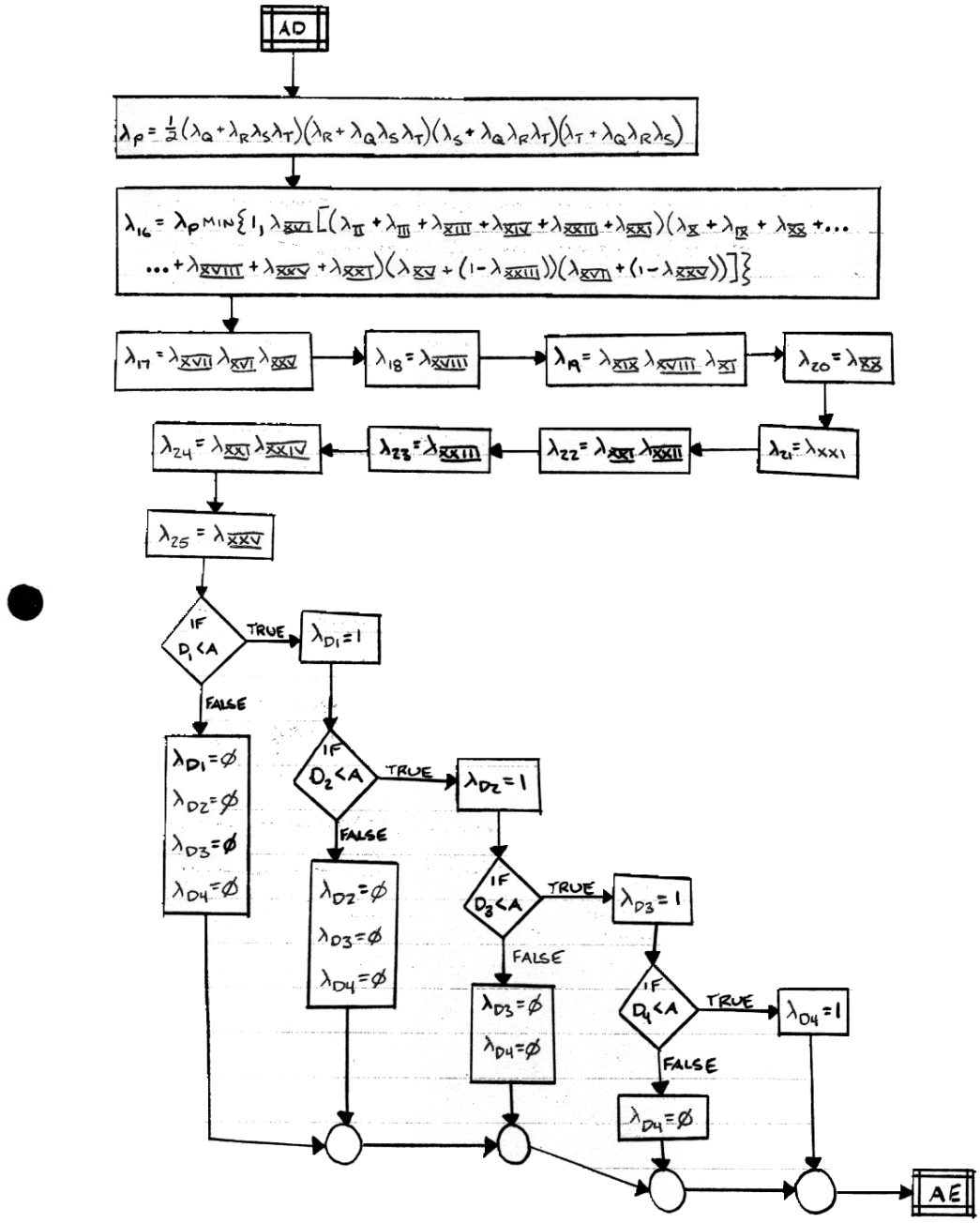
AD
$\lambda_P = \frac{1}{2}(\lambda_Q + \lambda_R\lambda_S\lambda_T)(\lambda_R + \lambda_Q\lambda_S\lambda_T)(\lambda_S + \lambda_Q\lambda_R\lambda_T)(\lambda_T + \lambda_Q\lambda_R\lambda_S)$
$\lambda_{16} = \lambda_P \text{MIN}\{1, \lambda_{XVI}[(\lambda_{II} + \lambda_{III} + \lambda_{XIII} + \lambda_{XIV} + \lambda_{XXIII} + \lambda_{XXI})(\lambda_X + \lambda_{IX} + \lambda_{XX} + \ldots$
$\ldots + \lambda_{XVIII} + \lambda_{XXV} + \lambda_{XXI})(\lambda_{XV} + (1-\lambda_{XXIII}))(\lambda_{XVI} + (1-\lambda_{XXV}))]\}$
$\lambda_{17} = \lambda_{XVII}\lambda_{XVI}\lambda_{XXV}$
$\lambda_{18} = \lambda_{XVIII}$
$\lambda_{19} = \lambda_{XIX}\lambda_{XVIII}\lambda_{XI}$
$\lambda_{20} = \lambda_{XX}$
$\lambda_{21} = \lambda_{XXI}$
$\lambda_{22} = \lambda_{XXI}\lambda_{XXII}$
$\lambda_{23} = \lambda_{XXIII}$
$\lambda_{24} = \lambda_{XXI}\lambda_{XXIV}$
$\lambda_{25} = \lambda_{XXV}$
IF $D_1 < A$
TRUE
$\lambda_{D1} = 1$
FALSE
$\lambda_{D1} = \emptyset$
$\lambda_{D2} = \emptyset$
$\lambda_{D3} = \emptyset$
$\lambda_{D4} = \emptyset$
IF $D_2 < A$
TRUE
$\lambda_{D2} = 1$
FALSE
$\lambda_{D2} = \emptyset$
$\lambda_{D3} = \emptyset$
$\lambda_{D4} = \emptyset$
IF $D_3 < A$
TRUE
$\lambda_{D3} = 1$
FALSE
$\lambda_{D3} = \emptyset$
$\lambda_{D4} = \emptyset$
IF $D_4 < A$
TRUE
$\lambda_{D4} = 1$
FALSE
$\lambda_{D4} = \emptyset$
AE

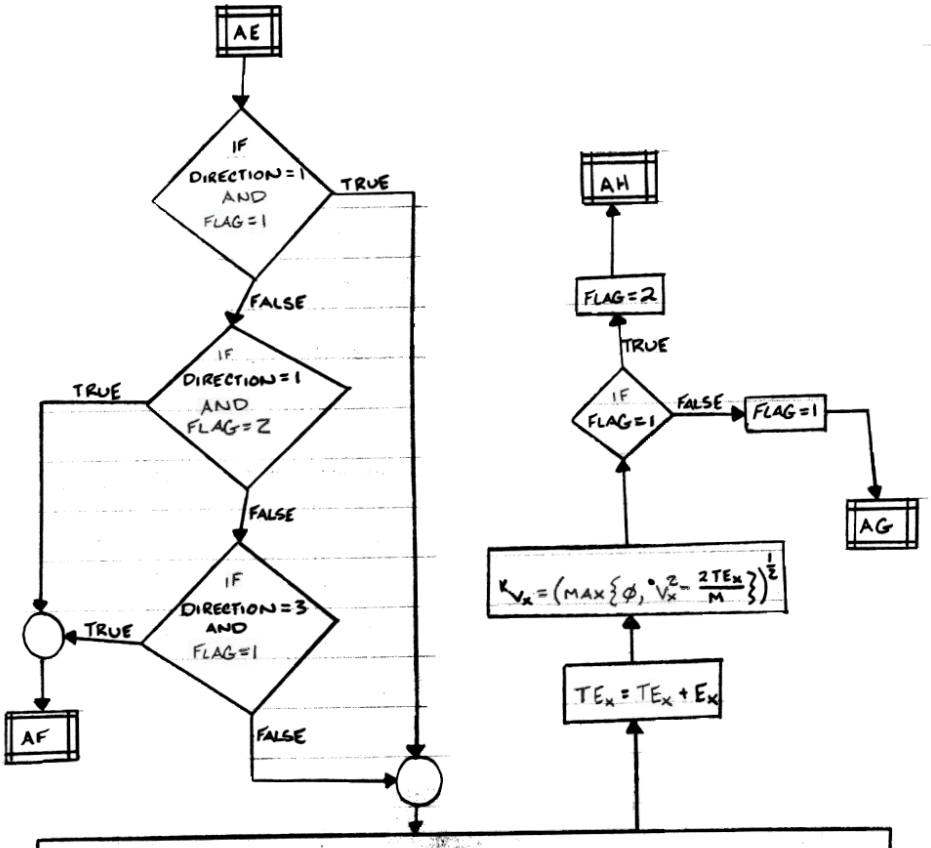

$$E_x = \lambda_0\Big[\lambda_1 E_{I} + \lambda_{D1}\lambda_6 E_{VI} + \lambda_{D2}\lambda_{11} E_{XI} + \lambda_{D3}\lambda_{16} E_{XVI} + \ldots$$
$$\ldots + \lambda_{D4}\lambda_{21} E_{XXI} + \lambda_{4L}\Big(\lambda_2 E_{II} + \lambda_3 E_{III} + \lambda_{D1}\{\lambda_4 E_{IV} + \ldots$$
$$\ldots + \lambda_5 E_{V}\} + \lambda_{D2}\{\lambda_{12} E_{XII} + \lambda_{13} E_{XIII}\} + \lambda_{D3}\{\lambda_{14} E_{XIV} + \ldots$$
$$\ldots + \lambda_{15} E_{XV}\} + \lambda_{D4}\{\lambda_{22} E_{XXII} + \lambda_{23} E_{XXIII}\}\Big) + \lambda_{4U}\Big(\lambda_9 E_{IX} + \ldots$$
$$\ldots + \lambda_{10} E_{X} + \lambda_{D1}\{\lambda_7 E_{VII} + \lambda_8 E_{VIII}\} + \lambda_{D2}\{\lambda_{19} E_{XIX} + \ldots$$
$$\ldots + \lambda_{20} E_{XX}\} + \lambda_{D3}\{\lambda_{17} E_{XVII} + \lambda_{18} E_{XVIII}\} + \lambda_{D4}\{\lambda_{25} E_{XXV} + \ldots$$
$$\ldots + \lambda_{24} E_{XXIV}\}\Big)\Big]$$

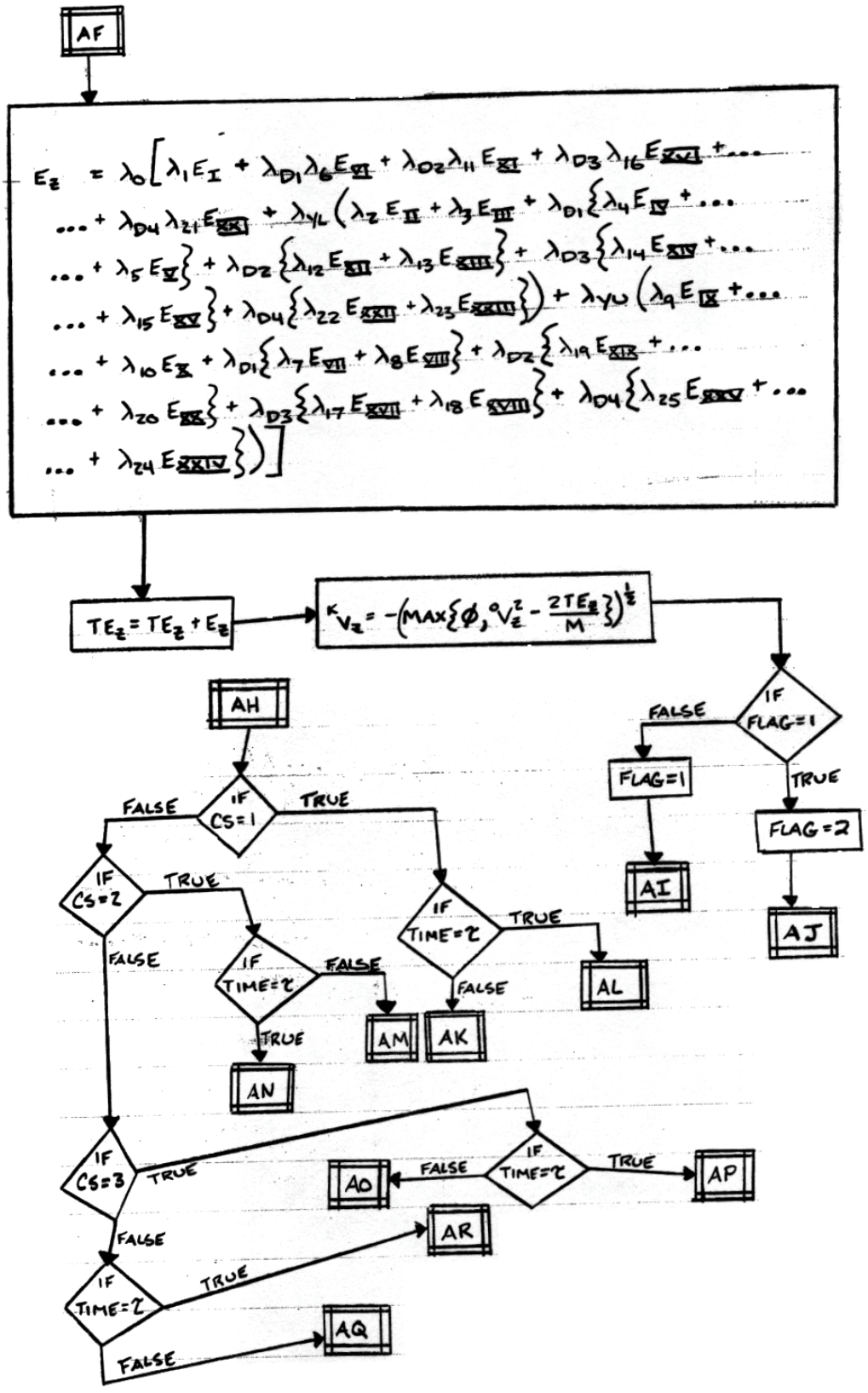
AF
$E_z = \lambda_0[\lambda_1 E_I + \lambda_{D1}\lambda_6 E_{VI} + \lambda_{D2}\lambda_{11} E_{XI} + \lambda_{D3}\lambda_{16} E_{XVI} + \ldots$
$\ldots + \lambda_{D4}\lambda_{21} E_{XXI} + \lambda_{YL}(\lambda_2 E_{II} + \lambda_3 E_{III} + \lambda_{D1}\{\lambda_4 E_{IV} + \ldots$
$\ldots + \lambda_5 E_V\} + \lambda_{D2}\{\lambda_{12} E_{XII} + \lambda_{13} E_{XIII}\} + \lambda_{D3}\{\lambda_{14} E_{XIV} + \ldots$
$\ldots + \lambda_{15} E_{XV}\} + \lambda_{D4}\{\lambda_{22} E_{XXII} + \lambda_{23} E_{XXIII}\}) + \lambda_{YU}(\lambda_9 E_{IX} + \ldots$
$\ldots + \lambda_{10} E_X + \lambda_{D1}\{\lambda_7 E_{VII} + \lambda_8 E_{VIII}\} + \lambda_{D2}\{\lambda_{19} E_{XIX} + \ldots$
$\ldots + \lambda_{20} E_{XX}\} + \lambda_{D3}\{\lambda_{17} E_{XVII} + \lambda_{18} E_{XVIII}\} + \lambda_{D4}\{\lambda_{25} E_{XXV} + \ldots$
$\ldots + \lambda_{24} E_{XXIV}\})]$
$TE_z = TE_z + E_z$
$K_{V_z} = -\left(MAX\{\phi, {}^{\circ}V_z^2 - \frac{2TE_z}{M}\}\right)^{\frac{1}{2}}$
IF FLAG=1
FALSE
TRUE
FLAG=1
FLAG=2
AI
AJ
AH
IF CS=1
FALSE
TRUE
IF CS=2
TRUE
FALSE
IF TIME=τ
FALSE
TRUE
AM
AK
IF TIME=τ
TRUE
FALSE
AL
AN
IF CS=3
TRUE
FALSE
AO
IF TIME=τ
FALSE
TRUE
AP
AR
IF TIME=τ
TRUE
FALSE
AQ

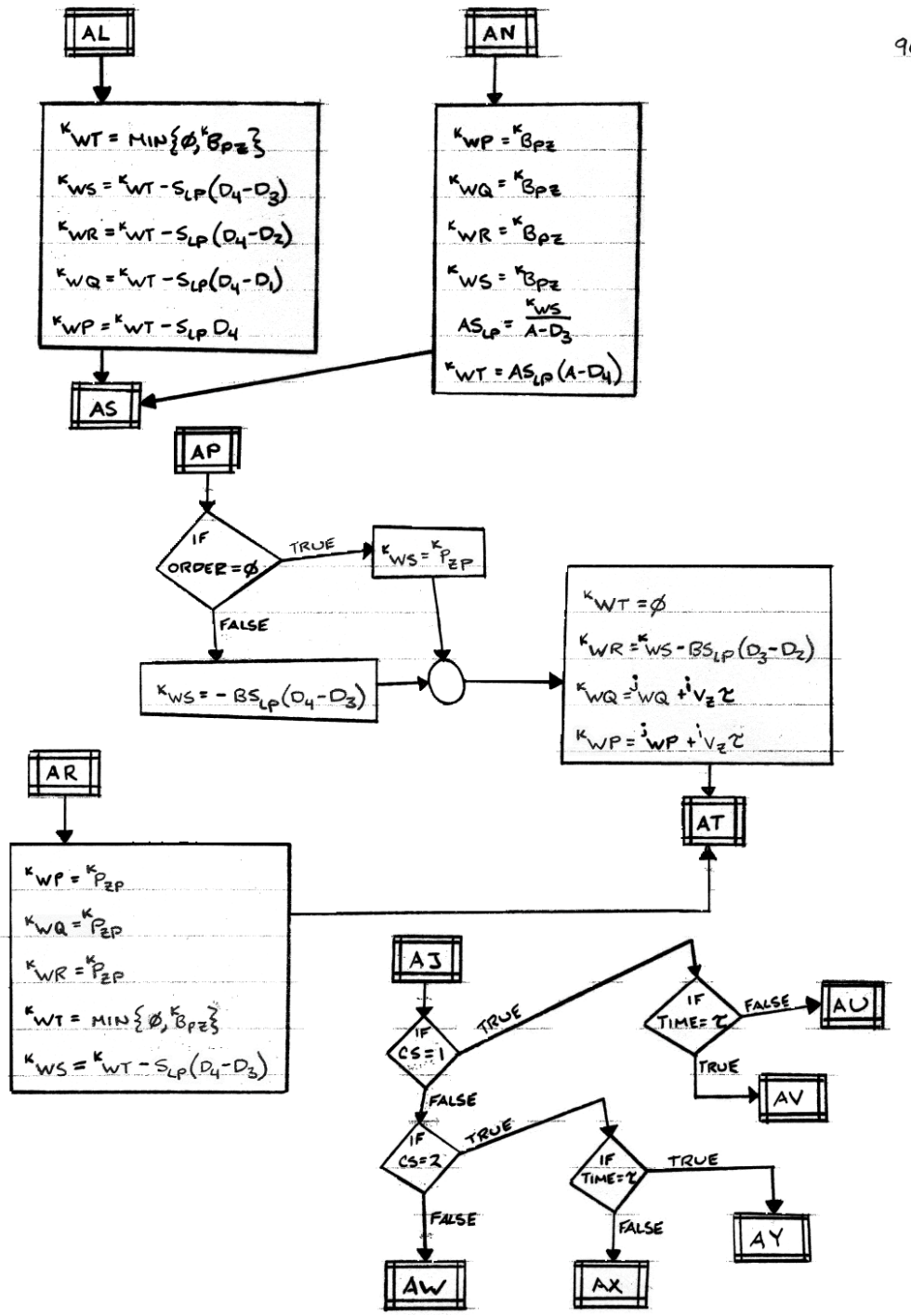
AL
AN
$^{K}WT = MIN\{\phi, {}^{K}B_{pz}\}$
$^{K}WS = {}^{K}WT - S_{LP}(D_4 - D_3)$
$^{K}WR = {}^{K}WT - S_{LP}(D_4 - D_2)$
$^{K}WQ = {}^{K}WT - S_{LP}(D_4 - D_1)$
$^{K}WP = {}^{K}WT - S_{LP} D_4$
$^{K}WP = {}^{K}B_{pz}$
$^{K}WQ = {}^{K}B_{pz}$
$^{K}WR = {}^{K}B_{pz}$
$^{K}WS = {}^{K}B_{pz}$
$AS_{LP} = \frac{^{K}WS}{A - D_3}$
$^{K}WT = AS_{LP}(A - D_4)$
AS
AP
IF ORDER = ϕ
TRUE
$^{K}WS = {}^{K}P_{ZP}$
FALSE
$^{K}WS = -BS_{LP}(D_4 - D_3)$
$^{K}WT = \phi$
$^{K}WR = {}^{K}WS - BS_{LP}(D_3 - D_2)$
$^{K}WQ = {}^{j}WQ + {}^{i}V_z\tau$
$^{K}WP = {}^{j}WP + {}^{i}V_z\tau$
AR
AT
$^{K}WP = {}^{K}P_{ZP}$
$^{K}WQ = {}^{K}P_{ZP}$
$^{K}WR = {}^{K}P_{ZP}$
$^{K}WT = MIN\{\phi, {}^{K}B_{pz}\}$
$^{K}WS = {}^{K}WT - S_{LP}(D_4 - D_3)$
AJ
IF CS = 1
TRUE
IF TIME = τ
FALSE
AU
TRUE
AV
FALSE
IF CS = 2
TRUE
IF TIME = τ
TRUE
AY
FALSE
FALSE
AW
AX

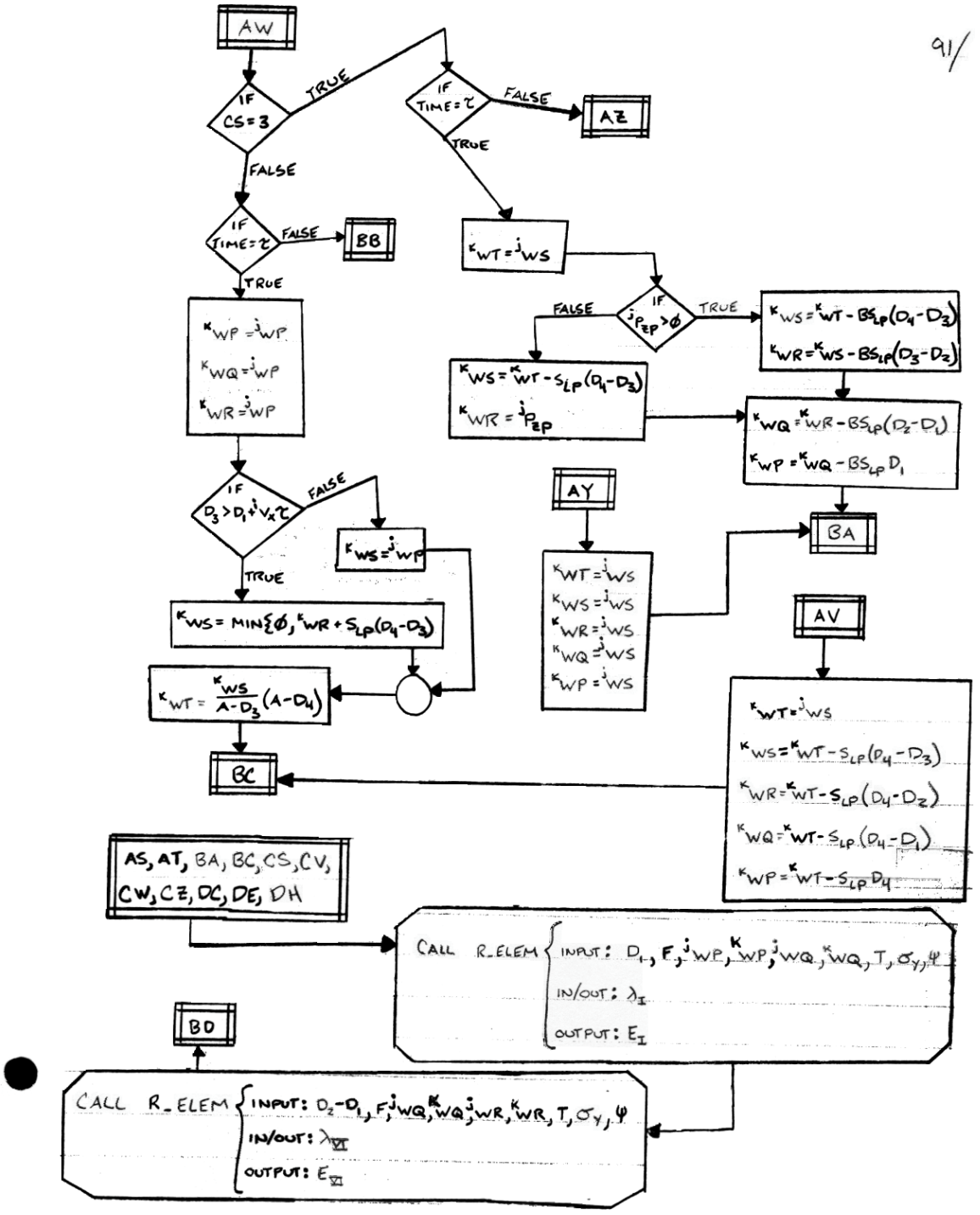
AW
IF CS=3
TRUE
FALSE
IF TIME=τ
FALSE
AZ
TRUE
IF TIME=τ
FALSE
BB
TRUE
$^{K}W_P = {}^{j}W_P$
$^{K}W_Q = {}^{j}W_P$
$^{K}W_R = {}^{j}W_P$
IF $D_3 > D_1 + {}^{j}V_x\tau$
FALSE
TRUE
$^{K}W_S = {}^{j}W_P$
$^{K}W_S = MIN\{\phi, {}^{K}W_R + S_{LP}(D_4 - D_3)\}$
$^{K}W_T = \frac{^{K}W_S}{A - D_3}(A - D_4)$
BC
$^{K}W_T = {}^{j}W_S$
IF $^{j}P_{EP} > \phi$
FALSE
TRUE
$^{K}W_S = {}^{K}W_T - S_{LP}(D_4 - D_3)$
$^{K}W_R = {}^{j}P_{EP}$
$^{K}W_S = {}^{K}W_T - BS_{LP}(D_4 - D_3)$
$^{K}W_R = {}^{K}W_S - BS_{LP}(D_3 - D_2)$
$^{K}W_Q = {}^{K}W_R - BS_{LP}(D_2 - D_1)$
$^{K}W_P = {}^{K}W_Q - BS_{LP}D_1$
AY
$^{K}W_T = {}^{j}W_S$
$^{K}W_S = {}^{j}W_S$
$^{K}W_R = {}^{j}W_S$
$^{K}W_Q = {}^{j}W_S$
$^{K}W_P = {}^{j}W_S$
BA
AV
$^{K}W_T = {}^{j}W_S$
$^{K}W_S = {}^{K}W_T - S_{LP}(D_4 - D_3)$
$^{K}W_R = {}^{K}W_T - S_{LP}(D_4 - D_2)$
$^{K}W_Q = {}^{K}W_T - S_{LP}(D_4 - D_1)$
$^{K}W_P = {}^{K}W_T - S_{LP}D_4$
AS, AT, BA, BC, CS, CV, CW, CZ, DC, DE, DH
CALL R_ELEM { INPUT: D_1, F, $^{j}W_P$, $^{K}W_P$, $^{j}W_Q$, $^{K}W_Q$, T, σ_y, ψ
IN/OUT: λ_I
OUTPUT: E_I
BD
CALL R_ELEM { INPUT: $D_2 - D_1$, F, $^{j}W_Q$, $^{K}W_Q$, $^{j}W_R$, $^{K}W_R$, T, σ_y, ψ
IN/OUT: λ_{VI}
OUTPUT: E_{VI}

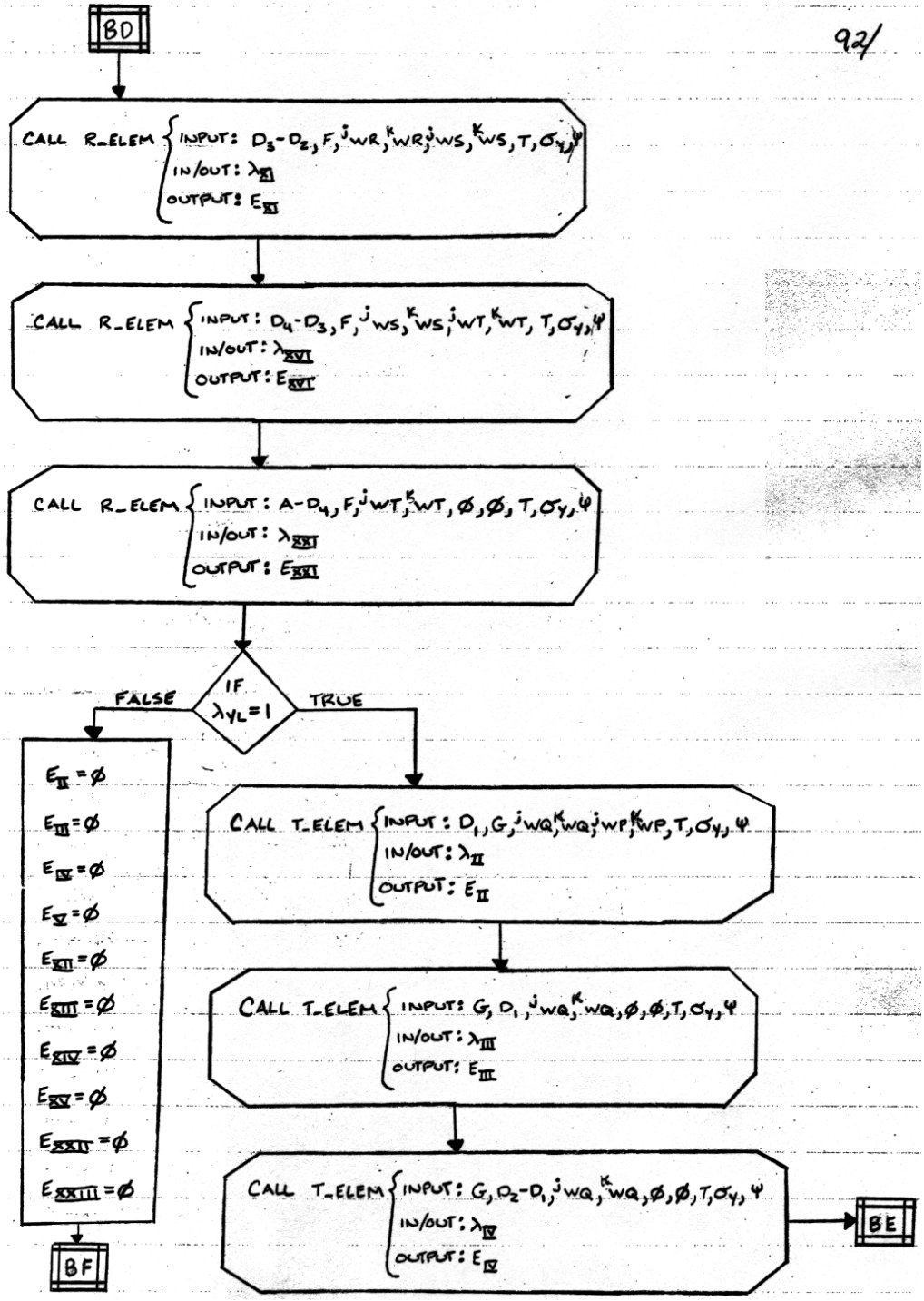
BD
CALL R_ELEM
INPUT: $D_3-D_2, F, {}^jWR, {}^KWR, {}^jWS, {}^KWS, T, \sigma_y, \psi$
IN/OUT: λ_{XI}
OUTPUT: E_{XI}
CALL R_ELEM
INPUT: $D_4-D_3, F, {}^jWS, {}^KWS, {}^jWT, {}^KWT, T, \sigma_y, \psi$
IN/OUT: λ_{XVI}
OUTPUT: E_{XVI}
CALL R_ELEM
INPUT: $A-D_4, F, {}^jWT, {}^KWT, \phi, \phi, T, \sigma_y, \psi$
IN/OUT: λ_{XXI}
OUTPUT: E_{XXI}
IF $\lambda_{YL}=1$
FALSE
TRUE
$E_{II}=\phi$
$E_{III}=\phi$
$E_{IV}=\phi$
$E_{V}=\phi$
$E_{XII}=\phi$
$E_{XIII}=\phi$
$E_{XIV}=\phi$
$E_{XV}=\phi$
$E_{XXII}=\phi$
$E_{XXIII}=\phi$
BF
CALL T_ELEM
INPUT: $D_1, G, {}^jWQ, {}^KWQ, {}^jWP, {}^KWP, T, \sigma_y, \psi$
IN/OUT: λ_{II}
OUTPUT: E_{II}
CALL T_ELEM
INPUT: $G, D_1, {}^jWQ, {}^KWQ, \phi, \phi, T, \sigma_y, \psi$
IN/OUT: λ_{III}
OUTPUT: E_{III}
CALL T_ELEM
INPUT: $G, D_2-D_1, {}^jWQ, {}^KWQ, \phi, \phi, T, \sigma_y, \psi$
IN/OUT: λ_{IV}
OUTPUT: E_{IV}
BE

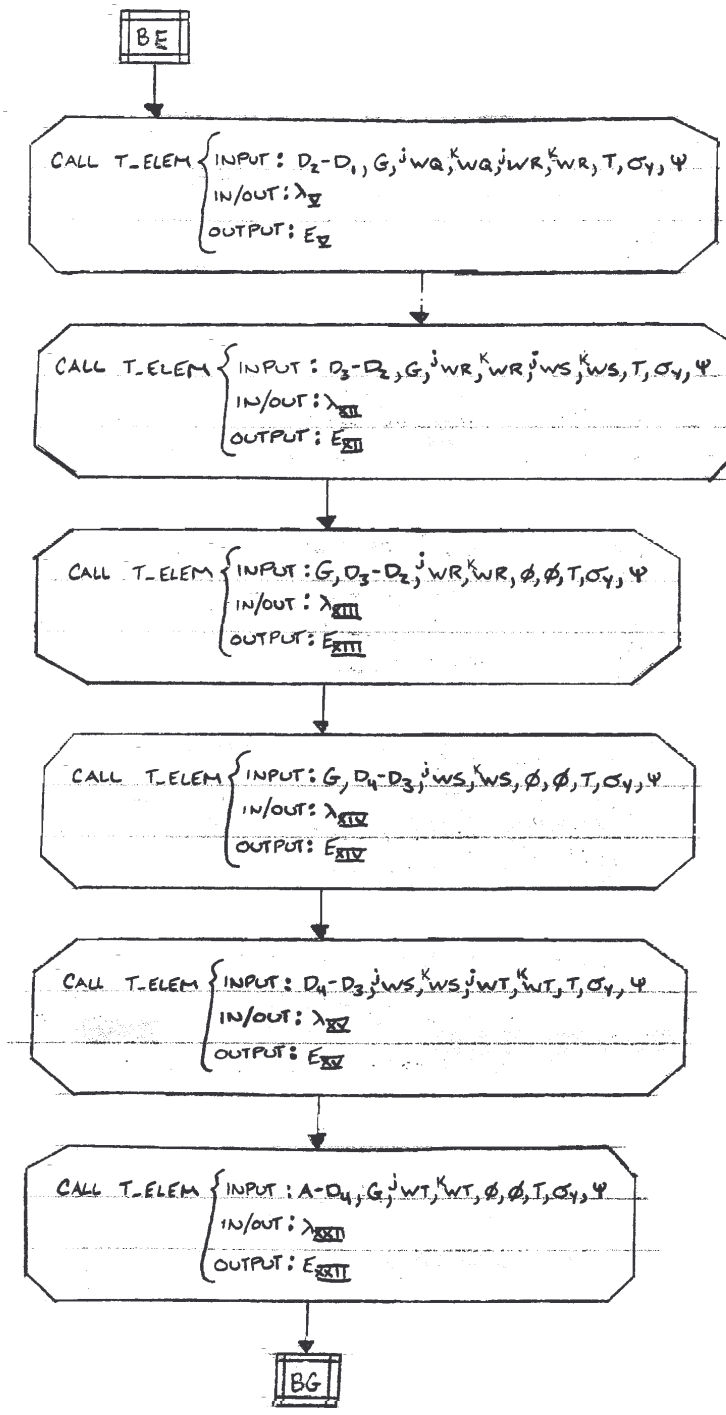
BE
CALL T_ELEM
INPUT : $D_2-D_1, G, {}^jWQ, {}^KWQ, {}^jWR, {}^KWR, T, \sigma_y, \Psi$
IN/OUT : λ_V
OUTPUT : E_V
CALL T_ELEM
INPUT : $D_3-D_2, G, {}^jWR, {}^KWR, {}^jWS, {}^KWS, T, \sigma_y, \Psi$
IN/OUT : λ_{VI}
OUTPUT : E_{VI}
CALL T_ELEM
INPUT : $G, D_3-D_2, {}^jWR, {}^KWR, \phi, \phi, T, \sigma_y, \Psi$
IN/OUT : λ_{VII}
OUTPUT : E_{VIII}
CALL T_ELEM
INPUT : $G, D_4-D_3, {}^jWS, {}^KWS, \phi, \phi, T, \sigma_y, \Psi$
IN/OUT : λ_{IX}
OUTPUT : E_{IX}
CALL T_ELEM
INPUT : $D_4-D_3, {}^jWS, {}^KWS, {}^jWT, {}^KWT, T, \sigma_y, \Psi$
IN/OUT : λ_X
OUTPUT : E_X
CALL T_ELEM
INPUT : $A-D_4, G, {}^jWT, {}^KWT, \phi, \phi, T, \sigma_y, \Psi$
IN/OUT : λ_{XI}
OUTPUT : E_{XII}
BG

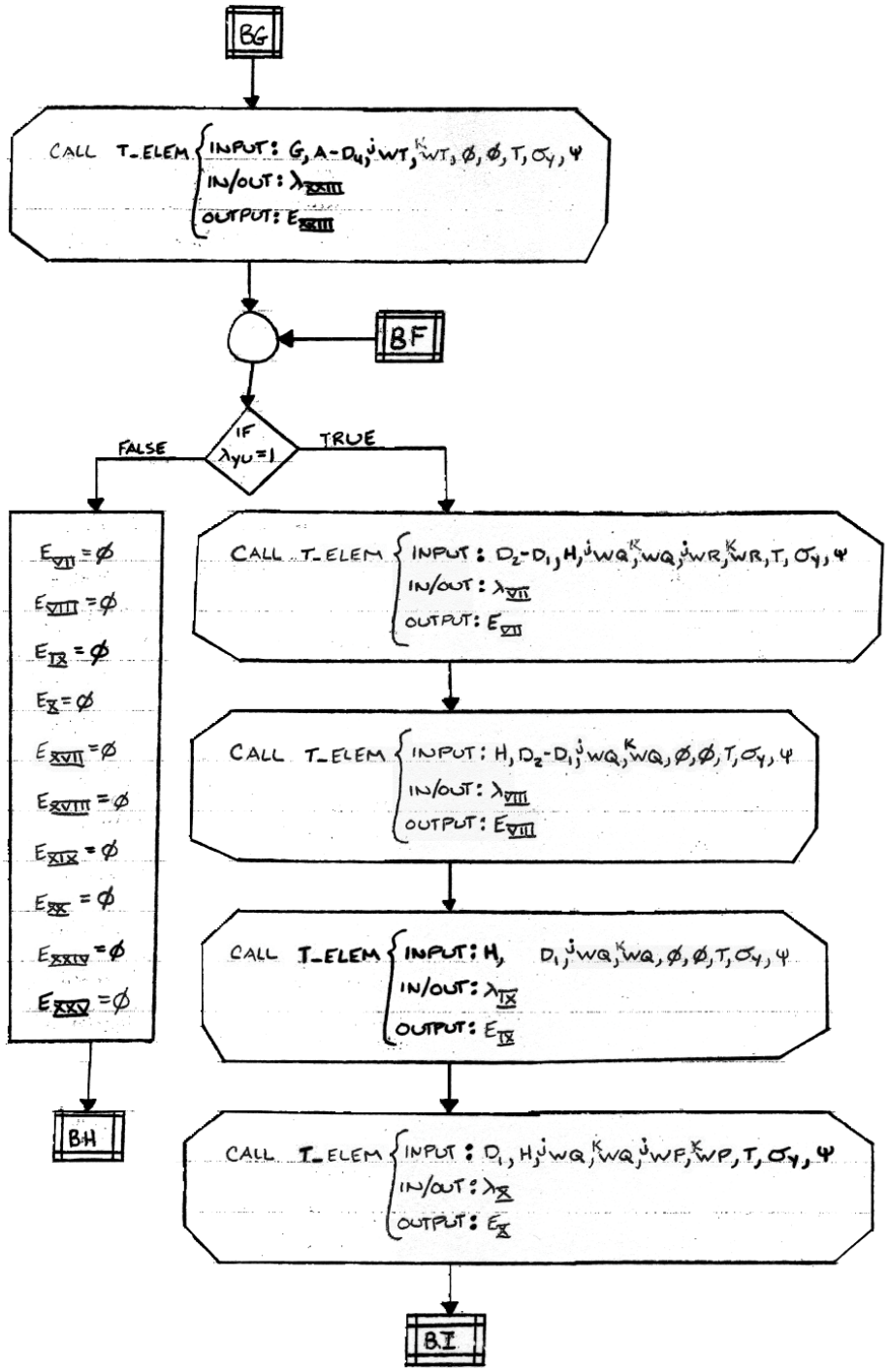
BG
CALL T_ELEM
INPUT: G, A-D4, jWT, kWT, ∅, ∅, T, σy, Ψ
IN/OUT: λXIII
OUTPUT: EXIII
BF
IF λyu=1
FALSE
TRUE
EVII = ∅
EVIII = ∅
EIX = ∅
EX = ∅
EXVII = ∅
EXVIII = ∅
EXIX = ∅
EXX = ∅
EXXIV = ∅
EXXV = ∅
BH
CALL T_ELEM
INPUT: D2-D1, H, jWQ, kWQ, jWR, kWR, T, σy, Ψ
IN/OUT: λVII
OUTPUT: EVII
CALL T_ELEM
INPUT: H, D2-D1, jWQ, kWQ, ∅, ∅, T, σy, Ψ
IN/OUT: λVIII
OUTPUT: EVIII
CALL T_ELEM
INPUT: H, D1, jWQ, kWQ, ∅, ∅, T, σy, Ψ
IN/OUT: λIX
OUTPUT: EIX
CALL T_ELEM
INPUT: D1, H, jWQ, kWQ, jWF, kWP, T, σy, Ψ
IN/OUT: λX
OUTPUT: EX
BI

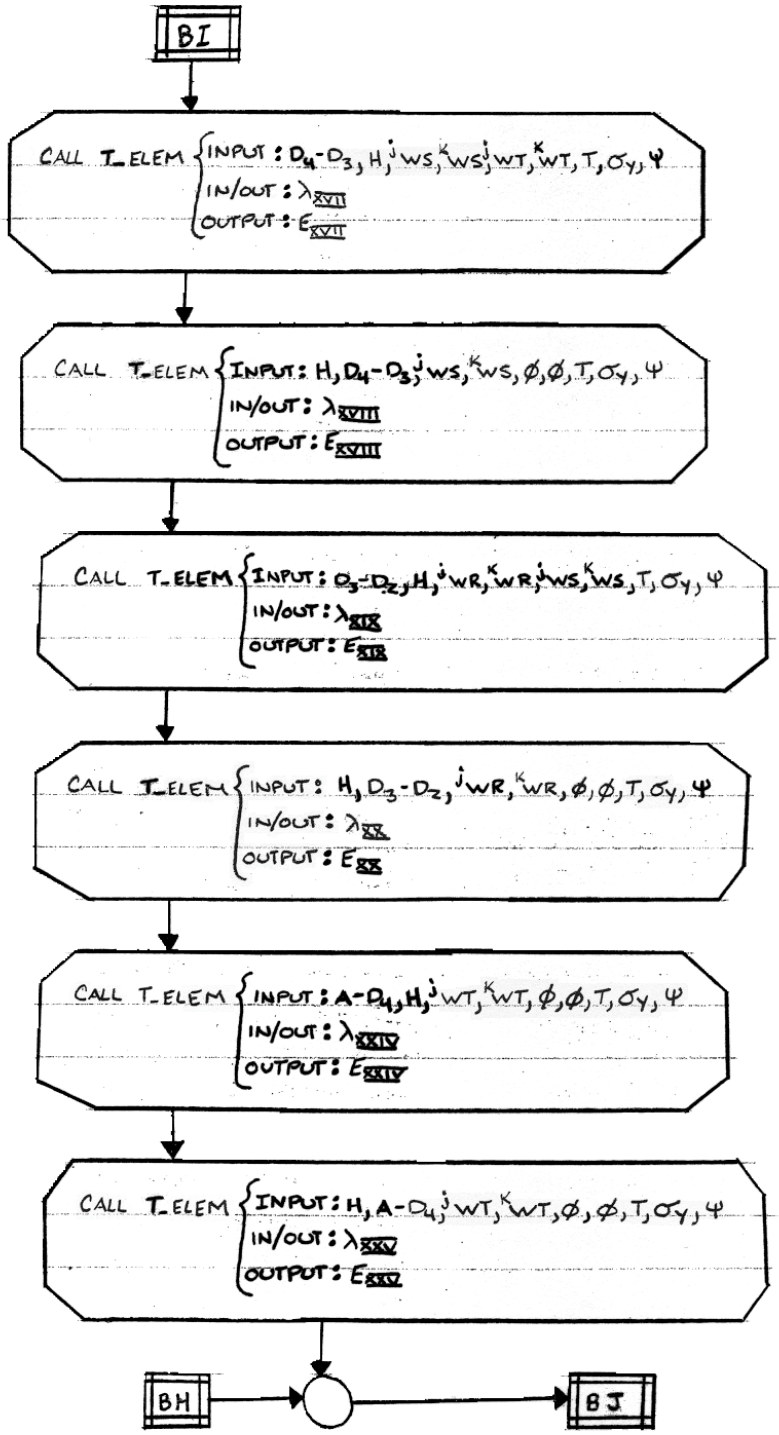
BI
CALL T_ELEM {INPUT : D_4-D_3, H_j, ^{j}WS, ^{K}WS, ^{j}WT, ^{K}WT, T, σ_y, ψ
IN/OUT : λ_{XVII}
OUTPUT : E_{XVII}
CALL T_ELEM {INPUT : H, D_4-D_3, ^{j}WS, ^{K}WS, ϕ, ϕ, T, σ_y, ψ
IN/OUT : λ_{XVIII}
OUTPUT : E_{XVIII}
CALL T_ELEM {INPUT : D_3-D_2, H_j, ^{j}WR, ^{K}WR, ^{j}WS, ^{K}WS, T, σ_y, ψ
IN/OUT : λ_{XIX}
OUTPUT : E_{XIX}
CALL T_ELEM {INPUT : H, D_3-D_2, ^{j}WR, ^{K}WR, ϕ, ϕ, T, σ_y, ψ
IN/OUT : λ_{XX}
OUTPUT : E_{XX}
CALL T_ELEM {INPUT : A-D_4, H_j, ^{j}WT, ^{K}WT, ϕ, ϕ, T, σ_y, ψ
IN/OUT : λ_{XXIV}
OUTPUT : E_{XXIV}
CALL T_ELEM {INPUT : H, A-D_4, ^{j}WT, ^{K}WT, ϕ, ϕ, T, σ_y, ψ
IN/OUT : λ_{XXV}
OUTPUT : E_{XXV}
BH
BJ

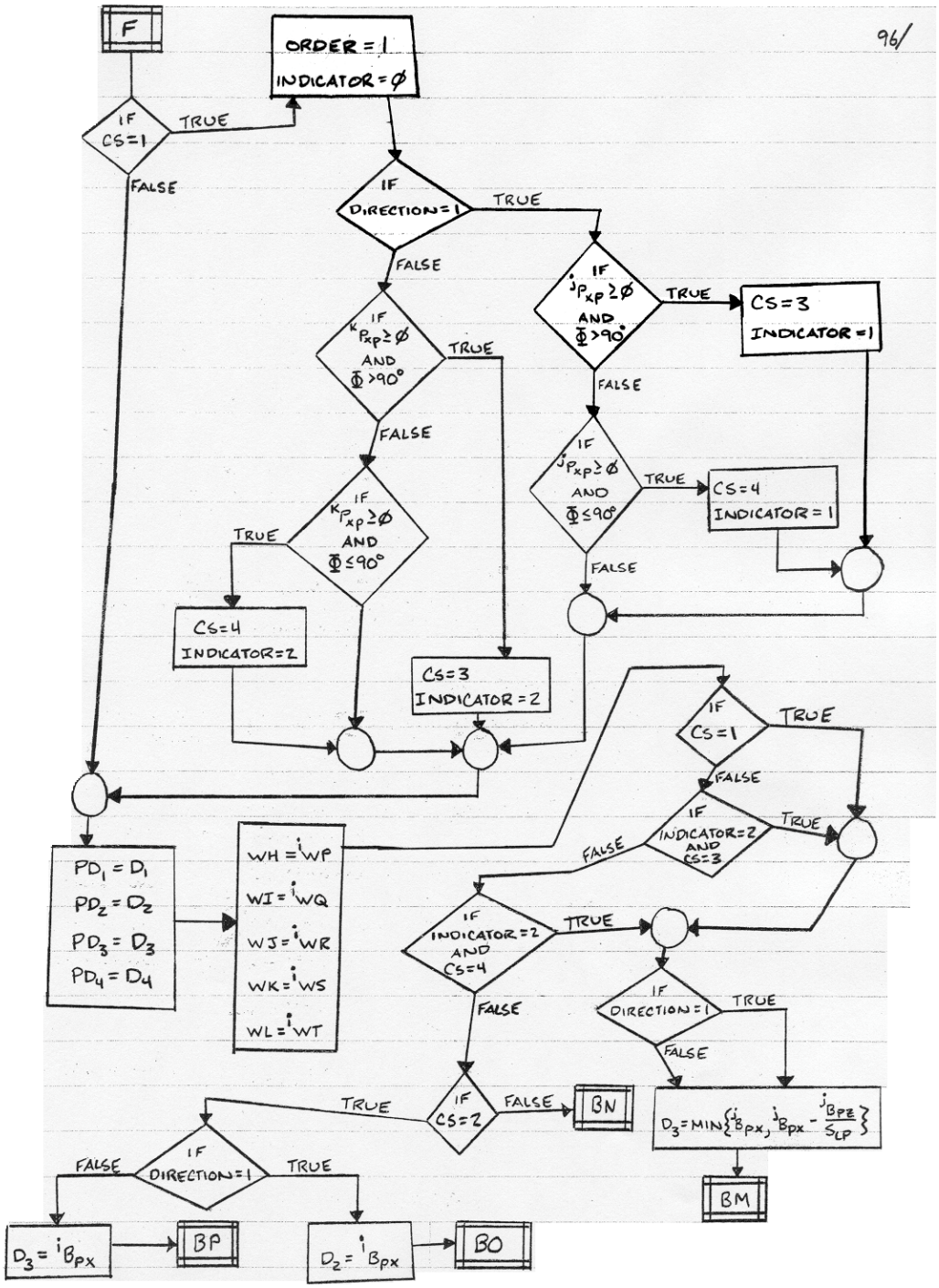
96/
F
ORDER = 1
INDICATOR = ∅
IF CS=1
TRUE
FALSE
IF DIRECTION=1
TRUE
FALSE
IF $^{j}P_{xp} \geq \emptyset$ AND $\Phi > 90°$
TRUE
CS=3
INDICATOR=1
FALSE
IF $^{k}P_{xp} \geq \emptyset$ AND $\Phi > 90°$
TRUE
FALSE
IF $^{j}P_{xp} \geq \emptyset$ AND $\Phi \leq 90°$
TRUE
CS=4
INDICATOR=1
FALSE
IF $^{k}P_{xp} \geq \emptyset$ AND $\Phi \leq 90°$
TRUE
CS=4
INDICATOR=2
CS=3
INDICATOR=2
IF CS=1
TRUE
FALSE
IF INDICATOR=2 AND CS=3
TRUE
FALSE
$PD_1 = D_1$
$PD_2 = D_2$
$PD_3 = D_3$
$PD_4 = D_4$
WH = ^{i}WP
WI = ^{i}WQ
WJ = ^{i}WR
WK = ^{i}WS
WL = ^{i}WT
IF INDICATOR=2 AND CS=4
TRUE
FALSE
IF DIRECTION=1
TRUE
FALSE
$D_3 = MIN\{^{i}B_{px}, {}^{j}B_{px} - \frac{^{j}B_{pE}}{S_{LP}}\}$
BM
IF CS=2
TRUE
FALSE
BN
IF DIRECTION=1
FALSE
TRUE
$D_3 = {}^{i}B_{px}$
BP
$D_2 = {}^{i}B_{px}$
BO

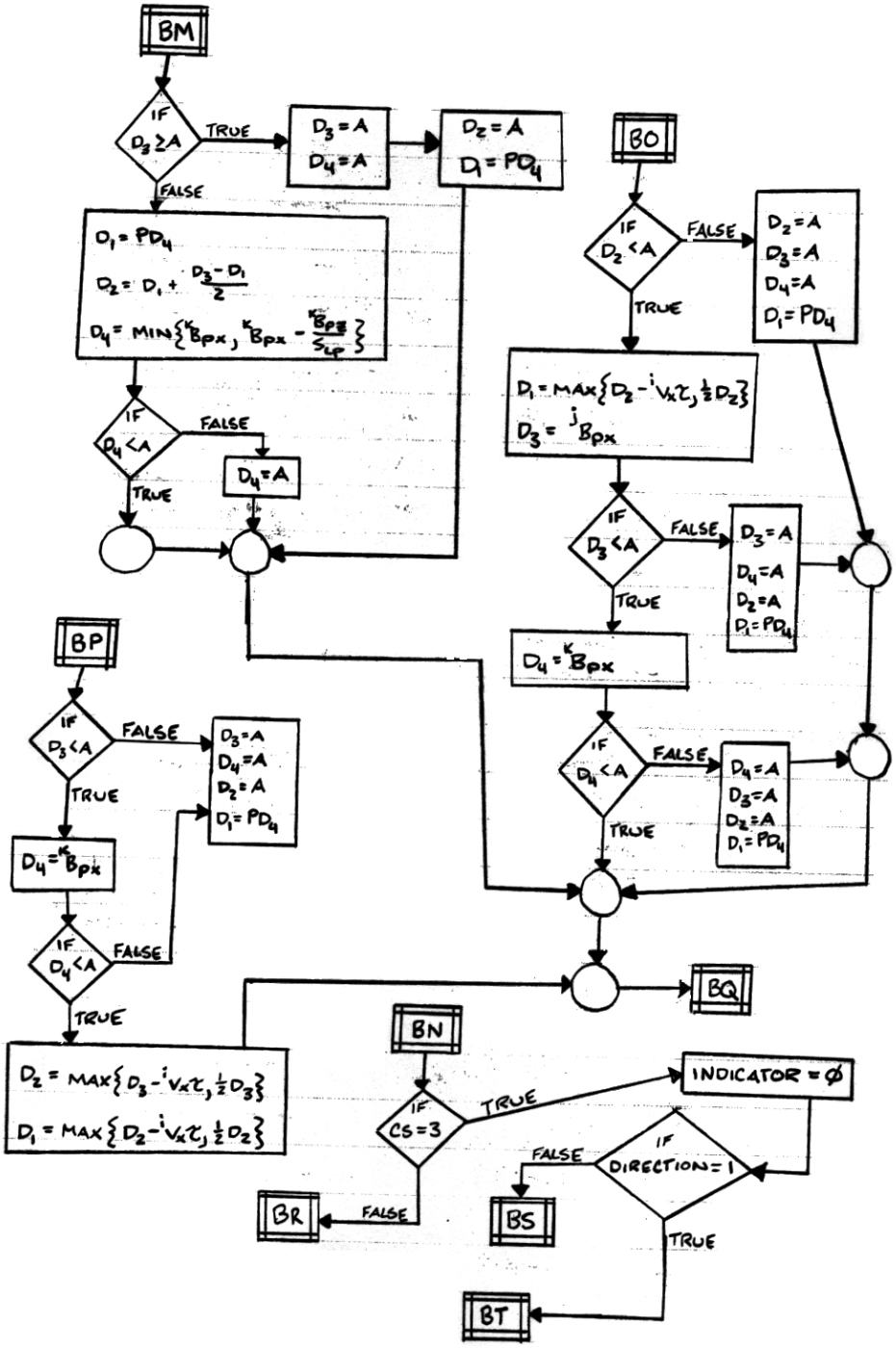
BM
IF $D_3 \geq A$
TRUE
$D_3 = A$
$D_4 = A$
$D_2 = A$
$D_1 = PD_4$
FALSE
$D_1 = PD_4$
$D_2 = D_1 + \frac{D_3 - D_1}{2}$
$D_4 = MIN\{{}^{k}B_{px}, {}^{k}B_{px} - \frac{{}^{k}B_{px}}{S_{up}}\}$
IF $D_4 < A$
FALSE
$D_4 = A$
TRUE
BO
IF $D_2 < A$
FALSE
$D_2 = A$
$D_3 = A$
$D_4 = A$
$D_1 = PD_4$
TRUE
$D_1 = MAX\{D_2 - {}^{i}V_x\tau, \frac{1}{2}D_2\}$
$D_3 = {}^{j}B_{px}$
IF $D_3 < A$
FALSE
$D_3 = A$
$D_4 = A$
$D_2 = A$
$D_1 = PD_4$
TRUE
$D_4 = {}^{k}B_{px}$
IF $D_4 < A$
FALSE
$D_4 = A$
$D_3 = A$
$D_2 = A$
$D_1 = PD_4$
TRUE
BP
IF $D_3 < A$
FALSE
$D_3 = A$
$D_4 = A$
$D_2 = A$
$D_1 = PD_4$
TRUE
$D_4 = {}^{k}B_{px}$
IF $D_4 < A$
FALSE
TRUE
$D_2 = MAX\{D_3 - {}^{i}V_x\tau, \frac{1}{2}D_3\}$
$D_1 = MAX\{D_2 - {}^{i}V_x\tau, \frac{1}{2}D_2\}$
BQ
BN
IF $CS = 3$
TRUE
INDICATOR = ϕ
IF DIRECTION = 1
FALSE
TRUE
BR
FALSE
BS
BT

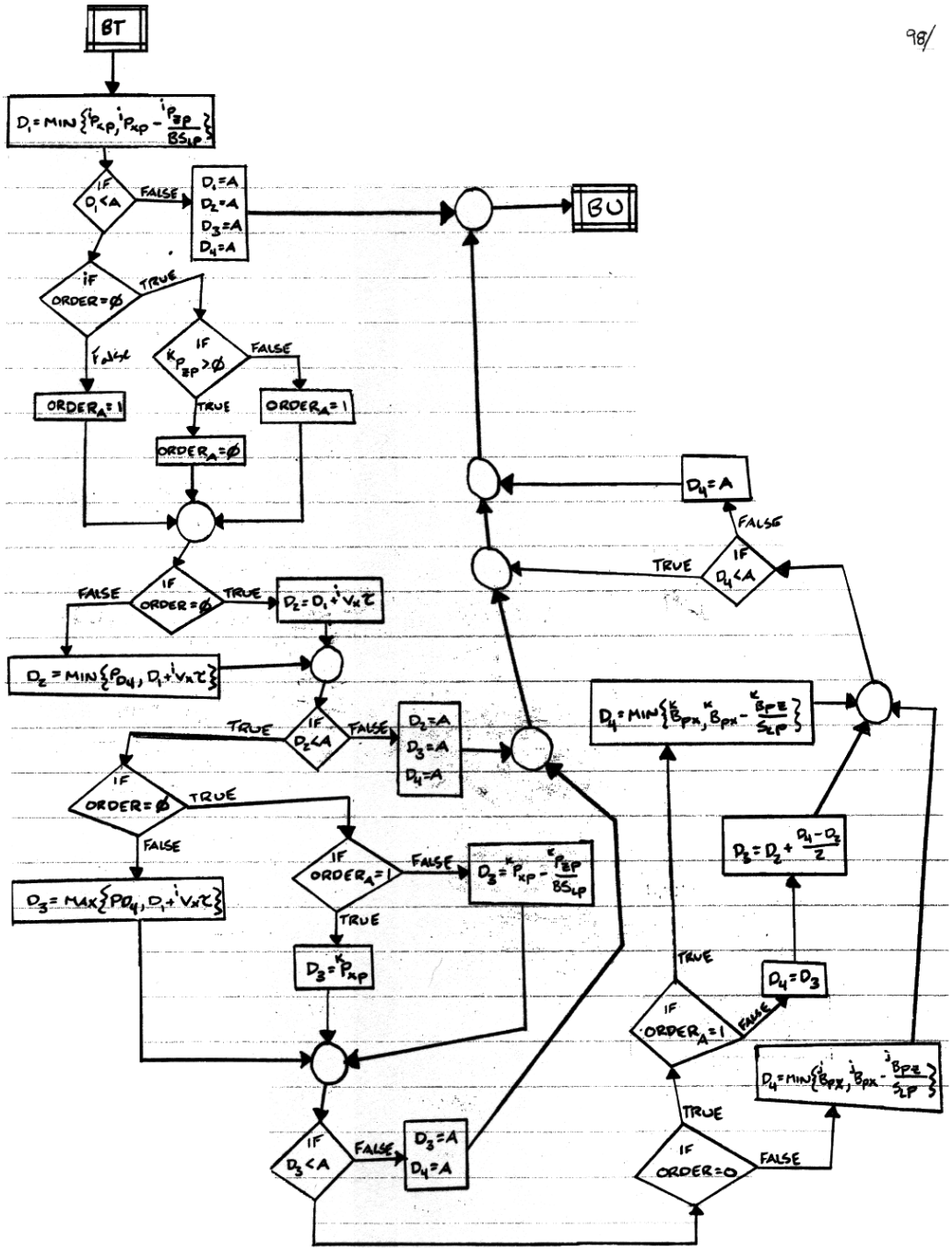
BT
$D_1 = MIN\{{}^iP_{xp}, {}^iP_{xp} - \frac{{}^iP_{sp}}{BS_{LP}}\}$
IF $D_1 < A$
FALSE
$D_1 = A$
$D_2 = A$
$D_3 = A$
$D_4 = A$
BU
IF ORDER = ∅
TRUE
FALSE
IF ${}^kP_{sp} > ∅$
FALSE
TRUE
$ORDER_A = 1$
$ORDER_A = ∅$
$ORDER_A = 1$
IF ORDER = ∅
FALSE
TRUE
$D_2 = D_1 + {}^iV_x\tau$
$D_2 = MIN\{P_{D4}, D_1 + {}^iV_x\tau\}$
IF $D_2 < A$
TRUE
FALSE
$D_2 = A$
$D_3 = A$
$D_4 = A$
IF ORDER = ∅
TRUE
FALSE
$D_3 = MAX\{PD_4, D_1 + {}^iV_x\tau\}$
IF $ORDER_A = 1$
FALSE
TRUE
$D_3 = {}^kP_{xp} - \frac{{}^cP_{sp}}{BS_{LP}}$
$D_3 = {}^kP_{xp}$
IF $D_3 < A$
FALSE
$D_3 = A$
$D_4 = A$
$D_4 = A$
FALSE
IF $D_4 < A$
TRUE
$D_4 = MIN\{{}^kB_{px}, {}^kB_{px} - \frac{{}^cP_{sp}}{S_{LP}}\}$
$D_3 = D_2 + \frac{D_4 - D_2}{2}$
$D_4 = D_3$
TRUE
IF $ORDER_A = 1$
FALSE
$D_4 = MIN\{{}^iB_{px}, {}^iB_{px} - \frac{{}^iB_{ps}}{S_{LP}}\}$
TRUE
IF ORDER = 0
FALSE

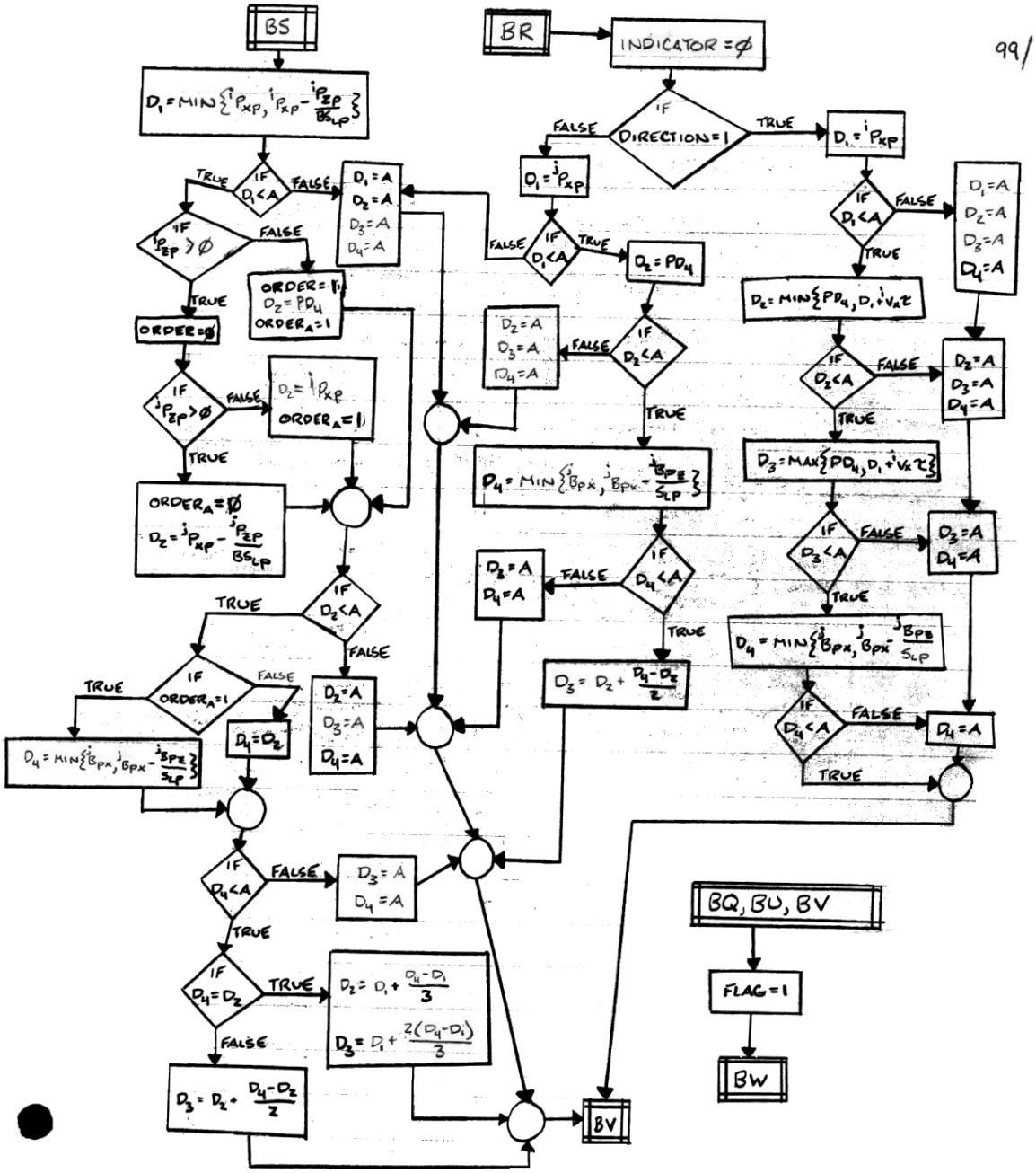
BS
BR
INDICATOR = ∅
99/
IF DIRECTION = 1
TRUE
FALSE
IF D1 < A
IF D2 < A
IF D3 < A
IF D4 < A
IF ORDER = ∅
IF ORDER_A = 1
IF D4 = D2
BQ, BU, BV
FLAG = 1
BW
BV

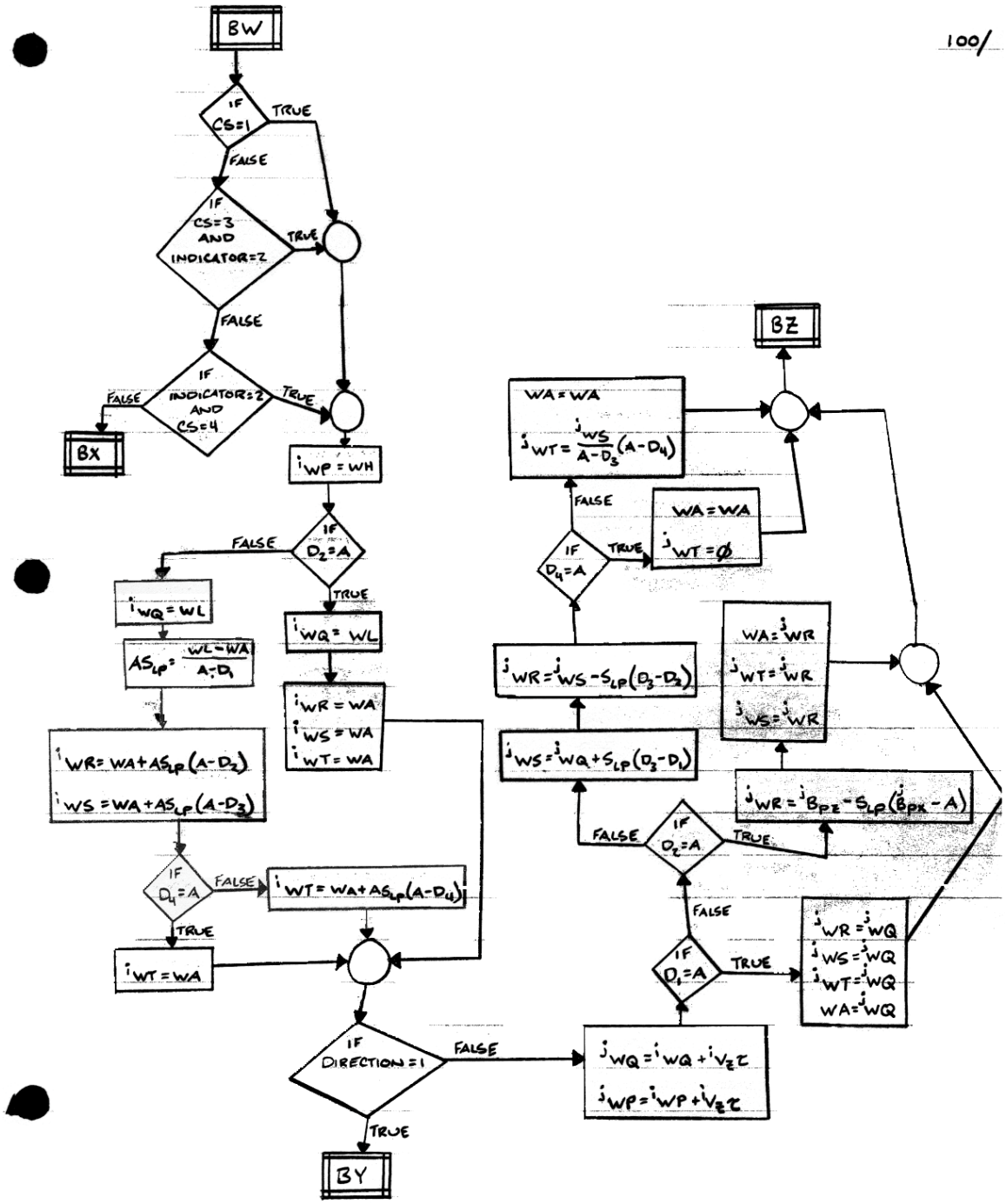
BW
IF CS=1
TRUE
FALSE
IF CS=3 AND INDICATOR=2
TRUE
FALSE
IF INDICATOR=2 AND CS=4
FALSE
TRUE
BX
$i_{WP} = WH$
IF $D_2 = A$
FALSE
TRUE
$i_{WQ} = WL$
$AS_{LP} = \frac{WL-WA}{A-D_1}$
$i_{WR} = WA + AS_{LP}(A-D_2)$
$i_{WS} = WA + AS_{LP}(A-D_3)$
$i_{WQ} = WL$
$i_{WR} = WA$
$i_{WS} = WA$
$i_{WT} = WA$
IF $D_4 = A$
FALSE
TRUE
$i_{WT} = WA + AS_{LP}(A-D_4)$
$i_{WT} = WA$
IF DIRECTION = 1
FALSE
TRUE
BY
$j_{WQ} = i_{WQ} + i_{V_E T}$
$j_{WP} = i_{WP} + i_{V_E T}$
IF $D_1 = A$
TRUE
FALSE
$j_{WR} = j_{WQ}$
$j_{WS} = j_{WQ}$
$j_{WT} = j_{WQ}$
$WA = j_{WQ}$
IF $D_2 = A$
TRUE
FALSE
$j_{WR} = j_{B_{PE}} - S_{LP}(j_{B_{PX}} - A)$
$WA = j_{WR}$
$j_{WT} = j_{WR}$
$j_{WS} = j_{WR}$
$j_{WS} = j_{WQ} + S_{LP}(D_3 - D_1)$
$j_{WR} = j_{WS} - S_{LP}(D_3 - D_2)$
IF $D_4 = A$
TRUE
FALSE
$j_{WT} = \emptyset$
WA = WA
$j_{WT} = \frac{j_{WS}}{A-D_3}(A-D_4)$
WA = WA
BZ

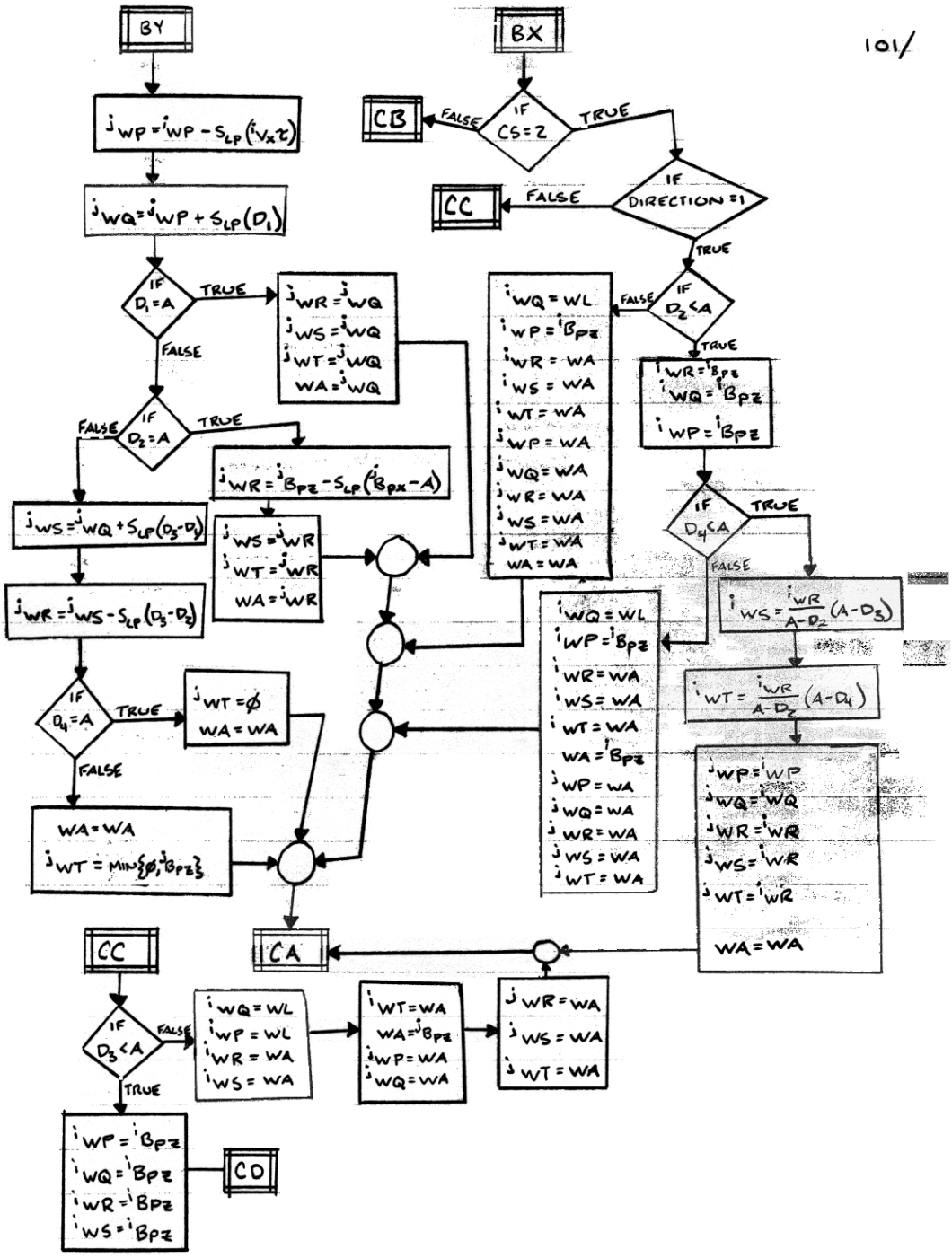
BY
BX
CB
CC
IF CS=Z
FALSE
TRUE
IF DIRECTION=1
IF D1=A
IF D2=A
IF D2<A
IF D4<A
IF D4=A
IF D3<A
CA
CD

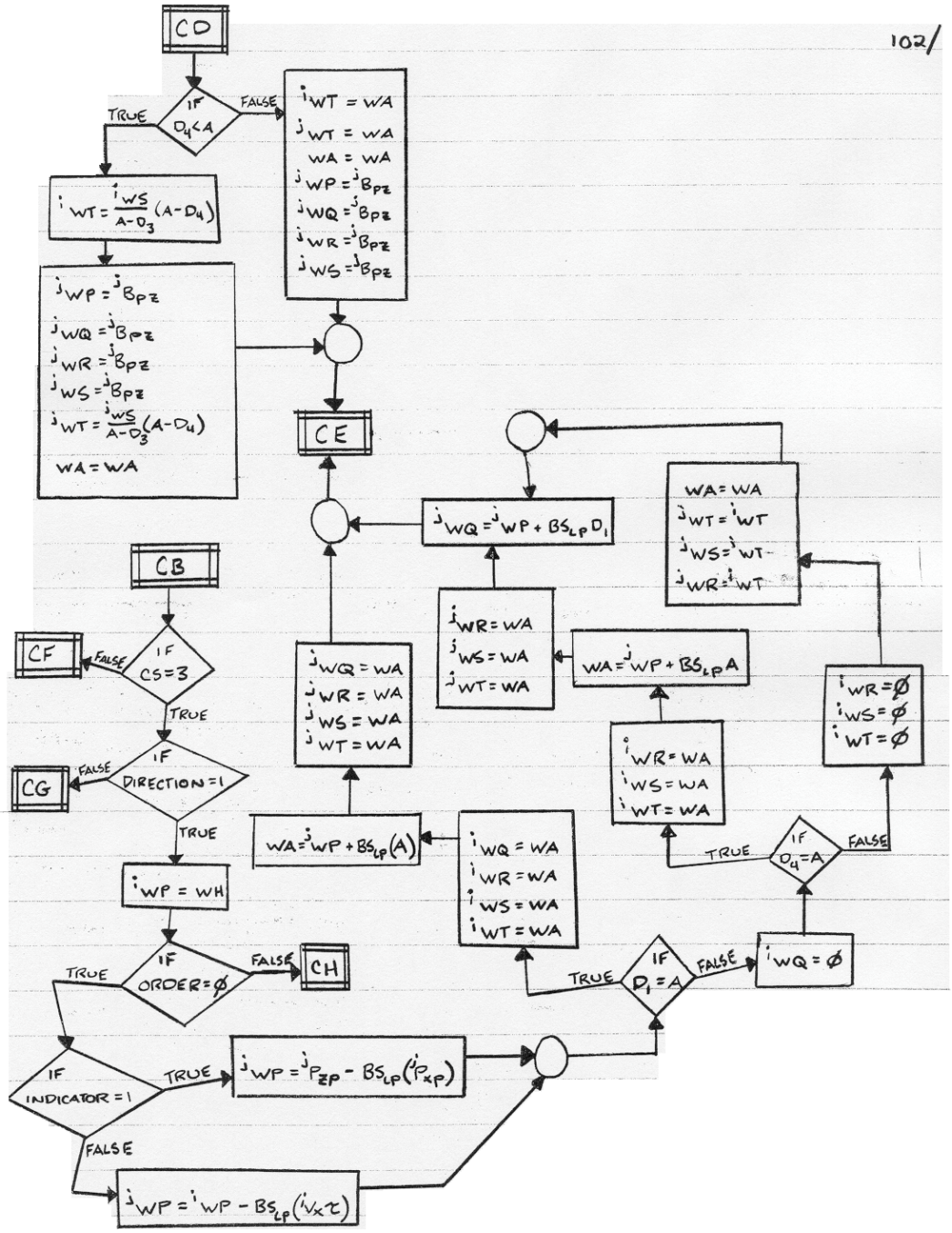
CD
IF D4<A
TRUE
FALSE
iWT = WA
jWT = WA
WA = WA
jWP = jBPZ
jWQ = jBPZ
jWR = jBPZ
jWS = jBPZ
iWT = iWS/(A-D3) (A-D4)
jWP = jBPZ
jWQ = jBPZ
jWR = jBPZ
jWS = jBPZ
jWT = jWS/(A-D3)(A-D4)
WA = WA
CE
jWQ = jWP + BSLP D1
WA = WA
jWT = iWT
jWS = jWT
jWR = jWT
CB
IF CS=3
CF
FALSE
TRUE
jWQ = WA
jWR = WA
jWS = WA
jWT = WA
jWR = WA
jWS = WA
jWT = WA
WA = jWP + BSLP A
iWR = Ø
iWS = Ø
iWT = Ø
IF DIRECTION=1
CG
FALSE
TRUE
iWR = WA
iWS = WA
iWT = WA
WA = jWP + BSLP (A)
iWQ = WA
iWR = WA
iWS = WA
iWT = WA
IF D4=A
TRUE
FALSE
iWP = WH
IF ORDER=Ø
TRUE
FALSE
CH
IF D1 = A
TRUE
FALSE
iWQ = Ø
IF INDICATOR = 1
TRUE
FALSE
jWP = jPZP - BSLP (iPXP)
jWP = iWP - BSLP (iVX τ)

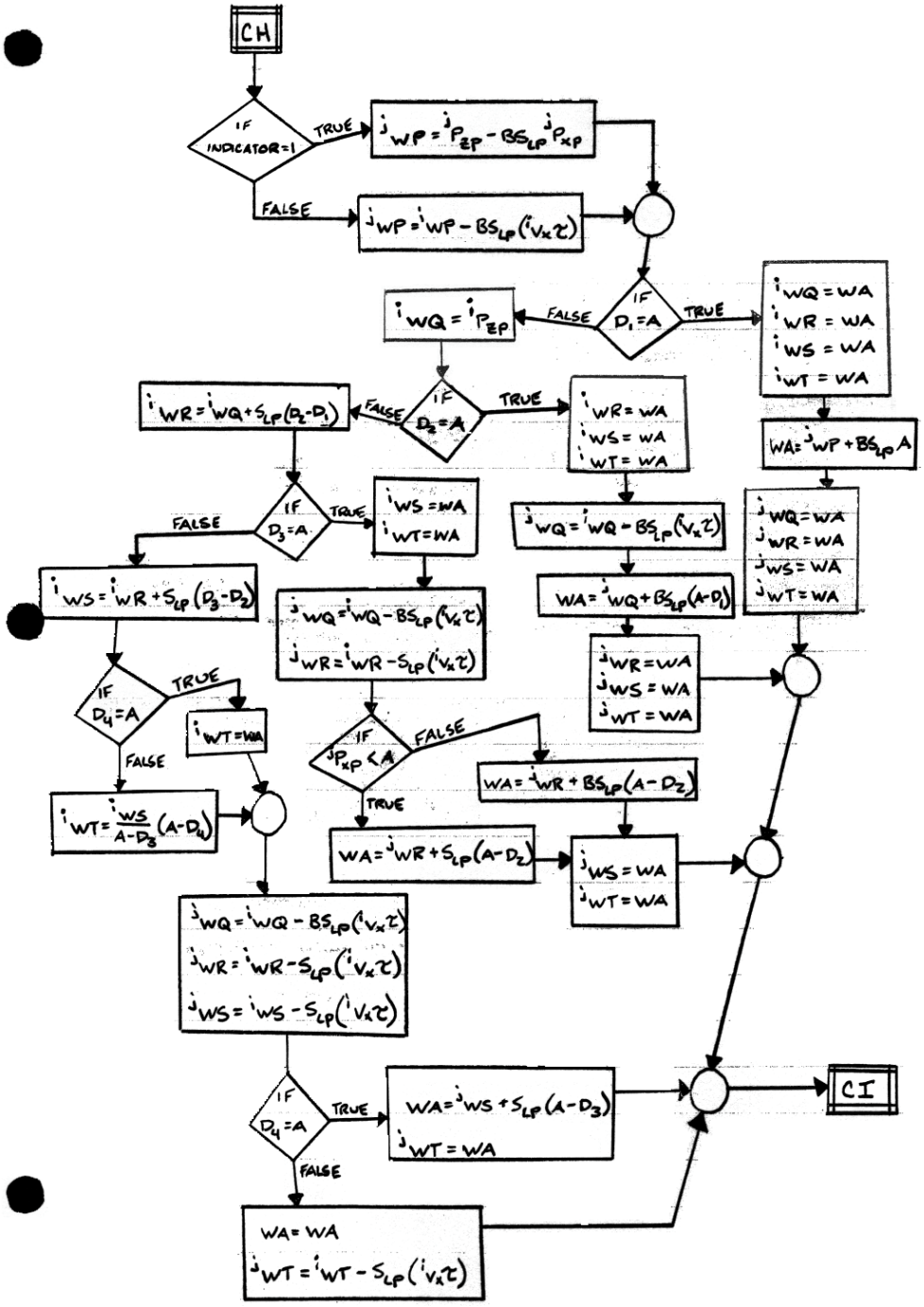
CH
IF INDICATOR=1
TRUE
FALSE
IF D1=A
TRUE
FALSE
IF D2=A
TRUE
FALSE
IF D3=A
TRUE
FALSE
IF D4=A
TRUE
FALSE
IF PxP<A
TRUE
FALSE
IF D4=A
TRUE
FALSE
CI

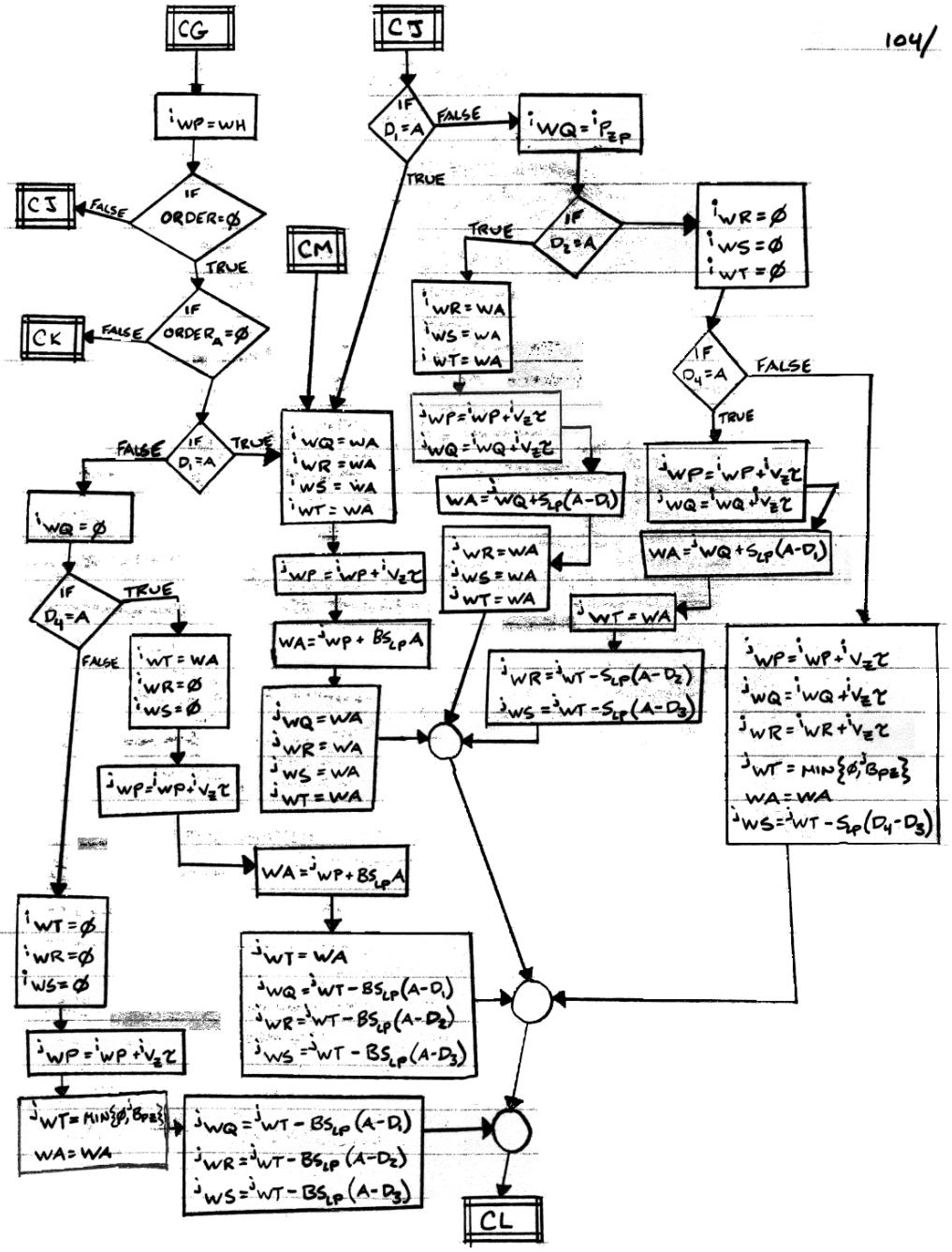
CG
CJ
CM
CK
CL
IF ORDER=Ø
IF ORDER_A=Ø
IF D_1=A
IF D_2=A
IF D_4=A
FALSE
TRUE
iWP=WH
iWQ=iP_ZP
iWR=Ø
iWS=Ø
iWT=Ø
iWR=WA
iWS=WA
iWT=WA
iWP=iWP+iV_Zτ
iWQ=iWQ+iV_Zτ
WA=iWQ+S_LP(A-D_1)
WA=iWP+BS_LPA
jWP=iWP+jV_Zτ
jWQ=iWQ+jV_Zτ
jWR=WA
jWS=WA
jWT=WA
jWR=jWT-S_LP(A-D_2)
jWS=jWT-S_LP(A-D_3)
jWP=iWP+jV_Zτ
jWQ=iWQ+jV_Zτ
jWR=iWR+jV_Zτ
jWT=MIN{Ø,jBP_Z}
WA=WA
jWS=jWT-S_LP(D_4-D_3)
iWQ=Ø
iWT=WA
iWR=Ø
iWS=Ø
iWT=Ø
iWR=Ø
iWS=Ø
jWQ=WA
jWR=WA
jWS=WA
jWT=WA
jWT=WA
jWQ=jWT-BS_LP(A-D_1)
jWR=jWT-BS_LP(A-D_2)
jWS=jWT-BS_LP(A-D_3)
jWT=MIN{Ø,jBP_Z}
WA=WA

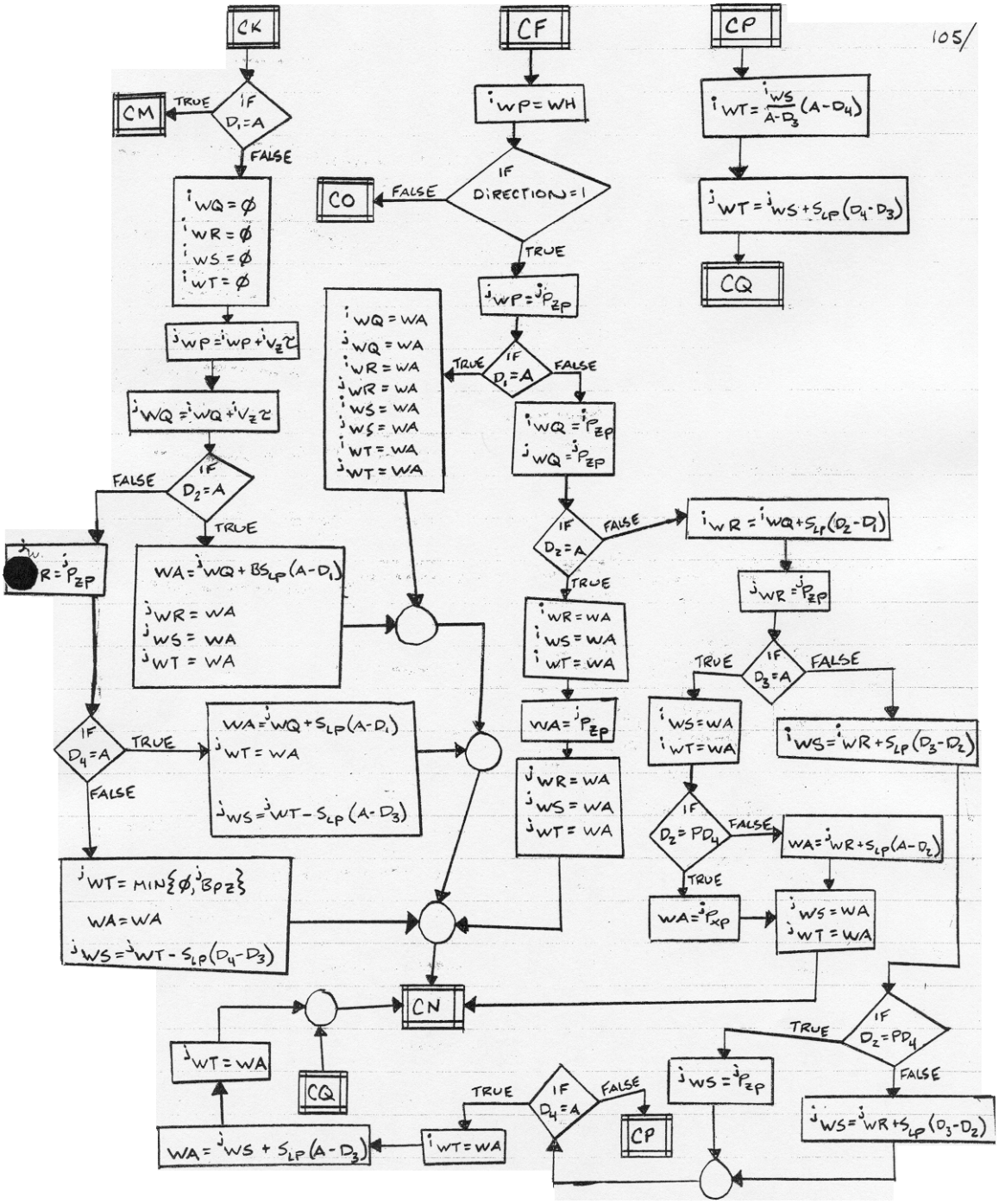
105/
CK
CF
CP
CM
TRUE
IF D1=A
FALSE
CO
FALSE
IF DIRECTION=1
TRUE
CQ
iWQ = ∅
iWR = ∅
iWS = ∅
iWT = ∅
iWP = WH
iWT = iWS/(A-D3) (A-D4)
jWT = jWS + SLP(D4-D3)
jWP = jPZP
jWP = iWP + iVZ
iWQ = WA
jWQ = WA
iWR = WA
jWR = WA
iWS = WA
jWS = WA
iWT = WA
jWT = WA
TRUE
IF D1=A
FALSE
iWQ = jPZP
jWQ = jPZP
jWQ = iWQ + iVZ
FALSE
IF D2=A
TRUE
IF D2=A
FALSE
iWR = iWQ + SLP(D2-D1)
jWR = jPZP
TRUE
IF D3=A
FALSE
jWR = jPZP
WA = jWQ + BSLP(A-D1)
jWR = WA
jWS = WA
jWT = WA
iWR = WA
iWS = WA
iWT = WA
TRUE
iWS = WA
iWT = WA
iWS = iWR + SLP(D3-D2)
IF D4=A
TRUE
FALSE
WA = jWQ + SLP(A-D1)
jWT = WA
jWS = jWT - SLP(A-D3)
WA = jPZP
jWR = WA
jWS = WA
jWT = WA
IF D2=PD4
FALSE
TRUE
WA = iWR + SLP(A-D2)
WA = jPXP
jWS = WA
jWT = WA
jWT = MIN{∅, jBPZ}
WA = WA
jWS = jWT - SLP(D4-D3)
CN
IF D2=PD4
TRUE
FALSE
jWS = jPZP
jWS = jWR + SLP(D3-D2)
jWT = WA
CQ
TRUE
IF D4=A
FALSE
CP
WA = jWS + SLP(A-D3)
iWT = WA

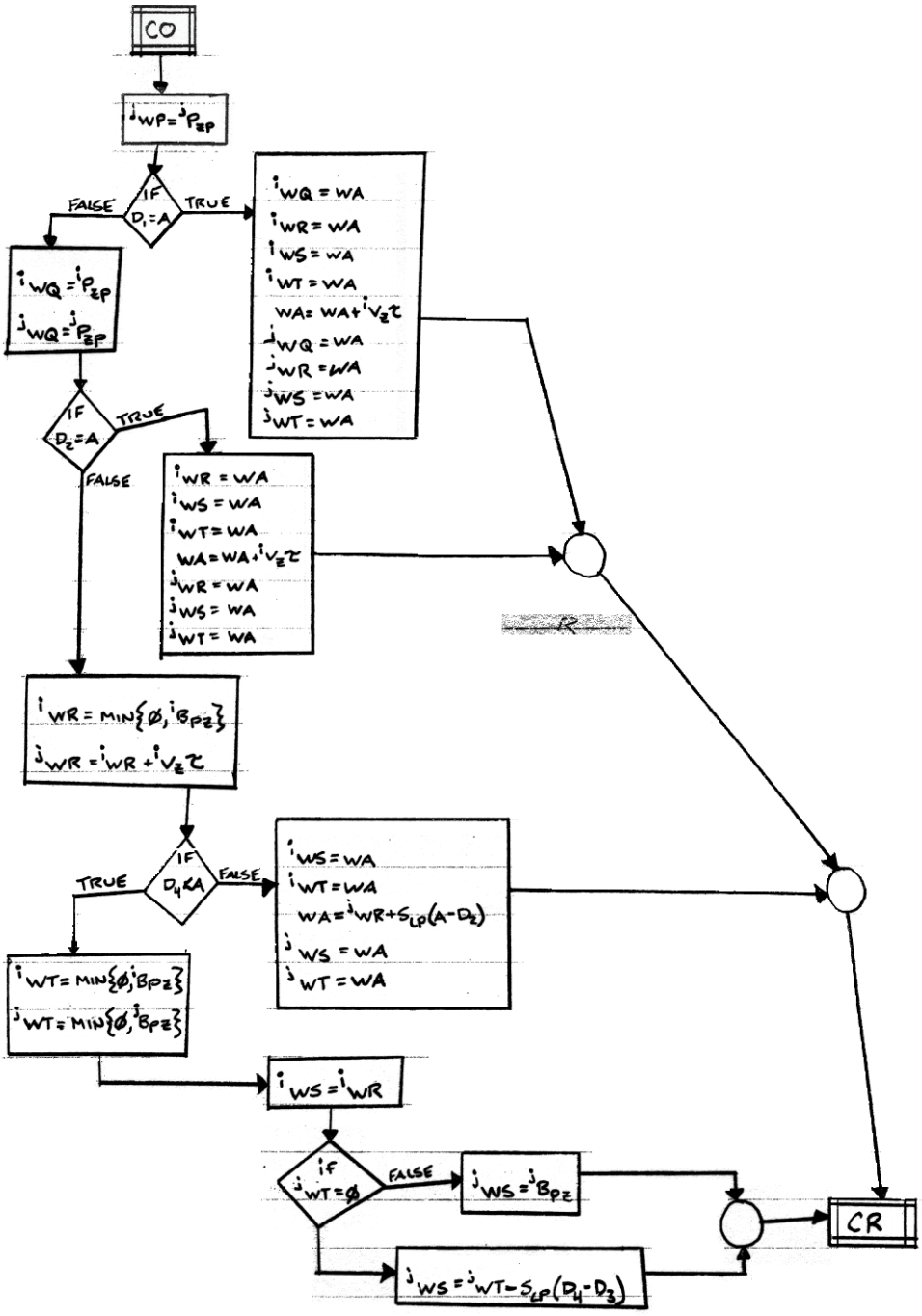
CO
$^{j}WP = {}^{j}P_{zP}$
IF $D_1 = A$
FALSE
TRUE
$^{i}WQ = {}^{i}P_{zP}$
$^{j}WQ = {}^{j}P_{zP}$
$^{i}WQ = WA$
$^{i}WR = WA$
$^{i}WS = WA$
$^{i}WT = WA$
$WA = WA + {}^{i}V_z\tau$
$^{j}WQ = WA$
$^{j}WR = WA$
$^{j}WS = WA$
$^{j}WT = WA$
IF $D_2 = A$
TRUE
FALSE
$^{i}WR = WA$
$^{i}WS = WA$
$^{i}WT = WA$
$WA = WA + {}^{i}V_z\tau$
$^{j}WR = WA$
$^{j}WS = WA$
$^{j}WT = WA$
$^{i}WR = MIN\{\emptyset, {}^{i}B_{pz}\}$
$^{j}WR = {}^{i}WR + {}^{i}V_z\tau$
IF $D_4 < A$
TRUE
FALSE
$^{i}WS = WA$
$^{i}WT = WA$
$WA = {}^{i}WR + S_{LP}(A - D_2)$
$^{j}WS = WA$
$^{j}WT = WA$
$^{i}WT = MIN\{\emptyset, {}^{i}B_{pz}\}$
$^{j}WT = MIN\{\emptyset, {}^{j}B_{pz}\}$
$^{i}WS = {}^{i}WR$
IF $^{j}WT = \emptyset$
FALSE
$^{j}WS = {}^{j}B_{pz}$
$^{j}WS = {}^{j}WT - S_{LP}(D_4 - D_3)$
CR

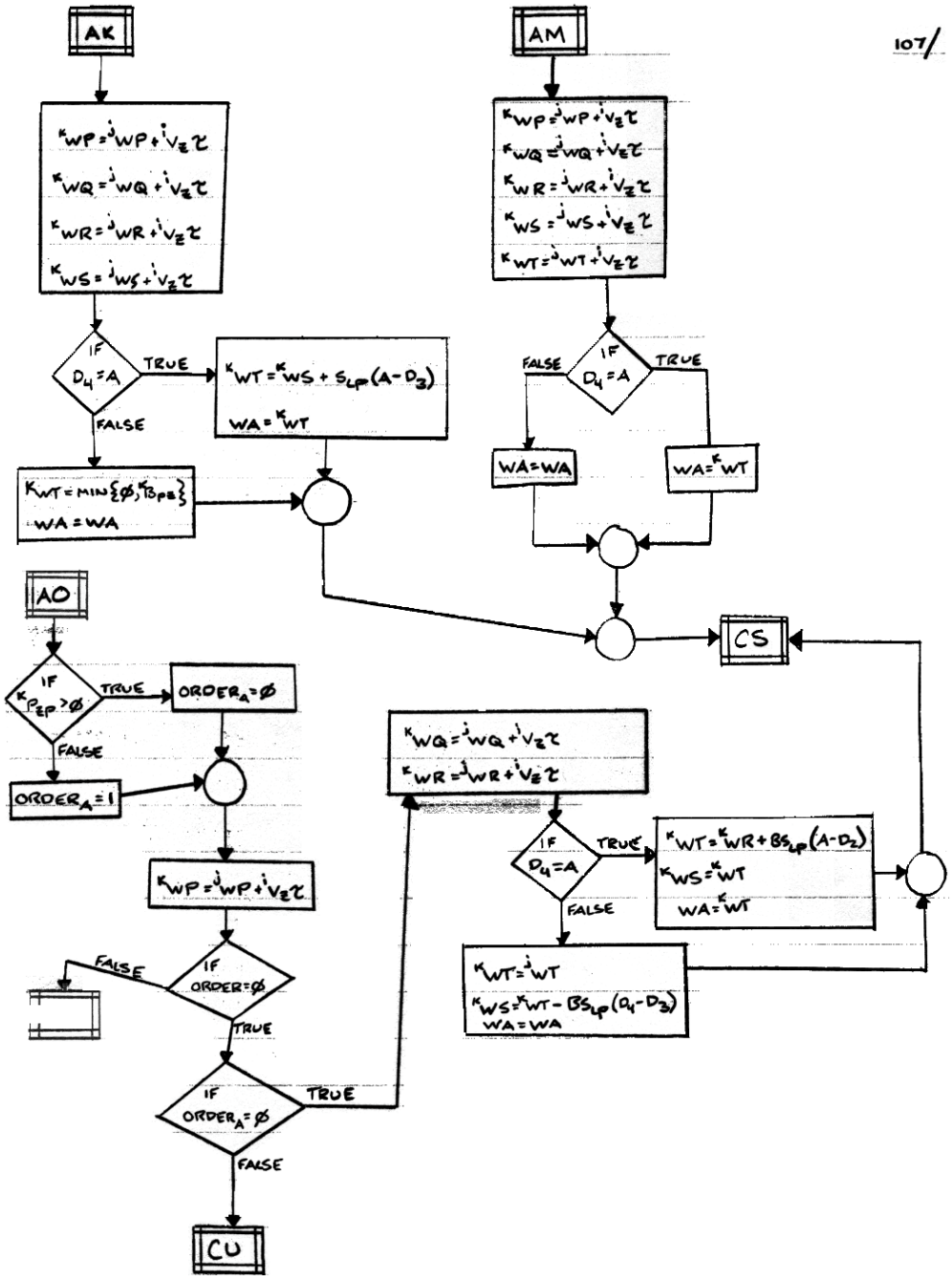
AK
AM
AO
CS
CU
IF
TRUE
FALSE
ORDER=Ø
ORDER_A=Ø
ORDER_A=1
WA=WA

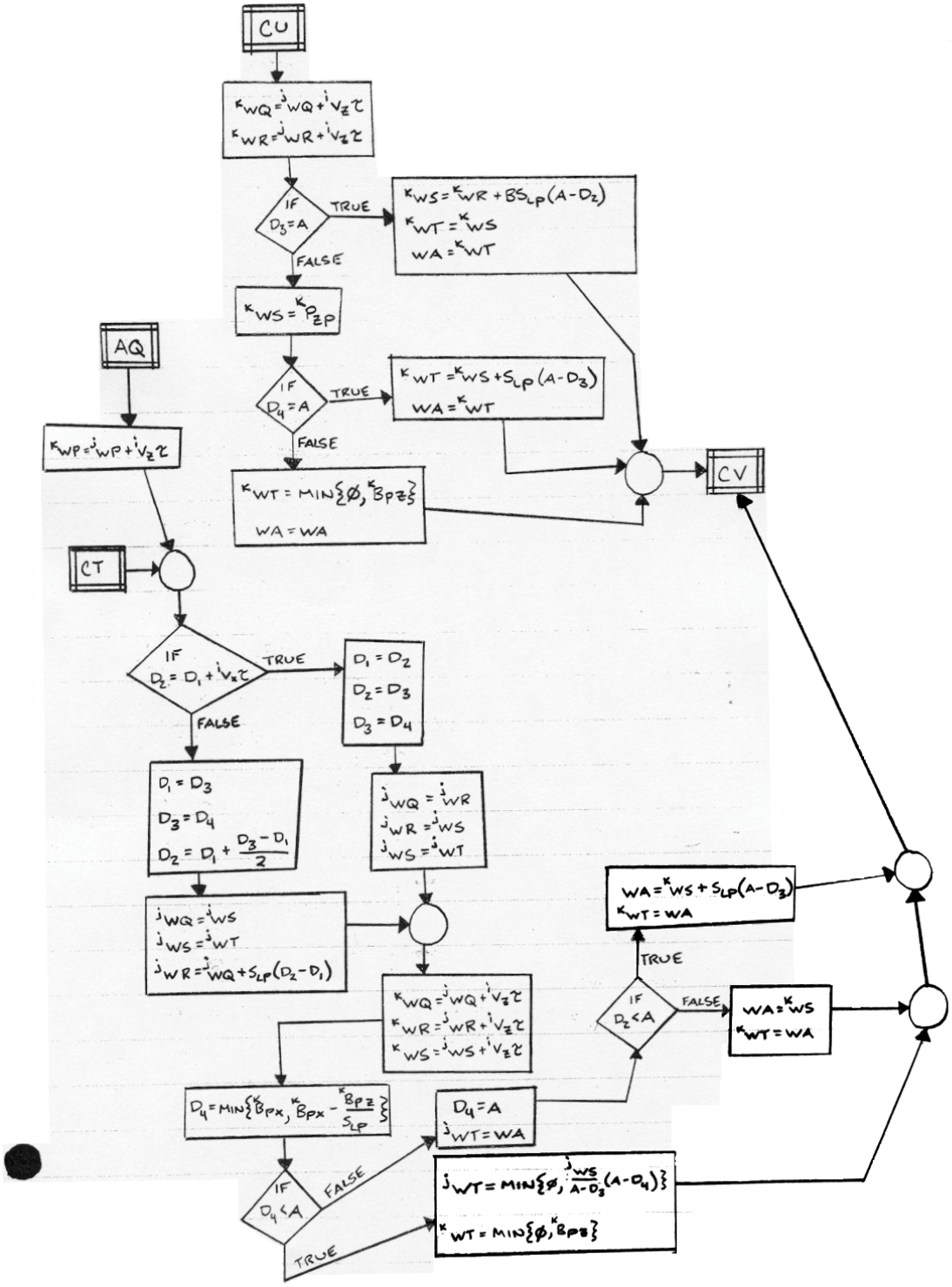
CU
$^{K}WQ = {}^{J}WQ + {}^{I}V_Z\tau$
$^{K}WR = {}^{J}WR + {}^{I}V_Z\tau$
IF $D_3 = A$
TRUE
$^{K}WS = {}^{K}WR + BS_{LP}(A - D_2)$
$^{K}WT = {}^{K}WS$
$WA = {}^{K}WT$
FALSE
$^{K}WS = {}^{K}P_{ZP}$
AQ
IF $D_4 = A$
TRUE
$^{K}WT = {}^{K}WS + S_{LP}(A - D_3)$
$WA = {}^{K}WT$
FALSE
$^{K}WP = {}^{J}WP + {}^{I}V_Z\tau$
$^{K}WT = MIN\{\phi, {}^{K}BPZ\}$
$WA = WA$
CV
CT
IF $D_2 = D_1 + {}^{I}V_Z\tau$
TRUE
$D_1 = D_2$
$D_2 = D_3$
$D_3 = D_4$
FALSE
$D_1 = D_3$
$D_3 = D_4$
$D_2 = D_1 + \frac{D_3 - D_1}{2}$
$^{J}WQ = {}^{J}WR$
$^{J}WR = {}^{J}WS$
$^{J}WS = {}^{J}WT$
$^{J}WQ = {}^{J}WS$
$^{J}WS = {}^{J}WT$
$^{J}WR = {}^{J}WQ + S_{LP}(D_2 - D_1)$
$WA = {}^{K}WS + S_{LP}(A - D_3)$
$^{K}WT = WA$
TRUE
IF $D_2 < A$
FALSE
$WA = {}^{K}WS$
$^{K}WT = WA$
$^{K}WQ = {}^{J}WQ + {}^{I}V_Z\tau$
$^{K}WR = {}^{J}WR + {}^{I}V_Z\tau$
$^{K}WS = {}^{J}WS + {}^{I}V_Z\tau$
$D_4 = MIN\{{}^{K}BPX, {}^{K}BPX - \frac{{}^{K}BPZ}{S_{LP}}\}$
$D_4 = A$
$^{J}WT = WA$
IF $D_4 < A$
FALSE
TRUE
$^{J}WT = MIN\{\phi, \frac{{}^{J}WS}{A - D_3}(A - D_4)\}$
$^{K}WT = MIN\{\phi, {}^{K}BPZ\}$

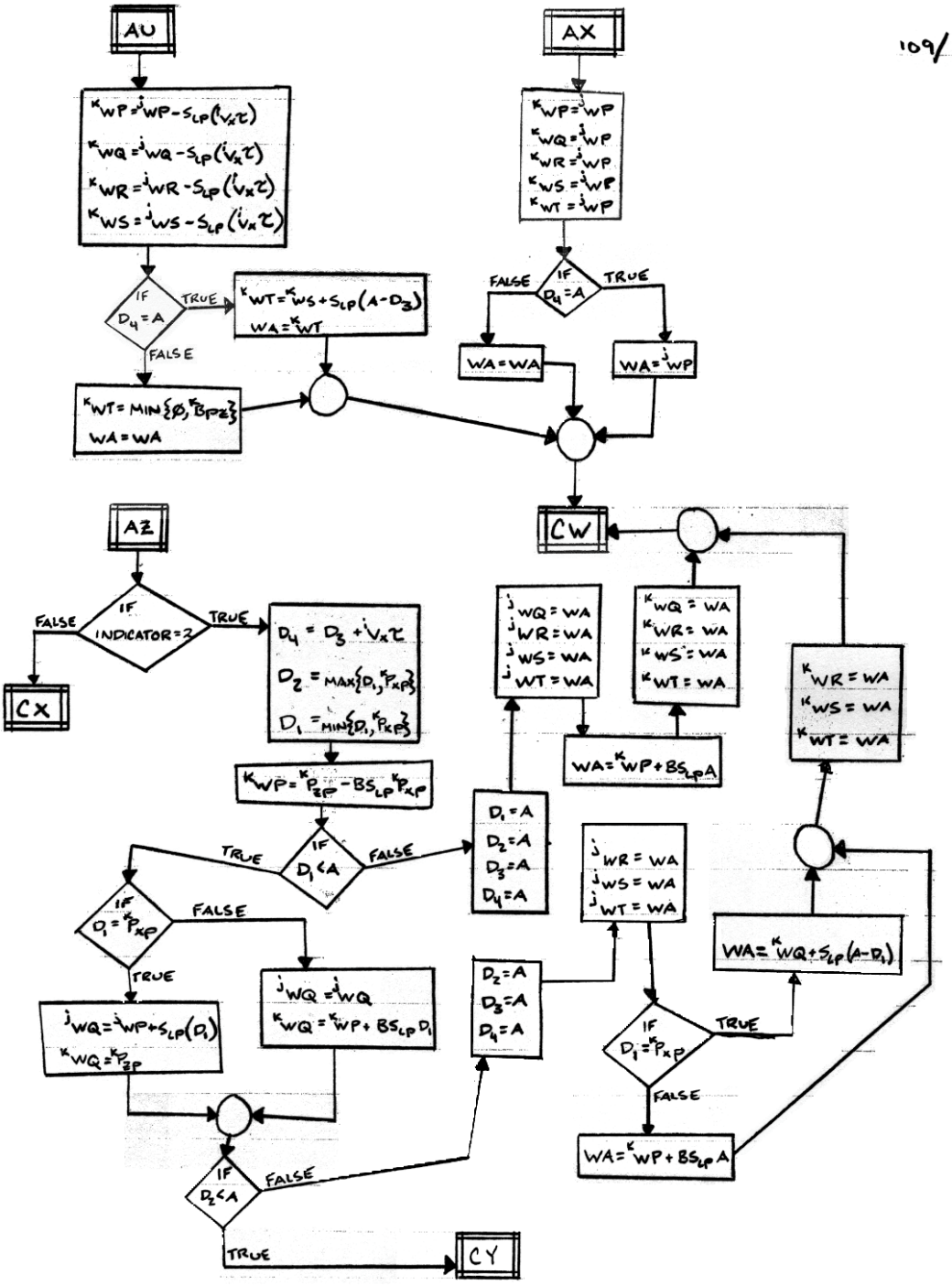
AU
AX
AZ
CW
CX
CY
IF D4 = A
TRUE
FALSE
IF INDICATOR = 2
IF D1 < A
IF D1 = KPXP
IF D2 < A
IF D1 = KPXP
WA = WA
WA = JWP
WA = KWT
WA = KWP + BSLP A
WA = KWQ + SLP (A - D1)
D1 = A
D2 = A
D3 = A
D4 = A

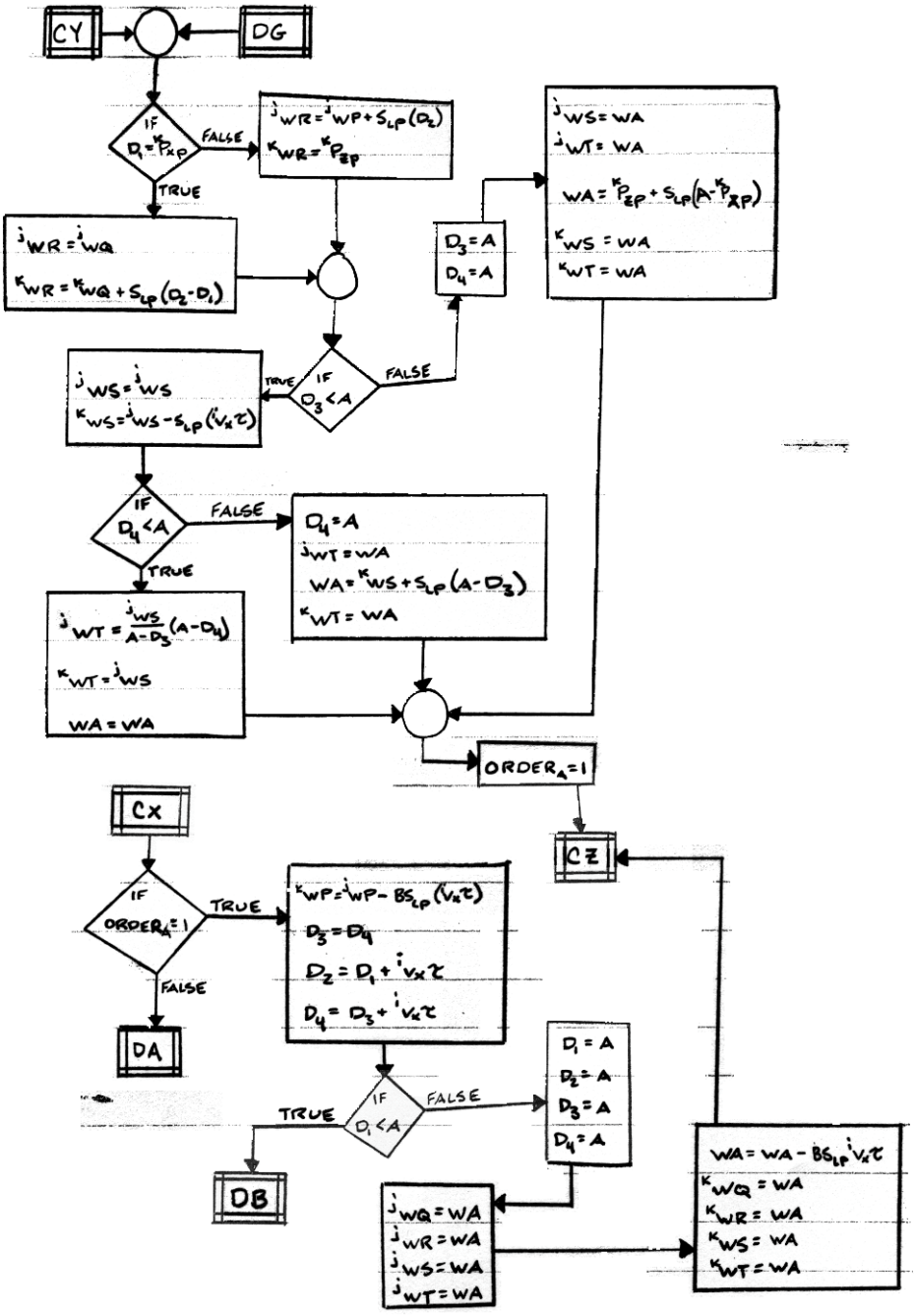
CY
DG
IF $D_1 = {}^{K}P_{XP}$
FALSE
TRUE
${}^{j}W_R = {}^{j}W_P + S_{LP}(D_2)$
${}^{K}W_R = {}^{K}P_{EP}$
${}^{j}W_R = {}^{j}W_Q$
${}^{K}W_R = {}^{K}W_Q + S_{LP}(D_2 - D_1)$
$D_3 = A$
$D_4 = A$
${}^{j}W_S = WA$
${}^{j}W_T = WA$
$WA = {}^{K}P_{EP} + S_{LP}(A - {}^{K}P_{XP})$
${}^{K}W_S = WA$
${}^{K}W_T = WA$
IF $D_3 < A$
TRUE
FALSE
${}^{j}W_S = {}^{j}W_S$
${}^{K}W_S = {}^{j}W_S - S_{LP}({}^{j}V_x \tau)$
IF $D_4 < A$
FALSE
TRUE
$D_4 = A$
${}^{j}W_T = WA$
$WA = {}^{K}W_S + S_{LP}(A - D_3)$
${}^{K}W_T = WA$
${}^{j}W_T = \frac{{}^{j}W_S}{A - D_3}(A - D_4)$
${}^{K}W_T = {}^{j}W_S$
$WA = WA$
$ORDER_A = 1$
CZ
CX
IF $ORDER_A = 1$
TRUE
FALSE
DA
${}^{K}W_P = {}^{j}W_P - BS_{LP}({}^{j}V_x \tau)$
$D_3 = D_4$
$D_2 = D_1 + {}^{j}V_x \tau$
$D_4 = D_3 + {}^{j}V_x \tau$
IF $D_1 < A$
TRUE
FALSE
DB
$D_1 = A$
$D_2 = A$
$D_3 = A$
$D_4 = A$
${}^{j}W_Q = WA$
${}^{j}W_R = WA$
${}^{j}W_S = WA$
${}^{j}W_T = WA$
$WA = WA - BS_{LP}{}^{j}V_x \tau$
${}^{K}W_Q = WA$
${}^{K}W_R = WA$
${}^{K}W_S = WA$
${}^{K}W_T = WA$

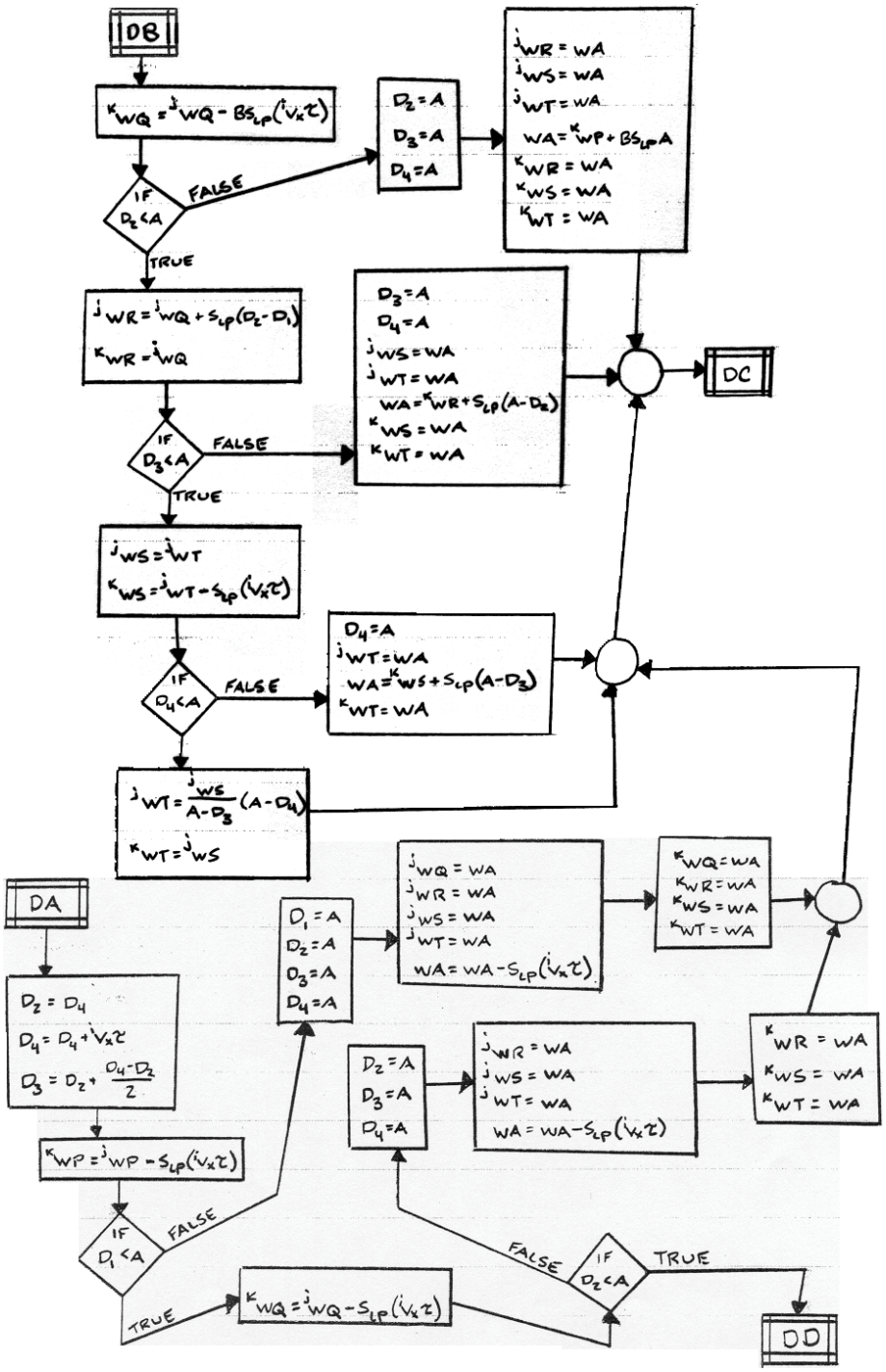
DB
$^{K}WQ = {}^{j}WQ - BS_{LP}(i_x\tau)$
IF $D_2 < A$
FALSE
$D_2 = A$
$D_3 = A$
$D_4 = A$
$^{j}WR = WA$
$^{j}WS = WA$
$^{j}WT = WA$
$WA = {}^{K}WP + BS_{LP}A$
$^{K}WR = WA$
$^{K}WS = WA$
$^{K}WT = WA$
TRUE
$^{j}WR = {}^{j}WQ + S_{LP}(D_2 - D_1)$
$^{K}WR = {}^{j}WQ$
IF $D_3 < A$
FALSE
$D_3 = A$
$D_4 = A$
$^{j}WS = WA$
$^{j}WT = WA$
$WA = {}^{K}WR + S_{LP}(A - D_2)$
$^{K}WS = WA$
$^{K}WT = WA$
DC
TRUE
$^{j}WS = {}^{j}WT$
$^{K}WS = {}^{j}WT - S_{LP}(i_x\tau)$
IF $D_4 < A$
FALSE
$D_4 = A$
$^{j}WT = WA$
$WA = {}^{K}WS + S_{LP}(A - D_3)$
$^{K}WT = WA$
$^{j}WT = \frac{^{j}WS}{A - D_3}(A - D_4)$
$^{K}WT = {}^{j}WS$
DA
$D_2 = D_4$
$D_4 = D_4 + i_x\tau$
$D_3 = D_2 + \frac{D_4 - D_2}{2}$
$^{K}WP = {}^{j}WP - S_{LP}(i_x\tau)$
IF $D_1 < A$
FALSE
TRUE
$^{K}WQ = {}^{j}WQ - S_{LP}(i_x\tau)$
$D_1 = A$
$D_2 = A$
$D_3 = A$
$D_4 = A$
$^{j}WQ = WA$
$^{j}WR = WA$
$^{j}WS = WA$
$^{j}WT = WA$
$WA = WA - S_{LP}(i_x\tau)$
$^{K}WQ = WA$
$^{K}WR = WA$
$^{K}WS = WA$
$^{K}WT = WA$
$D_2 = A$
$D_3 = A$
$D_4 = A$
$^{j}WR = WA$
$^{j}WS = WA$
$^{j}WT = WA$
$WA = WA - S_{LP}(i_x\tau)$
$^{K}WR = WA$
$^{K}WS = WA$
$^{K}WT = WA$
FALSE
IF $D_2 < A$
TRUE
DD

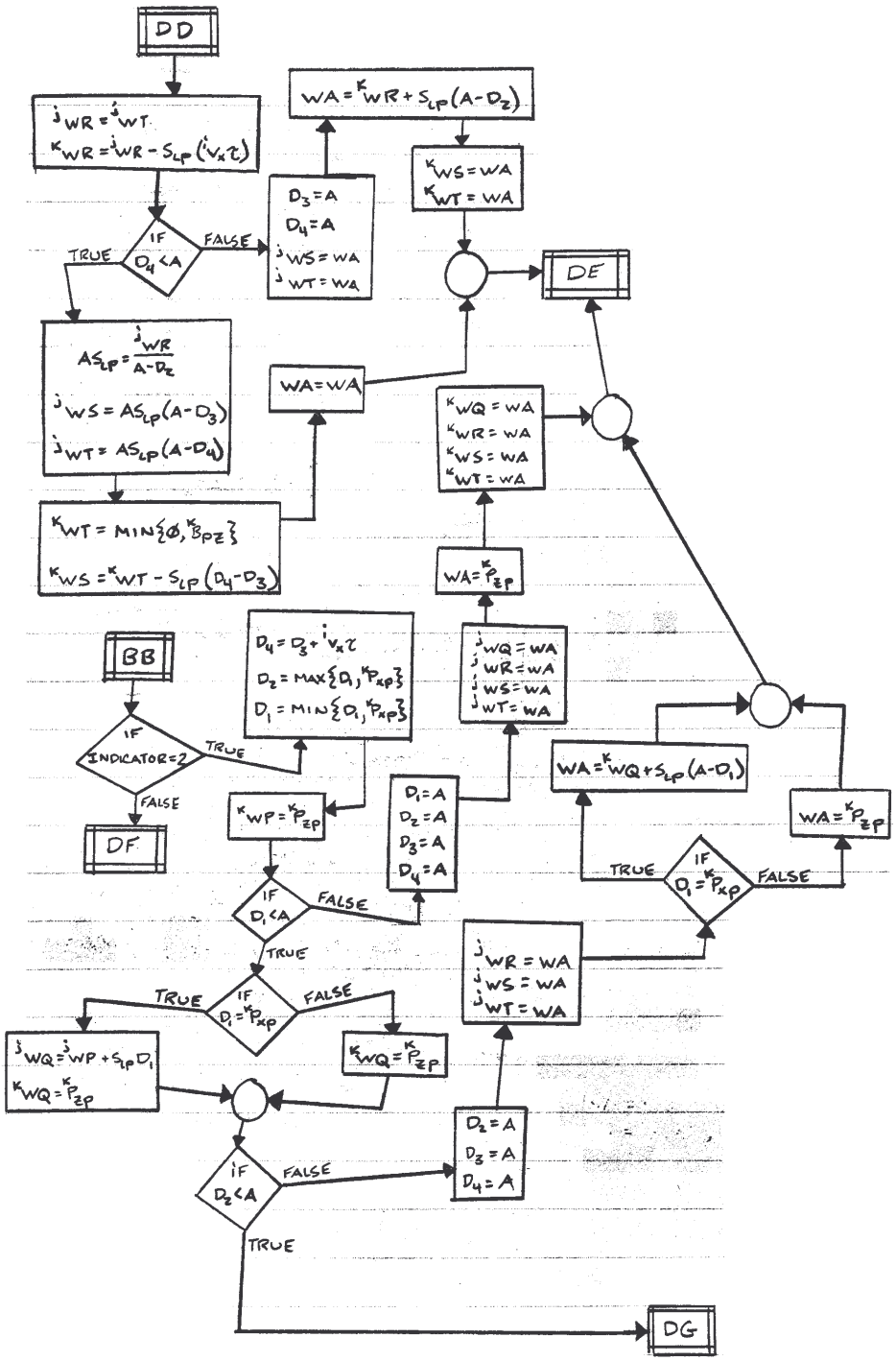
DD
$^{j}WR = {}^{j}WT$
$^{K}WR = {}^{j}WR - S_{LP}({}^{i}V_x\tau)$
IF $D_4 < A$
TRUE
FALSE
$D_3 = A$
$D_4 = A$
$^{j}WS = WA$
$^{j}WT = WA$
$WA = {}^{K}WR + S_{LP}(A - D_2)$
$^{K}WS = WA$
$^{K}WT = WA$
DE
$AS_{LP} = \frac{^{j}WR}{A - D_2}$
$^{j}WS = AS_{LP}(A - D_3)$
$^{j}WT = AS_{LP}(A - D_4)$
$WA = WA$
$^{K}WQ = WA$
$^{K}WR = WA$
$^{K}WS = WA$
$^{K}WT = WA$
$^{K}WT = MIN\{\emptyset, {}^{K}B_{PZ}\}$
$^{K}WS = {}^{K}WT - S_{LP}(D_4 - D_3)$
$WA = {}^{K}P_{ZP}$
BB
$D_4 = D_3 + {}^{i}V_x\tau$
$D_2 = MAX\{D_1, {}^{K}P_{XP}\}$
$D_1 = MIN\{D_1, {}^{K}P_{XP}\}$
$^{j}WQ = WA$
$^{j}WR = WA$
$^{j}WS = WA$
$^{j}WT = WA$
IF INDICATOR=2
TRUE
FALSE
DF
$^{K}WP = {}^{K}P_{ZP}$
$D_1 = A$
$D_2 = A$
$D_3 = A$
$D_4 = A$
$WA = {}^{K}WQ + S_{LP}(A - D_1)$
$WA = {}^{K}P_{ZP}$
IF $D_1 = {}^{K}P_{XP}$
TRUE
FALSE
IF $D_1 < A$
FALSE
TRUE
$^{j}WR = WA$
$^{j}WS = WA$
$^{j}WT = WA$
IF $D_1 = {}^{K}P_{XP}$
TRUE
FALSE
$^{j}WQ = {}^{j}WP + S_{LP}D_1$
$^{K}WQ = {}^{K}P_{ZP}$
$^{K}WQ = {}^{K}P_{ZP}$
$D_2 = A$
$D_3 = A$
$D_4 = A$
IF $D_2 < A$
FALSE
TRUE
DG

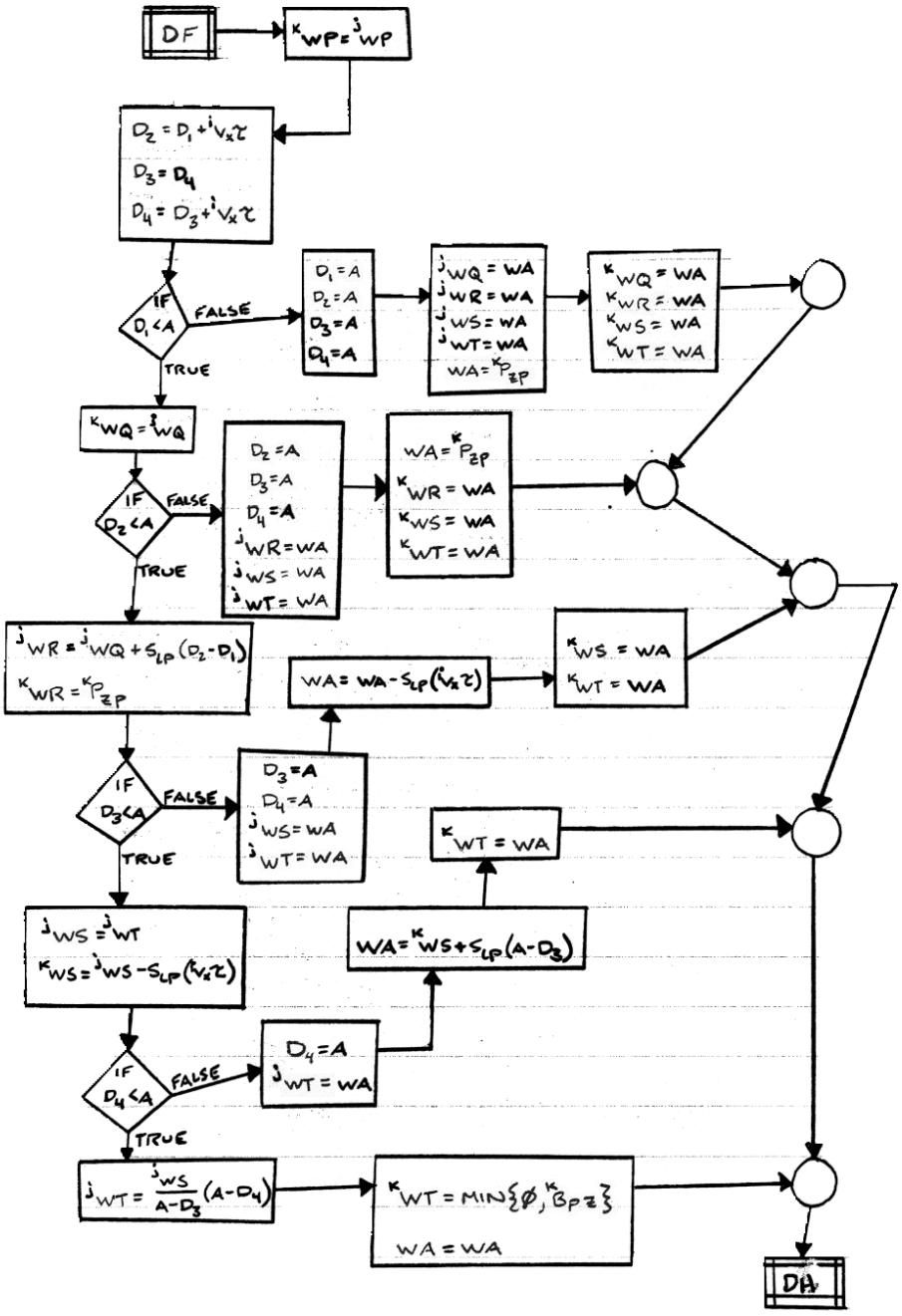
DF
$^{K}WP = {}^{j}WP$
$D_2 = D_1 + {}^{j}V_x\tau$
$D_3 = D_4$
$D_4 = D_3 + {}^{j}V_x\tau$
IF $D_1 < A$
FALSE
TRUE
$D_1 = A$
$D_2 = A$
$D_3 = A$
$D_4 = A$
$^{j}WQ = WA$
$^{j}WR = WA$
$^{j}WS = WA$
$^{j}WT = WA$
$WA = {}^{K}P_{ZP}$
$^{K}WQ = WA$
$^{K}WR = WA$
$^{K}WS = WA$
$^{K}WT = WA$
$^{K}WQ = {}^{j}WQ$
IF $D_2 < A$
FALSE
TRUE
$D_2 = A$
$D_3 = A$
$D_4 = A$
$^{j}WR = WA$
$^{j}WS = WA$
$^{j}WT = WA$
$WA = {}^{K}P_{ZP}$
$^{K}WR = WA$
$^{K}WS = WA$
$^{K}WT = WA$
$^{j}WR = {}^{j}WQ + S_{LP}(D_2 - D_1)$
$^{K}WR = {}^{K}P_{ZP}$
$WA = WA - S_{LP}({}^{j}V_x\tau)$
$^{K}WS = WA$
$^{K}WT = WA$
IF $D_3 < A$
FALSE
TRUE
$D_3 = A$
$D_4 = A$
$^{j}WS = WA$
$^{j}WT = WA$
$^{K}WT = WA$
$^{j}WS = {}^{j}WT$
$^{K}WS = {}^{j}WS - S_{LP}({}^{j}V_x\tau)$
$WA = {}^{K}WS + S_{LP}(A - D_3)$
IF $D_4 < A$
FALSE
TRUE
$D_4 = A$
$^{j}WT = WA$
$^{j}WT = \frac{^{j}WS}{A - D_3}(A - D_4)$
$^{K}WT = MIN\{\phi, {}^{K}B_{PZ}\}$
$WA = WA$
DH

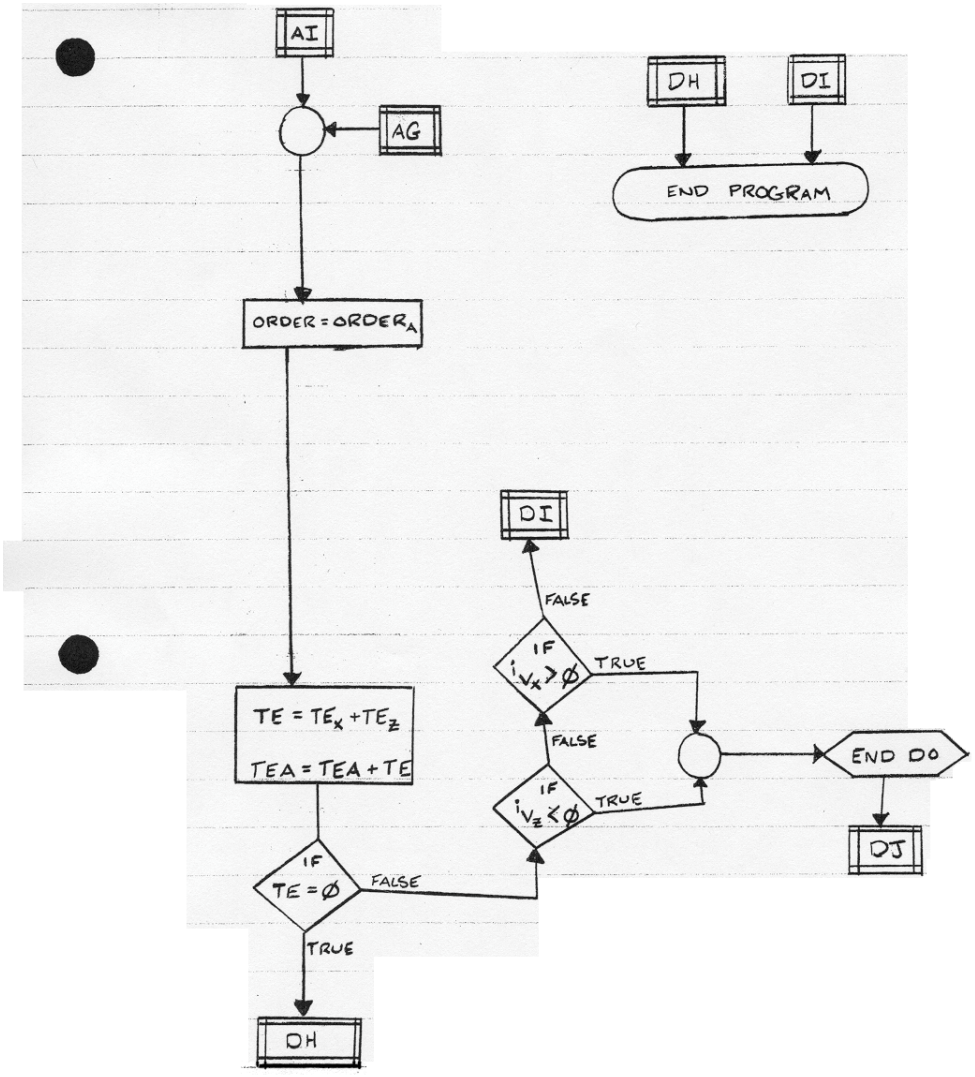
AI
AG
DH
DI
END PROGRAM
ORDER = ORDER_A
DI
FALSE
IF i_Vx > Ø
TRUE
TE = TE_X + TE_Z
TEA = TEA + TE
FALSE
END DO
IF i_Vz < Ø
TRUE
DJ
IF TE = Ø
FALSE
TRUE
DH

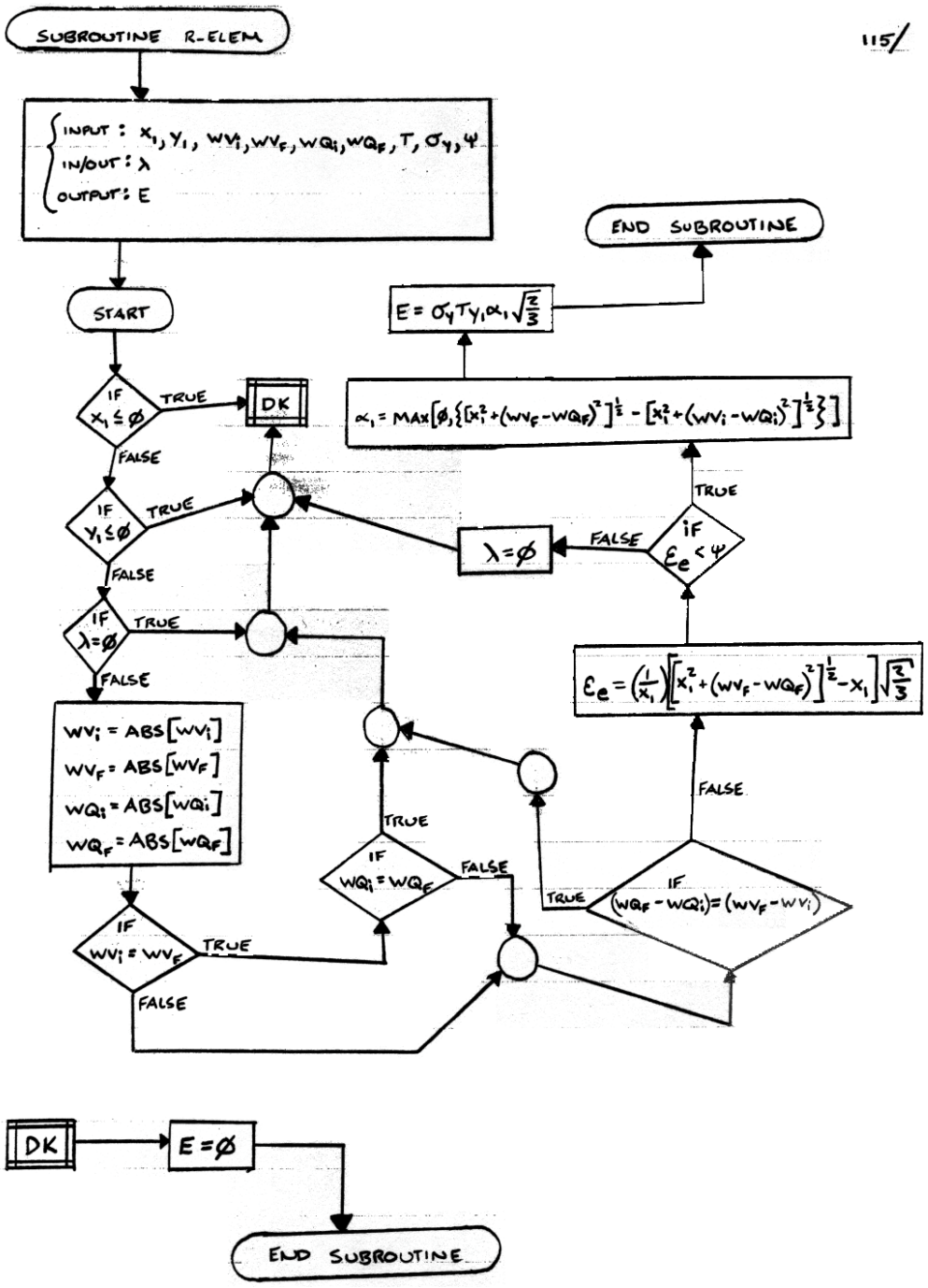
SUBROUTINE R-ELEM
INPUT : $x_1, y_1, wv_i, wv_F, wQ_i, wQ_F, T, \sigma_y, \psi$
IN/OUT : λ
OUTPUT : E
START
IF $x_1 \le \emptyset$
TRUE
DK
FALSE
IF $y_1 \le \emptyset$
TRUE
FALSE
IF $\lambda = \emptyset$
TRUE
FALSE
$wv_i = ABS[wv_i]$
$wv_F = ABS[wv_F]$
$wQ_i = ABS[wQ_i]$
$wQ_F = ABS[wQ_F]$
IF $wv_i = wv_F$
TRUE
FALSE
IF $wQ_i = wQ_F$
TRUE
FALSE
IF $(wQ_F - wQ_i) = (wv_F - wv_i)$
TRUE
FALSE
$\varepsilon_e = \left(\frac{1}{x_1}\right)\left[\left[x_1^2 + (wv_F - wQ_F)^2\right]^{\frac{1}{2}} - x_1\right]\sqrt{\frac{2}{3}}$
IF $\varepsilon_e < \psi$
TRUE
FALSE
$\lambda = \emptyset$
$\alpha_1 = MAX\left[\emptyset, \left\{\left[x_1^2 + (wv_F - wQ_F)^2\right]^{\frac{1}{2}} - \left[x_1^2 + (wv_i - wQ_i)^2\right]^{\frac{1}{2}}\right\}\right]$
$E = \sigma_y T y_1 \alpha_1 \sqrt{\frac{2}{3}}$
END SUBROUTINE
DK
$E = \emptyset$
END SUBROUTINE

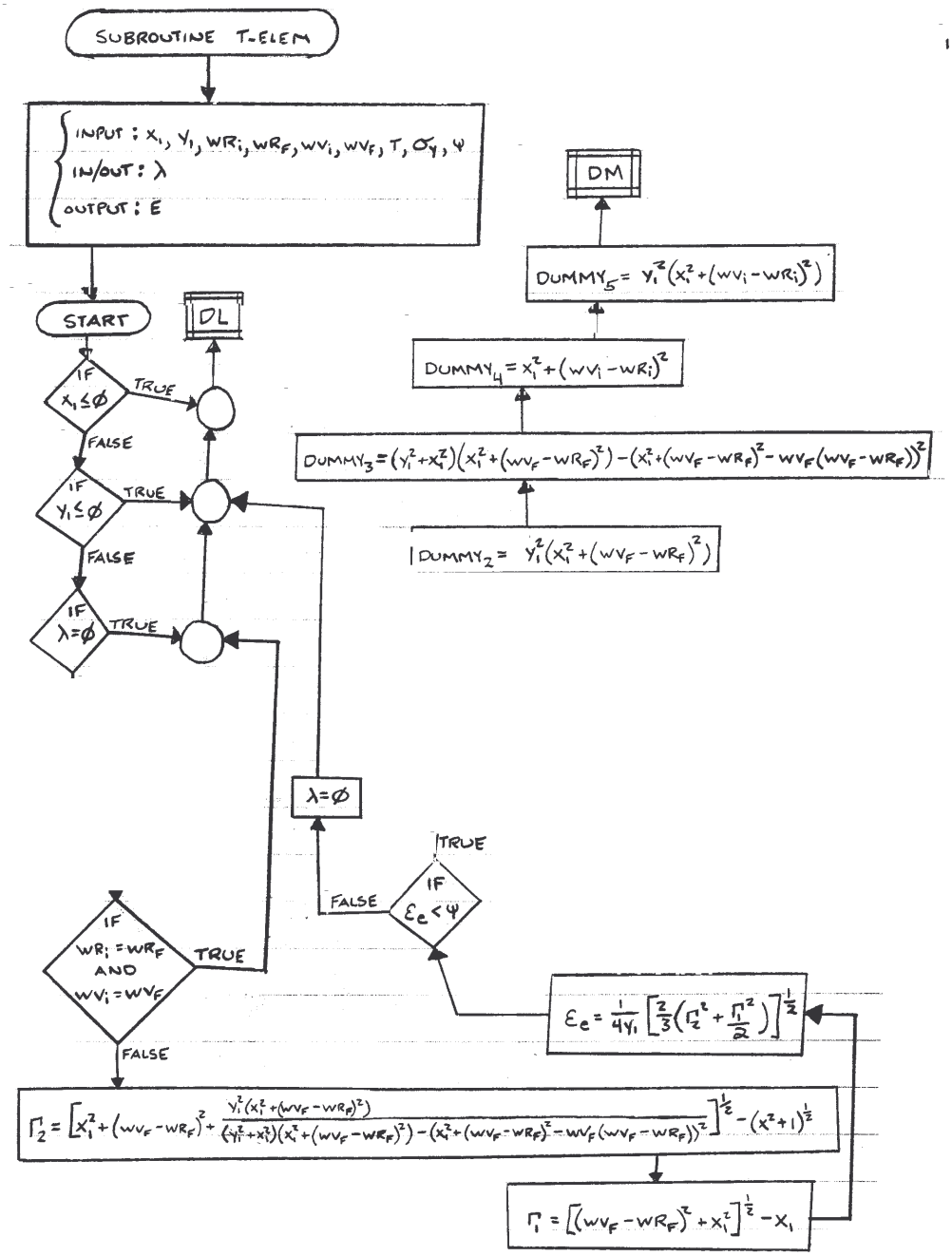
SUBROUTINE T-ELEM
INPUT : x_1, y_1, WR_i, WR_F, WV_i, WV_F, T, σ_y, ψ
IN/OUT : λ
OUTPUT : E
START
DL
DM
IF $x_1 \le \phi$ TRUE
FALSE
IF $y_1 \le \phi$ TRUE
FALSE
IF $\lambda = \phi$ TRUE
$DUMMY_5 = y_1^2\left(x_1^2 + (WV_i - WR_i)^2\right)$
$DUMMY_4 = x_1^2 + (WV_i - WR_i)^2$
$DUMMY_3 = (y_1^2 + x_1^2)\left(x_1^2 + (WV_F - WR_F)^2\right) - \left(x_1^2 + (WV_F - WR_F)^2 - WV_F(WV_F - WR_F)\right)^2$
$DUMMY_2 = y_1^2\left(x_1^2 + (WV_F - WR_F)^2\right)$
$\lambda = \phi$
TRUE
IF $\varepsilon_e < \psi$
FALSE
$\varepsilon_e = \frac{1}{4y_1}\left[\frac{2}{3}\left(\Gamma_2^2 + \frac{\Gamma_1^2}{2}\right)\right]^{\frac{1}{2}}$
IF $WR_i = WR_F$ AND $WV_i = WV_F$
TRUE
FALSE
$\Gamma_2 = \left[x_1^2 + (WV_F - WR_F)^2 + \frac{y_1^2(x_1^2 + (WV_F - WR_F)^2)}{(y_1^2 + x_1^2)(x_1^2 + (WV_F - WR_F)^2) - (x_1^2 + (WV_F - WR_F)^2 - WV_F(WV_F - WR_F))^2}\right]^{\frac{1}{2}} - (x^2 + 1)^{\frac{1}{2}}$
$\Gamma_1 = \left[(WV_F - WR_F)^2 + x_1^2\right]^{\frac{1}{2}} - x_1$

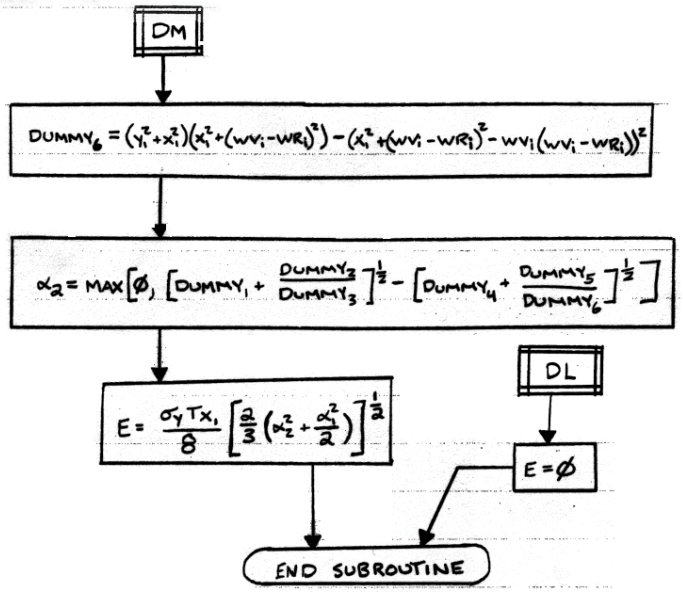
DM
$DUMMY_6 = (y_i^2+x_i^2)(x_i^2+(wv_i-wR_i)^2)-(x_i^2+(wv_i-wR_i)^2-wv_i(wv_i-wR_i))^2$
$\alpha_2 = MAX[\phi, [DUMMY_1 + \frac{DUMMY_3}{DUMMY_3}]^{\frac{1}{2}} - [DUMMY_4 + \frac{DUMMY_5}{DUMMY_6}]^{\frac{1}{2}}]$
DL
$E = \frac{\sigma_y T x_1}{8}\left[\frac{2}{3}\left(x_2^2+\frac{\alpha^2}{2}\right)\right]^{\frac{1}{2}}$
E = ϕ
END SUBROUTINE

100k dwt Single Hull Tanker from Kuroiwa (1996)

Information Book

For

Grounding and Collision Analysis

UPDATE: OCTOBER 31, 1999

A. J. Brown

Naval Architecture

L = 222 m B = 42 m D = 20.3 m T = 13.35 m Δ = 111015 MT

Profile and Plan

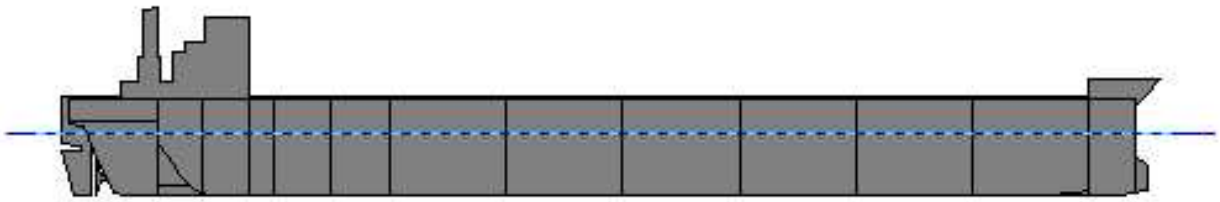

Weights and Stability

FullLoadDepart

Item	Weight MT	VCG m	LCG m-MS	TCG m-CL	FSMom m-MT
Light Ship	14,723	12.000	10.817A	0.000	----
Constant	300	14.000	80.000A	0.000	----
Cargo Oil	92,537	10.323	9.935F	0.000P	128,072
Fuel Oil	2,196	11.770	79.691A	0.000	778
Fresh Water	1,258	14.797	89.229A	0.000	0
SW Ballast	0	----	----	----	----
Misc. Weights	0	----	----	----	----
Displacement	111,015	10.635	4.042F	0.000S	128,850

Stability Calculation			**Trim Calculation**		
KMt	17.125	m	LCF Draft	13.350	m
VCG	10.635	m	LCB (even keel)	4.042F	m-MS
GMt (Solid)	6.490	m	LCF	2.261F	m-MS
FSc	1.161	m	MT1cm	1,335	m-MT
GMt (Corrected)	5.330	m	Trim	0.000	m
			List	0.0	deg

Drafts			**Strength Calculations**		
Draft at A.P.	13.350	m	Shear	0	MT at 0.000 m-MS
Draft at M.S.	13.350	m	Bending Moment	0	m-MT at 0.000 m-MS

Primary Subdivision
Cargo Block Longitudinal Bulkheads – 12.5 m from CL (CO-CUB-S and P)

	Compartment	Mir	# Sta	Aft m-MS	Fwd m-MS	Port m	Stbd m	Lower m	Upper m
1	FOREPEAK	N	7	105.000F	115.000F	HULL	HULL	HULL	HULL
2	NO.1 WBT S	N	11	80.000F	105.000F	CO-CUB-S	HULL	HULL	HULL
3	NO.1 COT C	N	11	80.000F	105.000F	CO-CUB-P	CO-CUB-S	HULL	HULL
4	NO.1 WBT P	N	11	80.000F	105.000F	HULL	CO-CUB-P	HULL	HULL
5	NO.2 WBT S	N	11	30.000F	80.000F	CO-CUB-S	HULL	HULL	HULL
6	NO.2 COT C	N	11	55.000F	80.000F	CO-CUB-P	CO-CUB-S	HULL	HULL
7	NO.2 WBT P	N	11	30.000F	80.000F	HULL	CO-CUB-P	HULL	HULL
8	NO.3 COT C	N	3	30.000F	55.000F	CO-CUB-P	CO-CUB-S	HULL	HULL
9	NO.4 COT S	N	3	5.000F	30.000F	CO-CUB-S	HULL	HULL	HULL
10	NO.4 COT C	N	3	5.000F	30.000F	CO-CUB-P	CO-CUB-S	HULL	HULL
11	NO.4 COT P	N	3	5.000F	30.000F	HULL	CO-CUB-P	HULL	HULL
12	NO.5 COT C	N	3	20.000A	5.000F	CO-CUB-P	CO-CUB-S	HULL	HULL
13	NO.4 WBT S	N	3	45.000A	5.000F	CO-CUB-S	HULL	HULL	HULL
14	NO.6 COT C	N	3	45.000A	20.000A	CO-CUB-P	CO-CUB-S	HULL	HULL
15	NO.4 WBT P	N	3	45.000A	5.000F	HULL	CO-CUB-P	HULL	HULL
16	NO.7 COT S	N	5	57.500A	45.000A	CO-CUB-S	HULL	HULL	HULL
17	NO.7 COT C	N	5	70.000A	45.000A	CO-CUB-P	CO-CUB-S	HULL	HULL
18	NO.7 COT P	N	5	57.500A	45.000A	HULL	CO-CUB-P	HULL	HULL
19	SLOP TANK S	N	3	70.000A	57.500A	CO-CUB-S	HULL	HULL	HULL
20	SLOP TANK P	N	3	70.000A	57.500A	HULL	CO-CUB-P	HULL	HULL
21	COFFERDAM	N	5	75.000A	70.000A	HULL	HULL	HULL	HULL
22	FO S	N	7	85.000A	75.000A	13.000S	HULL	HULL	HULL
23	ENGINE ROOM	N	7	95.000A	75.000A	13.000P	13.000S	2.000	HULL
24	ENG ROOM DB	N	5	95.000A	75.000A	HULL	HULL	HULL	2.000
25	FO P	N	7	85.000A	75.000A	HULL	13.000P	HULL	HULL
26	FRESH WTR S	N	5	95.000A	85.000A	13.000S	HULL	HULL	HULL
27	FRESH WTR P	N	5	95.000A	85.000A	HULL	13.000P	HULL	HULL
28	STRNG GEAR	N	7	114.000A	95.000A	HULL	HULL	16.000	HULL

Full Load cargo

FullLoadDepart

Cargo Oil Tank Name	Weight MT	% Full	Capacity MT	VCG m-BL	LCG m-MS	TCG m-CL	FSmom m-MT	Density MT/m3	Volume m3
NO.1 COT C	9,582	98.0	9,777	10.354	91.439F	0.000	13,010	0.9130	10,495
NO.2 COT C	11,316	98.0	11,547	10.330	67.500F	0.000	18,398	0.9130	12,394
NO.3 COT C	11,317	98.0	11,548	10.328	42.500F	0.000	18,394	0.9130	12,395
NO.4 COT S	3,789	98.0	3,867	10.230	17.500F	16.731S	1,173	0.9130	4,151
NO.4 COT C	11,318	98.0	11,549	10.328	17.500F	0.000	18,395	0.9130	12,396
NO.4 COT P	3,789	98.0	3,867	10.230	17.500F	16.731P	1,172	0.9130	4,151
NO.5 COT C	11,318	98.0	11,549	10.327	7.500A	0.000	18,396	0.9130	12,397
NO.6 COT C	11,318	98.0	11,549	10.328	32.500A	0.000	18,395	0.9130	12,397
NO.7 COT S	1,891	98.0	1,929	10.248	51.243A	16.722S	586	0.9130	2,071
NO.7 COT C	11,317	98.0	11,548	10.328	57.500A	0.000	18,395	0.9130	12,396
NO.7 COT P	1,891	98.0	1,929	10.248	51.243A	16.722P	586	0.9130	2,071
SLOP TANK S	1,845	98.0	1,883	10.424	63.690A	16.635S	586	0.9130	2,021
SLOP TANK P	1,845	98.0	1,883	10.424	63.690A	16.635P	586	0.9130	2,021
Totals	92,537	98.0	94,425	10.323	9.935F	0.000S	128,072		101,355

Ship Dimensions

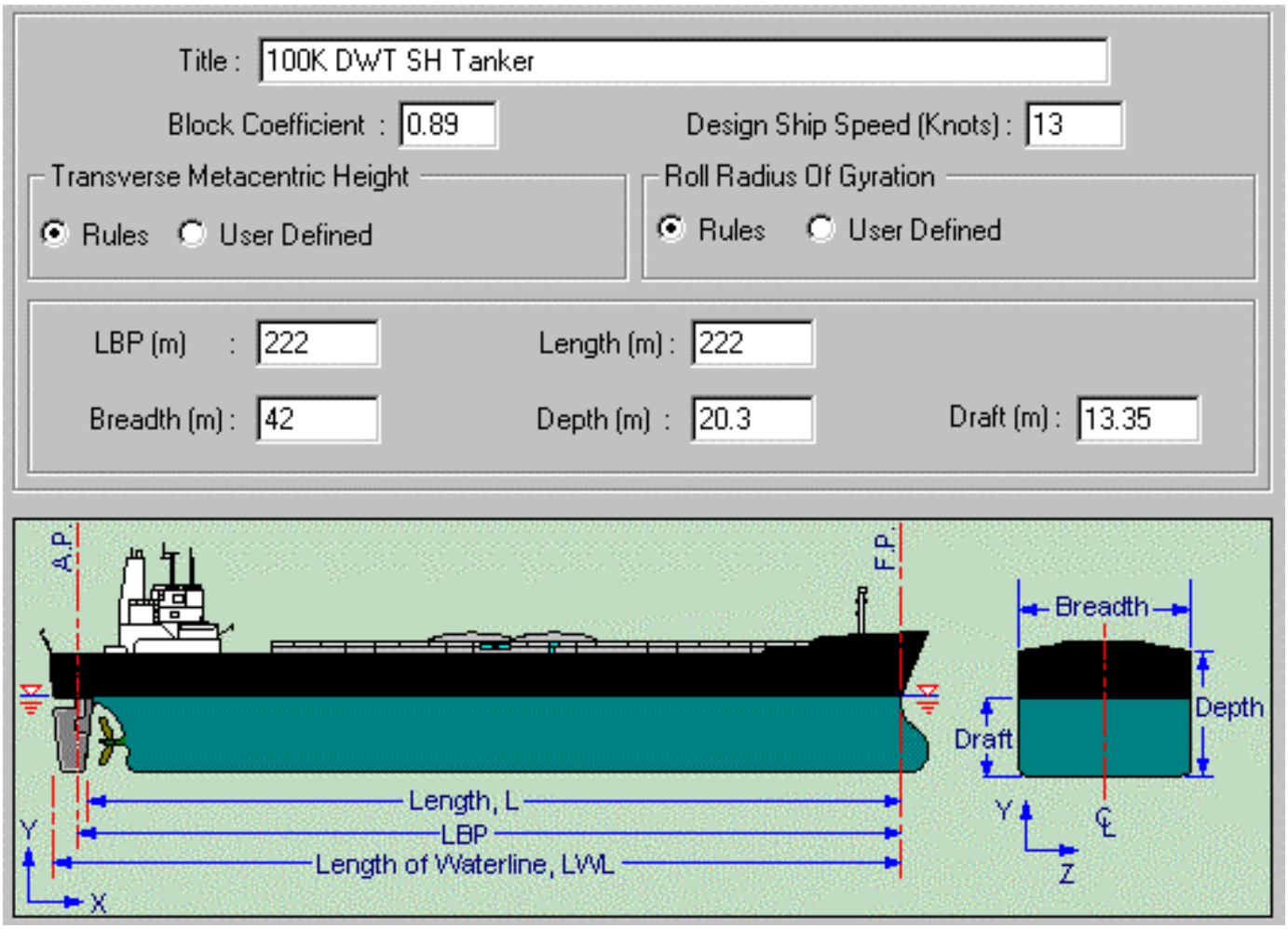

MIDSHIP GEOMETRY

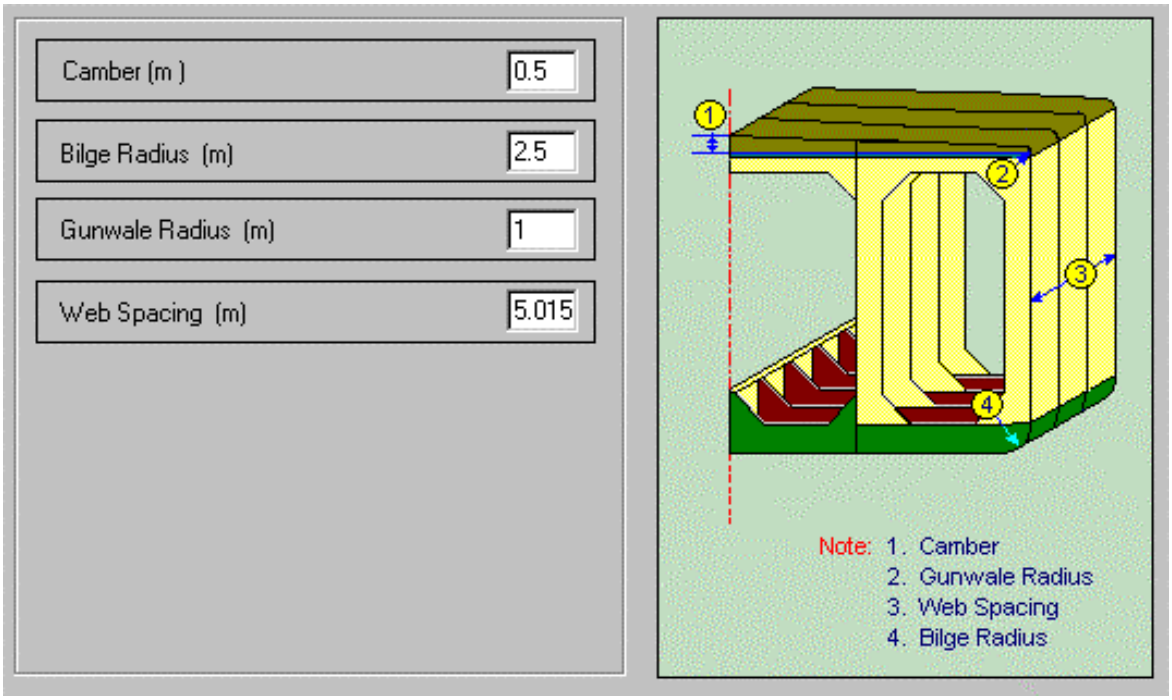

TANK DEFINITION

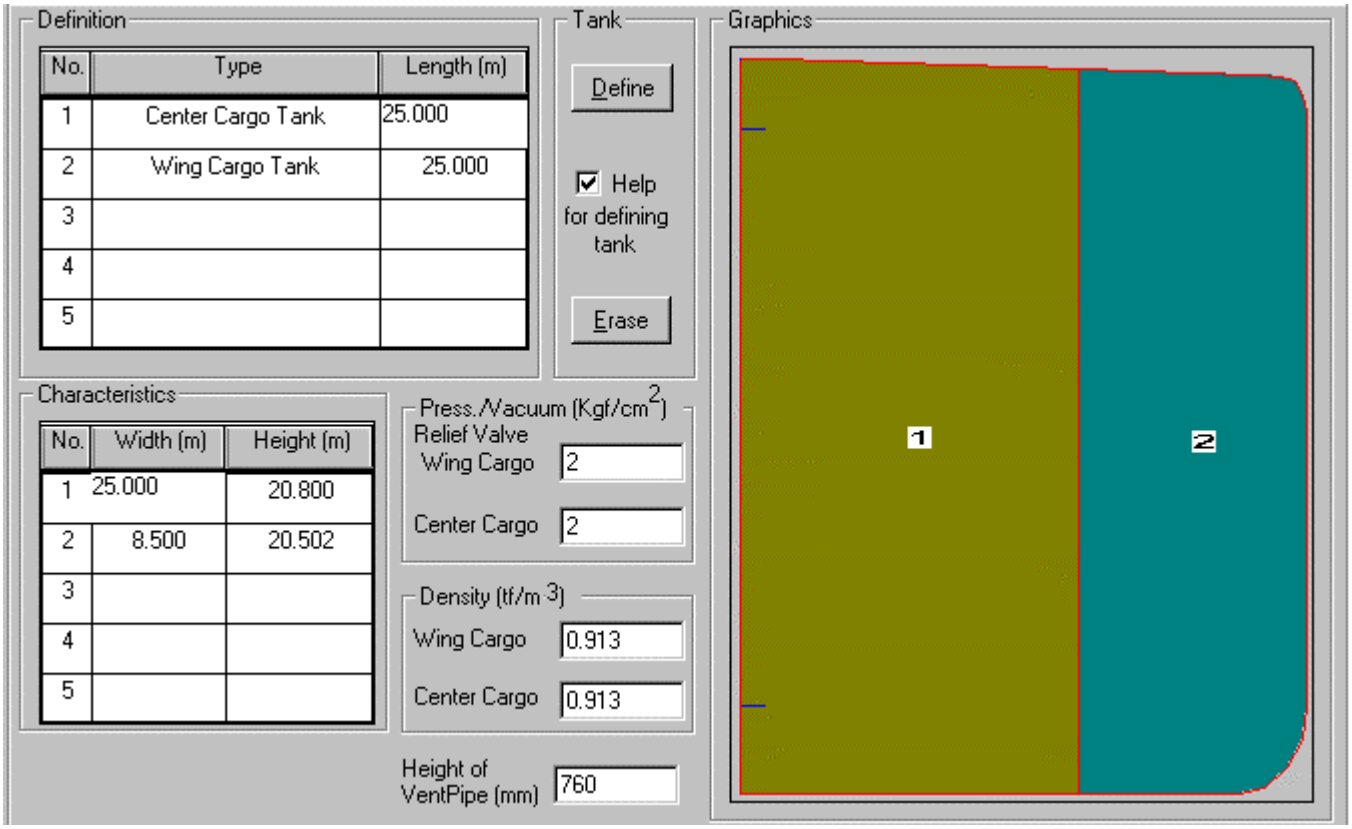

TRANSVERSE MEMBERS

Web Configuration

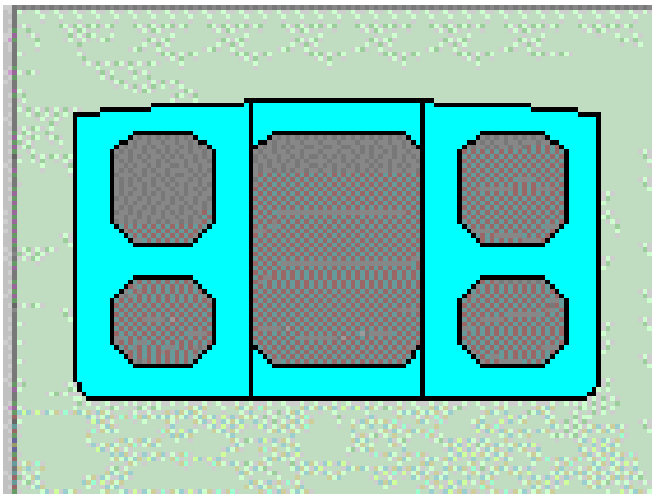

Spacing

Side Transverse (m) : 5.015

Deck Transverse (m) : 5.015

Vertical Web On Longitudinal Bulkhead (m) : 5.015

Strut

Number of Strut : 1

Span for main supporting member

○ User Defined

◉ Tank Configuration

Main Supporting Members – Side Transverse (Web)

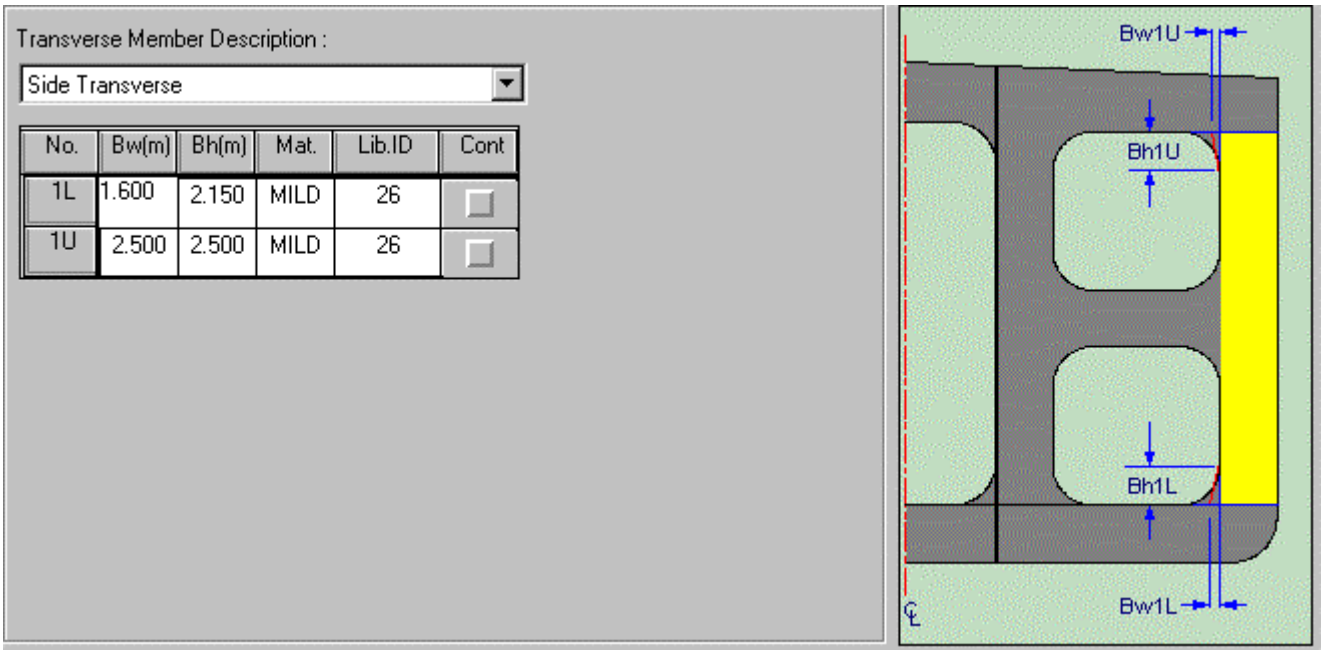

Web thickness: 15 mm

Main Supporting Members – Deck Transverse

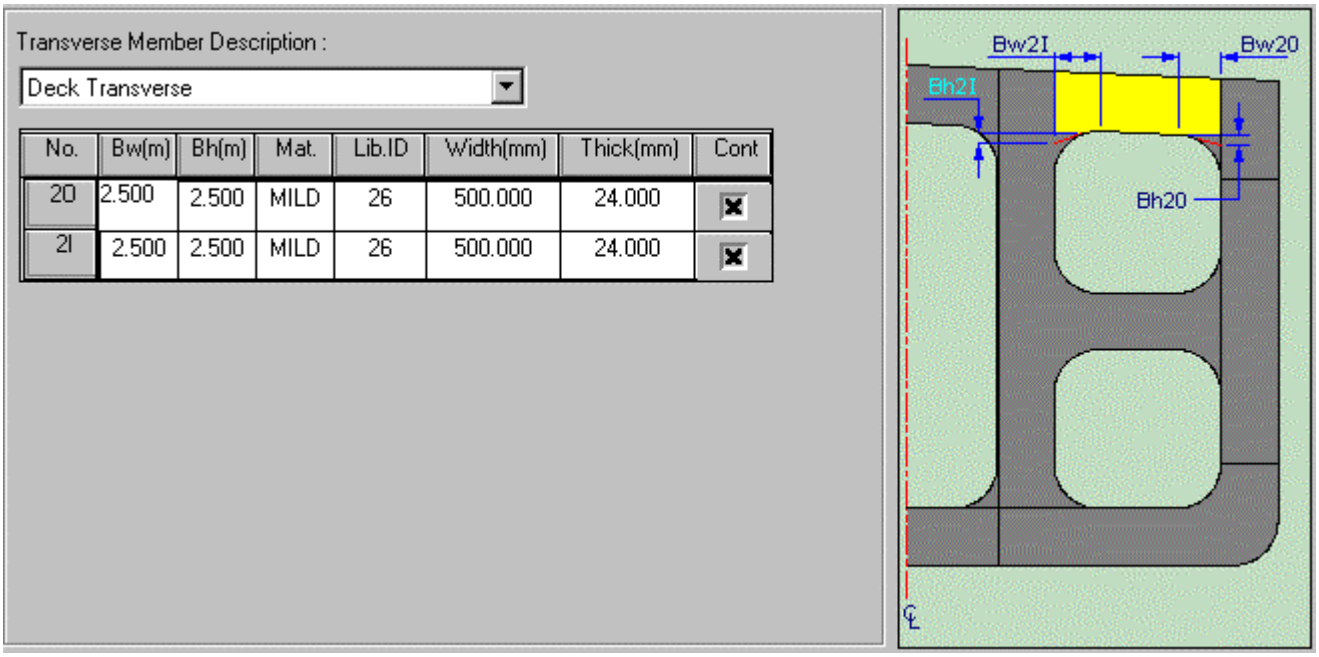

Deck Transverse web thickness: 15 mm

Main Supporting Members – Vertical Web on Longitudinal Bulkhead

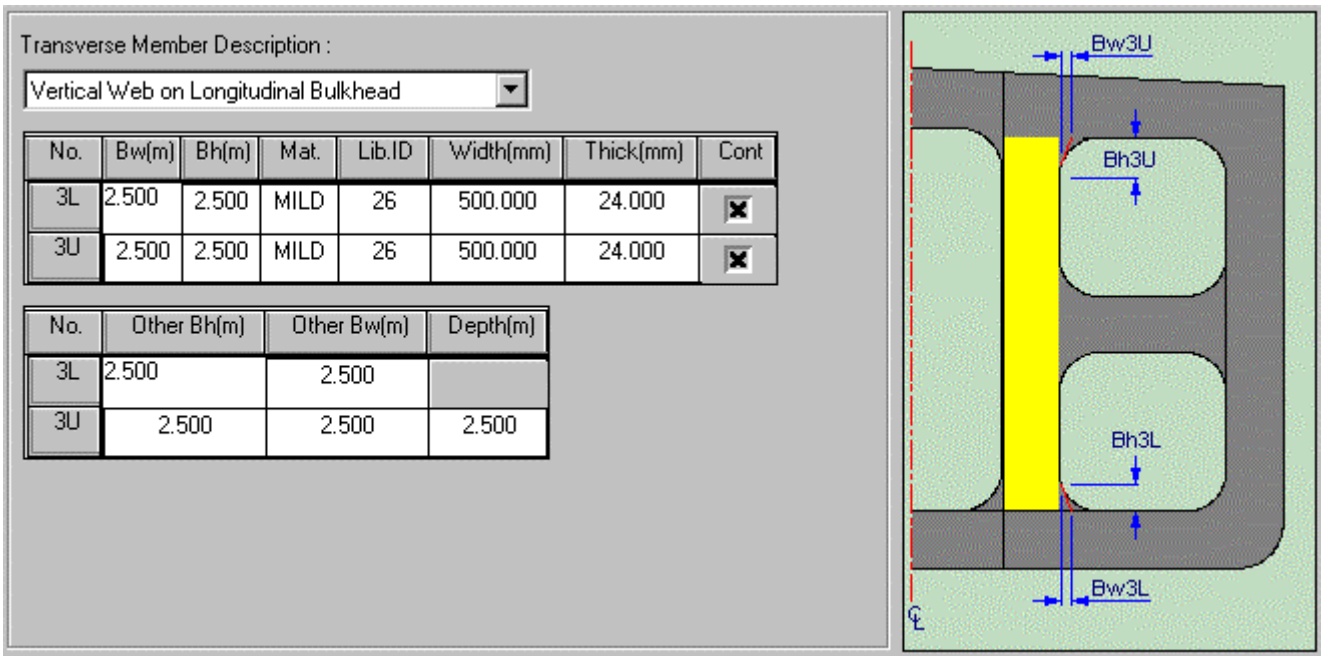

Vertical Web thickness: 15mm

Transverse Bulkhead

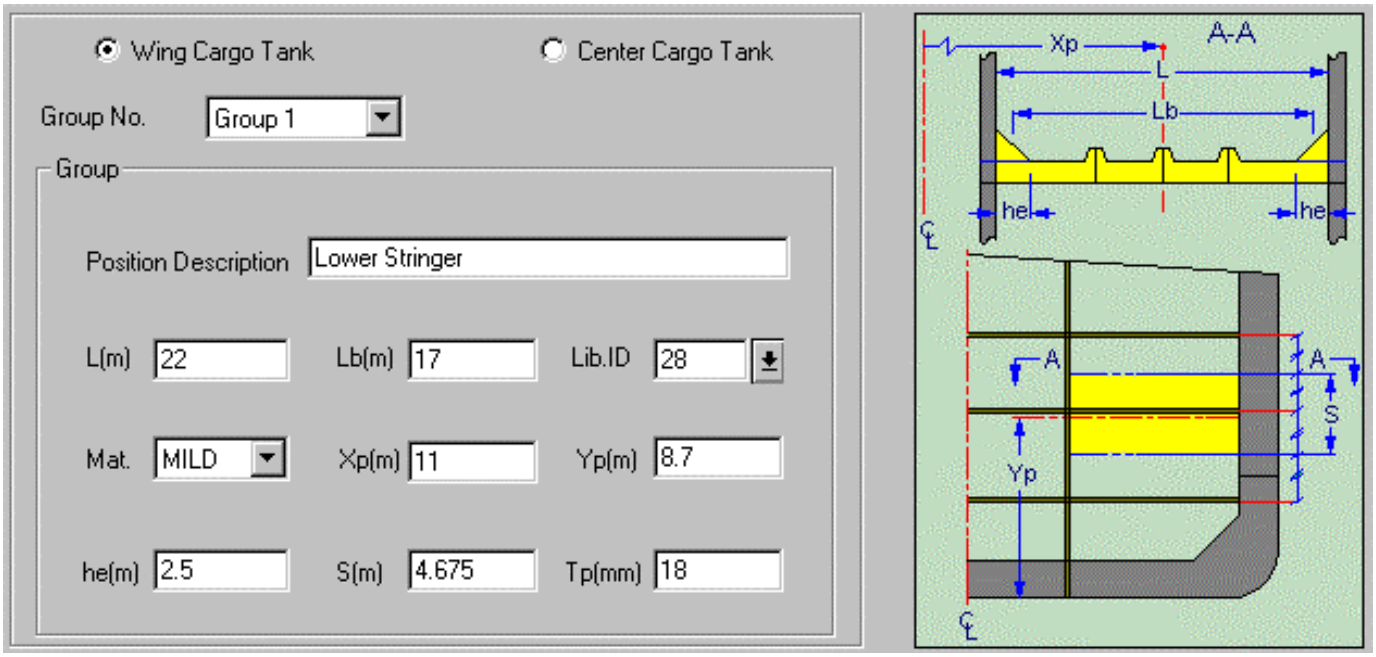

Horz Girder On Trn BHD. | Transverse BHD Plate/Stiffener | Vert Web On Trn BHD.

(•) Wing Cargo Tank ( ) Center Cargo Tank

Group No. Group 2

Group

Position Description: Upper Stringer

L(m)	22	Lb(m)	17	Lib.ID	29
Mat.	MILD	Xp(m)	11	Yp(m)	18.9
he(m)	2.5	S(m)	5.1	Tp(mm)	12

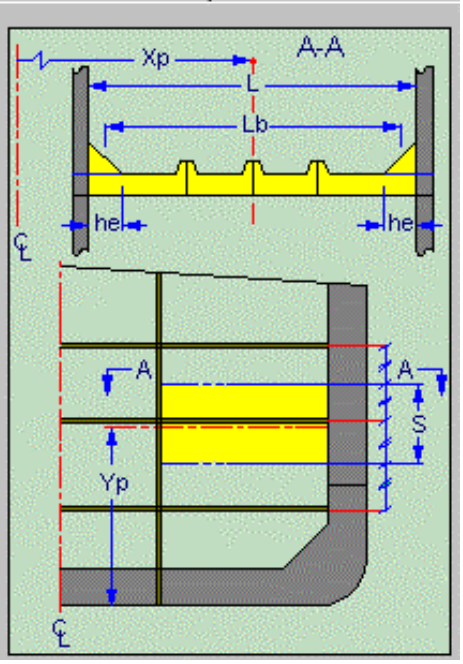

Horz Girder On Trn BHD. | Transverse BHD Plate/Stiffener | Vert Web On Trn BHD.

(•) Wing Cargo Tank ( ) Center Cargo Tank

Group No. Group 3

Group

Position Description: Stool Level

L(m)	22	Lb(m)	17	Lib.ID	28
Mat.	MILD	Xp(m)	11	Yp(m)	4.45
he(m)	2.5	S(m)	3.2	Tp(mm)	18

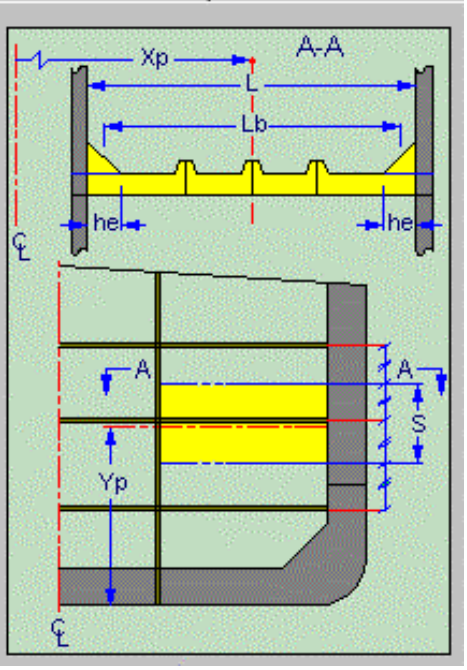

Horz Girder On Trn BHD. | Transverse BHD Plate/Stiffener | Vert Web On Trn BHD.

(•) Wing Cargo Tank ( ) Center Cargo Tank

Group No. Group 4

Group

Position Description: Middle Stringer

L(m): 22 Lb(m): 17 Lib.ID: 28

Mat.: MILD Xp(m): 11 Yp(m): 13.8

he(m): 2.5 S(m): 5.1 Tp(mm): 14

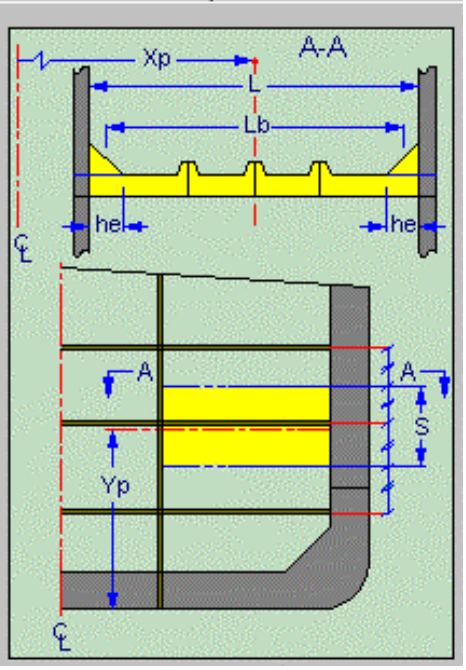

Horz Girder On Trn BHD. | **Transverse BHD Plate/Stiffener** | Vert Web On Trn BHD.

TB Group 1 Tank Type: Wing Cargo Tank

Description: Upper Xap (m): 152

Plate

Group: Plate 1 Zp (m): 11 SMax (mm): 850 Yp (m): 18.9

Description: TB Upper Thick.(mm): 12 Mat: MILD

Stiffener

No.	Type	Sp(mm)	Sl(m)	ZStfp(m)	YStfp(m)	Lib.ID	Mat.
1	1	850.00	5.100	11.000	21.450	11	MILD
2							
3							
4							
5							

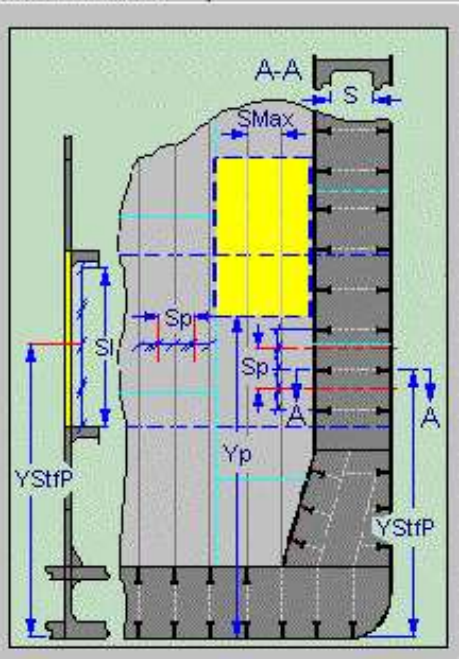

Horz Girder On Trn BHD. | **Transverse BHD Plate/Stiffener** | Vert Web On Trn BHD.

TB Group 2 | Tank Type: Wing Cargo Tank

Description: Middle | Xap (m): 152

Plate

Group: Plate 1 | Zp (m): 11 | SMax (mm): 850 | Yp (m): 13.8

Description: TB Middle | Thick.(mm): 14 | Mat: MILD

Stiffener

No.	Type	Sp(mm)	Sl(m)	ZStfp(m)	YStfp(m)	Lib.ID	Mat.
1	1	850.00	5.100	11.000	16.350	16	MILD
2							
3							
4							
5							

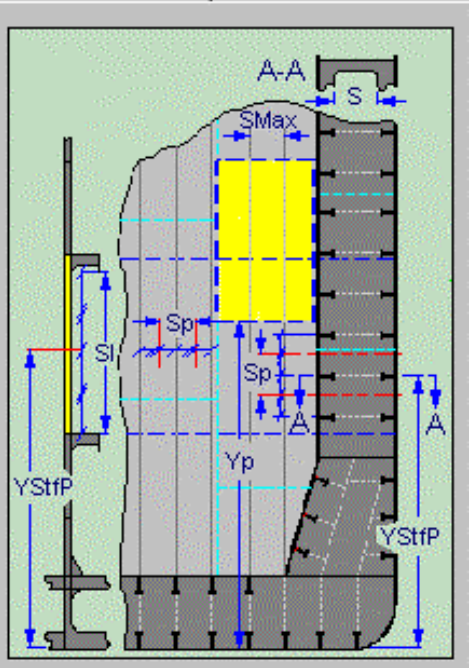

Horz Girder On Trn BHD. | **Transverse BHD Plate/Stiffener** | Vert Web On Trn BHD.

TB Group 3 | Tank Type: Wing Cargo Tank

Description: Lower | Xap (m): 152

Plate

Group: Plate 1 | Zp (m): 11 | SMax (mm): 850 | Yp (m): 8.7

Description: TB Lower | Thick.(mm): 16 | Mat: MILD

Stiffener

No.	Type	Sp(mm)	Sl(m)	ZStfp(m)	YStfp(m)	Lib.ID	Mat.
1	1	850.00	5.100	11.000	11.250	20	MILD
2							
3							
4							
5							

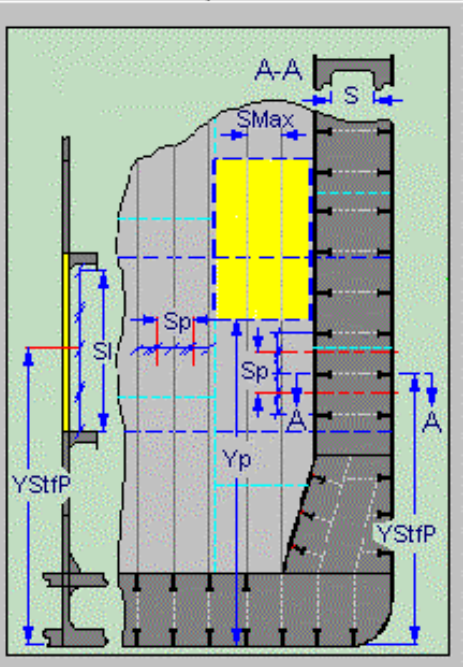

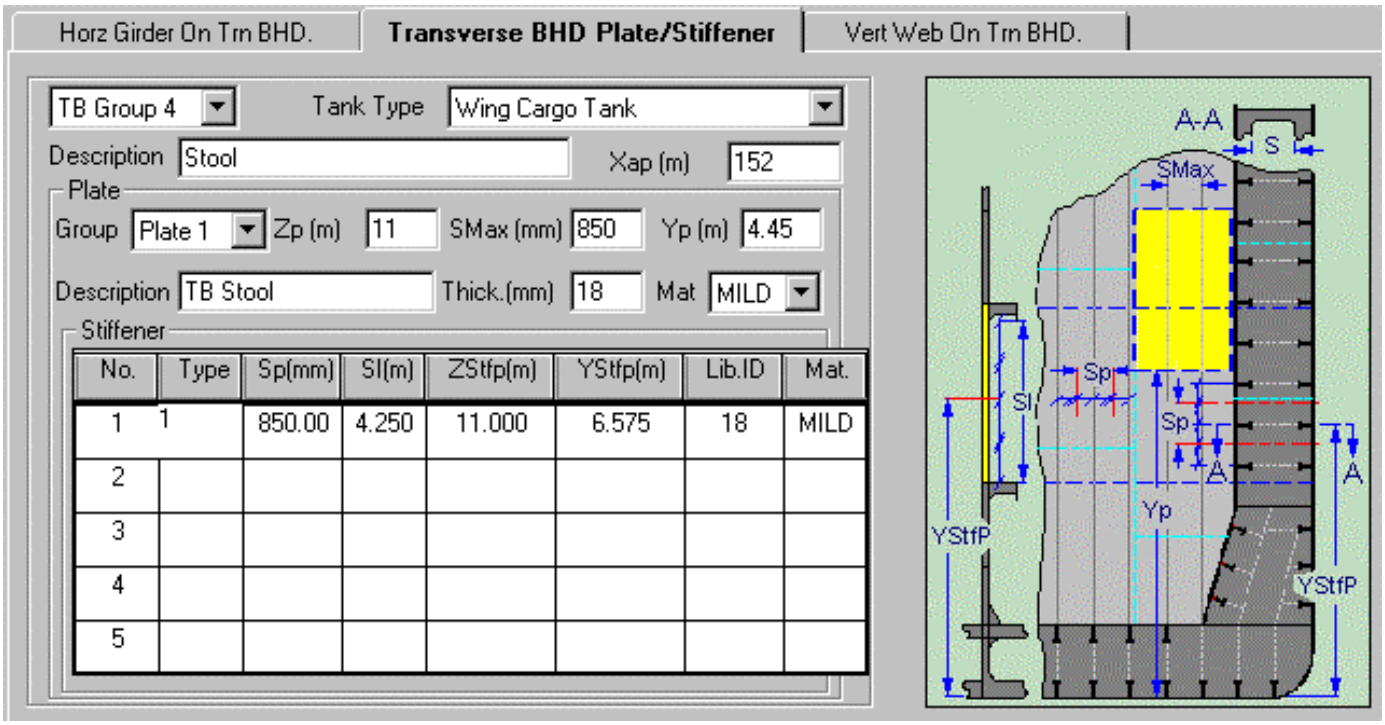
Horz Girder On Trn BHD.
Transverse BHD Plate/Stiffener
Vert Web On Trn BHD.
TB Group 4
Tank Type
Wing Cargo Tank
Description
Stool
Xap (m)
152
Plate
Group
Plate 1
Zp (m)
11
SMax (mm)
850
Yp (m)
4.45
Description
TB Stool
Thick.(mm)
18
Mat
MILD
Stiffener
No. Type Sp(mm) Sl(m) ZStfp(m) YStfp(m) Lib.ID Mat.
1 1 850.00 4.250 11.000 6.575 18 MILD
2
3
4
5
A-A
S
SMax
Sp
Sl
Sp
A
A
Yp
YStfP
YStfP

Struts

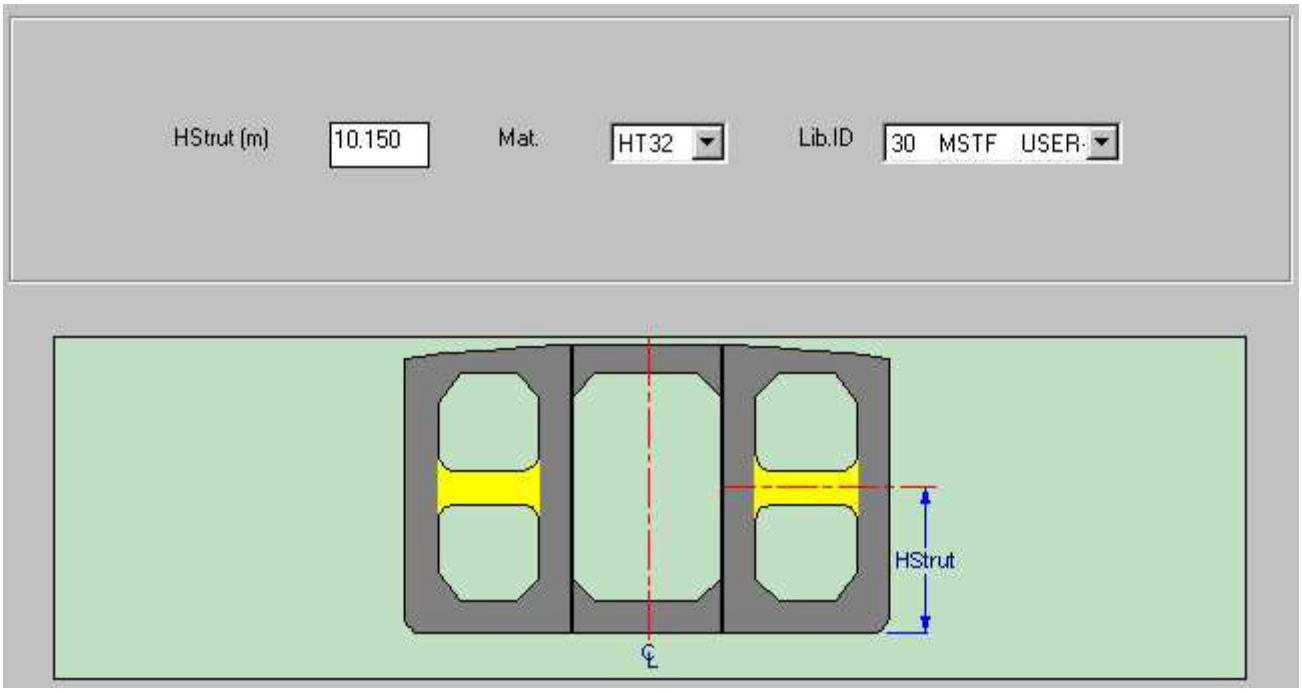
HStrut (m)
10.150
Mat.
HT32
Lib.ID
30 MSTF USER
HStrut
℄

Material Zones:

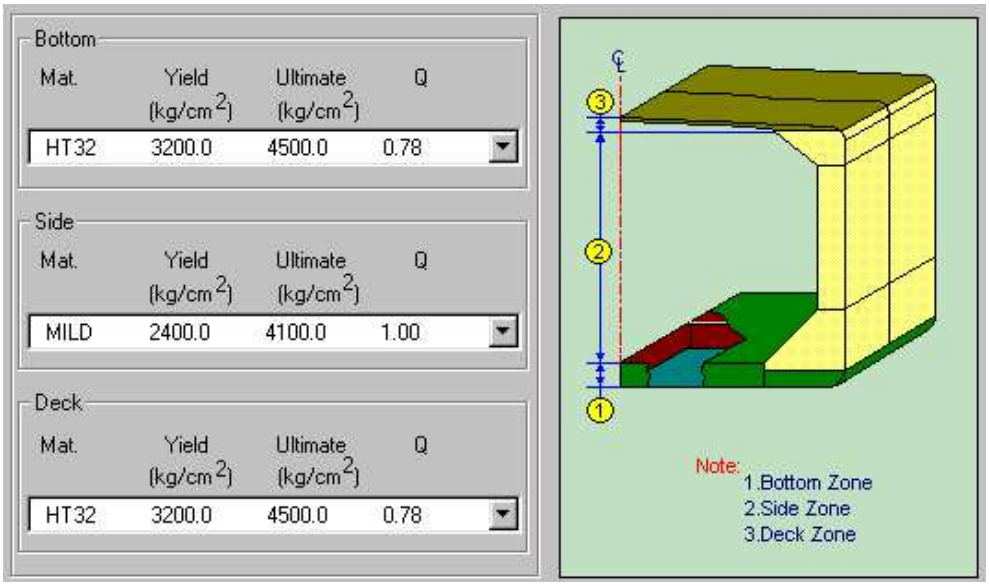

MATERIAL TABLE

==========

MAT #	MAT ID	YIELD STRESS	ULT STRESS	Q-FAC	Sm
(kgf/cm2)	(kgf/cm2)				
1	MILD	2400.	4100.	1.000	1.0
2	HT32	3200.	4500.	.780	.950
3	HT36	3600.	5000.	.720	.908
4	HT40	4000.	5200.	.680	.875

Stiffener Library:

#---- STIFFENER PROPERTIES; FILE:C:\SH_50\SH100\SH100.slb ; RECORDS: 29

#ID#	TYPE	ABS ID	DESCRIPTION	VAR 1	VAR 2	VAR 3	VAR 4	VAR 5	VAR 6
#(dimensions)				(mm)	(mm)	(mm)	(mm)	(mm)	(mm)
1	LANG	ILA200A	200x90x9x12 LIA	200.00	90.00	9.00	12.00	7.50	15.00
2	LANG	ILA225A	225x90x9x12 LIA	225.00	90.00	9.00	12.00	7.50	15.00
3	LANG	ILA250A	250x90x9x13 LIA	250.00	90.00	9.00	13.00	7.50	15.00
4	LANG	ILA250B	250x90x10.5x15 LIA	250.00	90.00	10.50	15.00	7.50	15.00
5	LANG	ILA250C	250x90x11.5x16 LIA	250.00	90.00	11.50	16.00	7.50	15.00
6	LANG	ILA275A	250x100x10.5x14 LIA	275.00	100.00	10.50	14.00	7.50	15.00
7	LANG	ILA300A	300x100x10.5x15 LIA	300.00	100.00	10.50	15.00	7.50	15.00
8	LANG	ILA300B	300x100x11.5x16 LIA	300.00	100.00	11.50	16.00	7.50	15.00
9	LANG	ILA325A	325x120x10.5x14 LIA	325.00	120.00	10.50	14.00	10.00	20.00
10	LANG	ILA325B	325x120x11.5x15 LIA	325.00	120.00	11.50	15.00	10.00	20.00
11	LANG	ILA350A	350x120x10.5x16 LIA	350.00	120.00	10.50	16.00	10.00	20.00
12	LANG	ILA350B	350x120x11.5x18 LIA	350.00	120.00	11.50	18.00	10.00	20.00
13	LANG	ILA375A	375x120x10.5x18 LIA	375.00	120.00	10.50	18.00	10.00	20.00
14	LANG	ILA375B	375x120x11.5x20 LIA	375.00	120.00	11.50	20.00	10.00	20.00
15	LANG	ILA400A	400x120x11.5x23 LIA	400.00	120.00	11.50	23.00	10.00	20.00
16	LANG	ILA425A	425x120x11.5x24 LIA	425.00	120.00	11.50	24.00	10.00	20.00
17	LANG	ILA450A	450x120x11.5x25 LIA	450.00	120.00	11.50	25.00	10.00	20.00
18	LANG	ILA475A	475x120x11.5x28 LIA	475.00	120.00	11.50	28.00	10.00	20.00
19	LANG	ILA475B	475x120x12.5x30 LIA	475.00	120.00	12.50	30.00	10.00	20.00
20	LANG	ILA500A	500x120x12.5x33 LIA	500.00	120.00	12.50	33.00	10.00	20.00
21	LANG	ILA500B	500x120x13.5x35 LIA	500.00	120.00	13.50	35.00	10.00	20.00
22	FLAT	USER-DEF	FB 400x28	400.00	28.00				
23	UANG	IUA150G	150X90X15 UIA	150.00	90.00	15.00	15.00	6.00	12.00
24	FLAT	USER-DEF	FB2000X12	2000.00	12.00				
25	FLAT	USER-DEF	FB2000X18	2000.00	18.00				
26	MSTF	USER-DEF	DECK WEB	3					
27	MSTF	USER-DEF	LBHD WEB	7					
28	MSTF	USER-DEF	BHD L STR	4					
29	MSTF	USER-DEF	BHD U STR	4					

User-Defined Shapes / Webs:

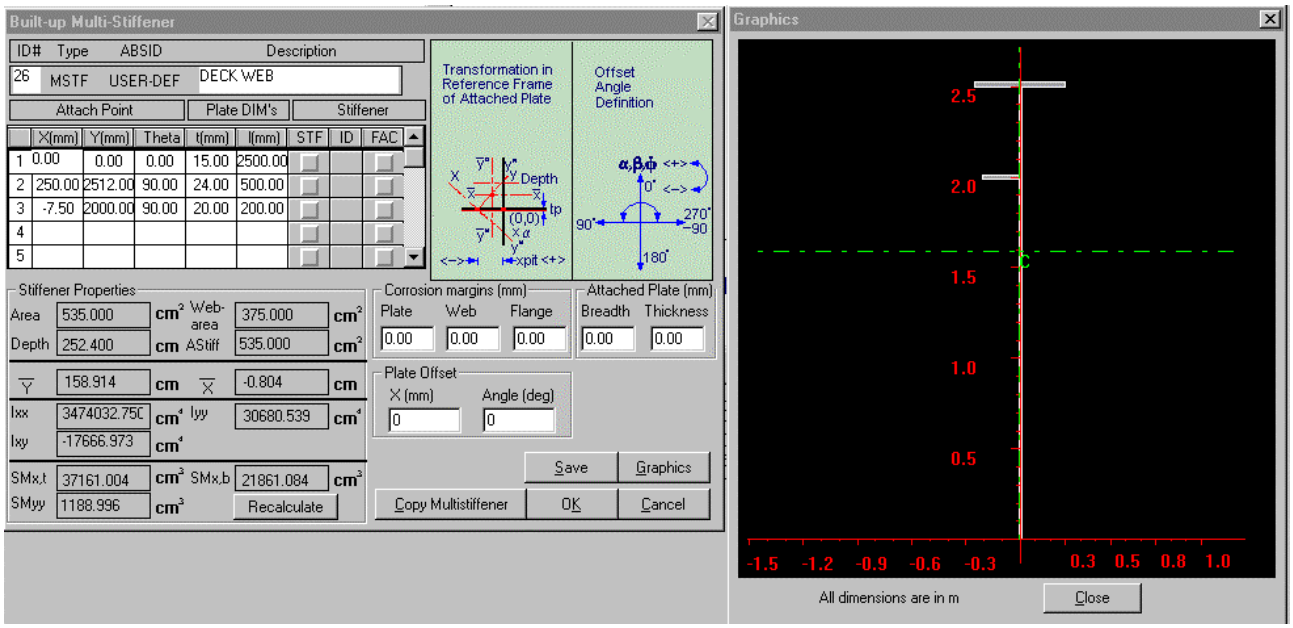

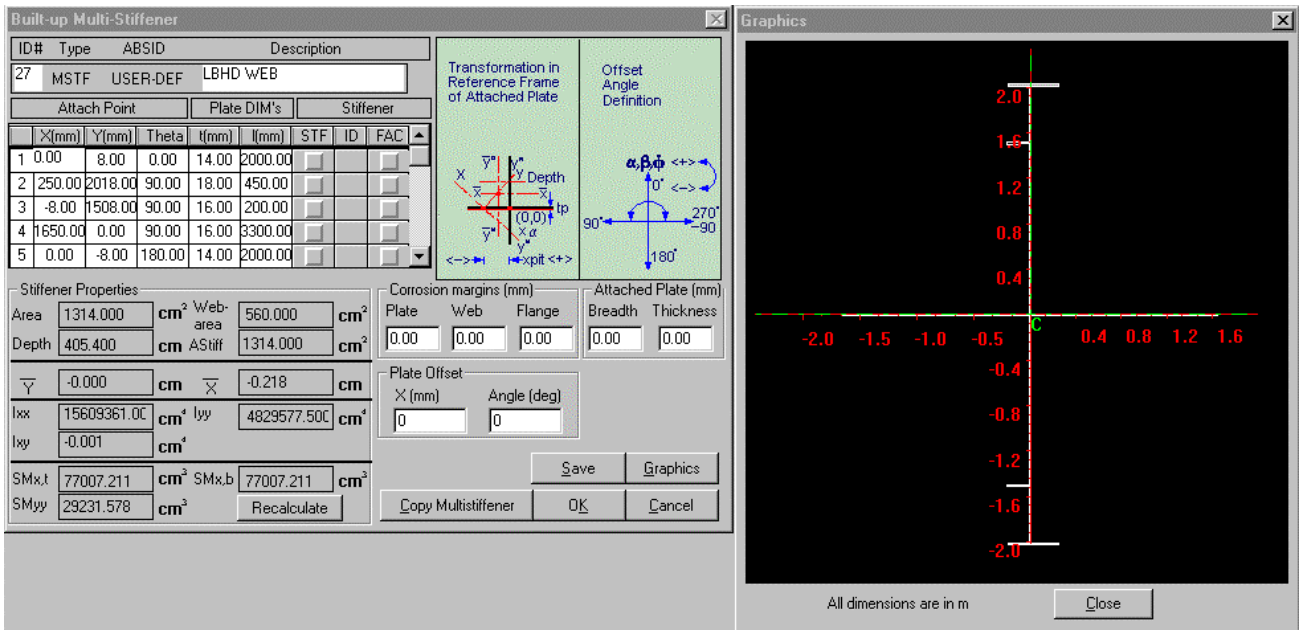

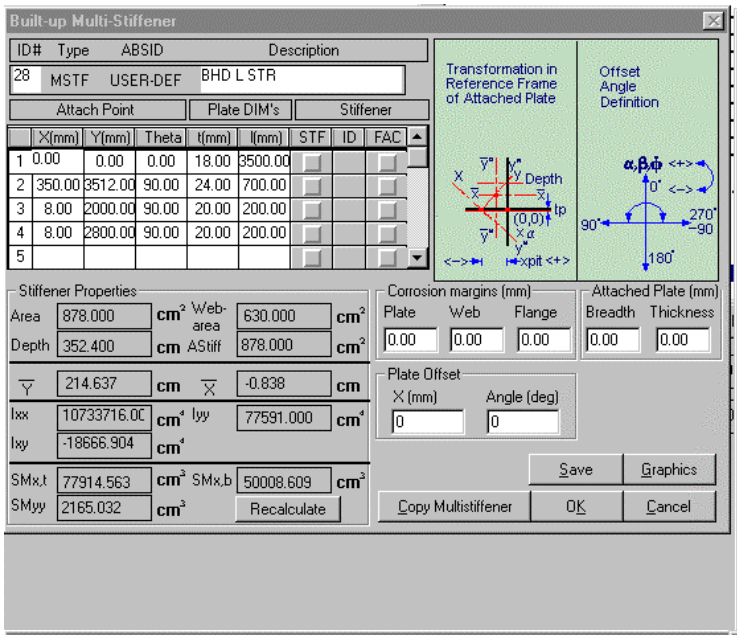
Built-up Multi-Stiffener
ID# Type ABSID Description
28 MSTF USER-DEF BHD L STR
Attach Point
Plate DIM's
Stiffener
X(mm) Y(mm) Theta t(mm) l(mm) STF ID FAC
1 0.00 0.00 0.00 18.00 3500.00
2 350.00 3512.00 90.00 24.00 700.00
3 8.00 2000.00 90.00 20.00 200.00
4 8.00 2800.00 90.00 20.00 200.00
5
Transformation in Reference Frame of Attached Plate
Offset Angle Definition
Depth
tp
xpit
Stiffener Properties
Area 878.000 cm²
Web-area 630.000 cm²
Depth 352.400 cm
AStiff 878.000 cm²
214.637 cm
-0.838 cm
Ixx 10733716.00 cm⁴
Iyy 77591.000 cm⁴
Ixy -18666.904 cm⁴
SMx,t 77914.563 cm³
SMx,b 50008.609 cm³
SMyy 2165.032 cm³
Recalculate
Corrosion margins (mm)
Plate Web Flange
0.00 0.00 0.00
Attached Plate (mm)
Breadth Thickness
0.00 0.00
Plate Offset
X (mm) Angle (deg)
0 0
Save
Graphics
Copy Multistiffener
OK
Cancel
Graphics
3.5
2.8
2.1
1.4
0.7
-2.0 -1.6 -1.2 -0.8 -0.4 0.3 0.6 0.9 1.2 1.5
All dimensions are in m
Close

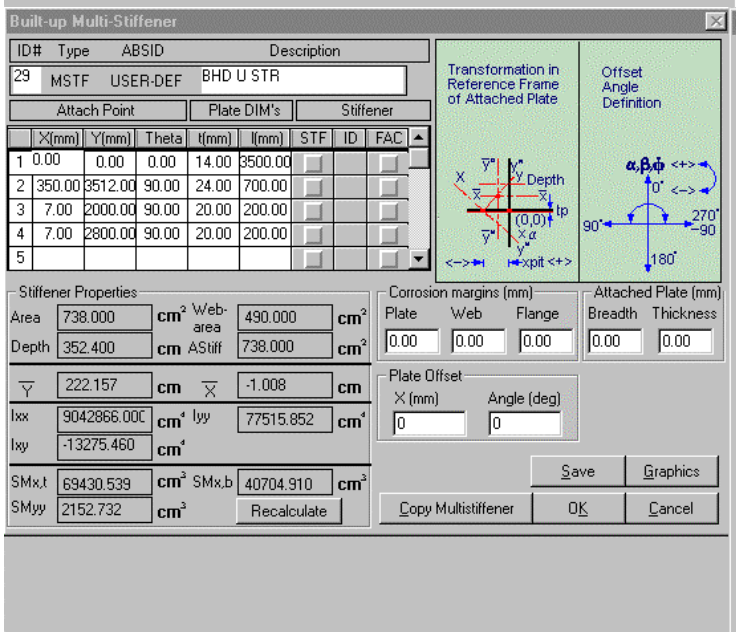
Built-up Multi-Stiffener
ID# Type ABSID Description
29 MSTF USER-DEF BHD U STR
Attach Point
Plate DIM's
Stiffener
X(mm) Y(mm) Theta t(mm) l(mm) STF ID FAC
1 0.00 0.00 0.00 14.00 3500.00
2 350.00 3512.00 90.00 24.00 700.00
3 7.00 2000.00 90.00 20.00 200.00
4 7.00 2800.00 90.00 20.00 200.00
5
Transformation in Reference Frame of Attached Plate
Offset Angle Definition
Depth
tp
xpit
Stiffener Properties
Area 738.000 cm²
Web-area 490.000 cm²
Depth 352.400 cm
AStiff 738.000 cm²
222.157 cm
-1.008 cm
Ixx 9042866.00 cm⁴
Iyy 77515.852 cm⁴
Ixy -13275.460 cm⁴
SMx,t 69430.539 cm³
SMx,b 40704.910 cm³
SMyy 2152.732 cm³
Recalculate
Corrosion margins (mm)
Plate Web Flange
0.00 0.00 0.00
Attached Plate (mm)
Breadth Thickness
0.00 0.00
Plate Offset
X (mm) Angle (deg)
0 0
Save
Graphics
Copy Multistiffener
OK
Cancel
Graphics
3.5
2.8
2.1
1.4
0.7
-2.0 -1.6 -1.2 -0.8 -0.4 0.3 0.6 0.9 1.2 1.5
All dimensions are in m
Close

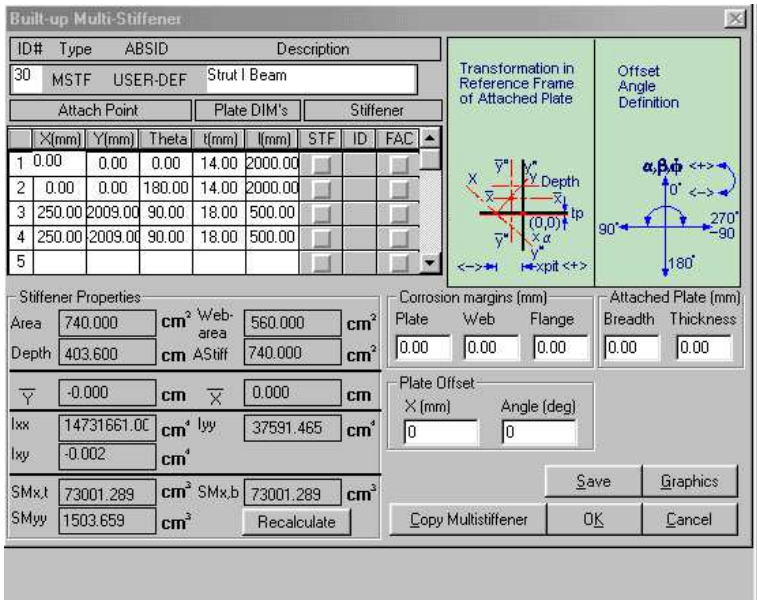
Built-up Multi-Stiffener
ID# Type ABSID Description
30 MSTF USER-DEF Strut I Beam
Attach Point
Plate DIM's
Stiffener
X(mm) Y(mm) Theta t(mm) l(mm) STF ID FAC
1 0.00 0.00 0.00 14.00 2000.00
2 0.00 0.00 180.00 14.00 2000.00
3 250.00 2009.00 90.00 18.00 500.00
4 250.00 2009.00 90.00 18.00 500.00
5
Transformation in Reference Frame of Attached Plate
Offset Angle Definition
Depth
tp
xpit
Stiffener Properties
Area 740.000 cm²
Web-area 560.000 cm²
Depth 403.600 cm
AStiff 740.000 cm²
-0.000 cm
0.000 cm
Ixx 14731661.00 cm⁴
Iyy 37591.465 cm⁴
Ixy -0.002 cm⁴
SMx,t 73001.289 cm³
SMx,b 73001.289 cm³
SMyy 1503.659 cm³
Recalculate
Corrosion margins (mm)
Plate Web Flange
0.00 0.00 0.00
Attached Plate (mm)
Breadth Thickness
0.00 0.00
Plate Offset
X (mm) Angle (deg)
0 0
Save
Graphics
Copy Multistiffener
OK
Cancel
Graphics
2.0
1.6
1.2
0.8
0.4
-2.0 -1.5 -1.0 -0.5 0.4 0.8 1.2 1.6
-0.4
-0.8
-1.2
-1.6
-2.0

Longitudinal Plate and Stiffener Elements

Local Plate IDs:

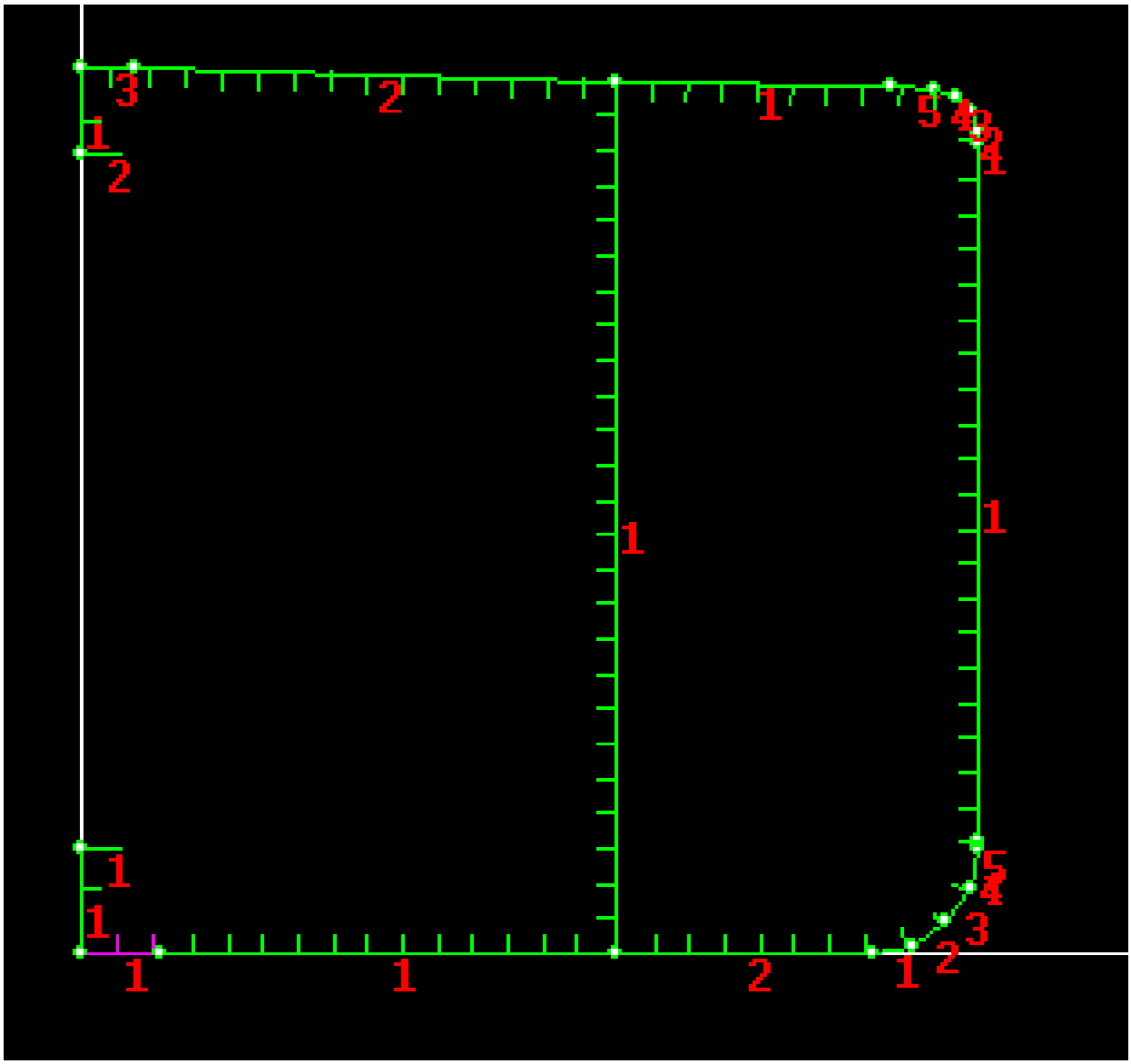

Global Plate Ids:

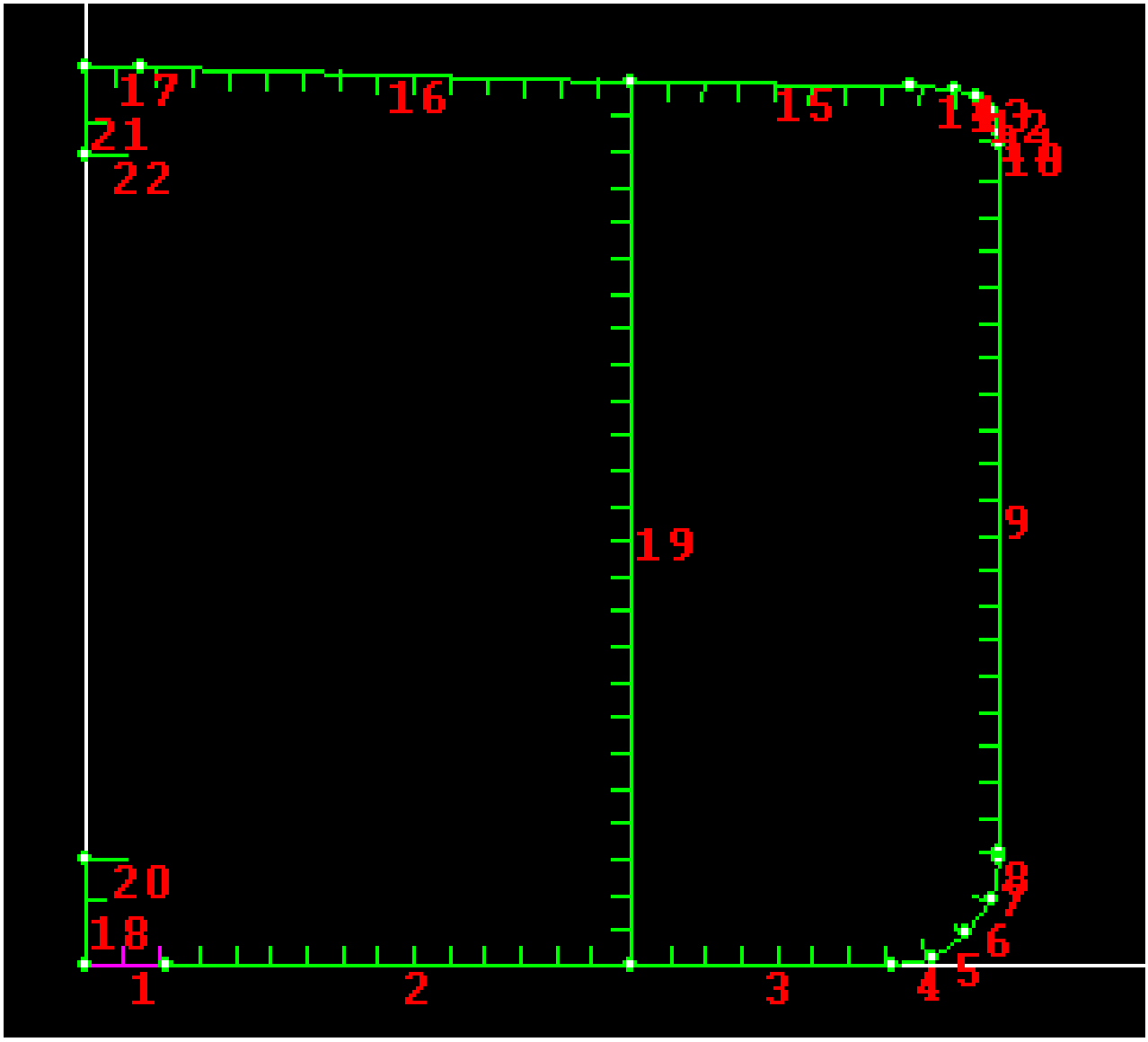

Plate:

DESCRIPTION	ID	B m	TP cm	A cm2	SPACING (m)	MATID	START X-COORD	START Y-COORD	END X-COORD	END Y-COORD
KEEL PLATE	KPL-01	1.8	2	360	0.96	3	0	0	1.8	0
BOTTOM	BTM-01	10.7	1.7	1819	0.96	3	1.8	0	12.5	0
BOTTOM	BTM-02	6	1.7	1020	0.92	3	12.5	0	18.5	0
BILGE	BLG-01	0.976	1.7	165.87	0.98	3	18.5	0	19.457	0.19
BILGE	BLG-02	0.975	1.7	165.82	0.976	3	19.457	0.19	20.268	0.732
BILGE	BLG-03	0.975	1.7	165.82	1.131	3	20.268	0.732	20.81	1.543
BILGE	BLG-04	0.976	1.7	165.87	1.231	3	20.81	1.543	21	2.5
BILGE	BLG-05	0.1	1.7	17	1.076	3	21	2.5	21	2.6
SIDE	SHL-01	16.4	1.6	2624	0.92	2	21	2.6	21	19
GUNWALE	GWR-01	0.3	1.7	51	0.92	2	21	19	21	19.3
GUNWALE	GWR-02	0.518	1.7	88	0.718	2	21	19.3	20.866	19.8
GUNWALE	GWR-03	0.518	1.7	87.99	0.518	2	20.866	19.8	20.5	20.166
GUNWALE	GWR-04	0.518	1.7	88	0.518	2	20.5	20.166	20	20.3
GUNWALE	GWR-05	1.001	1.7	170.2	0.901	2	20	20.3	19	20.348
UPPER DECK	DEC-01	6.502	1.7	1105.31	0.901	2	19	20.348	12.5	20.502
UPPER DECK	DEC-02	11.304	1.7	1921.67	0.904	2	12.5	20.502	1.2	20.8
UPPER DECK	DEC-03	1.2	1.7	204	0.904	2	1.2	20.8	0	20.8
N-TIGHT B. GDR	NBG-01	2.5	2.2	275	1.5	2	0	0	0	2.5
Other BULKHEAD	OTH-01	20.502	1.6	3280.32	0.822	2	12.5	0	12.5	20.502
MISC.	MSC-01	1	2	200	1	2	0	2.5	1	2.5
MISC.	MSC-02	2	1.7	170	1.25	2	0	20.8	0	18.8
MISC.	MSC-03	1	1.7	170	1	2	0	18.8	1	18.8

Local Stiffener Ids:

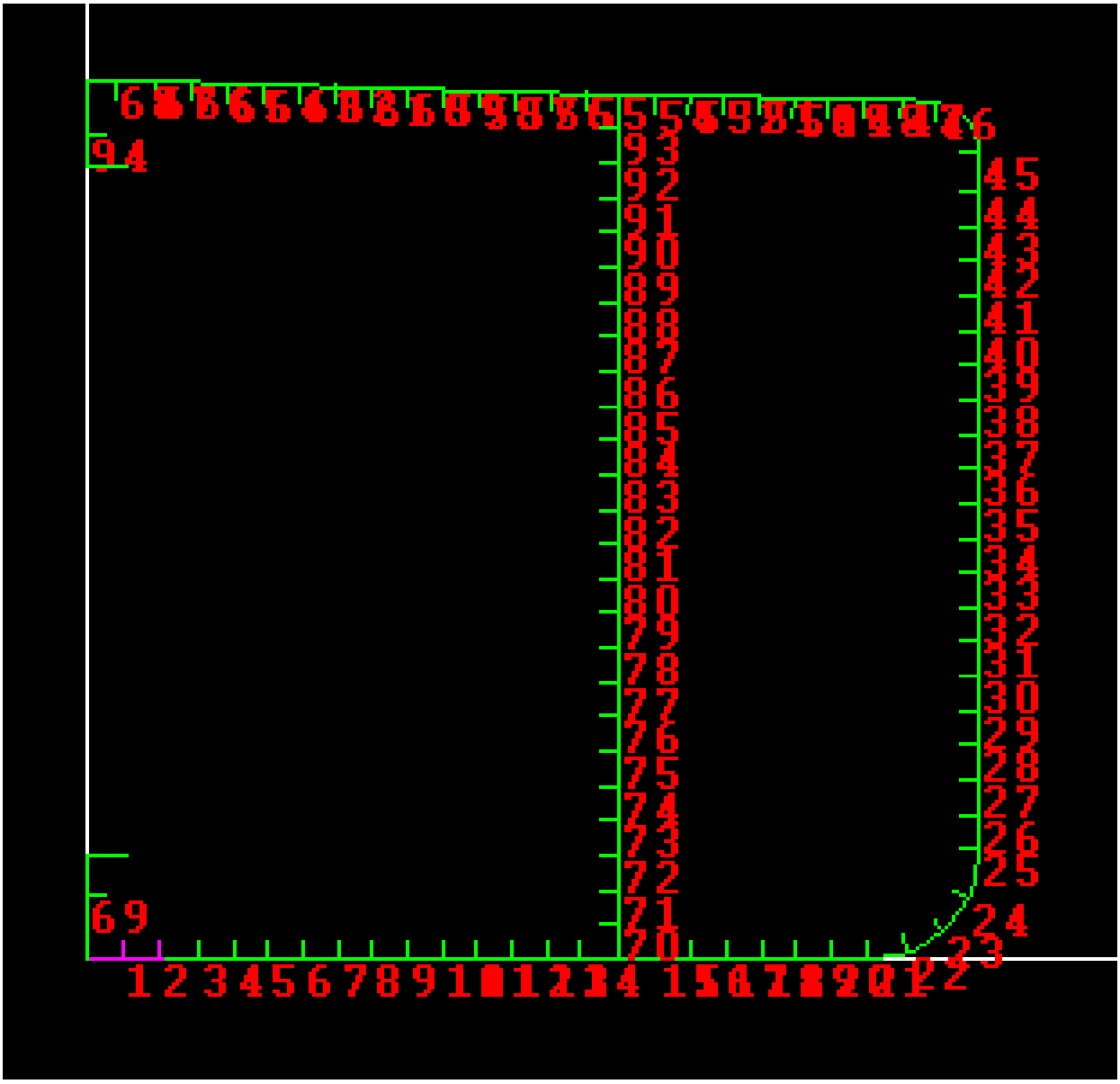

Global Stiffener IDs:

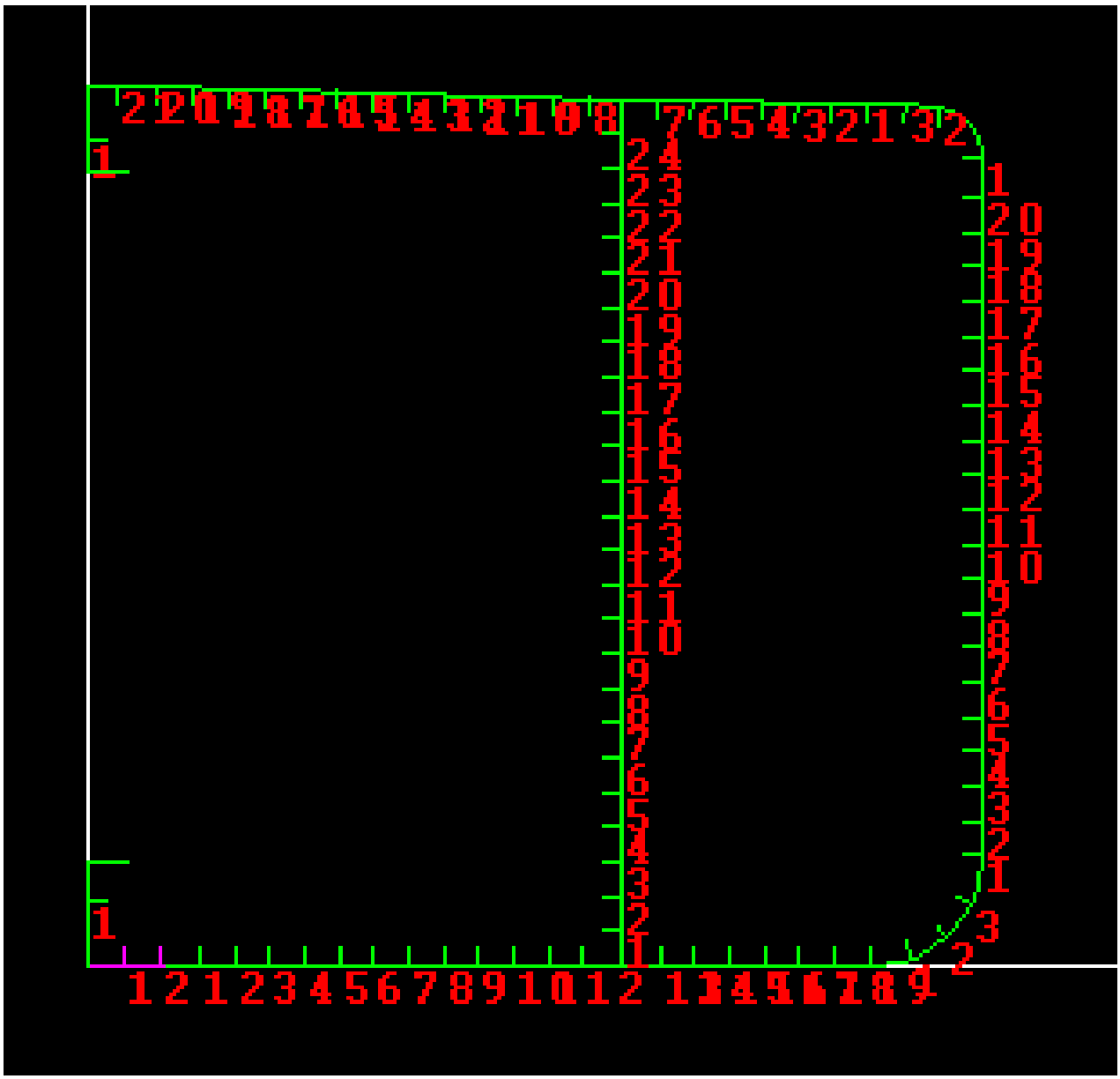

Stiffeners:

ID	MSID	XLB	A	STFSP	UNSPAN	MATID
			cm2	(m)	(m)	
KPL- 101	21	500x120x13.5x35 LIA	105.42	0.82	3.815	2
KPL- 102	21	500x120x13.5x35 LIA	105.42	0.89	3.815	2
BTM- 101	21	500x120x13.5x35 LIA	105.42	0.89	3.815	2
BTM- 102	21	500x120x13.5x35 LIA	105.42	0.82	3.815	2
BTM- 103	21	500x120x13.5x35 LIA	105.42	0.82	3.815	2
BTM- 104	21	500x120x13.5x35 LIA	105.42	0.82	3.815	2
BTM- 105	21	500x120x13.5x35 LIA	105.42	0.82	3.815	2
BTM- 106	21	500x120x13.5x35 LIA	105.42	0.82	3.815	2
BTM- 107	21	500x120x13.5x35 LIA	105.42	0.82	3.815	2
BTM- 108	21	500x120x13.5x35 LIA	105.42	0.82	3.815	2
BTM- 109	21	500x120x13.5x35 LIA	105.42	0.82	3.815	2
BTM- 110	21	500x120x13.5x35 LIA	105.42	0.82	3.815	2
BTM- 111	21	500x120x13.5x35 LIA	105.42	0.82	3.815	2
BTM- 112	21	500x120x13.5x35 LIA	105.42	0.85	3.815	2
BTM- 213	21	500x120x13.5x35 LIA	105.42	0.87	3.815	2
BTM- 214	21	500x120x13.5x35 LIA	105.42	0.82	3.815	2
BTM- 215	21	500x120x13.5x35 LIA	105.42	0.82	3.815	2
BTM- 216	21	500x120x13.5x35 LIA	105.42	0.82	3.815	2
BTM- 217	21	500x120x13.5x35 LIA	105.42	0.82	3.815	2
BTM- 218	21	500x120x13.5x35 LIA	105.42	0.82	3.815	2
BTM- 219	21	500x120x13.5x35 LIA	105.42	1.053	3.815	2
BLG- 101	0	500x120x13.5x35 LIA	105.42	0.488	3.815	2
BLG- 202	0	500x120x13.5x35 LIA	105.42	0.488	3.815	2
BLG- 303	0	500x120x13.5x35 LIA	105.42	0.488	3.815	2
SHL- 101	20	500x120x12.5x33 LIA	98.62	0.82	4.515	2
SHL- 102	20	500x120x12.5x33 LIA	98.62	0.82	4.515	2
SHL- 103	20	500x120x12.5x33 LIA	98.62	0.82	4.515	2
SHL- 104	20	500x120x12.5x33 LIA	98.62	0.82	4.515	2
SHL- 105	20	500x120x12.5x33 LIA	98.62	0.82	4.515	2
SHL- 106	20	500x120x12.5x33 LIA	98.62	0.82	4.515	2
SHL- 107	20	500x120x12.5x33 LIA	98.62	0.82	4.515	2
SHL- 108	20	500x120x12.5x33 LIA	98.62	0.82	4.515	2
SHL- 109	20	500x120x12.5x33 LIA	98.62	0.82	4.515	2
SHL- 110	20	500x120x12.5x33 LIA	98.62	0.82	4.515	2
SHL- 111	20	500x120x12.5x33 LIA	98.62	0.82	4.515	2
SHL- 112	20	500x120x12.5x33 LIA	98.62	0.82	4.515	2
SHL- 113	20	500x120x12.5x33 LIA	98.62	0.82	4.515	2
SHL- 114	20	500x120x12.5x33 LIA	98.62	0.82	4.515	2
SHL- 115	20	500x120x12.5x33 LIA	98.62	0.82	4.515	2
SHL- 116	20	500x120x12.5x33 LIA	98.62	0.82	4.515	2
SHL- 117	20	500x120x12.5x33 LIA	98.62	0.82	4.515	2
SHL- 118	20	500x120x12.5x33 LIA	98.62	0.82	4.515	2
SHL- 119	20	500x120x12.5x33 LIA	98.62	0.82	4.515	2
SHL- 120	20	500x120x12.5x33 LIA	98.62	0.82	4.515	2
GWR- 101	14	375x120x11.5x20 LIA	65.47	0.15	4.515	2
GWR- 502	14	375x120x11.5x20 LIA	65.47	0.82	4.515	2
GWR- 503	14	375x120x11.5x20 LIA	65.47	0.861	4.515	2
DEC- 101	18	475x120x11.5x28 LIA	85.65	0.861	4.515	2

DEC- 102	18	475x120x11.5x28 LIA	85.65	0.82	4.515	2
DEC- 103	18	475x120x11.5x28 LIA	85.65	0.82	4.515	2
DEC- 104	18	475x120x11.5x28 LIA	85.65	0.82	4.515	2
DEC- 105	18	475x120x11.5x28 LIA	85.65	0.82	4.515	2
DEC- 106	18	475x120x11.5x28 LIA	85.65	0.82	4.515	2
DEC- 107	18	475x120x11.5x28 LIA	85.65	0.841	4.515	2
DEC- 208	18	475x120x11.5x28 LIA	85.65	0.8	4.515	2
DEC- 209	18	475x120x11.5x28 LIA	85.65	0.85	4.515	2
DEC- 210	18	475x120x11.5x28 LIA	85.65	0.85	4.515	2
DEC- 211	18	475x120x11.5x28 LIA	85.65	0.85	4.515	2
DEC- 212	18	475x120x11.5x28 LIA	85.65	0.85	4.515	2
DEC- 213	18	475x120x11.5x28 LIA	85.65	0.85	4.515	2
DEC- 214	18	475x120x11.5x28 LIA	85.65	0.85	4.515	2
DEC- 215	18	475x120x11.5x28 LIA	85.65	0.85	4.515	2
DEC- 216	18	475x120x11.5x28 LIA	85.65	0.85	4.515	2
DEC- 217	18	475x120x11.5x28 LIA	85.65	0.85	4.515	2
DEC- 218	18	475x120x11.5x28 LIA	85.65	0.85	4.515	2
DEC- 219	18	475x120x11.5x28 LIA	85.65	0.85	4.515	2
DEC- 220	18	475x120x11.5x28 LIA	85.65	0.927	4.515	2
DEC- 321	18	475x120x11.5x28 LIA	85.65	0.6	4.515	2
NBG- 101	14	375x120x11.5x20 LIA	32.73	1.25	4.515	2
OTH- 101	20	500x120x12.5x33 LIA	98.62	0.82	4.515	2
OTH- 102	20	500x120x12.5x33 LIA	98.62	0.82	4.515	2
OTH- 103	20	500x120x12.5x33 LIA	98.62	0.82	4.515	2
OTH- 104	20	500x120x12.5x33 LIA	98.62	0.82	4.515	2
OTH- 105	20	500x120x12.5x33 LIA	98.62	0.82	4.515	2
OTH- 106	20	500x120x12.5x33 LIA	98.62	0.82	4.515	2
OTH- 107	20	500x120x12.5x33 LIA	98.62	0.82	4.515	2
OTH- 108	20	500x120x12.5x33 LIA	98.62	0.82	4.515	2
OTH- 109	20	500x120x12.5x33 LIA	98.62	0.82	4.515	2
OTH- 110	20	500x120x12.5x33 LIA	98.62	0.82	4.515	2
OTH- 111	20	500x120x12.5x33 LIA	98.62	0.82	4.515	2
OTH- 112	20	500x120x12.5x33 LIA	98.62	0.82	4.515	2
OTH- 113	20	500x120x12.5x33 LIA	98.62	0.82	4.515	2
OTH- 114	20	500x120x12.5x33 LIA	98.62	0.82	4.515	2
OTH- 115	20	500x120x12.5x33 LIA	98.62	0.82	4.515	2
OTH- 116	20	500x120x12.5x33 LIA	98.62	0.82	4.515	2
OTH- 117	20	500x120x12.5x33 LIA	98.62	0.82	4.515	2
OTH- 118	20	500x120x12.5x33 LIA	98.62	0.82	4.515	2
OTH- 119	20	500x120x12.5x33 LIA	98.62	0.82	4.515	2
OTH- 120	20	500x120x12.5x33 LIA	98.62	0.82	4.515	2
OTH- 121	20	500x120x12.5x33 LIA	98.62	0.82	4.515	2
OTH- 122	20	500x120x12.5x33 LIA	98.62	0.82	4.515	2
OTH- 123	20	500x120x12.5x33 LIA	98.62	0.82	4.515	2
OTH- 124	20	500x120x12.5x33 LIA	98.62	0.821	4.515	2
MSC- 201	14	375x120x11.5x20 LIA	32.73	1.5	5.015	2

Vita

John A. W. Sajdak was born in Pontiac, Michigan (USA) on January 28, 1978. His Primary Education was at Birmingham Brother Rice High School in Bloomfield Hills, Michigan.

He then attended Virginia Polytechnic Institute and State University (Virginia Tech), Blacksburg, USA for his undergraduate studies. Receiving a Bachelor of Science in Ocean Engineering in May 2001 and a Doctor of Philosophy in Loving His Wife in August 2004.